ΠΑΝΕΠΙΣΤΗΜΙΟ ΠΕΛΟΠΟΝΝΗΣΟΥ

ΣΧΟΛΗ ΜΗΧΑΝΙΚΩΝ

ΤΜΗΜΑ ΗΛΕΚΤΡΟΛΟΓΩΝ ΜΗΧΑΝΙΚΩΝ ΚΑΙ ΜΗΧΑΝΙΚΩΝ ΥΠΟΛΟΓΙΣΤΩΝ

ΠΤΥΧΙΑΚΗ ΕΡΓΑΣΙΑ

ΥΠΟΣΤΗΡΙΞΗ ΕΡΕΥΝΗΤΙΚΟΥ ΕΡΓΟΥ: ΕΛΛΗΝΙΚΗ ΚΑΙ ΑΓΓΛΙΚΗ ΕΠΙΣΤΗΜΟΝΙΚΗ ΟΡΟΛΟΓΙΑ, ΜΕΤΑΦΡΑΣΗ ΤΕΧΝΙΚΟΥ ΚΕΙΜΕΝΟΥ, ΣΥΛΛΟΓΗ ΚΑΙ ΟΡΓΑΝΩΣΗ ΒΙΒΛΙΟΓΡΑΦΙΑΣ

ΣΠΟΥΔΑΣΤΡΙΑ: ΜΗΛΑ ΔΗΜΗΤΡΑ (7173)

ΕΠΙΒΛΕΠΩΝ ΚΑΘΗΓΗΤΗΣ: ΧΑΡΑΛΑΜΠΑΚΟΣ ΒΑΣΙΛΕΙΟΣ

ΑΡΙΘΜΟΣ ΠΤΥΧΙΑΚΗΣ: 1737

ΠΑΤΡΑ 2021

Ευχαριστίες

Αρχικά, θα ήθελα να ευχαριστήσω τον εισηγητή της εργασίας μου κ. Γεώργιο Δημητρακάκη, για την ανάθεση της παρούσας πτυχιακής και για την εμπιστοσύνη που μου έδειξε για τη μετάφραση της διδακτορικής του διατριβής, αλλά και για την πολύτιμη βοήθεια και καθοδήγηση που μου παρείχε κατά την διάρκεια της πτυχιακής μου εργασίας. Τέλος θα ήθελα να ευχαριστήσω την οικογένειά μου για την υλική και ηθική υποστήριξη καθ' όλη την διάρκεια των σπουδών μου.

Περίληψη

Σε αυτή την πτυχιακή εργασία επιτυγχάνεται η υποστήριξη ερευνητικού έργου μέσα από τη μετάφραση μιας διδακτορικής διατριβής πάνω στο αντικείμενο των ηλεκτρονικών ισχύος, αλλά και με την υπόδειξη κατάλληλου λογισμικού αναζήτησης, συλλογής και οργάνωσης βιβλιογραφίας, έπειτα από σχετική διερεύνηση σε ένα σύνολο διάφορων αντίστοιχων εργαλείων. Επίσης, σπουδαίο μέρος της εργασίας αφιερώνεται στην ανάλυση της σημασίας γνώσης της τεχνικής ορολογίας στο επάγγελμα του ηλεκτρολόγου μηχανικού και στην μεθοδολογία ορθής μετάφρασης τεχνικού κειμένου.

Πιο συγκεκριμένα, γίνεται μετάφραση από τα ελληνικά στα αγγλικά της διδακτορικής διατριβής με τίτλο: «Διερεύνηση των απωλειών των μαγνητικών στοιχείων διαρρεόμενων από υψίσυχνα ρεύματα για εφαρμογές σε διατάξεις ηλεκτρονικών ισχύος» του Γεώργιου Δημητρακάκη, Δρ. Φυσικού του Παν/μίου Πατρών. Ακόμα γίνεται μετάφραση όλων των κειμένων εντός της διατριβής, και για όσα από τα σχήματα υπήρχε η δυνατότητα να αντικατασταθούν από καλύτερης ευκρίνειας αντικαταστάθηκαν ή επεξεργάστηκαν μέσω των λογισμικών Corel Photo Paint και Matlab. Για την παραπάνω μεταφραστική εργασία αντλήθηκαν πληροφορίες σχετικές με την αντιστοιχία ελληνικής και αγγλικής ορολογίας από online λεξικά και άλλες πηγές του διαδικτύου. Για τη δημιουργία των τελικών .docx και .pdf αρχείων έγινε χρήση σε υπολογιστή των λογισμικών Word και Visio του MS Office, καθώς και ένας online pdf combiner.

Στην συνέχεια της εργασίας γίνεται αναφορά στην μετάφραση επιστημονικών κειμένων, αλλά και στη σπουδαιότητα που αυτή έχει για τους ερευνητές. Επίσης γίνεται μια επισκόπηση στα οφέλη της οργάνωσης της βιβλιογραφίας στη συγγραφή πτυχιακών εργασιών. Επιπροσθέτως, γίνεται επιλογή του κατάλληλου λογισμικού, το οποίο λογισμικό αξιολογήθηκε συγκριτικά και με άλλα ώστε να επιλεγεί ως το λειτουργικότερο, με κριτήρια την εξυπηρέτηση των αναγκών οργάνωσης του δεδομένου υλικού, τη φιλικότητα προς το χρήστη, την προοπτική μελλοντικών updates κ.α.

Τέλος γίνεται αναζήτηση της διεθνούς βιβλιογραφίας στο γενικό αντικείμενο *Power electronics: converters, semi-conductors, switches, passive components,* που τέθηκε από τον ερευνητή κ. Δημητρακάκη, καθώς και μια πρόχειρη μελέτη για την

αξιολόγησή της. Το υλικό βρίσκεται σε ηλεκτρονική μορφή (.pdf αρχεία) και έγινε η αρχειοθέτησή του με τη χρήση του λογισμικού Reference Manager.

Περιεχόμενα

ΚΕΦΑΛΑΙΟ 1

ΜΕΤΑΦΡΑΣΗ ΕΞΕΙΔΙΚΕΥΜΕΝΟΥ ΚΕΙΜΕΝΟΥ

1.1. Γενικά στοιχεία

Η έρευνα στο πεδίο του ηλεκτρολόγου μηχανικού, όπως και σε κάθε επιστημονικό πεδίο, ξεκινάει πάντα με τη συλλογή, μελέτη, αξιολόγηση και ταξινόμηση της βιβλιογραφίας της σχετικής με το εκάστοτε ειδικό αντικείμενο. Με το όρο «βιβλιογραφία» εννοούμε οποιαδήποτε πληροφορία προέρχεται από αξιόπιστη πηγή. Τέτοιες πηγές είναι συνήθως οι δημοσιεύσεις σε διεθνή έγκριτα επιστημονικά περιοδικά και συνέδρια, τα βιβλία από γνωστούς εκδοτικούς οίκους, πανεπιστημιακές εκδόσεις, διδακτορικές διατριβές και πτυχιακές εργασίες, εξειδικευμένα websites (υπάρχουν και online επιστημονικά περιοδικά), εγχειρίδια κατασκευαστών κλπ., ενώ είναι αδιαμφισβήτητο γεγονός πως η πλειονότητα αυτών των πληροφοριών διατίθεται στα αγγλικά. Η διάχυση εξάλλου της παραγόμενης γνώσης (όταν κάτι τέτοιο είναι επιθυμητό και δεν επιδιώκεται η ανάπτυξη εμπορικού προϊόντος ή η κατοχύρωση κάποιας πατέντας) γίνεται μέσα από τα ίδια προαναφερθέντα μέσα και πάλι συνήθως στα αγγλικά.

Ένα ακόμα γεγονός είναι ότι μεταφράσεις των παραπάνω τεχνικών κειμένων βρίσκουμε συνήθως μόνο για κάποια βιβλία, με την ποιότητα της μετάφρασης να είναι συνάρτηση της σχετικότητας του μεταφραστή με το συγκεκριμένο αντικείμενο. Δεν είναι σπάνιο η μετάφραση σε σπουδαία επιστημονικά συγγράμματα να αγγίζει τα όρια του φαιδρού διότι – προφανώς– ο εκδοτικός οίκος ανέθεσε το έργο αυτό σε λάθος άνθρωπο. Διδακτορικές διατριβές και πτυχιακές εργασίες παραμένουν στη μητρική γλώσσα του συντάκτη τους (σπανίως ιδρύματα ανά τον κόσμο υποχρεώνουν ώστε η συγγραφή τους να γίνεται στα αγγλικά), ενώ τα τεχνικά εγχειρίδια, αν δεν είναι μόνο στα αγγλικά, προσφέρονται σε περιορισμένο αριθμό γλωσσών, με ελεγχόμενη και πάλι την ποιότητα της μετάφρασης.

Τέλος, πρέπει να αναφερθεί ότι ο νέος μηχανικός που καλείται ως υποψήφιος εργαζόμενος από εταιρίες του εξωτερικού ή και μεγάλες εταιρίες της ημεδαπής (πολυεθνικές ή όχι), συχνά οφείλει να συμπληρώσει online φόρμες, να δώσει συνεντεύξεις, να περάσει τεστ και να κάνει παρουσιάσεις στα αγγλικά, ενώ ζητείται (αν υπάρχει) αντίγραφο στα

αγγλικά της πτυχιακής εργασίας ή της διατριβής. Στη συνέχεια, μπορεί να του ζητηθεί ώστε όλη η γραπτή επικοινωνία στα πλαίσια της εργασίας του να είναι στα αγγλικά. Είναι προφανές πως για όλα τα παραπάνω απαιτείται καλή γνώση της αγγλικής, ευχέρεια στο γραπτό και προφορικό λόγο, αλλά και άριστη γνώση της ειδικής τεχνικής ορολογίας στα αγγλικά.

1.2. Η έννοια της μετάφρασης

Ο όρος μετάφραση, όπως καταγράφεται σήμερα, παρουσιάζει μία συγκεχυμένη και διφορούμενη χρήση δεδομένου ότι, ανάλογα με το γλωσσικό περιβάλλον στο οποίο τον συναντούμε, μπορεί να δηλώνει: τη διαδικασία μετάβασης από μία γλώσσα σε μία άλλη, άρα μία νοητική διεργασία, γνωστή και ως «μεταφράζειν», το αποτέλεσμα αυτής της διαδικασίας, άρα μία συγκεκριμένη γλωσσική οντότητα, το «μετέφρασα» δηλαδή, και τέλος, μία αφηρημένη έννοια που περιλαμβάνει τόσο τη διαδικασία όσο και το τελικό αποτέλεσμα της διαδικασίας αυτής. Όμως δεν έχει επικρατήσει κάποιος συγκεκριμένος ορισμός για την έννοια της μετάφρασης γι' αυτό και δημιουργείται και αυτή η σύγχυση. Σε πολλές επιστήμες, ο μελετητής όταν έρχεται αντιμέτωπος με κάποιο εμπόδιο του αντικειμένου του έχει τη δυνατότητα να ανατρέξει στη θεωρία και τους ορισμούς της επιστήμης του. Αντιθέτως, ο μεταφραστής δεν έχει αυτό το πλεονέκτημα. Παρόλα αυτά αν θέλαμε να ορίσουμε τι σημαίνει μετάφραση, θα λέγαμε ότι μετάφραση (στα αγγλικά translation) είναι η απόδοση προφορικού ή γραπτού λόγου από μια γλώσσα (πηγή) σε μια άλλη γλώσσα (στόχος). Ο όρος δηλώνει τόσο τη διαδικασία μεταφοράς όσο και το αποτέλεσμα, η στενή αυτή σημασία του όρου όμως αφορά μόνο τα γραπτά κείμενα. Όταν η μετάφραση είναι προφορική πρόκειται για διερμηνεία (στα αγγλικά interpretation). Η μετάφραση είναι η μεταφορά του νοήματος, της δομής και του ύφους των στοιχείων, φράσεων της γλώσσας-πηγής προς τη γλώσσα-στόχο. Είναι μία περίπλοκη και πολυδιάστατη διαδικασία η οποία απαιτεί ανάλυση, γνώση και κατανόηση της κάθε εμπλεκόμενης γλώσσας, αλλά και των πολιτιστικών και πολιτισμικών παραγόντων που συμβάλλουν στη δημιουργία και εξέλιξη της κάθε γλώσσας.

Η μετάφραση είναι μια παγκόσμια ανθρώπινη δραστηριότητα που καθίστατο αναγκαία σε όλες τις εποχές λόγω των πολλαπλών επαφών, οι οποίες επιβάλλονταν ανάμεσα σε κοινότητες ή σε άτομα που μιλούσαν διαφορετικές γλώσσες. Πριν από την επινόηση και τη διάδοση της γραφής η μετάφραση ήταν προφορική και γινόταν ταυτόχρονα με τη συνομιλία.

Σε κοινωνίες όπου είχε καθιερωθεί η γραφή, η μετάφραση ισοδυναμούσε με μετατροπή γραπτού κειμένου από τη μια γλώσσα στην άλλη. Η γραπτή μετάφραση, επειδή δεν υπήρχε και πίεση χρόνου επέτρεπε καλύτερη επεξεργασία ως προς το ύφος και τη χρήση ειδικών όρων.

Τόσο τα τεχνικά όσο και τα επιστημονικά κείμενα παρουσιάζουν άλλου είδους προβλήματα στη μετάφραση. Τα προβλήματα εστιάζονται κυρίως στην αναζήτηση και στην απόδοση των όρων. Τα προβλήματα αυτά θα αναλυθούν σε επόμενη ενότητα, σύμφωνα μάλιστα και με τις δυσκολίες που αντιμετωπίστηκαν στη μετάφραση της διδακτορικής διατριβής στα πλαίσια της παρούσας εργασίας. Κάθε επιστήμη έχει την δική της γλώσσα – ειδική γλώσσα– η όποια χρησιμοποιεί και ειδική ορολογία. Η ραγδαία πρόοδος όμως της τεχνολογίας έχει βοηθήσει αρκετά στο να αντιμετωπιστούν αυτού του είδους τα προβλήματα.

1.3. Τι είναι η ορολογία;

Η ανάγκη των επιστημόνων να επικοινωνούν και να εκφράζουν τις ιδέες τους και τις θεωρίες τους συνδέεται άμεσα με τη δημιουργία της ειδικής επιστημονικής γλώσσας, που είναι ευρέως γνωστή ως ορολογία, ιδιαίτερα στις μέρες μας, εξαιτίας της προόδου που σημειώνεται στις επιστήμες και στη συγκεκριμένη περίπτωση στον τομέα της ηλεκτρολογίας. Η επιστήμη του ηλεκτρολόγου μηχανικού και όλων των κλάδων που συνδέονται με την ηλεκτρολογία, όπως η ηλεκτρονική μηχανική, η αρχιτεκτονική υπολογιστών, οι τηλεπικοινωνίες κλπ, παρουσιάζουν ιδιαίτερη ζήτηση και ανάπτυξη. Μια τόσο εφαρμοσμένη επιστήμη όπως η ηλεκτρολογία χρησιμοποιεί τους δικούς της κώδικες, τη δική της γλώσσα, άρα και την δική της ορολογία. Επομένως, σύμφωνα με τα παραπάνω, ορολογία είναι ένα σύνολο μονάδων έκφρασης και επικοινωνίας (γλωσσικά εργαλεία, σύμβολα κλπ.) που επιτρέπει τη μεταφορά της εξειδικευμένης γνώσης.

Η εξέλιξη της επιστημονικής σκέψης έφερε την εξέλιξη της επιστήμης και η επιστήμη έφερε την εξέλιξη της επιστημονικής γλώσσας, η οποία στηρίζεται στην ορολογία. Η χρήση συγκεκριμένης ορολογίας προήλθε από την ανάγκη κατασκευής μια τεχνικής γλώσσας μέσω της οποίας κάθε επιστήμη θα είχε τη δυνατότητα να αναδομήσει την πραγματικότητα και να μετασχηματίσει την κοινή εμπειρία σε εξειδικευμένη γνώση.

Η ορολογία εμπλέκεται σε όλες τις επιμέρους επιστημονικές δραστηριότητες που αντιπροσωπεύουν και διαδίδουν την εξειδικευμένη γνώση, όπως η επιστημονική και τεχνική

μετάφραση, η διδασκαλία γλωσσών για ειδικούς σκοπούς, η γραφή τεχνικού λόγου, η διδασκαλία ειδικών θεμάτων, η τεκμηρίωση, οι τεχνολογίες που σχετίζονται με τις ειδικές γλώσσες, ο γλωσσικός σχεδιασμός, η τεχνική τυποποίηση κλπ. Με άλλα λόγια, όπου χρειάζονται ειδικές γνώσεις χρειάζεται ορολογία.

Οι ορολογικές εργασίες στη μετάφραση των ειδικών γλωσσών είναι:

1. Η αναζήτηση και εξαγωγή όρων από το μεταφραστέο κείμενο.
2. Η αναγνώριση της έννοιας και του συγκείμενου όπου ορίζεται η έννοια ή μαρτυρείται η χρήση της και ο προσδιορισμός των διακριτών χαρακτηριστικών από συγγενικές έννοιες.
3. Η αναγνώριση των διαφορετικών όρων που χρησιμοποιούνται για την υποδήλωση της έννοιας σε σχετικές γλωσσικές συλλογές και η άντληση ορολογικών πληροφοριών αξιοποιώντας ορολογικούς πόρους, όπως βάσεις ορολογικών δεδομένων π.χ. IATE [Interactive Terminology for Europe], (web site: https://iate.europa.eu)
4. Η επιλογή του πλέον κατάλληλου όρου.
5. Η αναφορά του βαθμού αποδεκτότητας για τους λοιπούς χρησιμοποιούμενους όρους στο πλαίσιο χρήσης και εφαρμογής.
6. Η καταγραφή των ορολογικών δεδομένων και προϊόντων των εργασιών ως μέρος της μετάφρασης ή για μελλοντική χρήση από μεταφραστή. Η συστηματική συλλογή ορολογικών πληροφοριών δίνει στους μεταφραστές τη δυνατότητα να παρακολουθούν και να επαναχρησιμοποιούν την εμπειρογνωσία τους, ενώ ταυτόχρονα διευκολύνει τη συνεργασία με άλλους μεταφραστές.

Στην Ελλάδα η Ορολογία εκπροσωπείται κυρίως από την ΕΛΕΤΟ [Ελληνική Εταιρεία Ορολογίας], (web site: http://www.eleto.gr). Λειτουργεί από το 1992 και είναι υπεύθυνη για τη δημιουργία ελληνικών όρων σε συγκεκριμένους τομείς και έχει σκοπό την προώθηση στον ελληνόφωνο χώρο της επιστήμης της Ορολογίας και την ανάπτυξη της ελληνικής ορολογίας σε όλους τους τομείς.

1.4. Τι είναι η εξειδικευμένη μετάφραση;

Για να μπορέσουμε να κατανοήσουμε τι σημαίνει εξειδικευμένη μετάφραση πρέπει πρώτα να καταλάβουμε τι είναι η εξειδικευμένη γλώσσα. Η εξειδικευμένη γλώσσα διαφέρει από την «κοινώς» ομιλούμενη γλώσσα, όσον αφορά την χρήση της, καθώς και τις πληροφορίες τις οποίες μεταφέρει. Σύμφωνα με την άποψη της Cabré [Common Language Versus Specialized Language] (1998, στο Coancă, 2011), θα μπορούσαμε να πούμε πως είναι ένα υποσύνολο της φυσικής γλώσσας, καθώς αποτελείται από ειδική ορολογία και ειδικό λεξιλόγιο, το οποίο σχετίζεται με συγκεκριμένο επάγγελμα ή δραστηριότητα, κάτι που δεν συναντάται στην φυσική γλώσσα. Με άλλα λόγια, κάθε κλάδος της επιστήμης και της τεχνικής έχει τη δική του γλώσσα που βασίζεται στη δική του ειδική ορολογία. Για παράδειγμα, ένας όρος που χρησιμοποιείται στη καθημερινή γλώσσα, αποκτά διαφορετική έννοια και γίνεται λιγότερο ακριβής σε σχέση με το αντίστοιχό του στην εξειδικευμένη γλώσσα.

Γενικά, αν θέλουμε να αποδώσουμε τη σημασία της μετάφρασης θα λέγαμε ότι είναι η διαδικασία κατά την οποία γίνεται απόπειρα ανασύνθεσης της ακριβέστερης ισοδύναμης προσέγγισης του μηνύματος της γλώσσας-πηγής στην γλώσσα-στόχο, πρώτα σε επίπεδο εννοιών και κατόπιν σε επίπεδο ύφους. Δηλαδή, αμφότερα τα κείμενα πρέπει να μεταδίδουν το ίδιο μήνυμα στον μεγαλύτερο βαθμό που τους επιτρέπουν οι φυσικοί περιορισμοί. Τέτοιοι περιορισμοί είναι το εννοιολογικό πλαίσιο, οι γραμματικοί κανόνες και των δύο γλωσσών, το συντακτικό, οι συγγραφικές συμβάσεις και οι αντίστοιχοι ιδιωματισμοί. Με βάση όλα τα παραπάνω μπορούμε να πούμε ότι η εξειδικευμένη μετάφραση είναι το αποτέλεσμα προσπαθειών για να ταξινομηθεί η δραστηριότητα της μετάφρασης μέσω τυπολογιών ή κατηγοριοποιήσεων, ώστε να κάνουν την σκέψη και την επικοινωνία στη μετάφραση ευκολότερη. Καλύπτει τα πεδία των εξειδικευμένων ζητημάτων, όπως είναι η επιστήμη και τεχνολογία, το μάρκετινγκ, τα οικονομικά, τα νομικά, η πολιτική, η ιατρική, τα μέσα μαζικής ενημέρωσης, καθώς και άλλους τομείς.

Προσπαθώντας να συνδυάσουμε στοιχεία από ορισμούς σχετικά με την εξειδικευμένη επικοινωνία και τη μετάφραση θα μπορούσαμε να πούμε ότι ένας αποδεκτός ορισμός της εξειδικευμένης μετάφρασης είναι: η εξωτερίκευση εξειδικευμένων γνωστικών συστημάτων και της γνωστικής επεξεργασίας, σταθμισμένα και επιλεγμένα από το κείμενο-πηγή, στοιχεία που υπόκεινται στην κρίση του μεταφραστή ή του αναγνώστη για το πώς θα τα χρησιμοποιήσει καθώς ο μεταφραστής θα πρέπει να εξαγάγει όλη την σχετική γνώση μέσω

της εσωτερίκευσης των εξειδικευμένων γνωστικών συστημάτων και της γνωστικής επεξεργασίας, με στόχο την διάχυση αυτής της γνώσης σε ένα άλλο γλωσσικό και πολιτισμικό πλαίσιο που ζητείται κάθε φορά.

Υπάρχουν όμως και κάποια κριτήρια τα οποία μας βοηθούν να πραγματοποιήσουμε με επιτυχία μια αποτελεσματική μετάφραση, δηλαδή κάποιες συγκεκριμένες ικανότητες. Σε αυτό εδώ το σημείο εμφανίζεται η έννοια της μεταφραστικής ικανότητας.

1.5. Η έννοια της μεταφραστικής ικανότητας

Όσοι ασχολούνται με τη μετάφραση ειδικών κειμένων, στην περίπτωσή μας τεχνικών κειμένων, θεωρούν ότι προτεραιότητα είναι μέσω της μετάφρασης να μεταδοθούν γνώσεις. Για να γίνει αυτό πρέπει ο μεταφραστής να ερευνήσει το αντικείμενο που πρόκειται να μεταφράσει. Άλλη περίπτωση είναι να είναι ήδη γνώστης του αντικειμένου και να έχει εμπειρία στην ανάγνωση και συγγραφή κειμένων σχετικών με αυτό και στις δύο γλώσσες (πηγή και στόχος)

Σύμφωνα με τον Kautz (2000: 89) ένα ουσιαστικό στοιχείο της ικανότητας του μεταφραστή αποτελεί η ερευνητική ικανότητα, καθώς τα 2/3 του χρόνου μετάφρασης αφιερώνονται στην έρευνα. Έμπειροι μεταφραστές χρησιμοποιούν τη βιβλιογραφία, που αναφέρεται στις υποσημειώσεις ή στο τέλος του προς μετάφραση κειμένου, ώστε να βρουν πληροφοριακά κείμενα για το αντικείμενο που μεταφράζουν.

Σύμφωνα με τη Μπατσαλιά (2008) [Γλωσσομάθεια και μεταφραστικές ικανότητες] ο μεταφραστής πρέπει να αποκτήσει τις παρακάτω δεξιότητες:

1. Αναγνώριση μέσω ανάλυσης και ερμηνείας του επικοινωνιακού σκοπού του πρωτοτύπου: οι καλοί μεταφραστές αναλύουν πλήρως κάθε πρόταση προτού δημιουργήσουν νέες στη γλώσσα – στόχο.
2. Αναγνώριση μέσω ανάλυσης όλων των εν δυνάμει ερμηνειών του πρωτοτύπου.
3. Ικανότητα επανασύλληψης των νοημάτων του πρωτοτύπου εντός των δεδομένων της γλωσσικής κοινότητας της γλώσσας – στόχου.
4. Ικανότητα διερεύνησης του γλωσσικού συστήματος της γλώσσας - στόχου για να αποδώσει σε επίπεδο ομιλίας όλα τα εν δυνάμει νοήματα και όλες τις εν δυνάμει ερμηνείες του πρωτοτύπου.

5. Ικανότητα χειρισμού της γλώσσας - στόχου με τέτοιο τρόπο ώστε οι λεξικολογικές, μορφολογικές, συντακτικές και υφολογικές επιλογές να είναι εναρμονισμένες με εκείνες τις συμβάσεις που διέπουν τη γλώσσα - στόχο στο συγκεκριμένο είδος κειμένου.

Η μετάφραση είναι επικοινωνιακή διαδικασία και ο επικοινωνιακός σκοπός είναι άρρηκτα συνδεδεμένος με το πρωτότυπο, ενώ παράλληλα απαιτεί την ανάπτυξη συγκεκριμένων δεξιοτήτων, οι οποίες δεν αποκτώνται αυτόματα και αυτονόητα κατά την εκμάθηση μιας γλώσσας. Ο μεταφραστής οφείλει να αναγνωρίζει τον επικοινωνιακό σκοπό του πρωτοτύπου και να διαθέτει στη γλώσσα - στόχο τόση επάρκεια, ώστε να προσαρμόσει τα γλωσσικά μέσα που χρησιμοποιεί στον εκάστοτε επικοινωνιακό σκοπό.

Τα μέσα της έρευνας των μεταφραστών είναι τα λεξικά, τα γλωσσάρια, οι εγκυκλοπαίδειες, τα παράλληλα κείμενα, τα πληροφοριακά κείμενα, οι πληροφοριοδότες (είναι κυρίως οι ειδικοί του πεδίου) και οι βάσεις δεδομένων. Στη διάθεση των μεταφραστών σήμερα υπάρχουν έντυπα και ηλεκτρονικά μέσα έρευνας και φυσικά υπάρχει το διαδίκτυο. Για να βρει κανείς πληροφορίες ή πηγές για κάποιο κείμενο που πρόκειται να μεταφράσει δε χρειάζεται να πάει σε κάποια βιβλιοθήκη, μπορεί όλα αυτά να τα βρει στο διαδίκτυο. Η ερευνητική ικανότητα είναι σημαντική τόσο στη διδασκαλία της μετάφρασης όσο και για την μεταφραστική πρακτική. Η απόδοση των μεταφραστών έχει αυξηθεί τα τελευταία χρόνια λόγω της εξέλιξης της τεχνολογίας που εμφανίζεται αρωγός της μεταφραστικής ικανότητας. Σήμερα ένας έμπειρος μεταφραστής μπορεί να μεταφράζει είκοσι σελίδες σε μία μέρα, αριθμός αδιανόητος την εποχή της γραφομηχανής. Η διασφάλιση της ποιότητας της μετάφρασης υποστηρίζεται από εργαλεία όπως ο αυτόματος ορθογραφικός έλεγχος, μεταφραστικές μνήμες κλπ, που δίνουν νέες δυνατότητες στην έρευνα. Η μεταφραστική ικανότητα αποκτάται με την άσκηση, την εμπειρία και την γνώση.

1.6. Ο ρόλος του μεταφραστή

Ο ρόλος του μεταφραστή είναι διπλός, αρχικά καλείται να παραγάγει ένα, πιστό στο πρωτότυπο, μετάφρασμα και κατά δεύτερον λειτουργεί και ως διαμεσολαβητής, μεταξύ πομπού-συγγραφέα και δέκτη-αναγνώστη. Οφείλει όμως και να γνωρίζει όχι μόνο τα συντακτικά, λεξιλογικά και υφολογικά στοιχεία των δύο γλωσσών, αλλά και τα πολιτισμικά

στοιχεία και επιρροές που επιδρούν πάνω στη γλώσσα προκειμένου να έχει πιο ολοκληρωμένες γνώσεις και να καταστεί έτσι ικανός να παράγει το επιθυμητό αποτέλεσμα. Πρέπει να είναι γνώστης όχι μόνο των γλωσσών μεταξύ των οποίων μεταφράζει, αλλά και να έχει γενικές και ειδικές γνώσεις πάνω στο αντικείμενο του εκάστοτε κειμένου προς μετάφραση. Πρέπει να είναι ικανός να χειριστεί άψογα τη γλώσσα–στόχο, αλλά και τη γλώσσα–πηγή και να χειρίζεται τη δεύτερη όπως τη μητρική του. Επιπρόσθετα, όπως επισημάνθηκε προηγουμένως, είναι καλό να γνωρίζει σε ποιόν απευθύνεται το κείμενο που θα παραγάγει για να του αποδώσει και το κατάλληλο ύφος. Ακριβώς όμως επειδή και η μετάφραση δεν είναι μια καθαρά μηχανική διαδικασία, απαιτεί και τη σωστή κρίση και τη διαίσθηση του μεταφραστή, καθώς δεν είναι μόνο τέχνη, αλλά και τεχνική. Ο μεταφραστής είναι αυτός που φέρνει κοντά τον συγγραφέα και τον αναγνώστη μεταφέροντας συνήθως κάποιο μήνυμα, κάποιες γνώσεις κ.α., ανάλογα πάντα με το ύφος του κειμένου.

Ο μεταφραστής μεταφράζει από τη γλώσσα–πηγή (συνήθως τη μητρική του) προς τη γλώσσα–στόχο (μία ξένη γλώσσα), ή και το αντίστροφο. Ανάλογα με τον τομέα στον οποίο ειδικεύεται (για παράδειγμα κείμενα τεχνικά, οικονομικά, νομικά, ιατρικά, λογοτεχνικά, κλπ) κάνει χρήση λεξικών, μεταφραστικών βάσεων ή και άλλων μεταφραστικών εργαλείων, που εξυπηρετούν τον ίδιο για να ολοκληρώσει το έργο το οποίο έχει αναλάβει. Μελετά αρκετά το πρωτότυπο κείμενο που του έχει δοθεί προκειμένου να συλλάβει το ύφος του κειμένου και τις γλωσσικές του ιδιαιτερότητες. Ακόμη, κάνει τη δική του έρευνα πάνω στο αντικείμενο του πρωτοτύπου, προκειμένου να μπορεί να αποδώσει ορθά τυχόν εξειδικευμένο λεξιλόγιο ή φράσεις που ίσως εκλείπουν ή διαφοροποιούνται από τη μία γλώσσα στην άλλη. Τελειώνοντας την εργασία του, επιλέγει τη σωστότερη κατ' αυτόν απόδοση του κειμένου και αντιπαραβάλλει το πρωτότυπο με το κείμενο της μετάφρασης για να επαληθεύσει ότι έχει αποδώσει σωστά το νόημα του κειμένου–πηγής. Ο μεταφραστής μέσα από το έργο του φέρνει σε επαφή ανθρώπους και πολιτισμούς που μιλούν διαφορετική γλώσσα και έχουν διαφορετική κουλτούρα και γι' αυτό το λόγο φέρει το βάρος και την ευθύνη για την ακριβή μεταφορά και απόδοση του νοήματος και στις δύο γλώσσες. Με αυτό τον τρόπο επιτυγχάνει το να καταστήσει κατανοητή μία λέξη, μία πρόταση ή ένα κείμενο, σε έναν αποδέκτη ο οποίος ίσως και να μην έχει καμία σχέση πολιτισμικά με το πλαίσιο στο οποίο γράφτηκε το πρωτότυπο και αυτός είναι και ο σκοπός του. Η απόδοση του μεταφράσματος βρίσκεται πάντα στη διακριτική ευχέρεια του μεταφραστή, ο οποίος πάντα αναλαμβάνει και το κόστος των επιλογών, του από τις οποίες κρίνεται και η αποτελεσματικότητα του.

Συχνά, όταν ένας μεταφραστής ξεκινά το έργο του, οι πρώτες σελίδες του μεταφράσματος χαρακτηρίζονται από απειρία και είναι συνήθως αυτές που χρήζουν

περισσότερης διόρθωσης. Έως ότου ο μεταφραστής γίνει ένα με το κείμενο, κατανοήσει τις επιταγές του και τις επιρροές που έχει αυτό δεχτεί, η ζύμωση στο νου του μεταφραστή είναι διαρκής και η πιστότητα της μετάφρασης βαίνει βελτιούμενη. Τέλος, σύμφωνα με τον Τριανταφυλλίδη [Λεξικό του Ιδρύματος Τριανταφυλλίδη, 1998], η μετάφραση δεν είναι μια απλή μεταφορά ενός κειμένου από τη μια γλώσσα στην άλλη, αλλά είναι μεταφορά πολιτιστικών στοιχείων από έναν πολιτισμό σε έναν άλλο.

Οι παραπάνω διαπιστώσεις σχετικά με τον ρόλο του μεταφραστή και τις δυσκολίες που συναντά όταν μεταφράζει ένα κείμενο από ένα γλωσσικό σύστημα σε κάποιο άλλο δείχνουν ότι η εννοιολογική ανάλυση στην οποία προβαίνει η ορολογία μπορεί να συνεισφέρει στην μετάφραση. Προβαίνοντας στην εννοιολογική ανάλυση ενός θεματικού πεδίου, ο μεταφραστής αποκτά γνώσεις για το πεδίο αυτό και μπορεί επίσης να διαπιστώσει τις ορολογικές αναντιστοιχίες που τυχόν υπάρχουν ανάμεσα στη γλώσσα του κειμένου και τη γλώσσα στην οποία μεταφράζει.

1.7. Εξοπλισμός και απαιτούμενες δεξιότητες ενός μεταφραστή

Απαραίτητα για έναν μεταφραστή είναι τα γενικά και εξειδικευμένα σε διάφορους θεματικούς τομείς λεξικά, σε έντυπη και ηλεκτρονική μορφή, καθώς και ειδικά προγράμματα λογισμικού που έχουν αναπτυχθεί για το σκοπό αυτό.

Ο μεταφραστής προκειμένου να φέρει εις πέρας το μεταφραστικό του έργο θα πρέπει να διακρίνεται από τις παρακάτω δεξιότητες:

- Επιμονή και υπομονή
- Πνευματική οξύτητα, επινοητικότητα
- Ετοιμολογία
- Ακρίβεια, ταχύτητα και υπευθυνότητα
- Ικανότητα στην έρευνα πηγών
- Γλωσσικές ικανότητες
- Προσοχή στην απόδοση της λεπτομέρειας
- Απόλυτη συγκέντρωση και διαύγεια πνεύματος
- Αντικειμενικότητα σε συνδυασμό με τη συνέπεια και την ευσυνειδησία
- Ικανότητα αντοχής στην πίεση που προκαλούν οι προθεσμίες και ο φόρτος εργασίας χωρίς να επηρεάζεται το αποτέλεσμα της εργασίας του.

1.8. Ο ρόλος του ορολόγου

Οι ορολόγοι διευκολύνουν τη διαδικασία έκδοσης ενός κειμένου και της μετάφρασής του, καθώς παρέχουν πιο εξειδικευμένες πληροφορίες μέσα από την έρευνα και τον εντοπισμό πληροφοριών πάνω στο αντικείμενο αυτό. Είναι επαγγελματίες που εξασφαλίζουν την ακρίβεια, καταλληλότητα και συνέπεια της χρήσης των όρων. Ορίζουν έννοιες, αναλύουν όρους βρίσκουν και επιλέγουν τα κατάλληλα τους ισοδύναμα σε άλλες γλώσσες. Τα ευρήματα τους χρησιμοποιούνται για να συντάξουν γλωσσάρια, να εμπλουτίσουν βάσεις δεδομένων που αφορούν την ορολογία και να τυποποιήσουν την ορολογία που χρησιμοποιείται σε έναν ορισμένο τομέα ή οργανισμό. Επίσης, ο ειδικός σε θέματα ορολογίας πρέπει να έχει συγκεκριμένες δεξιότητες. Πρέπει να είναι ιδιαίτερα καλός γνώστης της γλώσσας ή των γλωσσών που χειρίζεται. Ακόμη, οφείλει να γνωρίζει καλά τον κλάδο της γλωσσολογίας για να μπορεί να εκπληρώσει το έργο που του ανατίθεται και να χειρίζεται εξίσου καλά τον προφορικό και το γραπτό λόγο. Παραδείγματος χάριν, υπάρχουν περιπτώσεις κατά τις οποίες ο ορολόγος καλείται να επιλέξει ανάμεσα σε συνώνυμους όρους. Η επιλογή αυτή πρέπει να γίνεται με βάση τα κριτήρια της συχνότητας χρήσης του όρου αυτού. Ο ορισμός ή η κατασήμανση της έννοιας του όρου εξυπηρετεί τη διαφοροποίησή της έννοιας από συναφείς έννοιες. Δηλαδή, φανερώνει το σύνολο των ουσιωδών χαρακτηριστικών που τη συνιστούν, καθώς και το σύνολο των αντικειμένων που αντιπροσωπεύει. Όλες αυτές οι προϋποθέσεις συνθέτουν το προφίλ του ειδικού σε θέματα ορολογίας προκειμένου να επιτυγχάνεται το επιθυμητό αποτέλεσμα και ο λόγος που θα παράγει να έχει συνοχή.

1.9. Η σχέση μεταξύ μεταφραστή και ορολόγου

Όπως αναφέρθηκε και στις προηγούμενες παραγράφους, η μετάφραση αποτελεί μια περίπλοκη διαδικασία κατά την οποία ο μεταφραστής κάνει χρήση πολλών μέσων (λεξικά, διαδικτυακά μέσα κλπ) προκειμένου να τη φέρει εις πέρας. Ακόμη, ο ρόλος του είναι πολυδιάστατος και γι' αυτό οφείλει να είναι πλήρως καταρτισμένος επί του αντικειμένου το οποίο καλείται να μεταφράσει.

Ο ρόλος του μεταφραστή είναι να παράγει ένα ορθό μετάφρασμα, να μπορεί να αποδώσει πιστότερα υφολογικά, συντακτικά, και γραμματικά το πρωτότυπο στο μετάφρασμα.

Οφείλουμε όμως να λάβουμε υπόψη μας ότι κάθε κείμενο χρήζει διαφορετικής προσέγγισης. Σε ένα τεχνικό κείμενο, για παράδειγμα, ο μεταφραστής καλείται να αποδώσει το κείμενο με σαφήνεια και επιστημονική ακρίβεια. Αντίστοιχα, σε ένα ιατρικό ή νομικό κείμενο το οποίο περιλαμβάνει όρους του αντικειμένου, ο μεταφραστής καλείται να αποδώσει ένα παράγωγο το οποίο θα περιλαμβάνει τους κατάλληλους όρους και τη σημασιολογία που απαιτείται. Με λίγα λόγια, εάν κληθεί να μεταφράσει κείμενα με συγκεκριμένο διεπιστημονικό αντικείμενο, εκεί είναι που παίρνει τη θέση της η ορολογία. Επίσης, για την άντληση ορολογικών πληροφοριών ο μεταφραστής θα πρέπει να έχει τη δυνατότητα να μελετήσει και να ερευνήσει εξειδικευμένα, επιστημονικά και τεχνικά λεξικά, διεθνή πρότυπα, συλλογές και βάσεις δεδομένων της ορολογίας.

Εξαιτίας της πολυπλοκότητας των προβλημάτων που αντιμετωπίζει ο ορολόγος κατά την μεταφραστική διαδικασία έχει επισημανθεί η ανάγκη ύπαρξης ενός συστήματος που θα ελέγχει την ποιότητα ως προς την συλλογή, επεξεργασία και καταχώριση της ορολογίας έτσι ώστε να διευκολυνθεί το έργο του διαχειριστή του ορολογικού υλικού.

Σε αυτή τη περίπτωση, ο ορολόγος καλείται να μεταφράσει τους επιστημονικούς όρους και να βοηθήσει με αυτό τον τρόπο στη διεκπεραίωση του έργου. Και αυτό συμβαίνει διότι, ο ορολόγος έχει ως αντικείμενο εργασίας την εύρεση, επεξεργασία και διερεύνηση επιστημονικών και μη όρων. Επιπρόσθετα, παρακολουθεί και εντοπίζει τις συνεχείς αλλαγές της γλώσσας και την εμφάνιση νέων όρων σε αυτή. Βασικό του στόχο αποτελεί η συλλογή, η ανάλυση και η καταγραφή πληροφοριών σχετικά με μία ή περισσότερες έννοιες. Με τη δική του συμβολή προσδιορίζονται έννοιες και τομείς σε ένα συγκεκριμένο θεματικό πλαίσιο.

Λαμβάνοντας υπόψη τα παραπάνω στοιχεία κατανοούμε τη σχέση που υπάρχει μεταξύ μεταφραστή και ορολόγου, και πώς αυτοί οι δύο τομείς είναι άρρηκτα συνδεδεμένοι μεταξύ τους. Γι' αυτό το λόγο είναι απαραίτητη η συνύπαρξη και αλληλεπίδραση αυτών, προκειμένου να καταστεί εφικτή η ορθή μετάφραση ενός διεπιστημονικού κειμένου που αποτελείται από συγκεκριμένους όρους και έννοιες.

1.10. Προβλήματα μετάφρασης που προκύπτουν σε τεχνικά και επιστημονικά κείμενα

Παρότι είναι γνωστό πως η μετάφραση είναι η αντανάκλαση ενός κειμένου–πηγής σε ένα ισοδύναμο κείμενο–στόχο, στην πραγματικότητα τα πράγματα δεν είναι τόσο απλά. Μια μετάφραση δεν περιλαμβάνει απλά την μετάφραση των γλωσσικών δομών (συντακτικό και γραμματική), αλλά και τη μετάφραση λεξιλογικού και σημασιολογικού περιεχομένου, καθώς και τα στιλιστικά στοιχεία της γλώσσας πηγής, τα οποία πρέπει να «αναπαραχθούν» στην αντίστοιχη γλώσσα–στόχο. Ενώ η εν γένει μετάφραση συνεπάγεται μια κατανόηση του αυθεντικού κειμένου, καθώς και των εμπεριεχομένων εκφράσεων και μηνυμάτων που πρέπει να μεταφερθούν στη γλώσσα–στόχο, η εξειδικευμένη μετάφραση περιπλέκει κάπως τα πράγματα, καθώς οι μεταφραστές εκτός του ότι χρειάζεται πρώτα να κατανοήσουν το αρχικό κείμενο, θα πρέπει στη συνέχεια να αναγνωρίσουν την ορολογία που αφορά στο συγκεκριμένο εξειδικευμένο τομέα, ώστε να αναζητήσουν την αντίστοιχη ορολογία στη γλώσσα–στόχο και εν τέλει θα πρέπει να δημιουργήσουν ένα κείμενο στη γλώσσα–στόχο, το όποιο θα αναπαράγει το ίδιο περιεχόμενο και το όποιο θα χρησιμοποιεί όρους που θα προσομοιάζουν με αυτούς στο κείμενο–πηγή. Σύμφωνα με τους Hervey & Higgins (1992, στο Γούτσος, 2004: 99) δεν είναι δυνατόν να αναφερόμαστε γενικευτικά στον επιστημονικό και τεχνικό λόγο, εφόσον κάθε ειδικευμένο πεδίο έχει το δικό του ιδίωμα, την δική του τεχνική αργκό και τα ιδιαίτερα χαρακτηριστικά του είδους, με τα οποία ο μεταφραστής πρέπει να είναι εξοικειωμένος για να παραγάγει ένα πειστικό κείμενο–στόχο. Η πολυδιάσπαση των κειμένων σε είδη οδήγησε τους μελετητές να κάνουν λόγο για κείμενα με ειδικές γλώσσες.

Λαμβάνοντας υπόψη πως η γλώσσα είναι μεταβαλλόμενη και επηρεάζεται άμεσα από τις κοινωνικές και πολιτισμικές συνιστώσες της κάθε χώρας, ο μεταφραστής καλείται να φέρει εις πέρας το έργο του παρ' όλες τις δυσκολίες που θα συναντήσει στη διαδικασία της μετάφρασης. Στη σχέση που δημιουργείται ανάμεσα στη γλώσσα πηγή και τη γλώσσα στόχο υπάρχουν φορές που δε μπορεί να υπάρξει ακριβές μεταφραστικό ισοδύναμο. Ακόμη, οι ιδιωτισμοί και οι εκφράσεις που χρησιμοποιεί ένας λαός στη καθομιλουμένη, αποτελούν ξεκάθαρα παραδείγματα που μπορούν να περιπλέξουν περισσότερο τη μεταφραστική διαδικασία. Επιπρόσθετα, υπάρχουν και γραμματικές διαφορές σε κάθε γλώσσα. Σύμφωνα με τον Wilss (Μπατσαλιά & Σελλά-Μάζη, 1994:108-109) μεταφραστική δυσκολία συναντάμε όταν δεν είναι δυνατή μία λεξιλογική ή συντακτική μία προς μία αντιστοίχιση

μεταξύ του κειμένου–πηγή και του κειμένου–στόχος, διότι, στην περίπτωση αυτή, μία τέτοια «λέξη προς λέξη» μετάφραση θα επέφερε αρνητικά μεταφραστικά αποτελέσματα.

Ειδικότερα, οι κυριότερες μεταφραστικές δυσκολίες (οι δυσκολίες που παρατίθενται σε αυτό το σημείο θα αναλυθούν περαιτέρω σε επόμενη ενότητα, σύμφωνα με τις δυσκολίες που αντιμετωπίστηκαν στην παρούσα εργασία κατά τη μετάφραση της διδακτορικής διατριβής), εντοπίζονται στο επίπεδο της λέξης και των γραμματικών τύπων και είναι οι παρακάτω:

- Δυσκολία να αποδώσουμε μονολεκτικά το σημασιολογικό βάθος και πλάτος μιας λέξης του πρωτοτύπου.
- Αδυναμία να αποδοθούν για παράδειγμα, σχήματα λόγου που βασίζονται στη μορφή των λέξεων, κωμικά λογοπαίγνια, παρετυμολογήσεις κλπ της μεταφραζόμενης γλώσσας.
- Δυσκολίες που προκύπτουν από τη διαφορετική σειρά των λέξεων σε κάθε γλώσσα, για παράδειγμα διαφορετική θέση για το ρήμα, καθώς και δυσκολίες στη διατήρηση της δυναμικής θέσης μιας λέξης, όπως της εμφατικής τοποθέτησης μιας λέξης στην αρχή του λόγου ή της απομάκρυνσης του επιθετικού προσδιορισμού από το ουσιαστικό.

Τις περισσότερες φορές δεν είναι δυνατό να γίνει κατανοητός ένας όρος χωρίς ο μεταφραστής να λάβει υπόψη του τα συμφραζόμενα, τα οποία όμως δεν γίνονται κατανοητά από τον μη ειδικό. Η λύση στο πρόβλημα αυτό είναι η εκμάθηση του πεδίου από το μεταφραστή ή η συνεργασία του με τους ειδικούς του πεδίου. Αυτό αποτελεί το βασικό πλαίσιο διαμόρφωσης και ανάλυσης της μετάφρασης του επιστημονικού και τεχνικού λόγου. Σε όλα αυτά τα προβλήματα βρίσκει λύσεις η χρησιμοποίηση των τεχνολογικών εργαλείων (ηλεκτρονικά λεξικά, ηλεκτρονικά σώματα κειμένων και μεταφραστικές μνήμες).

1.11. Η ανάπτυξη της τεχνολογίας ως αναπόσπαστο εργαλείο στο μεταφραστικό έργο

Ήδη από τη δεκαετία του ’60, ο Wüster (1969, στο Κατσογιάννου & Ευθυμίου, 2004: 51) επεσήμανε την ανάγκη να χρησιμοποιηθεί η σύγχρονη τεχνολογία σε όφελος της εξειδικευμένης μετάφρασης. Ειδικότερα, αναφερόταν στη χρήση των υπολογιστών για την

σύνταξη ορολογικών λεξικών. Από τη δεκαετία του '80, εμφανίζεται ο όρος *μεταφραστική τεχνολογία*, που είναι το σύνολο των εφαρμογών της τεχνολογίας οι οποίες χρησιμοποιούνται στην εξειδικευμένη μετάφραση.

Από τότε μέχρι σήμερα, η τεχνολογία έχει κάνει μεγάλα άλματα και το έργο των μεταφραστών έχει βοηθηθεί πολύ από αυτή την πρόοδο. Με τη διάδοση του διαδικτύου έχει συντελεστεί μία ιστορική τομή, η οποία έχει αλλάξει καθοριστικά τον τρόπο εργασίας των μεταφραστών. Τα τελευταία χρόνια η μετάφραση με τη βοήθεια του ηλεκτρονικού υπολογιστή αποτελεί αναπόσπαστο κομμάτι της μεταφραστικής πρακτικής. Οι ορολογικές μνήμες μπορούν άνετα να χρησιμοποιηθούν, π.χ. στις θετικές επιστήμες και να λύσουν το πρόβλημα της τυποποίησης και της συνέπειας στις ελληνικές μεταφράσεις.

Η τεχνολογία συνεχώς εξελίσσεται επιδρώντας θετικά στη μετάφραση ως προς την ποιότητα, την πιστότητα και την ποσότητα και θεωρείται πλέον δομικό στοιχείο της μετάφρασης. Εκτός από τα κλασικά πλέον προγράμματα μηχανικής μετάφρασης, πληθαίνουν συνεχώς οι εφαρμογές που συνδέουν την ορολογία με όλους τους άλλους κλάδους της γλωσσικής τεχνολογίας: διαδικασίες όπως η αναζήτηση στο διαδίκτυο, η αξιοποίηση ηλεκτρονικών λεξικών και η χρήση προγραμμάτων ορθογραφικής και συντακτικής διόρθωσης υιοθετούνται από ένα ευρύ φάσμα χρηστών του διαδικτύου.

Η ανάπτυξη τέτοιων εφαρμογών οδήγησε στη δημιουργία της ορολογικής τεχνολογίας, που είναι συνδυασμός γνώσης και εμπειρίας από την ορολογία, την γλωσσολογία και την πληροφορική και ασχολείται με τη διαχείριση των ορολογικών δεδομένων. Οι σημαντικότεροι τομείς εφαρμογής της είναι σήμερα ο εντοπισμός όρων και η ανάκτηση πληροφορίας από ηλεκτρονικά σώματα κειμένων, η δημιουργία οντολογιών και λεξικών όρων κλπ.

Οι εφαρμογές της ορολογικής τεχνολογίας μπορούν να χωριστούν σε δυο κατηγορίες:

Α. Η πρώτη κατηγορία αποτελείται από τα εργαλεία που χρησιμοποιούνται για τον εντοπισμό των όρων σε κείμενα και η εξεύρεση των μεταφραστικών τους αντιστοίχων, για τη συλλογή γλωσσικών δεδομένων που μπορούν να ενσωματωθούν σε υπολογιστικά (τα οποία περιέχουν κωδικοποιημένα δεδομένα αποκλειστικά για χρήση από υπολογιστικές εφαρμογές π.χ. μηχανική μετάφραση) ή ηλεκτρονικά λεξικά, αλλά και για την ίδια τη δημιουργία λεξικών.

Β. Η δεύτερη μεγάλη κατηγορία εφαρμογών αποτελείται από τα γλωσσάρια, λεξικά ή άλλου είδους συλλογές όρων σε έντυπη ή σε ηλεκτρονική μορφή. Κυρίως οι διαδικτυακές βάσεις ορολογίας είναι αυτές που περιέχουν μεγάλο πλήθος όρων από διάφορα γνωστικά πεδία και παρέχουν ποικίλες δυνατότητες. Στον τομέα

αυτό οι πλέον δημοφιλείς εφαρμογές είναι οι τράπεζες όρων, δηλαδή ογκώδη υπολογιστικά συστήματα που βασίζονται σε ηλεκτρονικά λεξικά και σώματα κειμένων και λειτουργούν ως αποταμιευτικά ορολογικών δεδομένων. Πρόκειται για προϊόντα που δημιουργούνται με στόχο αφενός τη συγκέντρωση αξιόπιστων ορολογικών πόρων σε μορφή προσβάσιμη από μεγάλο αριθμό χρηστών και αφετέρου την οργανωμένη επεξεργασία τους που γίνεται με την βοήθεια των νέων τεχνολογιών.

Η εργασία εντοπισμού όρων είναι δύσκολη. Δεν υπάρχουν γενικά και καθορισμένα κριτήρια για τη διάκρισή τους. Η αυτόματη αναγνώριση επιστημονικής και τεχνικής ορολογίας είναι πρωταρχικής σημασίας για τη γλωσσική τεχνολογία γιατί μπορεί να βελτιώσει αισθητά την απόδοση των συστημάτων μηχανικής μετάφρασης, εξαγωγής πληροφοριών, αυτόματης κατηγοριοποίησης και δεικτοδότησης κειμένων και άλλων γλωσσικών εφαρμογών.

1.12. Παράγοντες που επηρεάζουν το κόστος μιας μετάφρασης

Το κόστος για τη μετάφραση ενός κειμένου συνήθως επηρεάζεται από τους εξής παράγοντες:

1. γλωσσικό συνδυασμό
2. ορολογία
3. προθεσμία
4. όγκος

Γλωσσικός συνδυασμός

Το κόστος μιας μετάφρασης ποικίλει ανάλογα με τον γλωσσικό συνδυασμό. Συνήθως στην Ελλάδα, οι μεταφράσεις προς τα Ελληνικά κοστίζουν λιγότερο από τις μεταφράσεις προς μια ξένη γλώσσα. Δηλαδή εάν θέλουμε να μεταφράσουμε ένα κείμενο από τα Αγγλικά προς τα Ελληνικά, τότε θα κοστίσει λιγότερα χρήματα απ' ό,τι εάν μεταφράσουμε το κείμενό από τα Ελληνικά προς τα Αγγλικά. Επίσης, πολλές φορές ορισμένοι γλωσσικοί συνδυασμοί κοστίζουν ακριβότερα ή φθηνότερα, ανάλογα με τη γεωγραφική θέση του πελάτη και του μεταφραστή. Για παράδειγμα, εάν βρισκόμαστε στην Ελλάδα και θέλουμε να μεταφράσουμε ένα κείμενο προς τα Ιαπωνικά, τότε είναι πολύ πιθανό να πληρώσουμε περισσότερα χρήματα απ' ό,τι αν ζητούσατε να μεταφραστεί το κείμενό μας σε οποιαδήποτε άλλη ευρωπαϊκή

γλώσσα. Αυτό συμβαίνει επειδή οι μεταφραστές ασιατικών γλωσσών στην Ευρώπη είναι δυσεύρετοι και άρα πιο ακριβοπληρωμένοι.

Ορολογία

Η φύση του ίδιου του κειμένου είναι άλλος ένας σημαντικός παράγοντας που καθορίζει αν το κόστος της μετάφρασής του θα είναι υψηλό ή χαμηλό. Αυτό σημαίνει ότι εάν το θέμα του κειμένου είναι άκρως εξειδικευμένο με δύσκολους όρους, περίπλοκη σύνταξη, εικόνες, πίνακες και παραρτήματα, όπως για παράδειγμα, ένα κείμενο σαν τη διατριβή που μεταφράστηκε για τις ανάγκες της παρούσας εργασίας και βρίσκεται στο παράρτημα της παρούσας πτυχιακής, εννοείται ότι ο μεταφραστής του θα ζητήσει πολύ υψηλότερη αμοιβή. Αντιθέτως, εάν το θέμα του κειμένου είναι απλό, χωρίς ειδικούς όρους ή περίπλοκη σύνταξη, (π.χ. ένα άρθρο γενικού ενδιαφέροντος), τότε το κόστος της μετάφρασης θα είναι χαμηλότερο.

Προθεσμία

Η δουλειά του μεταφραστή καθορίζεται μονίμως από ημερομηνίες παράδοσης. Τα πάντα έχουν μια προθεσμία. Για τις επείγουσες μεταφράσεις, η χρέωση πρέπει να είναι υψηλότερη από τη συνήθη ή τη συμφωνηθείσα αμοιβή. Πόσο υψηλότερη; Αυτό εξαρτάται από το μεταφραστή. Ορισμένοι μεταφραστές χρεώνουν από 50% έως και 100% επιπλέον τον πελάτη τους για κάθε επείγουσα ανάθεση, αλλά αυτό δεν ισχύει πάντα. Σε αυτήν την περίπτωση, εννοείται ότι εάν δε δοθεί στον επαγγελματία μεταφραστή ο απαραίτητος χρόνος που χρειάζεται για να διεκπεραιώσει σωστά την εργασία του και απαιτηθεί να είναι έτοιμη νωρίτερα, θα χρεώσει τον πελάτη του περισσότερο.

Σύμφωνα με τους γενικούς κανόνες της αγοράς, ένας επαγγελματίας μεταφραστής μπορεί να μεταφράσει 2.000 λέξεις (περίπου 8 σελίδες Α4) προς τη μητρική του γλώσσα σε ένα 8ωρο. Ομοίως, ένας επαγγελματίας διορθωτής μπορεί να διορθώσει 1.000 λέξεις (περίπου 4 σελίδες Α4) την ώρα. Αυτή η παραγωγή όμως ισχύει εάν ο μεταφραστής ή ο διορθωτής δεν έχει αναλάβει κανένα άλλο έργο εκείνη την ημέρα, πράγμα ακατόρθωτο στις μέρες μας.

Όγκος

Το κόστος μιας μετάφρασης ενδέχεται να αλλάξει ανάλογα με το μέγεθος του κειμένου. Εάν το κείμενο είναι αρκετά μεγάλο, τότε ισχύει η «έκπτωση μεγάλων έργων». Τι σημαίνει μεγάλο έργο; Ένα ή περισσότερα κείμενα με άθροισμα άνω των 10.000-20.000 λέξεων. Σε

αυτήν την περίπτωση είναι στη διακριτική ευχέρεια του μεταφραστή να κάνει κάποιου είδους έκπτωση, επειδή θα του ανατεθεί μια μεγάλη εργασία.

1.13. Το νομοθετικό πλαίσιο για την προστασία του μεταφραστικού έργου

Το αντικείμενο προστασίας είναι η μετάφραση όχι ως διανοητική διεργασία και διαδικασία, αλλά ως αποτέλεσμα της μεταφραστικής δραστηριότητας, ως προϊόν διανοίας.

Η προστατευόμενη από το δίκαιο πνευματικής ιδιοκτησίας μετάφραση είναι το έργο γραπτού λόγου (κείμενο) το οποίο αποτελεί την απόδοση ενός υφιστάμενου κειμένου από μία γλώσσα, ιδίωμα ή διάλεκτο σε άλλη γλώσσα, χωρίς αλλαγές εκτός από εκείνες που επιβάλλονται από τις γλωσσικές απαιτήσεις και υφολογικές ανάγκες του μεταφρασμένου κειμένου. Τέτοιες μεταφράσεις μπορεί να είναι: μετάφραση λογοτεχνικού έργου, επιστημονικού άρθρου κλπ.

Ο νόμος αναφέρει ρητά τις μεταφράσεις ανάμεσα στα εν δυνάμει προστατευόμενα έργα (άρθρο 2 παρ. 2 Ν. 2121/1993). Για την προστασία μίας μετάφρασης ως πνευματική ιδιοκτησία απαιτείται προσωπική πνευματική και δημιουργική συμβολή του μεταφραστή. Έτσι, δεν αποτελεί προστατευόμενο έργο η αυτόματη μετάφραση που πραγματοποιείται από λογισμικό, ιδίως όταν οι ανθρώπινες παρεμβάσεις είναι ελάχιστες και αγγίζουν τα όρια της απλής επιμέλειας κειμένου (π.χ. χρήση της εφαρμογής Googletranslator). Ομοίως υπολείπονται καταρχήν δημιουργικής διαδικασίας η απλή επιμέλεια ή η διόρθωση ενός κειμένου μιας μετάφρασης. Η μετάφραση, πέρα από το γεγονός ότι πρέπει να είναι προϊόν πνευματικής και δημιουργικής συμβολής ενός ανθρώπου, αποτελεί προστατευόμενο έργο εφόσον είναι πρωτότυπη. Σύμφωνα με την κρατούσα θεωρία της «στατιστικής μοναδικότητας» του έργου, *η πρωτοτυπία βασίζεται στην κρίση ότι κατά λογική πιθανολόγηση, κάτω από τις ίδιες ακριβώς συνθήκες και με τους ίδιους στόχους κανένας άλλος δημιουργός δεν θα ήταν σε θέση να δημιουργήσει όμοιο έργο, σημαδεύοντας με την προσωπικότητά του το έργο.*

1.14. Μεθοδολογία για την μετάφραση της διδακτορικής διατριβής

Στην παρούσα εργασία, όπως ήδη αναφέρθηκε στην εισαγωγή γίνεται μετάφραση της διδακτορικής διατριβής του Γεώργιου Δημητρακάκη, Δρ. Φυσικού του Πανεπιστήμιου Πατρών με τίτλο: *Διερεύνηση των απωλειών μαγνητικών στοιχειών διαρρεόμενων από υψίσυχνα ρεύματα για εφαρμογές σε διατάξεις ηλεκτρονικών ισχύος.* Η συγκεκριμένη διατριβή αποτελείται από 7 κεφάλαια και έχει έκταση περίπου 65.000 λέξεις. Η μετάφραση αυτής της διατριβής βρίσκεται ήδη από τον Ιανουάριο του 2021 αναρτημένη στη βάση δεδομένων Νημερτής του Πανεπιστημίου Πατρών, μαζί με το πρωτότυπο έργο στα ελληνικά, το οποίο είναι διαθέσιμο ήδη από το 2009.

Πρέπει να αναφερθεί επίσης ότι στο κείμενο υπάρχουν πίνακες, διαγράμματα, εικόνες αλλά και παραπομπές που παρεμβάλλονται στη φυσιολογική ροή του κειμένου. Τα κείμενα μεταφράστηκαν όλα ανεξαιρέτως. Οι πίνακες, τα διαγράμματα, και οι εικόνες επεξεργάστηκαν κατάλληλα με την βοήθεια των λογισμικών Corel Photo Paint και Matlab και συμπεριλήφθηκαν και αυτά στη μετάφραση. Η όλη παραπάνω διαδικασία της επεξεργασίας των σχημάτων της ήταν μια ιδιαιτέρως περίπλοκη και χρονοβόρα διαδικασία, γιατί πέρα από την μετάφραση έπρεπε να σχήματα να τροποποιηθούν καταλλήλως έτσι ώστε να συμπεριληφθούν και αυτά στην διατριβή. Τα σχήματα επεξεργάστηκαν έτσι ώστε οι εικόνες να έχουν το ίδιο μέγεθος με το πρωτότυπο, τα comments που εμπεριείχε η κάθε εικόνα μεταφράστηκαν για να έχουμε έτσι ένα ολοκληρωμένο αποτέλεσμα. Όλα αυτά έγιναν με την βοήθεια των παραπάνω λογισμικών. Σε όσες από τις εικόνες υπήρχε η έγχρωμη εκδοχή τους αντικαταστάθηκαν με το έγχρωμο αρχείο.

Το κείμενο της διατριβής είναι γραμμένο σε επίσημη γλώσσα και έντονο επιστημονικό λόγο, αφού απευθύνεται καθαρά σε γνώστες του αντικειμένου της επιστήμης της ηλεκτρολογίας. Επίσης το κείμενο χαρακτηρίζεται έντονα από ειδική τεχνική ορολογία πάνω σε θέματα ηλεκτρολογίας και ηλεκτρονικής.

Η μεθοδολογία που ακολουθήθηκε για την μετάφραση της διδακτορικής διατριβής περιλαμβάνει τρία στάδια. Στο πρώτο στάδιο, συγκεντρώθηκε και μελετήθηκε η σχετική βιβλιογραφία, έντυπη και ηλεκτρονική, ελληνική ή ξενόγλωσση (στην αγγλική γλώσσα) σχετική με την ορολογία που χρησιμοποιείται στη διατριβή για την μετάφραση αυτής. Στο δεύτερο στάδιο, εντοπίστηκαν και μελετήθηκαν οι βασικές έννοιες του κειμένου και οι όροι που εμφανίζονται στο κείμενο. Στο τρίτο στάδιο, συντάχθηκε ένας κατάλογος με τους

κυριότερους τεχνικούς όρους που παρουσιάζονται στο κείμενο. Παρακάτω θα περιγραφεί η διαδικασία ανάλυσης των δεδομένων.

Πιο συγκεκριμένα, για την δημιουργία και ολοκλήρωση της παρούσας πτυχιακής εργασίας, προκειμένου να δημιουργηθεί ένα ορθό μετάφρασμα, χρειάστηκε να χρησιμοποιηθεί ένα πλάνο εργασίας, το οποίο θα αποδεικνυόταν και αποτελεσματικό. Για αυτό το λόγο παρατίθενται και τα βήματα που ακολουθήθηκαν στην πορεία της μεταφραστικής διαδικασίας, αλλά και καθ' όλη τη διάρκεια της εργασίας.

Το πρώτο βήμα ήταν μια ανάγνωση ολόκληρης της διδακτορικής διατριβής, αφενός για να διαπιστωθεί επακριβώς ποια ήταν τα ζητήματα τα οποία πραγματεύεται και αφετέρου να εντοπιστούν σε πρώτη φάση όροι και φράσεις που λειτουργούσαν ως «πυρήνες» του νοήματος, συνεπώς θα έπρεπε να ληφθούν εξαρχής υπόψη και να κατανοηθεί πλήρως η σημασία τους, καθώς και να μελετηθούν πιθανές πολυσημίες ή νοηματικές διαφορές σε διαφορετικά συγκείμενα.

Αρχικά, βέβαια, έγινε μια προσπάθεια για τη μετάφραση των πρώτων σελίδων, λίγο πειραματικά, πριν από οποιαδήποτε πραγματολογική και θεωρητική έρευνα, πράγμα που αποδείχτηκε μεγάλο λάθος, καθώς ήταν φυσικό και επόμενο η μετάφραση να γίνεται λίγο μηχανικά, αφού δεν υπήρχε επακριβής γνώση του αντικειμένου, αλλά ούτε και άλλη οποιαδήποτε προηγούμενη μεταφραστική εμπειρία. Έπειτα, βάζοντας τη διαδικασία σε μια ορθή πορεία, έγινε ανάγνωση πληροφοριών, κειμένων και άρθρων σχετικού περιεχομένου, που επρόκειτο να βοηθήσουν τόσο στον εγκλιματισμό και την προσέγγιση προς τον μεταφραστικό κόσμο, όσο και στην εξοικείωση με τη χρήση του αντίστοιχου λεξιλογίου, τρόπου γραφής και ύφους που διακρίνει τέτοιου είδους κείμενα.

Σε αυτό το σημείο, το διαδίκτυο αποδείχτηκε πολύτιμη βοήθεια, καθώς προσφέρεται η πρόσβαση σε επιστημονικά, άρθρα έγκυρα ή λιγότερο έγκυρα (πράγμα αναπόφευκτο), ιστοσελίδες σχετικά με τη μετάφραση, την ορολογία, τη γλωσσολογία και πολλές άλλες βοηθητικές πληροφορίες. Βεβαίως, εκτός από τις διαδικτυακές πηγές πληροφόρησης, μελετήθηκε και η πανεπιστημιακή βιβλιογραφία η οποία είχε συγκεντρωθεί κατά τα χρόνια φοίτησης μου στο πρώην Τ.Ε.Ι Δυτικής Ελλάδος, συγκεκριμένα, στο τομέα της ηλεκτρολογίας, που ενδιέφερε στην προκειμένη φάση. Χάρη σε όλες αυτές τις πηγές, κατορθώθηκε να αντληθεί το απαραίτητο υλικό και να κατανοηθεί το κείμενο σε ικανοποιητικό βαθμό ώστε να μη γίνεται η μετάφραση μηχανικά. Επιπλέον, μέσα από αυτή την έρευνα δόθηκε η ευκαιρία να αποκομιστούν πολλές γνώσεις περί του θέματος της διατριβής, πέρα από τα όρια της μετάφρασης του συγκεκριμένου κειμένου, αλλά και της ιδιαιτερότητας που χαρακτηρίζει το ζήτημα της μετάφρασης σε σύγκριση με την ορολογία

και τις διαφορές που τις διέπουν. Το θέμα της διατριβής, το οποίο επιλέχτηκε για να μεταφραστεί, δεν ήταν ένα άγνωστο αντικείμενο προς εμένα. Μέσα από αυτή την μετάφραση υπήρξε διπλό προσωπικό όφελος. Αφενός εμπλουτίσθηκαν οι γνώσεις μου και κατανοήθηκαν μια σειρά ζητημάτων που σχετίζονται με τις απώλειες ισχύος σε μαγνητικά στοιχεία (πηνία–μετασχηματιστές) τα οποία χρησιμοποιούνται σε εφαρμογές ηλεκτρονικών ισχύος. Σχετικές γνώσεις δηλαδή είχαν αποκομιστεί μόνο αποσπασματικά κατά την διάρκεια των σπουδών στο τμήμα Ηλεκτρολόγων Μηχανικών Τ.Ε. πάνω σε θέματα συναφή με την διατριβή. Εξάλλου, μέσα από αυτή την πτυχιακή, δόθηκε η ευκαιρία ώστε να γίνει η μετάφραση της διδακτορικής διατριβής στα αγγλικά πράγμα σπάνιο, αφού τα περισσότερα ιδρύματα δεν υποχρεώνουν τη συγγραφή ή την μετάφραση των διδακτορικών διατριβών ή των πτυχιακών εργασιών σε κάποια άλλη γλώσσα παρά μόνο στην επίσημη γλώσσα του ιδρύματος ή ίσως στα αγγλικά αν πρόκειται για αλλοδαπό σπουδαστή. Έτσι μέσα από την μετάφραση έγινε εξάσκηση πάνω στην αγγλική ορολογία της ηλεκτρολογίας, μια επιστήμη η οποία είναι άρρηκτα συνδεδεμένη με την αγγλική γλώσσα, η οποία μάλιστα θα μας ακολουθεί κατά την άσκηση του επαγγέλματος.

Στη συνέχεια, προχωρώντας με μεγαλύτερη αποφασιστικότητα και σιγουριά στη μετάφραση του κειμένου, υπήρξαν πολλές στιγμές που συναντήθηκαν δυσκολίες, αφενός στην κατανόηση κάποιας φράσης και αφετέρου στην εύρεση κάποιου όρου, αλλά αντιμετωπίστηκαν με επιτυχία, είτε με την βοήθεια κάποιων online λεξικών ή άλλων πηγών του διαδικτύου, είτε με την σωστή καθοδήγηση και τα στοχευμένα σχόλια του συγγραφέα της διατριβής. Επίσης, πολλές φορές χρειάστηκε να αναθεωρηθεί το αρχικό μετάφρασμα, έτσι ώστε να βελτιωθεί όσο το δυνατόν περισσότερο. Σε αυτό συνέβαλαν αρκετά οι μεταφραστικές τεχνολογίες, τα online λεξικά καθώς, και διάφορα έντυπα, χάρη στα οποία έγινε ενημέρωση και εμπλουτισμός των γνώσεων ακόμα περισσότερο για το αντικείμενο του κειμένου και πολλές φορές χρειάστηκε να γίνει αλλαγή ως προς τη μετάφραση κάποιων όρων. Απώτερος στόχος ήταν πάντα το μεταφρασμένο στα αγγλικά κείμενο να προσεγγίζει στο μέγιστο δυνατό βαθμό το αρχικό κείμενο, τόσο σε ύφος όσο και σε νοηματική απόδοση.

1.15. Ανάλυση των μεταφραστικών δυσκολιών

Η μετάφραση τεχνικών κειμένων αποτελεί ένα ιδιαίτερα περίπλοκο είδος μετάφρασης. Η ορολογία των τεχνικών κειμένων είναι πολύ συγκεκριμένη, γι' αυτό και οι τεχνικές

μεταφράσεις παρουσιάζουν ιδιαίτερη δυσκολία. Προκειμένου να παραχθεί ένα ορθό μετάφρασμα έπρεπε να γίνεται διερεύνηση εις βάθος των επιλογών που δίνονταν για τη μετάφραση ποικίλων όρων μέσα στο κείμενο. Κατά κύριο λόγο, πηγές αποτέλεσαν online λεξικά εγχειρίδια κατασκευαστών και πολλοί διαδικτυακοί ιστότοποι. Έγινε η επιλογή κυρίως να μεταφραστούν οι όροι που συναντήθηκαν στο πρωτότυπο κείμενο με βάση την εγκυρότητα των πηγών, την προσωπική κρίση της μεταφράστριας και τέλος με βάση το κατά πόσο οι όροι αυτοί μπορούσαν να σταθούν ορθά μέσα στο σύνολο του μεταφράσματος το οποίο είχε παραχθεί.

Κατ΄ αυτόν τον τρόπο χρειάστηκε να γίνει έρευνα σε αρκετούς διαδικτυακούς τόπους για κάθε όρο, στη συνέχεια έγινε σύγκριση των ευρημάτων και έγινε ενσωμάτωση των όρων στο μετάφρασμα. Τα προβλήματα στη μετάφραση είναι ορισμένα αντικειμενικά εμπόδια που αντιμετωπίζουν όλοι οι μεταφραστές κατά τη μετάφραση τεχνικών κειμένων και η μεθοδολογική ικανότητα και η στρατηγική προσέγγισης, παίζουν σημαντικό ρόλο στην επίλυσή τους. Τα μεταφραστικά προβλήματα είναι φυσικά άμεσα συνδεδεμένα και συνυφασμένα με τις μεταφραστικές ικανότητες του μεταφραστή. Οι δυσκολίες που χρειάστηκε να αντιμετωπιστούν κατά την διαδικασία της μετάφραση ήταν κυρίως γλωσσικά προβλήματα (λεξιλογικά και συντακτικά), τα οποία και παρουσιάζονται αναλυτικά παρακάτω.

- <u>Λεξιλογικές δυσκολίες</u>

Είναι προφανές ότι σε ένα επίσημο τεχνικό κείμενο που περιέχει ειδική επιστημονική ορολογία είναι αναπόφευκτο να υπάρξουν μεταφραστικές δυσκολίες σε όρους που μεταφράζονται από την ελληνική προς την αγγλική γλώσσα. Η βασικότερη και σημαντικότερη δυσκολία όλων ήταν να αντιστοιχηθούν οι ηλεκτρολογικές έννοιες της ελληνικής με εκείνες της αγγλικής γλώσσας. Πολλές φορές, όπως διαπιστώθηκε, αυτή η διαδικασία δεν είναι τόσο απλή αφού αρκετές από τις λέξεις της ελληνικής γλώσσας εκφράζουν ένα πολύ διαφορετικό νόημα από τις αντίστοιχες της αγγλικής. Επίσης η ελληνική γλώσσα διαθέτει αρκετά πιο πλούσιο λεξιλόγιο από ότι η αγγλική δυσχεραίνοντας έτσι ακόμα περισσότερο το έργο της μετάφρασης όσον αφορά την επιλογή του κατάλληλου όρου έτσι ώστε να αποδίδεται στο ακέραιο το νόημα του πρωτότυπου κειμένου. Μάλιστα, σε κάποιες περιπτώσεις δεν ήταν αρκετό απλώς να ανοίξει κανείς ένα λεξικό και να αναζητήσει τη σημασία του όρου, αλλά έπρεπε να ερευνήσει προσεκτικά τη σημασία μιας λέξης, πώς

χρησιμοποιείται και με ποια πρόθεση συντάσσεται. Σε αρκετές περιπτώσεις δεν ήταν αρκετή μόνη η χρήση ενός λεξικού, αλλά χρειάστηκε να γίνει αναζήτηση και στο διαδίκτυο προκειμένου να αναζητηθεί η σημασία και η συνήθης χρήση ενός όρου, κυρίως μέσα από επιστημονικά άρθρα. Τέλος, κάποιοι όροι της ελληνικής προκειμένου να μεταφραστούν στην αγγλική χρειάστηκε να μεταφραστούν περιφραστικά, ώστε ο αναγνώστης να καταλαβαίνει πλήρως το νόημα του κειμένου δεν υπήρχε μονολεκτική απόδοση, οπότε δεν μπορούσε να γίνει αυτολεξεί μετάφραση. Κάποια χαρακτηριστικά παραδείγματα των όσων προαναφέρθηκαν παρατίθενται παρακάτω:

Στο ελληνικό κείμενο χρησιμοποιούνται αρκετές φορές οι λέξεις *υπόθεση*, *υποθετικά*. Οι αντίστοιχες στην αγγλική είναι οι λέξεις *hypothesis*, *hypothetical*. Αυτές οι λέξεις θα ταίριαζαν άψογα για τη φιλοσοφία, την πολιτική ή κάπου αλλού όπου αναφερόμαστε σε ένα υποθετικό σενάριο. Στα μαθηματικά και στη φυσική συνήθως χρησιμοποιούμε τη λέξη *assumption*.

Οι λέξεις *flux* και *flow* στα ελληνικά σημαίνουν *ροή* και οι δύο. Ωστόσο στην αγγλική χρησιμοποιούνται εντελώς διαφορετικά. Αναλυτικότερα, για τη ροή ρεύματος ή για τη ροή θερμότητας θα χρησιμοποιήσουμε τη λέξη *flow*. Η λέξη *flux* συναντάται κυρίως στον ορισμό των πεδίων (το πεδίο μπορεί να είναι για παράδειγμα ηλεκτρικό ή μαγνητικό, μπορεί όμως να είναι και πεδίο ροής δυνάμεων, ροής ρευστού ή ροής θερμότητας).

Ο όρος *μέγεθος* στην ελληνική γλώσσα χρησιμοποιείται με ποικίλους τρόπους, ως έννοια στα αγγλικά όμως υπάρχουν διαφορετικοί ορισμοί ενδεικτικά αναφέρονται κάποια χαρακτηριστικά παραδείγματα:

size: *μέγεθος*, συνήθως χρησιμοποιείται για ρούχα και παπούτσια.

magnitude: *μέγεθος*, χρησιμοποιείται κυρίως για να χαρακτηρίσουμε το μέτρο ενός μιγαδικού αριθμού ή για να χαρακτηρίσουμε το μέγεθος ενός φυσικού φαινομένου (για παράδειγμα το μέγεθος του σεισμού).

quantity: *ποσότητα*, χρησιμοποιείται κυρίως για τα φυσικά μεγέθη

Άλλο ένα σημείο που παρουσιάστηκε μια δυσκολία ήταν η επιλογή του κατάλληλου ορισμού για την έκφραση *συνήθης θερμοκρασία* οι διαθέσιμες επιλογές που δόθηκαν ύστερα από έρευνα σε διάφορα online λεξικά ήταν:

normal temperature: η έκφραση *normal temperature* χρησιμοποιείται στις περιπτώσεις όπου υπάρχει ακριβής ρύθμιση της θερμοκρασίας (π.χ. η θερμοκρασία στο σώμα μας).

ordinary temperature, *room temperature*: οι εκφράσεις *ordinary temperature* και *room temperature* έχουν αυστηρό ορισμό και οι δύο (15-25°C και 1-30 °C αντίστοιχα)

usual temperature: είναι η έκφραση η οποία μεταφράζει πλήρως την έκφραση από τα ελληνικά στα αγγλικά στη συγκεκριμένη περίπτωση εντός της διατριβής.

Παρ' όλα   αυτά όμως, για να μην έχουμε παρεννοήσεις στην μετάφραση από τον ξενόγλωσσο αναγνώστη, επελέγη να χρησιμοποιηθεί στην μετάφραση η έκφραση *room temperature* παρότι επιστημονικά δεν αποτελεί την ορθότερη επιλογή.

Ένα άλλο σημείο της μετάφρασης που απαιτεί διευκρίνιση είναι στη σημασία των όρων *width* και *height*. Η απάντηση βρίσκεται στη διεθνή επιστημονική βιβλιογραφία. Εκεί ονομάζεται *height* το πάχος του τυλίγματος στη διεύθυνση την κάθετη στον άξονα συμμετρίας (και στη μαγνητική ροή) και *width* το ύψος του τυλίγματος. Οπότε και στη μετάφραση της διατριβής διατηρήθηκε η ορολογία ως είθισται να χρησιμοποιείται.

Σε ένα τελευταίο παράδειγμα, ο όρος *μεταβολή* ήταν μια ιδιαίτερη περίπτωση ως προς την επιλογή του κατάλληλου όρου στα αγγλικά γιατί έπρεπε να γίνει αντιληπτό κάθε φορά με ποια έννοια χρησιμοποιείται. Στα αγγλικά η λέξη *change* σημαίνει αλλαγή από μια κατάσταση σε μία άλλη ή αλλαγή από μια τιμή σε μία άλλη. Όταν υπάρχει συνέχεια στη μεταβολή (στο χρόνο ή εντός ενός πεδίου τιμών, δηλαδή σάρωση τιμών) χρησιμοποιείται η λέξη *variance*. Οπότε απαιτείτο προσοχή για το ποιος όρος εκφράζει απόλυτα τον όρο *μεταβολή* κάθε φορά.

Σα γενικό συμπέρασμα από τα παραπάνω παραδείγματα που προαναφέρθηκαν, γίνεται αντιληπτό πως η ελληνική γλώσσα διαθέτει σαφώς πιο πλούσιο λεξιλόγιο από την αγγλική και υπήρχαν πολλές λέξεις οι οποίες δε μπορούσαν να μεταφερθούν επακριβώς στην αγγλική, οπότε σε αυτή την περίπτωση πρέπει κανείς να ανατρέξει στην καλύτερη δυνατή επιλογή λέξης, που όμως να μην αλλοιώνει την ουσία του κειμένου, ή να το περιγράφει περιφραστικά, ή να περιγράφει τη γενική εικόνα (το νόημα της πρότασης) βάζοντας έτσι και ο μεταφραστής την δική του πινελιά στο περιεχόμενο του κειμένου.

- <u>Συντακτικές δυσκολίες</u>

Όπως προαναφέρθηκε, η διατριβή είναι γραμμένη σε επίσημη γλώσσα και περιέχει πληθώρα επιστημονικών όρων, οπότε παρουσιάστηκαν αρκετές δυσκολίες όσον αφορά τη σύνταξη των προτάσεων. Το πιο συχνό λάθος το οποίο χρειάστηκε αρκετές φορές να επισημανθεί και να διορθωθεί ήταν πως αντί για το ουσιαστικό χρησιμοποιούνταν μετοχή. Πολλές φορές ήταν σωστό, αλλά κάποιες άλλες αλλοίωνε το νόημα της πρότασης. Σε άλλες περιπτώσεις γινόταν αντικατάσταση του ουσιαστικού με απαρέμφατο. Επίσης σε πολλές περιπτώσεις, μάλλον λόγω βιασύνης ή απροσεξίας, γινόταν χρήση του ενικού αριθμού εκεί

που υπήρχε πληθυντικός και άλλαζαν οι χρόνοι του κειμένου, κυρίως αντικαθιστώντας εσφαλμένα τον ενεστώτα με παρατατικό.

Στα διδακτορικά, στις πτυχιακές και σε άλλα επίσημα τεχνικά κείμενα είθισται τα κείμενα να γράφονται σε τρίτο πρόσωπο και σε παθητική φωνή (π.χ. *το ρεύμα αυξάνεται, ελήφθησαν οι μετρήσεις*) και όχι σε πρώτο πρόσωπο και σε ενεργητική φωνή (π.χ. *αυξάνουμε το ρεύμα, λάβαμε τις μετρήσεις*) ή χρησιμοποιώντας μετοχές (π.χ. *αυξάνοντας το ρεύμα προκύπτει ότι* και όχι *αν αυξήσουμε το ρεύμα προκύπτει ότι*). Αυτό είναι κάτι που δε επιτρέπεται να αλλάξει κατά τη μετάφραση. Βέβαια δεν είναι νόμος απαράβατος, μπορεί π.χ. να λέμε κάπου *με αύξηση του ρεύματος θα παρατηρήσουμε μια μεταβολή*, αντί για *με αύξηση του ρεύματος παρατηρείται μία μεταβολή*. Αν στο ελληνικό κείμενο έχει τρίτο πρόσωπο και όχι πρώτο, αν έχει μετοχή και όχι ρήμα, αν έχει παθητική φωνή και όχι ενεργητική, σωστό είναι η σύνταξη του πρωτότυπου να διατηρείται και στη μετάφραση.

Τέλος, σε αρκετές περιπτώσεις όπου κάποιες από τις προτάσεις του κειμένου ήταν αρκετά μεγάλες και με κάπως περίπλοκο νόημα, χρειάστηκε να χωριστούν σε μικρότερες προτάσεις με σκοπό την καλύτερη νοηματική απόδοσή τους. Η άνω τελεία χρησιμοποιήθηκε αρκετές φορές και αποδείχθηκε μια καλή λύση αντί για το πλήρες σπάσιμο μια πρότασης σε δύο ξεχωριστές. Αυτό όμως έγινε με ιδιαίτερη προσοχή γιατί χωρίζοντας μία μεγάλη πρόταση στα δύο υπάρχει ο κίνδυνος να αλλοιωθεί το νόημα της πρότασης και αυτό δεν πρέπει σε καμία περίπτωση να συμβαίνει χάριν ευκολίας.

Ιδιαίτερη προσοχή δόθηκε και στα σημεία στίξης. Χαρακτηριστικό παράδειγμα είναι πως ένα κόμμα, που μπορεί να παραληφθεί ή αντιθέτως να χρησιμοποιηθεί χωρίς να χρειάζεται, μπορεί να αλλάξει εντελώς το νόημα μια πρότασης ή να περιπλέξει την πρόταση και να μη βγαίνει νόημα. Γενικά στα κόμματα δόθηκε μεγάλη προσοχή και αποδείχτηκε ότι όπου υπάρχει κόμμα στην διατριβή δεν είναι τυχαίο. Βέβαια μεταξύ αγγλικής και ελληνικής γλώσσας υπάρχουν και πολλές διαφορές σε θέματα σύνταξης ή χρήσης των σημείων στίξης. Για παράδειγμα στον αγγλικό γραπτό λόγο, υπό συνθήκες, μπορεί να μπει κόμμα μετά από τη λέξη *and*, στα ελληνικά γραπτά όμως απαγορεύεται κατηγορηματικά το κόμμα μετά το συνδετικό *και* παρότι στον προφορικό λόγο αρκετές φορές έχει νόημα.

ΚΕΦΑΛΑΙΟ 2

ΟΡΓΑΝΩΣΗ ΤΗΣ ΒΙΒΛΙΟΓΡΑΦΙΑΣ

2.1. Εισαγωγικά: Ιστορικά στοιχεία για τη δημιουργία της βιβλιογραφίας

Για πολλά χρόνια, η εξέταση της Ιστορίας του Βιβλίου, όσον αφορά τη μελέτη του υλικού υποστρώματος και της εξέλιξης αυτού, μονοπωλούσε το ενδιαφέρον της ερευνητικής κοινότητας. Μόλις στα μέσα του 20ού αιώνα έγινε αντιληπτή η ανάγκη εξέτασης και μελέτης των κοινωνικών και πολιτιστικών συνθηκών που καθόρισαν και διαμόρφωσαν την παραγωγή και τη διάθεση των συγγραφικών έργων (Finkelstein, 2005).

Η Ιστορία της Επιστήμης της Βιβλιογραφίας είναι συνυφασμένη και εξελίσσεται παράλληλα με την εξιστόρηση των εξελίξεων των παρακάτω επιστημών:

- η Ιστορία της Γραφής και των μέσων αποτύπωσης
- η Ιστορία του Βιβλίου
- η Ιστορία της Τυπογραφίας και της Εκτύπωσης

Η ιστορία της βιβλιογραφίας ξεκινά από πάρα πολύ νωρίς με την ανάγκη του ανθρώπου να επικοινωνήσει και να ανταλλάξει πληροφορίες. Οι πρώτοι άνθρωποι χρησιμοποιούσαν τον προφορικό λόγο (όχι με τη σημερινή έκφραση, αλλά κυρίως με την χρήση κραυγών και διάφορων άλλων ήχων), αλλά και διάφορες χειρονομίες προκειμένου να επικοινωνήσουν μεταξύ τους. Δεν υπήρχε κανένας περιορισμός ως προς το τρόπο που θα μετέδιδαν την πληροφορία από τον έναν στο άλλο. Στη συνέχεια, οι άνθρωποι των σπηλαίων χρησιμοποιούσαν τις ζωγραφιές προκειμένου να απεικονίσουν αντικείμενα, να μεταφέρουν πληροφορία, να αποτυπώσουν ιστορίες εμπνευσμένες από την καθημερινότητα τους. Δεν λαμβάνονταν δηλαδή καμία μέριμνα ώστε να μεταφερθούν αυτούσια η πληροφορία, μιας και δεν ήταν αυτός ο σκοπός, ενώ η αναφορά και απόδοση της πνευματικής υπευθυνότητας της πληροφορίας δεν είχε συλληφθεί ακόμα ως ιδέα (Diringer, 1953). Στην Εικόνα 2.1 βλέπουμε μια χαρακτηριστική σπηλαιογραφία από το Σπήλαιο της Αλταμίρα από την παλαιολιθική εποχή. Οι παλαιότερες από τις σπηλαιογραφίες που υπάρχουν μέσα στο Σπήλαιο σύμφωνα με επιστημονικές μελέτες χρονολογούνται μέχρι και 36.000 χιλιάδες χρόνια πριν.

Εικόνα 2.1: *Πολύχρωμη σπηλαιογραφία από το Σπήλαιο της Αλταμίρα (Β. Ισπανία).*

Σε όλες αυτές τις περιπτώσεις είναι εμφανής η ανάγκη του ανθρώπου να καταγράψει και να μεταδώσει πληροφορία σε άλλους ανθρώπους. Βέβαια, σκοπός τους δεν ήταν να αποτελέσουν αυτά ιστορικά αντικείμενα και απόδειξη της ύπαρξης και των συνθηκών ζωής τους, αλλά κυρίως να εξυπηρετήσουν δικές τους καθημερινές και προσωπικές ανάγκες.

Μετά από πολλά χρόνια κάνει την εμφάνισή της η γραφή και το τοπίο της μετάδοσης της πληροφορίας αλλάζει σημαντικά. Κάθε μέσο (αρχικά χρησιμοποιήθηκαν κυρίως πέτρες και ξύλα) το οποίο μπορούσε να χαραχτεί ή να ζωγραφιστεί χρησιμοποιήθηκε για να καλύψει τις ανάγκες της εποχής για την αποτύπωση της πληροφορίας.

Αρχές της τρίτης χιλιετηρίδας π.Χ. (π.χ. στην Αίγυπτο και στην Μεσοποταμία) άρχισε η χρήση πήλινων κομματιών ως γραφικό μέσο (Diringer, 1953). Αργότερα χρησιμοποιήθηκε ο πάπυρος και η περγαμηνή, τα οποία τέλος αντικαταστάθηκαν από το χαρτί. Ανάλογα με το υλικό, το σύγγραμμα κάθε φορά είχε και διαφορετική μορφή. Για παράδειγμα, τα πήλινα κομμάτια ήταν αρχικά ασύμμετρα, αργότερα πήραν συγκεκριμένη μορφή για να δηλώσουν και το είδος της πληροφορίας που αποτύπωναν. Ο δε πάπυρος είχε κυλινδρική μορφή, η περγαμηνή ευνόησε τη δημιουργία των κωδίκων, ενώ το χαρτί οδήγησε στη σύλληψη της σημερινής μορφής του βιβλίου.

Εικόνα 2.2: Σουμεριακή επιγραφή σε αρχαϊκό τρόπο, 26ος αιώνας π.Χ

Εικόνα 2.3: Ένας από τους πάπυρους της Οξυρρύχου, επιστολή για αγοραπωλησίες στα ελληνικά, 2ος αι. μ.Χ.

Εικόνα 2.4: Νομικός κώδικας του Βινοντόλ σε περγαμηνή. Χρονολογείται από το 1288 π.Χ. και είναι γραμμένη στο γλαγολιτικό αλφάβητο.

Οι πληροφορίες που αποτυπώνονταν στα παραπάνω γραφικά μέσα ήταν άμεσα συνδεδεμένες με τις ανάγκες της εποχής. Στα πρώιμα στάδια ήταν κυρίως πληροφορίες που αφορούσαν στη τήρηση λογαριασμών και εμπορικών συναλλαγών και πρωτογενή δεδομένα που είχαν να κάνουν με τις ποσότητες των προϊόντων που διακινούνταν με το εμπόριο.

Μέχρι σε αυτό το χρονικό σημείο, δεν μπορεί να γίνει αναφορά σε σύνταξη καταλόγων υπό τη μορφή βιβλιογραφιών. Τα κείμενα που παράγονταν είχαν διοικητική και οικονομική υπόσταση, καθώς επίσης και το πλήθος τους δεν επέβαλε τη διαμόρφωση καταλόγων για λόγους εύρεσης. Κυρίως όμως, γιατί δεν είχε εκδηλωθεί ακόμα η συγκεκριμένη ανάγκη.

Οι πρώτοι κατάλογοι βιβλιογραφιών αρχίζουν να εμφανίζονται με την άνθιση της λογοτεχνικής παραγωγής. Ο παλαιότερος κατάλογος που έχει ανακαλυφθεί είναι από το 2000 π.Χ.. Ανήκει αυτή τη στιγμή στη συλλογή Nippur και εκτίθεται στο Pennsylvania University Museum. Αποκρυπτογραφήθηκε από τον Kramer και περιλαμβάνει ένα λογοτεχνικό

κατάλογο με 62 τίτλους, ο οποίος καταγράφει τους τίτλους λογοτεχνικών συγγραμμάτων των Σουμερίων (Diringer, 1953).

Στη συνέχεια, έκαναν την εμφάνισή τους οι ιδιωτικές συλλογές, οι συλλογές αυτές είχαν τη μορφή προσωπικής, ιδιωτικής βιβλιοθήκης. Η συλλογή αναπτυσσόταν, εμπλουτιζόταν και ανήκε σε πλούσιους ευγενείς ή αστούς και αποτελούσε στοιχείο προσωπικού πλούτου και ευημερίας. Η καταγραφή των τεκμηρίων της συλλογής μετατρεπόταν σε επιτακτική ανάγκη με σκοπό να καταγράψουν τα βιβλία που κάποιος είχε στην προσωπική του συλλογή, στην προσωπική του βιβλιοθήκη. Αργότερα, η βιβλιογραφία υπό τη μορφή σύνταξης καταλόγων με τα στοιχεία των τεκμηρίων της συλλογής υιοθετήθηκε για την καταγραφή των τεκμηρίων που υπήρχαν σε μια βιβλιοθήκη.

Οι πρώτοι κατάλογοι βιβλιοθηκών εμφανίζονται στην Αίγυπτο από τους φύλακες της βιβλιοθήκης της Αλεξάνδρειας.

- Ο Καλλίμαχος ο Κυρηναίος (246-235 π.Χ.) ο οποίος θεωρείται και ο πατέρας της Βιβλιογραφίας είναι ο πρώτος που συνέθεσε τους πίνακες, έναν κατάλογο από 120 συγγράμματα από όλες τις γνωστές τότε επιστήμες.
- Ο Αριστοφάνης ο Βυζάντιος (195-180 π.Χ.) συνέταξε μία λίστα με τα ονόματα των πιο αντιπροσωπευτικών Ελλήνων Ποιητών.

Για πρώτη φορά, αρχίζουν να αποδίδονται τα διάφορα έργα στους συγγραφείς τους και να θεωρείται σημαντική η πνευματική υπευθυνότητα. Μάλιστα στη Μεσαιωνική Ευρώπη έχουν βρεθεί παραδείγματα συνέχισης της σύνταξης καταλόγων βιβλιοθηκών. Ο κατάλογος της Cordova Βιβλιοθήκης περιλάμβανε 400.000 τόμους και η Fatimidis Βιβλιοθήκη στο Κάιρο 100.000 τόμους (Diringer, 1953).

Η επινόηση όμως της τυπογραφίας ήρθε για μία ακόμα φορά να αλλάξει τα δεδομένα της επιστήμης της βιβλιογραφίας σχετικά με τη σύνταξη των καταλόγων. Οι κατάλογοι αυτοί παρά τον εμπορικό τους χαρακτήρα, μια και σκοπός τους ήταν να προωθήσουν τις εκδόσεις, περιέχουν σημαντικά βιβλιογραφικά στοιχεία. Αυτά αποτελούν σημαντικές βιβλιογραφικές πηγές που προωθούν και συμβάλλουν στην εξέλιξη της έρευνας με τον εντοπισμό όλων των αναφορών που αφορούν σε ένα συγκεκριμένο θέμα Στην Ευρώπη, ο πρώτος κατάλογος εντοπίζεται στις απαρχές της τυπογραφίας. Αποτελεί τον πρώτο γνωστό κατάλογο και είναι τυπωμένος στη Μαγεντία (Γερμανία) σε μονόφυλλο, στα 1469. Ονομάζεται κατάλογος του P. Schoeffer και ήταν τυπωμένος στο τυπογραφείο Chr. Plantin. Σήμερα φυλάσσεται στο Μουσείο Musee Plantin στην Αμβέρσα.

Οι κατάλογοι των βιβλιοπωλών και των τυπογράφων έφεραν και αποτύπωναν όλα τα κύρια χαρακτηριστικά μιας βιβλιογραφίας. Περιλάμβαναν όλα τα στοιχεία εκείνα (τίτλο, όνομα συγγραφέα, έτος έκδοσης) που επιβάλλουν τα πρότυπα σύνταξης βιβλιογραφιών στις μέρες μας και οι κατάλογοι αυτοί ήταν οργανωμένοι θεματικά. Επίσης, συχνά περιλάμβαναν στοιχεία σχετικά με τη δομή του έργου και την ποσότητα, στοιχεία που απαντώνται σήμερα σε κάποια εξειδικευμένα είδη βιβλιογραφιών, χρησιμοποιώντας κριτήρια ταξινόμησης, όπως είναι κριτήρια αλφαβητικά και χρονολογικά.

Μέσα από αυτούς τους καταλόγους προκύπτουν και στοιχεία σχετικά με το ποια τεκμήρια ήταν πιο δημοφιλή, ποια κυκλοφορούσαν και προωθούνταν περισσότερο. Τα στοιχεία αυτά μπορούν επίσης να αποτελέσουν στοιχείο τεκμηρίωσης σχετικά με το πνευματικό επίπεδο των ανθρώπων της κάθε εποχής.

Συμπερασματικά, λοιπόν θα μπορούσαμε να πούμε πως:

- Η παραγωγή λογοτεχνικών κειμένων οδήγησε κυρίως στη διαμόρφωση των πρώτων καταλόγων βιβλιογραφιών.

- Ένας ακόμα λόγος για τη δημιουργία των πρώτων καταλόγων βιβλιογραφίας υπήρξε η εξέλιξη της ανάγκης αποτύπωσης της πληροφορίας και αντιγραφής της, αλλά και της ανάγκης εύρεσης και ευρύτερης διάδοσης της πληροφορίας.

- Δεν υπήρχαν κανόνες και πρότυπα στη σύνταξη των καταλόγων.

- Οι κατάλογοι συντάσσονταν για να ικανοποιήσουν προσωπικές ανάγκες.

- Οι κατάλογοι εξυπηρέτησαν και εξυπηρετούν τις ανάγκες του εμπορίου και της εκδοτικής παραγωγής του βιβλίου.

Η έννοια της βιβλιογραφίας στον ελλαδικό χώρο χρησιμοποιήθηκε για πρώτη φορά από τους Έλληνες γραφείς του 3ου μ.Χ. αιώνα για να δηλώσουν την εργασία της αντιγραφής των βιβλίων με το χέρι. Τον 12ο αιώνα, ο όρος υιοθετήθηκε για να δηλώσει την πνευματική διεργασία της συγγραφής βιβλίων, ενώ, μόλις τον 17ο αιώνα, έλαβε τη σημερινή του σημασία.

2.2. Αναδρομή: από την έντυπη στην ψηφιακή εποχή

Τα τελευταία χρόνια μετακινούμαστε από την έντυπη προς την ψηφιακή πληροφόρηση. Γενικά, είναι πλέον αποδεκτό πως η ψηφιακή πληροφόρηση υπερτερεί έναντι της έντυπης. Το ιστορικό της μετάβασης παρουσιάζει μεγάλο ενδιαφέρον. Στην αρχή, η χρήση των

υπολογιστών, όταν ξεκίνησαν να χρησιμοποιούνται μαζικά, ήταν απλώς για την παραγωγή έντυπων δημοσιευμάτων. Αυτά σε πρώτη φάση διακινούνται μόνο έντυπα, οι υπολογιστές δηλαδή ήταν μόνο το εργαλείο με το οποίο δημιουργούσαμε κάτι, δεν είχαν καμία σχέση με την παραπέρα διακίνησή του. Σε επόμενη φάση άρχισε να γίνεται διάθεση κειμένου, ίδιο με το έντυπο, σε ηλεκτρονική μορφή και με ηλεκτρονικά μέσα, είτε πρόκειται για άρθρα περιοδικών είτε για βιβλία ή άλλα κείμενα που στέλνονται σε εκδότες ή σε άλλους, καθώς στη φάση αυτή οι εκδότες ζητούσαν μαζί με το έντυπο και το ηλεκτρονικό κείμενο. Ώσπου τελικά φτάσαμε στο σημείο, πολλές φορές τώρα πια, να καταργείται το έντυπο και να γίνεται αποκλειστικά διάθεση ηλεκτρονικού κειμένου (π.χ. βάσεις δεδομένων, ηλεκτρονικά περιοδικά, κ.α.).

Οι πρώτες επιστημονικές ηλεκτρονικές δημοσιεύσεις, που ξεκίνησαν, δημιουργήθηκαν και διακινήθηκαν δηλαδή μέσω υπολογιστή, ήταν καταρχάς κάποια Request for Comment της IETF (Internet Engineering Task Force), που περιέγραφαν κάποια στοιχεία εξέλιξης κάποιων διαδικασιών, κυρίως σχετικά με το πρώιμο διαδίκτυο, το 1969. Καθώς δεν υπήρχε ο ιστός, διακινήθηκαν με δισκέτες ή άλλα μέσα, άλλα διακινήθηκαν αποκλειστικά ηλεκτρονικά.

Αργότερα, με τα E - Prints, στο Los Angeles Laboratory - (1991), άλλαξε πάλι ο τρόπος της επιστημονικής επικοινωνίας, εφαρμόζοντας ένα σύστημα όπου όλοι οι φυσικοί της ίδιας ειδικότητας τοποθετούσαν και αναζητούσαν τα άρθρα τους σε ένα κοινό μέρος, που αποκαλούνταν αποθετήριο (Educational Repository).

Ώσπου ερχόμαστε στη σημερινή εποχή. Ήδη από το 2003 εκτιμάται ότι το 93% του παραγόμενου περιεχομένου είναι ψηφιακό. Άρα ένα μόνο πολύ μικρό ποσοστό φτιάχνεται σε μέσα μη ψηφιακά, βέβαια αυτό δεν συνεπάγεται ότι όλο αυτό το περιεχόμενο διακινείται από εκεί και πέρα ψηφιακά, καθώς ένα μεγάλο μέρος του τυπώνεται ή αποτυπώνεται σε άλλα μέσα. Όμως στην εποχή μας που έχουμε την πλειοψηφία του υλικού ήδη ψηφιακά, είναι πολύ εύκολο να φροντίσουμε για την ψηφιακή διακίνηση και διατήρηση του περιεχομένου αυτού. Η ηλεκτρονική δημοσίευση άρχισε από την Αμερική, την Ασία και κυρίως την Ιαπωνία. Την ίδια χρονική περίοδο στην Ευρώπη επικρατούσε η έντυπη δημοσίευση.

Τα περιοδικά είναι ο κύριος φορέας επιστημονικής πληροφόρησης και ήταν από τα πρώτα που φρόντισαν να διακινούνται ηλεκτρονικά. Σε πρώτη φάση διακινήθηκαν σε CD, αλλά και πάλι με βάση τις συνδρομές, απλώς διακινούσαν τα CD αντί να στέλνουν έντυπα περιοδικά. Αρχικά πιο πολύ εφαρμοζόταν σε περιλήψεις άρθρων, πρακτικά συνεδρίων, εμπορικούς καταλόγους και άλλα αντίστοιχα εργαλεία για αναζήτηση, αλλά σιγά - σιγά επικράτησε και σε ορισμένα περιοδικά.

Πλέον, το μέσο διάθεσης τους έχει αλλάξει από CD στον ιστό, άρα δεν είναι απαραίτητο πια ένα φυσικό μέσο για να φέρει το ψηφιακό περιεχόμενο, αλλά μεταφέρεται στους αναγνώστες κατευθείαν μέσω του ιστού. Το διαδίκτυο είναι πια αρκετά διαδεδομένο, το μεγαλύτερο ποσοστό των ανθρώπων έχουν πλέον πρόσβαση σε αυτό και έχουν τη δυνατότητα να βρουν οποιαδήποτε πληροφορία απευθείας και από την πρώτη στιγμή που δημοσιεύεται. Λόγω του ότι μειώθηκε πολύ το σχετικό κόστος, κυκλοφορούν τώρα ηλεκτρονικά περιοδικά με συνδρομή αλλά και δωρεάν.

Οι μορφές με τις οποίες διακινούνται τα ηλεκτρονικά περιοδικά αυτή τη στιγμή ακολουθούν διάφορα πρότυπα όπως HTML, PDF, κλπ και άλλα που βασίζονται σε XML. Επίσης, έχουν ξεκινήσει και κάποια έργα ώστε να ψηφιοποιηθούν παλαιά τεύχη για να είναι και εκείνα διαθέσιμα ηλεκτρονικά μαζί με τα καινούργια που παράγονται και διατίθενται κατευθείαν ηλεκτρονικά. Χαρακτηριστικό τέτοιο έργο είναι το JSTOR (Journal Storage Project), που δημιουργεί ένα ηλεκτρονικό αρχείο των εντύπων περιοδικών (electronic archiving of printed journals http://www.jstor.org).

Στα περιοδικά λοιπόν αρχίζουμε να έχουμε εκτός από τα έντυπα και «παράλληλα εκδιδόμενα» περιοδικά, που έχουν έντυπη και ηλεκτρονική έκδοση διαθέσιμη στο κοινό, πιστά αντίγραφα η μια έκδοση της άλλης ή με μικροδιαφορές όπως πιθανή αναφορά σε άλλη ενημερωτική, πρόσκαιρη, πληροφορία. Έτσι μπορεί να έχουμε έντυπα περιοδικά με ηλεκτρονικά αντίγραφα ή ηλεκτρονικά περιοδικά με έντυπα αντίγραφα, όπου το αντίγραφο δεν έχει απαραίτητα όλη την πληροφορία, αλλά έχει όλη την πρωτεύουσα και ουσιαστική πληροφορία.

Και φτάνουμε σήμερα να έχουμε μόνο ηλεκτρονικά περιοδικά, περιοδικά με καθόλου έντυπη μορφή. Αυτά έχουν το πλεονέκτημα ότι έχουν πολύ μικρότερο κόστος δημιουργίας και μηδαμινό σχεδόν κόστος διακίνησης.

Βέβαια, όπως είναι φυσικό, όσο πιο περίπλοκα γίνονται τα πράγματα γενικά και τα περιοδικά ειδικότερα, τόσο πιο δύσχρηστα γίνονται, ιδίως για τους μεγαλύτερης ηλικίας αναγνώστες. Αν σκεφτούμε όμως τον όγκο της πληροφορίας που μπορούμε να έχουμε στο έντυπο και στο ηλεκτρονικό περιοδικό, βλέπουμε πως δεν υπάρχει άλλη λύση: ένας απλός δίσκος υπολογιστή μπορεί να χωρέσει τόση πληροφορία που σε έντυπη μορφή δεν χωράει σε πολλά κτήρια μαζί.

2.3. Τι είναι η βιβλιογραφία γενικά

Ο όρος βιβλιογραφία περιέχει πολλαπλές έννοιες, μερικές από αυτές παρατίθενται παρακάτω:

- Αποτελεί ένα κείμενο που περιέχει βιβλιογραφικές αναφορές σε πηγές πληροφόρησης.
- Εμπεριέχει τη μελέτη των βιβλιογραφικών βάσεων δεδομένων (bibliographical databases), της βιβλιομετρίας (bibliometrics or statistical bibliography), αλλά και της επιστημονικής επικοινωνίας (scholarly and scientific communication).
- Δηλώνει μια λίστα με βιβλιογραφικές παραπομπές που χρησιμοποιήθηκαν στο πλαίσιο συγγραφής ενός έργου.
- Συχνά ο όρος βιβλιογραφία υιοθετείται και στο πλαίσιο της ιστορίας του βιβλίου.

Αυτό έχει ως αποτέλεσμα να έχουν διατυπωθεί μία σειρά από ορισμοί για τον όρο βιβλιογραφία με σκοπό να εξυπηρετήσουν τις εκάστοτε ανάγκες (Feather, 2003).

Ο πιο κοινός ορισμός για την επιστήμη της βιβλιογραφίας αναφέρει πως: *η βιβλιογραφία είναι μια συστηματική καταγραφή πληροφοριών για βιβλία, οπτικοακουστικά υλικά και άλλες εκδόσεις, οργανωμένη σε μια λογική σειρά, που παρέχει στοιχεία για τον συγγραφέα του τεκμηρίου, τον τίτλο του, την ημερομηνία αλλά και την περιοχή δημοσίευσης, τον εκδότη, την έκδοση, τη σειρά, και το περιεχόμενο του τεκμηρίου.* Οι βιβλιογραφίες ποικίλουν καθώς μπορεί είτε να αναφέρονται στα έργα ενός μόνο συγγραφέα ή ενός θέματος είτε να περιέχουν στοιχεία για μια περιοχή κατά τη διάρκεια μιας χρονικής περιόδου.

Η βιβλιογραφία ως πρακτική, είναι η ακαδημαϊκή μελέτη των βιβλίων. Σε γενικές γραμμές, η βιβλιογραφία δεν ασχολείται με το περιεχόμενο των βιβλίων, αλλά με τις πηγές των βιβλίων που χρησιμοποιήθηκαν για την συγγραφή τους. Τα είδη των βιβλιογραφιών χωρίζονται σύμφωνα με:

1. Τη μορφή: ενδεικτική, αναλυτική, περιγραφική και κριτική βιβλιογραφία.
2. Το περιεχόμενο: γενική και ειδική βιβλιογραφία.
3. Την έκταση: εξαντλητική και κατ' επιλογή βιβλιογραφία.
4. Το χρόνο κάλυψης: τρέχουσα βιβλιογραφία, αναδρομική βιβλιογραφία.
5. Την ταξινόμηση: αλφαβητική, θεματική και χρονολογική βιβλιογραφία.

6. Τον τρόπο σύνταξης: άμεση βιβλιογραφία και έμμεση βιβλιογραφία.

Η βιβλιογραφία βρίσκεται συνήθως στο τέλος της κάθε δημοσίευσης και περιλαμβάνει όλες τις δημοσιεύσεις τις οποίες ο συγγραφέας χρησιμοποίησε και αν πρόκειται για επιστημονικό πόνημα η κάθε αναφορά εμφανίζεται ως παραπομπή μέσα στο κείμενο.Η βιβλιογραφία απαντάται συνηθέστερα σε δημοσιεύσεις μεγάλης κλίμακας, όπως μονογραφίες, κεφάλαια βιβλίων, πτυχιακές εργασίες. Σε μερικές περιπτώσεις απαντάται και σε περιοδικές δημοσιεύσεις, αλλά αυτό ποικίλει ανάλογα με το περιοδικό.

Κάποια από τα πεδία μιας βιβλιογραφικής αναφοράς είναι απαραίτητα για τον εντοπισμό και την αναγνώριση τους. Βέβαια τα πεδία των βιβλιογραφικών αναφορών είναι αντίστοιχα του τύπου της δημοσίευσης, π.χ. αν είναι ένα άρθρο περιοδικού ή μια μονογραφία. Κάποια άλλα είναι προαιρετικά, ανάλογα με τον τύπο αναφορών που χρησιμοποιούνται.

Όνομα συγγραφέα ή ονόματα συγγραφέων

Το όνομα του συγγραφέα θα πρέπει να αναγράφεται. Κάθε τύπος διαθέτει την δική του πρακτική, όταν ένα έργο είναι ανώνυμο ή όταν εκπονείται από κάποιο συλλογικό όργανο. Σε μερικούς τύπους, απαιτούνται όλα τα ονόματα των συγγραφέων, ενώ σε μερικούς άλλους χρησιμοποιείται το κ.α. – *et al*, υπό προϋποθέσεις.

Τίτλοι

Ο τίτλος της εργασίας είναι απαραίτητο να αναγράφεται. Άλλοι τίτλοι που χρειάζεται να αναφέρονται είναι οι τίτλοι των περιοδικών και των συνεδρίων.

Τοποθεσίες

Ο τόπος δημοσίευσης απουσιάζει τις περισσότερες, αν όχι όλες τις φορές από αναφορές περιοδικών, χρησιμοποιείται όμως σχεδόν πάντα στις μονογραφίες και συχνά στις αναφορές συνεδρίων.

Χρονολογίες

Το έτος δημοσίευσης είναι η χρονιά δημοσίευσης της εργασίας και απαιτείται περισσότερο στις μονογραφίες ή στις μη περιοδικές εκδόσεις γενικότερα. Στις περιπτώσεις συνεδρίων μπορεί να απαιτείται ο χρόνος διεξαγωγής του, ο οποίος δε ταυτίζεται πάντα με την ημερομηνία δημοσίευσης. Σε περιπτώσεις ηλεκτρονικών πηγών μπορεί να απαιτείται η αναγραφή της ημερομηνίας ηλεκτρονικής δημοσίευσης, τελευταίας ανανέωσης ή

ημερομηνίας πρόσβασης. Στα επιστημονικά περιοδικά συχνά αναφέρεται η ημερομηνία πρώτης υποβολής προς κρίση της εργασίας (date of first submission). Με τον όρο «πρώτη» καλύπτεται και η περίπτωση που η εργασία απορρίφθηκε αρχικά, αλλά επανυποβλήθηκε αργότερα έπειτα από βελτιώσεις – τροποποιήσεις.

Όνομα εκδότη/εκδοτικού οίκου

Πρόκειται για το όνομα του εκδότη ενός δημοσιευμένου έργου και το οποίο συνηθίζεται να εμφανίζεται σε όλες τις πηγές, πλην των περιοδικών.

Αριθμήσεις

α) Τόμου/τεύχους. Οι αριθμοί του τόμου και του τεύχους εμφανίζονται συνήθως στις αναφορές περιοδικών. Οι τόμοι βέβαια μπορεί να εμφανίζονται σε μονογραφίες, οι οποίες εκδίδονται σε δύο η περισσότερα τμήματα. Άλλη μια αρίθμηση είναι αυτή των σειρών.

β) Σελίδων. Η αρίθμηση των σελίδων γίνεται με την αναγραφή της συγκεκριμένης σελίδας (ή σελίδων, αν πρόκειται για περισσότερες) στην περίπτωση των μονογραφιών. Στην περίπτωση των περιοδικών χρειάζεται να αναγράφεται η αρχική και η τελική σελίδα του άρθρου.

Έκδοση

Φαινομενικά ένα μη χρήσιμο στοιχείο για τον εντοπισμό των πηγών, αλλά χρήσιμο για την αξιολόγηση τους. Η αρίθμηση της έκδοσης χρησιμεύει όταν ένα βιβλίο έχει περισσότερες από μια εκδόσεις και σε αυτή την περίπτωση έχει υποστεί κάποιες αλλαγές (μικρής κλίμακας συνήθως).

Ψηφιακή Ταυτότητα

Καθώς πλέον πολλά από τα άρθρα, βιβλία κλπ διακινούνται σε ψηφιακή μορφή, τα περισσότερα από αυτά χαρακτηρίζονται από έναν μοναδικό συνδυασμό χαρακτήρων (γράμματα και ψηφία), τα οποία καθορίζουν την ψηφιακή του ταυτότητα (Digital Object Identifier – DOI). Η ταυτότητα αυτή πλέον αναγράφεται συχνά μαζί με τα υπόλοιπα στοιχεία σε μια λίστα αναφορών.

2.4. Τι είναι οι βιβλιογραφικές αναφορές και γιατί είναι τόσο σημαντικές

Η συγγραφή οποιασδήποτε εργασίας (σεμιναρίου ή πτυχιακής) γίνεται έπειτα από βιβλιογραφική έρευνα και απαιτεί την αναφορά των δημοσιευμένων πηγών (βιβλίων ή κεφαλαίων βιβλίων, άρθρων περιοδικών, πηγών του διαδικτύου, κ.ά.) που χρησιμοποιήθηκαν. Η αναφορά των πηγών που χρησιμοποίησε ο συγγραφέας στηρίζεται σε ορισμένες αρχές και γίνεται με συγκεκριμένους τρόπους έτσι ώστε η πληροφορία να χρησιμοποιείται ορθά και νόμιμα. Ορισμένες από αυτές τις αρχές είναι:

- Εντιμότητα: ο συγγραφέας βεβαιώνει πως δεν έχει οικειοποιηθεί έργα ή ιδέες άλλων, δεν διαπράττει δηλαδή το αδίκημα της λογοκλοπής.
- Ελεγξιμότητα: ο αναγνώστης μπορεί να ελέγξει και να διαπιστώσει την εγκυρότητα και την ακρίβεια των πληροφοριών που παραθέτει ο συγγραφέας.

Άλλοι λόγοι για τους οποίους είναι απαραίτητη η χρήση των βιβλιογραφικών αναφορών:

- Ο συγγραφέας αποδεικνύει το εύρος και το βάθος της έρευνάς του προσδίδοντας αξία στην εργασία του.
- Ο συγγραφέας αποδεικνύει τη βαθιά γνώση του επιστημονικού του αντικειμένου, καθώς και την παρακολούθηση της τρέχουσας εξέλιξης του τομέα του.
- Ο αναγνώστης μπορεί να εντοπίσει και να διερευνήσει ένα επιστημονικό πεδίο και να βρει πηγές ενδιαφέροντος.

Ο τρόπος με τον οποίο γίνονται οι αναφορές των έργων από τα οποία άντλησε πληροφόρηση ο συγγραφέας καθορίζεται από πρότυπα που έχουν αναπτυχθεί διεθνώς από πανεπιστήμια, ενώσεις ή οργανισμούς και προέκυψαν από τις ανάγκες τεκμηρίωσης διαφόρων επιστημονικών πεδίων. Για παράδειγμα, στη διατριβή που μεταφράστηκε στα πλαίσια της παρούσας εργασίας εφαρμόζεται το φορμά της IEEE.

2.5. Τα είδη των βιβλιογραφικών αναφορών

Όλες οι βιβλιογραφικές αναφορές έργων εμφανίζονται σε μια εργασία με δύο μορφές: ως παραπομπές και ως βιβλιογραφία.

1. Με την παραπομπή (in-text citation) ο συγγραφέας παραθέτει σε σύντομη μορφή την αναφορά σε έργο άλλου συγγραφέα. Οι παραπομπές έχουν δύο μορφές: την αριθμητική αναφορά και την παρενθετική αναφορά.

   α. Η αριθμητική αναφορά έχει τη μορφή αριθμητικού εκθέτη ή αριθμού εντός αγκύλης δίπλα στην αναφορά ενός αποσπάσματος ή ιδέας μέσα στη ροή του κειμένου. Οι αριθμητικοί εκθέτες με τα πλήρη στοιχεία του έργου προς αναφορά βρίσκονται στο τέλος της σελίδας (υποσελίδιες παραπομπές–footnotes) ή στο τέλος του κειμένου (endnotes).

   β. Η παρενθετική αναφορά καταγράφει τα βασικά στοιχεία της πηγής αναφοράς (συγγραφέας - έτος έκδοσης ή συγγραφέας - σελίδες) στο σημείο του αποσπάσματος ή της αναφοράς εντός του κειμένου.

   Αν πρόκειται για άρθρο σε επιστημονικό περιοδικό / συνέδριο, υπάρχει πάντα σαφής οδηγία για το πώς πρέπει να αποτυπώνονται οι αναφορές. Σε γενικές γραμμές, χωρίς αυτό να αποτελεί απόλυτο κανόνα, στα αντικείμενα μηχανικού και θετικών επιστημών η αναφορά γίνεται με εκθέτη ή αγκύλη, ενώ για θεωρητικά αντικείμενα προτιμάται η παρενθετική αναφορά.

2. Η Βιβλιογραφία αποτελεί ξεχωριστό τμήμα της εργασίας, βρίσκεται στο τέλος της και περιλαμβάνει το σύνολο των έργων ή πηγών που συμβουλεύτηκε ο συγγραφέας ασχέτως αν έχει κάνει αναφορά σε αυτά μέσα στη ροή του κειμένου του. Στην ελληνική γλώσσα και συγγραφική πρακτική χρησιμοποιούμε γενικά τον όρο «Βιβλιογραφία» χωρίς να διακρίνουμε ανάμεσα σε Βιβλιογραφικές Παραπομπές (Reference List/Works Cited) και Βιβλιογραφία (Bibliography) όπως γίνεται στο εξωτερικό. Σύμφωνα με αυτή τη διάκριση οι Βιβλιογραφικές Παραπομπές περιέχουν μόνο το υλικό που έχει αναφερθεί με παρενθετικές ή αριθμητικές αναφορές εντός κειμένου ενώ η Βιβλιογραφία περιέχει όλες τις πηγές που έχει χρησιμοποιήσει ο συγγραφέας για να διαμορφώσει άποψη για το θέμα του και να στηρίξει τα επιχειρήματά του. Τα διάφορα πρότυπα σύνταξης βιβλιογραφικών

αναφορών ακολουθούν διαφορετική πρακτική στο θέμα αυτό και αντίστοιχα χρησιμοποιούν διαφορετική ορολογία. Αν π.χ. πρόκειται για πτυχιακή εργασία, κάθε φοιτητής/τρια, σε συνεργασία με τον επιβλέποντα καθηγητή, μπορεί να επιλέξει το πρότυπο που ταιριάζει στις απαιτήσεις της εργασίας του εάν αυτό δεν προσδιορίζεται σαφώς από τις οδηγίες συγγραφής πτυχιακών εργασιών που ισχύουν για το συγκεκριμένο τμήμα / ίδρυμα.

2.6. Γιατί πρέπει να αναφέρουμε τη βιβλιογραφία σε μια εργασία

Οι βιβλιογραφικές αναφορές είναι απαραίτητο στοιχείο κάθε ακαδημαϊκού κειμένου, ερευνητικού ή επιστημονικού συγγράμματος, για να μπορεί ο αναγνώστης να εντοπίσει τις πηγές αν το κρίνει απαραίτητο και να σιγουρευτεί ότι οι πληροφορίες είναι ακριβείς. Χρησιμοποιούνται για να δηλώσουν τις πηγές από τις οποίες ο συγγραφέας άντλησε πληροφορίες και στοιχεία που χρησιμοποιεί στο έργο του. Οι πηγές δείχνουν σεβασμό προς τα πνευματικά δικαιώματα του δημιουργού, ενώ ταυτόχρονα ενισχύουν και την αξιοπιστία του συγγράμματος. Επιπρόσθετα όταν χρησιμοποιούμε στοιχεία από άλλα συγγράμματα χωρίς να αναφέρουμε την πηγή, πράττουμε λογοκλοπή.

2.7. Πώς συντάσσουμε την βιβλιογραφία σε μια πτυχιακή εργασία

Η σύνταξη της βιβλιογραφίας δεν γίνεται τυχαία, αλλά ακολουθεί κάποιους κανόνες δομής. Πιο συγκεκριμένα γράφουμε πρώτα την ξένη βιβλιογραφία και μετά την ελληνική που χρησιμοποιήθηκε. Στη συνέχεια ακολουθούν τα βιβλία με αλφαβητική σειρά και με βάση το επώνυμο του συγγραφέα. Αν ένα βιβλίο δεν ανήκει σε κάποιο συγκεκριμένο συγγραφέα στη θέση του επωνύμου του συγγραφέα και σε παρένθεση γράφουμε χωρίς συγγραφέα. Τέλος, ακολουθούν, πάλι σε αλφαβητική σειρά, τα βιβλία με βάση τον τίτλο του βιβλίου. Πιο συγκεκριμένα πρέπει να αναγράφονται:

A. Για βιβλία:
- Το όνομα του συγγραφέα: επώνυμο, αρχικό του ονόματος
- Ο χρόνος έκδοσης (σε παρένθεση)

- Ο τίτλος του βιβλίου (συνηθίζεται να τον υπογραμμίζουμε ή να τον γράφουμε με έντονους χαρακτήρες «Bold» ή με πλάγιους χαρακτήρες «Italics»).
- Ο τόπος έκδοσης
- Ο εκδοτικός οίκος.

Τα δύο τελευταία μπορούν να αλλάξουν σειρά. Να προσέξουμε εδώ ότι: Μετά από το επώνυμο του συγγραφέα ακολουθεί κόμμα και μετά το όνομα ή το αρχικό του ονόματός του, τελεία.

Β. Για εγκυκλοπαίδειες:
- Ο χρόνος έκδοσης
- Ο τίτλος της εγκυκλοπαίδειας
- Ο τόπος έκδοσης και ο εκδοτικός οίκος
- Ο αριθμός του τόμου
- Ο αριθμός των σελίδων

Γ. Για άρθρα περιοδικών:
- Το ονοματεπώνυμο του συγγραφέα
- Ο χρόνος έκδοσης
- Ο τίτλος του άρθρου
- Το όνομα του περιοδικού
- Ο μήνας, ο τόμος, ο αριθμός του τεύχους
- Ο αριθμός των σελίδων

Δ. Άρθρα εφημερίδας:
- Το ονοματεπώνυμο του συγγραφέα
- Ο χρόνος έκδοσης
- Ο τίτλος του άρθρου
- Το όνομα της εφημερίδας
- Η ημέρα και ο μήνας δημοσίευσης του τεύχους
- Ο αριθμός της σελίδας

E. Βίντεο:

- Ο τίτλος
- Ο χρόνος έκδοσης
- Οι εκδόσεις
- Ο τόπος έκδοσης

ΣΤ. CD –ROMs:

- Ο τίτλος
- Ο χρόνος έκδοσης

Z. Διαδίκτυο (Internet):

- Το όνομα του συγγραφέα ή του φορέα
- Ο χρόνος δημοσίευσης
- Ο τίτλος
- Η διεύθυνση της ιστοσελίδας
- Ο τόπος έκδοσης
- Η ημερομηνία προσπέλασης

H. Ηλεκτρονικό ταχυδρομείο:

- Το όνομα του συγγραφέα ή του φορέα
- Ο χρόνος συγγραφής
- Ο τίτλος, το θέμα
- Η διεύθυνση e-mail του συντάκτη
- Η ημερομηνία

Θ. Συνεντεύξεις:

- Το όνομα αυτού/αυτής που έδωσε συνέντευξη
- Η χρονική περίοδος ή η ημερομηνία που πάρθηκε η συνέντευξη
- Η ιδιότητα/θέση αυτού/αυτής που δίνει τη συνέντευξη
- Ο τίτλος / το θέμα

I. Φυλλάδια, μπροσούρες:

- Ο τίτλος

- Ο χρόνος έκδοσης

- Ο εκδότης

- Ο τόπος έκδοσης

2.8. Σκοπός της βιβλιογραφίας σε μια πτυχιακή εργασία

Πρωταρχικό ρόλο στη συγγραφή μια πτυχιακής εργασίας παίζει η αναζήτηση της σχετικής βιβλιογραφίας. Η βιβλιογραφική επισκόπηση για ένα συγκεκριμένο θέμα συνήθως δεν είναι εύκολη διαδικασία, απαιτεί τέχνη, αφαιρετική ικανότητα και μέθοδο. Απαιτεί επίσης κόπο γατί ο φοιτητής θα πρέπει να επισκεφτεί βιβλιοθήκες και να αφιερώσει χρόνο στην αναζήτηση και στη συγκέντρωση του υλικού.

Στόχος της βιβλιογραφικής ανασκόπησης είναι κατά κύριο λόγο να βοηθήσει το φοιτητή να οργανώσει τις σκέψεις του, να ταξινομήσει τα κύρια ζητήματα που θέλει να εξετάσει αλλά και να θέσει τους στόχους της ερευνάς του. Πιο συγκεκριμένα, η αναζήτηση της βιβλιογραφίας διεξάγεται στην αρχή της εκπόνησης μιας πτυχιακής εργασίας και αποτελεί μια οργανωμένη καταγραφή:

α) της ερευνητικής περιοχής που εξετάζεται

β) των κρίσιμων ζητημάτων που σχετίζονται με αυτή και

γ) των μεθόδων αντιμετώπισης τυχόν προβλημάτων που μπορεί να παρουσιαστούν

Η οργάνωση και η καταγραφή της βιβλιογραφίας είναι διαδικασίες που διεξάγονται παράλληλα με την ανάγνωση των βιβλίων ή των άρθρων. Είναι σημαντικό κατά την ανάγνωση των βιβλιογραφικών πηγών ο φοιτητής να σημειώνει κάπου ή να αποτυπώνει μέσα στο κείμενο την περίληψή τους αμέσως μετά την ανάγνωση και αυτομάτως να αναδιοργανώνει στο μυαλό του την εικόνα της ευρύτερης ερευνητικής περιοχής.

Η βιβλιογραφία έχει σκοπό να παρουσιάσει στον αναγνώστη με δομημένο τρόπο την οργάνωση της περιοχής που διερευνά και πιο συγκεκριμένα να παρουσιάσει:

- τα γενικά χαρακτηριστικά του ευρύτερου προβλήματος που διερευνά

- τις σχετικές υποπεριοχές του ζητήματος

- την εικόνα της ερευνητικής προσπάθειας μέχρι στιγμής στην παγκόσμια βιβλιογραφία

- τα ζητήματα που μένουν ανοιχτά προς διερεύνηση

2.9. Πρότυπα βιβλιογραφικών αναφορών

Σε παγκόσμιο επίπεδο, έχουν αναπτυχθεί διάφορα συστήματα βιβλιογραφικών αναφορών για την απόδοση, σύμφωνα με την απαιτούμενη μορφή, των πηγών που χρησιμοποιήθηκαν για τη συγγραφή μιας εργασίας, τα οποία διαφέρουν ως προς τον τρόπο με τον οποίο δομείται και παρουσιάζεται η βιβλιογραφική πληροφορία. Όλα αυτά τα πρότυπα βιβλιογραφικών αναφορών, ενώ παρέχουν τις ίδιες πληροφορίες, δηλαδή όνομα συγγραφέα, τίτλο, τόπο έκδοσης και εκδότη, το καθένα έχει τις δικές του ιδιαίτερες απαιτήσεις. Φυσικά, θα πρέπει να χρησιμοποιείται ένα μόνο πρότυπο τη φορά. Ο τρόπος με τον οποίο γίνονται οι αναφορές των έργων από τα οποία άντλησε πληροφορίες ο συγγραφέας καθορίζεται από συστήματα ή στυλ που έχουν αναπτυχθεί διεθνώς από πανεπιστήμια, ενώσεις ή οργανισμούς και προέκυψαν από τις ανάγκες τεκμηρίωσης διαφόρων επιστημονικών πεδίων. Ορισμένα από τα πιο γνωστά και ευρέως διαδεδομένα είναι τα:

I) APA Style:

Το πρότυπο APA πήρε το όνομά του από τον Αμερικανικό Οργανισμό Ψυχολογίας (American Psychological Association) και χρονολογείται από τα τέλη της δεκαετίας του 1920, όταν μια ομάδα ακαδημαϊκών, της οποίας τα μέλη προέρχονταν από τα πεδία της Ψυχολογίας, της Ανθρωπολογίας και της Διοίκησης Επιχειρήσεων, συναντήθηκε με σκοπό τη δημιουργία ενός συστήματος βιβλιογραφικής αναφοράς. Σήμερα το συγκεκριμένο πρότυπο χρησιμοποιείται σε διάφορα επιστημονικά πεδία, κυρίως σε αυτό των Κοινωνικών Επιστημών.

Παραπομπές:

Οι παραπομπές στο κείμενο γίνονται σε όλα τα παρενθετικά πρότυπα με την τοποθέτηση του επιθέτου του συγγραφέα και της χρονιάς δημοσίευσης του έργου.

Βιβλιογραφία:

- Η βιβλιογραφία εισάγεται με τον τίτλο References κεντραρισμένο
- Οι αναφορές παρατίθενται αλφαβητικά με βάση το όνομα του πρώτου συγγραφέα και αριστερή στοίχιση και εισάγονται με εξοχή πρώτης γραμμής (hanging indent)
- Απαιτείται διπλό διάστιχο
- Περισσότερα έργα του ίδιου συγγραφέα αναφέρονται διαδοχικά με αύξουσα χρονολογική σειρά

II) MLA (Modern Language Association) Style:

Η μέθοδος MLA (Modern Language Association) δημιουργήθηκε στις ΗΠΑ το 1883 ως μια επαγγελματική ένωση για ακαδημαϊκούς των επιστημονικών πεδίων της Λογοτεχνίας και της Γλώσσας. Η δε 1η έκδοση οδηγού εκδόθηκε μόλις το 1977. Σήμερα χρησιμοποιείται η 7η έκδοση.

- Η βιβλιογραφία εισάγεται με κεντραρισμένο τον τίτλο Works Cited
- Οι αναφορές παρατίθενται αλφαβητικά με βάση το όνομα του πρώτου συγγραφέα
- Η στοίχιση είναι αριστερή
- Μεσολαβεί διπλό διάστιχο.
- Οι αναφορές εισάγονται με εξοχή πρώτης γραμμής (hanging indent).
- Σε όλες τις αναφορές έντυπες ή ηλεκτρονικές αναγράφεται ο τύπος του μέσου.
- Δεν απαιτούνται οι ηλεκτρονικές διευθύνσεις. Συστήνεται η χρήση της ηλεκτρονικής διεύθυνσης μόνο σε περίπτωση που η πηγή δε μπορεί να βρεθεί κάπου αλλού ή το απαιτεί ο καθηγητής.
- Για περισσότερα έργα του ίδιου συγγραφέα δίνεται το όνομα μόνο στην πρώτη αναφορά και στις επόμενες αντικαθίσταται από (---.). Τα έργα παρατίθενται αλφαβητικά με τον τίτλο.

III) Chicago Style:

Το Chicago Manual of Style παρέχει οδηγίες και συμβουλές όχι μόνο για τη σύνταξη αναφορών και βιβλιογραφίας, αλλά γενικά για τη μορφοποίηση και έκδοση επιστημονικών εργασιών και θεωρείται η βάση προτυποποίησης της ερευνητικής μεθοδολογίας στις ΗΠΑ. Στην πραγματικότητα αναφέρεται σε δύο διακριτά στυλ αναφορών:

Α) Το στυλ που εφαρμόζεται στις ανθρωπιστικές επιστήμες, ιστορία και τέχνες και παρέχει οδηγίες για τη σύνταξη των υποσημειώσεων και της βιβλιογραφίας (Notes/Bibliography system). Η αναφορά των πηγών με το στυλ Notes/Bibliography απαιτεί:

1. Έναν αριθμητικό δείκτη στη ροή του κειμένου και την αντίστοιχη σημείωση στο κάτω μέρος της σελίδας (footnote) ή στο τέλος της ενότητας (endnote).
2. Μια βιβλιογραφία (bibliography).

B) Το στυλ που εφαρμόζεται στις φυσικές και κοινωνικές επιστήμες και παρέχει οδηγίες για τη σύνταξη των παρενθετικών αναφορών της μορφής «Συγγραφέας – Ημερομηνία έκδοσης» (Author-Date system) και της λίστας των Βιβλιογραφικών Παραπομπών (reference list). Η αναφορά των πηγών με το στυλ Author-Date απαιτεί:

1. Μια παρενθετική αναφορά (in-text citation), που υποδεικνύει στον αναγνώστη ότι τα πλήρη στοιχεία της πηγής υπάρχουν στη λίστα των Βιβλιογραφικών Παραπομπών στο τέλος της εργασίας.
2. Μια λίστα Βιβλιογραφικών Παραπομπών (Reference list).

IV) Harvard Style:

Τα περισσότερα πρότυπα αναφοράς βασίζονται σε εγχειρίδια τα οποία εκδόθηκαν από ακαδημαϊκές ενώσεις ή εκδοτικές εταιρίες. Κάτι τέτοιο δεν ισχύει στην περίπτωση Harvard και συνεπώς υπάρχουν αρκετές εκδόσεις της συγκεκριμένης μεθόδου. Για το λόγο αυτό θα πρέπει να υπάρχει συνέπεια στον τρόπο παράθεσης της βιβλιογραφίας από το συγγραφέα εφόσον επιλέγει τη συγκεκριμένη μέθοδο.

- Οι αναφορές παρατίθενται αλφαβητικά με βάση το όνομα του πρώτου συγγραφέα.
- Η στοίχιση που ακολουθείται είναι αριστερή.
- Οι τίτλοι των βιβλίων παρατίθενται ολογράφως με πλάγια γράμματα.
- Μεσολαβεί διπλό διάστιχο μεταξύ των αναφορών και μονό διάστιχο στα πλαίσια της ίδιας αναφοράς εφόσον αυτή καταλαμβάνει πάνω από μία γραμμή.
- Περισσότερα έργα του ίδιου συγγραφέα αναφέρονται διαδοχικά και εδώ με αύξουσα χρονολογική σειρά.

V) NLM (National Library of Medicine) Style:

Η μέθοδος αυτή χρησιμοποιείται κατά κύριο λόγο στα επιστημονικά πεδία της Ιατρικής και της Κινησιολογίας. Ο τρόπος χρήσης της ποικίλει τόσο ως προς τον τρόπο παράθεσης πηγών μέσα στο κείμενο όσο και στη βιβλιογραφία. Κατά κύριο λόγο χρησιμοποιείται ο online οδηγός "Citing Medicine: The NLM Style Guide for Authors, Editors, and Publishers, 2nd edition".

Παραπομπές:

Οι παραπομπές στο κείμενο στα αριθμητικά πρότυπα γίνονται με αρίθμηση 1, 2, 3... είτε με αγκύλες είτε με τη χρήση εκθετών.

Βιβλιογραφία:

- Ο τίτλος μπορεί να εμφανίζεται ως: References, Literature Cited, Bibliography.
- Γίνεται χρήση αρίθμησης για κάθε αναφορά.
- Οι αναφορές στη βιβλιογραφία παρατίθενται με τη σειρά που εμφανίζονται στο κείμενο.

VI) IEEE (Institute of Electrical and Electronics Engineers)

Τον ολοκληρωμένο οδηγό μπορεί κανείς να τον βρει από την ιστοσελίδα της IEEE. Όσον αφορά τη βιβλιογραφία:

- Κάθε αναφορά ταυτοποιείται με συγκεκριμένο αριθμό που εσωκλείεται σε αγκύλες.
- Οι αριθμοί στοιχίζονται αριστερά σε στήλη.
- Ακολουθούν οι αναφορές με μονό διάστιχο οι οποίες στοιχίζονται αριστερά σχηματίζοντας δική τους στήλη δίπλα σε αυτή με τους αριθμούς.
- Οι αναφορές στη βιβλιογραφία παρατίθενται με τη σειρά που εμφανίζονται στο κείμενο.

ΚΕΦΑΛΑΙΟ 3

ΤΟ ΛΟΓΙΣΜΙΚΟ MENDELEY REFERENCE MANAGER ΩΣ Η ΒΕΛΤΙΣΤΗ ΕΠΙΛΟΓΗ ΓΙΑ ΤΗΝ ΟΡΓΑΝΩΣΗ ΒΙΒΛΙΟΓΡΑΦΙΑΣ

3.1. Εισαγωγικά

Η διαχείριση των βιβλιογραφικών αναφορών είναι μία από τις πιο περίπλοκες πτυχές που καλείται να αντιμετωπίσει ένας ερευνητής κατά την διάρκεια της συγγραφής οποιασδήποτε εργασίας, είτε προορίζεται για δημοσίευση είτε για εσωτερική διακίνηση. Η ολοένα και αυξανόμενη αναγνώριση της σημασίας της πνευματικής ιδιοκτησίας, της επιστημονικής ακεραιότητας και της δεοντολογίας στην ακαδημαϊκή κοινότητα, καθώς και οι τεράστιες ποσότητες πληροφοριών που μπορούν πλέον να μεταφέρονται ηλεκτρονικά, οδηγούν τους χρήστες στο να στέλνουν, να αντιγράφουν, να οργανώνουν και να διαχειρίζονται πληροφορίες και κείμενα δημιουργώντας νέες δικές τους αναφορές. Επιπλέον, υπάρχει μια ολοένα αυξανόμενη ανάγκη των ερευνητών να δημοσιεύουν τα ερευνητικά τους αποτελέσματα, καθώς με γνώμονα αυτά αξιολογείται το ερευνητικό έργο τους και καθορίζεται η ακαδημαϊκή εξέλιξή τους μέσα από την απήχηση των δημοσιεύσεων τους. Καθίσταται έτσι αναγκαία η εκπαίδευση των χρηστών στη χρήση σύγχρονων εργαλείων διαχείρισης αναφορών. Τα εργαλεία βιβλιογραφικής διαχείρισης χρησιμοποιούνται ευρέως από τους ερευνητές για την αποθήκευση, οργάνωση και διαχείριση των αναφορών για ερευνητικές εργασίες, διατριβές, άρθρα περιοδικών και άλλες δημοσιεύσεις. Πρόκειται για εργαλεία που μας βοηθούν να εντοπίσουμε βιβλιογραφία, να αποθηκεύσουμε απευθείας από δικτυακές βάσεις δεδομένων και ιστότοπους και να οργανώσουμε σε προσωπική βάση δεδομένων βιβλιογραφικές αναφορές, να ενσωματώσουμε αναφορές στις εργασίες μας, να δημιουργήσουμε βιβλιογραφίες και να τις μορφοποιήσουμε επιλέγοντας το ανάλογο στυλ εμφάνισης για την τελική δημοσίευση.

3.2. Λογισμικά διαχείρισης βιβλιογραφικών αναφορών

Η ορθή διαχείριση των βιβλιογραφικών αναφορών επιτρέπει σε έναν ερευνητή να βελτιώνει τη συγγραφή των εργασιών του, να εναρμονίζεται με τις οδηγίες των μέσων δημοσίευσης και να αναδεικνύει δεξιότητες κριτικής σκέψης. Επίσης, οι βιβλιογραφικές αναφορές αποτελούν ένα μέσο διάδοσης και αξιολόγησης της επιστημονικής παραγωγής. Συνεπώς είναι απαραίτητο για την απόδειξη της ποιότητας και την αναγνώριση μιας εργασίας να αναφέρονται οι πηγές που έχουν χρησιμοποιηθεί.

Οι βιβλιογραφικές αναφορές θα πρέπει να γίνονται οποτεδήποτε γίνεται αναφορά σε ιδέες, απόψεις, τοποθετήσεις ή κάθε άλλη έκφραση σκέψης και δημιουργίας άλλου μέσα σε ένα κείμενο. Ακόμη και αν δεν αναπαράγεται άμεσα ένα ξένο δημιούργημα, αλλά μια άποψη βασίζεται ή ακόμη κι αν αντιπαρατίθεται σε άλλες απόψεις, θα πρέπει να γίνεται σε αυτές η αντίστοιχή μνεία για το σκοπό της διαφύλαξης της επιστημονικής ακεραιότητας.

Για το λόγο αυτό υπάρχουν διάφορα εργαλεία βιβλιογραφικής διαχείρισης για την καλύτερη οργάνωση της βιβλιογραφικής πληροφορίας, ώστε αυτή να είναι δομημένη και επαναχρησιμοποιήσιμη. Τα προγράμματα διαχείρισης βιβλιογραφικών αναφορών (Reference Management Software) βοηθούν στη δημιουργία, καταγραφή και χρήση των βιβλιογραφικών αναφορών, ενώ ορισμένα επιτρέπουν την αναζήτηση και διασύνδεση δημοσιεύσεων, ώστε τελικά να αυξάνουν την παραγωγικότητα των συγγραφέων. Μπορεί να είναι online, τοπικά εγκατεστημένα ή και τα δύο συγχρόνως ενώ κάποια είναι εμπορικά (Refworks, EndNote) και κάποια ελεύθερα (Mendeley, Zotero, Colwiz). Υπάρχουν επίσης ιστοσελίδες που περιέχουν εργαλεία σύνταξης βιβλιογραφίας για άμεση χρήση (Citation Machine, Cite This Forme, Easy Bib, κ.ά.).

Τα εργαλεία διαχείρισης βιβλιογραφικών αναφορών παρέχουν τις ακόλουθες δυνατότητες:

- Εισαγωγή βιβλιογραφικών αναφορών απευθείας από δικτυακές βάσεις δεδομένων και ιστότοπους σε προσωπική βάση δεδομένων.
- Δημιουργία και οργάνωση της βιβλιογραφίας σε προσωπική βάση δεδομένων.
- Μορφοποίηση των βιβλιογραφικών αναφορών (MLA, APA, Chicago Style, κ.α.).
- Δημιουργία βιβλιογραφίας σε επιστημονικά συγγράμματα, άρθρα, εργασίες κλπ
- Αναζήτηση, αποθήκευση και οργάνωση αρχείων που αφορούν την έρευνα σε οποιαδήποτε μορφή (.pdf, .doc, .txt κλπ).

Τα λογισμικά διαχείρισης βιβλιογραφικών αναφορών είναι εφαρμογές που επιτρέπουν τη δημιουργία, διαχείριση και χρήση βιβλιογραφικών αναφορών, ώστε να αυξήσουν την παραγωγικότητα των συγγραφέων και των ερευνητών. Τα περισσότερα από αυτά έχουν την δυνατότητα να εισάγουν πληροφορία σύμφωνα με κάποια φίλτρα και να την μετατρέπουν στον επιθυμητό τύπο. Στο διαδίκτυο υπάρχουν πολλά τέτοια λογισμικά τα οποία είτε είναι συνδρομητικά είτε ελεύθερα προσβάσιμα για χρήση. Μερικά από αυτά τα ελεύθερα λογισμικά αναφέρονται παρακάτω:

1. MENDELEY:

Το Mendeley είναι μία ελεύθερη, desktop και web λύση, σχεδιασμένη για τη διαχείριση και το διαμοιρασμό ερευνητικών εργασιών, την ανάκτηση εγγράφων και δεδομένων έρευνας και την online συνεργασία. Συνδυάζει το Mendeley Desktop και μια εφαρμογή διαχείρισης PDF εγγράφων και αναφορών (διαθέσιμο για Windows, Mac και Linux) με το Mendeley Web, να είναι ένα online εργαλείο διαχείρισης ερευνητικών εργασιών και ένα κοινωνικό δίκτυο για ερευνητές. Το Mendeley είναι ένα λογισμικό ακαδημαϊκής χρήσης, το οποίο ευρετηριάζει και οργανώνει όλα τα έγγραφα σε μορφή PDF καθώς και τις ερευνητικές εργασίες της προσωπικής ψηφιακής βιβλιογραφίας. Συλλέγει όλες τις απαραίτητες πληροφορίες εγγράφων από το .pdf αρχεία επιτρέποντας έτσι την αναζήτηση, την οργάνωση και την παραπομπή πάνω σε αυτά.

Επιτρέπει αυτόματα επίσης την αναζήτηση σε PubMed, CrossRef, DOIs καθώς και σε άλλες πληροφορίες σχετικών εγγράφων. Η λειτουργία drag and drop μετατρέπει τη λειτουργία συλλογής και οργάνωσης δεδομένων εύκολη και γρήγορη. Ο εισαγωγέας Ιστού επιτρέπει γρήγορα και εύκολα την εισαγωγή εγγράφων από πηγές όπως το Google Scholar, την ACM, την IEEE και πολλές άλλες με το πάτημα απλά ενός κουμπιού.

Το λογισμικό απαιτεί τοπική εγκατάσταση σε ηλεκτρονικό υπολογιστή, ενώ λειτουργεί παράλληλα με Microsoft Office για τη δημιουργία παραπομπών σε διαφορετικά στυλ βιβλιογραφίας.

Εικόνα 2.5: Λογότυπο MENDELEY

2. ZOTERO:

Το Zotero είναι μια δωρεάν, ανοικτού κώδικα εφαρμογή/λογισμικό, το οποίο επιτρέπει στους χρήστες του να διαχειρίζονται βιβλιογραφικά δεδομένα και να αποθηκεύουν στιγμιότυπα οθόνης (snapshots) από ιστοσελίδες ή άλλα ηλεκτρονικά τεκμήρια. Επίσης δίνεται η δυνατότητα στους χρήστες του να δημιουργούν χειροκίνητα τη δική τους προσωπική βιβλιογραφική βάση δεδομένων με την εισαγωγή βιβλιογραφικών αναφορών απευθείας από άλλες βιβλιογραφικές βάσεις δεδομένων. Μέσα από μια ξεχωριστή του λειτουργία, επιτρέπει την αναφορά - παραπομπή σε κείμενο, κατά τη σύνταξη δοκιμίων και άρθρων (Microsoft Word και OpenOffice.org Writer), δημιουργώντας παράλληλα βιβλιογραφικές λίστες σε διάφορα στυλ (όπως το APA και η MLA).

Σε πολλές ερευνητικές ιστοσελίδες, όπως για παράδειγμα οι ψηφιακές βιβλιοθήκες, PubMed, Google Scholar, Google Books, Amazon.com και Βικιπαίδεια, το Zotero μπορεί να εντοπίσει ένα βιβλίο ή ένα άρθρο και με ένα κλικ να βρει και να σώσει την πλήρη βιβλιογραφική αναφορά σε ένα τοπικό αρχείο. Εάν η πηγή είναι ένα online άρθρο ή ιστοσελίδα, το Zotero μπορεί να αποθηκεύσει προαιρετικά ένα τοπικό αντίγραφο, ενώ οι χρήστες μπορούν στη συνέχεια να προσθέσουν πάνω σε αυτό σημειώσεις, ετικέτες, και δικά τους μεταδεδομένα. Οι επιλογές των τοπικών δεδομένων βιβλιογραφικής αναφοράς μπορούν στη συνέχεια να εξαχθούν σε μορφοποιημένες βιβλιογραφίες. Επιπλέον, όλες οι εγγραφές συμπεριλαμβανομένων όλων των βιβλιογραφικών πληροφοριών που δημιουργούνται από το χρήστη, μπορούν να συνοψιστούν σε μια έκθεση HTML.

Εικόνα 2.6: Λογότυπο ZOTERO

3. CiteULike:

Το CiteULike είναι μια δωρεάν υπηρεσία που βοηθά στην αποθήκευση και οργάνωση επιστημονικών εργασιών. Βλέποντας κάποιος ένα έγγραφο στο διαδίκτυο που είναι ενδιαφέρον, μέσα από ένα κλικ μπορεί να το προσθέσει στην προσωπική του βιβλιοθήκη. Το CiteULike εξάγει αυτόματα τα στοιχεία των παραπομπών στην προσωπική βιβλιοθήκη και έτσι δεν υπάρχει καμία ανάγκη να γίνεται ξανά η πληκτρολόγηση. Λειτουργούν όλα μέσα από το φυλλομετρητή, έτσι δεν υπάρχει καμία ανάγκη να εγκατασταθεί οποιοδήποτε λογισμικό, επειδή η βιβλιοθήκη είναι αποθηκευμένη σε διακομιστή (server) και μπορεί να υπάρχει πρόσβαση σε αυτή ανά πάσα στιγμή από οποιονδήποτε υπολογιστή με σύνδεση στο διαδίκτυο.

Εικόνα 2.7: Λογότυπο CITE U LIKE

4. COLWIZ

Το Colwiz είναι μια δωρεάν web εφαρμογή για desktop και κινητά με βάση ένα λογισμικό διαχείρισης της έρευνας, που σχεδιάστηκε από ερευνητές στο Πανεπιστήμιο της Οξφόρδης. Το Colwiz περιλαμβάνει εργαλεία διαχείρισης αναφοράς, συνεργασίας και δικτύωσης. Η βιβλιοθήκη Colwiz είναι μια εφαρμογή που επιτρέπει στους χρήστες να βρίσκουν, να διαβάζουν, να σχολιάζουν, να αποθηκεύουν και να μοιράζονται ερευνητικά άρθρα. Τα άρθρα μπορούν να αρχειοθετηθούν στη βιβλιοθήκη σε προσαρμόσιμους φακέλους. Ο οδηγός Colwiz Import Wizard μπορεί να προσθέσει αυτόματα δημοσιεύσεις στη βιβλιοθήκη Colwiz από άλλες κοινές βιβλιοθήκες αναφοράς (συμπεριλαμβανομένης της αναφοράς μόνο από το End Note, ενώ αναφορές και PDF από Mendeley και Zotero) ή μεμονωμένα από φακέλους, υποστηρίζοντας διάφορες μορφές αρχείων (π.χ. Bib TeX, PDF και RIS). Νέα ερευνητικά άρθρα μπορούν να βρεθούν με την ενσωματωμένη μηχανή αναζήτησης, η οποία παρέχει στους χρήστες άμεση πρόσβαση σε αναφορές από περισσότερες από 30 διαφορετικές βάσεις δεδομένων και αποθετήρια αρχείων. Οι χρήστες μπορούν να προσθέσουν σημειώσεις, συνδέσμους, άρθρα και άλλα υποστηρικτικά αρχεία σε κάθε αναφορά στη βιβλιοθήκη Colwiz. Ακόμα, επιτρέπει στους χρήστες να λαμβάνουν σημειώσεις και να επισημαίνουν το άρθρο απευθείας στο PDF, κάνοντας τέτοιου είδους σχολιασμούς με δυνατότητα κοινοποίησης και αναζήτησης. Ο δωρεάν λογαριασμός επιτρέπει στους χρήστες να προσθέσουν 5.000 καταχωρίσεις αναφοράς και 2 GB δωρεάν χώρο αποθήκευσης για αρχεία PDF.

Εικόνα 2.8: Λογότυπο COLWIZ

3.3. Επιλογή εργαλείου διαχείρισης αναφορών

Υπάρχουν λοιπόν διάφορα, ελεύθερα διαθέσιμα, εργαλεία διαχείρισης των βιβλιογραφικών αναφορών. Για να γίνει η επιλογή του κατάλληλου εργαλείου που ταιριάζει στις ανάγκες μας θα πρέπει να λάβουμε υπόψη τα ακόλουθα:

α)   Τον τρόπο πρόσβασης, ο οποίος μπορεί να είναι από επιτραπέζιο υπολογιστή μέχρι και φορητές συσκευές, αν απαιτείται εγκατάσταση λογισμικού, τη συμβατότητα με το λειτουργικό σύστημα που έχουμε και αν έχει δυνατότητα συγχρονισμού μέσω cloud, για την πρόσβαση στην εφαρμογή από διάφορες συσκευές (υπολογιστή, κινητό, tablet).

β)   Το αν η εφαρμογή είναι συμβατή με το σύνολο του περιεχομένου που θέλουμε να αποθηκεύσουμε και να διαχειριστούμε, όπως βιβλιογραφικές αναφορές (κείμενο με ειδικό φορμά), αρχεία με πλήρες κείμενο, εικόνες, αρχεία ήχου, στιγμιότυπα οθόνης κλπ.

γ)   Τη δυνατότητα εισαγωγής αναφορών με τρόπο αυτόματο ή διά χειρός, την αυτόματη εισαγωγή βιβλιογραφικών λεπτομερειών από καταλόγους βιβλιοθηκών, βάσεις δεδομένων, ιστότοπους κλπ.

δ)   Πού θα γίνεται η αποθήκευση των αναφορών. Πόσος δωρεάν αποθηκευτικός χώρος είναι διαθέσιμος online, πόσο κοστίζει ο επιπλέον χώρος.

ε)   Τον τρόπο οργάνωσης των αναφορών σε συλλογές και υποσυλλογές, τη χρήση ετικετών, το φιλτράρισμα, την αναζήτηση στο σώμα του κειμένου.

στ) Αν προσφέρει δυνατότητες κοινωνικής δικτύωσης των ερευνητών με την δημιουργία και την συμμετοχή σε ομάδες και διαμοιρασμού αναφορών και εγγράφων.

ζ)   Αν διαθέτει πρόσθετο παραπομπής για επεξεργαστή κειμένου που βοηθά στη δημιουργία παραπομπών σε κείμενο και παράγει αυτόματα βιβλιογραφία, αν είναι συμβατό με τον επεξεργαστή κειμένου που χρησιμοποιείται, καθώς και ποια είναι τα στυλ αναφοράς που υποστηρίζει.

η)   Τη βιωσιμότητα της εφαρμογής και την υποστήριξή της από τους δημιουργούς της. Δεν υπάρχει εγγύηση ότι ένα εργαλείο ελεύθερου λογισμικού θα είναι πάντα διαθέσιμο.

θ)   Τέλος θα πρέπει να ελέγξουμε αν είναι συμβατό με άλλα εργαλεία διαχείρισης και βέβαια, αν είναι εύκολο στη χρήση του και αν παρέχει υποστηρικτικό υλικό.

Στο διαδίκτυο υπάρχουν πολλοί συγκριτικοί πίνακες που μπορούμε να συμβουλευτούμε προκειμένου να επιλέξουμε το λογισμικό που ταιριάζει στις ανάγκες μας. Παρακάτω (Εικ. 3.1) παρατίθεται ένας πίνακας ο οποίος παρουσιάζει διάφορα λογισμικά που κυκλοφορούν

στην αγορά, είτε δωρεάν είτε με χρέωση, καθώς και τη συμβατότητά τους με τα ποικίλα λειτουργικά συστήματα (Windows, OSX, Linux, iOS, Android).

Software	Developer	First public release	Latest stable release date	Latest stable version	Cost (USD)	Free software	License	Notes
RefME	RefME	2014	Shut down in 2017		Free	No	Proprietary	Web, iOS and Android; Chrome and Safari Extensions available; discontinued
RefWorks	Ex Libris / ProQuest	2001	2018	3	Institutional subscription	No	Proprietary	web-based, browser-accessed, Word & Google Docs
refbase	refbase developers	2003-06-03	2014-02-28	0.9.6	Free	Yes	GNU GPL	web-based for institutional repositories/self-archiving[9]
Bebop	ALaRI Institute	2007-11-08	2009-11-10	1.1	Free	Yes	BSD	web-based BibTeX front-end (Apache, PHP, MySQL)
Wikindx	Mark Grimshaw	2004-02	2021-05-19	6.4.8	Free	Yes	ISC license	web-based
Paperpile	Stefan Washietl, Gregorgy Jordan, Andreas Gruber	2013	Continually updated online		US$2.99/month for academics, 9.99/month otherwise	No	Proprietary	web-application, integrates with Google Docs, collaboration & sharing features, currently only on Google Chrome
ReadCube Papers (now Papers)	ReadCube	2011-10	2021-03-09	v.4.23.3	US$ 3/month for students, 5/month academics	No	Proprietary	Web-app, Desktop (MacOS, Windows), Mobile (iOS and Android). Microsoft Word and Google Docs add-in. Browser extension (Chrome, Firefox, Edge, Safari)
EndNote	Clarivate Analytics	1988	2020-12-14	20	US$299.95[1]	No	Proprietary	The web version EndNote basic (formerly, EndNote Web) is free of charge
Pybliographer	pybliographer developers	1998-10-30 (0.2)	2018-04-03	1.4.0	Free	Yes	GNU GPL	Python/GTK2

Software	Developer	First public release	Latest stable release date	Latest stable version	Cost (USD)	Free software	License	Notes
Biblioscape	CG Information	1997	2015-06-22	10.0.3.6	US$79-299[1]	No	Proprietary	ODBC; web access in Pro ed; optional client/server; discontinued?
RefDB	refdb developers	2001-04-25	2007-11-05	0.9.9	Free	Yes	GNU GPL	network-transparent; XML/SGML bibliographies
Reference Manager	Thomson Reuters	1984	2010	12.0.3	Not for sale anymore, sales ceased December 31, 2015	No	Proprietary	network version; built-in web publishing tool; discontinued
Zotero	Roy Rosenzweig Center for History and New Media at GMU	2006	2021-01-11	5.0.95 [10]	Free / Online storage free up to 300 MB / Additional storage space available	Yes	AGPL	Multi-platform desktop version with connectors for Firefox, Chrome and Safari. Web-access to reference library also available through Zotero.org or through a personal cloud-based database folder on a user's computer (Google Drive, Dropbox, etc.).
JabRef	JabRef developers	2003-11-29	2020-03-10	5.0	Free	Yes	MIT license	Java BibTeX and BibLaTeX manager
Bibus	Bibus developers	2004-06-03	2013-05-23	1.5.1	Free	Yes	GNU GPL	discontinued?
Qiqqa	Qiqqa	2010-04	2016-09	v79	Free, Freemium and Premium versions	No	Proprietary	Desktop; Tablet; Web; Intranet
Sente	Third Street Software, Inc.	2004	Shut down in 2017	6.7.9	US$60–80[1] / Free for libraries up to 100 refs	No	Proprietary	Desktop and iPad, centralized backup/synching; discontinued
Bookends	Sonny Software	1988 (Mac) / 1983 (Apple II+)	2021-01-23	13.5.1[3]	US$59.99[1]	No	Proprietary	Desktop & iOS synced via iCloud, integrated web search, PDF download, auto-completion, Word plugin, BibTex support, PDF annotations stored as notes

Software	Developer	First public release	Latest stable release date	Latest stable version	Cost (USD)	Free software	License	Notes
colwiz	colwiz Ltd	2011	2016-05-09		Free / Online storage free up to 3 GB / Additional storage space available	No	Proprietary	Desktop (Win, Mac, Linux) & Web components, iOS and Android
Citavi	Swiss Academic Software	2006-02-13	2021-01-14	6.8.0.0	US$70-949 / Free for projects up to 100 references[4]	No	Proprietary	data can be saved locally on the computer, or, for team access, in the Citavi Cloud or an intranet Microsoft SQL Server;[5] search databases from interface[6]
WizFolio	WizPatent	2008-06	Shut down in 2017	Avatara	US$25 / Free Basic version	No	Proprietary	centrally hosted website; discontinued
BibBase	Christian Fritz	2005	2013-07	v3	Free	No	Proprietary	centrally hosted website, intended for publication pages
BibSonomy	University of Kassel	2006-01	2018-07-30	3.8.13	Free	Yes	AGPL, GPL, LGPL[2]	centrally hosted website
CiteULike	Oversity Limited	2004-11	Shut down in 2019-03-30[7]		Free	No	proprietary[8]	centrally hosted website
KBibTeX	KBibTeX developers	2005-08	2018-06-21	0.8.1	Free	Yes	GNU GPL	BibTeX front-end, using the KDE Software Compilation
BibDesk	BibDesk developers	2002-04	2021-02-22	1.8	Free	Yes	BSD	BibTeX front-end + repository; Cocoa-based; integration with Spotlight
Referencer	Referencer developers	2008-03-15	2014-02-27	1.2.2	Free	Yes	GNU GPL	BibTeX front-end
Mendeley	Elsevier	2008-08	2020	1.19.8	Free / Online storage free up to 2 GB / Additional storage space available	No	proprietary (OS API clients exist)	Account required, Desktop & Web components, Windows, Linux, macOS (not macOS 11 Big Sur)
SciRef	Scientific Programs	2012	2020-07-30	1.6.2	US$38.90 / Free trial version	No	Proprietary	

Εικόνα 3.1: Συγκριτικός πίνακας λογισμικών διαχείρισης αναφορών.

3.4. Η επιλογή του Mendeley Reference Manager ως εργαλείο διαχείρισης των βιβλιογραφικών αναφορών

Το Mendeley Reference Manager είναι μια ευρέως διαδεδομένη διαδικτυακή εφαρμογή διαχείρισης βιβλιογραφίας και ταυτόχρονα ένα κοινωνικό δίκτυο ερευνητών, που παρέχει τη δυνατότητα οργάνωσης της βιβλιογραφίας, αλλά και διαμοιρασμού βιβλιογραφικών αναφορών και εργασιών ανάμεσα σε ερευνητές. Είναι μια δωρεάν (freeware) εφαρμογή συμβατή με ποικιλία λειτουργικών συστημάτων και κινητών συσκευών (Windows, Mac, Linux, iOS, Android) που βοηθά στην οργάνωση και τη διαχείριση αναφορών. Διατίθεται σε τρεις εκδοχές (Desktop, Web και mobile), οι οποίες συγχρονίζονται μεταξύ τους. Το Reference Manager, αξιοποιώντας τη φιλοσοφία των μέσων κοινωνικής δικτύωσης, επιτρέπει στους χρήστες του να προωθήσουν την έρευνά τους συνδεόμενοι με άλλους ερευνητές ή ομάδες και να αναζητήσουν δημοσιεύσεις πάνω σε θέματα που τους ενδιαφέρουν. Μπορούμε να το χρησιμοποιήσουμε μέσω του υπολογιστή (σταθερού ή φορητού), του τηλεφώνου ή του tablet, εγκαθιστώντας την ανάλογη εφαρμογή ή μέσω περιηγητή. Η δημιουργία λογαριασμού και η εγκατάσταση της εφαρμογής είναι απλή διαδικασία. Ο λογαριασμός είναι απαραίτητος, προκειμένου να χρησιμοποιούμε τις διάφορες εκδοχές λογισμικού και να επιτυγχάνεται ο συγχρονισμός των δεδομένων μας.

Το Reference Manager (RM) διατίθεται σε δύο εκδόσεις ανάλογα με τις ανάγκες των χρηστών του.

- **Standard edition**

Στη δωρεάν έκδοση του RM δίνεται 2GB προσωπικός αποθηκευτικός χώρος και επιτρέπει την δημιουργία συνολικά πέντε (5) ιδιωτικών (Private) ομάδων ή ανοικτών ομάδων κατόπιν πρόσκλησης (Invite-only) με 100MB κοινό αποθηκευτικό χώρο και μέχρι 25 μέλη η καθεμία. Οι ανοικτές ομάδες Open που μπορούν να δημιουργηθούν είναι απεριόριστες.

- **Premium edition**

Το Mendeley προκειμένου να ανταποκριθεί στις αυξημένες ανάγκες των χρηστών του προσφέρει τη δυνατότητα αναβάθμισης του εκάστοτε λογαριασμού, έναντι αντιτίμου. Υπάρχουν διάφορα είδη αναβαθμίσεων (δυνατότητα περισσότερου αποθηκευτικού χώρου ή περισσότερων ιδιωτικών ομάδων) και η τιμή διαμορφώνεται ανάλογα με τις απαιτήσεις του κάθε χρήστη.

Πολλά πανεπιστημιακά ιδρύματα διαθέτουν συνδρομή σε κάποιο εργαλείο διαχείρισης αναφορών παρέχοντας στους φοιτητές τους ένα εργαλείο οργάνωσης των βιβλιογραφικών τους αναφορών βοηθώντας τους έτσι στην συγγραφή των εργασιών τους.

Η επιλογή του Mendeley ως πρόγραμμα οργάνωσης της βιβλιογραφίας στην παραπάνω εργασία έγινε αφού ελήφθησαν υπόψη τα εξής ιδιαίτερα χαρακτηριστικά του:

α)   Συγκεντρώνει και αποθηκεύει αρχεία .pdf από τον υπολογιστή, από βάσεις δεδομένων ή από άλλα εργαλεία διαχείρισης βιβλιογραφίας όπως τα EndNote, Papers, Zotero.

β)   Δίνεται η δυνατότητα να επεξεργάζεσαι και να κρατάς σημειώσεις στα έγγραφα.

γ)   Παρέχεται η δυνατότητα να δημιουργείς βιβλιογραφικές παραπομπές και βιβλιογραφία με όποιο πρότυπο επιλεγεί και μπορεί να μετατρέπει υφιστάμενες βιβλιογραφίες στο επιθυμητό πρότυπο.

δ)   Δίνεται η δυνατότητα να δημοσιεύονται αναφορές ή άρθρα και να ανταλλάσσονται με άλλους συγγραφείς ή ομάδες.

3.5. Τρόπος λειτουργίας του προγράμματος Reference Manager

Δημιουργία λογαριασμού (Create a Free Account)

Πραγματοποιείται επίσκεψη στην ιστοσελίδα www.mendeley.com με σκοπό τη δημιουργία ενός νέου λογαριασμού. Θα χρειαστεί να γίνει εγγραφή δηλώνοντας μια έγκυρη διεύθυνση ηλεκτρονικού ταχυδρομείου που χρησιμοποιούμε και κάποιες προσωπικές πληροφορίες. Επίσης δηλώνεται και η ακαδημαϊκή μας ιδιότητα. Στο επόμενο βήμα προαιρετικά δηλώνεται το εκπαιδευτικό ίδρυμα στο οποίο ανήκουμε. Θα ζητηθεί μέσω email να επιβεβαιωθεί η εγγραφή μας στο Mendeley, ώστε να ολοκληρωθεί η διαδικασία της εγγραφής. Κάθε φορά που πραγματοποιείται σύνδεση στο λογαριασμό που έχουμε δημιουργήσει θα γίνεται η εισαγωγή με το email και τον κωδικό (password) που δηλώθηκε κατά την εγγραφή.

Εγκατάσταση του εργαλείου στον Η/Υ (Mendeley Desktop Download)

Μόλις ολοκληρωθεί η διαδικασία της εγγραφής θα πρέπει να γίνει λήψη και εγκατάσταση της Desktop έκδοσης του Mendeley στον υπολογιστή, ανάλογα με το λειτουργικό σύστημα που διαθέτει ο υπολογιστής (https://www.mendeley.com/download-mendeley-desktop).

3.6. Η έκδοση Mendeley Desktop

Η Desktop έκδοση του RM μπορεί να εγκατασταθεί σε όσους Η/Υ επιθυμούμε. Κάθε φορά που γίνεται είσοδος στην εφαρμογή και γίνεται σύνδεση online, αυτή συγχρονίζεται με τον Web λογαριασμό, έτσι ώστε να ενημερωθεί με τις όποιες αλλαγές ή προσθήκες έχουν πραγματοποιηθεί. Μια καλή πρακτική είναι να γίνεται συγχρονισμός των βιβλιοθηκών κάθε φορά πριν κλειστεί η εφαρμογή, επιλέγοντας το σχετικό κουμπί **Sync** (⟳) που υπάρχει στη γραμμή εργαλείων του Desktop. Με αυτόν τον τρόπο οι όποιες αλλαγές πραγματοποιηθούν μεταφέρονται στο cloud του RM και θα είναι διαθέσιμες και στις υπόλοιπες εγκαταστάσεις του προγράμματος. Κατά την εγκατάστασή του, το RM εγκαθιστά ένα φάκελο στο δίσκο του Η/Υ για την αποθήκευση όλων των PDF αρχείων που κατεβαίνουν είτε από τον χρήστη είτε από το RM.

3.7. Τρόπος λειτουργίας της εφαρμογής Mendeley Desktop

3.7.1. Δομή και λειτουργίες του προγράμματος Mendeley Reference Manager

Το περιβάλλον του Mendeley Desktop χωρίζεται σε τρεις στήλες. Στην αριστερή στήλη απεικονίζεται η οργάνωση της βιβλιοθήκης σε φακέλους (Εικ. 3.2). Ο πίνακας αριστερά μας προσφέρει ένα μενού που μας επιτρέπει να περιηγηθούμε μέσα από διαφορετικές επιλογές φιλτραρίσματος στη βιβλιοθήκη μας.
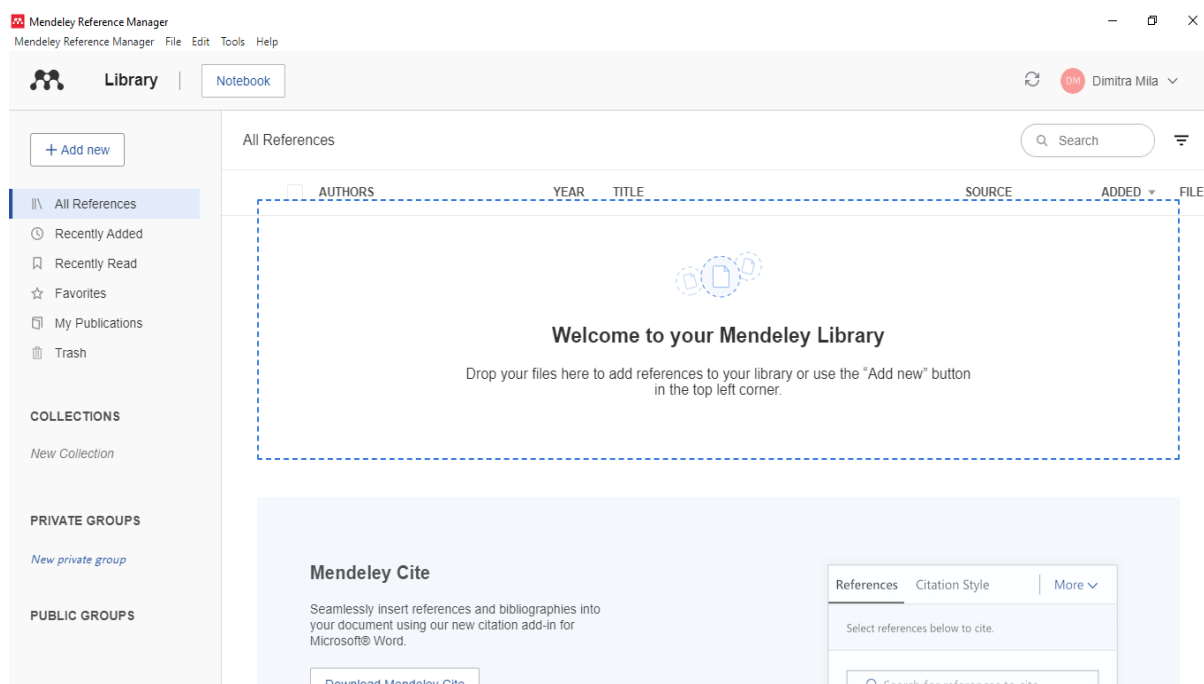
Εικόνα 3.2: Περιβάλλον εργασίας για την έκδοση Mendeley Desktop.

Επιλέγοντας διαφορετικούς φακέλους ή ομάδες που περιλαμβάνονται σε αυτή τη στήλη, θα εμφανιστούν στο κεντρικό πλαίσιο αντίστοιχες λίστες με καταχωρήσεις. Η ενότητα απαρτίζεται από τους εξής φακέλους:

- **All References:** Περιέχονται όλες οι αναφορές που υπάρχουν στη βιβλιοθήκη, ανεξάρτητα από το αν ανήκουν σε κάποιο φάκελο.

- **Recently Added:** Περιέχονται οι αναφορές που προστέθηκαν πρόσφατα στη βιβλιοθήκη.

- **Recently Read:** Περιέχονται οι αναφορές που διαβάστηκαν πρόσφατα μέσω του PDF Viewer.

- **Favorites:** Περιέχει τις αναφορές που έχουν οριστεί ως αγαπημένες.

- **My Publications:** Στο φάκελο αυτό μπορεί να γίνει εισαγωγή δημοσιεύσεων. Θα ζητηθεί όμως να γίνει επιβεβαίωση ότι είστε ο συγγραφέας και κάτοχος των πνευματικών δικαιωμάτων της δημοσίευσης.

- **Trash:** Στο φάκελο αυτό περιέχονται οι αναφορές που έχουν διαγραφεί. (Εικ. 3.3).
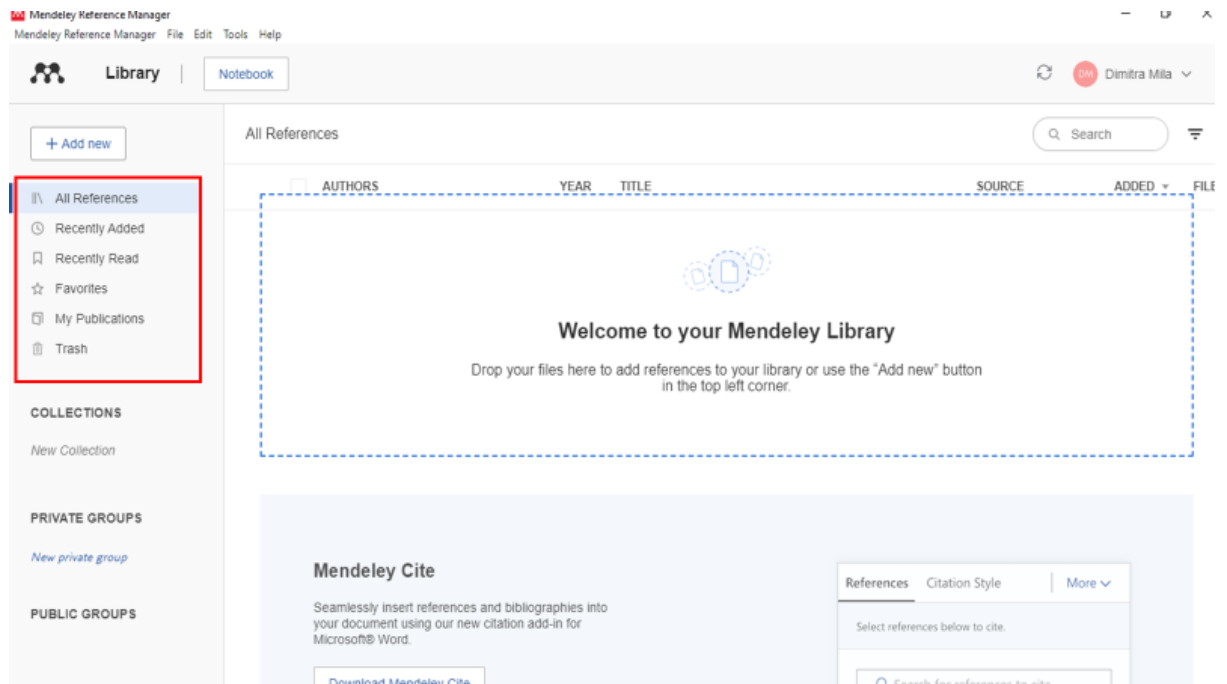
Εικόνα 3.3: Οργάνωση της βιβλιοθήκης σε φακέλους.

Επίσης, μέσω του προγράμματος δίνεται η δυνατότητα στους χρήστες να δημιουργούν τους δικούς τους φακέλους μέσα από την επιλογή **New Collection**. Ο χρήστης πληκτρολογεί το όνομα του φακέλου και πατώντας ENTER δημιουργείται ο φάκελος, στη συνέχεια επιλέγει από την κεντρική στήλη τις αναφορές που θέλει να εισαγάγει και τις σέρνει πάνω στο φάκελο που επιθυμεί (drag & drop) (Εικ. 3.4).
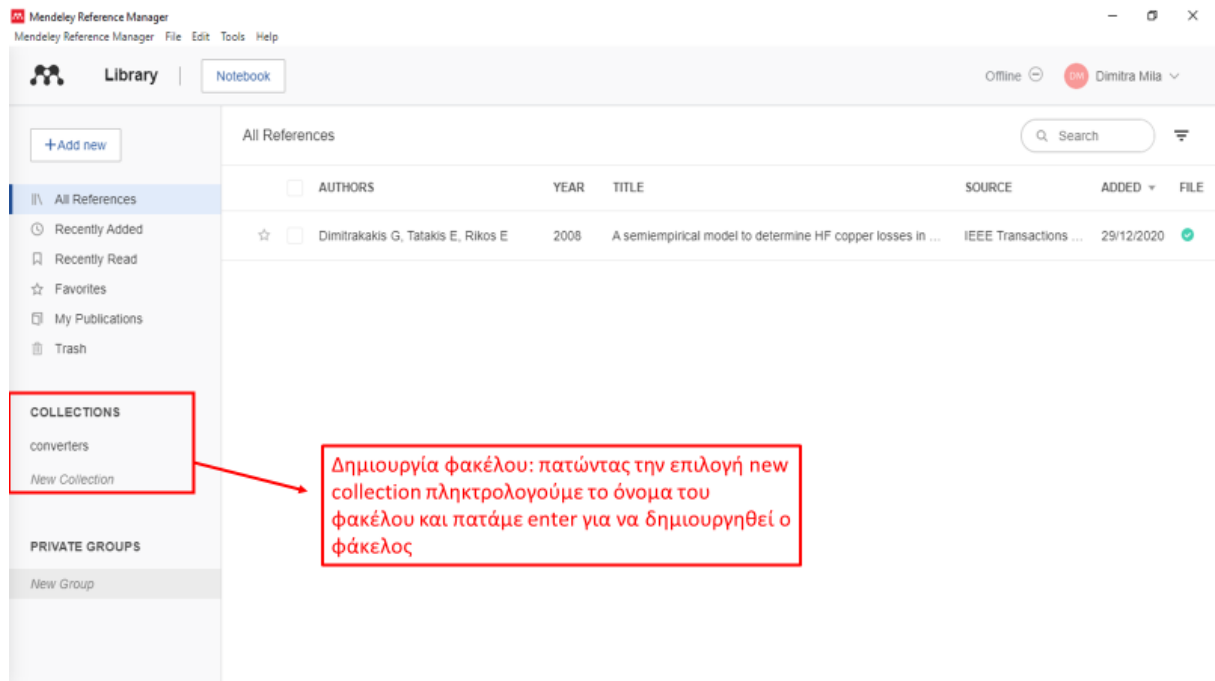
Εικόνα 3.4: Δημιουργία φακέλου.

Τέλος, το RM προσφέρει τη δυνατότητα δημιουργίας ομάδων συζήτησης (Groups). Στο πλαίσιο μίας ομάδας είναι δυνατή η συγκέντρωση βιβλιογραφίας, ο διαμοιρασμός και ο σχολιασμός των εγγράφων που μοιράζεται η ομάδα. Ο αριθμός των ομάδων που μπορούν να δημιουργηθούν εξαρτώνται από το είδος του λογαριασμού που έχει εγκατασταθεί στον Η/Υ (Standard ή Premium edition). Μέσω των ιδιωτικών ομάδων διευκολύνεται ο διαμοιρασμός αναφορών αλλά και εγγράφων πλήρους κειμένου. Προσφέρεται η δυνατότητα ανταλλαγής σχολίων στο πλήρες κείμενο των εγγράφων και σημειώσεων ορατών από όλα τα μέλη της ομάδας. Υπάρχει πάντα η δυνατότητα συζητήσεων/ανταλλαγής απόψεων ορατών μόνο από τα μέλη της ομάδας. Τα μέλη, προσκαλούνται από το δημιουργό της ομάδας και ενημερώνονται για την προσθήκη εγγράφων και σχολίων (Εικ. 3.5).
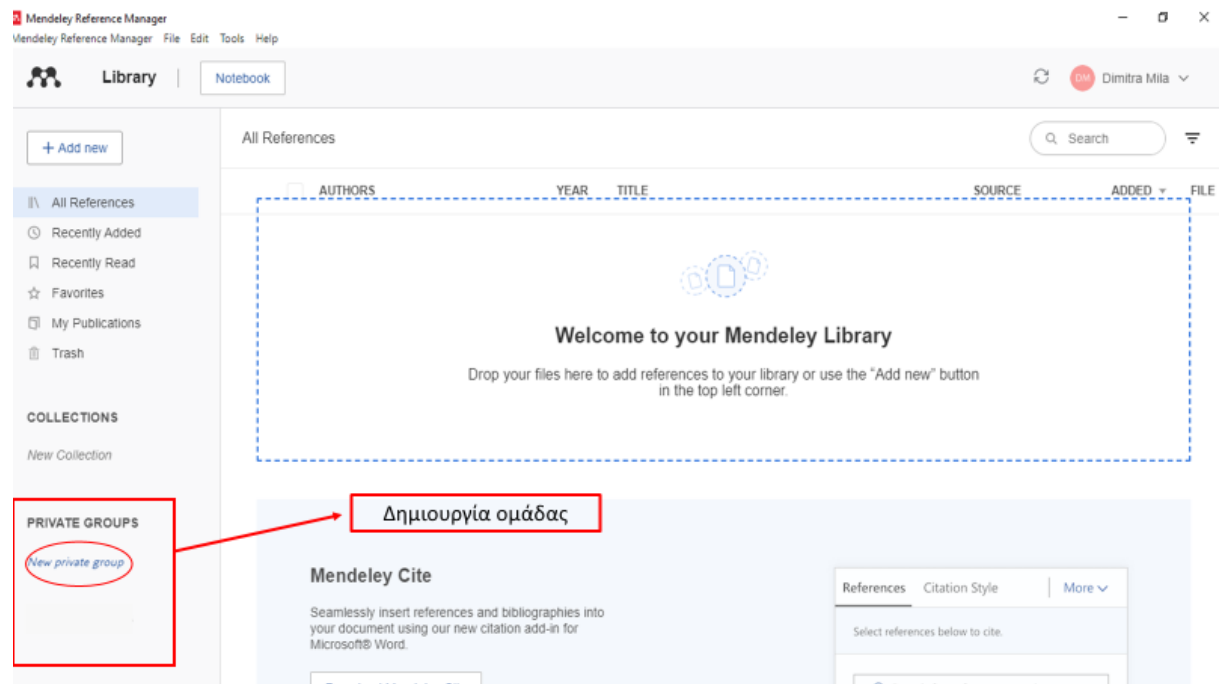
Εικόνα 3.5: Δημιουργία ομάδας.

Η κεντρική στήλη περιέχει τις αναφορές του φακέλου που έχουν επιλεγεί για να προβληθούν. Στην κορυφή της στήλης αυτής και κάτω από το όνομα του φακέλου υπάρχουν πέντε διαφορετικές επιλογές βάσει των οποίων μας επιτρέπεται η ταξινόμηση των αναφορών. Προκειμένου να γίνει επιλογή μιας συγκεκριμένης ταξινόμησης απλώς πατάμε πάνω στο αντίστοιχο tab (Εικ. 3.6):

- **Authors:** Βάσει του ονόματος του συγγραφέα.
- **Year:** Βάσει της χρονιάς δημοσίευσης/έκδοσης.
- **Title:** Βάσει του τίτλου της δημοσίευσης.
- **Added:** Βάσει της ημερομηνίας προσθήκης της εγγραφής στη βιβλιοθήκη.
- **Source: Β**άσει του τίτλου του περιοδικού.

Μπορούμε επίσης να χαρακτηρίσουμε μία αναφορά ως αγαπημένη τικάροντας την επιλογή ☆ . Το αστέρι γίνεται κίτρινο κάθε φορά που μια αναφορά χαρακτηρίζεται ως αγαπημένη.
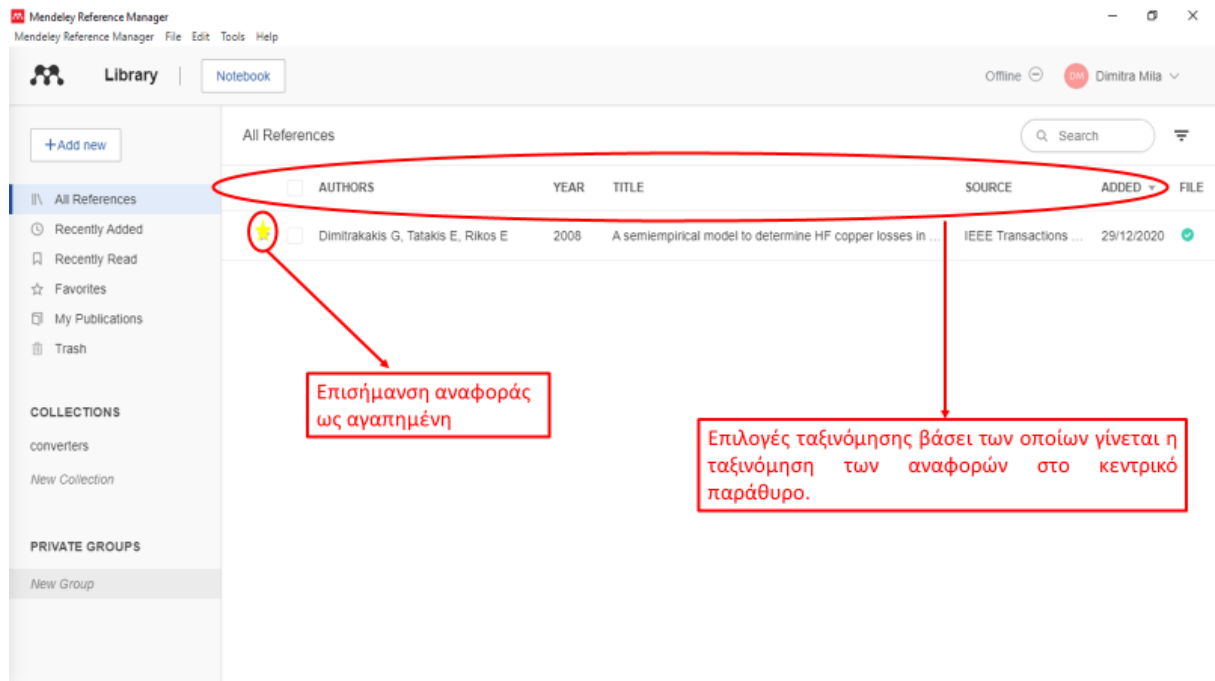
Εικόνα 3.6: Ταξινόμηση αναφορών στο κεντρικό παράθυρο του Reference Manager.

Στην τρίτη και τελευταία στήλη της εμφανιζόμενης εγγραφής του RM εμφανίζονται τα βιβλιογραφικά στοιχεία της αναφοράς που έχει επιλεγεί από το κεντρικό παράθυρο. Στην καρτέλα αυτή εμφανίζονται κάποιες βασικές πληροφορίες για την αναφορά που έχει επιλεγεί. Πιο συγκεκριμένα εμφανίζονται πληροφορίες όπως: ο τίτλος του άρθρου, το όνομα του συγγραφέα, το περιοδικό, το έτος που δημοσιεύτηκε η αναφορά, η περίληψη του άρθρου, οι λέξεις κλειδιά που μπορεί να περιλαμβάνονται και τα μόνιμα αναγνωριστικά της αναφοράς. Αν τυχόν χρειάζεται να γίνουν διορθώσεις, απλά επιλέγουμε με το ποντίκι το πεδίο που θέλουμε να τροποποιήσουμε και εισάγουμε τα στοιχεία που επιθυμούμε (Εικ. 3.7 (α)).

Στο πεδίο **Tag**, μπορούν να προστεθούν δικές μας λέξεις κλειδιά μέσα από τις οποίες μας επιτρέπεται να κάνουμε αναζήτηση στη βιβλιοθήκη, μέσω του πεδίου της αναζήτησης που υπάρχει στην εφαρμογή.

Τα αρχεία που επισυνάπτονται στην αναφορά εμφανίζονται στο πεδίο **Files** (Εικ. 3.7 (β)).

Στην καρτέλα **Annotations** εμφανίζονται σχόλια που έχουμε εισαγάγει μέσω του PDF Viewer μέσα στο PDF, ενώ στην καρτέλα **Notes**, δίνεται η δυνατότητα εισαγωγής των δικών μας σημειώσεων, που θέλουμε να κρατήσουμε για την αναφορά που έχει επιλεγεί για ανάγνωση (Εικ. 3.7 (γ)).
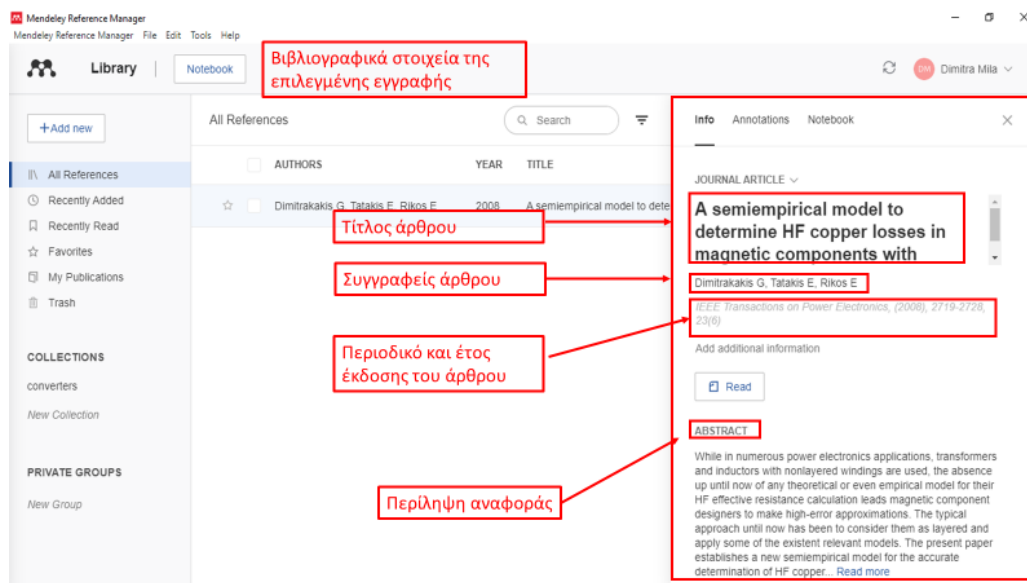
Εικόνα 3.7 (α): Ανάλυση των βιβλιογραφικών στοιχείων της αναφοράς.
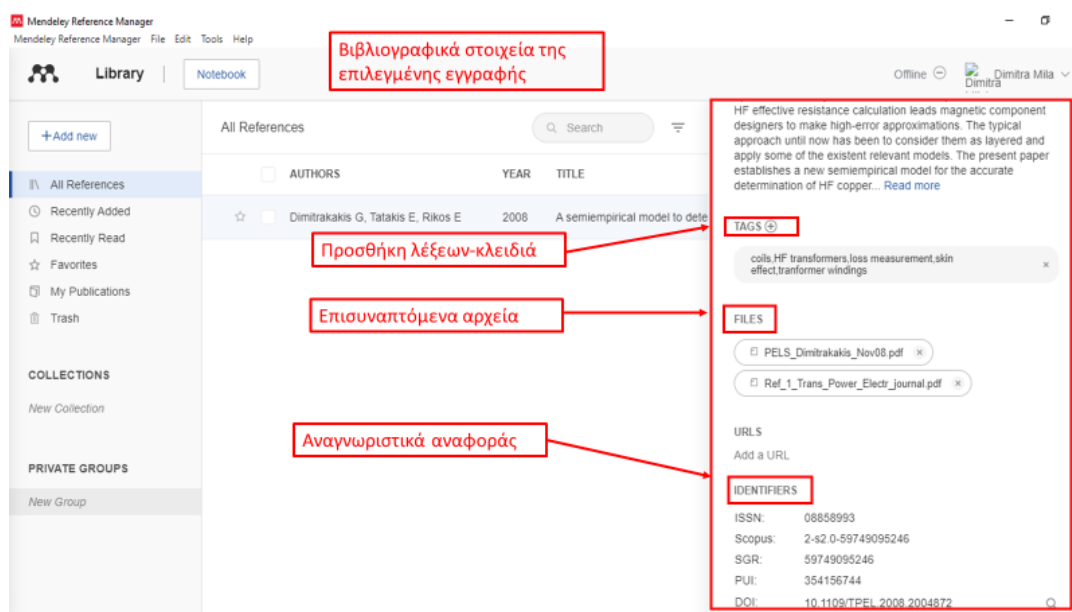
Εικόνα 3.7 (β): Ανάλυση των βιβλιογραφικών στοιχείων της αναφοράς.
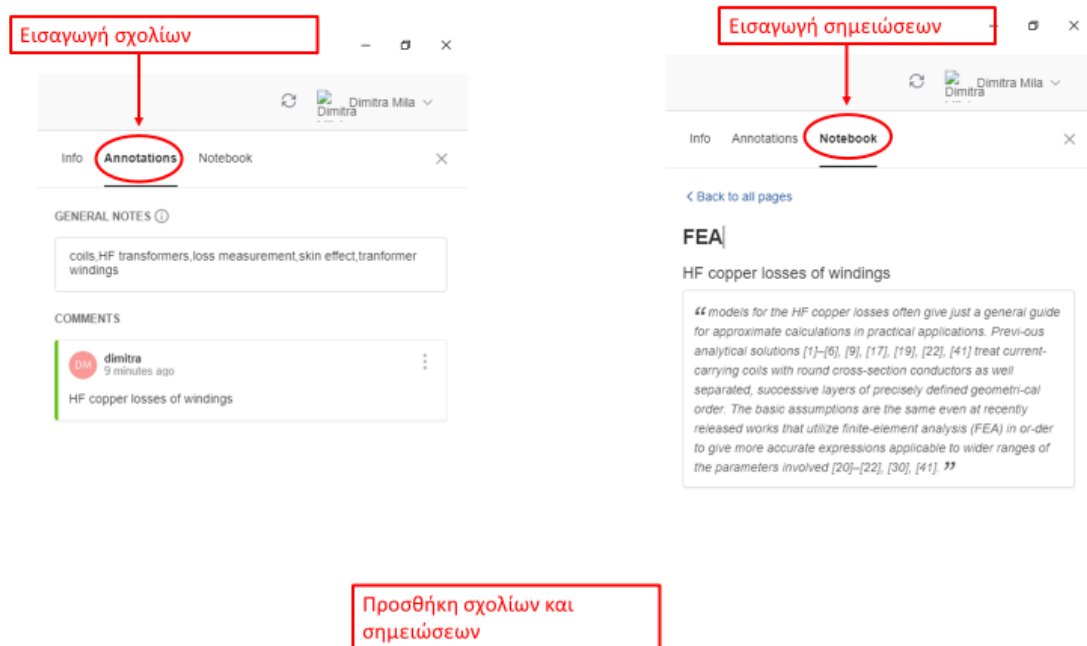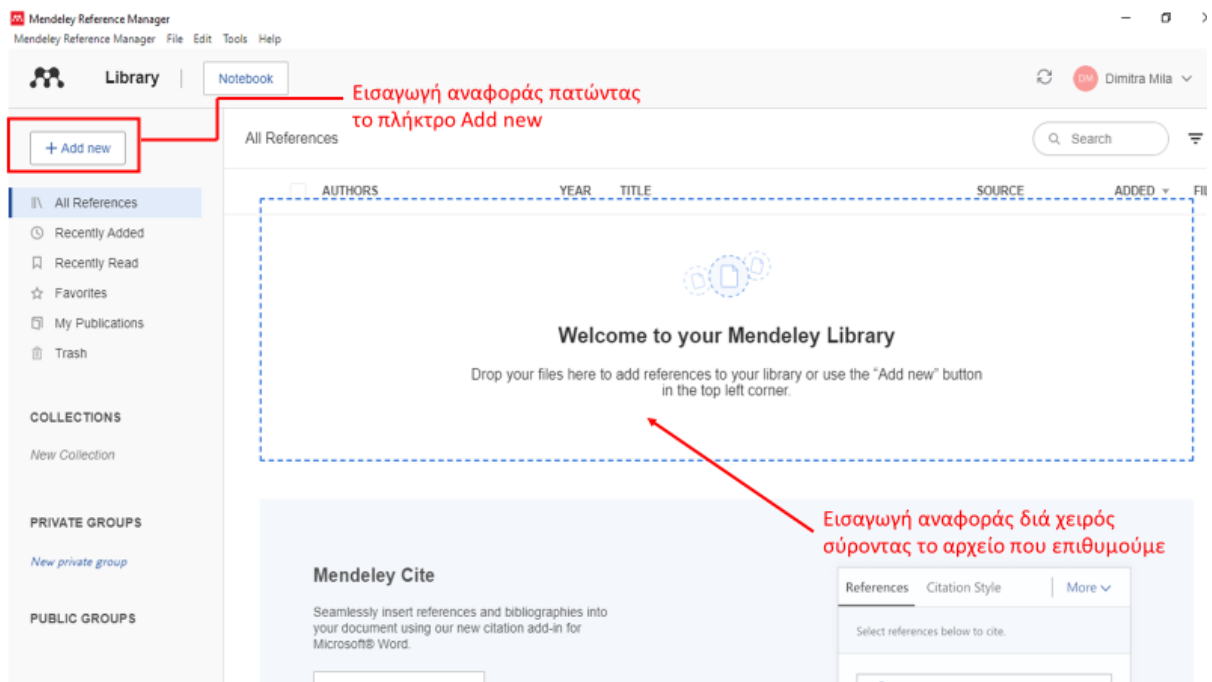
Εικόνα 3.7 (γ): Προσθήκη σχολίων και σημειώσεων.

Τέλος, στην πάνω δεξιά άκρη του Desktop υπάρχει ένα πλαίσιο αναζήτησης προκειμένου να εντοπιστούν οι αναφορές που έχουν αποθηκευτεί στη βιβλιοθήκη. Επιλέγοντας το φακό στο αριστερό άκρο του πλαισίου επιλέγουμε σε ποιο πεδίο θέλουμε να πραγματοποιηθεί η αναζήτηση (όνομα συγγραφέα, σχόλια που έχουμε εισαγάγει ως σημειώσεις σε αναφορές). Αν δεν επιλεγεί κάποιο συγκεκριμένο πεδίο, η αναζήτηση πραγματοποιείται ως λέξη-κλειδί σε όλα τα πεδία, καθώς και στο PDF αρχείο που ενδεχομένως συνοδεύει τις εγγραφές (Εικ. 3.8).
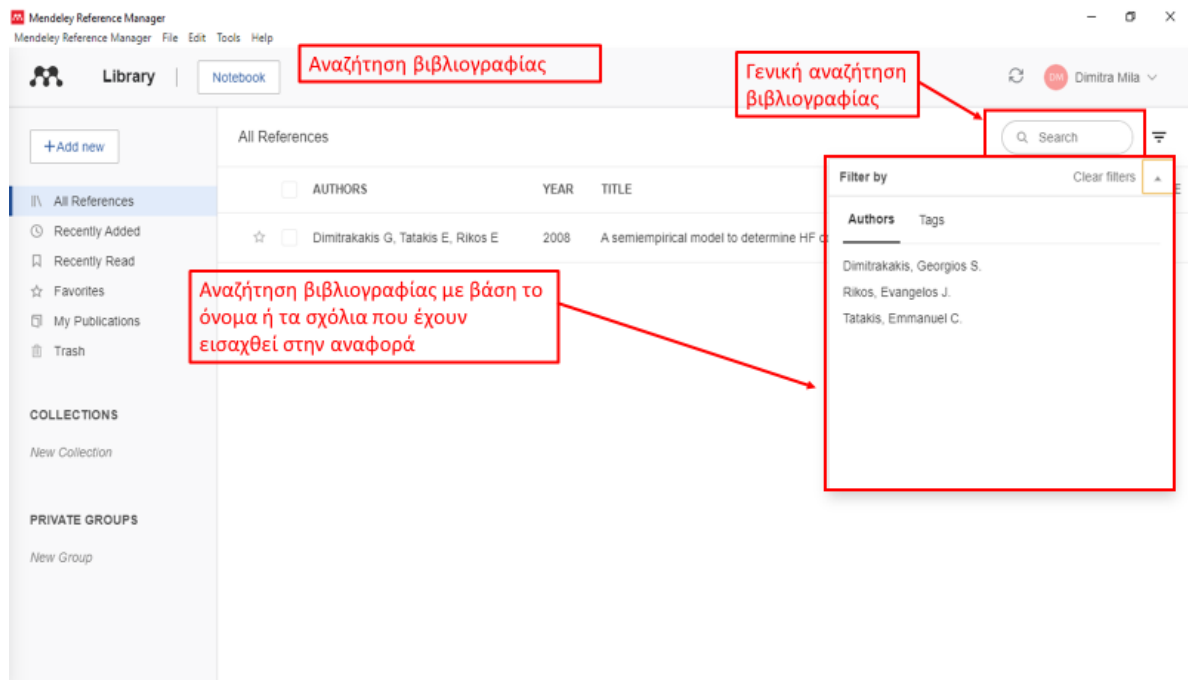
Εικόνα 3.8 : Πλαίσιο αναζήτησης της βιβλιογραφίας.

3.7.2. Εισαγωγή βιβλιογραφικών αναφορών στον κειμενογράφο

Για την εισαγωγή βιβλιογραφικών αναφορών στην εφαρμογή επιλέγουμε την επιλογή **Add New** και επιλέγουμε την αναφορά που επιθυμούμε να εισαγάγουμε στο πρόγραμμα. Με τον ίδιο τρόπο μπορεί να γίνει προσθήκη στη βιβλιοθήκη αρχείων τύπου XML, BibTex, RIS που περιέχουν εγγραφές από βιβλιογραφικές βάσεις ή άλλα προγράμματα διαχείρισης βιβλιογραφίας (EndNote, RefWorks κ.ά.). Διαφορετικά, η εισαγωγή της αναφοράς μπορεί να γίνει απλώς σύροντας τη προς το κεντρικό παράθυρο του RM, εφόσον τα αρχεία είναι αποθηκευμένα στον Η/Υ. Το RM αναγνωρίζει τις βιβλιογραφικές πληροφορίες που περιέχονται στα περισσότερα PDF αρχεία. Ως αποτέλεσμα γίνεται η εισαγωγή στη βιβλιοθήκη του πλήρους κειμένου των δημοσιεύσεων και ταυτόχρονα δημιουργείται και η σχετική εγγραφή με τις βιβλιογραφικές πληροφορίες του τεκμηρίου (Εικ. 3.9).

Εικόνα 3.9 : Εισαγωγή αναφοράς στην επιφάνεια εργασίας του Mendeley.

3.7.3. Εισαγωγή σχολίων και σημειώσεων (PDF Viewer)

Το RM δίνει τη δυνατότητα προσθήκης σχολίων και σημειώσεων στο πλήρες κείμενο (PDF αρχείο) των αναφορών της βιβλιοθήκης, εφόσον φυσικά έχει αποθηκευτεί. Κάνοντας διπλό κλικ με το ποντίκι στην αναφορά που επιθυμούμε. Το RM έχει δικό του PDF viewer οπότε ανοίγει το PDF σε μια νέα καρτέλα στο περιβάλλον της εφαρμογής από όπου μπορεί να γίνει εισαγωγή σχολίων και σημειώσεων (Εικ. 3.10). Επιλέγοντας από τα διαθέσιμα εικονίδια από τη γραμμή εργαλείων, μπορούμε να επιλέξουμε ένα χωρίο στο κείμενο, να το μαρκάρουμε με έντονη υπογράμμιση ή/και να εισαγάγουμε ένα σχόλιο. Στο σημείο τοποθετείται ένα bubble με διακριτό χρώμα που υποδεικνύει την ύπαρξη σχολίου. Τα σχόλια που εισήχθησαν μπορούμε να τα δούμε επιλέγοντας την αναφορά στην κεντρική στήλη στο Mendeley Desktop και κατόπιν την αντίστοιχη καρτέλα **Notes** στη δεξιά στήλη. Στο σημείο αυτό μπορεί να γίνει εισαγωγή εκτενέστερων και ευρύτερων σχολίων στο επάνω πλαίσιο που υπάρχει διαθέσιμο, ενώ ακριβώς από κάτω εμφανίζονται τα σχόλια (**Annotations**) που έχουν προστεθεί στο PDF.
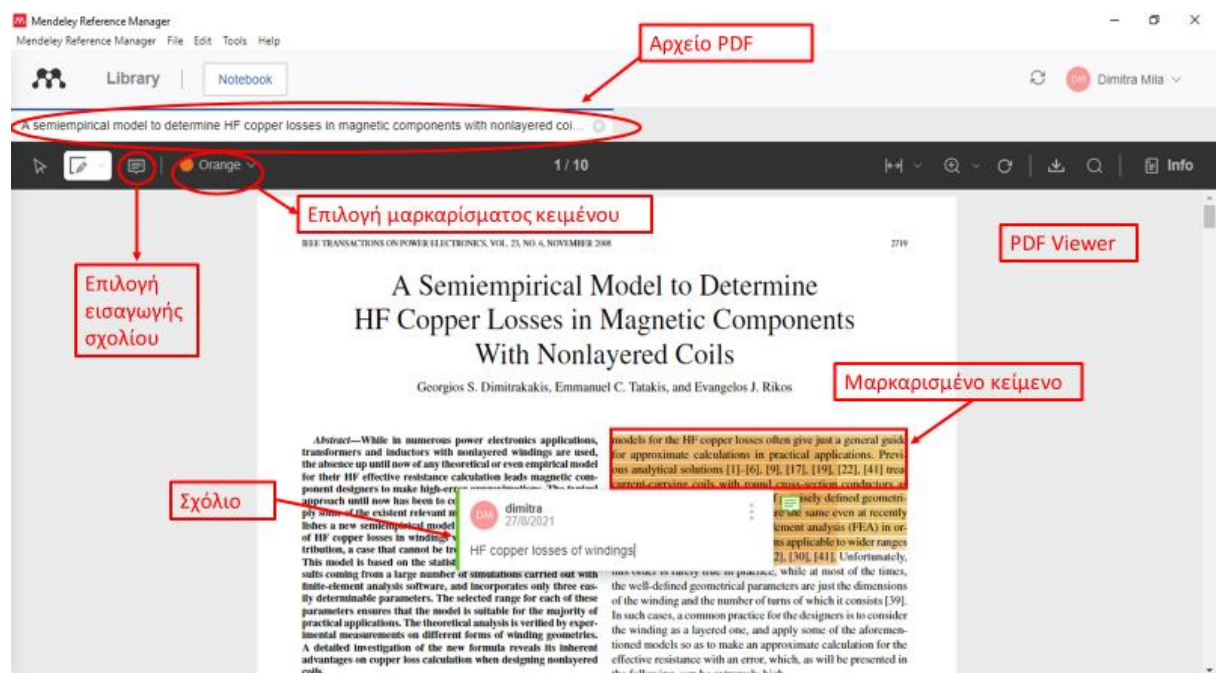
Εικόνα 3.10 : Εισαγωγή σχολίου και μαρκάρισμα κειμένου μέσω του PDF Viewer.

Όλη η παραπάνω διαδικασία που περιγράφηκε εφαρμόστηκε και στην οργάνωση της βιβλιογραφίας με θέμα: *Power electronics: converters, semi-conductors, switches, passive components*. Η σχετική βιβλιογραφία παραδόθηκε από το συγγραφέα της διατριβής σε ψηφιακή μορφή (αρχεία PDF) και έγινε η οργάνωση αυτής μέσω του προγράμματος Mendeley Reference Manager.

ΚΕΦΑΛΑΙΟ 4

ΣΥΜΠΕΡΑΣΜΑΤΑ

Ολοκληρώνοντας την παρούσα πτυχιακή εργασία γίνεται αντιληπτό πως η αγγλική γλώσσα είναι άρρηκτα συνδεδεμένη με την επιστήμη του ηλεκτρολόγου μηχανικού. Συνήθως μεταφράσεις τεχνικών κειμένων βρίσκουμε μόνο για κάποια βιβλία, με την ποιότητα της μετάφρασης να είναι συνάρτηση της σχετικότητας του μεταφραστή με το συγκεκριμένο αντικείμενο. Δεν είναι σπάνιο που πολλές φορές η μετάφραση σε σπουδαία επιστημονικά συγγράμματα αγγίζει τα όρια του φαιδρού διότι –προφανώς– ο εκδοτικός οίκος ανέθεσε το έργο αυτό σε λάθος άνθρωπο. Επίσης, διδακτορικές διατριβές και πτυχιακές εργασίες παραμένουν στη μητρική γλώσσα του συντάκτη τους (σπανίως ιδρύματα ανά τον κόσμο υποχρεώνουν ώστε η συγγραφή τους να γίνεται στα αγγλικά), ενώ τα τεχνικά εγχειρίδια, αν δεν είναι μόνο στα αγγλικά, προσφέρονται σε περιορισμένο αριθμό γλωσσών, με ελεγχόμενη και πάλι την ποιότητα της μετάφρασης. Οι δυσκολίες που συναντά ο μεταφραστής είναι πάρα πολλές τόσο συντακτικές όσο και δυσκολίες που αφορούν την ορθότερη απόδοση ενός όρου. Τις περισσότερες φορές δεν είναι δυνατό να γίνει κατανοητός ένας όρος χωρίς ο μεταφραστής να λάβει υπόψη του τα συμφραζόμενα, τα οποία όμως δεν γίνονται κατανοητά από τον μη ειδικό. Η λύση στο πρόβλημα αυτό είναι η εκμάθηση του πεδίου από το μεταφραστή ή η συνεργασία του με τους ειδικούς του πεδίου. Αυτό αποτελεί το βασικό πλαίσιο διαμόρφωσης και ανάλυσης της μετάφρασης του επιστημονικού και τεχνικού λόγου. Σε όλα αυτά τα προβλήματα βρίσκει λύσεις η χρησιμοποίηση των τεχνολογικών εργαλείων (ηλεκτρονικά λεξικά, ηλεκτρονικά σώματα κειμένων και μεταφραστικές μνήμες).

Μέσα από τη μετάφραση που έγινε στα πλαίσια της παρούσας εργασίας υπήρξε διπλό προσωπικό όφελος. Αφενός εμπλουτίσθηκαν οι γνώσεις μου σε μια σειρά ζητημάτων που σχετίζονται με τις απώλειες ισχύος σε μαγνητικά στοιχεία (πηνία– μετασχηματιστές) τα οποία χρησιμοποιούνται σε εφαρμογές ηλεκτρονικών ισχύος. Σχετικές γνώσεις που είχαν αποκομιστεί μόνο αποσπασματικά κατά την διάρκεια των σπουδών στο τμήμα Ηλεκτρολόγων Μηχανικών. Αφετέρου κατανοήθηκε η σπουδαιότητα της γνώσης της τεχνικής ορολογίας για την επιτυχή άσκηση του

επαγγέλματος του ηλεκτρολόγου μηχανικού. Έτσι, μέσα από τη μετάφραση έγινε βελτίωση του επιπέδου μου πάνω στην αγγλική ορολογία της ηλεκτρολογίας και εξάσκηση στη μετάφραση του τεχνικού κειμένου προκειμένου σε περίπτωση που μου ζητηθεί στο μέλλον ένα αντίστοιχο έργο να μπορέσω να το υλοποιήσω με επιτυχία.

Τέλος, για την ολοκλήρωση της πτυχιακής εργασίας χρειάστηκε να γίνει αναζήτηση και επιλογή του κατάλληλου λογισμικού. Τα λογισμικά διαχείρισης βιβλιογραφικών αναφορών είναι εφαρμογές που επιτρέπουν τη δημιουργία, διαχείριση και χρήση βιβλιογραφικών αναφορών, ώστε να αυξήσουν την παραγωγικότητα των συγγραφέων και των ερευνητών. Κατά την διαδικασία αναζήτησης του κατάλληλου λογισμικού οργάνωσης της βιβλιογραφίας χρειάστηκε να γίνει σύγκριση και αξιολόγηση μέσα από διάφορα λογισμικά, προκειμένου να γίνει η επιλογή του πιο εύχρηστου προγράμματος. Πέρα όμως, από την εύρεση του λογισμικού χρειάστηκε να γίνει και εκμάθηση του προγράμματος με σκοπό την ταξινόμηση της βιβλιογραφίας.

ΒΙΒΛΙΟΓΡΑΦΙΑ

- Coancă, M. (2011): Common Language Versus Specialized Language
  http://www.rebe.rau.ro/RePEc/rau/jisomg/SP11/JISOM-SP11-A22.pdf

- Diringer D. (1953). The Alphabet: A Key to the History of Mankind. *2ⁿᵈ* edition.

- Feather, J (2003). Bibliography. IN: *International Encyclopedia of Information and Library Science. 2ⁿᵈ*. ed. Ed. By John Feather & Paul Sturges. London: Routledge (s. 37-38)

- IATE - Η πολυγλωσσική βάση όρων της ΕΕ:
  http://iate.europa.eu/

- I.Finkelstein, From Canaanites to Israelites: When, How and Why, in Gabba, E. a.o. (eds.), Recenti tendenze nella ricostruzione della storia antica d'Israele, Rome 2005, 11-27
  (PDF) I. Finkelstein, From Canaanites to Israelites: When, How and Why, in Gabba, E. a.o. (eds.), Recenti tendenze nella ricostruzione della storia antica d'Israele, Rome 2005, 11-27. | Israel Finkelstein - Academia.edu

- Kautz U. (2002). Handbuch Didaktik des Übersetzens und Dolmetschens. München: Goethe Institut.

- Nida, A. E. & Taber, R. C. (1969). The Theory and Practice of Translation, With Special Reference to Bible Translating, 200. Brill: Leiden

- Ανανιάδου, Σ. & Ζερβάνου, Κ. (2004): «Αναγνώριση όρων σε υπολογιστικά συστήματα: Προβλήματα και μέθοδοι», στο Μ. Κατσογιάννου & Ε. Ευθυμίου (επιμ.) Ελληνική Ορολογία: Έρευνα και εφαρμογές, Αθήνα: Καστανιώτης

- Ανθή Βηδενμάιερ, Ερευνητική ικανότητα - Το μεγάλο μυστικό των μεταφραστών, Αριστοτέλειο Πανεπιστήμιο Θεσσαλονίκης
  https://www.frl.auth.gr/sites/metafrasi/PDF/Videnmayer.pdf

- Αποστόλου, Φ. (2011). Η διερμηνεία και η μετάφραση στην Ευρωπαϊκή Ένωση
  https://www.enl.auth.gr/gramma/gramma11/Apostolou3.pdf

- Γούτσος, Δ. (2004): «Προβλήματα μετάφρασης του επιστημονικού και τεχνικού λόγου», στο Μ. Κατσογιάννου & Ε. Ευθυμίου (επιμ.) Ελληνική Ορολογία: Έρευνα και εφαρμογές, Αθήνα: Καστανιώτης

- Γραμμενίδης, Σ., Δημητρούλια, Ξ., Κουρδής, Ε., Λουπάκη, Ε., Φλώρος, Γ., 2015. Διεπιστημονικές προσεγγίσεις της μετάφρασης. [ηλεκτρ. βιβλ.] Αθήνα Σύνδεσμος Ελληνικών Ακαδημαϊκών Βιβλιοθηκών.
  http://hdl.handle.net/11419/3901

- Δημητρούλια, Τ. (2005). Μετάφραση και κουλτούρα πολιτισμική στροφή στη μεταφρασεολογία και ο ρόλος των νέων τεχνολογιών. Σύγκριση, 16, 158-172. 82
  http://gcla.phil.uoa.gr/newfiles/syngrisi16/16.dimitroulia.pdf

- Δημητρούλια, Τ. (2006): «Η μεταφραστική τεχνολογία και η ελληνική γλώσσα», στο Πρακτικά 1ης Συνάντησης Νέων Μεταφρασεολόγων, Μεταφρασεολογικές Σπουδές και Έρευνα στην Ελλάδα, Θεσσαλονίκη, 1-3 Νοεμβρίου 2006
  www.enl.auth.gr/translation/PDF/Dimitroulia.pdf

- Δογορίτη, Ε. & Βυζάς, Θ. (2015): Ειδικές Γλώσσες & Μετάφραση για Επαγγελματικούς Σκοπούς, Αθήνα: Διόνικος.

- Εθνικό και Καποδιστριακό Πανεπιστήμιο
  http://www.lib.uoa.gr/fileadmin/user_upload/Efarmoges_bibliografikis_diacheirisis_Karypidoy-Frantzi.pdf

- ΕΛΕΤΟ – Ελληνική Εταιρία Ορολογίας (2010): ΟΡΟΓΡΑΜΜΑ Αρ.103, από
  http://www.eleto.gr/download/Orogramma/Or103_V04.pdf

- Ηλεκτρονικό Λεξικό της Κοινής νεοελληνικής γλώσσας του Μανόλη Τριανταφυλλίδη:
  http://www.greek-language.gr/greekLang/modern_greek/tools/lexica/triantafyllides/index.htm

- Ιορδανίδου, Α. (2004): «Η ορολογία στα λεξικά γενικής γλώσσας», στο Μ. Κατσογιάννου & Ε. Ευθυμίου (επιμ.): Ελληνική Ορολογία: Έρευνα και εφαρμογές, Αθήνα: Καστανιώτης

- Καλαμβόκα, Π. (2004): «Λεξικά Ορολογίας στο διαδίκτυο», στο Κατσογιάννου Μ. & Ευθυμίου Ε.(επιμ.) Ελληνική Ορολογία: Έρευνα και Εφαρμογές, Αθήνα: Καστανιώτης

- Καραγιάννης, Γ. (2004): «Ελληνική Ορολογία στην Κοινωνία της Πληροφορίας», στο Κατσογιάννου Μ. & Ευθυμίου Ε.(επιμ.) Ελληνική Ορολογία: Έρευνα και Εφαρμογές, Αθήνα: Καστανιώτης

- Κατσογιάννου, Μ. & Ευθυμίου, Ε. (2004): «Θεωρία, μέθοδοι και πρακτικές της Ορολογίας», στο Μ. Κατσογιάννου & Ε. Ευθυμίου (επιμ.) Ελληνική Ορολογία: Έρευνα και εφαρμογές, Αθήνα: Καστανιώτης

- Κατσογιάννου, Μ. (2004): «Λεξικά Ορολογίας: Μεθοδολογία, δομή και περιεχόμενο», στο Μ. Κατσογιάννου & Ε. Ευθυμίου (επιμ.) Ελληνική Ορολογία: Έρευνα και Εφαρμογές, Αθήνα: Καστανιώτης

- Κελάνδριας, Ι. Π. (2007). Ο ρόλος των μεταφραστικών οδηγιών στη διαμόρφωση της ειδικής ορολογίας. Συνέδριο «Ελληνική Γλώσσα και Ορολογία». ΕΛΕΤΟ – 6ο.

- Κελάνδριας, Ι. Π. (2013). Η ορολογική 'σύγκλιση' ως μεταφραστικό εργαλείο της ειδικής μετάφρασης. Συνέδριο «Ελληνική Γλώσσα και Ορολογία». ΕΛΕΤΟ – 9ο.
  Microsoft Word - 32-18-25_KelandriasPanagiotis_Paper_V03.doc (eleto.gr)

- Κεντρωτής, Γ. (1996). Θεωρία και πράξη της μετάφρασης. Αθήνα: Εκδόσεις Δίαυλος.

- Κοκκίνου Νεφέλη (2015-2016). Μετάφραση αποσπάσματος από το διδακτορικό: 'The translator as terminologist, with special regard to the EU context.' της Marta Fischer και μεταφραστικά σχόλια. Πτυχιακή εργασία, ΤΕΙ Ηπείρου, Τμήμα διοίκησης επιχειρήσεων.

- Κομνηνός Παπαευαγγέλου, Ε. Κων. (2016). Εξειδικευμένη μετάφραση και νέες τεχνολογίες: η αναζήτηση όρων με τη χρήση ηλεκτρονικών λεξικών, σωμάτων κειμένων και μεταφραστικών μνημών. Πτυχιακή εργασία, ΤΕΙ Ηπείρου, Τμήμα διοίκησης επιχειρήσεων.

- Κουτσιβίτης, Β. (1992). Η Θεωρία της μετάφρασης στην Ελλάδα. Αθήνα: Ελλ. Πανεπ. Εκδόσεις.

- Λαμπροπούλου, Π. (2010): «Γλωσσικοί πόροι και τεχνολογίες: Η σημερινή ελληνική πραγματικότητα», Ινστιτούτο Επεξεργασίας Λόγου/Ε.Κ. «Αθήνα», Ημερίδα παρουσίασης CLARIN-EL
  http://prep.clarin.gr/files/Labropoulou%20LRT%20surveys.pdf

- Λουπάκη, Ε. (2013): «Η θέση της ορολογίας στο μάθημα της μετάφρασης γενικών κειμένων», στο Ανακοινώσεις 9ου συνεδρίου Ελληνική γλώσσα και Ορολογία, Αθήνα: ΕΛΕΤΟ, σσ.146-156,
  Microsoft Word - 10-24-29_LoupakiElpida_Paper_V03.doc (eleto.gr)

- Μικρός, Γ. (2004): «Ηλεκτρονικά σώματα κειμένων και ορολογία», στο Μ. Κατσογιάννου & Ε. Ευθυμίου(επιμ.) Ελληνική Ορολογία: Έρευνα και εφαρμογές, Αθήνα: Καστανιώτης

- Μπαμπαΐτης Βασίλειος-Νικόλαος (2009). Ψηφιακές βιβλιοθήκες και ηλεκτρονικά βιβλία (e-Books). Διπλωματική εργασία, Αριστοτέλειο Πανεπιστήμιο Θεσσαλονίκης, Τμήμα Πληροφορικής.

- Μπατσαλιά, Φ. & Σέλλα-Μάζη. Ε. (1994). Γλωσσολογική προσέγγιση στη θεωρία και τη διδακτική της μετάφρασης. Αθήνα: Εκδόσεις Έλλην.

- Μπατσαλιά, Φ. (2001-2003). Παράμετροι της μεταφραστικής διαδικασίας και συγκριτική γλωσσολογία. Αθήνα: Εκδόσεις Παρουσία, Τόμος ΙΕ-ΙΣΤ΄.

- Οδηγός χρήσης Mendeley διαχείριση και οργάνωση της βιβλιογραφίας (2016)

- https://www.lib.auth.gr/sites/default/files/docs_files/MendeleyGuide_Greek_Final.pdf

- Παλασάκη, Β. (2007). «Τα σώματα κειμένων: Ένα εργαλείο για τα παραδείγματα εξειδικευμένων λέξεων». Αθήνα: Ελληνική Εταιρία Ορολογίας.
  Microsoft Word - 6th_22-03-PalasakiVasilikiPaper_V05.doc (eleto.gr)

- Πανεπιστήμιο Ιωαννίνων
  https://wwwlib.teiep.gr/images/stories

- Πανεπιστήμιο Κύπρου
  http://library.ucy.ac.cy/el/services/citation-management-tools

- Πανεπιστήμιο Πατρών

http://www.lis.upatras.gr/wp-content/uploads/2013/01/Citations_LIS_Guide.pdf

- Παπανδρέου Παναγιώτα (2016). Σχολιασμένη μετάφραση από τα Αγγλικά προς τα Ελληνικά Απόσπασμα από το άρθρο «The Refugee Surge in Europe: Economic Challenges». Μεταπτυχιακή εργασία, Αριστοτέλειο Πανεπιστήμιο Θεσσαλονίκης, Διατμηματικό Πρόγραμμα Μεταπτυχιακών Σπουδών Μετάφρασης και Διερμηνείας Κατεύθυνση: Μετάφραση.

- Πιπερίδης, Σ., Δεμοίρος, Ι., Μπούτσης, Σ. (2004): «Αυτόματη κατασκευή δίγλωσσων λεξικών», στο Μ. Κατσογιάννου & Ε. Ευθυμίου(επιμ.) Ελληνική Ορολογία: Έρευνα και εφαρμογές, Αθήνα: Κασταντώτης

- Πούγγουρας, Π. (2006). Η συμβολή της Ορολογίας στη μετάφραση ειδικών κειμένων: το παράδειγμα μίας ορολογικής εργασίας με αντικείμενο την ειδική γλώσσα της Κρυπτολογίας

http://www.enl.auth.gr/translation/PDF/Pougouras.pdf

- Ρ. Καρυπίδου- Α. Φραντζή (2017). Παρουσίαση στην Ημερίδα με θέμα «Οι Ψηφιακές Συλλογές της ΒΚΠ στις υπηρεσίες της εκπαίδευσης και της έρευνας» η οποία διοργανώθηκε από τη Βιβλιοθήκη & Κέντρο Πληροφόρησης του Εθνικού και Καποδιστριακού Πανεπιστημίου Αθηνών»

- Σκούρτου Ε. (1997). Θέματα Διγλωσσίας και Εκπαίδευσης. Αθήνα: Νήσος

- Τεχνολογικό Εκπαιδευτικό Ίδρυμα Ηπείρου Βιβλιοθήκη και Κέντρο Πληροφόρησης (2017). Οδηγός Βιβλιογραφικών Παραπομπών και σύνταξης Βιβλιογραφίας.
Βιβλιογραφικεσ παραπομπεσ και συνταξη βιβλιογραφιασ (uoi.gr)

- Τριανταφυλλίδης, Β. Δ. (2011). «Η μέθοδος Στανισλάφσκι στη μετάφραση ή η αβάσταχτη μοναξιά του μεταφραστή».
http://www.apiliotis.gr/ArticlesList.aspx?C=367&A=382

- Φλώρου, Ελ. Μετάφραση ιατρικής ορολογίας από την Αγγλική προς την Ελληνική γλώσσα: Προβλήματα και Στρατηγικές
https://www.frl.auth.gr/sites/metafrasi/PDF/florou.pdf

- Χαραλαμπάκης, Χ. (2011). Λεξικογραφία και ορολογία: Συμπεράσματα από τη σύγκριση δύο σύγχρονων νεοελληνικών λεξικών. ΕΛΕΤΟ – 8ο Συνέδριο «Ελληνική Γλώσσα και Ορολογία», 10-12 Νοεμβρίου 2011. [Microsoft Word - 00b_CharalambakisChristoforos_Paper_V02.doc (eleto.gr)](#)

- Χίου, Θ. (2007). Ημερίδα Εργασίας με τίτλο «Αναβάθμιση του μεταφραστικού επαγγέλματος σε Ελλάδα και Κύπρο και πνευματικά δικαιώματα» https://www.iprights.gr/gnomes/136-pneymatika-dikaiomata-kai-metafrash-dikigoros-pneymatiki-idiokthsia-chiou-theodoros-xioy

ΕΥΡΕΤΗΡΙΟ ΕΙΚΟΝΩΝ

- Εικόνα 2.1.:

  https://www.maxmag.gr/politismos/palaiolithiki-techni-sto-spilaio-tis-altamira/

- Εικόνα 2.2.:

  https://www.freeminds.gr/taxideuontas_alfavhtario/

- Εικόνα 2.3.:

  https://el.wikipedia.org/wiki/%CE%A0%CE%AC%CF%80%CF%85%CF%81%CE%BF%CE%B9_%CF%84%CE%B7%CF%82_%CE%9F%CE%BE%CF%85%CF%81%CF%81%CF%8D%CE%B3%CF%87%CE%BF%CF%85

- Εικόνα 2.4.:

  https://el.wikipedia.org/wiki/%CE%A0%CE%B5%CF%81%CE%B3%CE%B1%CE%BC%CE%B7%CE%BD%CE%AE

- Εικόνα 2.5.:

  https://commons.wikimedia.org/wiki/File:Mendeley_Logo_Vertical.png

- Εικόνα 2.6.:

  https://www.logo.wine/logo/Zotero

- Εικόνα 2.7.:

  https://www.educatorstechnology.com/2019/04/5-handy-tools-for-research-students.html

- Εικόνα 2.8.:

  https://innovation.ox.ac.uk/success-stories/colwiz-accelerating-global-research/

- Εικόνα 3.1.:

  https://en.wikipedia.org/wiki/Comparison_of_reference_management_software

ΠΑΡΑΡΤΗΜΑ

INVESTIGATION OF LOSSES IN MAGNETIC COMPONENTS WITH HIGH-FREQUENCY CURRENT FLOW FOR POWER ELECTRONIC CONVERTER APPLICATIONS

DOCTORAL DISSERTATION

GEORGIOS S. DIMITRAKAKIS

PHYSICIST

UNIVERSITY OF PATRAS

DEPARTMENT OF ELECTRICAL AND COMPUTER

ENGINEERING

DISSERTATION NUMBER: 221

JUNE 2009

ΠΙΣΤΟΠΟΙΗΣΗ

Πιστοποιείται ότι η παρούσα διατριβή με θέμα

"Διερεύνηση των Απωλειών Μαγνητικών Στοιχείων Διαρρεόμενων από Υψίσυχνα Ρεύματα για Εφαρμογές σε Διατάξεις Ηλεκτρονικών Ισχύος"

του κ. Γεώργιου Σ. Δημητρακάκη Πτυχιούχου Φυσικού, παρουσιάστηκε στο Τμήμα Ηλεκτρολόγων Μηχανικών και Τεχνολογίας Υπολογιστών του Πανεπιστημίου Πατρών τη 15η Ιουνίου 2009 και εξετάστηκε και εγκρίθηκε από την ακόλουθη Εξεταστική Επιτροπή:

1) Εμμανουήλ Τατάκης, Αναπληρωτής Καθηγητής Πανεπιστημίου Πατρών
2) Αθανάσιος Σαφάκας, Καθηγητής Πανεπιστημίου Πατρών
3) Κωνσταντίνος Σώρρας, Αναπληρωτής Καθηγητής Πανεπιστημίου Πατρών
4) Νικόλαος Σπύρου, Καθηγητής Πανεπιστημίου Πατρών
5) Ιωάννης Μήλιας - Αργείτης, Αναπληρωτής Καθηγητής Πανεπιστημίου Πατρών
6) Αντώνιος Κλαδάς, Καθηγητής Ε.Μ.Π.
7) Χαράλαμπος Δημουλιάς, Λέκτορας Α.Π.Θ.
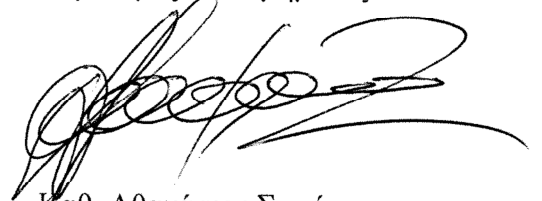
Πάτρα, 15 Ιουνίου 2009

Το Επιβλέπον Μέλος Δ.Ε.Π.

Αναπλ. Καθ. Εμμανουήλ Τατάκης

Ο Πρόεδρος του Τμήματος

Καθ. Αθανάσιος Σαφάκας

PREFACE

This doctoral dissertation was prepared at the Electromechanical Energy Conversion Laboratory of the Electrical and Computer Engineering Department of the University of Patras. Ittreatsof a series of issues related to the power losses in magnetic components (inductors - transformers) used in power electronic applications, both theoretically and experimentally.

This dissertation consists of the introduction, eight (8) chapters and the appendixes.In the introduction a general description of the problems arising with the use of magnetic components in power electronic converters is provided and the objectives of the dissertation are clarified. In the appendixes, which are at the end of the dissertation, some issues have been briefly developed that are directly related to the subject of the dissertation, but are not included in the material of any of its chapters.

In the first chapter there is a general description of the physical effects that take place in the magnetic components when they carry a current variable in time, i.e. the hysteresis effect and the development of eddy currents in the core, as well as the development of eddy currents in their windings (skin and proximity effects).

In the second chapter there is a brief description of the issue of the magnetic properties of matter and in particular ofthe materials that are of keen interest in the power electronic applications (ferrites). The most important models of macroscopic description of magnetic hysteresis are presented and the basic structure of the expressions commonly used to calculate the core losses in magnetic components is given.

In the third chapter the various factors that affect the copper losses of magnetic components are outlined and the most important works from the international literature on the subject of calculating these losses are mentioned.

In the fourth chapter, using finite element software, the accuracy and application limits of the most important theoretical works on copper losses in windings consisting of layers are investigated. Then, with the help of the software, the edge effect in layered windings, which, potentially, can lead to a significant increase in copper losses, is investigated, while also the effective resistance of a winding with round cross-section conductors when they are placed in hexagonal configuration is calculated.

In thefifth chapter the work to develop a new model for calculating the copper losses in magnetic component windings when the round cross-round conductors that make them up are

randomly placed within the available space (window) is described. The conditions and limits of the model application are clearly defined, and the proposed expression is investigated in terms of the coincidence of its result with both the results of the simulations and the experimental measurements obtained. Moreover, the sensitivity of the new expression to variations in the only one of the parameters that may present an error in its determination is investigated and an approximate low frequency expression is proposed.

In the sixth chapter the design of a resonant inverter for the production of high frequency sinusoidal voltage, suitable as an excitation source of magnetic components for taking measurements in them is presented.Through the theoretical and experimental study that is carried out, the appropriate dimensioning of the components that form the power and control circuits is achieved, in order to achieve the expansion of the operating frequency range, the minimization of the harmonic distortion of the output voltage and the maximization of the amplitude.

In the seventh chaptera series of issues related to conducting experimental measurements on magnetic components is analyzed and the most appropriate methodologies to measure the losses in them and to acquire the hysteresis loop of the core's magnetic material are proposed. Further than that, some correction methodologies are proposed when the measurements for the acquisition of the hysteresis loop present a known phase error or when, based on Dowell's model, the effective resistance of a winding is calculated for a temperature higher than the ambient temperature, as typically happens during the operation of magnetic components.

In the eighth chapter the conclusionsdeduced from the preparation of the dissertation are summarized and its original elements are pointed out.

Closing this short preface, I would like first of all to thank the Chairman of the three-member advisory committee and supervisor of this dissertation, Associate Professor Mr. Tatakis Emmanuel, for his multifaceted cooperation, as well as for his full support and continuous scientific guidancethat he offered me throughout its elaboration.

I would also like to thank the members of the three-member advisory committee, Professor Mr. Safakas Athanasios and Associate Professor Mr. Sorras Konstantinos, for their valuable advice, which contributed significantly to the level improvement of the dissertation.

I must also refer to the postgraduate students of our Laboratory, current and former, without the support and company of whom the postgraduate studies would be a definitely less successful and clearly less enjoyable course in time.I warmly thank them all.

CONTENTS

CHAPTER 7

ISSUES RELATED TO MEASUREMENTS ON MAGNETIC COMPONENTS   **199**

CHAPTER 8

RECAPITULATION − CONCLUSIONS   **231**

REFERENCES   **237**

SYMBOLS – ABBREVIATIONS   **251**

INTRODUCTION – OBJECTIVES

1. Introduction

Power electronic converters are used in a wide range of applications, such as power supply of electronic devices, speed control of motor systems, etc. During the development of these converters, special attention is paid to aspects such as high efficiency and reliability extended life span, low cost, small volume and weight, improved power factor, minimum harmonic noise towards the grid, reduced electromagnetic interference to the environment, ease of production line build up, etc.

Most electronic power converters contain passive components (capacitors - inductors - transformers) which, as the case may be, serve various purposes, such as filtering of the voltage or current harmonics (both towards the converter output and towards the power supply grid) or variation of the level of a voltage and the transfer of electric power through electric isolation. The first purpose is served through the ability of capacitors and inductors to store energy (in the form of electric and magnetic field respectively), while the second thanks to two basic principles of electromagnetism, namely the creation of a magnetic field by an electric current and the creation of an electric field from a changing magnetic field.

The passive components largely determine parameters of the converters, such as weight, volume and cost. Regarding the capacitors we are interested in features such as their size, capacitance and voltage tolerance, but their parasitic inductances (ESL – Equivalent Series Inductance) and resistances (ESR – Equivalent Series Resistance) are equally important. These parasitic elements are usually of low value, and in particular the ohmic losses in a capacitor are so low that they are usually considered as negligible. Of course, despite their low values, in some cases the parasitic elements of the capacitors have a significant effect on the operating characteristics of the converters, such as, for example, the ripple amplitude of the output voltage of the switched-mode power supplies. However, the same does not apply to magnetic components, which, together with semiconductor switches, are the main cause of power loss in a converter. The development of heat in the magnetic components is due to the ohmic losses that occur in the windings (copper losses) and due to the hysteresis and eddy current losses that appear in their magnetic cores (core losses).

The ohmic losses are due to the flow of electric current in the conductive material of their coils, which is usually copper. Part of the electric energy is converted into heat through the

process of impact of the conduction electrons with the lattice points of the crystal structure of the metal. For given dimensions of the current carrying conductors the power loss increases excessively with increasing frequency. This is because the appearance of the skin and proximity effects leads to a concentration of the current in just a small surface part of their cross section. This fact leads to a significant reduction of their effective cross section and increase of their ohmic resistance [5], [9], [12], [41], [47], [74], [91].

At the beginning of the previous century the use of magnetic components at high frequency operation devices was an object mainly related to the evolution of radio communications and the fitting of their windings on a substrate of dielectric material was an adequate design solution [7], [10], [123]. However, in power electronic devices, the required high power density requires the use of a magnetic material core. In this way the magnetic field energy –temporary– storage capacity is multiplied. Moreover, the magnetic flux is driven into a specific path and thus the electromagnetic emission to the surroundings is avoided, while at the same time the size of the components is significantly reduced.

However, the problem that arises with the use of a magnetic core is the appearance of power losses in it in the form of heat. The magnetic hysteresis is one of the two effects that lead to the appearance of losses in a ferromagnetic material when it is subject to a periodically varying magnetic excitation [8], [13], [26], [27], [66], [80]. The other effect is the development of eddy currents in the core volume and the consequent ohmic losses [22], [44], [75], [129]. Simple iron alloys, such as those used in systems connected to the grid (e.g. distribution transformers and electric motors), exhibit very high hysteresis losses per cycle (they have a large hysteresis loop area) and, in addition, at typical power electronic converter operating frequencies it is impossible to apply the technique of reducing the eddy current losses by laminating the core. Hence, some new materials were invented, such as ferrites, which, despite the drawback of relatively low magnetic saturation induction, show extremely low losses [124], [131], [133], [140], [142]. Of course, although the use of ferrites provided a solution to the problem of core losses by reducing them to tolerable levels, it did not completely eliminate them, so we see that in an optimally designed magnetic component the core losses are of the same order as the copper losses [68], [124], [143].

Although in some applications the conditions for the operation of magnetic components are strictly defined, in most cases their various operating parameters (e.g. frequency, voltage, current, temperature) constantly change. Moreover, the response of the converters (and therefore of the magnetic components as well) to transient phenomena is almost always critical. Due to these facts, and in combination with the fact that the presence of magnetic

components in a power electronics topology plays an important role in the determination of the efficiency of the converter, the need for some appropriate analytical models and applied practical methods for the precise calculation of their losses in the various operating conditions becomes imperative. Despite many years of development in the field of power electronic applications, the calculation of losses in magnetic components is often based on the accumulated knowledge, as expressed through various empirical rules, also combined with experimental data provided by ferrite manufacturers [1], [10], [123]−[125], [128], [133], [143]. These empirical equations usually describe the operation of magnetic components within narrow limits of variation of the various parameters, without any general loss calculation methods covering all design options. Therefore, each magnetic component for each different application and for each different operating state is essentially a different problem that requires special treatment [7]−[9], [12], [13], [22], [26], [29], [41], [47], [143]. Studying the international literature, we observe that the accuracy and simplicity in formulating the results of any theoretical model are in conflict with its generality and usually the effort is focused on the direction of emergence the first two.

Of course, we should not forget that power losses are not the only problem associated with the presence of magnetic components in power electronic converters. In several cases some other parameters are also important, such as the electromagnetic emission to the environment, the distortion of the voltage – current waveforms due to the non-linear relation between magnetic intensity and magnetic induction in the core material, as well as the oscillations in voltage and current when the parasitic capacitances of the magnetic component are combined with the switching operation of the converter. Finally, the leakage inductance in transformers is a feature that, depending on the application, can be an advantage or a serious problem. In the present dissertation, however, the above issues are raised only for a rough outline and the emphasis is on the issue of losses.

2. Objectives of this dissertation

From the brief introduction right above the importance of having knowledge of the phenomena that take place in magnetic components when they carry high-frequency currents gets clear. But this knowledge should not be general and superficial. It is necessary to have a correct perception of the extent and the way in which each phenomenon affects the operation of the magnetic components and consequently the operation of the other stages of the

converters in which they are included. There must be reliable, accurate and easy-to-use models for someone to be able to calculate critical quantities in magnetic components, such as the losses, even before the implementation of a converter device. Very important too is the possibility of having the appropriate device and a valid, accurate method for obtaining reliable experimental measurements, to allow the verification of theoretical models and the obtention of information that cannot be derived from theoretical approaches.

The above context also includes the objectives of this dissertation. The most important of these is **the development of a new model for the calculation of copper losses at high frequencies when the conductors in the windings present a random arrangement in the available space**. The case of windings with conductors arranged in a random manner, although a common design choice, is not described by the well-known models for the copper losses, thus forcing magnetic component designers to resort to approximate methods that lead to significant errors. Moreover, for the case of uniformly arranged conductors, some special phenomena which have an effect on copper losses are investigated. The aim of this investigation is to carry out a **qualitative and quantitative analysis of the edge effect in the windings of magnetic components as well as to examine the special situation that occurs in relation to the proximity effect when the conductors are placed in a hexagonal arrangement.** The purpose of this analysis is to investigate the extent and manner in which high frequency effects occur in these cases and to clarify their effect on copper losses.

Another goal is also to **validate the reliability and clarify the limits of application of the most important of the models for the copper loss calculation,** in order to eliminate the relevant confusion around this issue. Finally, another fundamental goal of the dissertation is the **development of a complete set-up and a methodology for obtaining reliable experimental measurements on magnetic components**, to make possible the experimental determination of the losses, as well as other parameters, necessary for the prediction, through various existing models, of the behavior of magnetic components in real operating conditions.

In order for the above objectives to be clearly included into the wider context of the existing scientific knowledge, the literature review precedes the rest of the work. Through this review the various models for describing and calculating the losses in magnetic components are recorded and evaluated.

Thus, the first step in the context of the dissertation was to gather from the international literature the most important works on magnetic component losses. This material is presented

in a concise, but at the same time complete and understandable way, along with a comparative list of the works dealing with similar issues, in order to highlight their advantages and disadvantages.

The study of the literature, which took place throughout the elaboration of the dissertation, in the beginning served the need of obtaining general information on the given subject and the direction of the research effort to those sectors that are a suitable ground for the output of original scientific results. The ultimate goal of this work, however, is for the reader of the dissertation to be able to easily come to a conclusion about whether a proposed method, model, or theoretical result found in the literature is appropriate for his own purposes or not.

Then, with the help of finite element software, the accuracy of the results and the application limits of the classical copper loss calculation models are determined, the effects that take place in the windings of the magnetic components in the area near the yoke are analyzed qualitatively and quantitatively and finally, the impact of the proximity effect on windings of round cross-section conductors with a hexagonal arrangement is investigated. The aim is to present the results both by formulating simple, descriptive conclusions and by presenting parametric diagrams that graphically illustrate the dependence of critical quantities as a function of various geometric quantities and frequency.

The use of finite element software also supports the establishment of the new model, which aims to the accurate determination of the high-frequency copper losses in magnetic component windings the conductors of which are randomly distributed within the available space. The purpose is for the parameters of the new model to be quantities that are easily calculable, that is, to be related to quantities that are either known to the magnetics designer or very easy to be measured.

The goal of developing a complete set-up, as well as a reliable methodology for taking measurements on magnetic components, is achieved by carrying out two separate works. One work is the design and analysis of a resonant converter for excitation of magnetic components with high frequency sinusoidal voltage. The aim is to make the detailed theoretical and experimental analysis of the operation of the converter the basis for the possibility to manufacture it with the desirable specifications, in terms of operating frequency, output power and harmonic content of the output voltage. The second work is related to the analysis of the various error factors involved in the experimental procedure and to the corresponding suggestions for the selection of the most appropriate methodology to

take measurements, reduce the errors and correct the result in some cases if the error of specific parameters is known.

It should be noted that the division of the dissertation into chapters and the choice for the order of their presentation do not strictly follow the order in which its objectives were stated above and have been made to facilitate the reader in understanding the various issues it deals with.

CHAPTER 1

ELECTROMAGNETIC EFFECTS IN MAGNETIC COMPONENTS

1.1. General issues

The particular behavior of magnetic components (transformers and inductors) when they carry high-frequency sinusoidal currents, is a matter that concerned researchers since the early decades of the 20th century [3], [4], [5]−[7], when the electromagnetic theory had taken its final form from J. Maxwell [2], [130]. Effects taking place in the windings, such as skin and proximity effect, the difficulty in modeling the ferromagnetic material of the core, as well as the absence of reliable confirmation experiments, had kept relatively low the level of various theoretical studies (such as S. Butterworth's work on copper losses of solenoid coils [5]−[7]). As a result, the usual tactic was to draw up some set of simple, mainly empirical rules, necessarily of limited scope, to assist magnetic component designers [123]. Such manuals, which include, both the results of various theoretical studies and the accumulated empirical knowledge on magnetic components design, are widely used today [124], [128], [143].

In 1966, P. Dowell presented an extremely important theoretical work [12], later used unaltered or with modifications to describe the different electromagnetic quantities of the winding (distribution of currents and fields, power losses) [14], [20], [24], [68], [79], [100], [108], [124], [128]. Before that, various works had preceded on the same issue, based mainly on the direct analytical solution of Maxwell equations [4], [11], but were difficult to apply on practical problems, in contrast with the results of Dowell's work, which are well-known for their simplicity.

Similarly, about the magnetic material of the core, further than various modeling efforts that will be mentioned in the following, on the major issue of loss prediction, magnetic component designers, to this day, usually use one of the forms of the Steinmetz equation [1], which gives the specific losses of a material as a function of frequency and magnetic induction for a limited range of values of these two parameters. This equation is combined

with various data given by the manufacturers of materials and by various approximate methods the calculation is adapted to the specific conditions of each problem (core geometry, voltage-current waveforms, etc.).

The appearance and development of electronic power components, as well as the need for ever greater power densities (increase of the required power – decrease in the volume of devices), has led to the design of power converters with non-sinusoidal currents of high frequencies (hundreds of kHz). In this direction have also contributed new technologies for the manufacturing of ferromagnetic materials (e.g. ferrites) with the desired characteristics [124], [133], [140], [142], as well as the development of resonance topologies [84], [88], [110], [112], [113], [116], [117], [120], [135], [139], which enable low switching losses on semiconductor components, even at frequencies of the order of MHz. At the same time, there was an effort to study and model the magnetic components that operate under the above conditions, with main objective the design optimization and prediction of critical quantities, such as throughput power, efficiency and temperature rise [17], [18], [20], [24]. New experimental measurement techniques, also assisted by the evolution of computers and measuring systems [28], [38], [40], [57], enabled a more thorough study of the different types of core and the development of models that describe the behavior of these materials under periodic magnetic excitation conditions [26], [43].

Given the modern theoretical tools and the constantly increasing computing power of computers, new efforts were made on magnetic component modeling and on the improvement of some already existent theories. These works extend on three main axes:

(a) Analytical solution of Maxwell equations, e.g.: [54], [98], [134].

(b) Solution following successive assumptions – simplifications that limit the complexity of the problem, e.g.: [21], [33], [45], [71], [72].

(c) Use of finite element methods in a computer to extract reliable results, e.g.: [56], [70], [107], [159], [160].

Each of the previous approaches has problems and limitations. The method (a) is disadvantaged by the fact that its application is limited only to cases where the symmetry of the problem allows the straight-forward solution of the Maxwell equations. Methods (b) generally suffer low accuracy and cannot lead to general solutions because they focus on specific problems. Their usual starting point is the selection of some assembly and functional parameters through empirical rules and the application of the method for the description and

optimal selection of the others. The methods (c), although accurate, must be applied on a case-by-case basis and require, even with the most sophisticated commercial software, high computational power and runtime, which increase excessively when time is entered as a problem variable.

The result of the several works to date is a series of theoretical studies in the frequency range up to approximately 250kHz, for sinusoidal and non-sinusoidal voltage and current waveforms. Their validation is mainly performed with finite element method (especially in the most recent publications), while reliable experimental measurements appear only for the lowest frequencies. For frequencies above the 250kHz limit, a qualitative study of the effect of various geometric parameters on the losses of magnetic components (e.g. in flat PCB coil transformers) is mainly carried out using finite element software [34], [35]. In relatively recent works [79], [83] there is an effort to calculate and model the copper losses for frequencies up to approximately 1MHz and for non-sinusoidal waveforms, but limited to specific operating conditions and winding geometries.

Detailed studies have also been carried out on fundamental frequencies up to 400Hz, at which the largest amounts of electrical energy are produced and transmitted (e.g. [136], [144]). In these works the study of effects for frequencies of approximately 1 or 2kHz is considered sufficient to include any harmonic content of the voltage-current waveforms.

The difficulties in creating satisfactorily accurate and as possible general models are due to the very strong nonlinearities and the simultaneous and interrelated contribution of the core and winding to the abovementioned electromagnetic effects, which complicate the analysis of the problem. Some characteristic problems that lead to the absence of substantial theoretical studies on frequencies greater than a few hundred kHz are:

- The development of eddy currents in ferrites for frequencies above a limit (from 150 to 250 kHz for the usual types of ferrites used in electronic power converters).
- The occurrence of electromagnetic oscillations (standing waves) in the core volume and the appearance of the skin effect for the eddy currents of the core for frequencies of the order of MHz.
- The edge effect (significant increase in the current density at the ends of the winding, especially when it consists of foils).
- The development of capacitive currents in the winding, already from one fifth of the resonance frequency of the magnetic component (see §5.5.).

Moreover, it should be noted that the wide variety of design options and topologies makes each magnetic component a specific problem.

The first three chapters of the dissertation present some of the most important studies that have been done in the effort to understand the effects that take place in magnetic components when they carry high frequency currents. This presentation is concise and its aim is not to reproduce the original works, but mainly to list the basic principles on which they are based, their philosophy of development, and some of the their important conclusions, since, even today, many of them are keys to an optimal inductor and transformer design. Moreover, throughout the dissertation, where necessary, there are references to the related literature, to support a better comprehension of what is written.

The collection of literature has been continuous throughout the elaboration of this dissertation, while its study and classification proved to be a work much harder than initially estimated. Purpose of this continuous literature update was, on the one hand, to direct the work towards those areas of the given cognitive object in which there was a favorable field for original research activity, and on the other hand the acquisition of knowledge of current developments, both in the field of theoretical analysis of the relevant subjects and in that of experimental measurement methods and practical applications of theoretical results.

1.2. Introduction to electromagnetic effects

1.2.1. General issues

In Ch. 2 and Ch. 3 is the quotation of various efforts, which have been made to date by the scientific community to find and formulate the rules governing the electromagnetic effects that take place in magnetic components. Before that, however, a brief, primarily qualitative description of them would be informative. These effects are the skin effect and the proximity effect, which occur in conductors that carry high-frequency currents and the effects of hysteresis and eddy currents and the resulting losses, occurring in a material when it is subject to a changing magnetic field. The first two are also effects of the appearance of eddy currents in the current carrying conductors when they are under the action of a changing magnetic field. The hysteresis occurs in materials with non-zero magnetization.

Further than the need to describe these basic effects, as the operating frequencies of power converters increase new problems arise for the magnetic component designers, which

are also summarily described in the subsequent sections. One example is the development of electromagnetic oscillations in the volume of magnetic cores.

1.2.2. Eddy currents

It is readily concluded from Maxwell equations [2], [130] that the existence of a changing electric field E imposes the creation of a magnetic field B with magnitude proportional to the time derivative of E and direction perpendicular to it everywhere in space, while the exactly reverse relation also applies. These interactions are described by the following equations, which are two of Maxwell's four general form equations in integral form:

$$\oint H \mathrm{d}l = \int_S \left(J + \frac{\partial D}{\partial t} \right) \mathrm{d}s = I_{total} \tag{1.1}$$

$$\oint E \mathrm{d}l = -\int_S \frac{\partial B}{\partial t} \mathrm{d}s \tag{1.2}$$

In these equations, which correspond to Ampere's and Faraday's laws respectively (in Ampere's law Maxwell added the displacement current $\partial D / \partial t$), H is the magnetic intensity, B is the magnetic induction or, as otherwise named, magnetic flux density, J is the conductivity current density, D is the electric displacement, while $\mathrm{d}l$ and $\mathrm{d}s$ are the vector differentials of length and surface respectively. In both equations, the surface S is any open surface that is terminated on the closed curve on which the left-hand side is integrated and I_{total} in (1.1) is the total current that penetrates this surface.

Hence, when a material is under the action of an alternating magnetic field, it is inevitably also under the action of the resulting alternating electric field. If the material is conductive, the result will be the creation of some closed internal currents and the consequent heat generation due to ohmic losses. This energy comes from the cause of generation of the

---

[1] Referring to the "cause of generation of the alternating field", we want to separate the case examined here, in which a conductive material remains stationary in a changing magnetic field, in which case the energy of losses due to eddy currents comes from the field generation system, in contrast to the one in which the conductor moves within a static magnetic field, in which case the loss energy comes from the means that supplies the conductor with kinetic energy. Obviously there can be a combination of the two cases.

alternating magnetic field[1]. The power of these losses depends on the conductivity of the material, but also on geometric parameters and is approximately proportional to the square of the frequency, although the exact dependence on frequency is a function of various factors, among which the frequency itself [83], [124]. The loss of energy is not the only result of eddy currents, but also important is the creation of a magnetic field that opposes the externally imposed field and weakens it, which, in respect of a magnetic core, practically means a reduction in the effective magnetic permeability [55].

For magnetic cores, resolving the problem of losses due to eddy currents is basically achieved in two ways: a) For low frequency applications (less than 1kHz) it is sufficient to laminate the conductive material along the direction in which the field is applied to decrease losses by a large percentage. b) High frequency applications require the use of specific ferromagnetic materials (e.g. ferrites) that have extremely low conductivity (almost negligible) up to a frequency limit. Typical values for this limit range from a few tens of kHz to a few hundred kHz, while in modern materials for power electronic applications this limit is set in the range of a few (2 to 4) MHz. The reason for this increase in electric conductivity with frequency is analyzed in Ch. 2, which refers to the losses of the magnetic material of the core of magnetic components.

However, as it has already been mentioned, losses due to eddy currents also appear in the windings of magnetic components, an issue analyzed in the following paragraphs.

1.2.3. The skin effect in an isolated current carrying conductor

At high frequencies, the current carried by a conductor is not evenly distributed throughout its cross-section, as when we have direct (dc)[2] current, but tends to be distributed in a thin outer shell. This effect is a result of the varying magnetic flux within the conductor due to the self current of the conductor, which only encloses part of this current. The solution of Maxwell equations shows that the eddy currents are developed in such a way as to amplify the current near the surface and damp it down towards the center of the cross-section of the conductor. An equivalent aspect comes from the observation that those areas of the cross-section of the conductor enclosed by a larger number of flux lines have a greater inductive reactance to the cause of the alternating field[2], which is the electric current. Thus, a redistribution of the current density on the cross-section of the conductor is caused, so that areas with a lower inductive reactance (near the surface) are charged with more current. This fact, in a circular cross-section conductor, leads to a maximum current density on the surface and minimum in the centre (see Fig. 1.1, §1.2.4). For a square cross-section of the conductor

we have a maximum density at the corners, lower at the sides and minimum in the centre while for other geometrics we have corresponding distributions [123].

The redistribution of the current results in an increase in the R_{ac}/R_{dc} ratio above unity, where R_{ac} is the effective resistance of the conductor when it carries a sinusoidal current of given frequency and R_{dc} its resistance when it carries a direct current. This is to be expected, since some parts of the conductor contribute less to the current transmission and therefore the effective cross-section of the conductor decreases. Further than the increasing resistance, the redistribution of the current is always such that the coupling of the magnetic flux with the conductive material is decreased, compared to the case where the current is direct. Due to this, the energy of the magnetic field in the conductor volume decreases (outside the conductor it remains constant for a given current intensity). Therefore, the total magnetic field energy –inside and outside the conductor– decreases, which is equivalent to a decrease in the total self-inductance of the conductor.

The increase in the effective resistance R_{ac} and the decrease of the inductance L_{ac} rise with the frequency f of the current, as well as with the specific conductance σ, the magnetic permeability μ and the dimensions of the cross-section of the conductor (Appendix I). An important quantity for the description of the skin effect is the skin depth δ, defined as the depth from the surface of the isolated circular cross-section conductor in which, for sinusoidal quantities, the current density has taken the value $1/e$ of the value on the surface, where e is the base of the naperian logarithms (an equivalent definition is given in Ch. 4). Skin effect δ is a function of σ, μ and f [129] and is given by the equation:

$$\delta = \frac{1}{\sqrt{\sigma \pi \mu f}} \tag{1.3}$$

---

2   The term "alternating" is used improperly here, while more correct would be the expression "changing" or "time-varying". However, since the existence of a constant term in the waveform of a periodic electromagnetic excitation can often be studied separately in terms of its effects and the periodic variation of a quantity can be given by the sum of "alternating" sinusoidal terms of a Fourier series, this catachresis is justified (since usually we do refer to periodic quantities) and we find it in many scientific writings. For the same reason, in many points of the text, we will say "direct" or "dc" meaning "constant in time" since, referring to periodic electromagnetic quantities, the constant term of the Fourier series (the average value) has prevailed to be referred to as "direct" or "dc" component.

For example, for a temperature of 20$^{\text{o}}$C, at the frequency of 50Hz the skin depth for copper is 9.3mm, while at 1 kHz is 2.1mm and at 50kHz is 0.3mm.

1.2.4. The proximity effect

We have therefore seen that a wording for the description of the skin effect would be to say that the eddy currents are superimposed on the current of the conductor and this results to the final distribution of the current density, while another would be to say that the current is redistributed in such a way that the conductive material is partially screened against the varying magnetic field. However, these formulations highlight the generality of the effect and indicate that there will be a redistribution of the current even if the magnetic flux that penetrates the conductor is not due to the current of the conductor itself but due to the current of adjacent conductors. This case of actually the same effect determines what we call the proximity effect, i.e. the redistribution of the current density in the cross-section of a conductor due to the magnetic field created by adjacent current carrying conductors. When a current carrying conductor is in proximity to other conductors that carry a current of similar (or even higher) intensity, the magnetic field and current density distributions in it are mainly determined by the influence of these adjacent conductors and depending on the geometry of the relative position of the conductors they may have any form. Of course, in the general case, this influence peters out when the distances of the adjacent conductors from the conductor in question increase. However, for a large number of conductors whose distances from their adjacent conductors are of the order of the dimensions of their cross-section the proximity effect on each of them is definitely much greater than the skin effect. The result is again the concentration of the current in the areas of the cross-section of the conductor where the magnetic field appears stronger and this in turn results in higher effective resistance. As an example, in an infinite solenoid inductor carrying an alternating current, the magnetic intensity is maximum within the inductor and zero outside, with a gradual reduction as we run through the winding from the inside to the outside of the inductor. The proximity effect, in this case, will result in an increased concentration of current at the inner side of each layer of the winding i.e. the side of the cross-section of the conductors closer to the inductor symmetry axis, there where the magnetic intensity is higher (see Appendix III).

In Fig. 1.1 [124] we see in a descriptive way the effect of the two effects (proximity and skin) on a conductor that carries an alternating current. In case (b) the adjacent conductors carry the same current and produce a magnetic field with the direction shown in the figure. The continuous line for the current distribution in case (b) corresponds to moderately high frequencies, for which, according to the author of [124], the ratio of the radius of the conductor to the skin depth is lower than 2 ($r/\delta<2$), while the case of higher frequencies is presented with a dashed line. Parameter *x* represents the distance from the center of the cross section. In fact, as it comes up from the analysis in Ch.4 and Ch.5, the linear profile in magnetic intensity and current density at *x* direction, perpendicular to the direction of the proximity field, is a condition overturned at considerably lower frequencies.

It should be noted that it is appropriate to use the r/δ ratio as a parameter for describing the effects associated with the development of eddy currents in circular cross-section
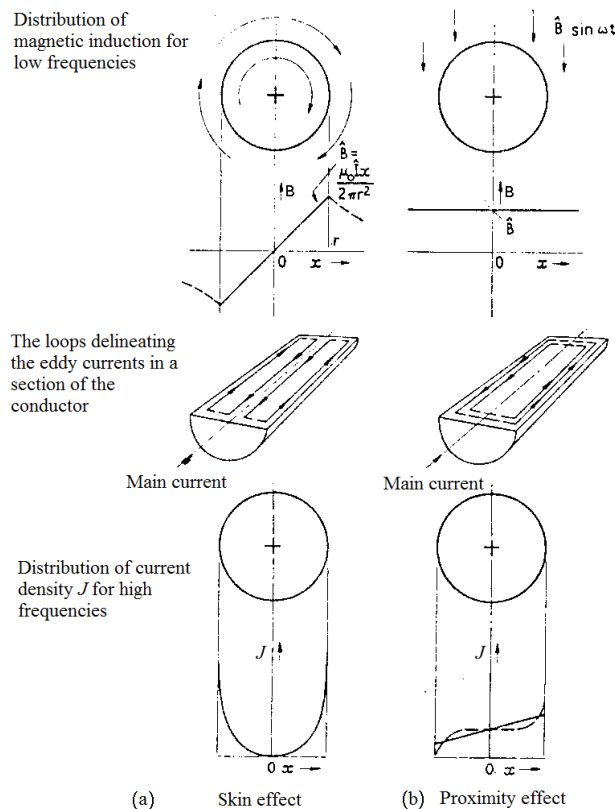

Figure 1.1: The skin and proximity effects in a circular cross-section current carrying conductor [124].

current carrying conductors since, in the absence of additional effects (e.g. capacitive currents), it is the value of the above ratio which determines the relative change of several quantities and not the absolute value of the frequency. For other conductor geometries, instead of *r*, a corresponding critical dimension of their cross-section is used. The above convention, which is also adopted in this dissertation, is found in almost all relevant scientific work.

In conclusion of this introductory presentation on eddy currents in current carrying conductors, it should be noted that technological development in the field of superconductive materials leaves no room for hope that we will see any large-scale applications in the near future and therefore the use of copper will definitely be the best option for many more years to come. Materials that maintain their superconducting properties at temperatures close to ambient temperature, except that their production cost is high, they are still in the phase of research development and do not have the required mechanical properties to replace the conductors, while even the low depth cooling they require in some cases (e.g. ceramic superconductive materials at -40°C) makes their use extremely problematic. Moreover, the requirement for cooling at temperatures close to the absolute zero of various other alloys, in order to have superconducting properties, so far restricts their use only to sophisticated applications, such as the windings of electromagnets in large particle accelerators. Still, under development are some new promising technologies, such as the exotic nano-materials (e.g. carbon-based nano-tubes) and graphene structures. Some of these materials are characterized, among other things, by appropriate conductivity values and have already begun to be experimentally used in applications where the achievement of small sizes is of high priority, such as the creation of integrated circuits and the transmission of electrical signals in applications of microelectronics (logic circuits, LCD screens etc.). It is therefore not excluded that we will see in the near future "magnetic nano-elements" for the creation of microscopic power supplies embedded in integrated circuits or even wider scale applications of these materials in the fields of electronic and electrical engineering.

At the same time, for applications in which skin and proximity effects become important, researchers are looking for the advantages of using aluminum instead of copper [14], [156]. The lower specific conductivity of aluminum leads to higher skin depths, a fact that significantly balances its undoubted disadvantage at low frequencies. When in a given application the frequencies are very high and in the windings there is no dc component of the current, the use of aluminum, which in recent years has become much cheaper than copper, potentially gives an economically preferable solution. The problems in the use of aluminum,

so far, are focused on its metallurgical processing and the difficulty in creating welds and electrical connections.

1.2.5. Magnetic hysteresis

The magnetic properties of atoms are due to the possibility of magnetic dipole moment in them, which in turn is due to the quantum spin quantity of the elementary particles and the movement of electric charges on an atomic scale [127], [145]. The important thing is that the magnetic moments of atoms appear quantized at various energy levels (in magnitude and by direction) and under the action of an external cause (e.g. magnetic field) they can jump from one level to some other, absorbing the required amount of energy for this change [126]. However, in the majority of materials, at room temperature, the application of any external magnetic field cannot result in any significant change in their macroscopic magnetic state. This is because of the absence of magnetic dipole moment in atoms, or because their magnetic dipole moments remain randomly oriented due to their thermal energy.

The macroscopic magnetic properties of solid magnetic materials, with a chemical composition usually based on iron (Fe), nickel (Ni) or cobalt (Co), are due to the autogenous existence of microscopic regions (Weiss regions) in which the atomic dipole moments appear oriented to one common direction and therefore, each such (saturated) region exhibits an elementary magnetic dipole moment. In the general case, a magnetic material sample appears magnetically neutral, as these elementary magnetic dipole moments are randomly oriented. With application of an external magnetic field, the elementary magnetic moments can be oriented according to it, to a degree that depends, both on the value of the applied field, and on other material-related factors. This orientation, for some materials, is maintained in a large percentage of the dipoles even after the field is removed, which results in the sample appearing magnetized. Contrariwise, heating or a strong mechanical shock in a magnetized sample can restore the random distribution of elementary magnetic moments and the material then appears altogether magnetically neutral. The laws governing the effects related to magnetization processes are statistical in nature, while their detailed formulation and understanding also requires the knowledge of quantum physics and –if we refer to solid materials– solid-state physics [126], [127].

As for how this orientation spreads to a macroscopic sample when the external magnetic field varies, various theories have been proposed, some of which will be cited in the next paragraph. What is interesting here is that this change absorbs some energy derived from the external cause, which is stored in the elementary magnetic dipoles, while at the same time

some energy is converted into heat. In the reverse change of the dipoles magnetic state, with the application of a new external cause, a percentage of the previously stored energy is also converted into heat, making the whole process an irreversible change, as termed in physics.

In the absence of eddy currents, the magnetic intensity $\boldsymbol{H}$ is proportional to the current i used externally for the field creation and is given by the equation:

$$\oint \boldsymbol{H} dl = i \tag{1.4}$$

If there is some conductive material in space and eddy currents appear, to the current i we should add the term i_{eddy} which represents the ampere-turns of eddy currents through an open surface which is terminated on the closed curve for which the integral of (1.4) is calculated. In the presence of magnetic material, the equation between $\boldsymbol{H}$ and $\boldsymbol{B}$ is as follows:

$$\boldsymbol{B} = \mu_0(\boldsymbol{H} + \boldsymbol{M}) \tag{1.5}$$

where $\boldsymbol{M}$ is the magnetization of the material. The existence of the material and the effect of magnetization on the magnetic field can be taken into account by introducing the magnetic permeability μ of the material and then the previous equation becomes:
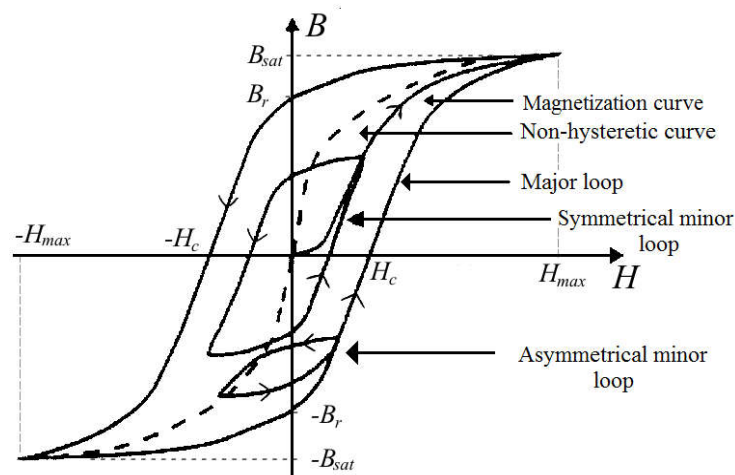

Figure 1.2: The curves related to the hysteresis effect on a macroscopic scale.

$$\boldsymbol{B=\mu H} \qquad\qquad\qquad (1.6)$$

The magnetic permeability μ_0 of the free space has a value of $4\pi 10^{-7}$H/m and the magnetic permeability of a material is often expressed by the relative magnetic permeability μ_r, which is the ratio of μ to μ_0 ($\mu_r=\mu/\mu_0$). The important thing about the hysteresis effect is that magnetic permeability is not constant, but depends (for an isotropic material) from H, from the magnetization history of the material and from its temperature[3].

For the macroscopic description of the effect we use the plot of the magnetic induction B as a function of the magnetic intensity H. In Fig. 1.2 appears, among other relevant curves, a typical hysteresis loop (major or main loop). The main loop, when the variation of H is "slow", is often referred to as a static loop. A sinusoidal time variation of H between the values $\pm H_{max}$ will result in a periodic sweep of the static loop, with the sense of rotation marked on the graph, if the frequency is sufficiently low (e.g. 50 Hz if we refer to ferrites). Quite important are the intersection points of the loop with the axes marked as B_r (remanence or retentively) and H_c (coercive force, coercive field or demagnetizing force), as well as the saturation induction B_{sat}. The saturation effect is also very important for the magnetic component designers, since it is an important restrictive factor in the capabilities of magnetic components. In the saturation range, despite any increases in H, magnetization does not increase and the slope of the $B(H)$ curve tends to the value μ_0. Division of the slope of the magnetization curve at any point on the H–B plane with μ_0 results in the differential permeability:

$$\mu_d = \frac{1}{\mu_0}\frac{\mathrm{d}B}{\mathrm{d}H} \qquad\qquad\qquad (1.7)$$

---

[3] For anisotropic materials, their magnetic properties (and therefore the hysteresis loop) vary depending on the direction examined each time. Declaring as vectors the quantities $\boldsymbol{B}$, $\boldsymbol{H}$, $\boldsymbol{M}$, the magnetic permeability should also be declared as a tensor. But we avoid this here because we discuss about isotropic materials. In various points, we also study the magnitudes B, H, M of the quantities without causing confusion with the corresponding vectors.

At high frequencies, the shape of the hysteresis loop may vary, with the greatest change in the increase of H_c, which makes it appear more flattened [75]. At even higher frequencies, and/or for non-sinusoidal current waveforms, the shape of the loop may be, in short, irregular [38]. The energy per unit volume delivered by the external cause of the field change, during the process of hysteretic magnetization of a material, is given by the equation:

$$W_m = \int_{B_1}^{B_2} H \mathrm{d}B \tag{1.8}$$

where B_1 and B_2 are the initial and the final value of the magnetic induction respectively. Percentage of this energy is absorbed to change the magnetization of the material, while the rest is converted into heat. Therefore, the energy consumed per unit volume for a full magnetization cycle is given by the area of the hysteresis loop.

But a model for the magnetic hysteresis, such as those that will be cited in Ch. 2, except the major loop, should also describe a number of other curves at the H–B plane which are also shown in Fig. 1.2:

- Referring to a closed magnetic path within the material (material sample without gap), the magnetization curve is traced by gradually increasing the magnetic intensity, starting from a state at which the material appears magnetically neutral. Its slope near the beginning of the axes determines what in the international literature is referred to as the initial magnetic permeability μ_i, a quantity involved in the expression of several magnetic properties of the material or of a core made of it [124], [140], [142].

- A symmetrical minor loop is traced in the same way as the major, but it differs in that the endmost magnetic intensity values are lower than $\pm H_{max}$ and respectively the maximum value achieved for magnetic induction B is considerably lower than the saturation induction.

- An asymmetric minor loop will occur if during tracking the main loop or a symmetrical minor loop there is a temporary change in the direction of H variation. If, for example, while tracking the major loop with increasing H and before it reaches the value $+H_c$, a reduction toward negative values happens and then again an increase, a symmetric minor loop, such as that of Fig. 1.2, will be traced. Hence, the condition for the existence of minor loops in the case of periodic H variation is that there are more than two changes of the sign of the $\mathrm{d}H/\mathrm{d}t$ time derivative of H within one period. Such an operating state is

typical in power electronic applications, as the magnetic components are carry currents with periodic variation in time (usually not sinusoidal, but e.g. pulsating, triangular [saw-tooth] or trapezoidal [partially linear]), but often with a significant ripple. This ripple may be either due to external factors, such as electromagnetic noise, or internal factors, such as oscillations related to the presence of parasitic inductances and capacitances in a circuit that performs high frequency switching operation.

- The non-hysteretic curve describes the suppositive magnetization path of the material in a case where it would be done without losses. Experimentally, it is taken indirectly, acquiring many hysteresis loops, for various levels of excitation. It is used in circuit simulation software products, such as PSpice, to calculate the harmonic distortion of the voltage-current waveforms due to the presence of magnetic components in a circuit.

CHAPTER 2

CORE LOSSES IN MAGNETIC COMPONENTS

2.1. Introduction

The use of magnetic core in a magnetic component is dictated by the need to increase the inductance of a circuit, to amplify and drive the magnetic flux and to store energy in a specific space (by inserting an appropriate gap). The various problems arising with the placement of a core in the magnetic components have already been briefly reported. In the following, therefore, there will be briefly analyzed, mainly on the basis of the knowledge offered by the international literature, issues such as the loss of energy due to hysteresis and eddy currents, the damping of the magnetic field due to eddy currents and the deformation of voltage and current waveforms due to the non linear character of the magnetization curve. We will also give a brief description of the most important macroscopic models describing the magnetization of materials.

The aim is to illustrate the complexity of the mechanisms responsible for the above effects, as well as of the laws governing them, but also to make it clear that the different models of their description on a macroscopic scale are usually nothing but tough approximations, each providing satisfactory results only in a limited scope.

2.2. Magnetic properties of matter

As mentioned earlier, the magnetic properties of matter atoms have their origins in the movement of electrons on an atomic scale and in the quantum quantity of spin [126], [127], [145]. The contribution of the magnetic dipole moment of the atomic nucleuses and that of the conductivity electrons of conductors to the effect of magnetism comes in particular cases of generally lower importance. The quantity of the magnetic dipole moment is used to describe the (magnetic) properties that the space acquires in the vicinity of an atom, but it is

right to be treated as a quantum vector quantity and not to be confused with the vector quantities we use to represent magnetic fields on a macroscopic scale.

However, one can come up with equations for the well-known quantities *H*, *B*, *M* which describe the magnetic properties on a macroscopic scale, starting from the atomic magnetic dipole moment and by applying laws of quantum mechanics, statistical physics and solid state physics. In the volume of a material where atoms have a periodic spatial arrangement (crystal lattice), the structure of the material appears as the sequential iteration of an elementary atom arrangement, which we call the primitive cell of the lattice. It is relatively easy to examine the properties of the material considering the primitive cell as the smallest area that can be studied separately. This way, the magnetic dipole moment of a cell is calculated and then the macroscopic magnetic properties of a sample are based on the study of its crystal structure. A certain fact is that the given each time arrangement of the atoms in a cell, combined with the requirement of minimum magnetic energy, favor the orientation of the magnetic dipole moment of the cell at specific directions, so that an anisotropy arises in the magnetic properties on a primitive cell scale. This anisotropy will only emerge macroscopically in a monocrystal (a sample of material in which there is no disturbance of the crystal structure).

In ferromagnetic materials (in §2.3. there will be reference to the different categories of magnetic materials), magnetic saturation is achieved when the magnetic moments of all the primitive cells of the crystal lattice are aligned according to the external field. If we assume a saturated sample like that of the case (a) of Fig. 2.1 [127] and calculate the magnetic energy contained therein, we will find that it is higher than the corresponding energy of the sample in case (b), in which the sample consists of two saturated domains with opposite magnetization, while in case (c) the energy is even lower. The cases (d) and (e) correspond to zero magnetic energy [145]. In the light of the principle of minimal energy, which governs all autogenous physical processes, we conclude that the existence of magnetic domains in a material (Weiss domains) is the natural outcome of a system.
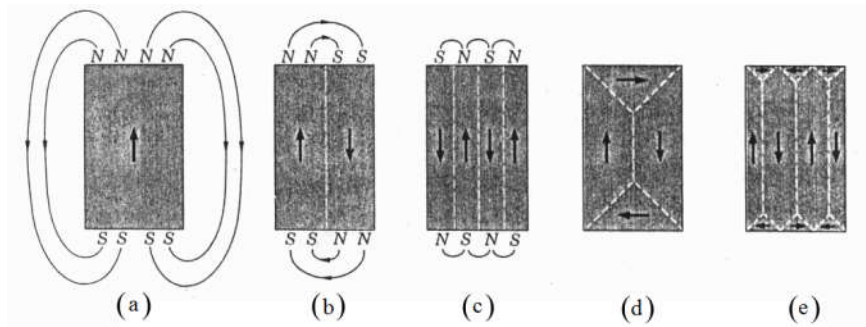
Figure 2.1: The origin of magnetic domains is related to the tendency of a system to be in minimum energy state [127].

Magnetic domains are separated from each other by separative zones, which in the international literature are named domain walls or Bloch walls [145]. In these zones the change in the direction of the vector of magnetization is gradual from the one area to the other, since such a gradual transition, with the wall thickness equal to many constants of the crystal lattice (about 300 for iron), shows much less energy than in the case of a sharp change in magnetization between two adjacent cells of the lattice. In a sample in which the crystal structure exhibits discontinuities (these discontinuities [dislocations] may be of various kinds [146], [147]), it is observed that they favor the development of magnetic domain walls in the same area of space. Moreover, it is quite possible for a domain wall to be terminated on a crystalline dislocation. When this is the case, a displacement of the magnetic domain walls often also entails the displacement of these crystalline dislocations. It would be wrong to consider these displacements as similar to the relative movement with friction of two objects, but, intuitively, one can understand that they are accompanied by forces of "friction" that oppose them.

When applying a weak external field (of the order of mT) to a sample of ferromagnetic material consisted of magnetic domains, what happens is a reversible or, if we borrow a term from mechanics, "elastic" displacement of the domain walls, which will return to their original position if the external field is removed. With stronger fields, we have irreversible displacements of the walls, while for very strong fields, approaching the saturation of the sample, a turn of the magnetization vector is also observed in the domains.

Apparently, during the change in the form of the domains, an exchange of energy between adjacent domains, accompanied by losses, takes place. Some energy will also be lost due to the "friction" mentioned above during displacement of the walls, while rotation of the

magnetization vectors will also lead to losses. As the frequency increases, the Bloch wall displacement acquires an oscillation character with the "friction" forces being the damping factor in this movement. It should also be noted that there is a resonant frequency for the vector magnetization in a cell of the crystalline lattice (of the order of 2MHz for ferrites commonly used in power electronic devices). If this value is approached in magnetic component operating conditions, a turn of the magnetization vector and extremely high losses are observed, even for low magnetic intensity values [31], [32], [133] (while it was mentioned earlier that turning the magnetization in a magnetic domain occurs only by applying a strong external field). Depending on the dimensions of the core, at frequencies of the same order, we may also have the development of standing electromagnetic waves in its volume, an effect that we will analyze in the next.

It is therefore understood that **for each material, above some frequency, the calculation and theoretical analysis of losses under conditions of periodic magnetic excitation is not a simple case of combining hysteresis and eddy currents, in the same way these phenomena are described for low frequencies.** However, since modern requirements in the field of power electronic converters gradually lead to an increase in operating frequencies to even higher than 1MHz (§3.3.3.), a corresponding progress in the field of material manufacturing has been achieved to enable such applications. As an example, we mention Ferroxcube 3F3, 3F35 and 3F4 ferrite grades for applications at switching frequencies up to 500kHz, 1MHz and 3MHz respectively [32], [142], as well as Epcos ferrite N49 for frequencies up to 1MHz [140].

Thus, without a deeper investigation of the physics of these effects, we identify the causes of hysteresis as related to three different factors:

a) Interaction between magnetic domains.
b) Anisotropy.
c) Internal "friction" forces with the displacement of various discontinuities in the volume of the material.

The dominant effect each time is different for the various materials and of course depends on the level and frequency of the excitation imposed by the external field.

In literature there are various methods to approach the subject of material magnetization and model the hysteresis loop. Several of them are simple attempts to find appropriate expressions by some curve fitting procedure so as their results to approximate some experimental data and fall short of generality, while some other, which take into account all

the effects related to energy levels on a microscopic scale, become particularly "heavy" for application to practical problems.

Although the detailed description of the previously mentioned issues is a whole chapter of the solid-state physics and therefore does not belong to the purposes of this presentation, in the next paragraph we will outline these mechanisms by shortly describing four of the most important macroscopic models for magnetic hysteresis. We will see that each of them gives more weight on only some of these mechanisms and therefore applies to only a specific category of materials.

2.3. Magnetic materials – ferrites

By studying the behavior of a macroscopic sample when applying an external field to it, magnetic materials can be divided –at first– into three categories: diamagnetic, paramagnetic and ferromagnetic.

The diamagnetic materials, with the application of an external magnetic field, are weakly magnetized, with the vector of magnetization having the same direction as the external field and magnitude of opposite sign. The majority of the materials have diamagnetic properties, while the most intensely diamagnetic material is the bismuth (Bi). Organic compounds and water also have diamagnetic properties.

Paramagnetic (materials with unpaired electrons in the outer shell of their atoms) with the application of an external field are magnetized weakly at the same direction with it. Their atoms have permanent magnetic dipole moment, but with the application of an external magnetic field only a low percentage of them are aligned with the field. Examples of paramagnetic materials are aluminum (Al) and platinum (Pt).

Finally, ferromagnetic materials are strongly magnetized in the same direction as the external field. Without going into details about the first two categories we will notice that the ferromagnetic materials are those of practical interest, since they have a high positive value for the relative magnetic permeability μ_r (up to 20.000) and are used in various applications, such as permanent magnets, magnetic components (inductors – transformers), electric motors, information magnetic storage, etc. It should also be noted that one major difference between diamagnetic, paramagnetic and ferromagnetic materials, in addition to the magnitude of their

magnetization, is that, for the first two categories, magnetization vanishes when the external field is removed.

Ferromagnetic materials can also be divided into categories depending on their magnetic properties. A general separation classifies them in hard and soft, with the first characterization referring to those with high remanent magnetization B_r (as a percentage of the saturation magnetization) and high demagnetizing force H_c, while the opposite applies to the soft materials. Hard materials are used for the manufacture of permanent magnets and in applications where the "memory" of the material's magnetization history is necessary (magnetic recording), while the soft ones in applications requiring low hysteresis losses (e.g. magnetic components), since the area of their hysteresis loop is small.

The deeper study of the mechanisms under which elementary magnetic moments interact, both between them and with an external field, leads to the definition of two more categories of materials, which are the ferrimagnetic and the anti-ferromagnetic. Ferrimagnetic materials have the macroscopic properties of the ferromagnetic ones, but generally exhibit significantly weaker magnetization, while in anti-ferromagnetic materials the magnetization caused by the application of an external field is practically negligible.

Ferrites are ferrimagnetic materials (iron oxides) which began to be experimentally manufactured in the late 1920s and began to be widely used only after World War II. They have the generic formula X-Fe_2O_4, where X is some, or a combination in various proportions of some of the following metals: iron (Fe), manganese (Mn), cobalt (Co), nickel (Ni), copper (Cu), zinc (Zn), magnesium (Mg) and cadmium (Cd). The impurities selected each time give their name to the ferrite. Thus, for example, we can say that the most important for practical applications are manganese – zinc ferrites (Mn-Zn) and nickel – zinc ferrites (Ni-Zn).

Although hard ferrites have also been manufactured, the focus is on the soft ones that generally have lower saturation magnetism than raw iron, but have a number of other advantages. As such we can mention the low values for B_r and H_c (and therefore the small hysteresis loop area), high relative magnetic permeability and low electrical conductivity up to some frequency limit (different for each material), which is a necessary condition for the reduction of losses due to eddy currents.

The reason why electrical conductivity increases in ferrites with an increase in frequency is related to the fact that a macroscopic sample of the material consists of microscopic grains (crystallites) which are separated from each other by a thin insulation layer of very high resistance. The capacitance between them actually short-circuits the insulation layer at high frequencies, so then the specific resistance of the sample approximately takes the value of the

specific resistance of a crystallite. Typical values for it are 0.001Ωm for Mn-Zn ferrites and 30Ωm for Ni-Zn ferrites [35], [133]. The frequency for which the electrical conductivity begins to become significant is different for each type of ferrite and may be a few tens of kHz or a few hundreds of kHz (in most of the cases) or greater, especially for newer materials.

Ni-Zn ferrites have μ_i<1000 (the value of μ_i is indicative and differs greatly from $\mu_\alpha = \Delta B / \mu_0 \Delta H$ [amplitude permeability] often used in calculations for various applications), high specific resistance and moderate temperature stability (μ_r generally drops with temperature). They are preferred mainly in telecommunication applications (low power, high induction, broad bandwidth) for frequencies from 0.5 to 100MHz. Mn-Zn ferrites have μ_i from 1000 to 5000 and specific resistance lower than that of Ni-Zn, which is greatly reduced at frequencies well below those in Ni-Zn ferrites. They also generally present lower B_{sat} than Ni-Zn ferrites [35], [133]. They are mainly used in applications between 1kHz and 2MHz, such as magnetic components in power electronic converters.

Other alternatives, further than ferrites, are amorphous metals (processed in glass phase) and powered iron alloys, which have lower cost, greater B_{sat}, but generally exhibit more losses than ferrites [35].

2.4. Electromagnetic oscillations in the core volume

In ferrites the relative magnetic permeability μ_r as well as the electrical conductivity are functions of frequency, with a decreasing dependence for μ_r and ascending for σ, while the relative dielectric constant ε_r also varies with frequency. The manufacturer usually gives the curves describing the dependence of μ_r on frequency for the frequency range in which each ferrite is used [140], [142], but generally the corresponding information about σ and ε_r are not provided. Curves for these two quantities are provided, for example, in [124], but only for some of the available ferrite grades.

In ferrites, as in any material medium, there is a finite propagation speed of an electromagnetic disturbance. The value of this speed depends on $\mu=\mu_r\mu_0$ and $\varepsilon=\varepsilon_r\varepsilon_0$ (absolute magnetic permeability and absolute dielectric constant respectively) as well as on frequency. The propagation of such a disturbance shall be subject to reflections on the discontinuities of the material and to attenuation if the material exhibits losses. It is therefore possible for standing waves to appear in the volume of the material (resonance), which will result in an

excessive rise of the losses [34], [60], [124], [133]. In resonance state the amplitude of the induced electrical field becomes maximum and therefore the induced eddy currents produce a magnetic field that tends to cancel the magnetic flux. So, not only do losses increase, but the conditions of normal operation of the magnetic component are generally cancelled. For these reasons, it is obvious that such a situation is not desirable.

With increasing frequency, the first resonance will occur if half of the wavelength λ, for the specific material, becomes equal to the minimum dimension of the cross-section of the core. The wavelength is given by the well-known equation:

$$\lambda = \frac{1}{f\sqrt{\mu_0 \mu_{eff} \varepsilon}} \tag{2.1}$$

where of course the effective (relative) magnetic permeability μ_{eff} and the dielectric constant ε correspond to the specific frequency f, with the first one depending on the existence of a gap in the core (it is $\mu_{eff} \cong l_{eff}/l_g$ when l_g is the gap length and l_{eff} the length of the effective magnetic path in the ferrite, with $l_g << l_{eff}$, see §7.3.2.). For ferrites and core sizes commonly used in power electronic applications, the frequencies at which resonance occurs range from values just under 1MHz to approximately 5MHz [34], [133]. Therefore, one must be careful about the occurrence of this effect if he selects high operating frequencies, as it begins to affect the function of the magnetic component and to increase the losses from a frequency that is approximately half (or lower) of the one at which the resonance occurs. A simple method, however, to deal with the problem is to insert a gap in the core which reduces the effective magnetic permeability. In practice, the existence of any gap shifts the frequency of resonance to a value much higher than those for which the use of the material is considered prohibitive due to losses. For example, it is stated in [133] that for a specific core shape of the ferrite grade 3F3 for which the first resonance frequency is at 4.5MHz, a 0.05mm gap shifts it to 30MHz (it is reminded that the specific material is suggested by the manufacturer as suitable for frequencies up to 500kHz).

2.5. Models for the macroscopic magnetic behavior of ferromagnetic materials

The mechanisms that affect the hysteresis effect are on a case-by-case basis (depending on the material: polycrystalline or amorphous, isotropic or anisotropic) complex and their analytical study is not an easy task. Therefore, the creation of a model is often based on a simplified representation of the average behavior of the material. Therefore, based on this average behavior, the magnetization mechanisms, i.e. the rotation of local magnetic moments or the movement of the magnetic domain walls, are modeled. In accordance with what was reported in Ch. 1, any model must also include other important characteristics of the magnetization process such as saturation, reversible (non-hysteretic) and non-reversible processes [80]. In the following, the most important of the macroscopic models for magnetic hysteresis will be presented, as well as some other approaches to the modeling of the same effect.

*- **Preisach** model (1935)*

This model [8] is based on the view – assumption that the material consists of independent (non-interactive) particles, each of which has only two possible magnetization values, +m and –m. On the basis of the model's assumptions, at the position of each particle, the result of interaction with adjacent particles is a "net" field h_i (interacting field).

The key to the model is a distribution function, called the Preisach density function and describes the statistical magnetic behavior of a random sample of a large number of particles, which are considered infinitely small. The approximate form of this function is experimentally obtained and is different depending on the material under study. It has been shown [42], [80] that for some materials this function may have the following form:

$$p(h_i, h_c) = \frac{M_s}{2\pi\sigma_c\sigma_i} \exp\left[-\frac{\left(h_c - \overline{h_c}\right)^2}{2\sigma_c^2}\right] \exp\left[-\frac{h_i^2}{2\sigma_i^2}\right] \tag{2.2}$$

in which, except the local field h_i the demagnetizing force h_c also appears, while $\overline{h_c}$ is its average value for all particles. The σ_c and σ_i variables are the distribution widths for h_c and h_i respectively. In this formulation, the parameter of the classic Preisach model to be determined

during the experimental procedure, is M_s (saturation magnetization of the sample), while $\bar{h}_c$, σ_i, σ_c are adjustable parameters.

In order to directly take into account the interaction between particles, it was proposed [33] that the local field h_i at the position of a particle, such as its value is configured by the presence of other particles, may be associated with the macroscopically observed magnetization M through a constant ratio α ($h_i=\alpha M$), which arises as another adjustable parameter in the new formulation of the model (moving Preisach model).

- *Stoner–Wohlfarth* model (1948)

The Stoner-Wohlfarth model describes the magnetization curves of a polycrystalline material consisting of small particles that do not interact with each other and are characterized by uniaxial anisotropy. These particles are smaller than the minimum required for the formation of a magnetic domain. The magnetization of each such particle is considered to have a constant value, but its direction may vary. Anisotropy is determined by the existence, for each particle, of an axis of preferred orientation of the magnetization with its direction forming an angle ϕ relative to the vector of the external field [$\phi \in (0, \pi)$] and with a Gaussian distribution $F(\phi)$ describing the statistical behavior of the quantity ϕ in a random sample consisting of several particles:

$$F(\phi) = \frac{1}{\sqrt{2\pi}\sigma} \exp \frac{-\left(\phi - \bar{\phi}\right)^2}{2\sigma^2} \tag{2.3}$$

In this equation $\bar{\phi}$ is the average value of the angle between the field and the preferred axis of the material particles and therefore constitutes the direction of the easy magnetization axis, as it is called, of the macroscopic sample, while σ is a constant associated with $\bar{\phi}$ (it describes the standard deviation of the distribution).

This model may describe the reversible and non-reversible changes in the energy state of a particle with changes in H, due to the corresponding changes in its magnetization direction. The behavior of a macroscopic sample is derived from the statistical study of this particle behavior.

*- **Globus** model(1976)*

This model [13] refers to the soft ferrites for which Globus made some observations and after a few assumptions, concluded that the magnetization of a macroscopic sample exhibits the same behavior as that of a microscopic, spherical sample consisting of two domains with magnetization at angles 0° and 180° relative to the external field. The change in the overall magnetization of this sample is determined by the movement of the separative wall between the two domains. The three basic equations of the model give the intensity *H* of the field and the magnetization for non-reversible and reversible variations (the separative membrane may also be "elastically" distorted) and are trigonometric composite functions of the separative wall's position (this position is determined by angle *θ*):

$$H = \frac{g + \gamma \cos\theta}{M_s R \sin^2\theta} \tag{2.4}$$

$$M = \frac{1}{2M_s}\cos\theta\left(2 + \sin^2\theta\right) \qquad \text{non-reversible variations} \tag{2.5}$$

$$M_{rev} = \frac{3M_s^2 D}{8\gamma} H \qquad \text{reversible variations} \tag{2.6}$$

In these equations, *g* is a proportionality constant between the length of the circumference of the separative membrane between the domains and the friction force when moving it, *γ* is a quantity associated with the energy of the separative membrane, M_s is the saturation magnetization of the globule, *D* a constant and *R* the radius of the globule.

*- **Jiles – Atherton** model (1986)*

It describes isotropic, polycrystalline materials consisting of grains, each of which consists of many magnetic domains [26]. Any domain has a magnetization with constant direction and magnitude. Its walls can be deformed "elastically" by applying an external field (reversible variations) or even can be displaced (non-reversible variations), thus increasing the size of the domain in relation to adjacent domains. Domains the magnetization of which has a vector with small angle in relation to the variation of the external field are more favored by this variation by absorbing energy, available for their expansion. The fundamental idea of the model is based on the assumption that the intensity of the magnetic field at the position of a domain depends not only on the externally applied field ***H***, but also on the magnetization of

the adjacent domains (interaction between domains). On a macroscopic scale, the effective magnetic intensity H_e will be given by the equation:

H_e=H+αM (2.7)

where M is the magnetization of the material and α a constant which is found experimentally. If b is a constant that determines the width of the loop and M_s a constant that determines the saturation level, the non-hysteretic curve for an isotropic ferromagnetic material (from which the major loop can then be extracted) can be described by the equation:

$$M = M_s \left[\coth\left(\frac{H_e}{b}\right) - \left(\frac{b}{H_e}\right) \right]$$ (2.8)

Without going into the details of the above models, we will make some general remarks:

- These models succeed, with variable degree of success each, to describe the various curves associated with the effect of magnetization in ferromagnetic materials. Each one focuses on different material characteristics and therefore they find application in different materials and for different practical applications. We will just mention that the Stoner–Wohlfarth model is more suitable to the hard magnetic materials, that of Jiles–Atherton to the medium ferrites, Globus model to the soft ferrites, while Preisach's one to thin foils of hard magnetic material, in magnetic recording applications [80].

- For the application of each model very important are their various parameters, some of which are determined straight experimentally and others by further calculations. The number of a model's parameters and the easy determination of their values are of major importance for the engineer who is interested to rely on it and draw conclusions useful for a particular application. In practice, having experimentally taken as many of the magnetization curves required to identify some of the model's parameters (e.g. static loop, first magnetization curve, non-hysteretic curve), one looks for the appropriate values of the others, for the model's predictions to describe what is experimentally observed. Thus, a model cannot describe the magnetization curves of all the materials, whatever values we choose for these adjustable parameters, and therefore there is so far no general model covering all the materials. Also, a model

that was originally constructed for a particular category of materials may often, with an appropriate selection of its parameters, describe quite satisfactorily the behavior of other materials.

- Oversimplification in the consideration of the several effects often leads to erroneous results. So, for example, instead of the Globus model that refers to soft ferrites, magnetic component designers usually use the Jiles–Atherton model, which gives for these materials more accurate results than the previous one, if of course, appropriate values have been selected for the model parameters.

- After the original enouncement of the models, several researchers, including sometimes their own inventors, supplemented them by giving them a modified form, to take into account more accurately some effects, broadening this way their scope of application. Subject to such modifications became mainly the most popular of these: the models of Preisach, Jiles–Atherton, but also that of Stoner–Wohlfarth [82]. As examples, we mention the dynamic model of Jiles–Atherton, based on the corresponding static one which, through an additional parameter, takes into account the friction forces at the movement of the walls of magnetic domains and the dynamic models of Mayergoyz and Bertotti [43] based on Preisach's static model.

In addition to the above classic models that describe the macroscopic magnetic behavior of ferromagnetic materials, various other efforts have been made through the years with little or greater success. With the help of two examples below, we can see the possibility to treat the physical effects in a completely theoretical way, by making some assumptions about them and then to rely on some mathematical tools in order to predict the various curves that describe them.

In [62] the idea is based on the ability of any closed, flat curve to be described as a complex function. If the form of the major loop at the fundamental frequency is known and with the assumption that at the same values of dB/dt correspond parts of the loop with the same slope, this model can accurately predict the form of the minor loops. It is only necessary to know the applied voltage waveform and to have with good accuracy the electrical characteristics (inductance, resistance) of the excitation circuit for the form of $H(t)$ to be accurately predicted. Unfortunately, the use of the model is limited to this prediction only, when the harmonic content is not very high (especially that of the high-order harmonics) and

it cannot, for example, offer any clue about how the form of the loop will change with frequency.

In another attempt to model the magnetic hysteresis [67] the required data is the static major hysteresis loop $B(H)$, from which we can have the corresponding loop $\mu_0 M(H)$ and then, for its two branches, the curves $d(\mu_0 M)/dH$ as functions of H. The model is applied for the prediction of the minor loops when the waveform in time of either the magnetic induction or the magnetic intensity is known. It is based on the knowledge of the dM/dH derivative at all points of the major loop to predict the form of the minor loop at any position of the first one. This model is simple in its formulation and application, but finds application only for iron cores excited at low frequency (50Hz) with the frequency of harmonics not exceeding 800Hz [67]. In fact, the prediction achieved for the form of the minor loops (and the hysteresis losses) is approximate and not satisfactory if high accuracy is required.

2.6. Eddy current losses – expressions for the total core losses

The effects of magnetization and hysteresis, as we have seen, are affected by a variety of factors, the study of which led to the development of simple, descriptive models. The effect of the appearance of eddy currents, however, although also affected by various factors (the dimensions of the sample for example), is subject exclusively to laws known to us by Maxwell's electromagnetic theory and thus its understanding and complete description can only be based on the accurate solution of the relevant equations. However, it turns out that a number of factors, related to the microscopic structure of materials, introduce problems, for the solution of which the electromagnetic theory is not sufficient. The spatial anisotropy of the various materials or their elementary particles, in terms of their electrical and magnetic properties, the change of these properties with frequency and temperature and the coupling of the electric and the changing magnetic field in the scale of elementary magnetic dipoles are just a few of them. Finally, for the needs of practical applications one again ends up with simple equations (models), often different for various materials and various electromagnetic excitation conditions. These equations usually result from experimental observations in typical applications or even from some simple assumptions. Moreover, the experimental determination of eddy current losses has as a condition the separation of the hysteresis losses from them, which is rarely an easy task. For these reasons, the experimental verification and

definition of the application field of the various models for eddy current losses are extremely difficult, while in the expressions for the core losses in literature the two types of losses often appear together.

Regarding the increase in core losses with frequency, one can understand the reasons that lead to it, although the exact analytical expression describing it in each specific case is not self-evident. At low frequencies, where no additional effects take place, the hysteresis losses are proportional to the frequency, since they are proportional to the area of the hysteresis loop and therefore they depend proportionally on how many times the loop is swept per time unit. Respectively, since the induced voltage between two elementary surfaces of the material is proportional to the time derivative of the magnetic induction and the eddy current losses are proportional to the product of the voltage times the corresponding current, the eddy current losses will be proportional to the square of the frequency.

A first remark is that, for a sinusoidal excitation, the specific losses (losses per volume unit) of the core of magnetic components can be given approximately by an equation of the form:

$$P_v = P_{v,hyst} + P_{v,eddy} = C_1(f,T)\Delta B^{x(f,T)} f + C_2(f,T)\Delta B^{y(f,T)} f^2 \tag{2.9}$$

where $P_{v,hyst}$ and $P_{v,eddy}$ are the specific losses of hysteresis and eddy currents respectively and ΔB the difference between the maximum and minimum magnetic induction values. The coefficients C_1 and C_2 are functions of the material properties, frequency f and temperature T, while exponents x, y are also functions of frequency and temperature, generally different for each material. Regarding the dependence of specific losses on temperature, it is noted that in several types of ferrites they are minimized when the temperature takes a given value [28], which is usually in the range between 60 and 85ºC [140], [142], a typical temperature range for full load operation. On first approach and generally in practical applications where the frequency does not change significantly, the coefficients C_1 and C_2 and the exponents x, y are considered as constant. In fact, for many materials, including ferrites, the exponents x, y are approximately equal to 2 in a wide frequency range [133]. It is also obvious that for relatively low frequencies (typically f<100kHz for several ferrite grades) at which the electrical conductivity of ferrites is very low and the intensity of the induced electrical field in the core volume is also relatively low, C_2 value is about zero.

By studying several experimental data in literature, one can see that for the same ΔB and f the losses depend on the waveform of the applied excitation. Experimental measurements show that high values of the dH/dt magnetic intensity time derivative in large parts of the signal period result in the extension of the hysteresis loop [16], [38]. In other words, the form of the loop is determined not only by the extreme values of the magnetic intensity, but also by the manner, in time, in which the magnetic intensity changes from one value to another. In general, if one wants to use (2.9) for various waveforms other than sinusoidal, he should determine for which frequency band of the basic harmonic applies it and for these frequencies to determine the correct values of C_1, C_2, x, y (which will generally be different from the corresponding values for sinusoidal excitation).

Of course, equation (2.9) is just one way to express an experimental result, which is the variation of the specific losses of a material with changes in parameters f, ΔB, T. Similar expressions have been enounced since the end of the 19th century [1]. In modern literature one finds expressions such as the one we find in [133]:

$$P_v = C_m f^{x'} \Delta B^{y'} \left(a - bT + cT^2\right)$$

(2.10)

where the study has been carried out for very small ring-shaped cores, so that, due to the small dimensions of the sample, the development of eddy currents is limited (without them being always negligible), especially at the frequencies of several hundred kHz. Again, the issue is the experimental determination, for each material, of the constants C_m, x', y', a, b, c for the various frequency ranges, where in the case of non-sinusoidal excitation, f represents the fundamental frequency and ΔB the peak-to-peak value of the magnetic induction. It is noted at this point that the existence of a constant term for the magnetic induction, in general, leads to different core losses than for the same ΔB without it, since the swept loop is different. Therefore, the excitation conditions should be clearly defined when relations such as (2.9) and (2.10) are used. Moreover, a different option to express the core losses is the use of the amplitude of the fundamental harmonic of the magnetic induction instead of its total amplitude [63]. In an attempt to avoid dividing the frequency spectrum into areas, (2.10) can be alternatively written as follows [133]:

$$P = C_m f^{x(f)} \Delta B^{y(f)} \left(c_1 - c_2 T + c_3 T^2\right)$$

(2.11)

where c_1, c_2, c_3 are positive constants.

We have seen that the equation (2.9) is considered very simplified to lead to accurate results and gives the true dimension of the problem only at low frequencies. In order to extend its application to higher frequencies one must consider, as is actually the case, that all the constants that appear in it are far from being "constants" but depend on frequency and temperature, without considering any anisotropies (we always refer to samples that macroscopically appear isotropic, as is the case for materials selected in magnetic component applications).

It is therefore observed that the eddy current losses, above some frequency limit, follow a dependence that declines from the quadratic law that appears in (2.9). To describe this effect, it is recommended [27], [39] that the specific eddy current losses may be calculated from two terms, the classical and the excess or anomalous:

$$P_{cl}(t) = C_{cl}\left(\frac{dB}{dt}\right)^2 \rightarrow P_{cl}(t) = C'_{cl} f \int_0^T \left(\frac{dB}{dt}\right)^2 dt \qquad (2.12)$$

$$P_{ex}(t) = C_{ex}\left|\frac{dB}{dt}\right|^{3/2} \rightarrow P_{ex}(t) = C'_{ex} f \int_0^T \left|\frac{dB}{dt}\right|^{3/2} dt \qquad (2.13)$$

where T is the period of the applied voltage and C_{cl}, C_{ex}, C'_{cl} and C'_{ex} are constants dependent on the conductivity and geometry of the sample. Exponent 3/2 in (2.13) resulted from experimental measurements. The frequency dependence is now determined by how this appears in the term dB/dt. Thus, for sinusoidal B, it comes up that the specific eddy current losses are given by the expression:

$$P_{v,eddy} = P_{cl} + P_{ex} = K_1(fB)^2 + K_2(fB)^{3/2} \qquad (2.14)$$

with K_1, K_2 constants. For other waveforms some corresponding expressions are valid. From (2.12) and (2.13) it is also apparent that high values for the magnetic induction derivative for large parts of the signal period will result in increased eddy current losses, a presumable result, since for the same time intervals we will have high electric field intensities in the core volume. The above results were initially extracted for the case when the core consists of soft

magnetic material sheets, although they were later used to model losses in ferrite cores [44], [53], [94], which are mainly used in power electronic devices.

For the separation of the three –now– terms of losses, the method, proposed and detailed in [44], is based on the assumptions that the hysteresis losses are proportional to the frequency (i.e. that the hysteresis losses per cycle are constant) and that the exponents in P_{cl} and P_{ex} dependence on frequency remain constant (e.g. 2 and 3/2 in (2.14)). Then, if the losses are measured at a very low frequency to determine the hysteresis losses (the method is not applied if there are minor loops) and the total losses are known (usually given by the manufacturer of the ferrite up to a frequency limit), it is a simple computational task to determine the proportionality coefficients for P_{cl} and P_{ex} (e.g. K_1 and K_2 if we refer to (2.14)) and thus the separation of the three terms. However, based on what was explained previously about the variation of the hysteresis loop shape with frequency, but also with the form of the time function of the imposed excitation, we understand that the first assumption is already uncertain, especially if the frequency increases beyond 1kHz. For this reason, appreciable effort has been made [30], [52], [104] to correlate the results obtained for sinusoidal excitation with those for non-sinusoidal excitation, such as square pulses, but still only in the case of iron sheets.

Moreover, as the use of (2.12) and (2.13) to distinguish between the different loss mechanisms is not possible when the hysteresis loop also has minor loops, some studies have been carried out on the issue of their combination with any of the hysteresis models [69], [75] with the prospect to overall model the core losses. The end result of such studies is often the modeling of core losses based on various equivalent circuits, for only limited application fields (e.g. [53], [64], [66]). These equivalent circuits can then be introduced into some circuit simulation software so that, in addition to the distortion of the voltage and current waveforms due to the non-linear relation between B and H, the losses are calculated.

In closing this chapter, we should mention an important finding, which results from the study of literature on the issue of core losses in magnetic components. We see that the physical mechanisms governing the occurrence of these losses change both with the frequency and the amplitude of the excitation and also depend, both on the particular form of the variation in time of some quantities (magnetic induction and magnetic intensity), as well as from the existence of a constant term in them. In fact, the exact character of energy interactions and the occurrence of losses, in terms of the above parameters, for a material of given chemical composition, may vary depending on its magnetization history or on its crystal structure. It is therefore impossible for the study of core losses to rely on the harmonic

analysis of the applied excitation and to seek the effect of each harmonic component, as independent from that of the other harmonics [104]. The only point of caution in non-sinusoidal excitation conditions is, as mentioned above, whether the amplitude of the fundamental magnetic induction harmonic or its total amplitude [63] will be used in the various calculations for the core losses, with a constant concern to predict and avoid saturation.

CHAPTER 3

COPPER LOSSES IN MAGNETIC COMPONENETS

3.1. General view

The research community was asked to study the effect of losses in magnetic components from the mid-19th century, with the discovery of alternating electric power. From that time already, it had become clear that materials subject to alternating magnetic excitation exhibit some sort of losses, causing their heating. The particular state established on an alternating current flowed winding, with regard to ohmic losses, had not yet been realized, as the use of alternating power was limited in the sector of the electricity generation, electric power transmission on a small scale and electric actuation (electric machines and transformers). In these applications the effects of changing magnetic flux within the volume of current carrying conductors are not easily perceived, mainly due to the low frequency of operation. Modern applications (e.g. radio signal transmission), led to the use of high frequency signals and to the appearance of increased power densities in the various electrical and later (mainly post-war) electronic devices. As a result, the relevant phenomena and the revelation of new problems with theoretical and practical interest emerged (e.g. the effect of parasitic capacitances).

The electromagnetic theory, completed by Maxwell as early as the beginning of the 20th century [2], was a complete tool for describing the phenomena, but so difficult to use, that it left no room for analytical solution of the problems. The difficulty to find a satisfactory solution using Maxwell equations is mainly due to the following factors:

- Electromagnetic quantities are time-varying, which makes it difficult to solve the equations and it gets even worse when the time dependencies are unknown. This is because, among other things, an effect of the phenomena under study is also the harmonic distortion of the waveforms (voltage, current, magnetic flux) due to the non-linear relation between magnetic intensity H and magnetic induction B. Moreover, regardless of the variation in the waveforms resulting in cases of sinusoidal electromagnetic excitation,

it is important to mention that sinusoidal excitation, which is also the easiest of all cases in terms of study, is encountered in relatively limited number of applications.

- The spatial geometry of the practical problem is usually complex enough to make it almost impossible even to set up equations or to formulate boundary conditions without simplifications or omissions.

Hence, an effort was launched by the researchers to record the phenomena in the greatest possible detail and then interpret them, in order to satisfy the need to complete the scientific knowledge on this new field, but also the requirement of magnetic designers for simple and easy-to-use rules, on the basis of which it could be possible to optimize the design of these components.

The outbreak of World War II boosted the development of radio telecommunications, as well as other sectors of electrical circuit design, in which the magnetic components largely determine the cost, performance and reliability of the devices. The design of the magnetic components was based on the trial and error method, until the final product satisfies the predefined requirements. Thanks to this process, valuable experience was gathered by the engineers – designers of that time. To better use and archive this knowledge, relevant handbooks were written, containing a wealth of numerical data in the form of diagrams, tables and empirical equations. These equations were easily extracted by the method of finding coefficients and exponents, so that the resulting function coincides with the experimental data (curve fitting). Based on these handbooks, there were also several step-by-step simple methodologies, for the quick, easy and successful design of the appropriate magnetic component. The "Radio Engineer's Handbook" - 1943 [123] is one that covers many more design sectors further than the magnetic components. Among other things, the contribution of such handbooks to the subsequent theoretical analysis of phenomena was important, since they offered ready experimental material for the establishment of new descriptive models. At the same time, appeared several periodicals such as "Wireless Engineer" or "Electrical Engineering" etc. that were intended to keep the international scientific and technical community informed of the many important findings of that time.

The effects of losses in the winding and core of a magnetic component are interrelated, since what happens in the one area directly affects the other. In most cases, however, with some simple assumptions, which are not far from the reality of practical applications, we can study the two effects independently. It therefore remains as the last issue to examine, whether the assumptions made lead to incorrect results, with the obvious role of the experiment in the

verification of any theoretical construction. During the experimental procedure, the interrelation between core and winding often emerges as the major obstacle to the reliable measurement acquisition. Thus, nowadays the finite element method is widely used to study the phenomena that take place in the core and in the winding and for the extraction of data not easy to be obtained with experimental methods (§4.3.).

It is worth mentioning at this point that before the discovery of suitable ferromagnetic materials with reduced losses in high frequency applications, inductors and transformers were usually wound on a substrate of dielectric material in the desired shape. Thus, the first studies exclusively focused on the problem of the variation the ohmic resistance of the windings, as well as the effect of parasitic capacitances, on the operating characteristics of magnetic components under conditions of periodically varying electromagnetic excitation. The calculation and the modeling of parasitic capacitances in the windings of magnetic components is an issue that will generally not concern us in this dissertation, since it becomes important at frequencies considerably higher than those encountered in usual power electronic device applications.

In Ch. 4 of the dissertation there is an investigation of the reliability and boundaries of application of the three considered as classic models for copper losses in magnetic components (S. Butterworth - 1922 [5]−[7], P. Dowell - 1966 [12], J. Ferreira - 1994 [47]). This investigation is preceded by a detailed description of the three models. In addition to these models, however, which for various reasons have been widely accepted by magnetic components designers, numerous attempts have been made to describe copper losses in magnetic components. The exact objective and the way in which this effort is made each time differs. Some directly apply the Dowell and Ferreira models to make optimal magnetic components design, taking into account, for example, only the fundamental current component, or the frequency is considered low enough for Dowell's formula to be replaced by the first terms of the corresponding Taylor series. In some others, improvements are made to Dowell's model to describe losses under conditions not included in the above model, e.g. when the excitation is non-sinusoidal or when the various windings of a transformer carry current in different parts of a period.

Except the works that, one way or another, are connected to any of the classic models (usually that of Dowell) there are also great efforts to develop entirely new models, based either on direct analytical solution of Maxwell's equations, or on the method to approximate with some equation results derived from analysis with finite element software. Moreover, many works provide a qualitative description of critical quantities in specific problems (e.g.

the edge effect and the fringing field effect), also mainly with the use of finite element software.

Thus, on the subject of copper losses, there are a plenty of works, the most important of which will be mentioned further below. As we will see, their degree of success is related, both to the assumptions made when a problem is defined and to the methodology followed in order to solve it. Similarly, the degree of acceptance of their results by the magnetic component designers is mainly related to their accuracy, as well as to the ease of use, since the resulting expressions are often too awkward to be practically applied.

3.2. Losses in round cross-section conductor windings

3.2.1. Analytical solutions

An approach more general than Dowell's, which can be applied to various winding geometries and different types of current waveforms, is proposed in [29]. Using different magnetomotive force diagrams (MMF)[1], for the different parts of a period, the losses in the case of transformers in which different windings do not conduct simultaneously can be calculated. A typical example of such transformers is those used in Flyback converters, in which in part of the period only the primary carries current, storing energy in the core gap, while in the next part of the period it is only the secondary with current and the previously stored energy is transferred to the inverter's load circuit. For cases where the operating conditions and geometry of the problem are such as those assumed in Dowell's model, the expression for the F_R resistance factor of the proposed method reduces to that of Dowell (F_R is the ratio of the effective resistance R_{ac} of a winding for a given frequency of sinusoidal current to the resistance R_{dc} in direct current, $F_R=R_{ac}/R_{dc}$). The same method found in [29] is also used in [36] for the extraction of an equivalent circuit for transformers.

In [41] the electromagnetic problem of a set of parallel conductors with infinite length, extending along the z direction (perpendicular to the x–y plane), which are under the effect of a homogeneous time-alternating magnetic field, is analyzed as a two-dimensional problem (at

---

[1] In the absence of magnetic materials, the magnetomotive force (MMF) is proportional to the amplitude of the magnetic intensity.

the *x–y* plane). In order to accurately express the interaction between conductors, the analysis treats each conductor with its induced eddy currents as a magnetic dipole. The basic condition for the method to be applicable is the knowledge of the precise position of all conductors. It finds easy application and gives a satisfactorily accurate result in the case of a single layer of current carrying conductors, which are uniformly positioned with equal distances between adjacent conductors and for frequencies only moderately high, for which it is $r/\delta < 0.8$ [143].

In [74] the increase in losses in Litz wire and simple stranded wire is being considered as a result of the skin and proximity effects, as they take place on both strand scale and wire scale. Nevertheless, only strand scale proximity effect is taken into account for the extraction of the final results. The solution presented is recommended for the frequency band for which it is $r/\delta < 1$.

In [81] a detailed solution is presented, on the basis of the Bessel functions, for windings with round cross-section Litz wire layers. The conductors inside a winding are placed in a square layout. The solution proposed takes into account the local proximity field in a strand, which is due to the currents of adjacent strands inside the wire and it is supposed that there is no skin effect on strands. The proximity field due to the currents of the remaining conductors of the winding is considered uniform at the *y* direction (the direction of the symmetry axis of the magnetic component) and that its value varies linearly at the *x* direction (perpendicular to *y*). From this assumption it comes clear (see also §.4.3. and §5.4.2.) that in this case, the given solution cannot be applied for high frequencies.

In [143] the authors propose, for moderately high frequencies ($r/\delta < 0.8$), a method based on the superposition of three different suppositive fields, in order to better describe the two-dimensional field within a round cross-section conductor that forms part of a layered winding. These three fields are as follows: a) A circular one, due to the current of the conductor under study itself, b) A field at direction *y* (with a value dependent on *x*), describing the effect of distant conductors and c) A hyperbolic field, describing the effect of the conductors in direct adjacency to the conductor under study. Each separate layer of the geometry examined consists of equidistant turns, with equal radius of their round cross-section. All the layers are geometrically separated from each other (as in all models that consider layers) and each one extends along the direction *y*. In addition to these limitations, all the geometric parameters that determine a layer may have different values in each layer. More specifically, these parameters are the radius of the conductor and the filling factor η of one layer (as defined in Dowell's work, see §4.2.3.), as well as the precise location of a layer in *x–y* directions. The ability to vary the position of a layer in the *y* direction in practice

means that the conductors of a layer can show a relative dislocation with respect to the conductors of the adjacent layers. In this way, the square layout of the conductors in the winding, which is a typical concept in almost all the relevant models, here is a simple sub-case. What is remarkable is that the required sums to calculate the hyperbolic terms make the above method extremely difficult to implement.

3.2.2. Solutions with numerical methods

The evolution in computer technology enabled use of the finite elements method to accurately determine the magnetic field and power density distributions in winding geometries that were not easy to study with analytical methods. Models obtained from analytical methods were re-examined and corrections were proposed that improve their accuracy and make them applicable to a wider range of the parameters involved [70], [91], [95], [143]. New expressions were also proposed for the effective parameters of a winding (resistance, magnetic permeability) [83], [98], [99], [106], [109], [119].

A significant work is [83] in which the extraction of the results is based on the assumption that the losses P_{ac} due to the eddy currents in the winding (skin and proximity effect) are proportional to the square of the time derivative of the magnetic induction:

$$P_{ac}(t) \sim \left(\frac{\mathrm{d}B}{\mathrm{d}t} \right)^2 \tag{3.1}$$

as well as on the assumption that the field extends only along the y direction of the symmetry axis of the magnetic component. The main step in the method proposed in [83] is to do a magnetostatic analysis with finite element software to find the field distribution in the window area (leakage field) and in particular in the area occupied by copper. For more than one winding the goal is to determine the way the field that each one creates penetrates both itself and the other windings. Each winding is considered as a uniform current density area. The results take the form of an eigenmatrix, descriptive of the assembly, which for two windings is of 2×2 dimensions, while corresponding are its dimensions for more windings. The great advantage of the above method is that it can give results even for magnetic components whose various windings do not carry current simultaneously, as in [29]. Moreover, it gives results regardless of the position geometry of the windings within the window area, while also the winding current functions may be non-sinusoidal, as long as they

are known. Secondary phenomena, such as the increase in losses in the winding when it is near the gap and penetrated by locally created magnetic flux (fringing field, see §3.4.1), may also be taken into account. A great conclusion that results with the application of this method is, among other things, that proper interleaving of the windings can significantly reduce the losses, especially if they are more than two and/or carry current non-simultaneously.

The authors in [99] propose a model for a wide range of frequencies based on analysis results from finite element software (FEA), but the functions involved and the frequency or geometry dependent coefficients make it unattractive for anyone who wishes to make quick calculations. Similar, in terms of the form of the results, is the situation in [109].

As a final example, in [98] and [119] FEA is also applied in order to distinguish between low and high scale interactions between the conductors within a winding.

In closing this paragraph, it is worth noting that the complexity of the final expressions in most of the previous works or the restrictions on the parameters involved (e.g. the frequency) stand so far as sufficient reasons for the magnetic components designers to continue to usually apply Dowell's model for an easy and quick calculation of losses.

3.3. Losses in conductive foil windings and printed circuit board windings

3.3.1. General issues

When designing a magnetic component for an electronic power converter, one chooses the most suitable of the available round cross-section wires, depending on the current value and the operating frequency and always in relation to the available magnetic cores. Windings with square or rectangular cross-section wire, with cross-section dimensions of 1mm or less, are not encountered in applications of high frequencies and low / moderate power levels (up to approximately 500W), as the placement of such a wire would offer no advantage, while instead it would lead to a low copper filling factor. This is because the small dimensions of its cross-section would make it a tricky task to arrange the turns in a layer without rotation of the wire. On the contrary, in grid frequency and high current applications, rectangular cross-section conductors are used to achieve a high copper filling factor and reduce the leakage.

In power electronic applications, when the current or operating frequency increases, a stranded conductor is usually used. However, when the value of the current becomes too high the construction of a stranded wire with a large number of strands, but also its placement in

the available window area, with the help of a coil former (bobbin), becomes extremely problematic. In this case it is more practical to make a winding with copper foils.

Finally, in modern applications, in which the reduction in the size of magnetic components is often the most basic requirement, it is now typical to use planar magnetic components with printed circuit board (PCB) windings [34], [35], [65], [90], [92], [93], [114], [118], [148], [150], [151], [153], [154]. We will therefore present below some works dealing with the high-frequency copper losses in copper foil windings and PCB windings.

3.3.2. Copper foil windings that occupy the entire height of the window

For windings with copper foils that occupy the entire height of the magnetic component window, the conditions of the one-dimensional analysis are met with very good accuracy and the expressions of [9], [12] give an accurate result. Therefore, the relevant work found in the literature focuses on the investigation of copper losses, based on the expressions given in [9], [12], in variations of parameters, such as the exact thickness of the foils.

In [15] the analysis is based on Dowell's model. It appears that, for a winding with copper foils, the optimal thickness Δ_n of the n-th layer (reduced to δ, where δ is the skin depth) in order to minimize R_{ac}, when $n \geq 3$, is:

$$\Delta_n = [n(n-1)]^{-1/4}, \qquad n \geq 3 \tag{3.2}$$

whereas for the second and the first layer, for which the above equation does not apply, it appears that in order to minimize the losses it must be $\Delta_2 = 0.8$ and $\Delta_1 \geq 1.2$. However, this important result is difficult to be applied in practice with conductors of different dimensions in each layer. Yet, with the same reasoning and assumptions, the optimal relative conductor thickness for the total number of layers m is calculated as:

$$\Delta_{optimum} = \sqrt[4]{3} \big/ \sqrt{m} \tag{3.3}$$

and if the number of layers m is quite high the total losses for this case are approximately 12% greater than the case with the layer-by-layer optimization [15]. For low m values the difference is low. The same actually results are also obtained in [14], [65] and [71].

In the previous analysis the independent variable is the thickness of the conductor of each layer, while in other similar studies the role of this parameter can be taken by some other one.

However, this treatment of the problem is unilateral and appropriate only in applications with poor requirements, in terms of overall efficiency, performance and cost, since the rough determination of the other parameters of the assembly can lead to the opposite result. For example, a rule valid for all kinds of windings and not only for foils is that a bad choice in the interleaving scheme of the windings can lead to increased losses, regardless of the choice for the thickness of the conductors. Therefore, what is important in the end for the magnetic components designer is the optimization when it takes into account many parameters together (see Appendix II).

3.3.3. Planar magnetic components with PCB windings

In recent years, the need to reduce the size of power supplies, especially in electronic devices, such as computers, has become more pressing than ever. The passive components (magnetic components – capacitors) make up a significant part of the total volume of such a device and the basic technique to reduce their size is to increase the operating frequency. With the frequency ranging from 700kHz to 10MHz, it is possible for the power density in the magnetic components to be many times higher than what is encountered with the usual switching frequencies in power converters (100 - 200kHz) [34], [35], [90]. The final result is power supplies with a throughput power density which, for a power of a few tens or a few hundreds of Watts, may be even greater than $6W/cm^3$, whilst in a linear power supply corresponding typical values are lower than $0.12W/cm^3$ [149]. Another ability also offered by very high switching operating frequencies is the creation of low power supply devices (of the order of 1W) in the form of integrated circuit [151].

However, in order to depress the profile of the power supplies, it is necessary to use planar magnetic components, with a typical thickness of 1cm, in which the winding consists of conductive tracks on the board on which can be located both the circuit powered and the power supply itself [34], [35], [65], [90], [92], [93], [114], [118], [148], [153], [154]. In the case of a transformer, for example, the primary and secondary (or secondaries) may be printed on the two sides of the board or on the several layers it may contain. In Fig. 3.1 are the photographs of two commercial power supplies [151] with an approximate thickness of 1cm, which is obviously determined by the thickness of the planar magnetics. With the usual core types (e.g. E, UI, P, etc.) and use of round cross-section conductors or copper foils for the windings, it is not possible to reduce the height of the magnetic component that much.

In the planar magnetics the ratio of their outer surface area to the throughput power takes values considerably higher than those in the classical core geometries, thus allowing for more
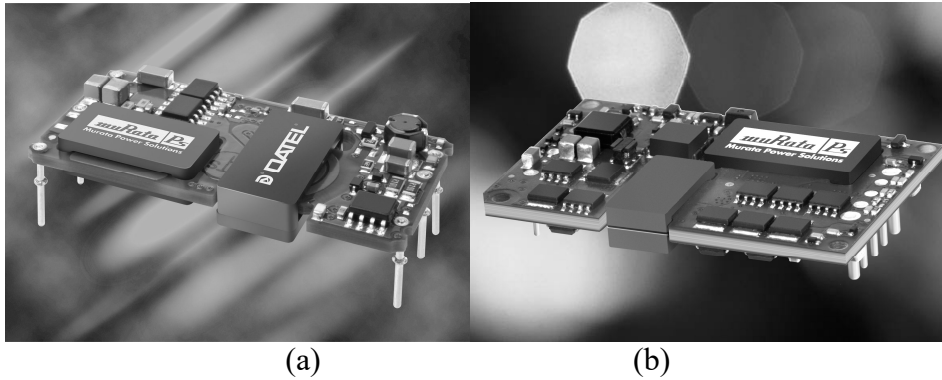
(a)   (b)

Figure 3.1: Commercial proposals for low profile power supplies, which include planar magnetics. (a): 30W, dc-dc, forward converter, $2.3 \times 4.9 \times 0.9$ cm (~3W/cm^3) (b): 165W, dc-dc, $3.7 \times 5.8 \times 1$ cm (~7.5W/cm^3). In both cases the efficiency is 90% [151].

efficient cooling, even without forced convection. Moreover, the large planar outer surface of planar cores enables the placement of external heat sinks if required. In most cases there is the possibility of openings on the core for air convection in the slot where the printed winding is placed. Thus, for the windings, cooling is much easier than in a common winding, given the large surface they present in contact with the air. It is reminded that the heat transfer coefficient from a thermal conductive surface (e.g. metallic) with air convection is approximately equal to 15W/m^{2}grad.

For a spiral winding on the board, one-dimensional analysis can give a quite accurate result for high-frequency copper losses [148]. Thus, one easily finds that they can be extremely low, always compared to the classical geometries of magnetic components, since there is usually just one layer (it is noted that the losses are approximately proportional to the square of the number of layers (eq. 3.11)). This makes planar geometry ideal for applications where an inductor is required to have current with a significant high-frequency ripple; to reduce the DC losses we can increase the thickness of the conductive tracks of the winding with just a small extra cost in losses due to eddy currents [65].

For an even greater size reduction, in the case of inductors, integrated (coupled) magnetics are used [92], [114], [153], [155]. The method of integrating magnetic components, although particularly useful in cases of planar magnetics, is also applied to the usual geometries of magnetic cores and lies in placing on the same core more than one inductor, when the phase shift between their currents favors such a choice. Usually these are two inductors with the alternating components of their currents showing a phase shift of 180$^\text{o}$, but they may be more. In such a case the magnetic flux in some part of the core may be

minimized or even zeroed, resulting in a significant reduction in core losses or even in the possibility to cut out part of the core, which would otherwise have zero magnetic flux. It is also shown [114] that by integrating the magnetic components, it is easier to use topologies and converter control methods that lead to a reduction in losses in the switching components, such as turn on – turn off of the components under zero voltage or zero current (ZVS or ZCS). Furthermore, it is mentioned that for operating frequencies of the power supplies higher than 1MHz and for power levels lower than 100W, the researchers are looking for the possible advantages of planar magnetic components without core [93].

With the size of the power supply sufficiently small, it can be placed in close proximity to the powered circuit (e.g. logic circuits, remote sensors, etc.), resulting in a drastic reduction of power lines and the ohmic losses in them. In typical localized power supplies, the semiconductor switches are operated at frequencies up to 10MHz for a power of less than 10W [90]. For example, in [150] a product is launched for 8.2W power, with an operating frequency of 4MHz and a transfer power density of $2.3W/cm^3$. For power supplies with resonant or semi-resonant converters and for a power higher than a few tens of watts, operating frequencies in commercial applications usually range between 700kHz and 2MHz, while devices that operate at higher frequencies are still in a research stage. Of course, planar magnetics are not only used in applications with frequencies of the order of MHz. A planar transformer for a power of 200W and an operating frequency 200kHz, for example, can have a thickness typically equal to 0.7cm and large dimensions of the order of a few cm [148].

However, the planar magnetics also have some disadvantages. Converters operating at frequencies above 1MHz, typically use Forward or Flyback semi-resonant topologies, thus requiring a gap in the magnetic components, whether it is an inductor or an isolation transformer [34]. Moreover, in magnetic components, regardless of the necessity or not for energy storage, a small gap is often inserted in order to ensure that the magnetic permeability of the core and therefore the inductance of the component, are not affected by the temperature. However, unlike the usual core types, in which the gap field affects a small part of the winding where it locally increases the losses (§3.4.1), in the planar magnetics the phenomenon may be largely extent. In order to reduce this problem, in the design of the core, it is necessary to have a slot for the windings quite deep (relative to the thickness of the board) in order to allow the windings to be placed away from the gap. However, this design is accompanied by a low copper filling factor of the slot and a low coupling coefficient between the windings [34], [92]. There are, of course, other design solutions to reduce the problems

caused by the existence of a gap, each one of which has its own pros and cons. The choice of the optimal solution each time is dictated by the requirements of each application.

With regard to the core losses, it is reminded that, at frequencies above 1MHz, phenomena such as the resonance of the magnetic domain walls, but also resonances in the volume of the core, become potentially constrain factors for the good operation of the magnetic components and for the loss suppression under acceptable levels [35], (§2.4.). The materials used to ensure good operating conditions at these frequencies usually have other problems, such as low values for the magnetic permeability and saturation induction.

Additional problems in planar magnetics are the relatively high values for the leakage inductance (as already mentioned) and parasitic capacitances [35], quantities which are critical for the proper operation of resonant or semi-resonant topologies. As their elimination is not practically possible, the problem is translated into a necessity for the precise determination of their values and an effort to keep them as constant as possible, regardless of the temperature, frequency or loading conditions of the device, so that they can be taken into account in the resonant components L and C [105], [117], [120], [122], [148], [154]. Given the design of the windings on a PCB, it is easy to maintain constant values for these quantities throughout the production line.

Finally, the normally high frequency of operation, the existence of a gap and the proximity of the power supply device to the logic circuits in the applications where planar magnetics are used make more necessary some electromagnetic shielding in order to avoid the diffusion of electromagnetic noise.

3.4. Special issues related to magnetic component copper losses

Except the efforts to describe the high frequency effects in normal winding geometries, some special issues, such as the fringing field effect in the area near the gap and the edge effect, as well as the exact geometric arrangement of the conductors in a winding with round cross-section conductors have attracted the interest of the researchers. This is due to the potentially high variation in the losses that may cause the phenomena that occur in these cases.

3.4.1. The gap fringing field effect

It has been previously mentioned that the inductors in power electronic applications, but also the transformers used in Flyback type converters, usually have a gap in their core. An example of exception is the magnetic components in toroidal cores, made of materials with generally lower magnetic permeability compared to ferrites. For a magnetic component that has a core with an effective magnetic path length l_{eff} equal to a few tens of cm, the typical gap length l_g is usually less than 1mm, but can be up to a few (4-5) mm, depending on the requirements of the given application. The existence of a gap in the core serves the storage of energy in the magnetic component in the form of magnetic field. Another purpose served by the insertion of the gap is to stabilize the effective magnetic permeability μ_{eff} of the core and hence the inductance of the magnetic component. Without gap, the quantity that is of practical interest is $\mu_\alpha = \Delta B / \mu_0 \Delta H$ (see §7.3.2), which is of the same order as μ_i (§1.2.5), although these two quantities are not equal to each other. However, μ_i and μ_a are sensitive to temperature variations, while in particular μ_a, which is the critical quantity, also depends on the frequency and amplitude of excitation. By inserting a gap, the effective magnetic permeability of the core becomes, in short, independent of the exact magnetic properties of the material (as long as it is $\mu_i >> \mu_0$) and it is [131] (also see §7.3.2.):

$$\mu_{eff} \approx l_{eff}/l_g \tag{3.4}$$

where of course, if the material does not enter saturation, it will be $\mu_a = \mu_{eff}$. The problem that arises with the insertion of a gap, however, is that the strong gap field is not limited to the gap space, but extends to the areas close to it, where there may be conductors of the winding. In such a case they develop locally, in the areas where the gap field intersects the winding, strong eddy currents, resulting in local increase in temperature, but also in the overall increase in the effective resistance of the winding.

Regarding this phenomenon, it appears from the study of the literature that a thorough investigation has been done. Qualitative results [24], [51], [59], [71] and analytical expressions [89], [97], [102], [143] clearly delimit the area of fringing field effect and clarify the conditions under which a local overheating (hot spot) of the winding is possible. The general conclusions resulting from the above works can be summarized in the following points:

   - The fringing field effect is more important in conductive foil windings.

- The area outside the gap in which the field is located extends to a distance from it approximately equal to its length.

- Regarding a winding with round cross-section conductors, in practice only two turns close to the gap are affected.

In the end, the effect of this phenomenon on the total winding resistance proves to be of minor importance and a possible hot spot is highlighted as the most serious potential problem it may cause.

The proposed solutions (e.g. winding combining the use of Litz wire and a common solid wire of round cross-section [143] or winding of conductive foils in a shape resembling the form of the field [51]) are not always realistic or easy to implement. Thus, in the end, the well known general rules of the distribution of the gap in all three core legs (instead of just the middle one, as it is when we try to avoid electromagnetic interferences) and the placement of the winding at a sufficient distance from the gap are designated as the most useful design advice in practice. Another suggestion to completely avoid this effect is the use of magnetic materials with a distributed gap [90].

3.4.2. The edge effect

In a winding of conductive foils, for the magnetic flux through the conductors to extend only in the direction y of the magnetic component symmetry axis and the current density to vary only at x direction, perpendicular to y, they (the conductors) must occupy the entire width of the window. In other words, the width of the conductive foil must be equal to that of the window (as "width" we take the long dimension of the cross section of the foil, which is parallel to the y axis). In this case the effective resistance is accurately calculated from the expressions given in [9] and [12]. However, if the conductors are not tangent to the core yokes, but their edges are away from it, the magnetic flux around the edges has components, both in y and x direction and entering to the conductors intersects their surfaces at an angle (Ch.4). This results in the distortion of the one-dimensional character of the field and the current density in the conductors, so the one-dimensional models [9], [12] do not apply. The same applies to a winding with conductors of round cross-section, with the difference that in this case there are other additional reasons that lead to a two-dimensional form of the field with increasing frequency, encountered at the entire winding and not only at its edges (Ch.4).

The literature sporadically provides some results on the edge effect, which often lead to conflicting conclusions:

In [9], [24], [37], [124] it is reported that an increase in losses in conductive foil windings is caused when there is a component of the field perpendicular to its surface.

In [50] and [72] the approach attempted is identical: the edge effect in windings of conductive foils, at high frequencies for which it is $h/\delta>3$ (h is the thickness of the foil), is treated with electrostatic assumptions for the calculation of current density and reports a high increase in losses, a result that is also supported in [71]. In the same works, some exponential series (in terms of frequency) is used for low frequencies, while for the intermediate frequency range an asymptotic solution is proposed.

In [46] FEA is applied for the study of the configuration where the primary and secondary both consist of a conductive foil. It is concluded that there is an optimal distance between the two windings and that the losses are minimized when both are of the same width and are placed symmetrically within the window, with equal distances from both the top and bottom yoke.

Probably the most extensive works on the subject are found in [70], [87], [91], [107], at which FEA is also applied. In [70], [107] the edge effect in a single conductive foil layer is studied. Based on the results, it is reported that there is an increase in losses at low frequencies, while at high frequencies it is stated that a decrease occurs, which depends on the distance between the primary and the secondary under study. In [91] the general conclusion that the edge effect in conductive foil winding leads to an increase in losses at low frequencies and a decrease at high frequencies, is supported on the basis of numerical data from FEA derived for some specific values of the parameters m, h/δ and η_e, where m is the number of layers, h the thickness of the foil and η_e is the percentage of the width of the window that it occupies. In the same work, a first attempt is also made to describe the edge effect in windings with round cross-section conductors. The numerical results for F_R of a particular winding with $m=3$ are presented and some general conclusions are drawn regarding the observed total decrease of losses and the possibility of a hot spot, due to the increase of losses in a turn. In [87] the edge effect in a conductive foil single layer winding is studied with FEA and the method of least squares is applied to find a modified form of Dowell expression, which gives the resistance factor F_R in this case. The application of this expression cannot be done directly; the intermediate steps of calculating some parameters must precede and based on these results, the values of some factors must be taken from a table. In this work it is reported as a typical case the increase of losses in the whole frequency range, up to the value $h/\delta=10$, opposite to the results of the same authors presented in [70], [91].

All the above analyses contribute significantly to the understanding of the edge effect in windings with conductive foil or with round cross-section wire. However, it is clear that what is missing from the literature is a detailed and aggregated presentation, giving clear indications of the scale of the edge effect on the copper losses of magnetic components, something which is one of the subjects of Ch. 4 of this dissertation.

3.4.3. Winding conductors of round cross-section arranged in hexagonal configuration

An additional issue related to copper losses is that of the exact arrangement of the conductors (turns) in a round cross-section wire winding. In all the works mentioned so far a "standard" geometry is considered: the conductors are placed in a square configuration (i.e. the centers of the cross-section of adjacent conductors are located at the vertices of an imaginary square) or sometimes, when the interior of a Litz wire is studied, in hexagonal configuration. The exception to this rule is the model presented in [143], in which, as mentioned (§3.2.1), the conductor configuration maintains the general design of the separated layers, but any configuration in a form between the square and the hexagonal is possible. In [74], [83], in which the losses at moderately high frequencies are studied (see also §3.2.1.), the exact configuration of the conductors is not critical. Finally, in [111] it is explained that layered windings with hexagonal configuration of the conductors show increased losses compared to windings with a square configuration, given that the total copper factor in the winding (or "copper filling factor") remains constant. However, as we will see in Ch. 4, in practical applications in which the hexagonal configuration leads to a tightly wound coil with an increased copper factor, the losses may be considerably lower than those encountered at the classic square configuration.

3.5. Copper losses for non-sinusoidal currents

The studies presented so far were developed for sinusoidal current waveforms and in addition to the various geometric parameters, such as the shape and cross-section area of the conductors, special attention was also paid to the variation with frequency in the effective resistance. Fourier analysis is a way to extend the application of previous results to the case of non-sinusoidal waveforms. However, other methods have been proposed to bypass Fourier analysis, each of which has advantages and disadvantages. This section includes a brief

presentation of some important studies, which attempt to solve the problem of the copper loss calculation for non-sinusoidal waveforms.

The case of sinusoidal currents in magnetic components has various applications, but not that much in the field of power electronic converters. In modern power converters the magnetic components mainly carry pulsed currents, saw tooth or partially sinusoidal and partially linear as in semi-resonant converters [139]. Therefore, one must be able to calculate the ohmic losses under these conditions in order to make the best design choices.

In chapters Ch.1 and Ch.2 we saw the mechanisms that govern the appearance of losses in the core of a magnetic component and it was concluded that it is impossible to look for the effect of each harmonic component of the magnetic excitation on these losses as independent of the other harmonics.

On the contrary, in the calculation of copper losses for non-sinusoidal current waveforms, the typically used method is the Fourier analysis of them, the calculation of the effective resistance for each harmonic frequency and then the sum of the individual terms of the copper losses corresponding to the various harmonics. This method can be justified from a physical point of view in any case. The ohmic losses in the conductors are due to the loss of energy in the form of heat during the impact of conduction electrons with the lattice points of the crystal structure of the conductors or, more generally, with the elementary particles of the material (atoms), since we may also have amorphous materials [145], [146]. The physical laws, which govern the phenomena that occur during these collisions, are characterized by times of the order of the electron relaxation times (approximately 10^{-14} sec at room temperatures, up to 10^{-9} sec at temperatures close to absolute zero). Thus, for the current harmonic frequencies that do not exceed a few GHz, the application of the method is absolutely correct, let alone for the frequencies of interest in power electronic applications (up to a few MHz). It should be noted at this point that Ohm's law is not valid for significant electric field variations that take place at times lower than the relaxation times of electrons [146]. In books of applied electromagnetism, such as [129], [138], one can find the conditions required to ensure that the superposition principle is a proper theoretical approach in the case of propagation of an electromagnetic interference in a medium, even when it shows losses.

If we decompose the waveform $i(t)$ of the current to its constituent sinusoidal waveforms according to Fourier analysis (Appendix IV), it maybe written in the form:

$$i(t) = I_{dc} + \sum_{n=1}^{\infty} I_n^{\max} \cos(n\omega t + \phi_n) \tag{3.5}$$

where I_{dc} is the constant term of the current, while the amplitude $I_n^{\max}$ of the n-th term is a function of n and ω, with ω the radian frequency of the first harmonic and is generally decreasing with respect to n (although not necessarily monotonically decreasing). For example, in the common case where $i(t)$ consists of rectangular frequency pulses $f=1/T$, with a minimum value of 0 (for a time interval T-T_h) and a maximum value of I_h (for a time interval T_h) and therefore with a duty cycle $D = T_h/T$, $I_n^{\max}$ will be given by the equation:

$$I_n^{\max} = \frac{2I_h}{\pi n} \sin(\frac{n\omega T_h}{2}) \tag{3.6}$$

The power P_{Cu} of the ohmic losses, in any case, will be:

$$P_{Cu} = R_{dc} I_{dc}^2 + \sum_{n=1}^{\infty} I_{n,rms}^2 R_n \tag{3.7}$$

where $I_{n,rms} = I_n^{\max}/\sqrt{2}$ is the rms value of the n-th Fourier term of the current and R_n the resistance at frequency $\omega_n = n\omega$. Finally, the total effective resistance of the winding R_{eff} will be given by the equation:

$$R_{eff} = P_{Cu}/I_{rms}^2 \tag{3.8}$$

where:

$$I_{rms} = \sqrt{I_{dc}^2 + \sum_{n=1}^{\infty} I_{n,rms}^2} \tag{3.9}$$

As a first example of application of the above analysis, the losses in windings of copper foils that carry pulsed currents are studied in [24]. The parameters considered are as follows:
- The total number of layers m of the winding.

- The duty cycle *D* of the current pulse series.

- The times t_r (rise time) and t_f (fall time) of the rise and fall of the current pulse (there is no overshoot), which are taken equal and appear as percentages of the total current period. It is obvious that as these times decrease, the harmonic content of the pulse series increases.

- The ratio h/δ of the thickness *h* of the conductor to the skin depth δ at the fundamental frequency.

It turns out that there is an optimal thickness h_{opt} for which the losses become minimum. For example, if it is 0.1<*D*<0.8 and t_r=t_f=0.5%, h_{opt} is given by the equation [24]:

$$h_{opt} = 3.075 \frac{\delta\sqrt{D}}{m} \quad , \qquad m>1 \tag{3.10}$$

What matters is that, in a similar way, one may examine the optimization of the winding's design, for various waveforms of current, involving each time in his study the parameters of interest and ending up in equations such as (3.10).

In the same work, an analysis is carried out in regard to when it is advantageous, in terms of losses, to use a round cross-section wire or a symmetrical stranded conductor (Litz). It is concluded that for a diameter of the solid wire up to 2δ, the use of Litz wire instead of the solid wire leads to a reduction in losses and is preferable. For higher frequencies, however, the possibility arising for the development of eddy currents in the entire volume of the Litz wire, together with the relative increase in the dc resistance of the Litz wire to be used, eventually increase the losses to a value greater than the resulting for a solid wire of round cross-section. A corresponding analysis is found in [74], as well as in [5] for a simple stranded conductor.

We will close this review on the issue of losses in windings that carry non-sinusoidal currents, with reference to work [79], in which the authors, based on Dowell's expression, bypass the Fourier analysis and proceed to direct approximate calculation of the effective resistance R_{eff} for a given waveform of current. The only required parameters, except the frequency *f*, are the rms values of the current I_{rms} and of its first derivative with respect to time I'_{rms}.

For frequencies with the radius *r* of the round cross-section conductor or the thickness *h* of the conductive foil not much higher than the skin depth δ (up to approximately 1.5δ),

Dowell's expression for the resistance factor F_R in a winding of m of layers (see §4.2.3) can be approximated as follows [79]:

$$F_R \cong 1 + \frac{G}{3} Z^4 \tag{3.11}$$

where:

$$G = \frac{5m^2 - 1}{15} \tag{3.12}$$

$$Z = h/\delta, \qquad \text{conductive foils} \tag{3.13a}$$

$$Z = (r/\delta)\sqrt{\pi\eta}, \qquad \text{round cross-section conductors} \tag{3.13b}$$

As we have seen, a random periodic current waveform may be decomposed to its Fourier terms. Given that it is $\delta \sim 1/\sqrt{f}$ (see eq. 1.3), the resistance factor F_{Rn} for the frequency of the n-th harmonic, will be given by (3.11) if Z is replaced with $\sqrt{n}Z_1$, where Z_1 is Z for $\delta = \delta_1$, with δ_1 the skin depth at the fundamental frequency. From (3.11) it follows that:

$$F_{Rn} = 1 + \frac{G}{3} n^2 Z_1^4 \tag{3.14}$$

While from (3.5), (3.7) and (3.8) follows:

$$\frac{R_{eff}}{R_{dc}} \cong \frac{I_{dc}^2 + \sum_{n=1}^{\infty} F_{R_n} I_{n,rms}^2}{I_{rms}^2} \tag{3.15}$$

If in this equation F_{Rn} is replaced from (3.14), with a few simple operations, it follows that:

$$\frac{R_{eff}}{R_{dc}} \cong 1 + \frac{G}{3} Z_1^4 \left[\frac{I'_{rms}}{\omega I_{rms}} \right]^2 \tag{3.16}$$

Equation (3.16) helps to easily determine the effective resistance for a random waveform of current, since finding the I_{rms} and $I_{rms}^{'}$ is a relatively simple task. It is a satisfactory approximation when the thickness of the conductor is close to the value δ_1 of the skin depth at the fundamental frequency and the harmonic content of the waveform of the current is not particularly high.

A great conclusion that one can come up with starting with (3.16) is that if the thickness of the conductive foil is chosen such that the winding shows the minimum effective resistance, for any current waveform with a low harmonic content (and in any case for a sinusoidal one), it will be:

$$\left(\frac{R_{eff}}{R_{dc}} \right)^{foil}_{opt} \cong \frac{4}{3}, \qquad \text{conductive foils} \tag{3.1a}$$

$$\left(\frac{R_{eff}}{R_{dc}} \right)^{round}_{opt} \cong \frac{3}{2}, \qquad \text{round cross-section conductors} \tag{3.17b}$$

CHAPTER 4

INVESTIGATION OF COPPER LOSSES IN LAYRED COILS

4.1. Introduction

Copper losses in magnetic coils depend on several geometrical parameters, as well as on frequency, in a way that makes their analytical modeling a quite difficult task. In this chapter a software tool is used, which implements finite-element-analysis (FEA) to solve electromagnetic problems in order to investigate a series of issues critical to the accurate determination of copper losses in layered coils. Some of the issues investigated are the impact of the edge effect and the winding pitch on the overall copper losses. The effective resistance of windings with a hexagonal conductor arrangement is also investigated and the accuracy of the results as well as the validity range of the classic models for copper losses in windings with round solid wire are specified. The results of this work help us to fully understand the real impact of the two-dimensional effects in layered windings of real rather than ideal magnetic components. They constitute a tool for the accurate calculation of losses, which is necessary for an optimized magnetic component design in power electronic applications.

The most extensive works on the issue of losses in copper coils, which stood as reference points for the theoretical approach of it, where those of S. Butterworth (1922) [5]−[7], E. Bennet και S. Larson (1940) [9], P. Dowell (1966) [12] and J. Ferreira (1994) [47], as also enhanced by M. Bartoli *et al.* [49], [58]. Each of these was broadly used in the design of transformers and inductors for the frequency range at which the capacitive currents of the coils can be neglected [14], [20], [24], [68], [79], [100], [108], [114], [123], [124], [128], [143]. For the establishment of the former analyses, several assumptions and approximations are introduced, which invalidate their predictions over numerous practical applications. These assumptions have to do with the geometry of the coil and the corresponding form of the magnetic flux in the window of a magnetic component, part of which crosses through the conductor located there[1] (about the leakage flux in a transformer

window see Appendix III). More specifically, the assumption of a leakage flux through the conductors parallel to the symmetry axis of the magnetic component (one-dimensional field analysis) often does not apply. The actual flux through the conductors has such a form that, until now, seems very difficult to be successfully treated by any analytical method in a complete way.

Several authors have criticized the forementioned models (mainly Dowell's) and have attempted to give expressions for a more accurate description of experimental or simulation results [29], [36], [48], [41], [70], [74], [81], [83], [87], [91], [96], [99], [106], [143]. These works contribute much to the better understanding of high-frequency copper losses. However, when they do not remain within the limitations of the initial models by taking some extra two-dimensional effects into consideration, they often focus only on part of the possible winding configurations or lead to quite complicated expressions. Moreover, the attempts so far of investigating layered windings seem to partially supplement the basic theoretical analysis of Dowell. Most of the times, their results are in the form of complicated formulas and coefficient tables. Besides that, they do not offer clear indications of when Dowell's formula is valid without modifications, or what the application limits of the new, each time, proposed expression are, for the establishment of which, cases with poor or no practical value are often analyzed. As examples may stand the cases of [109], in which the purpose of the whole work is based on the unsubstantiated argument that in practical applications values for the filling factor n (§4.2.3) lower than 0.66 are typical and [91], [95] in which, in order to support the conclusions presented, the case $n = 0.3$ is analyzed.

After Dowell's work, what happens so far is that round wire coil copper loss calculations are carried out using his expression (the one most often used), with many magnetic component designers not being aware of the possible error introduced, since literature offers only some scattered information about Dowell's model inaccuracy for coils not compactly wound [36], [48], [70], [74], [91], [96], [109], [143]. Ferreira's formula is often described as inaccurate [83], [100], without detailed reference to the magnitude of deviation from reality or from the corresponding one of Dowell, an issue thoroughly investigated in this chapter.

---

[1] In the case of transformers, this flux is described in the international literature as "leakage flux". However, as the investigation of copper losses involves both, transformers and coils, this term is commonly used in literature, in general, to describe the flow in the window of a magnetic component, without distinguishing between transformers and inductors. This same convention is also followed in this dissertation.

The air-gap fringing field effect (§3.4.1) seems to have sufficiently been studied in literature [24], [51], [59], [71], [89], [97], [102], [143]. Considering the edge effect (§3.4.2) [9], [24], [37], [46], [50], [70], [71], [72], [87], [91], [107], [124] there is a generally approved impression that it increases the losses which, as will be presented, is only partially true.

Under this scope, FEA software is the key to investigate and quantify the effect of the mechanism of copper losses at those frequencies that are high enough that, depending on the dimensions of the conductors, eddy currents are developed within the conductors. This chapter first summarizes the basic models for the calculation of copper losses. Then, with the use of FEA software, a detailed investigation of the distribution of current density and magnetic flux in round conductor layered, square conductor layered, as well as foil windings is carried out. As a result of this extensive work, some qualitative, easily comprehensive conclusions help to fully understand the extent of impact of 2-D effects on the losses encountered in layered windings.

4.2. Basics models for the copper losses in magnetic components

4.2.1. General considerations

The most commonly considered as classical works on the issue of copper losses in magnetic components are those of Butterworth [5]−[7], Dowell [12] and Ferreira [47]. Their object is the calculation of the effective resistance R_{ac} of solenoid coils with round conductors when a sinusoidal current of a given frequency f flows through them. Such a winding is divided into segments, each of which extends between a point of zero and another of maximum magnetomotive force (MMF) and which, in Dowell's work, are referred to as "winding portions" (Appendix III). To calculate the total increase in resistance of a winding of a magnetic component someone should identify the various portions of the winding and calculate, based on the number of layers and the value of the filling factor η (§4.2.3), the R_{ac} for each of them and finally, in the case of parts connected in series, to sum up these resistances. An inductor winding is such a portion, while in a transformer there are at least two or more, depending on the way selected for the interleaving of the primary and secondary winding/windings (Appendix III).

At this point, attention should be paid as, in the case of a transformer, in order to be able to separate the windings into portions, it is assumed that the primary and secondary ampere-turns are fully compensated and therefore the magnetic flux in the core is zero. This approximation is valid when the secondary windings are short-circuited, while the magnetic permeability of the core must be very large, ideally infinite. However, the deviation from the above approximation when a transformer is loaded is generally small and decreases as the magnetizing current decreases. It is also noted that in the loaded operation mode of an ungapped transformer, in which the primary and secondary ampere-turns are nearly equal (they are never exactly equal), only 7% (typically) of the instantaneous magnetic energy of the magnetic component is in the core, while the rest corresponds to the leakage field [92].

From the final expressions obtained someone can calculate the resistance factor $F_R = R_{ac}/R_{dc}$, where R_{dc} is the resistance at direct current of constant value. The basic assumption in any case is that the coil is formed by successive layers with a large number of turns, equal for all the layers and with the same distance d_t between adjacent turns. For the calculation of F_R in these models, the values of four parameters are necessary: the frequency f, the radius of the round conductor r, the number of layers m and the filling factor η, as defined in Dowell's work [12]. In the following we will see some more details on these three models.

4.2.2. S. Butterworth's work (1922)

Butterworth's work [5]-[7] is worth mentioning for three main reasons:

a) It was a pioneer work on the detailed study of copper losses in windings with HF current flow. Preceded works [referenced in [5]-[7]) were mainly experimental, without achieving a satisfactory theoretical background in the study of copper losses.

b) His work, as it was, or with improvements or modifications [10], has been a guide to the copper losses calculation in the design of magnetic components [123] for about forty years, until the presentation of Dowell's work in 1966.

c) Subsequent works that were included by the researchers in a broader family of analytical solutions based on the Bessel functions, such as Ferreira's one, have actually led to the same result.

Butterworth's work, compactly presented in [123], is mainly an attempt to describe with an analytical solution the available by that time experimental data on the effective resistance of solenoid coils with round conductors, in the absence of magnetic core. He derived formulas for the R_{ac} calculation of single layer (regardless of winding density), as well as

multilayer coils with widely spaced turns in their layers. Some years later, R. Mudhurst [10] focused on single layer coils and after a series of measurements he proposed some corrections.

Among the issues discussed in this chapter is also the comparative presentation of Butterworth's work with that of Dowell and Ferreira, which aim at the calculation of R_{ac} of coils with magnetic core. For this we will consider its results for the case at which the assumed conditions ensure that the radial component of magnetic field has minimum effect on the ohmic losses. Hence, we will consider his results only for the case when $l/D>10$, where l is the length of the air cored solenoid and D is its diameter. According to [5]–[7] this condition approximates what is called in literature an infinitely long solenoid, with MMF being equal to zero right outside the solenoid and with l/D ratio values higher than 10 not leading to any prominent changes on R_{ac} (compared to the case $l/D=10$). In the following, s is the center-to-center distance between adjacent turns of one layer (or otherwise, as it is called, winding pitch) and d is the diameter of the round conductor ($d=2r$). For a single layer solenoid, regardless of the value of d/s and for $l/D>10$, Butterworth ended to the following expression:

$$F_R = a(r/\delta, d/s) \cdot H(r/\delta) + K_1 \cdot \gamma(r/\delta, d/s) \cdot (d/s)^2 \cdot G(r/\delta) \qquad (4.1)$$

For sparse windings ($d/s<0.6$) of one or multiple layers and always for $l/D>10$, the corresponding expression is

$$F_R = H(r/\delta) + K_2 \cdot [p(m) \cdot m \cdot (d/s)]^2 \cdot G(r/\delta) \qquad (4.2)$$

where H and G were indicated respectively as the skin effect and proximity effect terms and K_1, K_2 are constants. In [5]–[7] one can find the analytical expressions of all the quantities appearing in (4.1) and (4.2). Note that in the two previous expressions, for the sake of uniformity with the following, the dependence on frequency is expressed by the ratio r/δ instead of the quantity z used by Butterworth, which is directly proportional to r/δ ($z=2\sqrt{2\pi}\,r/\delta$). Moreover, it must be noticed that Dowell's η parameter (see eq. 4.6) is proportional to the ratio d/s used by Butterworth. The reason that Butterworth did not derive a formula for the F_R of compactly wound coils (with $d/s>0.6$) is that the basic assumption in his calculations was that the proximity field within the copper has direction parallel to the

symmetry axis of the solenoid. As we will see in the following, this assumption is only true for windings sufficiently sparse, and thus, in the general case, the influence of adjacent conductors on the flux form within a conductor is not properly taken into account, so the result for the ohmic losses is greater than real.

4.2.3. P. Dowell's work (1966)

Dowell's analysis [12] on the HF copper losses offers a compact formula for the calculation of F_R for coils with round conductors, of a single or multiple layers. The coil must be wound on a high-permeable magnetic core and extend across the whole window width. This condition ensures (only partially, as we will see in §4.3.3) that the magnetic flux inside the copper has a direction parallel to the y axis of the magnetic component and that there is no edge effect, i.e. there is no field component in the x axis direction, which is perpendicular to y, at the ends of the coil, close to the core yokes. The several windings of it, regarding the case of a transformer, are wound successively, one over the other, along the x-axis. Furthermore, given that the field extends only in the y axis and its value depends only on x, application of Ampere's law for Dowell's model results in that the space between layers is a constant MMF area. For the facilitation of his calculations, instead of round conductors, he considered the existence of equivalent conductors with square cross section of the same area. The real part of his final expression gives the F_R, of a winding portion which extends between a zero and a maximum MMF point (Appendix III), as:

$$F_R = \frac{R_{ac}}{R_{dc}} = Z \frac{\sinh 2Z + \sin 2Z}{\cosh 2Z - \cos 2Z} + \frac{2(m^2 - 1)}{3} \cdot \frac{\sinh Z - \sin Z}{\cosh Z + \cos Z} \qquad (4.3)$$

where:

$$Z = (r/\delta)\sqrt{\pi\eta} \qquad (4.4)$$

The length h of the cross-sectional dimension of the hypothetical square cross-section conductors assumed by Dowell results from the requirement that the cross-sectional area of the hypothetical conductor should be equal to that of the real conductor of round cross-section and radius r:

$$\pi r^2 = h^2 \Rightarrow h = r\sqrt{\pi} \tag{4.5}$$

It is self-meant that despite the hypothetical - computational change in the shape of the cross-section of the conductors, their positions (the positions of the centers of their cross section) remain the same so that the overall winding profile remains unaltered. It is clear that as we sweep the cross section of a layer with square conductors along the *y* direction, we encounter copper only at a fraction of the path. This percentage Dowell called it layer filling factor η. With a simple geometric view, it turns out that when the winding pitch of a layer with circular cross-section conductors is *s*, then the following expression applies:

$$\eta = \frac{r\sqrt{\pi}}{s} \tag{4.6}$$

If someone ignores the existence of the insulating coating, which in any case covers a conductive wire of round cross-section in magnetic components and assuming that the adjacent turns in one layer are in contact with each other, it will be *s = 2r* and the maximum possible value for η is η_{max}=0.886.

It comes up from (4.4), (4.5) and (4.6), that for foil windings (η=1) eq. (4.3) can be applied by substituting $Z=h/\delta$, with *h* in this case the foil thickness. It has to be mentioned that Dowell's result for the sub-case η=1 coincides with the formula given in [9], which was a work exclusively on foil windings. Dowell's originality was just that he assumed the same flux and current density forms as in foils (i.e. *y* oriented flux, current density dependent only on *x*) when the conductive layer is only partially filled with copper, i.e., when it consists of square cross-section conductors

Finally, it is to be noted that the imaginary part of Dowell's final expression gives the inductance coefficient of the current carrying winding [12], which in the classic equivalent circuit of a transformer coincides with a percentage of the leakage inductance L_σ.

The relevant results show the drop of inductance with frequency, which is due to the reduction of leakage flux within the copper. This phenomenon is of great importance in applications where the value of L_σ of a transformer is a critical parameter, e.g. in the case of resonant converters in which transformer and inductor parasitic components are used as resonators [105], [117], [122], [148], [154]. However, although the reduction of the magnetic field energy in the copper volume can be very significant, as a whole the induction of leakage

L_σ decreases only by a small percentage [12], [24]. The reason for this lies in the fact that, even in a tight winding with circular cross-section conductors, the copper filling factor is of the order of 40-50% [124], while most of the leakage flux in the window area is usually out of the copper, in the space between different windings (high MMF areas) or between the layers of the same winding. Further than the above reference, the phenomenon of the inductance drop with frequency will not concern us in this dissertation.

In works as [14], [20], [24], [68], [79], [100], [108], [114], [124], [128] Dowell's formula is applied for the optimization of magnetic components design. The fact that this 1-D analysis is not accurate at high frequencies or for low values of the layer filing factor η (considering round wire windings) is often discussed, but the authors make just some general reference on this issue. In [91], [96], [109], referring to [48], the authors report that Dowell's formula is considered accurate for a winding pitch equal to 1.5 wire diameter, interpreting in [91], [109] this condition as $\eta>0.66$, whereas the correct expression should be $\eta>0.59$. In [36] the 1-D analysis is approved for $\eta>0.50$. In [91], [74] it is reported that for low frequencies the one-dimensional analysis can generally be considered accurate, while the same argument is stated in [70] and moreover it is mentioned that the error of the one-dimensional analysis can be up to +50% when $\eta<0.44$. Also, in [91] the error of Dowell's 1-D analysis is reported for some specific values of the *m*, *r/δ* and η parameters. It is evident that, although Dowell's formula is widely approved, its application limits and error magnitude are not explicitly specified. One goal, among others, of the work presented in this chapter of the dissertation is to provide clear indications of the validity of Dowell's 1-D analysis, as well as of Butterworth's 2-D model and Ferreira's one, which is briefly presented in the next paragraph.

4.2.4. J. Ferreira's work (1994)

In the next few decades after its presentation, Dowell's work has been nearly exclusively used to calculate the ohmic losses of magnetic components. From the experimental results, however, it became apparent that, for low values of the filling factor η or for high frequencies, it gave values for the F_R generally larger than the real ones.

Nearly thirty years later, Ferreira presented a copper loss calculation model that bypasses the approximation of square cross-section conductors and considers the actual round cross-section conductors [47]. The basic assumptions are the same as those of Dowell (identical layers placed consecutively across the *x*-axis, many turns per layer, magnetic core, winding between zero and maximum MMF. The critical assumption for this model is that the flux within a conductor due to the adjacent current carrying conductors is parallel to the symmetry

axis *y*, whereas any component in the *x* direction is only a result of the current density of the conductor itself. He applied the principle of superposition based on the orthogonality (independence) of the two effects, skin and proximity, arguing that he first observed this condition (orthogonality), while it is already mentioned above that this separation had been applied by Butterworth seventy years earlier. His final expression for F_R did not contain as a parameter the distance between adjacent conductors of one layer and it was found that its result has an extremely high error [49], [58]. In order to improve its accuracy, the authors in [49], [58] introduced Dowell's filling factor η in the initial formula:

$$F_R = \frac{q}{2}\left[r_{skin} - 2\pi\eta^2\left(\frac{4(m^2-1)}{3}+1\right)r_{prox}\right]$$
(4.7)

where:

$$q = \frac{\sqrt{2}r}{\delta}$$
(4.8)

and:

$$r_{skin} = \frac{\mathrm{ber}(q)\mathrm{bei}'(q) - \mathrm{bei}(q)\mathrm{ber}'(q)}{[\mathrm{ber}'(q)]^2 + [\mathrm{bei}'(q)]^2} \qquad r_{prox} = \frac{\mathrm{ber}_2(q)\mathrm{ber}'(q) + \mathrm{bei}_2(q)\mathrm{bei}'(q)}{[\mathrm{ber}(q)]^2 + [\mathrm{bei}(q)]^2}$$
(4.9)

with r_{skin} and r_{prox} the skin and proximity effect terms, respectively. The expressions describing the skin effect, as well as the series expansions of the Bessel functions appearing in (4.9), are found in Appendix I.

4.3. Solving electromagnetic problems with finite-element-analysis software

4.3.1. Introduction

In the next paragraphs of this chapter, as well as in the next chapter, we export a series of conclusions about the copper losses in magnetic components. These conclusions are based on

simulations, made with an electromagnetic problems software solver, which applies the finite element method.

This section first summarizes the general philosophy adopted in the scientific community on the subject of computer simulations. Then follows a brief description of the design methodology followed by the user, as well as the general operating principles of the algorithms applied by the software used to calculate the required electromagnetic quantities (Vector Fields Opera-2D). More details on specific issues, further than the brief description given below, can be found in the software instruction manual [141].

4.3.2. General issues about simulation of physical systems on a computer

In various fields of modern scientific research, some systems are simulated by computers. These systems either have a large number of expressions that describe them or exhibit complex or chaotic behavior (e.g. study of mechanical strength of materials and constructions, study of the Earth's atmosphere or systems of celestial bodies and particles on an atomic scale).

From the study of the literature on the subject of this dissertation, it becomes apparent that computer simulation has become more and more important over the years. The software most commonly used is circuit simulation software (prediction of voltages and currents in electrical circuits) and finite-element-analysis software to solve electromagnetic problems (prediction of electromagnetic quantities in space) and problems of thermodynamics (heat diffusion study) or fluid mechanics (e.g., study of flux in refrigerant liquid circuits). Researchers resort to the computer simulation method when it is difficult to obtain reliable measurements, when they want to predict several quantities prior to the construction of an object (device or component) or when knowledge of results is required for a wide range of different operating conditions, that are in practice not easy to vary in a controlled manner.

Unfortunately, in many cases, simulation escapes the strict framework of necessity and ends up being a shelter for those who do not want to be involved in the time-consuming procedure of experimental confirmation. There would be nothing to blame about this tactic if it was assured that the simulation could 100% substitute the experiment in any case. But this cannot be true, since the conditions that apply to a simulated system are impossible to be transferred with perfect fidelity to any software environment. The construction of a simulation model is done only through a series of approximations, both by the user of the software and then by the software itself. These approximations inevitably make the results of the simulation to differ from the real ones. Several quantities are considered constant without

being so, simplifications and rejections of "negligible" terms are made, in order to regress the size of the problem several symmetries are considered, often true in practice only approximately, while for the modeling of specific parts of the problem, ready-made model blocks from software libraries are used, without always matching reality. In many cases, researchers accept, for the sake of time saving and convenience, any error in the results of the simulations (especially if the limits within which it varies are approximately known). In many other cases, however, rough simulations are made with poor modeling of the physical systems, perhaps even with a low correlation level to the object of study, in order to invest some scientific work with the mantle of confirmation, which is occasionally called by its initiators as ... "experimental".

The final conclusion is that computer simulation is a very useful tool and indispensable for the advancement of science, but in no way substitutes the experiment and any conclusion resulting from simulation processes must be under question until confirmed by reliable experimental measurements. For the experimental measurements the critical parameter to be known is the margin of error of their results.

At this point, it is necessary to comment on the use of finite-element software for the extraction of the conclusions presented later in this chapter, as well as for the establishment of the new model presented in Ch. 5. Through the analysis presented in these two chapters of the dissertation it comes clear that the use of finite-element software for this study was a necessity and that without this great computing tool the export of the corresponding results would be impossible. An assumed methodology for obtaining experimental results corresponding to the numerical data on which the conclusions of these chapters are based would require much time to devise and even more time to implement, certainly much more than what can be spent on a doctoral research. Even more complicated and time-consuming would be the effort to an analytical solution of the problems discussed later in this chapter, and, as explained in Ch. 5, the problem of a random arrangement of the conductors investigated there, simply and logically, cannot have an analytical solution.

A properly structured model, with a satisfactory mesh of finite elements, gives very accurate results for the simulated problem. The question is whether the user of the software, (as well as any other prospective reader of the results) fully understands what is it exactly being simulated, if the boundary conditions selected are the right ones, what is the impact of the several approximations made and finally, whether the model built on the software environment corresponds, even approximately, to the actual physical problem. In order to have a clear answer to all of the above questions, an effort was made in the presentation, as

this is performed in Ch. 4 and Ch. 5, so that all the parameters related to the models simulated are listed, together with clarifying comments on the relevant cases of magnetic components in practical applications.

4.3.3. Simulation of magnetic components in two dimensions with the Vector Fields - Opera 2D software

4.3.3.1. Locating areas with different physical properties

The magnetic components are devices which in many cases can be represented by two-dimensional models. In order to reflect reality –at least approximately– such a representation should be subject to any of the following two conditions:

(a) The magnetic component has a cylindrical symmetry. There is no magnetic field component in the azimuth direction (the direction of e_θ in a cylindrical coordinate system with unit vectors e_r, e_z, e_θ) and its distribution is the same for any cross section of the component that includes the axis of symmetry.

(b) The magnetic component has a big length in direction z (its x, y dimensions are much smaller than its z dimension) and its cross-section perpendicular to that direction is fixed independent of the z-position. In such a case it is a satisfactory approximation to assume that the distribution of the field on the cross-section of the component does not change at the various positions along the z direction and that the field has no component in this direction (x-y symmetry). The three-dimensional phenomena that may occur at the edges of the component are not taken into account and are considered negligible when the simulation model is correlated to the physical problem, since they affect only a small part of the component.

If the "x-y symmetry" is selected by the user the problem is solved with the vector potential A as the unknown quantity. If the "axial symmetry" is selected, the unknown quantity in the differential equations system being solved is the modified vector potential $r_m A$, where r_m is the radial coordinate in the cylindrical coordinate system.

For the magnetic components simulated in the context of this dissertation and in which the various electromagnetic quantities in the volume of their current carrying conductors are studied, x-y symmetry has been assumed, although the cylindrical symmetry is closer to the actual geometry of the problem. This assumption does not significantly affect the end result, provided that in the actual component the thickness of a conductor (in x dimension) is much smaller than the average radius of the component (less than 5% [9]). This condition generally applies in practice and the numerical result of the simulation practically does not differ

between the two cases of symmetry. The *x-y* symmetry was selected so that the results of this analysis are directly comparable to those found in literature, as in the vast majority of works on the issue of copper losses in magnetic component windings the same approximation is found.

After designing the different areas of the model, the software user determines the physical properties of each area. In general, an area of the model belongs to one of the following three categories:

(a) Areas with non-zero conductivity σ and magnetic permeability μ different from that of the vacuum, e.g. ferromagnetic materials and materials in which eddy currents develop.

(b) Magnetic field generating areas, i.e. current carrying conductors. The excitation of these conductors can be achieved either by a voltage source, thus the value for the resulting current is determined as a result of the solution, taking into account the interaction with the other parts of the model, or by a current source. The details of the voltage or current sources are defined by the user.

(c) Areas not occupied by materials but by vacuum or air ($\sigma=0$, $\mu=\mu_0$).

For the purposes of the study done in this dissertation, the relative permeability of the core of the magnetic components was decided to be constant (linear magnetic material) and equal to $\mu_r=2000$. It is noted that the results of test simulations showed that higher or even lower values (up to $\mu_r=150$) do not lead to remarkable changes on the leakage flux path or on the effective resistance of the windings. This argument complies with the results presented in [71]. Hence, no further investigation (e.g. for $\mu_r<150$) was made in this dissertation.

The software can solve various types of problems, such as static electricity or magnetism problems, rotating machines, charged particle beams, transient states etc. For the study of magnetic components in the present work, harmonic analysis of steady state is made, in which the excitation applied, as well as all the electromagnetic values, are sinusoidal time functions. Unlike other cases of problems, such as the problems of transient phenomena, if the sinusoidal steady state is analyzed, it is not necessary to apply initial conditions, (values of several quantities for $t=0$). In all the simulations, the excitation comes from a voltage source applied to a primary winding (copper foil), which is otherwise of no interest in the study, except to the extent that it is always taken care to be at a sufficient distance from the short circuited secondary winding under study, so that its presence does not affect the electromagnetic quantities in the area of interest.

Moreover, given that magnetic field analysis is performed, insulating materials, such as the conductors coating (e.g. in enameled wires) or the bobbin for the fitting of the winding in the core window, are not separate areas in the models, but instead they are simulated as air areas. Note that two-dimensional magnetic analysis does not account for conduction or displacement currents on the *x-y* plane, and therefore capacitive currents between the conductors are not considered.

4.3.3.2. The expressions being solved

In the case of harmonic low frequency magnetic analysis (there is no loss of energy to the vacuum space in the form of electromagnetic radiation) the software solves the Helmholtz vector equation with unknown quantity the magnetic vector potential *A*:

$$\nabla \times \left(\frac{1}{\mu} \nabla \times \boldsymbol{A} \right) = \boldsymbol{J}_s + \boldsymbol{J}_v - \sigma \frac{\partial \boldsymbol{A}}{\partial t} \tag{4.10}$$

In the previous expression the current density has been analyzed in three terms: $\boldsymbol{J}_s$ are the imposed currents (current source excitation), $\boldsymbol{J}_v$ are the currents flowing on external circuits (excitation from voltage sources and currents flowing in windings which form closed circuits and are connected to some load) and $\sigma(\partial A/\partial t)$ are the induced currents (e.g. eddy currents) flowing either in closed circuits of the previous category or in conductive objects that do not form an external circuit. In two dimensions (problem with *x-y* symmetry) only the *z* components of the above three terms are present and (4.10) is simplified as follows:

$$-\nabla \cdot \frac{1}{\mu} \nabla A_z = J_{sz} + J_{vz} - \sigma \frac{\partial A_z}{\partial t} \tag{4.11}$$

In the problems discussed in the dissertation, as mentioned above, the excitation comes from a voltage source and therefore $\boldsymbol{J}_s$=0. The secondary winding under study is in any case shorted, i.e. it is connected to an external circuit with resistance equal to the minimum acceptable by the software (1μΩ), since zero resistance is not acceptable. Having selected the length of the models in the *z* dimension to be 1000mm and in conjunction with the cross-sectional dimensions of the conductors in the *x-y* plane, it comes that 1μΩ is a negligible resistance compared to that of the winding conductors. From the solution of the problem, the

distribution of $A_z(x, y)$ at the *x-y* plane of the *z* vector potential component is found and then the *x* and *y* components of the magnetic induction are given by the relations:

$$B_x = \frac{\partial A_z}{\partial y} \qquad \text{and} \qquad B_y = -\frac{\partial A_z}{\partial x} \qquad (4.12)$$

4.3.3.3. Boundary conditions

Applying boundary conditions when solving electromagnetic problems limits the physical problem and ensures the reliability of the results. In particular, in a finite-element-analysis software simulation model, the boundary conditions can be applied for four reasons:

(a) To offer a way of reducing the size of the finite element model in cases where the total problem shows some symmetry.

(b) To approximate the magnetic field over long distances from the problem area (remote field boundaries).

(c) In some cases of electromagnetic problems they are used to represent the excitation sources.

(d) To ensure the uniqueness of the solution.

In the context of this work, the application of boundary conditions serves the purposes (a) and (d).

To ensure the uniqueness of the resulting solution, a node of the finite mesh or a surface of an area (side) of the model is required to have a predetermined value for the potential, which is the unknown quantity in the differential equations. For magnetic analysis in two dimensions which is of our interest here, the above condition is equivalent to a fixed value for the vector potential on at least one side of one of the areas. In the software environment, the boundary conditions are expressed by imposing either a zero vertical component ($B_n=0$) or a zero parallel component ($B_t=0$) of the field on the side of an area. So, the aforementioned condition is satisfied if a zero vertical component is imposed on one side of an area of the model. If there is no such side in the areas of the object being simulated (i.e. satisfying the condition $B_n=0$) the condition can be applied to a side of the model's external limits. These external limits must be far enough from the object to be simulated so that the solution in the area of the study object won't be affected by any boundary condition applied to them. A satisfactory distance is usually equal to five to ten times the largest dimension of the object being simulated.
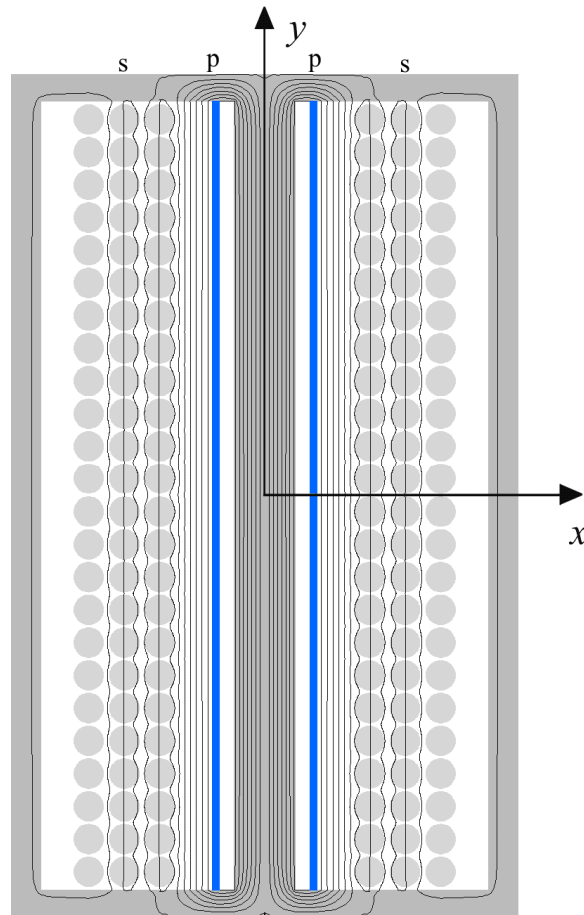
Figure 4.1: A typical form of transformer model simulated. By exploiting the symmetries about the *x* and *y* axes and by applying the appropriate boundary conditions, only a quarter of the total geometry is finally simulated. This particular illustration of flux lines corresponds to $r/\delta = 1$.

The application of boundary conditions to take into account some symmetries and to reduce the size of the model can be demonstrated through an example. Figure 4.1 shows the cross-section of a transformer with a primary winding consisting of a thin conductive foil and a secondary consisting of three layers of round cross-section conductors with twenty-four turns each. As can be seen from the printed magnetic field flux lines, this problem has mirror symmetry at both the *y* and the *x* axes.

The currents flowing in the symmetrical to the *y*-axis areas are opposite and the field on the *y*-axis is tangent with it ($B_n=0$). Correspondingly, the currents in areas symmetrical to the *x*-axis are on the same direction and the field everywhere on the *x*-axis is perpendicular to it ($B_t=0$). Hence, by applying the two above-mentioned boundary conditions to *x* and *y* axes and by setting them both as outer boundaries of the model, we can finally simulate only a quarter of the total problem (e.g. that enclosed in the first quadrant of the figure).

In the geometries simulated for the study presented in the following paragraphs of Ch. 4, both symmetries have been taken into account and thus each model includes one-quarter of the total geometry. In Ch. 5 however, where the windings under study have a random conductor arrangement, there is no symmetry about the *x*-axis. Hence, only the symmetry about the *y*-axis (which of course only applies approximately) is taken into account, and therefore half of the total geometry is simulated (see Fig. 5.1).

4.3.3.4. Finite element mesh and accuracy of the solution

The Finite Element method to solve a problem that extends in two dimensions lies in dividing the plane into a finite set of triangular elements (finite elements) and in the subsequent solution of the problem for each node of the mesh, which results from the lines that define these elements (finite mesh). Each area of the model is bounded by sides, which can be either straight or curved lines. The user is asked to define a number of subdivisions of each side, which are either evenly distributed over the entire side length or, with a convergence factor, they get gradually shorter as the given side is swept in one direction. When creating the mesh, these subdivisions correspond to element sides and the possibility of densifying the elements towards one end of a side allows a denser mesh in areas of interest for which high accuracy is required. The Delaunay method is used to create the finite mesh, while the Galerkin method of weighted residuals [141] is applied for the solution of (4.11) at each node of the mesh.

When solving the problem, it is approximated that the vector potential values vary linearly from one node to another and therefore the field calculated by the curl of the vector potential (eq. 4.12) will be constant within each element. To improve accuracy, the user can select to change the above condition and vary the vector potential between successive nodes as the interpolation of the values valid at the nodes with the application of a second-order polynomial.

The solution of the problem includes the values of the vector potential at each node and the values for the current density in each element of the mesh. The illustration and extraction of the results can be done graphically and/or in lookup tables, for specific points or areas of the plane or along lines defined by the user or presented as graphs with color scale zones or curves of equal values for a given quantity. For example, curves of equal vector potential correspond to magnetic flux lines (as in Fig. 4.1).

The Finite Element method gives values for the derivatives of the vector potential (i.e. for the magnetic field) that are discontinuous from one element to the other. Hence, the software

calculates an average value of the corresponding values in the elements surrounding a node and this value is applied to the given node. This procedure does not, of course, refer to nodes located on area boundaries, where discontinuities in the magnetic field value are eventually encountered. The comparison between the magnetic field values in an element before and after the calculation of the mean value at the three nodes that define it determines the local error of the solution for the given element. This error is a quantity that can be mapped, just like the other quantities (e.g. the magnetic field and the current density), so that the user can detect large error areas directly with a simple visual check. In order to have an overall picture of the error in the entire simulated model, it is possible to calculate its RMS value for all the model elements (the square root of the average of the squares of the errors of all the elements). A second option is the calculation of the weighted average error, in which the weighting factor is the area of the elements, i.e. small area elements contribute less compared to large area elements.

It is clear that by reducing the size of the elements in a part of the model, the accuracy of the solution is locally increased. So, it is possible, if this option is selected by the user, for the software to locate the areas of increased error, i.e. the areas where intense field variations are observed and through a repetitive process to automatically redesign the mesh with smaller elements. This process stops when a predefined number of iterations is completed or when the number of model elements reaches the maximum permissible according to the program license, or when the total RMS error of the solution drops below a user-specified value. In the first two cases the execution of the program is stopped. In the models simulated for the dissertation's requirements, the typical number of elements ranged from 70.000 to 100.000 (with the software license available, the maximum allowed number of items was 400.000).

It should be noted that automatic refinement of the mesh in areas of increased error does not always ensure the convergence of the solution; it is possible to have an error rise, instead of the expected drop, with the reduction of the elements size in large error areas. A divergent solution can arise, for example, when some areas of the model have edges. In such a case, convergence can be achieved if during the design a tiny blunt of the edge is inserted by adding a very small (compared to the model dimensions) side (straight line or arc) there where otherwise would be a corner. Such design tricks actually have a negligible effect on the final accuracy of the results, and after their implementation they usually go unnoticed.

The aforementioned error values are the upper error limits of the actual error and an inadequate division of the plane into large elements not only will lead to false results for the electromagnetic quantities, but will also lead to a vague picture of the actual error values.

One last remark is that for linear magnetic materials the local error in an element is mainly related to its size and the size of its adjacent elements and less to the size of the elements (and the error value) in other areas of the model. If the model includes non-linear magnetic materials (this is not the case in the present study), the correlation of the local error with the total error, and thus with the size of the elements in any part of the model, is certainly more important, but it is hard to be exactly estimated.

A point of special attention is the fact that, even for a satisfactory prima facie overall accuracy of the model, as preselected by the user of the software, the automatic refinement of the mesh in areas with high error may not be sufficient in critical areas of the model. In the study carried out in the present work such areas of increased interest are the conductors of the magnetic components. The automatic refinement of the mesh implemented by the software does not ensure that the elements of the finite mesh in the conductors have dimensions smaller than the skin depth at the test frequency. For finite elements with dimensions comparable to the skin depth (or greater), the final results regarding the form of the magnetic field, the current density distribution and the power consumption may be grossly misleading. Therefore, the initially selected options of the software user (the number of subdivisions on the sides of the several areas) must ensure that the area corresponding to the conductors is divided into finite elements sufficiently small, even for the highest frequency for which the simulation is run. Figure 4.2 shows a detail of one of the models simulated for magnetic components with a winding consisting of circular cross-section conductors (that of Fig. 4.1), in which the finite element mesh appears. At the maximum frequency for which the operation of the magnetic component was simulated, the relation $r=5\delta$ applies, where r is the radius of the cross-section of the conductor and δ the skin depth at that frequency. It comes obvious from the figure that even at this frequency the skin depth remains approximately three times the typical dimensions of the finite elements within the conductor. It is obvious that any modification of the model in the direction of increasing the accuracy of the solution, either by increasing the mesh elements or by altering the character of the interpolation of values from node to node (polynomial second order rather than linear) significantly increases both the simulation time and the size of the result file.
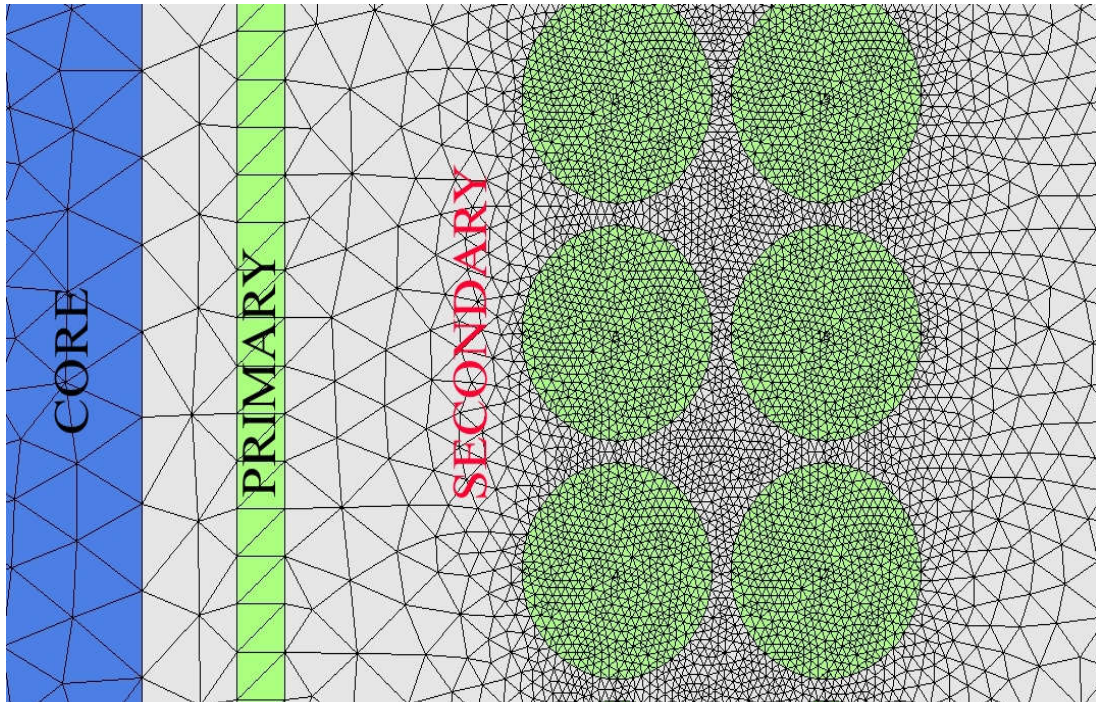
Figure 4.2: Detail of the model of Fig. 4.1 in which the finite element mesh appears. When designing the model, it has been selected for 76 elements to be placed on the circumference of each conductor.

Finally, it should be noted that with regard to the computer used, the practical requirements for reducing the runtime of the simulations are a high speed clock for the processor, large RAM and the ability to increase the virtual memory of the system. In any case, if the simulation time and the size of the result file remain within reasonable limits, for a carefully designed model, the total RMS error of the solution is around 1%. This value is also the standard value for the total RMS error of the solution in the models simulated. Therefore, the whole analysis in the dissertation based on simulations made with the finite element software describes results that are subject to an uncertainty of this order.

4.4. Validity range of the classic theoretical models

4.4.1. General considerations

While accurate experimental measurements are the most reliable way to contrast between theoretical models and practical applications, computer-aided simulation is the appropriate way to validate a model created by analytical methods. Two critical factors in this process are

the accuracy of the method that the software utilizes to solve a problem and the feasibility of reproducing in its environment the conditions under which a model is established. Considering FEA, the first factor is out of question, since Maxwell's equations are solved, regardless of the automated method that the software uses to solve the differential equations system or to create the finite-element mesh. As for the second factor, reproduction of the model conditions and selection of the proper boundary conditions is mainly a matter of the software user skills rather than the facilities or limitations of the software itself.

In the following paragraphs, with the help of the FEA software, a detailed investigation of the current density and magnetic flux distributions, as well as the value of the resistance factor F_R is made in windings formed by conductor layers. At first, the case of square cross section conductors is investigated to check the accuracy of Dowell's model, which was developed describing exactly this geometry. Dowell's model, however, is used to calculate F_R in windings consisting of circular cross-section conductors as well. So next, the above mentioned quantities are investigated for circular cross-section windings and the results of the three models (Butterworth - Dowell - Ferreira) are compared with those of the simulations, so that the precision of the models and the limits of their application come clear. It should be noted that all the results - conclusions presented in this study refer to the case when $d_t = d_l$, with d_t the distance between adjacent turns of one layer and d_l the spacing between successive layers, i.e. when the conductors are placed in a square layout. In §4.4.3 reference is made to the case when $d_t \neq d_l$.

4.4.2. Coils with square cross-section conductors and foils

As a first task, for the requirements of the analysis in this part of the dissertation, numerous FEA simulations were carried out in order to check the validity of the models about copper losses in layered windings under sinusoidal excitation. The first issue of study was the leakage flux, current density and effective resistance of coils wound with square cross-section conductors or conductive foils extending across the whole width of the core window.

It is true that square cross-section conductors (as well as rectangular cross-section ones [119]) in magnetic component coils are not actually met often in practice (they are used in high-power-low-frequency applications for the achievement of high copper filling factor), but study of this case was necessary to investigate the validity of Dowell's result, since his formula was extracted within the scope of such conductors. Moreover, as already mentioned,

a foil winding may be considered as a sub-case of square conductors layer, at the limit where $\eta \rightarrow 1$.

The maximum number of layers at the simulations was $m_{max}=3$ and at the maximum frequency it was $(h/\delta)_{max}=5$, with h the edge of the square conductor or the thickness of the foil. Windings with filling factor values from $\eta=1$ to as low as 0.475 were studied. The reasons why it was chosen to investigate the above ranges for these three parameters are related to the values usually obtained by the respective parameters in practical applications (with circular cross-section conductors) and are analyzed in the following paragraph. For the facilitation of presentation, the error of Dowell's 1-D analysis in respect to the simulation results is expressed in terms of the quantity:

$$E_S = \frac{F_R^{1D} - F_R^{FEA}}{F_R^{FEA}} \times 100\% \tag{4.13}$$

where F_R^{1D} and F_R^{FEA} are the results for the resistance factor F_R of one-dimensional analysis and those of the computer-aided FEA, respectively.
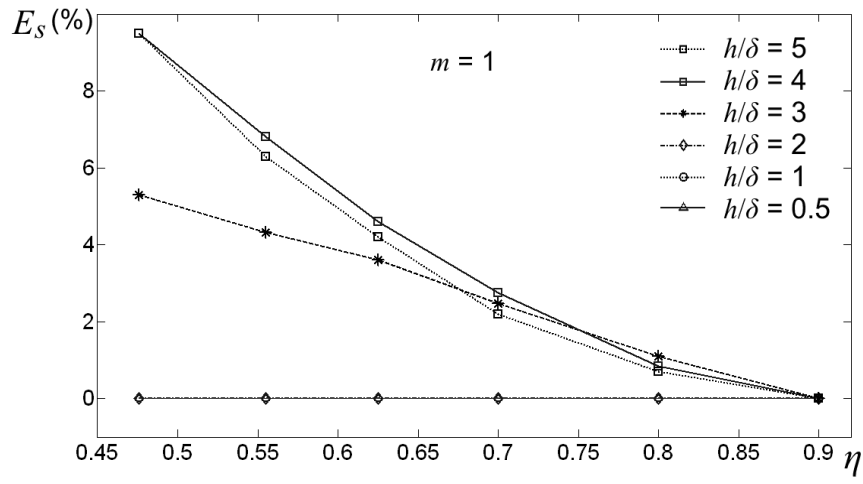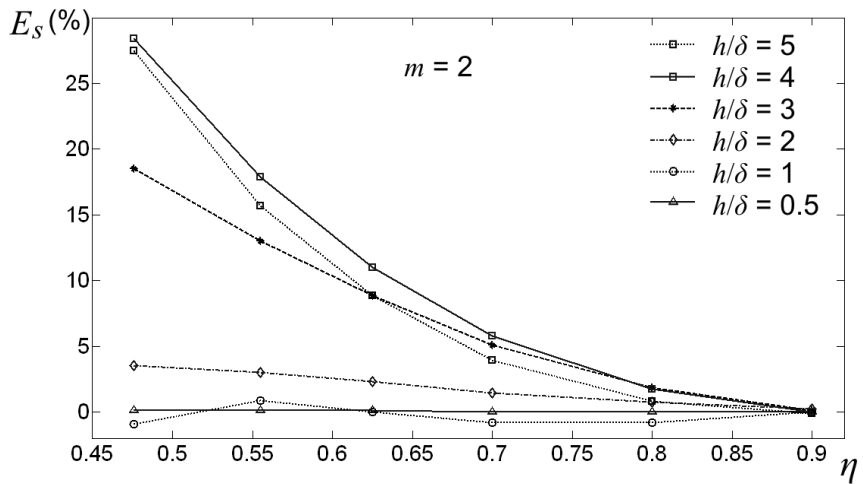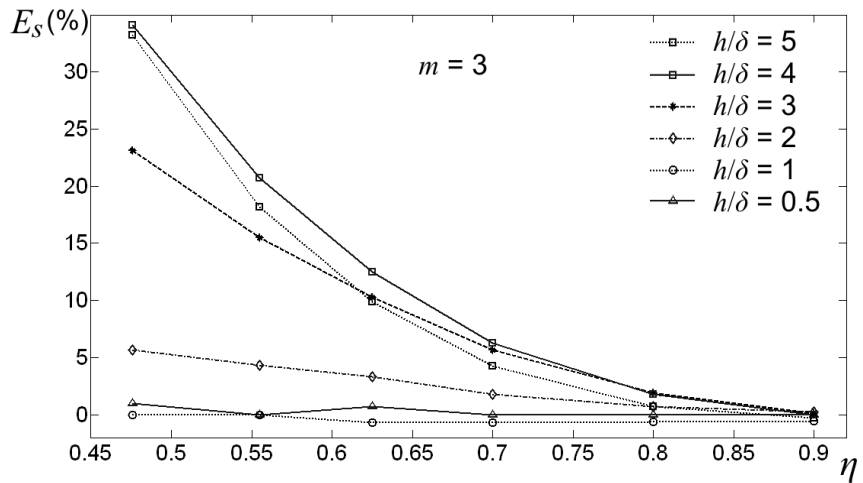
Figure 4.3: The error E_s of the result of (4.3) (Dowell's equation) relative to the FEA results for square cross-section conductors (eq. 4.13), as a function of the filling factor η, with h/δ as a parameter, for the number of layers (a) $m=1$ (b) $m=2$ and (c) $m=3$. In case (a) E_s for $h/\delta=0.5$, 1 and 2 is equal to zero.

In Fig. 4.3 the error E_S of Dowell's prediction is plotted compared to the FEA result versus filling factor η for the cases $m=1$, $m=2$ and $m=3$, having the ratio h/δ as a parameter.

From the study of the total set of results for the aforementioned ranges of the parameters, in general, the following conclusions are derived:

- For foil windings ($\eta=1$) occupying the full window width, F_R is calculated with negligible error by Dowell's model, regardless of the number of the layers or the frequency. The leakage flux is parallel to *y*-axis of the magnetic component and the current density distribution depends only on *x*-dimension, just as it was assumed in [12].

- For square cross-section conductors the 1-D solution generally overestimates the losses. Further than this general finding, we may see that E_S decreases as η increases or/and h/δ, *m* decrease. For any *m* and h/δ values it is $E_S<5\%$ if $\eta>0.75$. Moreover, for any *m* and η values it is $E_S<1\%$ if $h/\delta<1$.

It is evident from the results of the previous simulations that the accuracy of Dowell's formula depends on the degree of fulfillment of the condition that only a *y*-component of the leakage flux is present. The current distribution, which screens the bulk of copper from magnetic flux, has of course the same form (depends only on *x*). With decreasing η and increasing frequency 2-D effects take place, the effective cross section increases, and Dowell's model becomes inaccurate. This attribute is clearly demonstrated in Fig. 4.4, where a two-layer winding with $\eta=0.625$ is shown, simulated at (a) $h/\delta=1$ and (b) $h/\delta=2$. Due to the relatively small filling factor value the magnetic flux and current density distribution show a 2-D form in the conductors even for $h/\delta=1$. At $h/\delta=2$ the deviation from Dowell's 1-D assumed forms is much more prominent.

Strictly talking, Dowell's formula gives the losses in layers of square conductors including the limiting case of foils. It was derived under simple electromagnetic considerations and accurately describes the current density distribution and losses for those filling factor η values at which the flux is exclusively *y*-directed. Under this scope, the parameter η has a very clear physical sense when applying Ampere's law on the whole length of a long coil with many turns per layer, to calculate the value of the magnetic intensity $H(x)$ at a position *x* of the winding [12]. This calculation indicates that proximity effect over a conductor is due to all the other conductors in the winding and a small change in the path of integration at *y*-direction does not considerably alter the final result.
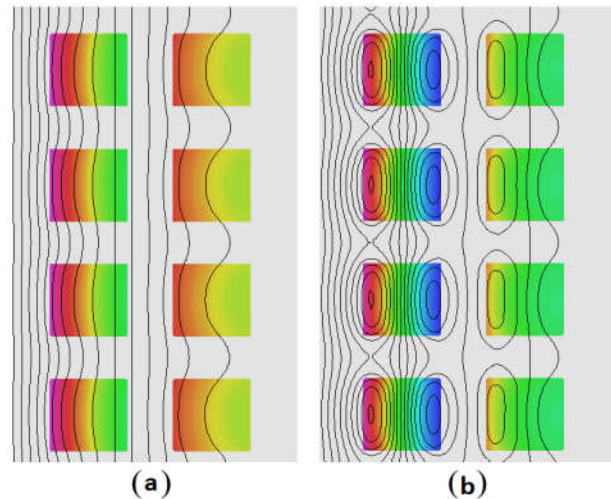
Figure 4.4: Instantaneous current density and flux lines for square conductor winding with two layers, which has been simulated for (a) $h/\delta=1$ and (b) $h/\delta=2$. Red colored areas are with high current densities. The flux pattern in (b) indicates the existence of areas with oppositely directed currents (color blue stands for negative current).

Yet, despite the simple reasoning behind Dowell's work, in the publications [95], [96] the author attempts to bring out two supposed physical inconsistencies of this model. He presents as the first error of the model the supposed violation of Ampere's law in Dowell's calculations leading to the final expression. To support his claim, the author shows how the result changes by changing the integration path (in *y*-direction) to calculate the total ampere-turns that determine the MMF value at some *x* position when this integration path (always in the *y* direction) contains only a few turns (one-two). Obviously, in such a case, the result for MMF is different, but this case is not relevant to Dowell's model, which has clearly been formulated for the case of layers with many conductors and with integration on the whole length of the layer [12]. In order to confirm the above reasoning, someone can refer to works such as [5]-[7], [41], in which the skin effect in a layer with a finite - specific number of conductors is treated, not under the scope of determining the total MMF at a point in space, but considering each conductor as a discrete unit that interacts with each one of the other conductors. For the calculation of F_R of each separate turn, the effects from all the other turns are summed. There, it becomes clear how quickly the effect of the other turns of the layer is damped down with the distance from the turn under study. In the case now that the winding is in a magnetic core and the corresponding calculations involve the application of the image theory, it is realized that, since the number of turns is not very small (for example, it is not

just three or four), it does not matter what their exact number is but only their pitch (i.e., Dowell's layer filling factor η) and the number of layers.

In another attempt to doubt the theoretical basis of Dowell's model, the author in [95], [96] argues that the appearance of the quantity $\delta/\sqrt{\eta}$ in the final F_R expression, where the corresponding equation for a copper foil (for example) has just the skin depth δ (eq. 4.3 and 4.4), constitutes a violation of the electromagnetic theory. This happens –as claimed– because this way the skin depth, which is normally a feature of the physical properties of a material (eq. 1.3), becomes a quantity dependent on the geometric parameters of the winding, such as the filling factor. It is also noted in [95], [96] that, in various works in literature, the quantity $\delta/\sqrt{\eta}$ is referred to as equivalent or effective skin depth, while we should recall that in other works, for the expression of the same thing, some authors name the product ηf active or equivalent frequency. However, in this case too, there is no relation between Dowell's model and any suppositive violations of the electromagnetic theory. The definition of skin depth refers to the case of an electromagnetic wave incident on a solid, flat, infinite, conductive surface. The depth at which the intensity of the radiation has the value of $1/e$ of the corresponding undisturbed radiation (away from the conductive surface), but also the resulting current density has the value $1/e$ of the corresponding on the surface, is defined as skin depth. When the conductive area is not solid, e.g. a layer of conductors in a magnetic component, the depth for which this reduction will occur is necessarily related to the degree of filling of the surrounding space by conductive material (and thus by current density) and has nothing to do with the definition of any physical quantity.

4.4.3. Coils with round wire

For coils with round conductors, a large number of simulations were carried out in order to have a satisfactory sweep of the parameters involved, so as to cover all the cases referring to practical applications. More specifically, the ranges of r/δ, m and η had as follows: $0 < r/\delta \le 5$, $1 \le m \le 3$ and $0.443 \le \eta \le 0.865$. The layers simulated had a reasonably large number of conductors, (of the order of 50). The study excluded the first few conductors in the vicinity of the ferrite yoke since, no matter how small is the distance of the end conductors (of its first conductors) from the ferrite, there is always an imperceptible edge effect, which slightly changes their state. The primary winding (a single sheet extending across the whole window width) was kept far from the short-circuited secondary under study, at a distance

approximately equal to five times the radius of the secondary conductors ($5r$), despite that simulations showed only negligible effect even for a distance equal to $2r$.

At this point some remarks are necessary about the selected range for the critical parameters η, r/δ and m. As we have seen in Ch. 3, optimization reasons lead to power electronic converter designs with magnetic components operating at a fundamental frequency for which it is approximately F_R=1.5 for round conductor windings [14], [79], [124], [128] and respectively F_R=1.33 for foil windings [79]. These F_R values correspond to frequencies for which r/δ (or h/δ) is approximately equal to unity, or a bit lower than that. In most of the cases the harmonic content of the current waveform gathers within the first few harmonics, although at some power electronics applications harmonics of the order of the 15th may have non-negligible magnitude. Under this point of view, study of the copper losses with $(r/\delta)_{max}$=5 is more than sufficient. Moreover, for a magnetic component designed for a switching frequency at which it is r/δ=1, it is quite possible that current harmonics of order higher than 25, if present, flow as capacitive currents in through the volume of the winding. On the other hand, in layered windings with carefully wound wires, the distance d_t between adjacent turns is in no case much greater than twice the thickness of the wire's insulation, which is about 5%-15% of its radius. If we also account for some extra distance further than the insulation and suppose a total distance (copper to copper) between adjacent turns of d_t=0.6r, it will be η>0.68. Hence, the selected ranges for η and r/δ are satisfactory for studying most of the practical application designs with layered windings. If the designer consciously chooses not to pay attention on the winding method, there will be a non-layered configuration. However, this case is not described by the aforementioned models and is analyzed in Ch. 5 of this dissertation.

Finally, about the number of layers m, it should be noted that the study of windings containing up to three layers is considered sufficient to determine how, as the various parameters vary, adjacent turns of the same layer or different layers interact, so that the magnetic flux and current density distributions take their given two-dimensional form. However, regarding the exact values for the resistance factor F_R when m>3, no information is obtained from the analysis performed for $m \leq 3$, but it comes clear that there is a deviation trend of Dowell's one-dimensional analysis from the simulation results with an increase in m. Thus, given the results of the one-dimensional analysis (for $m \leq 3$), for m>3 an approximate calculation of the actual F_R can be made, although the most appropriate treatment would be the simulation for the specific each time number of layers.

In the following, the quantity E_R will be used for the expression of the deviation of each of the three basic models from the FEA results, which is exactly the same as E_S in (4.13), that is:

$$E_R = \frac{F_R^{\text{model}} - F_R^{\text{FEA}}}{F_R^{\text{FEA}}} \times 100\% \tag{4.14}$$

where F_R^{model} and F_R^{FEA} are the F_R results for the resistance factor of any of the three models and the FEA respectively, in the case of the of the circular cross-section conductors.

In Figures 4.5 to 4.7 there are diagrams comparatively showing the results of the three models and FEA for m=1, 2 and 3, for some of the values of the filling factor studied. The dash-dotted curve refers to Butterworth's formula (4.2).

Moreover, for a more detailed presentation of Dowell's model accuracy, Fig. 4.8 shows the error E_R of (4.3) relative to the FEA simulation results as a function of the filling factor η, with the ratio r/δ as a parameter. Notice that for $m>1$, at high frequencies ($r/\delta>3$), Dowell's model accuracy slightly improves with frequency in contrary to the general attribute and the fact that, for large values of η the result it gives marginally underestimates the losses (typically 5%).

The conclusions derived from this work can me summarized as follows:

(*i*) Butterworth's formula for single layer infinitely long coils with any spacing (equation 4.1):

- In the whole η range studied, F_R is calculated with nearly negligible error, even for sparse windings with $\eta \cong 0.5$.

(*ii*) Butterworth's formula for multilayer, infinitely long windings with widely spaced turns in a layer (eq. 4.2):

- In the whole η range studied, F_R is calculated with an approximate error of $E_R \cong +6\%$ at r/δ=1, but gives a considerable overestimation at higher r/δ values. This error reduces considerably at the low η range ($\eta<0.6$), but still remains unacceptable for the calculations to be considered as even approximate (typically between 20% and 30%, depending on the given r/δ value).
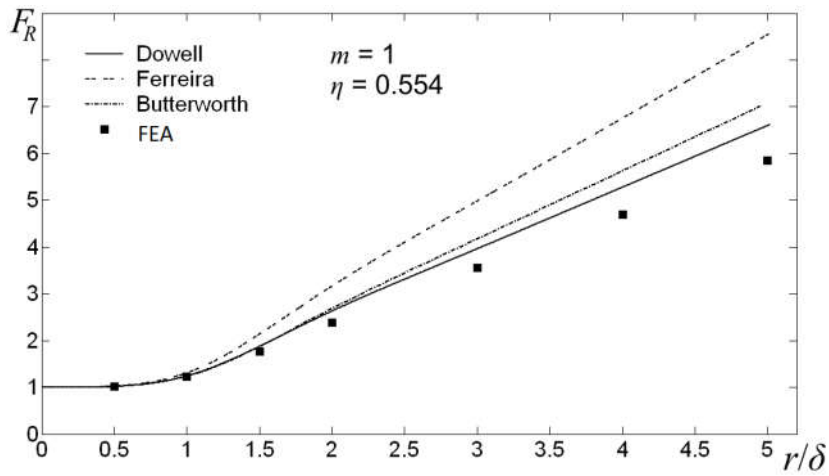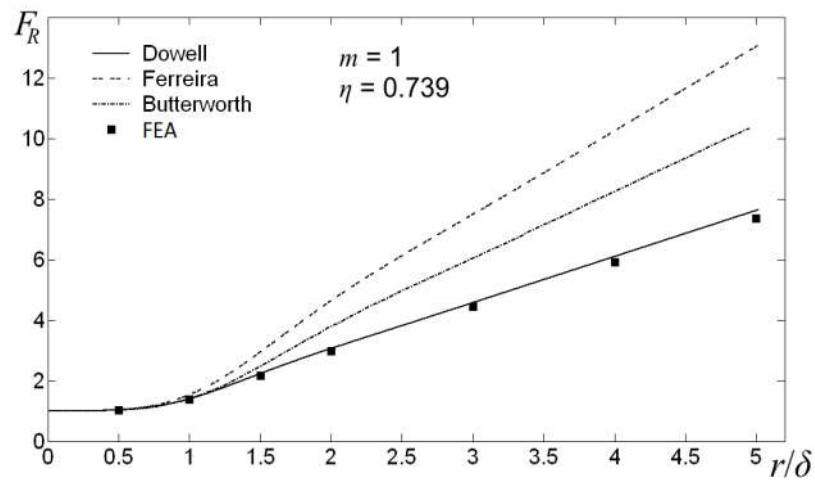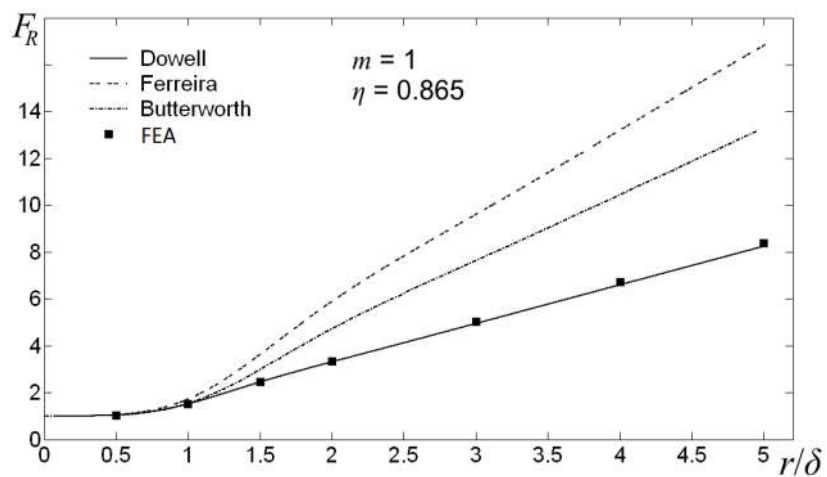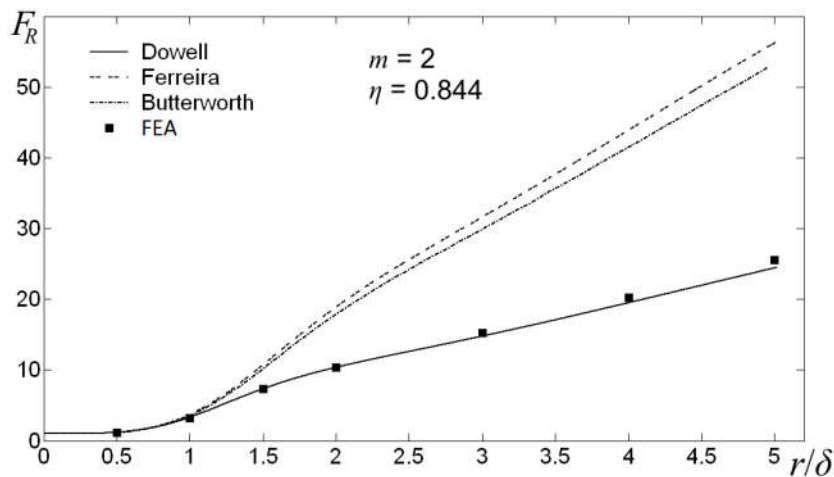
Figure 4.5: Comparative graph of the results of the three basic models for copper losses and those of FEA software simulation, for round conductor coils, with $m=1$ for (a) $\eta=0.554$, (b) $\eta=0.739$ and (c) $\eta=0.865$.
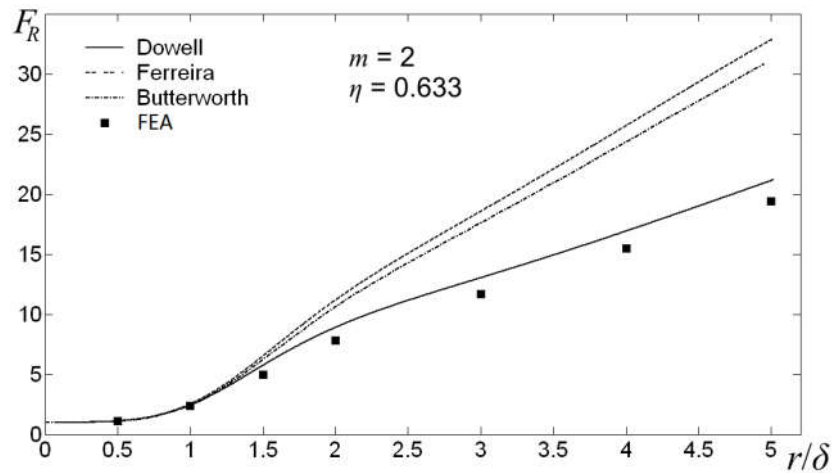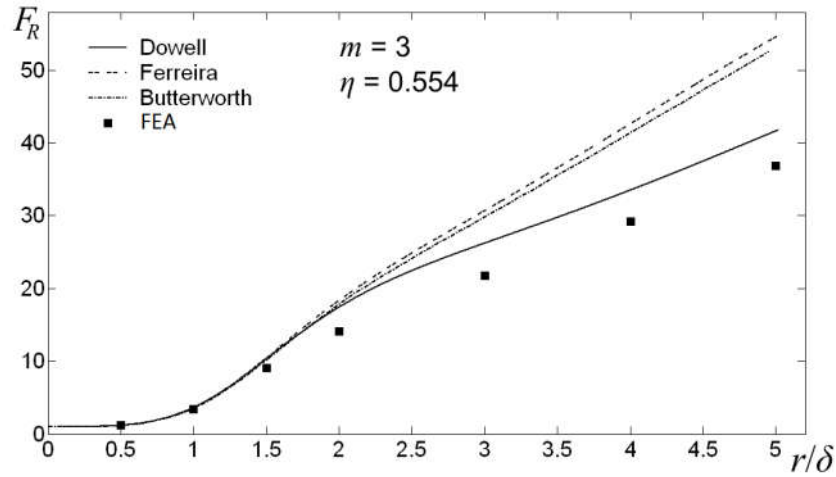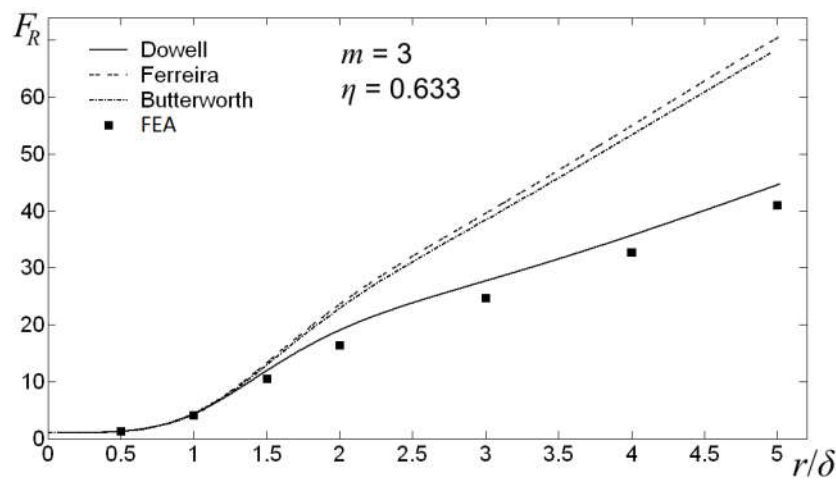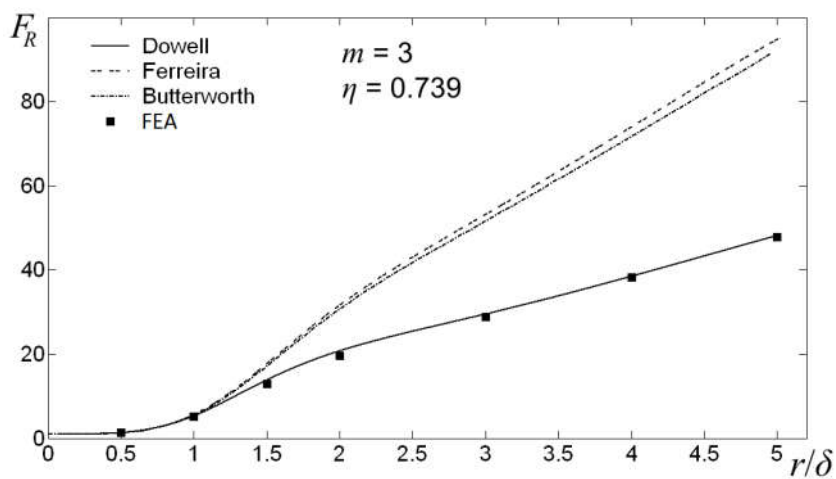
(a)
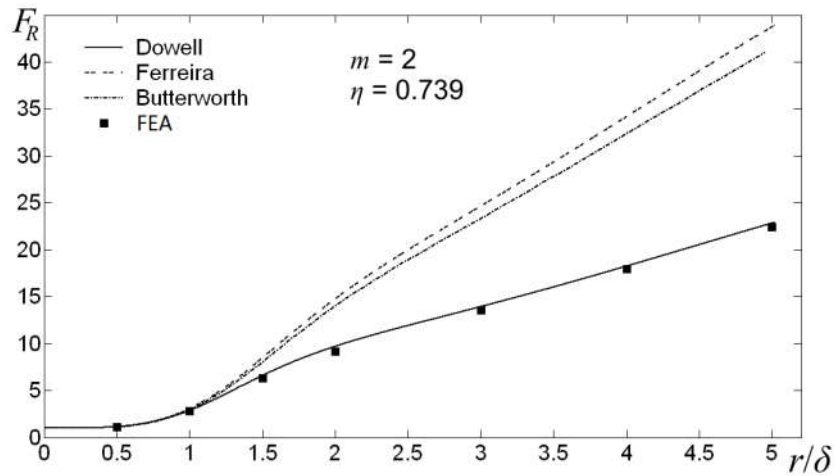
(b)

(c)

Figure 4.6: Comparative graph of the results of the three basic models for copper losses and those of FEA software simulation, for round conductor coils, with *m*=2 for (a) *η*=0.663, (b) *η*=0.739 and (c) *η*=0.844.

(a)

(b)

(c)

Figure 4.7: Comparative graph of the results of the three basic models for copper losses and those of FEA software simulation, for round conductor coils, with *m*=3 for (a) *η*=0.554, (b) *η*=0.633 and (c) *η*=0.739.
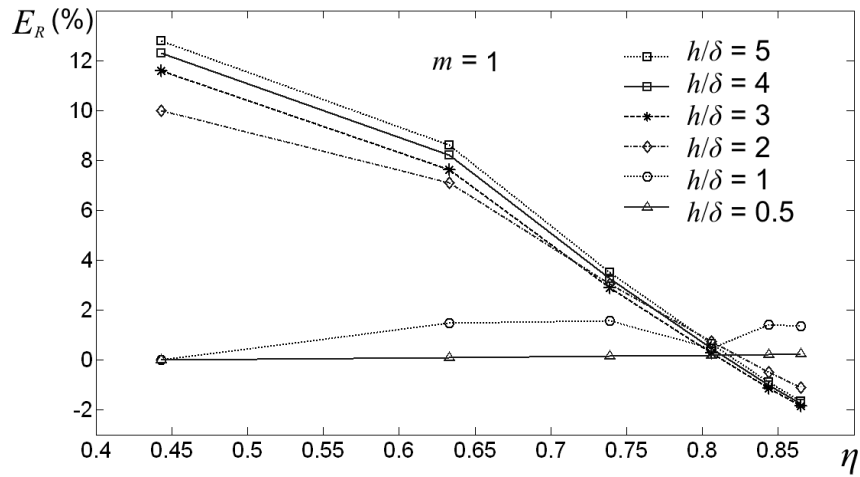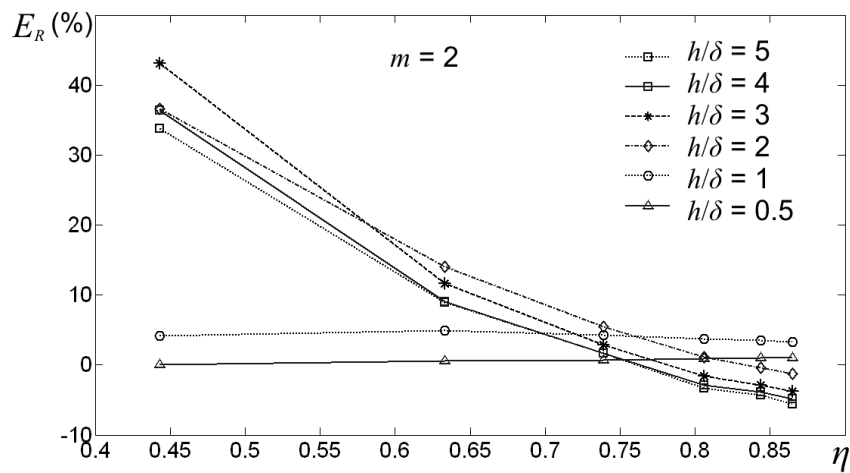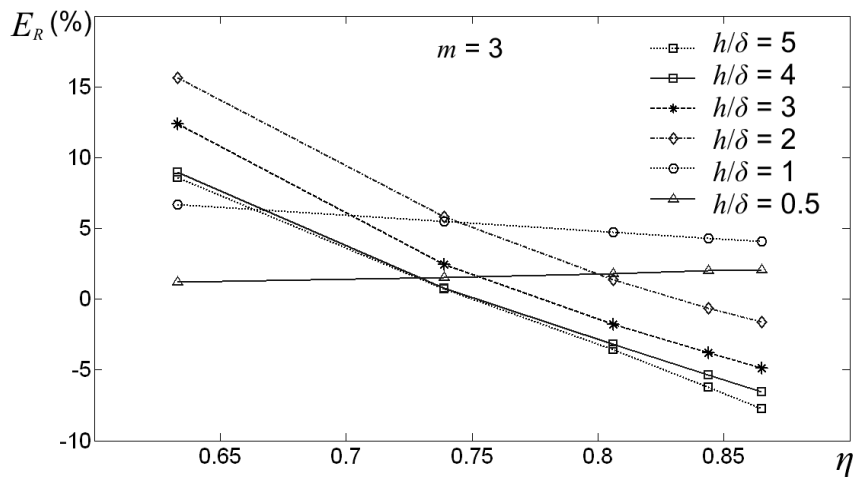
Figure 4.8: The error E_R of (4.3) (Dowell's equation) from the result of FEA for round conductors, (eq. 4.14), versus filling factor η, with r/δ as a parameter, for (a) $m=1$, (b) $m=2$ and (c) $m=3$.

 (*iii*) Ferreira's formula (eq. 4.7):

- Regardless of the specific η και r/δ values, for $m>1$ Ferreira's formula and Butterworth's formula (4.2) give approximately the same results.

(*iv*) Dowell's formula (eq. 4.3):

- For $\eta>0.75$ its result practically coincides with the simulation results, with E_R remaining in the approximate range of $\pm 5\%$. For lower η values E_R takes positive values and increases, as η decreases and/or m, r/δ increase. However, for $r/\delta<1$ this overestimation generally remains lower than $+5\%$.

It can be readily concluded that, even though all three models generally overestimate the losses, Dowell's formula is far more accurate, even when low filling factors are involved. It is evident that using (4.2) and (4.7) (referred in literature as "Bessel solutions") lead to a high error, which is because of the assumption that any *x*-component of the flux within a conductor is only due to the current in it and that proximity effect (which is any case is the dominant effect) gives only a *y*-oriented flux [5], [47]. This assumption is untrue except when very sparse windings or low frequencies are involved (see §5.4.2). This fact is clearly demonstrated in Fig. 4.9, at which the magnetic flux lines are shown at the winding space from where a conductor has been removed. While the absence of one conductor does not considerably alter the general pattern of the current density distribution in the neighboring ones (this is easily verified by simply viewing the result of the simulation), the magnetic flux in the empty space is generally more than just *y*-oriented, although this attribute is less keen for low *f* and η values. We can see that in Fig. 4.9(a) ($\eta=0.633$, $r/\delta=1$) the flux form is much closer to Ferreira's model assumption than in Fig. 4.9(b) ($\eta=0.633$, $r/\delta=2$).

It is necessary here to remind that, in all three analytical models discussed, MMF is assumed constant between successive layers and thus F_R does not depend on the interlayer distance d_l, something also cited in [109]. However, from the simulations carried out, it comes up that in fact d_l affects the MMF diagram, the current distribution in the conductors and eventually the F_R. From the case at which the layers are very close to each other ($d_l=0.05r$) up to that of very distant layers ($d_l>5r$), F_R is reduced by about 10% at the most prominent case of very low η values. At high η values the effect is negligible.
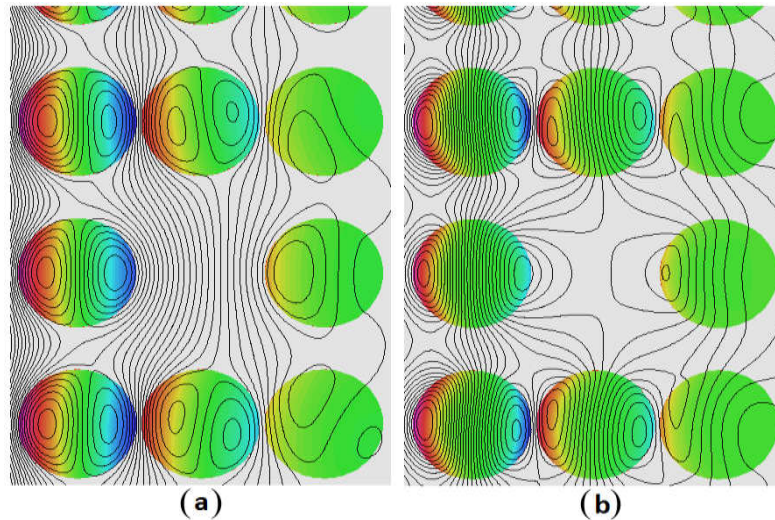
Figure 4.9: Flux lines in the space of a missing conductor in a winding with *m=3*, *η=0.633* for (a) *r/δ=1* and (b) *r/δ=2*.

4.5. The edge effect in magnetic components

4.5.1. General considerations

The edge effect in windings of magnetic components in some cases has a negative impact on copper losses, but in many others, as we will show in the following, it does not really affect them or it even improves the overall performance of magnetic components, despite that potentially it may cause some hot spot. Even so, authors so far do not pay much attention to the real impact of edge effect, giving the general impression that it is something that has to be eliminated by all means. Unfortunately all this information is scattered in literature (§3.4.2) and most of the times the relevant research suffers lack of generality (as for example when focusing on single layer foils) and lack of simplicity, considering the involved parameters and the form of results (expressions and tables of coefficients). The purpose of this work is not to repeat previously extracted results, but to give some important hints in the direction of a better understanding of the edge effect.

For this, several simulations were carried out, for copper foil coils as well as for round conductor coils, where the frequency and all the geometrical parameters were subject to variation - investigation. More specifically, these parameters, as well as their ranges, have as follows (also see Fig. 4.10): distance of the winding from the ferrite yoke d_f ($0.5 \leq d_f/h \leq 5$ for

foils and $0.5 \leq d_f/r \leq 15$ for round conductors), interlayer distance d_l ($0.1 \leq d_l/h \leq 2$ for foils and $0.05 \leq d_l/r \leq 0.8$ for round conductors), number of layers m ($1 \leq m \leq 4$) and frequency f ($0 \leq h/\delta \leq 5$ for foils and $0 \leq r/\delta \leq 5$ for round conductors). Moreover, for round wire windings, several η values were investigated ($0.633 < \eta < 0.865$).

The windings under study are symmetrically placed within the full width of the available window, i.e., the distance d_f from the ferrite yoke is the same on top and bottom of the magnetic component (also see Fig. 4.11). Hence, here also applies the symmetry with respect to the *x*-axis, as well as to the *y*-axis and only a quarter of the total geometry is simulated. The selected maximum values for the quantities d_f/r (or d_f/h) and d_l/r (or d_l/h) where imposed by the fact that greater values are quite unlikely to be met in practice. Magnetic component designers make an effort so that copper occupies as much as possible of the window width, within the requirements for electrical insulation from the core, for ease of construction and to protect conductors from a damage of their insulation films (e.g. with the use of a coil former). On the other hand, a foil winding with interlayer insulation of twice the thickness of the foil, further than the resultant low copper factor, shows extremely high leakage inductance (Appendix III) and any thicker insulation is generally avoided. Typical interlayer insulation films are much thinner than one conductor layer. However, this is not the case considering the distance between different windings, e.g. the primary and secondary winding of a transformer. Requirements for electrical isolation make it necessary in this case to place some special insulating films, inevitably though in expense of increasing the leakage flux. It should be noted, however, that in some cases, for reasons of electromagnetic shielding;, it is necessary to place some conductive film between the primary and secondary winding in a transformer [128], but the analysis carried out in the dissertation does not include this case.
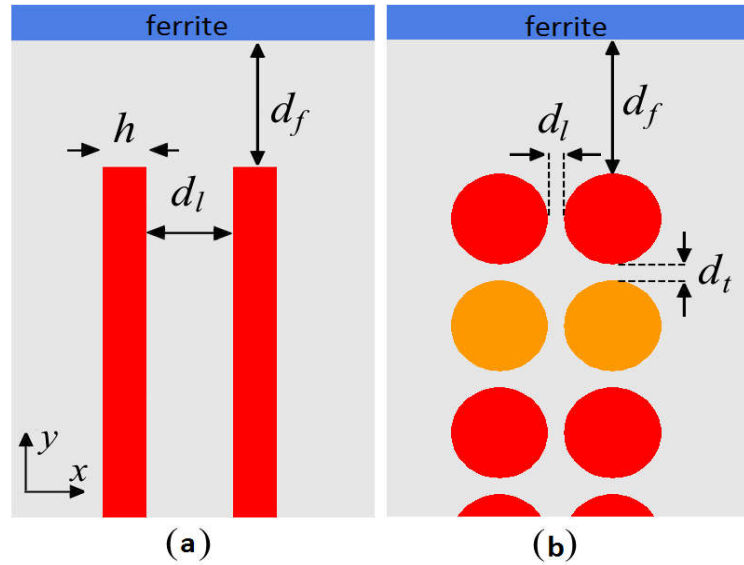
Figure 4.10: Definition of the geometrical quantities d_f, d_l, d_t and h for the description of high frequency effects. In (b) the array with $\sigma_a = 2$ is colored orange.

Regarding the number of layers m, the same remark applies, i.e. the study for $m \leq 4$ gives the general picture of the edge effect impact variation with variations of this parameter. For accurate results when $m > 4$ one has to make simulations for that particular each time number of layers.

The study of the several effects was made upon the whole of the winding, for each layer separately, for separate groups of conductors or either specific conductors. The F_R result in any of the above cases (with edge effect) is compared to that for no edge effect present (without edge effect) and is expressed by the quantity:

$$DF_R = \frac{F_R^{\text{with EF}} - F_R^{\text{without EF}}}{F_R^{\text{without EF}}} \times 100\% \tag{4.15}$$

It is reminded at this point that, especially in the case of conductive foils, the quantity $F_R^{\text{without EF}}$ appearing in (4.15) is equal to the result of Dowell's one-dimensional analysis (denoted as F_R^{1D} in (4.13)).

Finally, before any detailed conclusions of this work are presented, two basic remarks about the applied conditions in the FEA simulations for the study of the edge effect should be made:

(a)   In any case, the winding under study is short-circuited and the excitation primary foil, which is geometrically in contact with the ferrite, is considered distant enough so as not to affect the field geometry around the winding edges where the 2-D effects take place. After several simulations, it is concluded that, for this condition to hold true, the distance d_{ps} between the short circuited secondary and the excitation primary should be greater than the distance d_f between the winding and the ferrite yoke (Fig. 4.11). Special attention must be paid to this condition, since the proximity of the winding under study with the excitation primary considerably alters the flux form in the vicinity of the conductor edges and eventually the encountered losses. This effect is even more prominent when the excitation primary is also placed at a distance from the ferrite yoke [70], [107], [109]. Moreover, the core on the side of the winding under study being opposite to the side where the excitation primary is, is also distant enough, at a d_{sf} distance (not marked in Fig. 4.10, see Fig. 4.11), which is of the order of d_f too. This is to exclude the possibility of a flux distortion and the correlative small change in losses, as that described in [107].
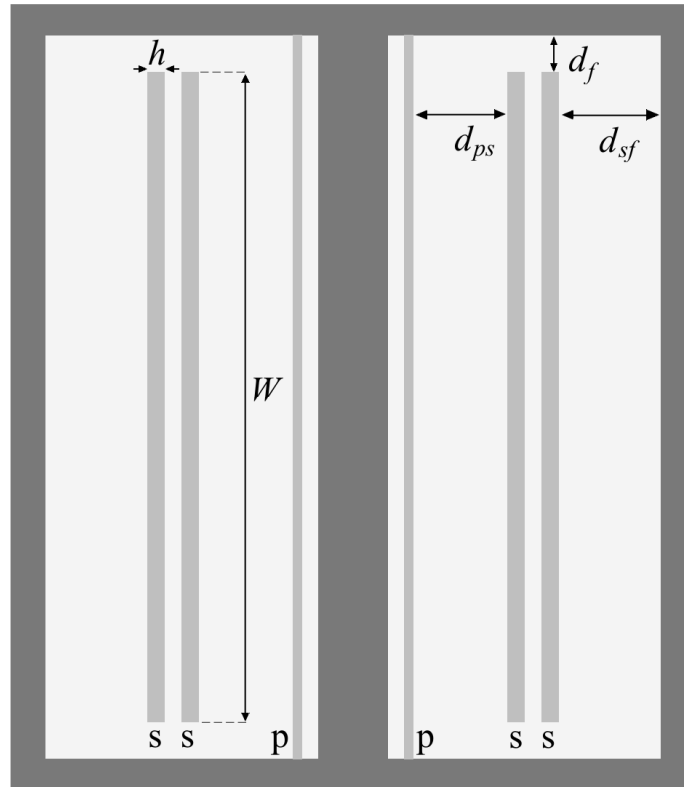
Figure 4.11: Typical geometric arrangement for studying the edge effect with FEA. The geometry is similar if the secondary winding (s) under study is composed of circular cross-section conductors.

(b)   The height W of a conductive sheet in y direction (Fig. 4.11) and its thickness h have fixed values and their ratio has the fixed value $W/h=90$. The significance of the W/h ratio will be demonstrated further below with the analysis of the results.

4.5.2. The edge effect in windings with copper foils

Indicative of the simulation results are the graphical examples given in the diagrams of Figures 4.12 to 4.14. Figure 4.12 shows DF_R plotted as a function of d_f/h, with h/δ as a parameter, for $m = 1, 2$ and 4. In Figure 4.13, for $m = 2$, DF_R is plotted as a function of d_l/h, with d_f/h as a parameter when $h/\delta=0.5, 1$ and 4, while in Fig. 4.14 is the corresponding diagram for $m = 4$ and for $h/\delta=1, 3$ and 5.
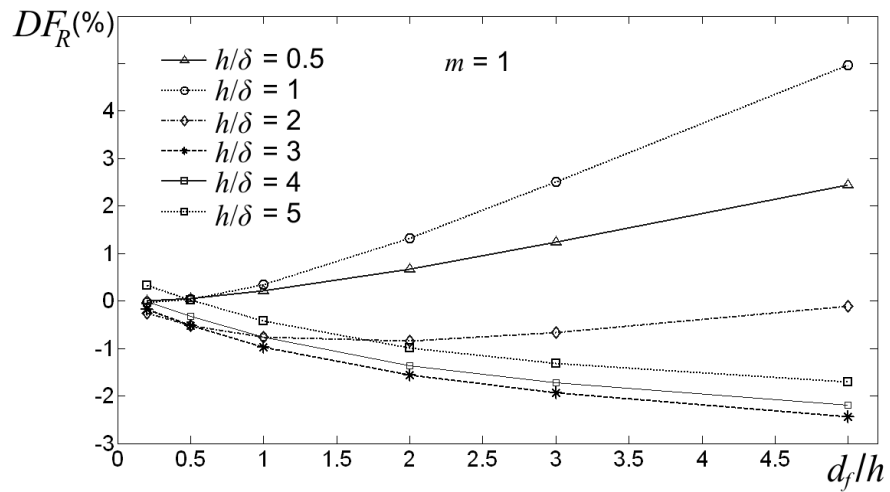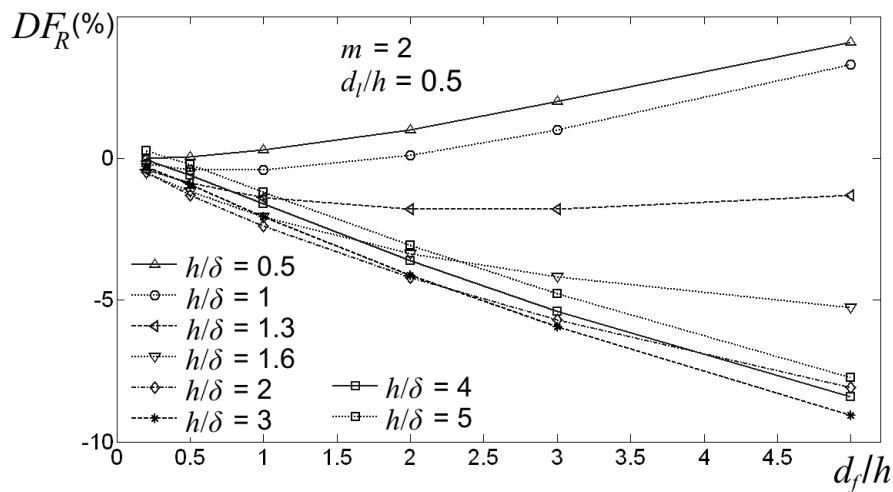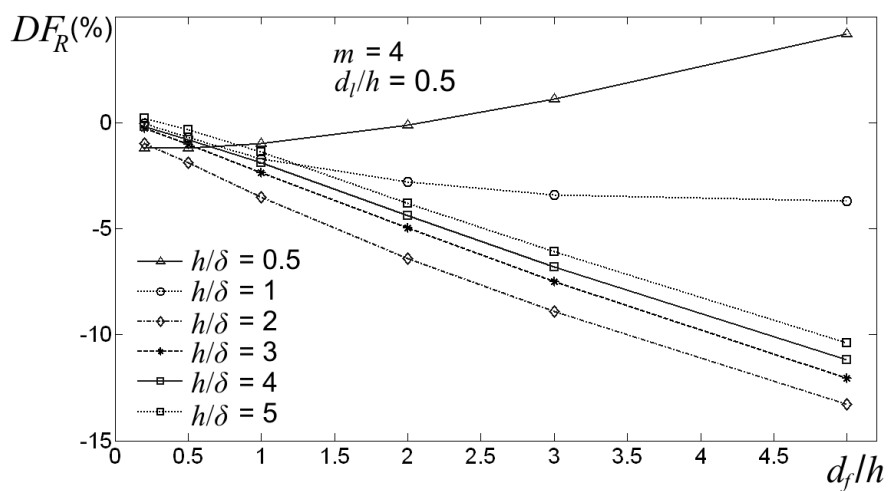
Figure 4.12: Plot of DF_R versus d_f/h, with h/δ as parameter, for copper foil windings with (a) $m=1$, (b) $m=2$ and (c) $m=4$.
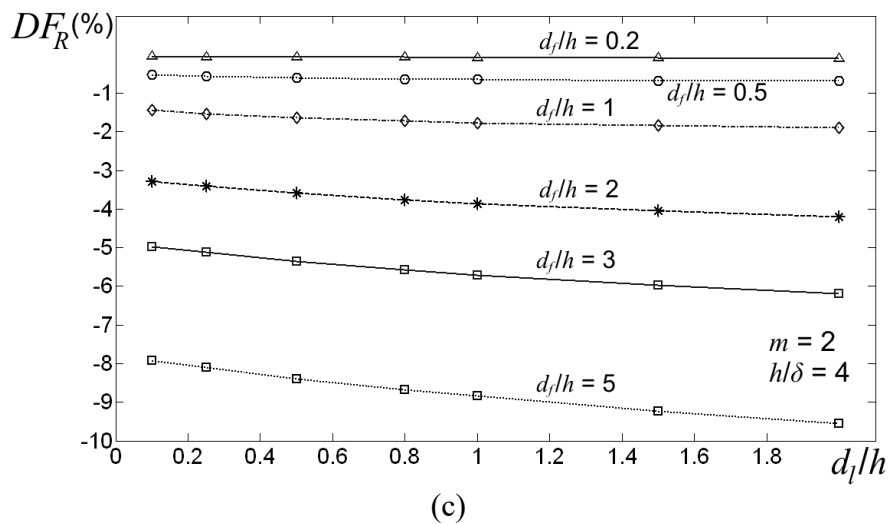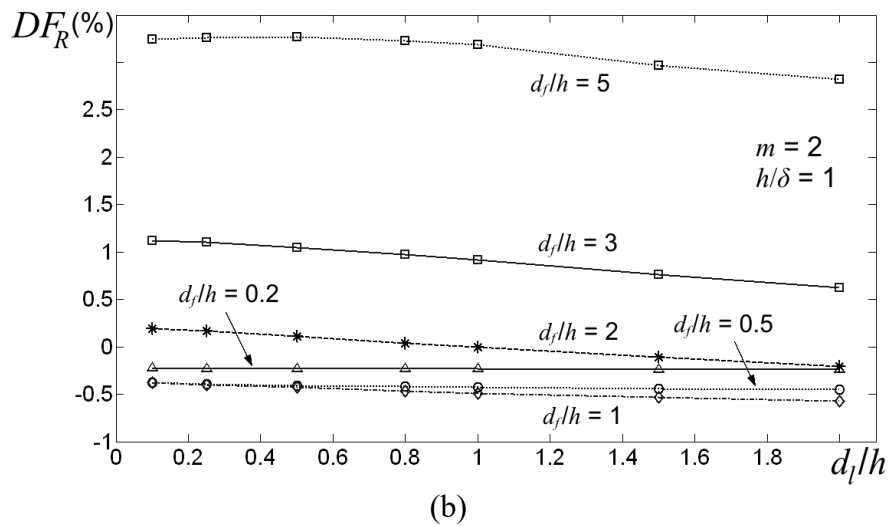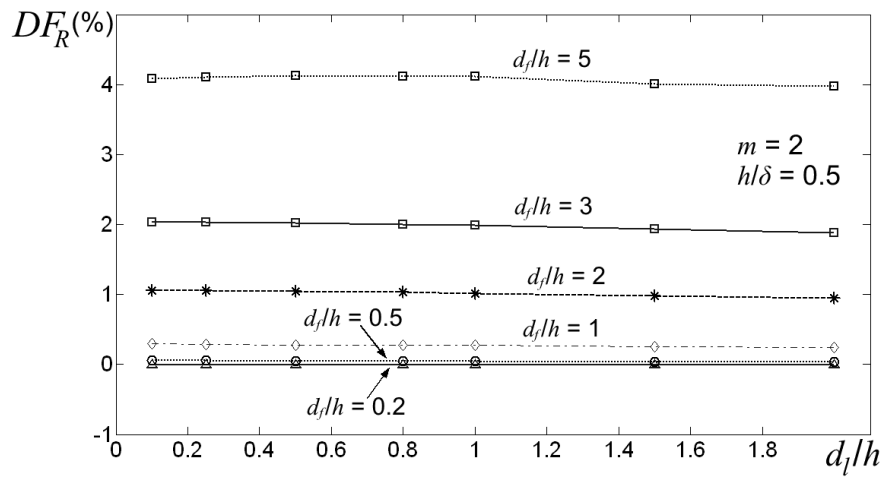
Figure 4.13: Plot of DF_R versus d_l/h, with d_f/h as parameter, for copper foil windings with $m=2$, for (a) $h/\delta=0.5$, (b) $h/\delta=1$ and (c) $h/\delta=4$.
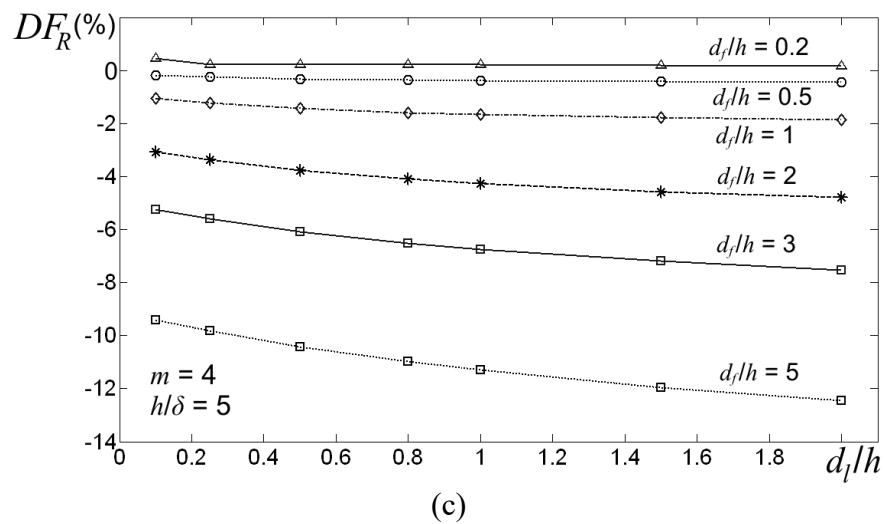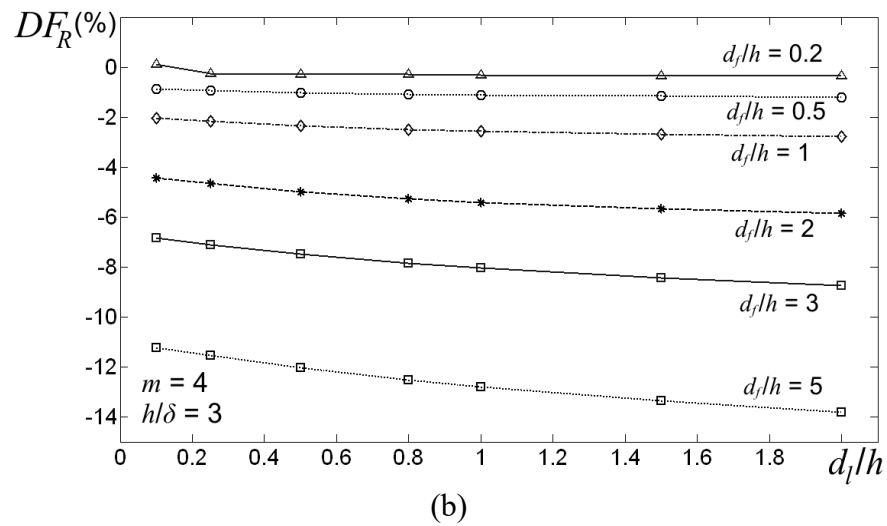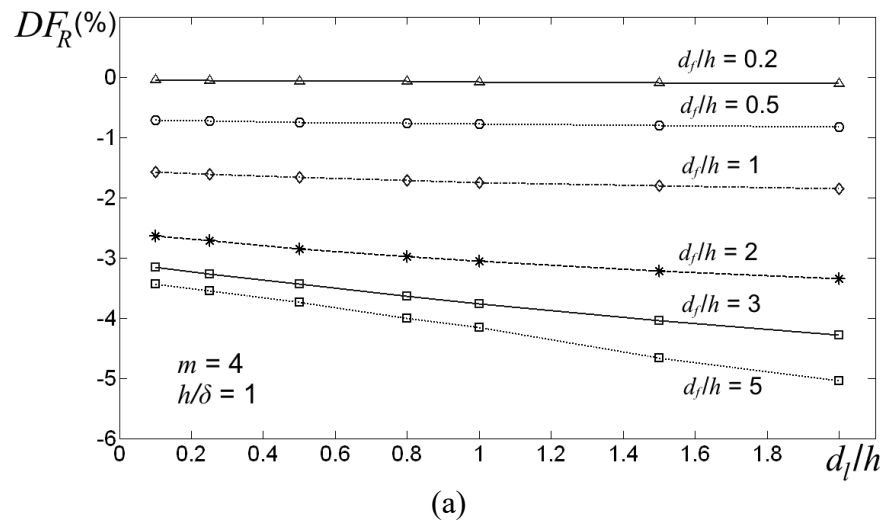
Figure 4.14: Plot of DF_R versus d_l/h, with d_f/h as parameter, for copper foil windings with $m=4$, for (a) $h/\delta=1$, (b) $h/\delta=3$ and (c) $h/\delta=5$.

Thus, regarding the dependence of the resistance factor of a winding with m layers on variations of the several parameters, the most important conclusions resulting from the analysis of the total numerical results are summarized in the following:

- Parameter d_f/h:
  (a) Generally, for $d_f/h<1$ the edge effect can be ignored ($|DF_R|<5\%$).
  (b) For $1<d_f/h<5$, as d_f/h increases DF_R increases towards negative values, (i.e. there is a relative drop in active resistance), expect for low h/δ values ($h/\delta<0.8$ when $m>2$), where a slight increase of DF_R is observed (Fig. 4.12).

- Parameter d_l/h: Up to the studied limit where the interlayer distance is twice the thickness of the foil ($d_l/h=2$), this parameter shows little effect on the extent of 2-D effects in the vicinity of the foil edges. Only a slight increase in the negative values of DF_R as d_l/h increases is observed and respectively a slight reduction in the positive values of DF_R at relatively low frequencies (Fig. 4.13 and Fig. 4.14).

- Parameter h/δ: As mentioned above, at low frequencies ($h/\delta<0.8$ when $m>2$) DF_R takes positive values, up to +5%. For frequencies higher than this, up to $h/\delta=2$, the edge effect becomes gradually more important (with negative values of DF_R), and for higher frequencies ($h/\delta>2$) no extra impact is observed or even there is a small reduction in absolute DF_R values.

- Number of layers m: For increasing m the absolute values of DF_R show a slight increase as well. However, the most important notice is that with decreasing m the frequency range for which the edge effect leads to moderately increased losses (positive DF_R) is extended to a somewhat higher limit (Fig. 4.12). For $m=2$ this attribute is present up to the approximate limit of $h/\delta=1.2$, and for $m=1$ the respective frequency limit is $h/\delta=2$.

It is also necessary to mention that the study of each single layer separately shows that the several layers do not contribute similarly to DF_R. Moreover, as expected, the general trend in the change of effective resistance is imposed mainly by the layers placed at regions of high MMF values, since these layers contribute relatively more to the increase of resistance at high frequencies (Appendix III).

The previous discussion gives a general view of the most important aspects of the edge effect in foil windings. The main conclusion is that in most of the practical applications the edge effect not only does not increase the losses, but also improves the overall performance

of the coil at the harmonic frequencies, if $h/\delta \cong 1$ is selected for the fundamental frequency. However, for frequencies with $h/\delta \cong 1$ and $h/\delta < 1$, where normally the greatest portion of throughput power is to be transferred, a moderate increase in losses occurs.

At this point it is necessary to clear out that when the ratio W/h increases, the edge effect becomes less important to the total effective resistance of the winding. This is because 2-D effects take place in a generally small depth y_e (see Fig. 4.15) from the edges of the foils (in y-direction). This depth is typically equal to a few times the copper skin depth at a given frequency. For as long as W/h is not very small ($W/h > 50$), the result of a change in this ratio on the value of DF_R is approximately inversely proportional, something that was easily verified through relevant test simulations. All the above numerical results refer to foil with $W/h=90$. This means, for example, that for $W/h=180$ all the previously presented DF_R values should be halved to get the actual result.

One way to investigate the geometrical extent of the edge effect in a winding is to study the amplitude of the ratio B_x/B_y of the x and y components of the magnetic field, in y-direction, along the sides of the foils. Figure 4.15 depicts part of a model simulated with $m=4$ and $d_f/h=3$, in which the flux lines for $h/\delta=1$ are also illustrated. In Figure 4.16(a) the $B_{x,max}/B_{y,max}$ ratio of the amplitudes of the x and y components of the magnetic field is plotted versus distance y_e from the edge, with y_e expressed in skin depth δ units (ratio y_e/δ appears). The specific plot corresponds to $m=4$, $d_f/h=5$, $d_l/h=2$ and refers to B_x and B_y components as they are in the inner side of the first foil layer, i.e. the side with the highest MMF values, the one that faces the excitation primary (in Fig. 4.15 this side is in position $x=15$mm). In Fig. 4.16(b) is the corresponding plot for $d_f/h=2$.
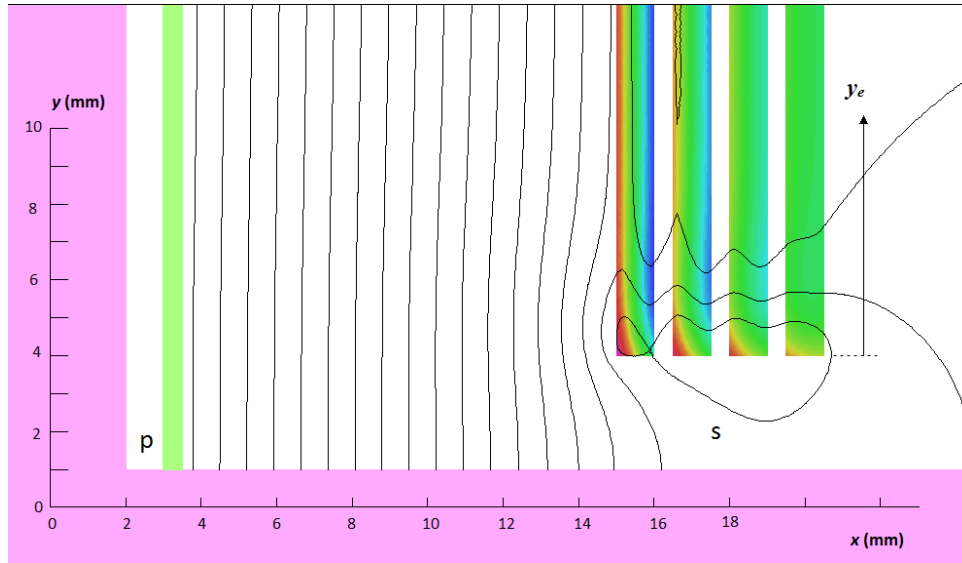
Figure 4.15: Model section that has been simulated for studying the edge effect in copper foil windings ($m=4$, $d_f/h=3$, $d_l/h=0.5$). This specific depiction of the flux lines and the current density in the secondary winding under study corresponds to $h/\delta=1$.

It is evident from these graphs that in a depth of about $y_e=4\delta$ the field component normal to the foil becomes a negligible fraction of the parallel one. We also see that the ratio $B_{x,max}/B_{y,max}$ takes higher values for a higher d_f/h, i.e., for greater distances of the edge from the ferrite. The study of the corresponding behavior of $B_{x,max}/B_{y,max}$ for other positions in the winding, further than the innermost foil side, or for windings with different m or/and d_l/h, indicates that the resultant dependence on d_f/h and h/δ is similar. What changes is the specific $B_{x,max}/B_{y,max}$ values encountered. Notice that B_x and B_y are generally not in phase and since one is interested in their relative magnitudes it is more appropriate to study the ratio of their amplitudes $B_{x,max}/B_{y,max}$ rather than the amplitude $(B_x/B_y)_{max}$ of their ratio.

Expect the ratio B_x/B_y, in order to get a complete picture of the edge effect extent, it is also necessary to investigate the current density distribution J as a function of y_e. In Fig. 4.17 J_{norm} is the amplitude of J ($J(x,y)$, same as B_x and B_y, is a sinusoidal time function) normalized at the value $J(x=15, y_e \gg 1)$. It corresponds to a winding with $m=4$, where the interlayer distances are half the foil thickness ($d_l/h=0.5$) and the inner side of the first foil (the one facing the excitation primary, area of maximum MMF) is at $x=15$ (Fig. 4.15). The value mentioned above, used for the normalization of J, is the highest value that occurs at the first foil, (and at the whole of the winding too), far away from the foil edge (i.e. at high y_e
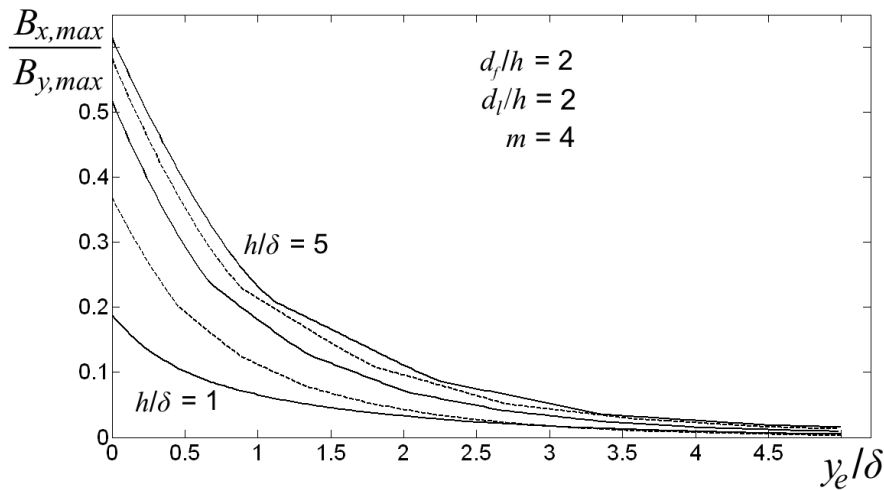
114

(a)

(b)

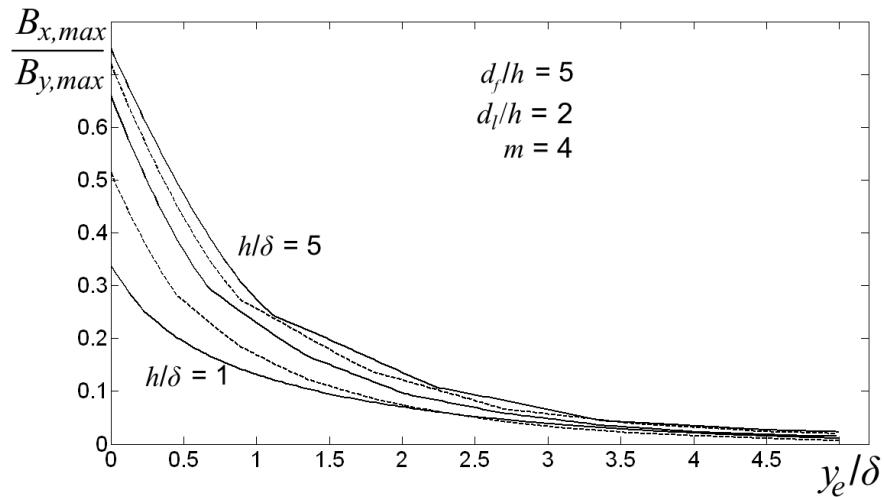**Figure 4.16:** Plot of the ratio $B_{x,max}/B_{y,max}$ along the side of a foil layer versus the distance y_e from the edge, with the ratio h/δ as a parameter for (a) $d_f/h=5$ and (b) $d_f/h=2$.

values), where the edge effect does not affect the current density and magnetic field. In Fig. 4.17 the distance y_e (in δ units) appears as a parameter.
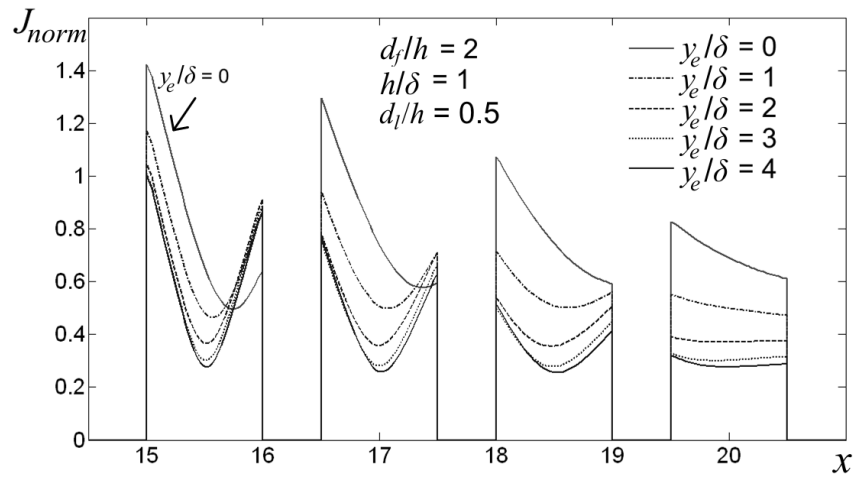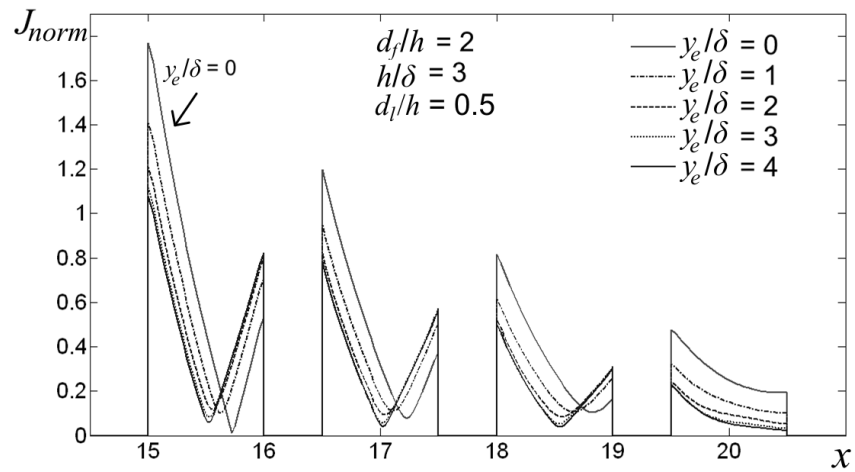
Figure 4.17: Normalized current density distribution (J_{norm}) x profile, with y_e as a parameter, at several frequencies and distances of the edge from the ferrite yoke, for a winding with m=4, d_l/h=0.5.

A general conclusion coming up from these plots is that in a depth $y_e=3\delta$ up to $y_e=4\delta$ the current density x-profile takes its non-affected by the edge effect form. We can also see (Fig. 4.17(a) and Fig. 4.17(b)) that as the frequency increases, except from tha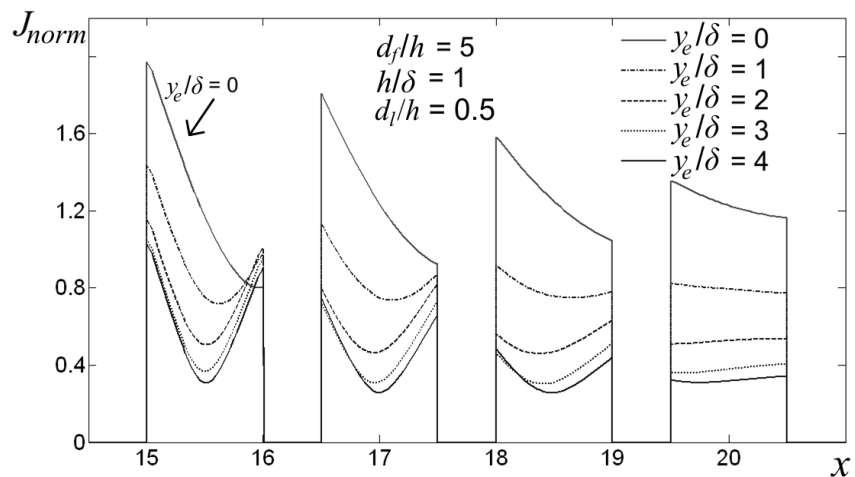t part of the conductor where higher J values occur (higher compared to the undisturbed profile at high y_e values), there is also another part where there is a major reduction of J. This attribute is more prominent at the foils that experience the highest MMF values and therefore contribute more to the final F_R result. It may explain the resultant F_R reduction as well as the observed relative difference between the impact of the edge effect on the several layers, compared to the no edge effect case, i.e. the reduction of losses that occurs for the foils at high MMF areas and increase for those at low MMF areas. At last, by comparing Fig. 4.17(a) και Fig. 4.17(c) it is evident that the local J increase at the edges for relatively low frequencies is more prominent for higher d_f/h values, hence the edge effect gets more important.

4.5.3. The edge effect in coils with round wires

The detailed study of numerous cases of layered coils with round cross-section conductors led to two major conclusions:

- In all the cases studied, the result on a winding with many turns per layer is the reduction of the overall resistance of the winding.
- For $d_f/r<1$ the edge effect can be ignored, whereas for $d_f/r>10$ it has no extra impact on copper losses further than what is observed at $d_f/r=10$.

Further than these two main conclusions some extra hints should be added that can help the designer judge the actual impact of the edge effect on copper losses, quite helpful, especially when there are only a few turns per layer. If we define as an ''array'' of conductors those ones, in all layers, with the same distance from the ferrite yoke (Fig. 4.10), for the sake of presentation, we need to establish two auxiliary quantities. At first, in the same way this was done in (4.15) for the general case of a conductor or group of conductors, we define DF_{Ra} as the relative difference of the resistance factor F_{Ra} of a conductor array compared to the case when no edge effect is present, expressed as a percentage:

$$DF_{Ra} = \frac{F_{Ra}^{\text{with EF}} - F_{Ra}^{\text{without EF}}}{F_{Ra}^{\text{without EF}}} \times 100\% \qquad (4.16)$$

The F_{Ra} value for an array is calculated as the average of the resistance factors of all the conductors in this array and the term $F_{Ra}^{\text{without EF}}$, that appears in (4.16), equals the F_R of the whole winding at the absence of edge effect (Appendix III). Second quantity to define is σ_a (Fig. 4.10), the integer index that describes the position of the array in the winding. For example the end array closer to the ferrite yoke has σ_a=1, the right innermost has σ_a=2 etc.

In Figures 4.18 to 4.20 some typical results of the simulations are presented. The following conclusions help to better understand the act of edge effect on copper losses:

- For sparse windings (η<0.65) DF_{Ra} is negative for all arrays at all frequencies. This attribute is the same at compact windings only at the low frequency range, up to r/δ=1.

- Focusing on each conductor separately, it is easily seen that the 2-D field and current distribution effects are more prominent at the conductors belonging to the innermost layer, i.e. the layer at the higher MMF values, closer to the excitation primary, especially if it is for the first few arrays. Besides that, the general concept is that DF_{Ra} follows a profile as that shown at Figures 4.18 to 4.20, i.e., a positive value for the first few arrays and then negative. These positive values are nearly negligible for r/δ=1 (typically +5%) or negative values occur, and may be up to +40% at r/δ=5. Attention must be given to the fact that, at high frequencies, the first few wire turns of the innermost layer may show increased losses (compared to the no edge effect case) of up to 85%. For the conductor arrays placed deep in the winding, DF_{Ra} of course tends to zero.

- Keeping in mind that in a multilayer winding it is the innermost layer mainly affected, the case of a single layer winding is the one at which the edge effect shows a maximum impact, which, even so, is still negligible at r/δ=1.
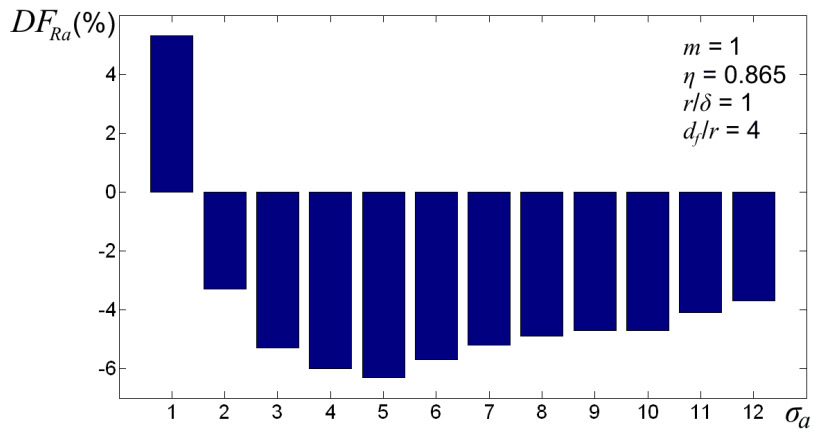
(a)
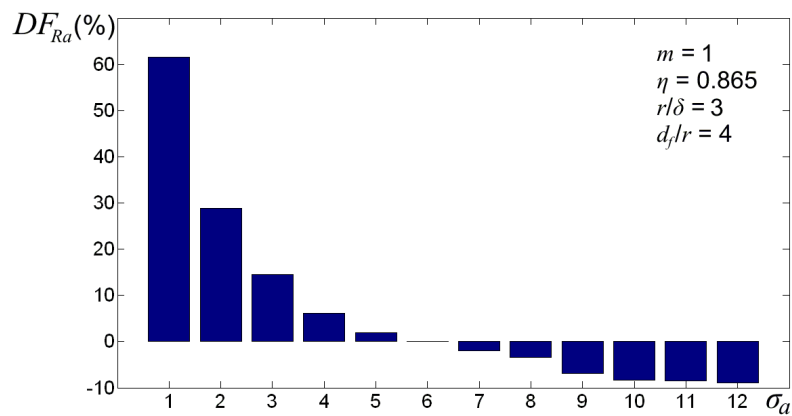
(b)
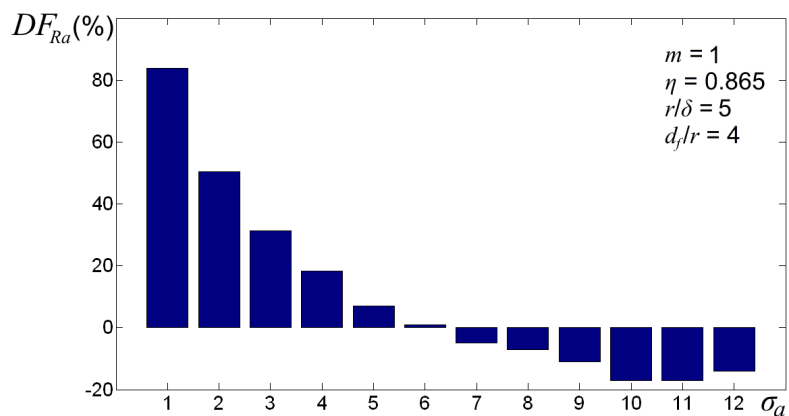
(c)

Figure 4.18: Relative difference DF_{Ra} of the resistance factor of a conductor array under the act of the edge effect, (eq. 4.16), as a function of the y position of the array in the winding (index σ_a), when $m=1$, $\eta=0.865$, $d_f/r=4$, for (a) $r/\delta=1$ (b) $r/\delta=3$ and (c) $r/\delta=5$.

119

(a)

(b)

(c)

Figure 4.19: Relative difference DF_{Ra} of the resistance factor of a conductor array under the act of the edge effect, (eq. 4.16), as a function of the y position of the array in the winding (index σ_a), when $m=2$, $\eta=0.865$, $d_f/r=4$, for (a) $r/\delta=1$ (b) $r/\delta=3$ and (c) $r/\delta=5$.
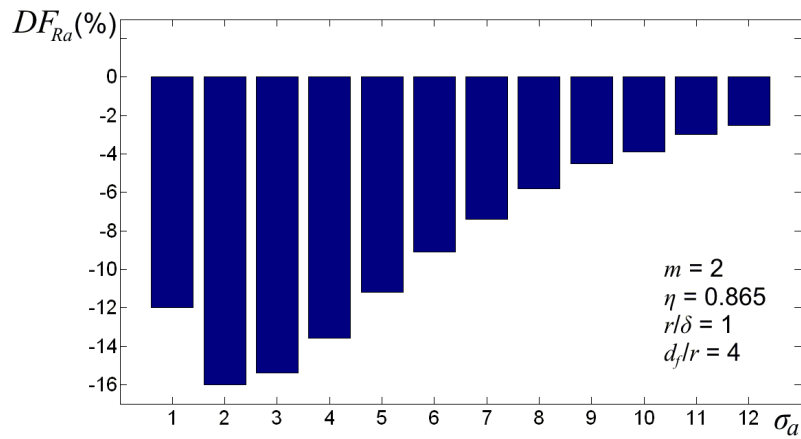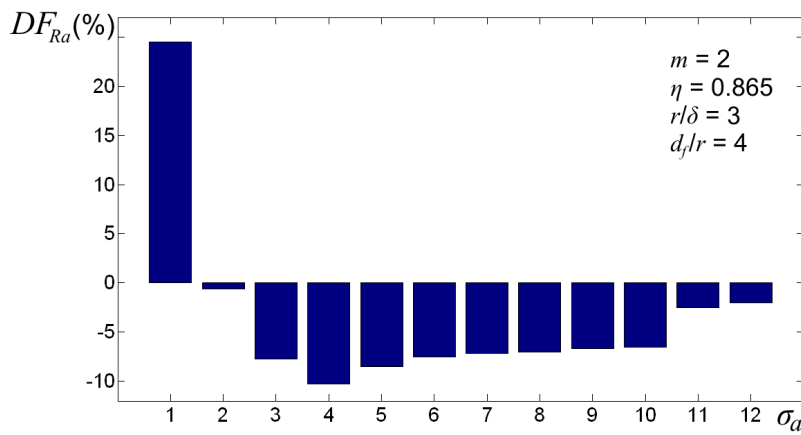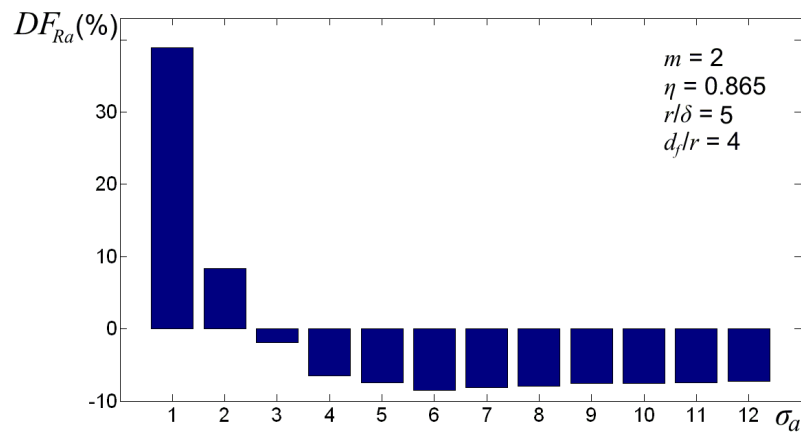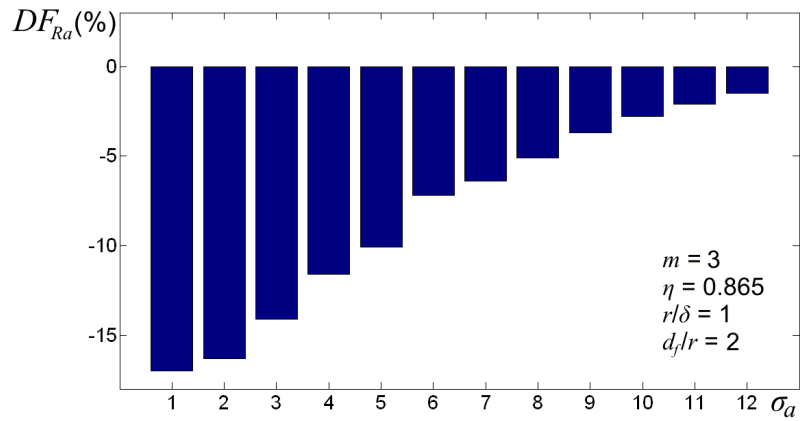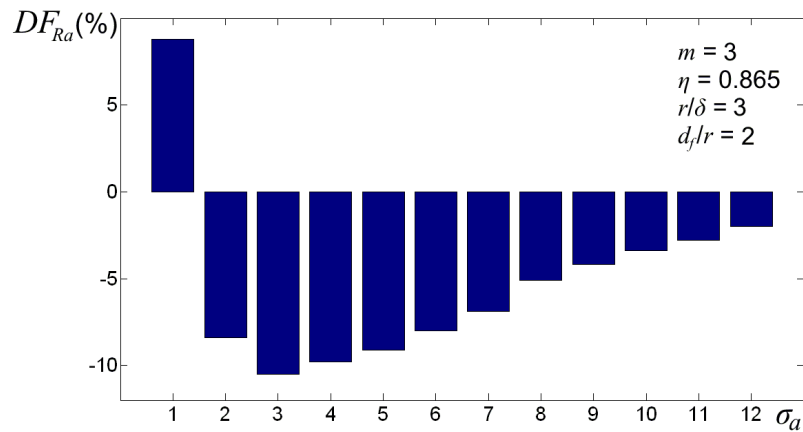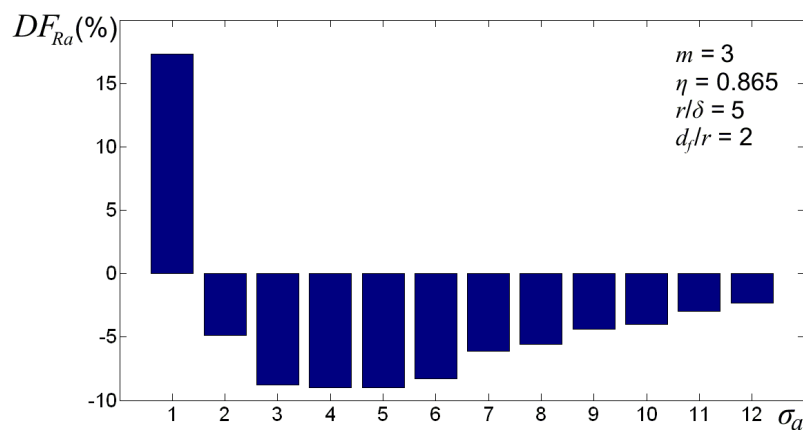
(a)

(b)

(c)

Figure 4.20: Relative difference DF_{Ra} of the resistance factor of a conductor array under the act of the edge effect, (eq. 4.16), as a function of the *y* position of the array in the winding (index σ_a), when *m*=3, η=0.865, d_f/r=2, for (a) r/δ=1 (b) r/δ=3 and (c) r/δ=5.

Conclusively, it may be said that the edge effect on windings with round conductors actually causes one single problem, that of a possible overheat of a few wire turns at the edges of the winding (especially the ones of the innermost layer). Although heat diffuses to all directions, the fact that these few turns are placed at the external parts of the winding means that effective cooling can be realized without additional means further than just air convection. The most important notice though should be that, for an optimized design, at which it is approximately $r/\delta \cong 1$ at the fundamental frequency and the current waveform has only a moderate harmonic content, it is rather unlikely to have a hot spot, not even on a single layer winding.

4.6. Coils with round wire in hexagonal configuration

The final issue studied in this chapter is the case of compact coils carefully wound, at which each conductor has an insulating film, yet there is no special insulating sheet between layers and the turns of a layer fall into the grooves formed by those of the innermost one. This sort of winding, not described by any of the existent models, is not uncommon, especially when the diameter of the conductor is large enough to favor such a tight winding to be constructed easily [124]. The simulations made for this case show that resistance factor F_R is reduced (compared to separate layers with $d_t=d_l$, i.e. at square fit configuration of the conductors) by about 8% to15% for $\eta>0.75$ and by 10 to 30% when $\eta<0.75$.

Such a winding is shown in Fig. 4.21(b), where it can be seen that part of the leakage flux is common between successive layers offering this way a beneficial interlayer proximity effect that increases the effective cross section of each conductor. This is in contrary to the typically analyzed square fit configuration (Fig. 4.21(a)), at which no such interaction is present. Notice that the winding of Fig. 4.21(b) has the same layer filling factor (parameter η) as that in Fig. 4.21(a) ($\eta=0.865$) but a higher overall copper filling factor. In Figures 4.21(c) and 4.21(d) a similar comparison is presented for $\eta=0.633$. For the winding of Fig. 4.21(b) F_R is lower than that of Fig. 4.21(a) by 8% at $r/\delta=1$ and by 15% when $r/\delta>3$, whereas the winding of Fig. 4.21(d) has an F_R about 25% lower than that of Fig. 4.21(c) at all frequencies.
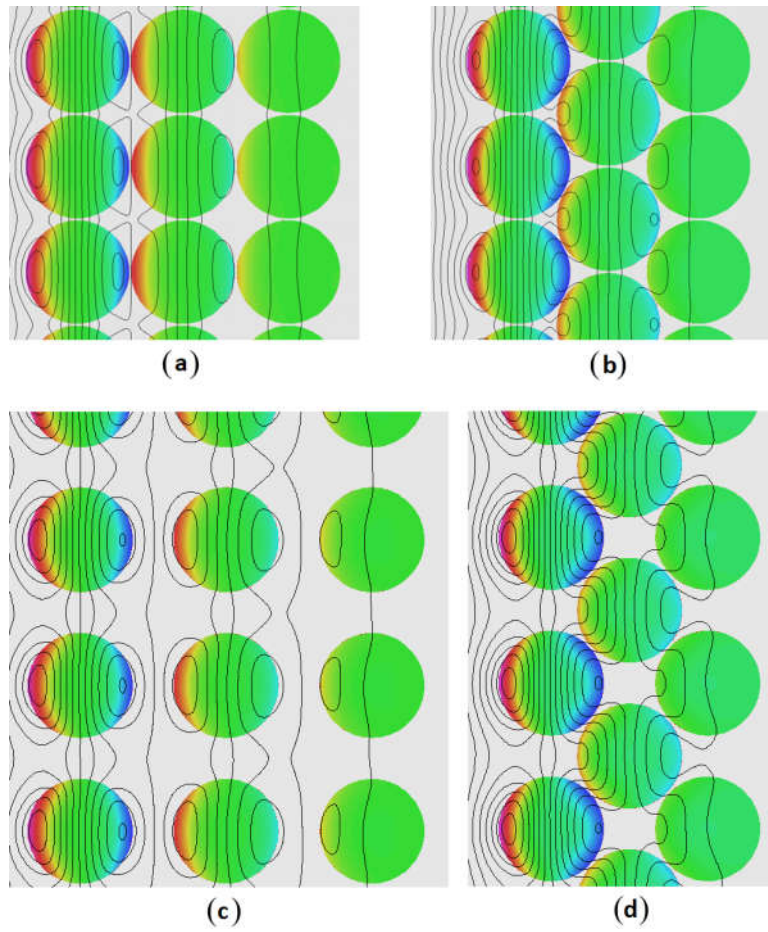
Figure 4.21: Flux lines and current density for windings with *m=3*, at *r/δ=2*, configured by the square fit scheme ((a) και (c)) and the corresponding hexagonal fit ((b) and (d)) having the same layer filling factor but a higher overall copper filling factor.

CHAPTER 5

A NEW MODEL FOR THE HIGH FREQUENCY LOSSES IN WINDINGS WITH RANDOM CONDUCTOR DISTRIBUTION

5.1. Introduction

The majority of power electronic converters and electromechanical energy conversion systems incorporate the use of copper coils, which can be part of inductors, transformers or some other sort of current-carrying group of conductors. These components show a significant amount of power loss in the form of ohmic loss in the conductors which, with increasing frequency, appear to be increased due to the skin and proximity effects. Although there is always an attempt to optimize these components in terms of power loss (among other specifications, like low cost, small volume, and the ease of assembly), the models for the high frequency copper losses often give just a general guide for approximate calculations in practical applications.

Previous analytical solutions [5]−[7], [12], [41], [47], [81], [143] (see Ch. 3) treat current-carrying coils with round cross-section conductors as well separated, successive layers of precisely defined geometrical order. This basic assumption still holds even at recently released works that utilize finite-element analysis (FEA) in order to give more accurate expressions applicable to wider ranges of the parameters involved [92], [98], [109], [119], [143]. An exception to this rule is the set of works [74], [83] in which the precise layout of the conductors is of minor importance, but their effects are only applicable to frequencies at which the r/δ ratio gets relatively small values ($r/\delta<0.8$).

Unfortunately, this fine order is rarely true in practice, while at most of the times, the well-defined geometrical parameters are just the dimensions of the winding and the number of turns of which it consists. In such cases, a common practice for the designers is to consider the winding as a layered one and apply some of the aforementioned models so as to make an approximate calculation for the effective resistance, with an error, which, as will be presented in the following, can be extremely high.

In this chapter of the dissertation a new semi-empirical model is proposed, for the determination of high frequency copper losses of windings that show an arbitrary conductor distribution within their cross-section space, a case that cannot be studied by any analytical method. The new model is based on the statistical analysis of numerical results coming from a large number of simulations carried out with finite element analysis software and is verified by experimental measurements on two different types of winding geometries. The new formula is simple and further than the three parameters adopted it has no complicated geometrical or frequency dependencies. It is ready to use if the dimensions of the winding and the number of turns are known quantities. A detailed investigation of the new formula reveals its inherent advantages on copper loss calculation when the design of a magnetic component involves non layered coils.

However, it should be made clear that **the present work does not intend to make a direct comparison between layered or periodically configured winding structures with randomly configured ones**. Moreover, it has already been well established to the research community [124], [128] that with a carefully wound layered coil, one can achieve much higher copper filling factor than with a random winding. Thus, **randomly wound coils are not an optimum design choice in any way but, since they are widely met in practice, a closed-form formula for their effective resistance calculation seems necessary**.

5.2. Formulation of the new model for high-frequency ohmic losses in windings with random conductor distribution

5.2.1. General conditions, parameters and field of application

The idea for a model describing the effective resistance of coils with round conductors arbitrarily distributed in their cross section comes up by the fact that this sort of winding seems to be the rule rather than the exception [124]. Layered windings with interlayer insulation and with special care taken so as to avoid overlapping of adjacent turns in one layer are mainly designed either for low frequency and high power applications (e.g. distribution network transformers) or for high voltage applications, where there is a high possibility of electric flash due to penetration of the wire insulation, such as the choke of the fluorescent lamp ignition circuit. However, this sort of wire winding needs special equipment to be achieved and it is time-consuming as a manual work, e.g. by installing a relatively rigid

insulating layer, either between all successive layers, or after wounding every two-three layers [124]. And that is why it is rarely met in practice, unless the wire's diameter is big enough to favor such a design [124]. Moreover, casual measurements on several laboratory converters with magnetic components gave us much evidence that when applying Dowell's formula on non layered windings, the result appreciably overestimates copper losses. The point here is that the random conductor distribution cannot be studied theoretically in any way to obtain an analytical solution. This logical conclusion is enhanced by the remark presented in [99], [143], that for any analytical solution to exist upon the basis of the orthogonality of some field components, the current density distribution inside a conductor should have some symmetry (odd or even) related to a given axis, an attribute incompatible with random geometries. Other analytical approximations, as in [41], that require the exact positions of all wires in order to make the relevant summations that describe the interaction between them are obviously also inapplicable to randomly wound coils. Therefore, the only way out is a statistical analysis on a large number of FEA results.

The electromagnetic problem that will be presented in the following is considered two-dimensional, i.e. it describes either magnetic components with axial symmetry (y is the symmetry axis) and a mean radius that is much greater than the radius r of the conductor, or, ideally, magnetic components that extend infinitely toward the z direction, perpendicular to the x–y plane (see §4.3.3.1). It is obvious that in a real solenoid winding the several turns do not all have the same length, but we can assume for the sake of the analysis that they all have a length equal to an average length l_T, which is the average value of the lengths of all turns, a typical assumption that we see in both Dowell's work and other works and which does not significantly affect the end result. The winding under study is considered to lie in the window space of an ungapped core, with high magnetic permeability (μ_r=2000) and zero losses (absence of eddy currents and magnetic hysteresis). As indicated by relevant FEA simulations, these conditions regarding the core are not critical to the analysis of winding losses, provided that μ_r>150 (see also §4.3.3.1).

A primary requirement for the establishment of the new model is the proper selection of its parameters. These parameters should be easily determinable, and thus should be directly related to known quantities.

The ratio r/δ, appearing in nearly all the previous works related to high frequency copper losses seems to be the most appropriate choice for the F_R frequency dependence (see §1.2.4).

In order now to express the geometrical dependencies, we first have to assume a winding with rectangular cross section of dimensions $X{\times}Y$, as illustrated in Fig. 5.1. The winding consists of N turns of round cross-section wire, randomly distributed in the $X{\times}Y$ area. To ensure that no excess losses appear on the conductors close to the core yoke (similar to those described in Ch. 4 for the edge effect observed on layered windings), Y must be approximately equal to the window width Y_w. According to simulation results, a small declension from this condition, of the order of the conductor radius r (as, for instance, to account for an insulation sheet or the coil former in real magnetic components), does not affect the final result. The winding should extend in the x-direction between a zero and a maximum MMF point (see Appendix III). This condition is approximated in the simulations
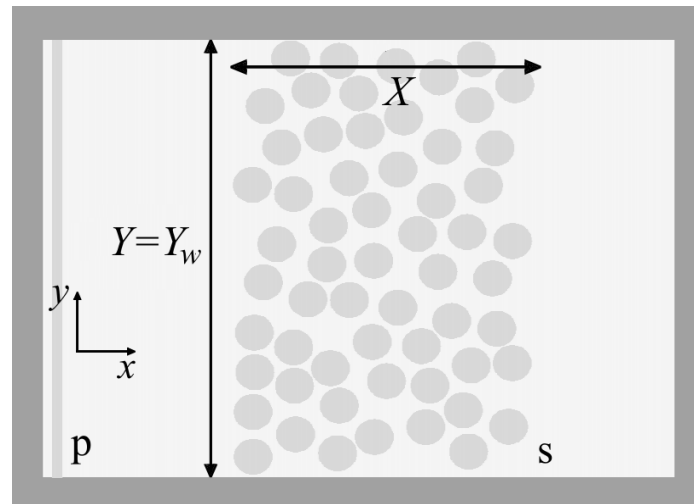
Figure 5.1: Typical random winding configuration simulated with $X/r{=}16$ and $F_{Cu}{=}0.46$.

by short-circuiting the secondary winding (s) under study, while an inner (i.e. near y-axis) primary winding (p), consisting of a conductive sheet, placed well away from the winding of interest (at least 8 times the radius r of the conductor), produces a high frequency sinusoidal excitation.

The two geometrical parameters adopted for the F_R expression are the ratio X/r and the copper factor F_{Cu}:

$$F_{Cu}=N\pi r^2/(XY) \tag{5.1}$$

i.e. the ratio of the copper cross-section area to the total winding cross-section area. The selection of these two parameters is fully justified by the simplicity and accuracy of the final formula. At this point, it is necessary to notice that the window portion, not occupied by the winding (Fig. 5.1), is not taken into account for the copper factor calculation, i.e. X is the height of just the winding and not that of the overall available window space.

In the simulations carried out, parameter r/δ ranged between 0.3 and 5, X/r ranged between 10 and 40, while F_{Cu} ranged between 0.23 and 0.65. **These ranges of the involved parameters define the validity range of the proposed model**.

At this point it is necessary to remind that for the optimum performance of magnetic components, F_R should be about 1.5 [79], [128], a value that, in general, corresponds to a frequency at which r/δ is approximately about unity. For non sinusoidal current waveforms, the total losses are to be determined by Fourier analysis and when $r/\delta \cong 1$ is selected for the fundamental frequency, as mentioned in Ch. 4, F_R knowledge up to the $r/\delta = 5$ limit is adequate for up to the 25th harmonic. Moreover, the application of the new model cannot be extended to the area $r/\delta < 0.3$, (not included in the study anyway) as the final expression for F_R does not converge to unity for $r/\delta \to 0$, which would be a necessary condition for such an (arbitrary) extension. Moreover, typical values for F_{Cu} in practical applications range close to 0.40 [128]. Taking all these into account, the options selected for the ranges of these two model parameters (r/δ and F_{Cu}) were considered satisfactory for most of the practical applications.

Regarding the parameter X/r some clarifications are necessary:

Taking into account the available standard core sizes [47], [140] and the available copper wire gauges [124] and how they are usually combined in practical applications, depending on the frequency and current flowing through the magnetic components, it comes clear that the study for $10 < X/r < 40$ covers a large part of these applications. Of course, values outside this range cannot be excluded as improbable.

The range $X/r < 10$ was excluded from the study when developing the proposed model for three main reasons:

(a) For a winding of such a small height, from a practical point of view, it is quite possible that the turns are placed in well arranged layers, either separated from each other (if insulating interlayer films are used) or in an approximately hexagonal fit of the conductors, since the required work is not particularly time consuming. Moreover, for example, a winding with $X/r \cong 2$ obviously corresponds to one layer of conductors and

another to $X/r \cong 3.7$ corresponds to two layers of conductors in hexagonal configuration. It is clear that at these X/r values a "random" winding is meaningless.

(b) As explained in §5.4.3, a typical value for the error with which X/r can be determined (using for example a caliper) is $\Delta(X/r)=\pm 1$. For $X/r<10$ such an uncertainty about the value of this parameter would lead to a very high error of the value obtained for the resistance factor by applying an expression such as the final expression (5.5), which is anyway not valid in this X/r range.

(c) It is explained in §5.2.3 that the result for the resistance factor F_R for a given set of values of the three parameters was obtained as the average from three different simulations, the results of which ranged by $\pm 3\%$ around the mean value. For $X/r<10$ however, the margins of this fluctuation increase rapidly as X/r decreases, especially for relatively small values of the F_{Cu} parameter. Of course, a statistical average for F_R could also be defined in this case (with more than three simulations however), but it is clear that any model in this X/r range would be by default unreliable.

With respect to the area $X/r>40$, the main remark is that the deviation of the final expression of the new model from the simulation results does not show any specific X/r behavior (§5.4.1). This fact implies that the model may also be valid for $X/r>40$, especially for X/r values that are not much greater than 40. However, strictly speaking, this is just a guess for the verification of which, a thorough study by either simulations or experimental measurements is necessary.

5.2.2. Matlab code to determine the random coordinates of the conductors

In order to take into account the existence of the insulation film of the wire, as indeed is the case, the algorithm that randomly determines the coordinates of the conductors within the cross-section of the winding (implemented in the Matlab math software) does not allow distances between the conductors less than 10% of their radius, but also not less than 5% of their radius from the ferrite yoke. These conditions are not critical to the generality of the new model and, given the random pattern of conductor distribution in space, we realize that it simply sets a limit to the highest possible F_{Cu} value. However, this limit is anyway much higher than the F_{Cu} range (0.35 - 0.55) that is of direct interest to us. Moreover, in a practical application, the conductor distance from the ferrite is definitely greater than $0.05r$, about the order of r, due to the presence of a coil former or a special insulation sheet and therefore the above condition is not a actual limitation. It is just necessary that Y is correctly determined, so that the determination of the copper factor F_{Cu} is also correct.

In the context of the algorithm, the rectangular area $X \times Y$ corresponding to the cross-section of the winding is first specified. Subsequently, on the basis of the conditions mentioned, the random coordinates of the centers of the cross sections of N conductors are determined so that the conductors remain at a distance of at least $0.1r$ between them and $0.05r$ from the y limits of that region, i.e. from the boundaries between the window and the core yokes.

However, with the random positioning of conductors the maximum copper factor that can be achieved is approximately equal to 0.43. In order to implement higher values for F_{Cu} it becomes necessary to apply an extra condition. Thus, if from X, Y, N and r results $F_{Cu} > 0.43$, after the random positioning of the first conductor, it is required from the code that the second one is not far from the first more than a given distance ($0.1r+b$), where b is user-defined. For all the other conductors it is required that each of them is not more than ($0.1r+b$) far from two of the already positioned conductors. In any case the minimum possible distance between two conductors remains equal to $0.1r$.

Application of the above bond now makes the distribution of conductors in the winding pseudorandom and in addition, it creates a new theoretical problem that requires a solution. To understand this problem, it is logical to conclude that for a given F_{Cu}, as b increases, the probability to have a conductor distribution satisfying the condition of the given F_{Cu} value (i.e., a given number of N conductors being randomly located in a given $X \times Y$ area) decreases and for b values greater than a limit (stated further below) this probability is zeroed (if it is $F_{Cu} > 0.43$). This is because, as b increases, the bond gets loose enough that, over some specific b value it has no longer any effect on the final arrangement of the conductors. Hence, application of the bond in this case does not alter the result of the code execution compared to the case where it is not applied. At the other extreme, as b decreases (always for given N, X, Y values), for values of b below a certain limit, the rectangular region $X \times Y$ is not completely occupied by conductors and although in the sub-region occupied by the conductors their distribution remains random, in the whole area $X \times Y$ this is obviously not true (part of this area is empty space).

This problem is resolved with statistical approach. In order to match between F_{Cu} and b_p values, where b_p is the value of b which ensures a random distribution of conductors over the entire cross-sectional area of the winding, the code for calculating random coordinates runs for different values of parameter b, with an appropriate step to ensure a good sweep of its range. In accordance with the above discussion, it was observed that values for b greater than about $0.96r$ result in conductor distributions with $F_{Cu} \cong 0.43$ and therefore the result of the

code execution is equivalent to that obtained without applying the bond. Correspondingly, values of b lower than $0.07r$ result in an almost layered layout, of approximately hexagonal fit. Finally, the $0.96r > b > 0.06r$ range is swept with a $0.03r$ step and for each b value the code runs one hundred times. In this version of the executed code only the dimensions X and Y are given, whereas the number N of the conductors finally placed in the given area can be any and is the result of the code execution. Thus, for each b value a result N_m is obtained for the number N of the conductors, which occurs with the statistically highest probability. This value of b represents the required b_p value for the given F_{Cu} as determined by X, Y, N_m. The results obtained show that the b_p value obtained for a given F_{Cu} is not dependent on the specific X, Y values if the ratios X/r and Y/r remain higher than 10. This is also the fourth reason, together with the three others already mentioned in paragraph 5.2.1, due to which no analysis was performed for $X/r < 10$.

A remark on the above reasoning is that, given the small step of variance of b, some values of F_{Cu} lead to two different values for b_p (i.e., two adjacent ones that differ by $0.03r$). The small difference between these two values ensures that it is not of critical importance to select either of them. In other words, the analysis described results in a small range of b values within which lies the required b_p. The width of this range is of the order of the step of b (i.e., $0.03r$). In order to reduce the width of this range (not considered as necessary for this study), three conditions should be applied in the b_p statistical survey methodology:

a) Increase the relative dimensions of the cross section of the winding with respect to the radius of the conductors, i.e. for a given r, increase X, Y (and therefore increase N for any value F_{Cu}). This would allow a better (ideally, nearly continuous) sweep of the F_{Cu} parameter.

b) Reduce the sweep step of the parameter b.

c) Increase the statistical sample, that is, to execute the code more than one hundred times for each b value.

In Fig. 5.2 is presented, for two combinations of X/r and Y/r ratios, the probability P_b of a conductor distribution with F_{Cu} copper factor to occur as a result of running the code for a given value of the b/r ratio. In Fig. 5.3 the points defining the three curves correspond to

(a)

(b)
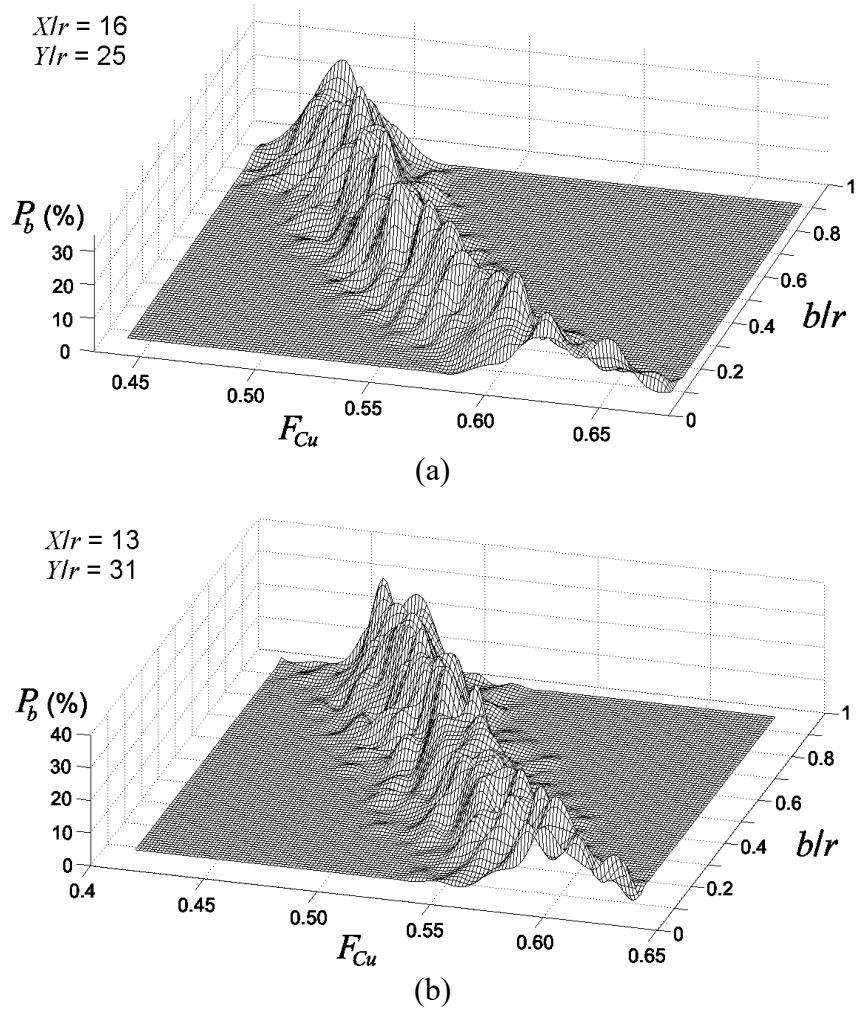
Figure 5.2: Plots of the probability P_b to obtain a random conductor distribution with F_{Cu} filling factor, for a given value of parameter b (here is the ratio b/r), for the cases (a) $X/r=16$, $Y/r=25$ and (b) $X/r=13$, $Y/r=31$.

the value pairs (b_p/r, F_{Cu}) used to implement the simulation models. The pairs for $X/r=16$, $Y/r=25$ and $X/r=13$, $Y/r=31$ were selected as the local maxima of the probability distributions of Fig. 5.2. In a case where the conditions a) to c) mentioned earlier would be satisfied, the locus of the local maxima of the probability distributions P_b would be a function independent of X/r and Y/r, so the three curves of Fig. 5.3, but also any corresponding curves for other X/r and Y/r values, would coincide.

At this point it should be noted that for each of the random conductor distributions that eventually occur, and if it is $X \neq Y$, two sets of simulations with different X/r values can be realized. This is achieved with a 90° rotation of the resulting distribution on the *x–y* plane, thereby transposing X and Y. This rotation on the *x–y* plane was practically realized when designing the models by changing the geometry of the window and the relative positioning of the excitation winding, leaving the positions of the turns of the random winding unaffected. In other words, the axes *x* and *y* of the model were transposed, instead of transposing the X and Y dimensions of the winding. In this way, much time was saved that would otherwise be required both in the statistical study to calculate the pairs (*x*, *y*) in order to create random conductor distributions, as well as to design the models in the FEA software environment.

5.2.3. Simulation results

For each set of values of the three parameters r/δ, X/r, F_{Cu}, three different simulations were carried out. This was achieved by simulating three different (random) spatial conductor
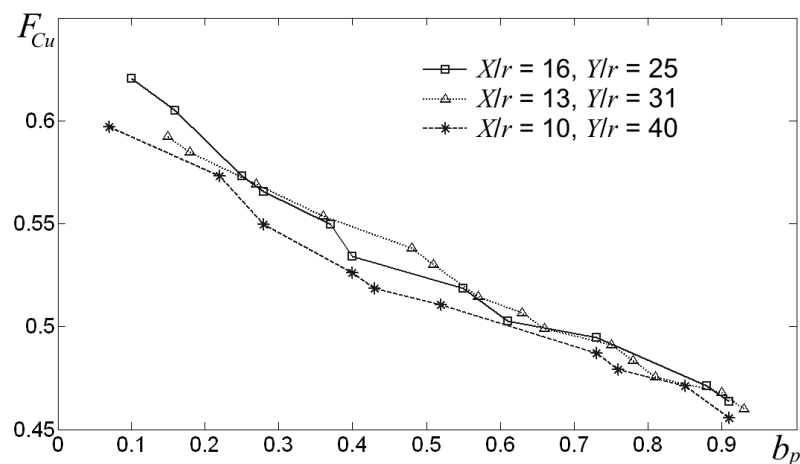
Figure 5.3: Plot of the F_{Cu} values of the simulated windings, as a function of the b_p values used in the calculation of the coordinates of the conductors, for the cases $X/r=16$, $Y/r=25$, $X/r=13$, $Y/r=31$ and $X/r=10$, $Y/r=40$.

distributions for each set of X, Y, f and N values, while r is kept constant throughout the process of simulations. Finally, averaging of the F_R result for each r/δ, X/r, F_{Cu} triad eliminates some imperceptible fluctuation, which at high frequencies ($r/\delta>2$) can be up to ±3% (typically ±2%). As an example, in Fig. 5.4 we can see the three different, random

spatial distributions simulated for the combination of $X/r=20$, $F_{Cu}=0.40$. In Fig. 5.5, for two different cases of parameter values X/r and F_{Cu}, the deviation D_s of the results of the three simulations is plotted each time relative to their average. The average of the three D_s values corresponding to an r/δ value is of course zero. We notice that at low frequencies the conductor distribution in space is of no importance and therefore the three results coincide.

From the simulations performed, (and after calculating the average values according to the above analysis) 1300 points were totally obtained within the limits of the (r/δ, X/r, F_{Cu}) space mentioned earlier. Figure 5.6 shows some indicative results for some values of the X/r and F_{Cu} parameters (they correspond to about 300 points).
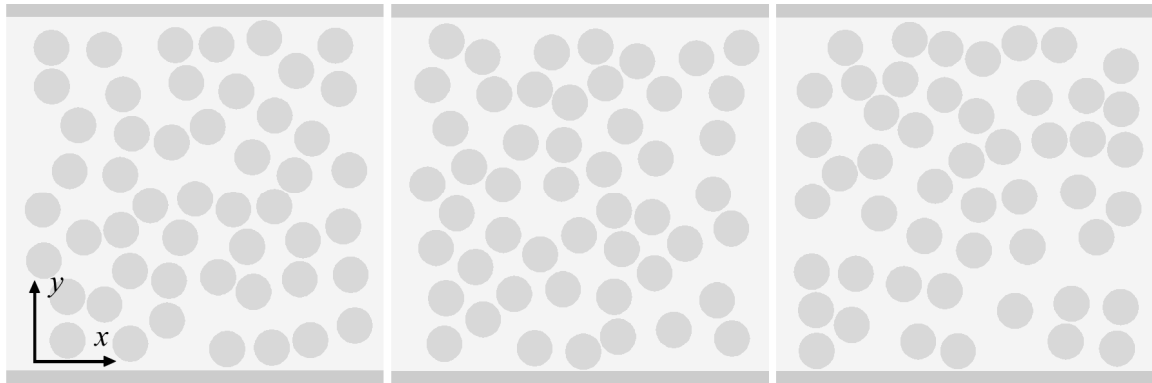
Figure 5.4: Three different spatial conductor distributions simulated for $X/r=20$, $F_{Cu}=0.40$.
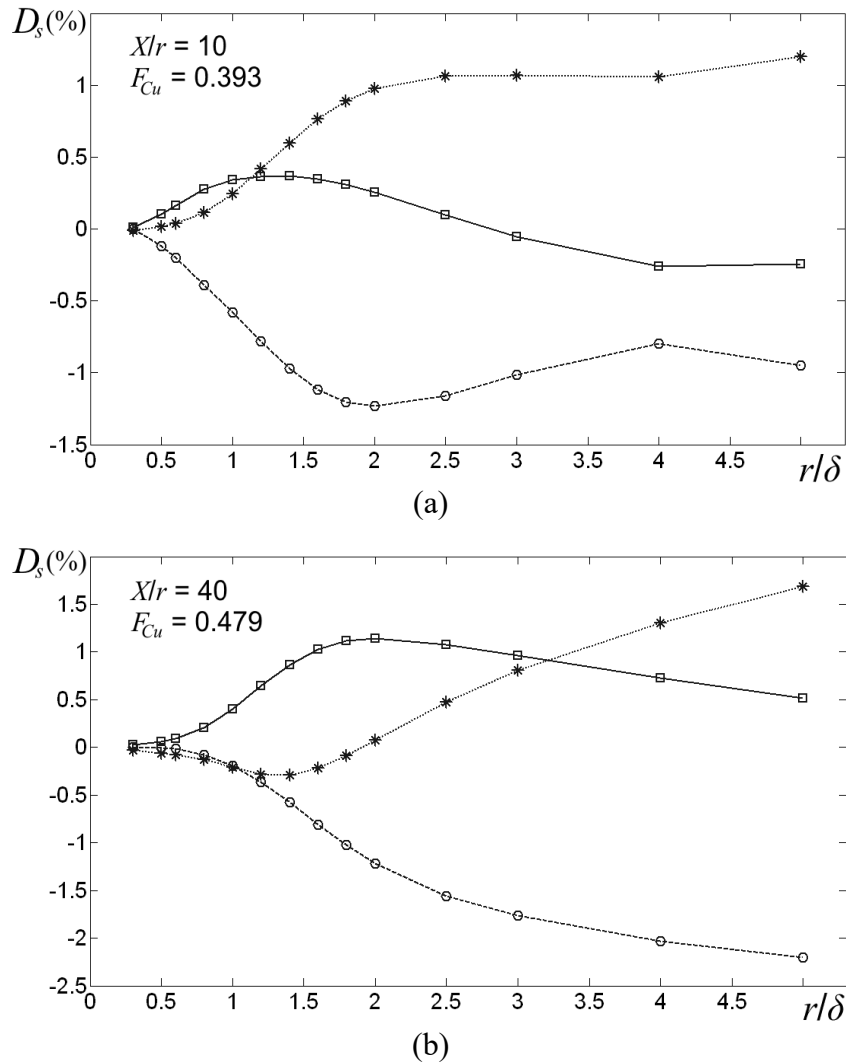
Figure 5.5: The deviation D_s of the results (F_R) of the three simulations for different spatial distributions from their average, for the cases (a) X/r=10, F_{Cu}=0.393 and (b) X/r=40, F_{Cu}=0.479.
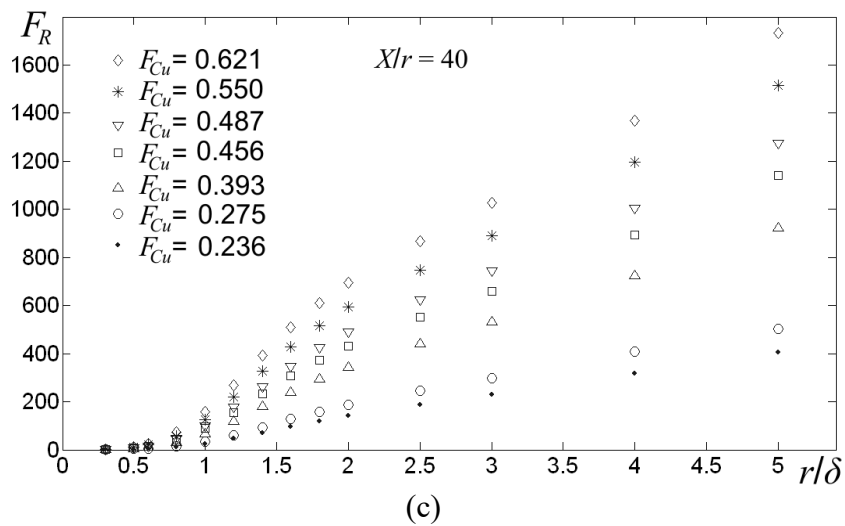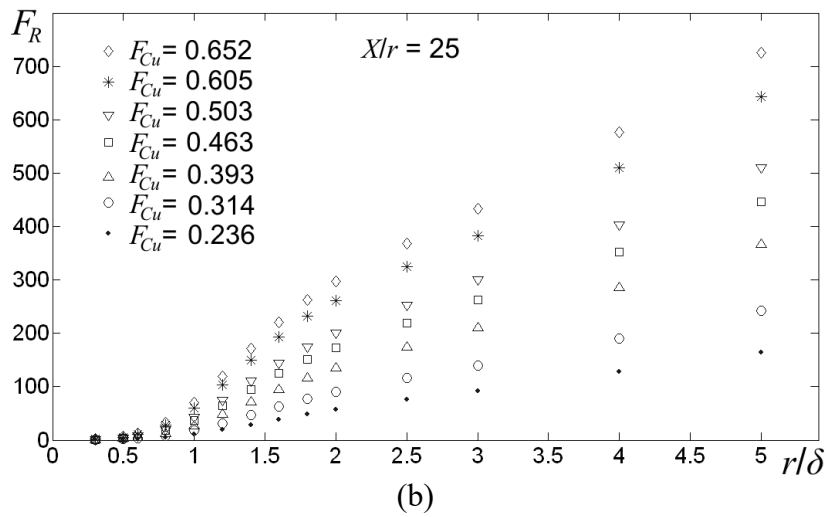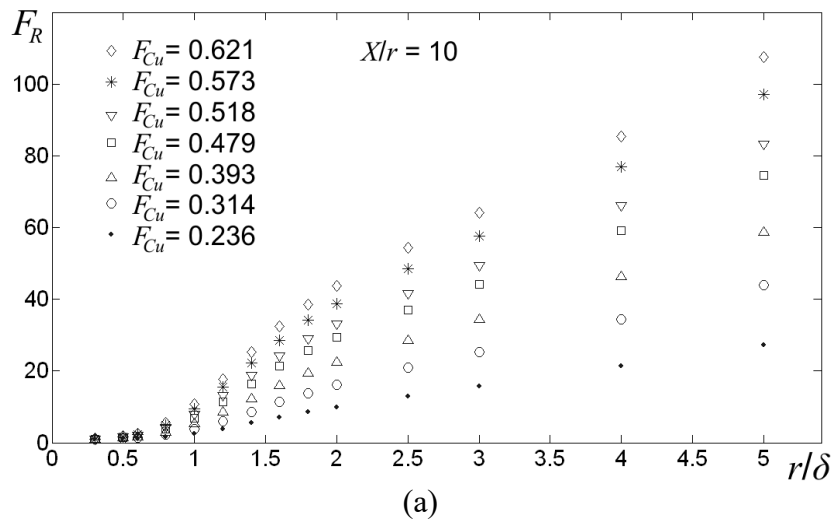
Figure 5.6: The results of the simulations for different filling factor F_{Cu} values, as a function of r/δ, for (a) X/r=10 (b) X/r=25 and (c) X/r=40.

5.3. Derivation of the final expression for the resistance factor

The final step in the direction of statistical treatment of the FEA data is the selection of an appropriate expression for F_R that will stand as a base function over which, through a curve fitting process, some correction function to be applied will be determined, thus resulting in the final equation.

A logical assumption in the reasoning for choosing the appropriate base function is that the dependence of the resistance factor F_R of coils with random distribution of the conductors on the r/δ ratio, regardless of its specific form, is expected to have the general dependence found in Dowell's equation. This general form indicates that at low frequencies (approximately $r/\delta < 0.8$) F_R is proportional to $(r/\delta)^4$, at high frequencies (approximately $r/\delta > 2$) it is proportional to (r/δ) and in the intermediate region it is proportional to $(r/\delta)^2$. This assumption is also supported by the fact that this general dependence of the resistance factor on the r/δ parameter (or h/δ when conductive sheets are studied) is highlighted in various works in the literature in which copper losses are studied, irrespective of the specific each time geometry of the problem [12], [47], [50], [72], [99], [109]. Thus, Dowell's expression is a reasonable choice for the required base function.

However, in order to make use of Dowell's expression in the present analysis, Dowell's model parameters must be correlated with those selected to describe the problem of random distribution of conductors. This correlation is based on the observation that in the case of a layered winding in which the distance between successive turns of a layer is equal to the distance between successive layers, i.e. when the conductors are in a square arrangement, the winding - as a total - has a uniform current density distribution. In other words, there are no areas of the cross-section of the winding which, compared to the rest of the cross-section, have higher or lower current density. Likewise, in a random distribution of conductors the current density distribution (always in a winding scale) also exhibits the same behavior. Moreover, in this specific case of layered winding (i.e. with a square arrangement of conductors), the parameters m and η of Dowell's model, with simple geometric considerations, can be directly related to the parameters adopted in the present analysis for non-layred windings, with the following equations:

$$\eta = \sqrt{F_{Cu}} \qquad \text{and} \qquad m^2 = \left(\frac{X}{r}\right)^2 \frac{F_{Cu}}{\pi} \tag{5.2}$$

It should be underlined at this point that in a layered winding with square arrangement of conductors except η and m, F_{Cu} and X also have a physical meaning (the total copper factor and the thickness of the winding, respectively), yet the opposite is not true. That is, in a winding with random distribution of the conductors, since there are no layers, either the layer filling factor or the number of layers make no sense.

If the expressions in (5.2) are substituted in Dowell's model formula (eq. 4.3) we obtain the following expression:

$$F_R = \Psi \frac{\sinh 2\Psi + \sin 2\Psi}{\cosh 2\Psi - \cos 2\Psi} + \frac{2}{3}(A-1)\Psi \frac{\sinh \Psi - \sin \Psi}{\cosh \Psi + \cos \Psi} \tag{5.3}$$

where:

$$\Psi = \frac{r\sqrt{\pi}}{\delta} \sqrt[4]{F_{Cu}} \quad \text{and} \quad A = \left(\frac{X}{r}\right)^2 \frac{F_{Cu}}{\pi} \tag{5.4}$$

Therefore, equation (5.3) is the aforementioned base function that is expected to facilitate the curve-fitting process, based on error minimization methods between the equation and the results of the FEA, which can be implemented using commercial software.

Studying (5.3), it is reasonable to suppose that the quantities Ψ and A may stand as global variables for the expression of high frequency losses of non-layred windings. This fact, if true, would considerably simplify the process of finding the proper form of the correction function to be applied on (5.3), so as to obtain a simple final expression for F_R accurately describing the FEA data with just two variables. In order to confirm or refute the previous hypothesis, we have to investigate the behavior of F_R with regard to Ψ and A.

Figure 5.7 shows, for some of the X/r values adopted in the simulations, the F_R result plotted as a function of A, when $\Psi=6$. It is evident that for any A value, F_R is somewhat lower when X/r is higher. A more detailed study of the simulation results reveals that this attribute is independent of the Ψ value, and despite the small relative amplitude of the resulting difference, it indicates clearly that A cannot stand as a free variable. This means that a hypothetical $F_R(A, \Psi)$ function would map any (A,Ψ) pair to more than one F_R values, i.e. it would not be a function. Thus, F_R necessarily has to be expressed as a function of the three fundamental parameters r/δ, X/r and F_{Cu}.
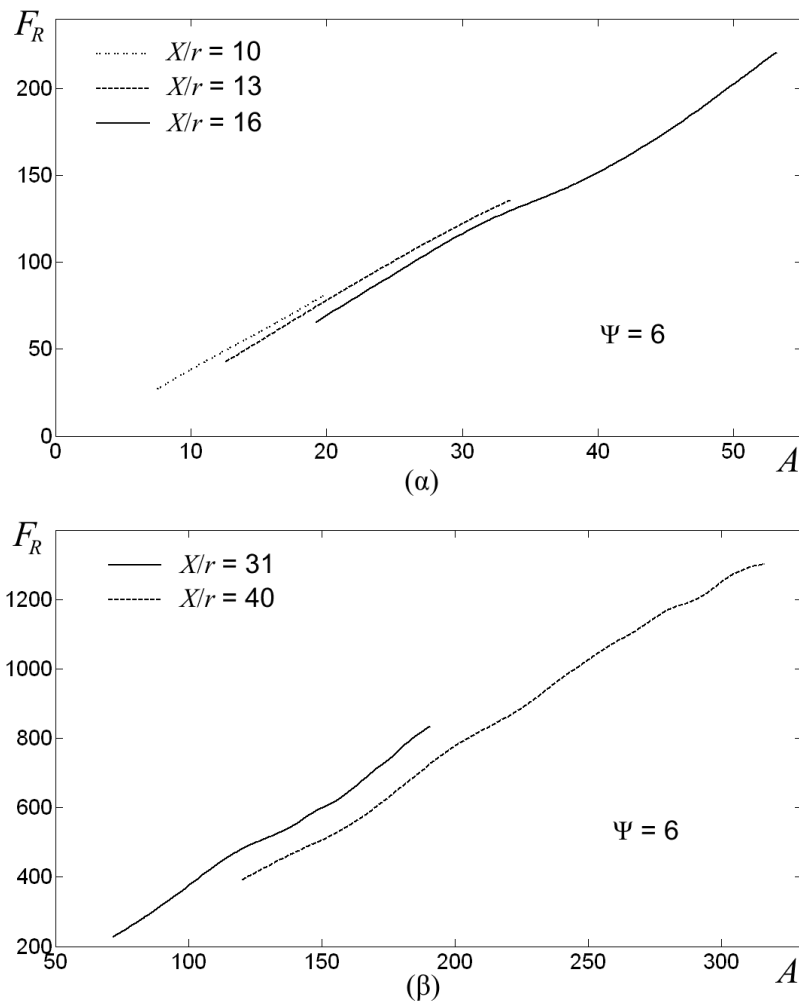
Figure 5.7: Plot of the random winding simulation results showing the resistance factor F_R as a function of the quantity A, when $\Psi=6$, for (a) $X/r=10$, 13, 16 and (b) $X/r=31$, 40.

Within this scope and with the base function (5.3) as starting point, there was a thorough mathematical processing of the numerical results, with application of the least squares method in three dimensions, with the help of the LabFit, Mathcad and Matlab software, in search of the appropriate final expression for F_R of windings with random conductor distribution. The purpose of this investigation was to find the appropriate corrective interventions in (5.3) for the final expression to be as simple as possible, describing at the same time the results of the simulations with the lowest possible error. The cases examined were the following: To apply a correction function to (5.3) (multiplier term); to have a cumulative correction term, alone or in combination with a multiplication factor, applicable to one or both of the terms of (5.3); the correction of any form (multiplier or exponent or

140

both) to be incorporated in the quantity Ψ. In any case, the various corrective terms (multiplicative, cumulative or exponential coefficients) were functions of the three parameters of the model, the form of which was subject to investigation.

Finally, this process led to the following expression for the high frequency resistance factor in non-layered windings, which was considered as the optimal choice in terms of both simplicity and accuracy:

$$F_R = \Psi \frac{\sinh 2\Psi + \sin 2\Psi}{\cosh 2\Psi - \cos 2\Psi} + g\left(\frac{r}{\delta}, F_{Cu}\right)\frac{2}{3}\left[\left(\frac{X}{r}\right)^2 \frac{F_{Cu}}{\pi} - 1\right]\Psi \frac{\sinh \Psi - \sin \Psi}{\cosh \Psi + \cos \Psi} \qquad (5.5)$$

where:

$$g\left(\frac{r}{\delta}, F_{Cu}\right) = \left(1 - \frac{p_1}{F_{Cu}}\right)\cdot\left(\frac{r}{\delta}\right)^{\left(p_2 - \frac{p_3}{F_{Cu}}\right)} \qquad (5.6)$$

with p_1=0.03782, p_2=0.15456, p_3=0.06279. The first term in (5.5) could be eliminated at the curve-fitting process without much of extra total error for the F_R function, but remains to better describe the data when the three parameters take relatively low values. To clear out this fact, one should consider that for small values of all three parameters, the first term in (5.5) contributes nearly 30% to the final result. Figure 5.8 shows the plot of the function g for the range of values of r/δ and F_{Cu}, as determined according to the proposed model, while in Fig. 5.9 we see a series of indicative graphs of (5.5), where one of the three parameters is kept constant in each one of the graphs.

It is also to be mentioned that in the mathematical processing of the numerical data in search of the appropriate form for the corrective function g, expressions, such as e.g. ratios of polynomial expressions of r/δ, X/r and F_{Cu}, which slightly reduced the overall absolute error of the final F_R expression in comparison to the FEA data, but this was achieved only at the expense of its simplicity, with a huge number of determinable fixed rate coefficients, which in some cases exceeded ten. This investigation did not lead to any expression that would be advantageous compared to (5.6).

Closing this paragraph, we should mention that at an early stage of the work on the formulation of the new model, which failed to take proper account of the analysis presented above on the possibility of A and Ψ to be the appropriate reference quantities, an initial expression for F_R was proposed [166]. Although this expression presents a low overall average error (about 3%) relative to the simulation results available at that time (about 800 points, i.e., much less than those available at the end of the work) it has some sinusoidal terms that contain A.
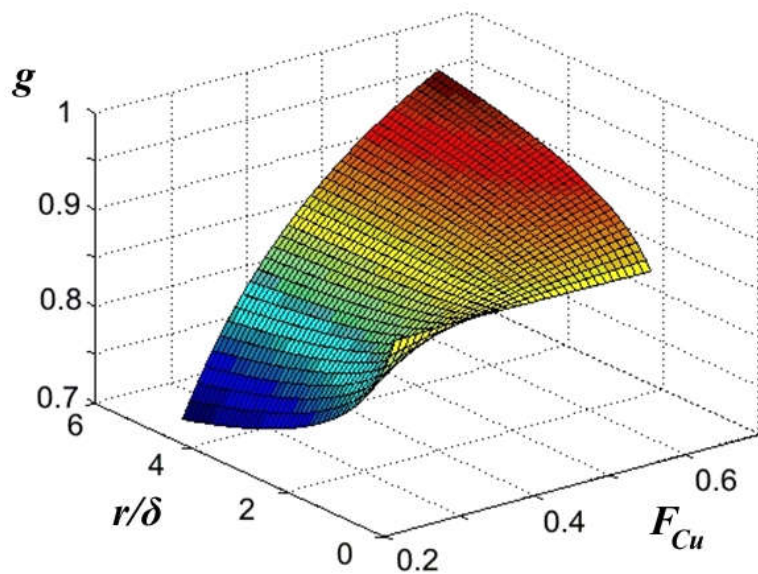

Figure 5.8: Plot of the correction function *g*.
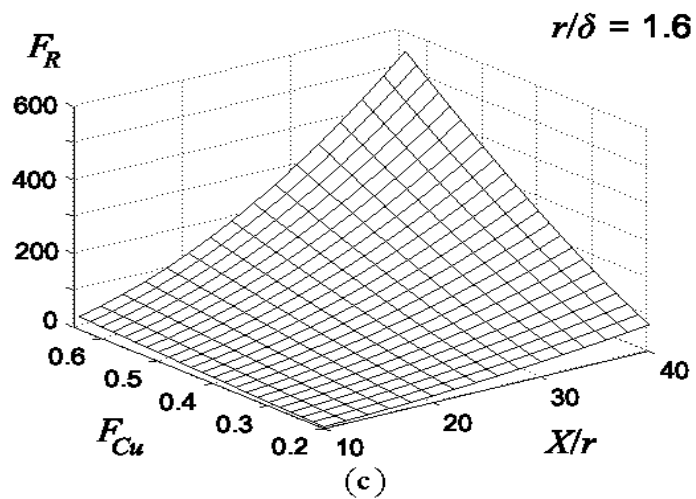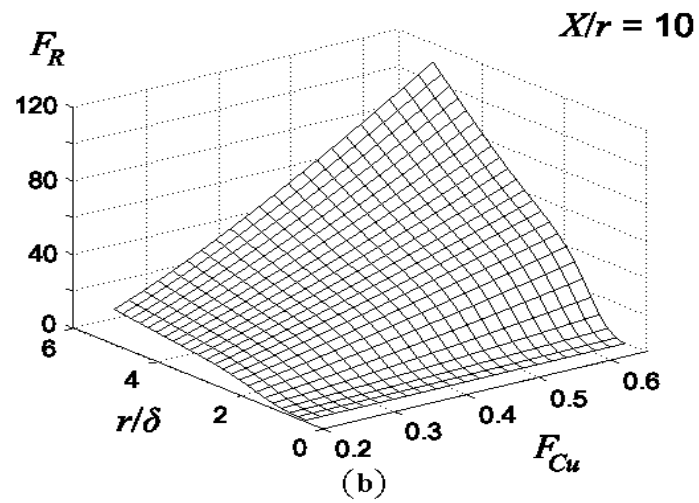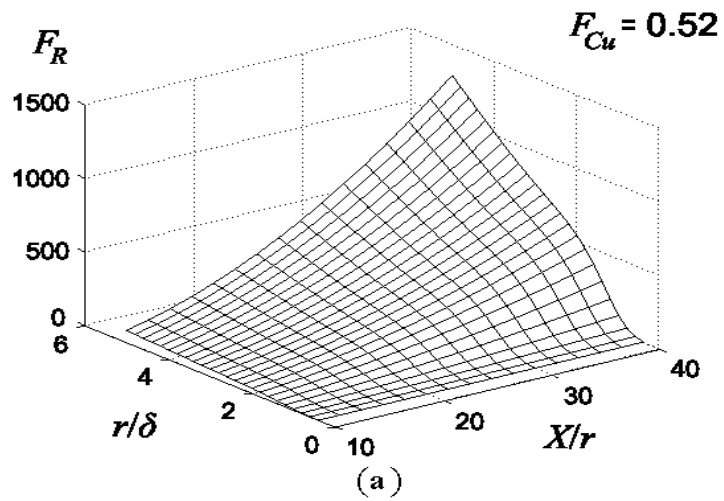
Figure 5.9: Indicative graphs of (5.5) when each of the three parameters of the new model remains constant.

143

However, such a behavior of F_R is characterized by a physical inconsistency. Simple logic, but also a simple overview of the simulation results, indicate that F_R is a monotonically increasing function for any of the three fundamental parameters r/δ, F_{Cu}, X/r and the same should apply to the dependence of F_R on A and Ψ that are products of these quantities, regardless of the power to which they are raised. Although the aforementioned sinusoidal terms do not generally lead to negative values for the F_R derivative with respect to A (i.e., F_R remains monotonically increasing), the periodic variation of F_R with respect to A in a generally increasing behavior is physically unacceptable and hence the expression proposed in [166] must be rejected.

5.4. Investigation of the new semi-empirical formula

5.4.1. Deviation from the simulation results

Expression (5.5) describes the simulation results with a total mean absolute error of 3%. A detailed illustration of the error with which (5.5) fits the simulation data is given in the set of graphs presented in Fig. 5.10, Fig. 5.11 and Fig. 5.12.

In these figures, the absolute value E of the error of (5.5) with respect to the simulation data is presented as a function of F_{Cu}, with X/r as a parameter, for some representative values of r/δ. It can be seen that at low frequencies, i.e., for low values of the r/δ ratio (Fig.5.10(a) and Fig. 5.10(b)), the match is nearly perfect (2% typical). For the frequency range within which the greatest part of the throughput power transfer occurs in most of the power electronic converters (since $r/\delta=1$ is the approximate choice for the fundamental frequency) the error is 5% typical (Fig. 5.10(c)). In the upper frequency range of the proposed model (Fig. 5.11 and Fig. 5.12) the typical deviation between (5.5) and the simulation data still remains at 5% except for low F_{Cu} values ($F_{Cu}<0.4$) for which it is about 10%. Another conclusion that indirectly arises from the general study of the deviation between (5.5) and the simulation data is that this error shows no clear attribute related to X/r. This fact justifies the absence of X/r from g.
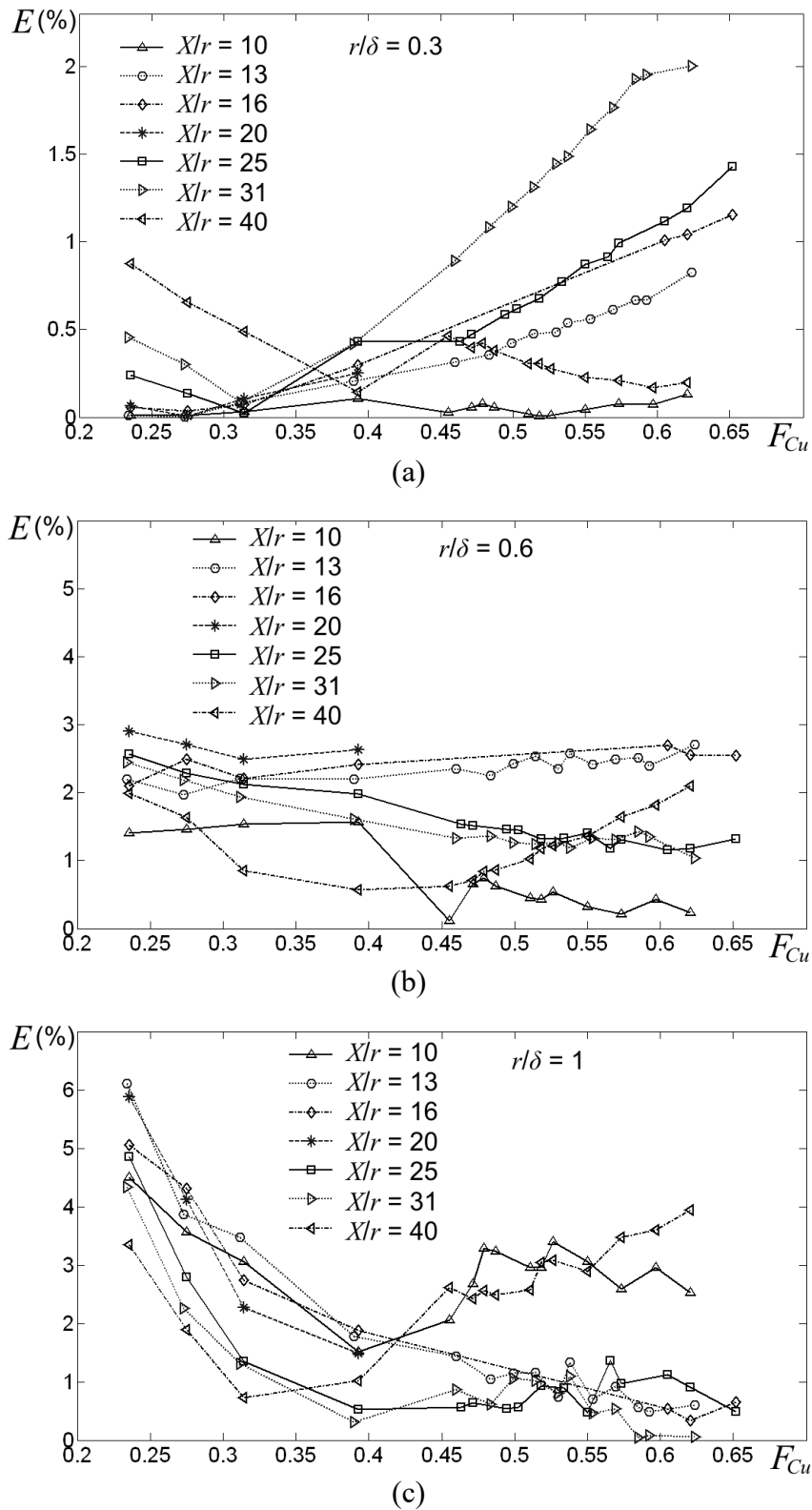
Figure 5.10: Absolute value E of the error of (5.5) relative to the simulation results as a function of F_{Cu}, for (a) r/δ=0.3, (b) r/δ=0.6 and (c) r/δ=1.
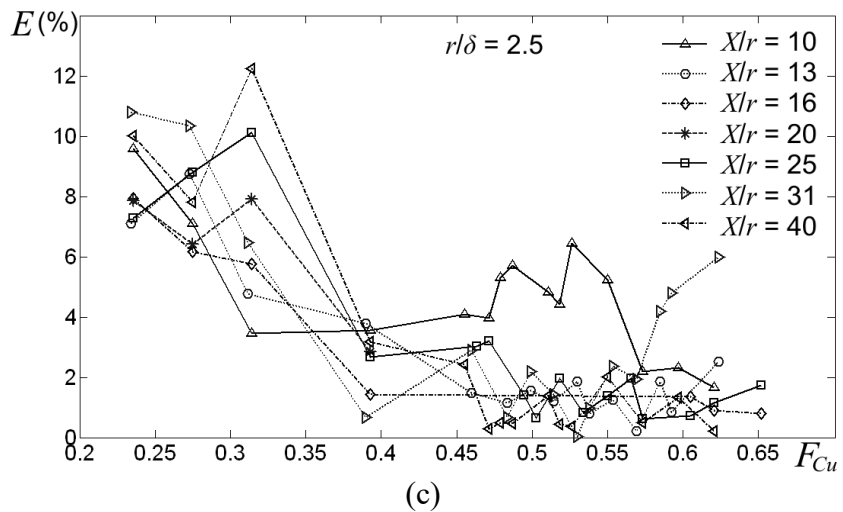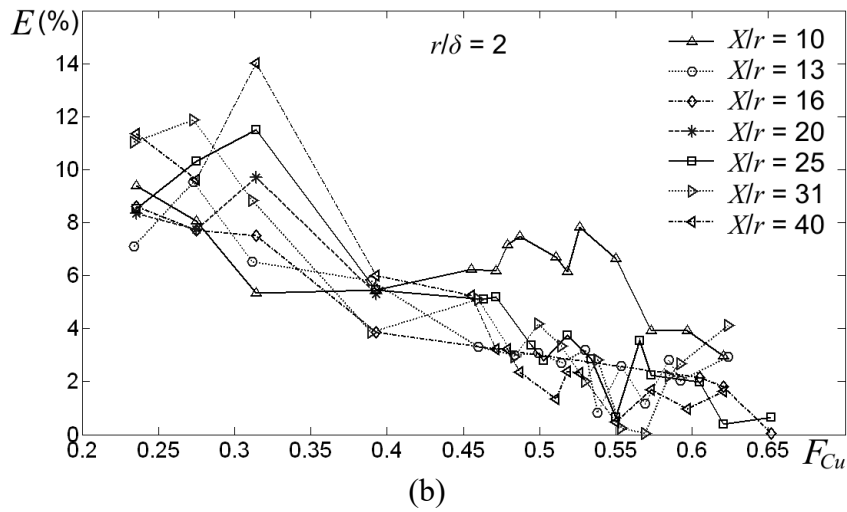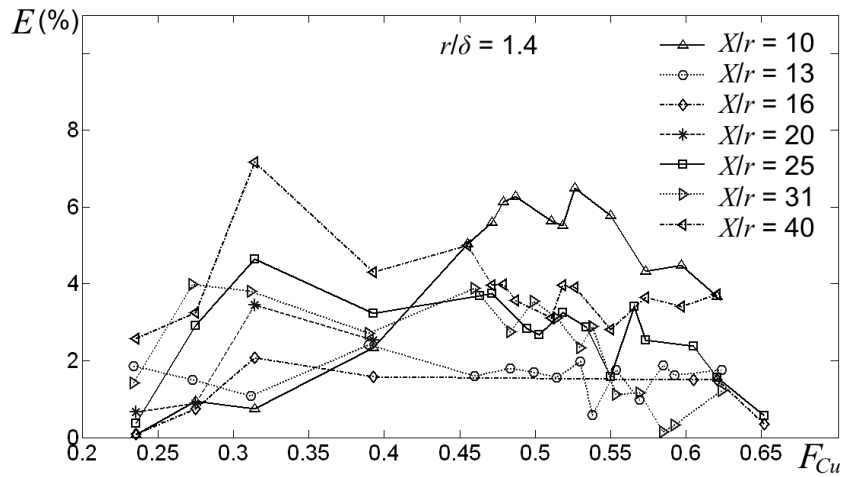
Figure 5.11: Absolute value E of the error of (5.5) relative to the simulation results as a function of F_{Cu}, for (a) $r/\delta=1.4$, (b) $r/\delta=2$ and (c) $r/\delta=2.5$.

146
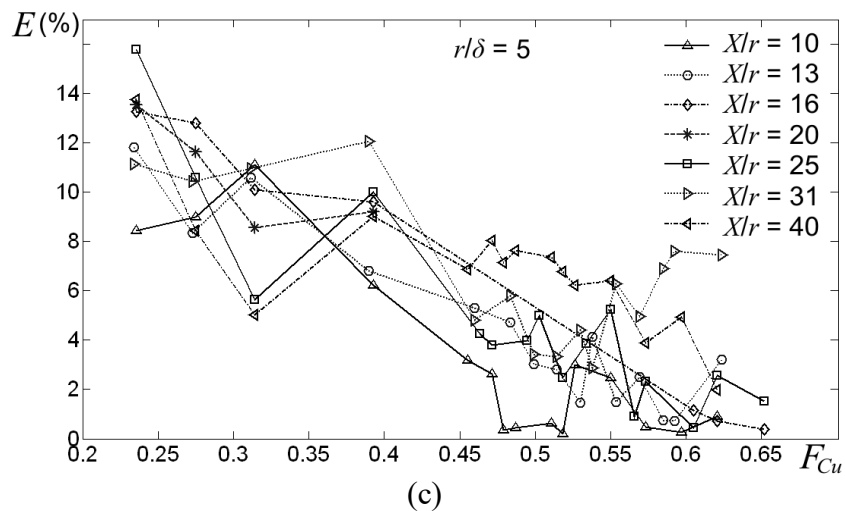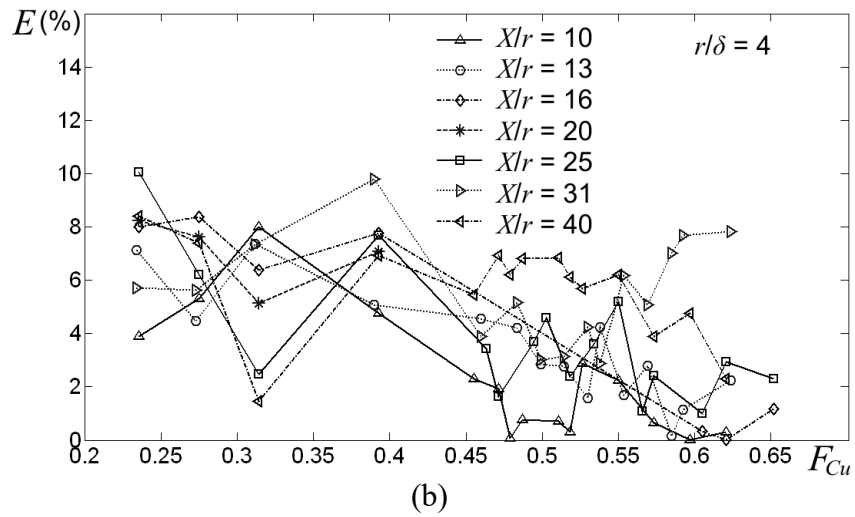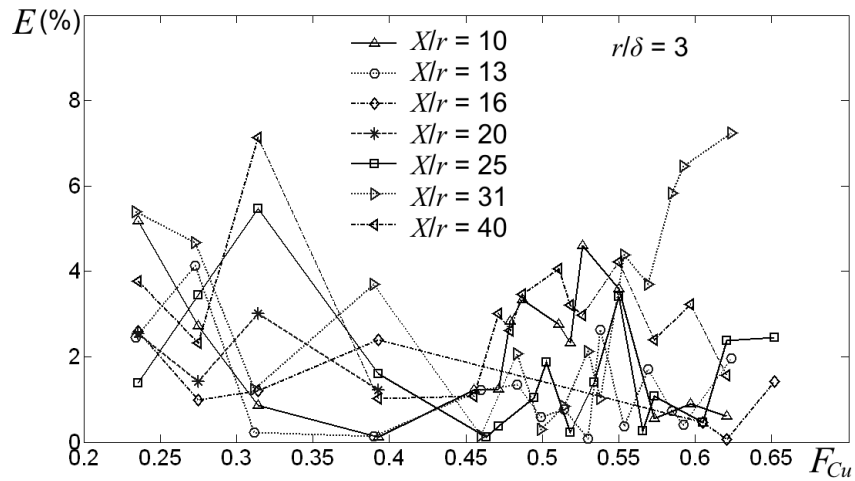
Figure 5.12: Absolute value E of the error of (5.5) relative to the simulation results as a function of F_{Cu}, for (a) $r/\delta=3$, (b) $r/\delta=4$ and (c) $r/\delta=5$.

5.4.2. Low frequency approximation

Expression (5.5) was extracted under the scope of accurately describing the simulation data, which, as mentioned earlier, sweep the range (0.3, 5) of the parameter r/δ. However, for low frequencies ($r/\delta < 0.7$), (5.5) can be simplified if its hyperbolic function terms are replaced by their Taylor series expansions [79], and terms up to third order are kept:

$$\frac{\sinh 2\Psi + \sin 2\Psi}{\cosh 2\Psi - \cos 2\Psi} \cong \frac{1}{\Psi} + \frac{4}{45}\Psi^3 \quad \text{και} \quad \frac{\sinh \Psi - \sin \Psi}{\cosh \Psi + \cos \Psi} \cong \frac{1}{6}\Psi^3 \tag{5.7}$$

If the expressions in (5.7) are substituted in (5.5) we obtain the following approximate expression for F_R at low frequencies:

$$F_R \cong 1 + \pi^2 F_{Cu} \left\{ \frac{4}{45} + \frac{g\left(\frac{r}{\delta}, F_{Cu}\right)}{9} \left[\left(\frac{X}{r}\right)^2 \frac{F_{Cu}}{\pi} - 1 \right] \right\} \left(\frac{r}{\delta}\right)^4 \tag{5.8}$$

Since none of the parameters F_{Cu} and X/r is very small ($F_{Cu} > 0.23$, $X/r > 10$) the following inequalities are valid:

$$\frac{4}{45} << \frac{g\left(\frac{r}{\delta}, F_{Cu}\right)}{9} \left[\left(\frac{X}{r}\right)^2 \frac{F_{Cu}}{\pi} - 1 \right] \tag{5.9a}$$

$$\left(\frac{X}{r}\right)^2 \frac{F_{Cu}}{\pi} >> 1 \tag{5.9b}$$

and (5.8) can be further simplified as follows:

$$F_R \cong 1 + g\left(\frac{r}{\delta}, F_{Cu}\right) \frac{\pi F_{Cu}^2}{9} \left(\frac{X}{r}\right)^2 \left(\frac{r}{\delta}\right)^4 \tag{5.10}$$

Table 5.1 gives the deviation Δ_a of the result of (5.10) from that of (5.5), for different indicative values of the parameters F_{Cu}, X/r, and r/δ, while in Fig. 5.13 some graphical

representations of (5.5) together with the low frequency approximation given in (5.10). From the Δ_a values listed in Table 5.1 it comes clear that the deviation of the low frequency approximation from the full expression increases significantly as r/δ and F_{Cu} increase, since they are included in the quantity Ψ, which is the variable in the expansions of (5.7). The corresponding increase with increments of X/r is relatively small, since (5.9a) and (5.9b) are almost always quite good approximations. In conclusion, we can say that (5.10) can be considered as a good approximation of (5.5) when $r/\delta<0.7$.

It would be interesting at this point to compare (5.10) with the existing formula for copper losses at low frequencies as found in [74], which can be expressed in terms of the parameters appearing in the present analysis as:

$$F_R = 1 + \frac{\pi F_{Cu}^{\ 2}}{9}\left(\frac{X}{r}\right)^2\left(\frac{r}{\delta}\right)^4 \tag{5.11}$$

TABLE 5.1
Indicative values of the deviation Δ_a of the low frequency approximation (5.10)
from the complete expression (5.5).

X/r	F_{Cu}	r/δ	$\Delta_a(\%)$	X/r	F_{Cu}	r/δ	Δ_a (%)	X/r	F_{Cu}	r/δ	Δ_a (%)
10	0.30	0.5	**0.3**	25	0.30	0.5	**0.5**	40	0.30	0.5	**0.6**
10	0.30	0.7	**1.5**	25	0.30	0.7	**2.4**	40	0.30	0.7	**2.7**
10	0.30	1	**9.1**	25	0.30	1	**11.4**	40	0.30	1	**11.7**
10	0.45	0.5	**0.5**	25	0.45	0.5	**0.9**	40	0.45	0.5	**1.0**
10	0.45	0.7	**3.1**	25	0.45	0.7	**4.0**	40	0.45	0.7	**4.2**
10	0.45	1	**16.0**	25	0.45	1	**17.6**	40	0.45	1	**17.8**
10	0.60	0.5	**0.9**	25	0.60	0.5	**1.3**	40	0.60	0.5	**1.4**
10	0.60	0.7	**4.7**	25	0.60	0.7	**5.5**	40	0.60	0.7	**5.6**
10	0.60	1	**22.4**	25	0.60	1	**23.6**	40	0.60	1	**23.8**

(a)

(b)

(c)
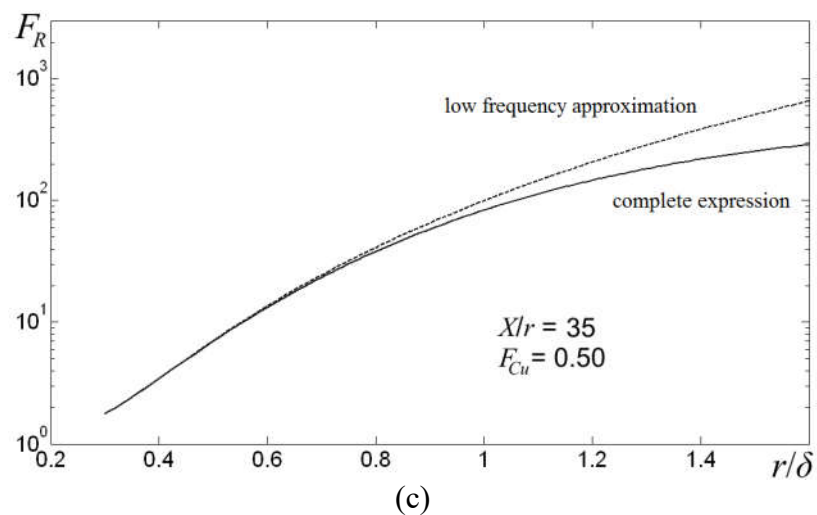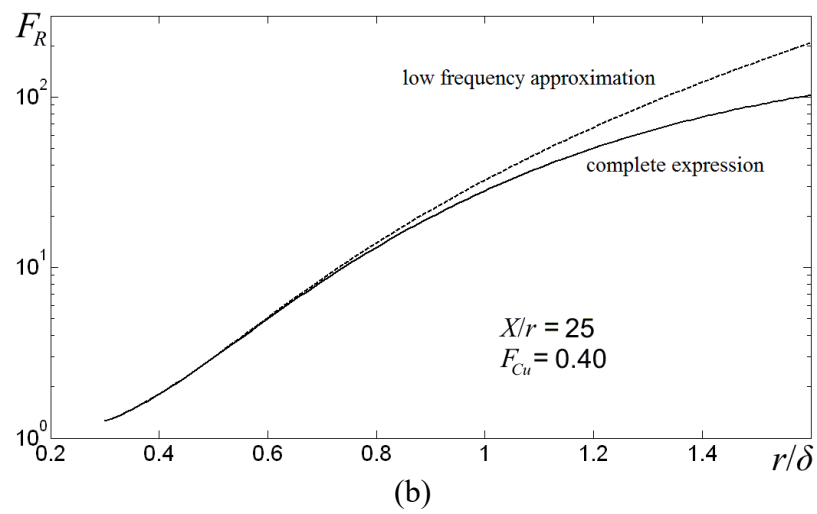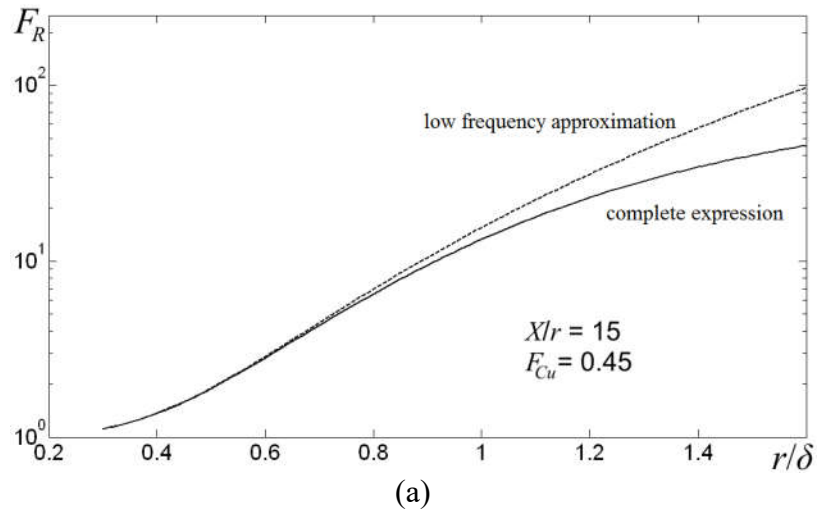
Figure 5.13: Plot of F_R versus r/δ, as obtained from the complete expression of the new model (5.5) and its low frequency approximation (5.10), for (a) X/r=15, F_{Cu}=0.45, (b) X/r=25, F_{Cu}=0.40 and (c) X/r=35, F_{Cu}=0.50.

Expression (5.11) was derived in [74] under the assumption of a flux field through the conductors that has no *x* component and is proposed as valid for $r/\delta<0.7$, while (5.10) –or the complete expression (5.5)– describes the simulation data with a fairly low error at low frequencies (Fig. 5.10(a) and Fig. 5.10(b)). The assumption now of a clearly *y*-oriented flux, which indisputably holds true for $r/\delta<0.3$ (strictly valid only for $r/\delta\rightarrow0$), for higher frequencies gradually becomes a rough approximation, a fact easily verified by FEA simulations.

Let us point out here that although the "low frequency range" has as unique criterion the assumption of one-dimensional field form in the conductors, it is defined as desired by the various researchers. For example, in [143] it is defined as $r/\delta<0.8$, in [119] as $r/\delta<1$, while in [5] as $r/\delta<0.2$. In Fig. 5.14 we see the magnetic flux in a winding with random conductor distribution for r/δ values equal to 0.3, 0.5, 0.6 and 0.8, where, as the frequency gradually increases, the declension from the above assumption is obvious. Two-dimensional effects lead to a lower effective resistance than calculated by the one-dimensional field approximation, and we may conclude that function *g* in (5.10) stands as a correction factor (with respect to (5.11)) that quantifies these two-dimensional effects (it is reminded that it is
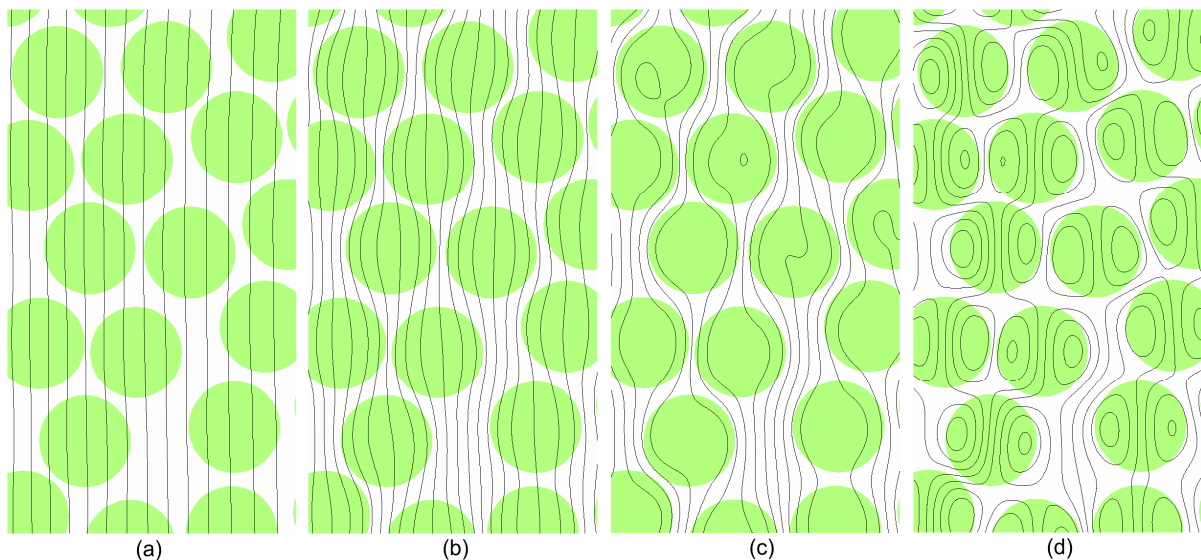
Figure 5.14: Flux lines of the leakage field in a winding with random conductor distribution, simulated for (a) $r/\delta=0.3$, (b) $r/\delta=0.5$, (c) $r/\delta=0.6$, (d) $r/\delta=0.8$.

$g<1$ for any of F_{Cu}, r/δ pair). Moreover, it should be marked that in [74], as the study is limited to the low frequency range, the precise arrangement of the conductors within the winding is not critical.

5.4.3. Sensitivity of the new expression in variations of *X/r* parameter

It would also be informative to study the sensitivity of (5.5) in variations of *X/r*, since this is essentially the only parameter of the model which may be determined with some measurement error.

Within the scope of the proposed model none of the F_{Cu} and *X/r* is very small. Therefore, in order to facilitate the present investigation, we can assume that:

$$F_R \cong \frac{2}{3}\left(\frac{X}{r}\right)^2 \frac{gF_{Cu}}{\pi} \Psi \frac{\sinh\Psi - \sin\Psi}{\cosh\Psi + \cos\Psi} \qquad (5.12)$$

Below is the Taylor expansion of the term with the hyperbolic and trigonometric functions appearing in (5.12), keeping this time, for more accuracy, one term more than the corresponding expression given in (5.7):

$$\frac{\sinh\Psi - \sin\Psi}{\cosh\Psi + \cos\Psi} \cong \frac{1}{6}\Psi^3 - \frac{17}{2520}\Psi^7 \qquad (5.13)$$

With the values of the other geometric parameters (*N*, *Y*, *r*) constant, F_{Cu} is inversely proportional to *X/r*. Taking this into account, as well as (5.13), (5.12) can be written as follows:

$$F_R \cong \lambda_1 - \frac{\lambda_2}{X/r}, \qquad r/\delta = \text{constant} \qquad (5.14)$$

where λ_1 and λ_2 are positive constant quantities (dependent on *N*, *Y*, *r*, *r/δ*, here considered as constant). This dependence can also be visually verified in Fig. 5.9(a) and Fig. 5.9(c). When constructing a magnetic component with a non-layered winding *X/r* can be determined easily and precisely by measurement with an error of the order of $\Delta(X/r)=\pm 1$ or even smaller. Under this scope and given that all other quantities involved (*N*, *Y*, *r*, *r/δ*) are precisely defined, the typical error with which F_R is calculated is:

$$\frac{\Delta F_R}{F_R} = \frac{\dfrac{\partial F_R}{\partial[(X/r)]}\Delta(X/r)}{F_R} \cong \frac{1}{\dfrac{\lambda_1}{\lambda_2}(X/r)^2 - (X/r)}\Delta(X/r) \tag{5.15}$$

while the following equation is valid:

$$\frac{\lambda_1}{\lambda_2} = \frac{2520}{6\cdot17}\cdot\frac{(Y/r)}{(r/\delta)^4 N\pi^3} \tag{5.16}$$

Expression (5.15) makes it clear that the F_R calculation with use of (5.5) gets more accurate as X/r increases, despite that in (5.5) F_R is approximately proportional to $(X/r)^2$. This is due to the fact that X/r is a continuous variable with an error of approximately constant amplitude, but also due to the inverse proportionality between X/r and F_{Cu}. We also notice that for given values of X/r and $\Delta(X/r)$, the result is more accurate when λ_1/λ_2 ratio is greater. It follows from (5.16) that high λ_1/λ_2 values correspond to low frequencies (small r/δ values) and low F_{Cu} values (for given X/r, this means high Y/r values and small N values), i.e. to that part of the field of application of the new model for which (for any given X/r) the proximity effect has a lower impact and the resistance factor has a relatively lower value.

5.4.4. Application of the new model in the case of stranded conductor

Taking into account the conditions under which the new model was formulated, it is expected to apply even to randomly wound coils with simple stranded wire, given that all strands carry equal and in-phase currents (i.e. skin and proximity effect do not exist on wire scale but only on strand scale).

In a winding with N in number, equally long, circular cross-section solid conductor turns, each of which has a resistance factor $F_{Rt,k}$, $k=1,2,\dots N$, the resistance factor F_R of the winding is equal to the average of the individual resistance factors i.e.:

$$F_R = \frac{1}{N}\sum_{k=1}^{N} F_{Rt,k} \tag{5.17}$$

This is the case studied in this chapter and is described in (5.5), since the N turns are randomly placed within the cross-section of the winding.

So let's now consider a winding that consists of N_c turns of wire, which in turn consists of n identical strands of circular cross-section of radius r. If the dc resistance of a strand-turn is $R_{dc,st\text{-}t}$ and the total dc resistance of a strand is $R_{dc,st}$, the total dc resistance of the winding will be:

$$R_{dc} = N_c R_{dc,st\text{-}t}/n = R_{dc,st}/n \qquad (5.18)$$

It is assumed that each strand is covered by an insulation film and that the stranded wire has been twisted before it is placed in the winding. Under these conditions, all strands are equivalent in terms of the effect of the magnetic field on them and of the change in their effective resistance.

In order to show that (5.5) can be used to calculate the F_R of this winding, we must first make a by default correct assumption, that the resistance of each turn of a strand, out of the totally $N=nN_c$ present in the winding, varies by a factor $F_{Rst\text{-}t,ij}$ generally different from the other strand turns, where $i=1, 2,…n$ and $j=1, 2,…N_c$. Subscripts i and j indicate that $F_{Rst\text{-}t,ij}$ corresponds to that part of strand i, which is within the turn j of the wire. Now, let each of the n strands have a total (i.e., in its whole length) active resistance $R_{st,i}$ and a resistance factor $F_{Rst,i}$. Given the aforementioned equivalence of the strands, they all have the same resistance factor F_{Rst}, which is equal to the F_R resistance factor of the winding, i.e.:

$$F_{Rst,1} = F_{Rst,2} = … = F_{Rst,n} = F_{Rst} = F_R \qquad (5.19)$$

However, the active resistance of a strand equals the sum of the active resistances of its individual segments (turns of strand) at the various turns of the wire and its resistance factor is equal to the average of the resistance factors of these (in series) subsections:

$$F_{Rst,i} = \frac{1}{N_c} \sum_{j=1}^{N_c} F_{Rst\text{-}t,ij} \qquad (5.20)$$

Since the effective resistance and the resistance factor are components with equal values for all strands, the result of (5.20) does not change if we take the average of the resistance factors of all strands. Hence, also taking into account (5.19), we can write:

$$F_{Rst,i} = F_{Rst} = F_R = \frac{1}{n}\sum_{i=1}^{n}\frac{1}{N_c}\sum_{j=1}^{N_c}F_{Rst-t,ij} = \frac{1}{nN_c}\left[\sum_{i=1}^{n}\sum_{j=1}^{N_c}F_{Rst-t,ij}\right] \qquad (5.21)$$

The term in the bracket equals the sum of the resistance factors of all strand turns in the winding and nN_c is their total number, thus (5.21) gives the average of the resistance factors of all strand turns, just like (5.17) gives the resistance factor of a solid wire winding as the average of the resistance factors of all turns. It is noted that the exact value for the twisting pitch of the stranded conductor, which previously was implicitly assumed equal to the length of a turn of the magnetic element, does not affect the final result.

We conclude that the expression (5.5) is also applied in the case of a stranded conductor, suffice it for the calculations of the parameters r/δ, F_{Cu} and X/r to use the values of the total number of strand turns $N=nN_c$ and the strand radius r.

5.5. Experimental validation of the new model

For the validation of the proposed semi-empirical expression (5.5), power loss measurements were taken during the experiments carried out over two transformers wound on ungapped cores with different center pole cross-section shapes. In both transformers, the core shape (type E and ETD) does not perfectly fulfill the condition of axial symmetry for the winding and the leakage flux through it. It was necessary though to confirm the new model's applicability on those two common cases, (instead of, for example, experiments on type P cores that show a perfectly symmetric cylindrical geometry or at least PH, PQ or RM that are close enough to P in form), despite that in literature, there is already evidence that the three dimensional effects taking place at the area close to core yoke do not considerably affect the copper losses [83], [97]. Moreover, the windings under study were deliberately wound in a random manner from the start so as to make sure that the F_{Cu} calculated for each of them corresponds to the actual value throughout the winding. If this was not the case, in the winding there could be some non-uniformity with locally different F_{Cu} values. Such a situation is not unusual in actual windings, since, at the beginning of the winding process, the existence of the bobbin always favors a careful, tight and almost stratified winding. In this case (which of course is not included in the new model) there would –possibly– be, an

increase or decrease of the F_{Cu} (compared to the totally uniform random arrangement) depending respectively on whether the areas of increased F_{Cu} would be in high or low MMF.

Thus, two sets of measurements were carried out on two different transformers. For the first set of the measurements, a transformer with copper wire of diameter d=0.56mm and turns ratio of N_p:N_s=220:332 was wound on an E65/32/27 core of the Ferroxcube 3F3 ferrite grade with the short-circuited secondary (s) wound over the primary (p) i.e. externally. The coil dimensions inside the bobbin were Y_p=Y_s=39.1mm, X_p/r= 14.9 and X_s/r=18.4. The dc resistances were measured under constant current flow conditions as $R_{dc,p}$=1.815Ω and $R_{dc,s}$=3.170Ω.

To ensure that at the frequencies of measurements, capacitive currents could be considered negligible, the leakage flux connection was inspected for resonance with the use of a frequency generator and a Summit Dmm 740 hand oscilloscope. This inspection indicated that up to the limit of 900kHz, there was an approximately linear with the frequency increase of the measured impedance amplitude and thus, capacitive currents were insignificant. At this point, we have to notice that when we investigated the capacitive behavior of the reverse short circuit (short-circuited primary - excitation in the secondary), the first capacitance currents appeared at a different, much lower frequency (approximately 300kHz). This remark is in accordance with the finding in the international literature [157] that the parasitic capacitance between transformer windings changes according to the transformation ratio. However, the interesting feature is that, by continuing the investigation at higher frequencies (within the maximum frequency generator limit), the first resonance was observed at a frequency approximately five times the frequency at which the first capacitive currents appeared (in the "right" connection the resonance was at a frequency beyond the device capabilities). This finding contradicts the suggestion in [83] that the operation of magnetic components at a frequency lower than 1/3 of the first resonance frequency ensures the absence of capacitive currents.

The excitation of the primary winding with sinusoidal voltage at frequencies from 43 to 510kHz was achieved with the use of the current-fed resonant converter analytically presented in Ch. 6. The method of measurement is similar to that shown in Ch. 7 and is based on the acquisition of the $v_p(t)$ and $i_p(t)$ waveforms from a HP 54820A Infinium digital oscilloscope, where $v_p(t)$ is the voltage applied on the primary winding and $i_p(t)$ the current flowing through it. Further on, the oscilloscope performs the calculation of dissipated power as $P_{Cu} = \langle v_p(t) \cdot i_p(t) \rangle$ for an integer number of periods. Sensing of the voltage is achieved

with the use of an active differential probe, and for the current, an identical probe was used to sense the voltage on a low-inductance shunt resistor.

As explained in Ch. 6 and Ch. 7, the inductive character and precise value of this shunt resistor is a matter of special attention. For this set of measurements and the one described further next, resistors (Vishay – Sfernice, thick film technology) with values between 10Ω and100Ω were used. Their values were accurately measured under constant current flow conditions and their inductance is lower than 0.1μH (according to data sheet).

For each frequency, several measurements were taken at different dissipated power levels. The whole process should be fast, and power losses should not exceed 25W otherwise, heating of the winding leads to a slight reduction of the measured resistance, as explained in §7.4.2. Measurements over 260kHz (r/δ=2.18) indicated that 3F3 ferrite grade is unsuitable at this frequency range for the purpose of the specific experiment due to core losses, while the resistance calculations suppose negligible core losses. It should be explained here that though short-circuited, the secondary does not totally cancel the ampere turns of the primary, an attribute clearly seen in the FEA simulation results as well. Even for the nearly perfect cancellation of the primary ampere turns, which happens as the frequency increases, the leakage flux path still crosses part of the core yoke. All other precautions described in Ch. 6 were also taken in order to ensure reliable measurements.

From the coil data given earlier, we get $F_{Cu,p}$=0.3326, $F_{Cu,s}$=0.4063 and r/δ ranges from 0.887 to 2.18. With use of the classical equivalent circuit for the transformer's leakage connection, the result of applying (5.5) for the calculation of the total resistance R_l, as seen from the primary side, is given by the expression

$$R_l = F_{R,p}R_{dc,p} + \left(\frac{N_p}{N_s}\right)^2 F_{R,s}R_{dc,s} \qquad (5.22)$$

In Fig. 5.15(a), the result of (5.22), normalized at the value $R_{l,dc}$=3.207Ω, resulting for $F_{R,p}=F_{R,s}$=1 (low frequencies), is plotted as a function of r/δ (solid line), and the measurements are shown as experimental points. It is evident that the measurements verify the model up to the r/δ=2.18 limit.

It would be interesting here to give an example of the error introduced when someone attempts to approximate such a winding with a layered one and proceed with Dowell's formula. The primary winding can be approximated as layered with either m_p=7, η_p=0.400 or

m_p=6, η_p=0.465 and the secondary as m_s=9, η_s=0.468 or m_s=8, η_s=0.527. From the four possible combinations, we choose to plot in the graph of Fig. 5.15(a) the highest result and the lowest result, corresponding to m_p=7, m_s=9 and m_p=6, m_s=8. It can be seen that in any case, the result would be an overestimation of R_l of the order of 60%.

In order to raise more evidence supporting the validity of (5.5), a second experiment was conducted, identical to the previous one, using an ETD49/25/16 core of the Ferroxcube 3C85 ferrite grade. The values of the several parameters were: d=0.50mm, N_p=N_s=327, Y_p=Y_s=33.0mm, X_p=X_s=4.1mm, i.e. X_p/r=X_s/r=16.4 and $F_{Cu,p}$=$F_{Cu,s}$=0.4745. The primary and the secondary dc resistances were measured as $R_{dc,p}$=2.14Ω and $R_{dc,s}$=2.78Ω thus, $R_{l,dc}$=4.92Ω. The capacitive currents of the leakage connection were negligible for frequencies up to 850kHz.

As shown in Fig. 5.15(b), the measurements verify the model's validity for frequencies up to r/δ=1.53 (f=160kHz). In this case, the ratio $R_l/R_{l,dc}$ is equal to the F_R of the primary and secondary winding since they both have identical geometrical characteristics (X/r and F_{Cu}). The available ferrite grade did not favor to obtain reliable measurements at higher frequencies, while the use of a wire with greater radius (in order to achieve greater r/δ values) was not favorable either due to the small R_{dc} and X/r values occurring, which may potentially lead to measurements errors.

In the same figure, the dashed lines show, just like in Fig. 5.15(a), the R_l values resulting after approximating the windings as layered and applying Dowell's model. They correspond to the values m_p=m_s=8 (η=0.55) and m_p=m_s=7 (η=0.63). The error in this case is about 25% at r/δ=1.5, and increases at higher frequencies (not plotted here).

Note that for a winding with X/r=16.4, in no case would one consider in the layered form approximation that m=9 (not possible) or m=6 (too much empty space between the suppositive layers not justified by the insulation enamel of the wires). As also mentioned in [124], when approximating a random winding as layered, it is a common practice to consider the minimum interlayer distance (i.e., maximum number of layers). It is therefore quite unlikely to get with this approximation, even by chance, a result that would approach the actual one.
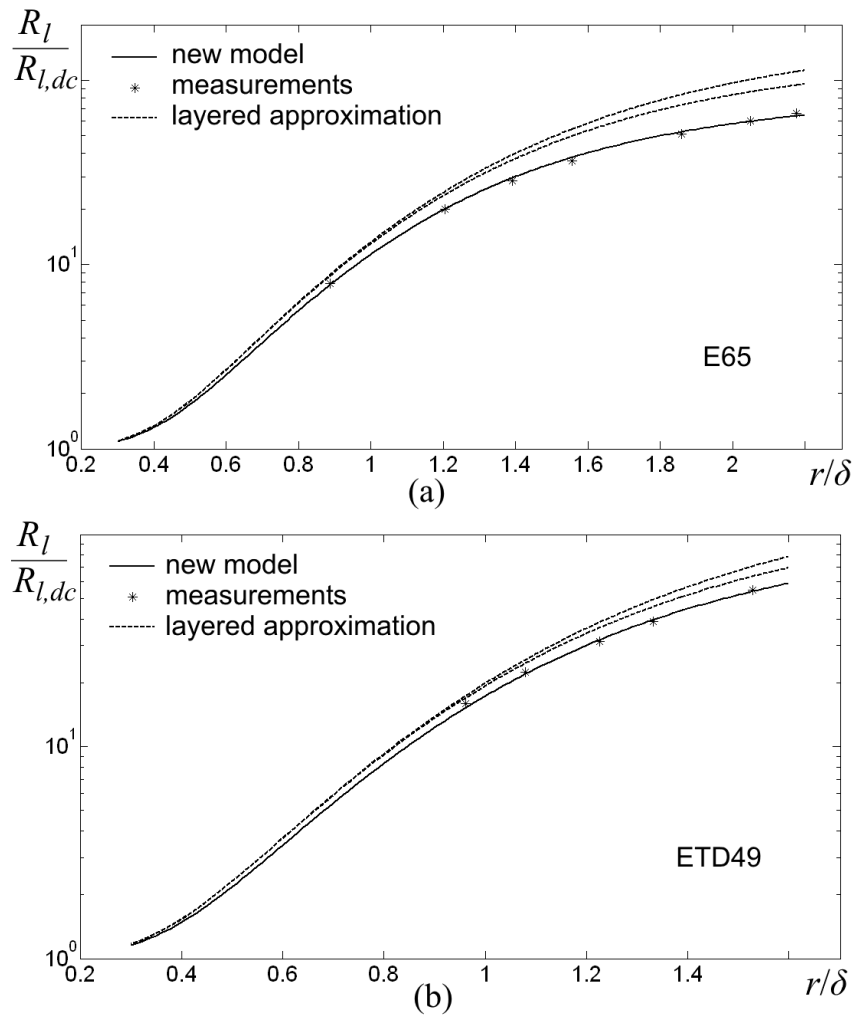
Figure 5.15: Effective resistance R_l normalized at the dc value $R_{l,dc}$ for the leakage connection of the random winding transformers under test, as approximated by applying (4.3) (Dowell's formula) for different numbers of suppositive layers that could possibly describe these random windings (dashed lines), as calculated by the new formula (solid line) and according to measurements.

It should be explained at this point that the error made in the above, typical so far, approximation of magnetic component designers is not only due to a weakness of Dowell's model or, more correctly, it is not due to some Dowell's error at all. One would say that for the values of η which appear in the hypothetical windings that approximate the transformer windings in the above experiments (from 0.40 to 0.63) Dowell's model is anyway inaccurate (§4.4.3.) giving a result higher than the real one and that this is the reason for the error we see in Fig. 5.15. It is also true that with a model for layer windings more accurate than Dowell's, the result for F_R would certainly be closer to the actual. The above reasoning is only partly true for two important reasons: The first one is related to the fact that Dowell's model is

159

indeed what designers use almost exclusively, as more accurate models, such as this of [109], are so complicated in their application that they are not suitable for quick calculations. Yet, the second and most important reason is related to the arbitrary choice for the number *m* of the suppositive layers that varies within a range that broadens as *X/r* increases. Let's have a look at some simple examples: For a winding with *X/r=12* one would say *m=5* (most likely) or *m=4* (less probable), while *m=6* is excluded because *r* does not include the wire insulation film and therefore such a winding does not fit into a space with *X/r=12*. For *X/r=25* one would say that *m=11*, but also maybe *m=10* or *m=12*. Finally, for *X/r=40* it would be a reasonable choice to say that *m=18* or 19, without being "absurd" to assume *m=17* or *m=16*. That is, we make a rough, completely arbitrary choice for *m*. Knowing that the result (irrespective of the model used) is sensitive to changes in *m* (of course, we don't forget in the above reasoning that an increase in *m* decreases η and this partially compensates the change of the result, since F_R is an increasing function of both *m* and η) we understand that the whole approach is completely arbitrary and it is not known at all whether its result is close to reality or not. Moreover, as previously mentioned, if it is Dowell's model used, none of the above *m* values would lead to a result close to the actual one. In conclusion, we may say that the error of this approach is not due to the accuracy of whatever model used to calculate the F_R value, but due to the fact of the preceding arbitrary assumption of the existence of imaginary layers there where no layers exist, which makes absolutely no physical or even practical sense.

As an end of this paragraph, it is necessary to point out a practical issue about the determination of the winding height *X*. For a core center pole with a circular cross section, accurate knowledge of *X* is just a matter of careful measurement. This is not the case when the core has a rectangular center pole. Especially for the inner winding in immediate contact with the bobbin (Fig. 5.16) two facts must be taken into account [124]: a) Bowing of the wire at the corners leaves some empty space, not occupied by copper, at the bottom of the winding over the faces of the bobbin. This formation is more prominent as the diameter of the wire gets greater and its extent can be visually estimated or measured when winding the first few turns. b) Over the edges of the coil former, the wire is normally wound in a tighter manner, thus making the winding thinner in total compared to the winding height over the faces ($X_c < X_f$).
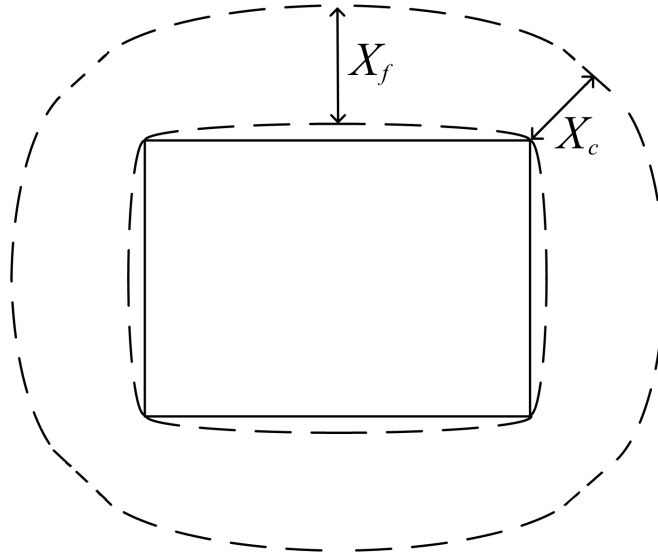
Figure 5.16: General pattern of a winding placed in a coil former with rectangular cross section

For the winding on the E core presented here, the two results for F_R when adopting one of the two values X_c or X_f for the sum of both primary and secondary heights (X_p+X_s) did not differ by more than 5% (remember that F_{Cu} is inversely proportional to X when N, Y and r are constant) and it was considered satisfactory to keep as the correct value for use in (5.5) the average of the two.

CHAPTER 6

DESIGN AND CONSTRUCTION OF A CURRENT-FED RESONANT INVERTER FOR MEASUREMENTS IN MAGNETIC COMPONENTS AT HIGH FREQUENCIES

6.1. Introduction

This chapter deals with the selection of an appropriate topology, as well as with the theoretical analysis and construction details of an inverter suitable as an excitation source of magnetic components with high quality voltage for measurements in the frequency range from a few kHz to 1 MHz. The interaction between the power part and the control circuit is investigated both with simulations and experimental verification of the theoretically derived equations that describe the inverter's operation. The result of this investigation is the appropriate dimensioning of the components in the two circuits (power and control) so as to optimize the inverter's performance, with maximum amplitude and minimum harmonic content of the output voltage, as well as with a maximum possible range of operating frequencies.

The trend towards increasing integration of electronic devices has pushed extremely high the necessary throughput power density of switch mode power supplies. In order to make feasible an appreciable miniaturization of these circuitries, in combination with higher output power (throughput power), switching frequencies that are quite higher than the regular values of about 250kHz have started to be subject of investigation by magnetic component designers. New converter designs based on resonant topologies [84], [88], [110], [112], [113], [116], [117], [120], [135], [139] and the use of planar magnetics [34], [35], [90], [114], [118], [143], [148] (see §3.3.3) or ferromagnetic materials with improved features [34], [35], [45], [74], [90], [149], [151] are very promising for future applications, even in the megahertz range. However, in both classic topologies (e.g., pulse width modulation

converters – PWM) and recently developed ones (e.g., resonant topologies), an appreciable portion of the overall losses still appears on the magnetic components.

The necessity to make accurate experimental measurements on high-frequency magnetics is on top priority in R&D phase and goes hand in hand with finite-element software analysis [35], [77], [114], [118]. Computer tools, although easy to use and very practical in avoiding multiple-attempt design and successive prototype improvements, cannot take into account all the factors that affect the operation of high-frequency converters. Moreover, some of these factors are not known beforehand thus, the experiment still remains the only reliable way for the final verification of any theoretical or computational prediction.

Testing of magnetic components is standardized by manufacturers of ferrite materials and is normally carried out either for specific conditions, regarding frequency, magnetic flux, and temperature, or with all other parameters constant when one of them sweeps a well-defined range [140], [142]. The excitation is sinusoidal and is applied on ring cores [140], [142], thus leaving on the magnetic component designers the proper approximations to be done for evaluating the actual results for other sorts of waveforms and different core shapes [28], [38], [94], [101], [103]. In any way, the data sheets provided by ferrite manufacturers often do not give a fully satisfactory picture of what has to be expected with regard to the general behavior and the power losses under the specific conditions that are to be encountered in practical applications.

From the aforementioned discussion, it becomes clear that some means of taking measurements under the standard sinusoidal excitation, but at the given desired conditions concerning frequency, temperature, magnetic flux, and core shape, would be undoubtedly a very useful tool. Given the possibility of taking measurements under any conditions, some standard approaches can be circumvented. Such approaches are, for example, the interpolation of the data given by the ferrite manufacturers to calculate the specific losses when the operating conditions are not described by any of the given curves or the arbitrary extension of these curves when the operating conditions are completely out of the covered range of the various parameters (also see §7.2.2).

However, it must be pointed that in magnetic components, further than the issue of ferrite core losses, copper losses represent a great portion too [79], [114], [128], [143] and their evaluation in a wide frequency range and for the given each time coil is of crucial importance. This argument is enhanced by the fact that the most widely used theoretical or semi-empirical formulas for high frequency copper losses are for ideal winding geometries [12], [47], [99], [109], [143], and even so, they generally show limited accuracy.

Until now, there are two alternatives in order to take measurements under sinusoidal excitation: One is the use of an impedance analyzer set [73], [78], [101], [105], [118]. The other is to combine a sinusoidal waveform generator with a linear power amplifier for the excitation of the device under test (hereafter "load" or DUT) and use a separate measuring system for data recording [34], [38], [57], [94], [115], [121]. Yet, both solutions have serious technical restraints.

Studying the specifications of commercial impedance analyzers, it becomes clear that they suffer from two drawbacks:

a) Only a few spot frequencies within their total frequency range are available for measurements.

b) The applied voltage drops with frequency and has a maximum value of just a few volts at high frequencies.

On the other hand, linear power amplifiers, at the frequencies of interest for power electronic applications, show a rapidly increasing distortion and a decreasing attainable amplitude of the output voltage as the frequency rises. Of course, the most important drawback of both previously mentioned devices is their high cost, which ranges between some hundreds and a few thousands of euros. For more sophisticated – more powerful products, the cost rises extremely high. In any way, measurements taken from devices excited with any of the two previous methods are of limited worth, since they are often far from describing actual operating conditions, which are characterized by high magnetic flux densities in the cores, high currents in the windings, and possibly high temperatures.

Some researchers have used in the past a current-fed resonant inverter as a low-cost solution to high-frequency sinusoidal excitation of magnetic components [57], [85]. The use of the inverter in these works was limited to a maximum frequency of 100kHz and a peak voltage of 50V. The harmonic content of the output waveform was considered acceptable even when there was a 7th harmonic equal to 2% of the fundamental. The specific inverter (a variant of the classical push-pull topology) first appears in the literature in [23], where it was used to apply 50kHz ac voltage on a clearly resistive load, at 1kW power. The main issue of study of this work was the voltage gain of the inverter, whereas the quality of the output waveform was of no interest. Thus, the switches driving method, combined with the values of the components in the resonant circuit, led to a highly distorted output voltage.

Further on in this chapter we discuss the pros and cons of key inverter topologies for the achievement of sinusoidal oscillation, and the advantages of the push-pull topology are highlighted. The topology proposed in [23] is theoretically analyzed and the factors affecting

the quality and value of the output voltage are thoroughly investigated. The combined effect on the performance of the inverter of both the power part component selection and the response speed of the control circuit is revealed by the analysis and is verified by measurements and simulations. The limitations over the rise of frequency are also pointed out and a fast control board is combined with low-loss resonant inductors to achieve a perfectly sinusoidal voltage in the range between some tens of kHz and 1 MHz, with the rms voltage at the high-frequency end equal to 450V.

6.2. Selection of appropriate topology

The only way to bypass the drawbacks of market devices is to construct a sinusoidal voltage or current resonant converter, with the obvious requirement to overcome the previously mentioned technical limitations and with the cost being kept sufficiently low at the same time. This last condition can be true for a laboratory made device, thus leaving the cost of the measuring set, which is normally already available, as the only relative expense. The point is to create a sinusoidal current through an LC circuit and then, according to the impedance of the load at the specific frequency, to either connect it in series with the LC circuit (low load impedance) or in parallel with it (high load impedance).
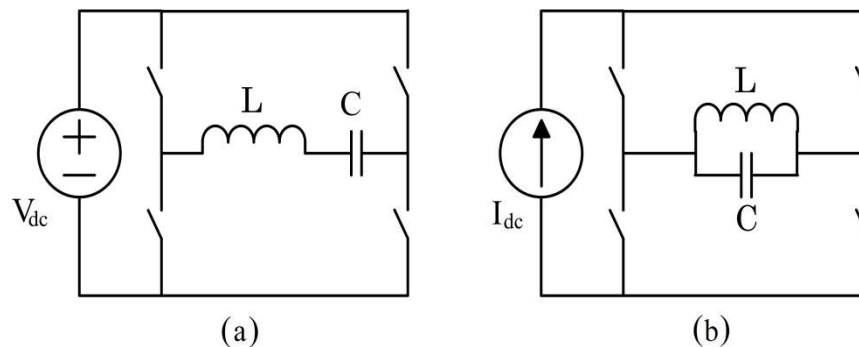
Figure 6.1: Basic resonant topologies for sinusoidal oscillation.

The two basic circuits to achieve forced resonance conditions are presented in Fig. 6.1. Figure 6.1(a) shows the full-bridge topology, in which a series LC circuit is triggered by voltage pulses [110], [112], [116], [117], [120], [122]. In this topology the output voltage can be very high, as it is limited only by the voltage ratings of the components L and C (the cut-off switches are at V_{dc} voltage), but the current is limited by the rated value of the semiconductor switches. The resonant current flows through the V_{dc} voltage source, thus

166

making it part of the resonant tank. The current monitoring, required to control the oscillator, greatly complicates its implementation. In any case, semiconductors made for large currents generally have long turn on - turn off times and the result is a slow inverter, with high switching and conduction losses, which is equivalent to a severe limitation of the maximum operating frequency. The same reasons also lead to poor quality output waveforms, since the losses on the switches, which carry the resonant current, introduce a considerable damping factor [158].

In Fig. 6.1(b) the resonant tank, consisting of an LC loop, is fed with current pulses on a full bridge topology. The cut-off switches are under the output voltage, which is generally expected to be quite high. Current I_{dc} is a relatively low current, equal to the average of the two switches' current pulses and is responsible for the power loss compensation in the resonant tank. Losses on the switches, which are not part of the resonant tank here, do not affect the quality of the output waveform.

In conclusion, the topology of Fig. 6.1(a) is more suitable for high output voltages, whereas that of Fig. 6.1(b) is preferable when the most important requirements are high output current, high frequency and output low harmonic content. The half bridge topology, in which two of the switches in both of the previous topologies are replaced by capacitors (in the voltage supply topology) or inductors (in the current supply topology), has almost the same analysis and is not taken as a separate case.

Figure 6.2 shows the center tapped, push-pull, full-wave topology to achieve resonance conditions. It seems to be the most appropriate as it incorporates the advantages of the topology in Fig. 6.1(b) using only two switches. The operation of the two switches provides the resonant tank with the excess power required to maintain the oscillation and this is achieved by pulses the amplitude of which is very low compared to the resonant current. In addition, as will be apparent from the oscillograms and the results of the simulations presented below, the semiconductor switches turn on at zero voltage. With the losses on the switches sufficiently low and the output voltage distortion dependent only on the losses occurring in the resonant inductors, the frequency can get very high values. It is worth noting that the maximum voltage on the switches is not preset. Under certain conditions it may be
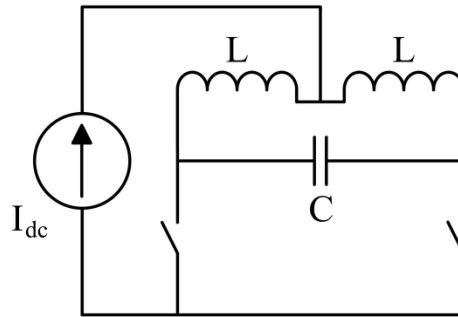
Figure 6.2: The push-pull topology for the achievement of resonance.

equal to the output voltage amplitude although in general it is lower (§6.8). The current source is easily implemented with a variable DC supply in series with a high value inductance.

What has to be pointed out is that, in any of the previous topologies, for a sinusoidal oscillation to be achieved, the switching frequency f_s has to coincide with the self-resonance frequency f_{res} of the resonant tank, as this is defined by the values of the LC components, possible parasitic LC components and any present damping factors. In [135] there is a detailed discussion about resonant converters operating at $f_s \neq f_{res}$, where it becomes clear that the resonating current or voltage harmonic distortion is very much affected by any deviation of f_s from f_{res}. In the following, if not else mentioned, it will be $f=f_s=f_{res}$.

6.3. General description of the inverter

In Fig. 6.3 is the schematic of the power part of the inverter selected for the implementation of the sinusoidal voltage excitation of magnetic components. A resonant tank formed by the main capacitor C_m, the auxiliary capacitors C_a and C_b and the two inductors L_a and L_b, is fed with constant current I_s and is forced to oscillation by the switching operation of the two semiconductor switches T_a and T_b. In series with the switches are the diodes D_a and D_b that block a negative current from flowing through the MOSFETS when the voltage on them tends to become negative. The DUT is connected at the ends of C_m (nodes A and B). For the simplification of calculations L_a and L_b will be considered as equal, but this fact proves to be of no critical importance for the operation of the inverter, while also, unless

stated otherwise, it will be assumed to be $C_a=C_b$. The current source I_s consists of a variable dc voltage supply in series with a relatively high inductance L_s ($L_s>>L_a$), thus I_s can be varied manually. For the inverter developed in this thesis, an inductor with $L_s=600$mH and saturation current 0.6A proved to be a satisfactory choice, whereas the value of L_a in no case exceeded 1mH. During the various tests, the maximum resonating currents encountered had rms values of the order of 5A, whereas the amplitude of the current pulses in the switches was typically lower than 0.3A and thus, the current I_s, which is equal to the average of the pulses of the semiconductor switches, also did not exceed 0.3A.

For ideal resonant inductors and a purely resistive load R_L, there is a proportional relation between I_s and the peak value V_{op} of the output voltage [23]:

$$I_s = \frac{\pi}{2} \cdot \frac{1}{R_L D} \cdot \frac{V_{op}}{2}$$

(6.1)
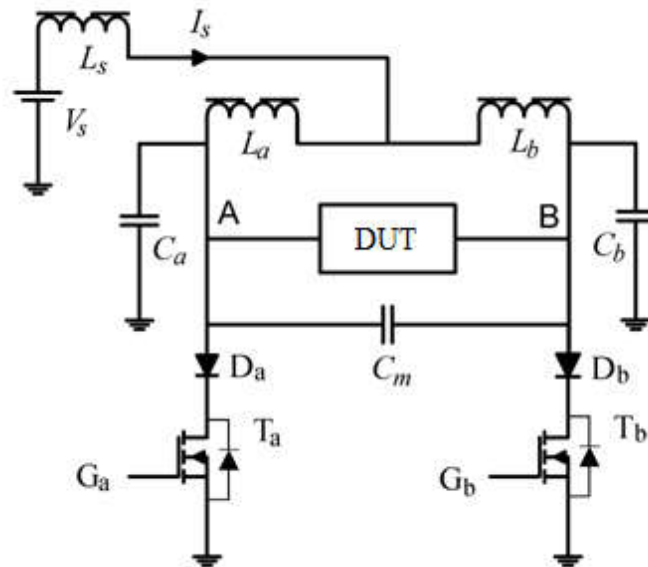
Figure 6.3: Power part of the inverter.

which means that the variation of V_{op} is achieved by varying the current I_s. As we will see next in this chapter, in the case of non-ideal coils or/and non-ohmic load, the total losses can be incorporated in the value of the –hypothetical– R_L load resistance, while its inductive part can be incorporated in the value of the inductive resonance $2L_a$ and the analysis of the inverter function remains the same. In (6.1) D is the duty cycle of the switches, i.e., the ratio of their conduction time t_{on} to the oscillation period $T=1/f$ ($D=t_{on}/T$)[1]. For ideal inductors, constant control board time delay t_d (t_d is explained in §6.4.2), and constant T and C_a, the duty cycle D of the switches depends only on the resistance R_L of the load. That is, a change of I_s only affects V_{op} proportionally, according to the dependence we see in (6.1), and not D. The capacitors C_a and C_b help to avoid a possible conduction overlap of the two switches, which would cause a temporary short-circuit discharge of C_m during their simultaneous conduction [23]. Such an operation mode would distort the output voltage and would overload the switches with high value current spikes on their turn on and voltage spikes on their turn off [23]. Moreover, without C_a and C_b, there would anyway be surges on the switches on their turn off due to the constant current flowing through the resonant tank, which now finds a conductive path to the ground through the two auxiliary capacitors. In addition, these two capacitors contribute to the soft turn off of the semiconductor switches, providing a relatively low voltage rise over them during the transient turn off effect. Their series connection, with the ground reference as the common node, brings them in parallel to the main capacitor C_m, making them actually part of the resonant tank.

For $L_a=L_b$ and $C_a=C_b$, the total inductance in the resonant tank is $2L_a$, and the total capacitance is $C_m+0.5C_a$. If we ignore the, insignificant in the general case, effect of damping factors (at an open output operation, damping is mainly related to the losses in the resonant inductors), the frequency of the output voltage, which is the self-resonance frequency of the LC loop, is given by:

---

[1] In the case of the present inverter, the conduction interval on the MOSFET semiconductor switches is only part of their command interval, that is, the time at which the applied voltage between the gate and the source of a switch is positive ($V_{GS}>0$). While the end of the conduction interval is signaled by the end of the command period (withdrawal of the voltage pulse from the switch's gate), its beginning is determined by factors related to the components of the power and control circuits (see §6.4.1 and Fig. 6.6).

$$f = \frac{1}{2\pi\sqrt{2L_a(C_m + 0.5C_a)}}$$ (6.2)

For the variation of frequency, a change of the passive components in the LC loop is required. Having a few inductor couples and some capacitors available, there can be a quite satisfactory frequency sweep, up to the maximum limit of the apparatus, if all the LC combinations are made. This sweep is not continuous; however, there can always be an LC combination that is adequate for the oscillation frequency to be very close to the desired one, if not matching. It is reminded that L_a and L_b may have different values and that any L_t inductor can be connected directly to the output, in parallel to the DUT, for finer frequency adjustment, provided that the L_a and L_b are quite lower than L_s (L_t has no such restriction).

Yet, in these cases, the total equivalent inductance of the resonant tank should be correctly calculated and is equal to $L_t(L_a+L_b)/(L_a+L_b+L_t)$, instead of $L_a+L_b=2L_a$, which we consider in the general case.

The control circuit triggers the power circuit with an initial random oscillation and then,
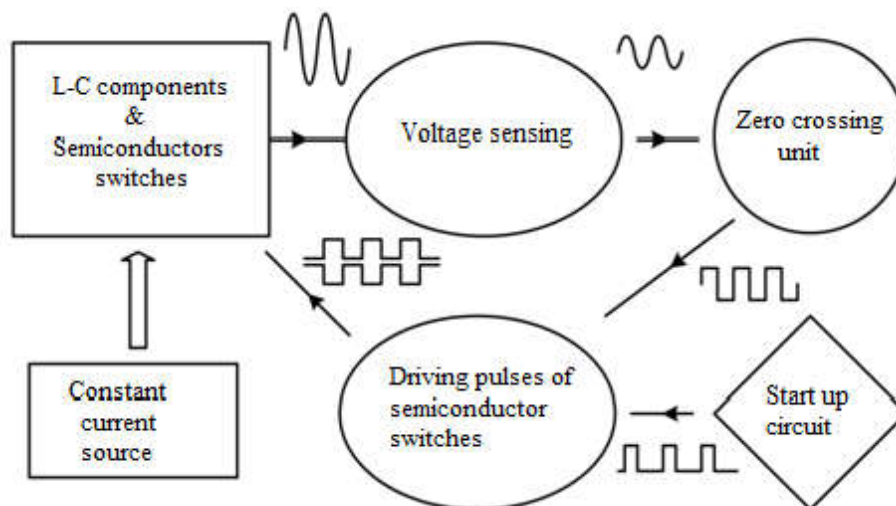
Figure 6.4: Block diagram of the inverter for high-frequency sinusoidal excitation of magnetic components.

with the intervention of the user (opening switch), changes mode and tunes the operation of

the power switches at the eigenfrequency of the resonant tank. The only input necessary for its operation is the inverter's output-voltage waveform. The block diagram of the overall system is in Fig. 6.4.

6.4. Design of the inverter

6.4.1. Control circuit

The control circuit of the inverter, shown in Fig. 6.5, was designed to provide both the device's startup operation and its control in steady state. For this reason, it can either operate as a closed loop, designed to feed the two power switches with complementary pulses, or feed them with triggering pulses that offer the necessary initial disturbance in the resonant tank for the start of the oscillation process. After a low amplitude ac voltage is achieved, the operation can be set to the closed-loop mode if the user opens the switch S1 in the start-up circuit.

The logic of the closed loop is to simply feed the MOSFET gates with 180° pulses (i.e. a semi-period long) that change value at each output voltage zero crossing (Fig. 6.6). In practice, this is done with a time delay t_d, which, for the inverter to function properly, must remain below $T/4$ (§6.6.3). The rising edge of such a pulse reaches the gate of a MOSFET at a time when the voltage on the MOSFET-diode series combination (i.e. the voltage at the corresponding node A or B) is negative. The switch will turn on as soon as the voltage on it becomes zero, tending to get positive values.

It is noted that in the following the time t_s, which is required for the transient turn-off effects of the switches, will be included in the time delay t_d. This interval time, from the withdrawal of the voltage pulse from the gate of a MOSFET to null drain current

172
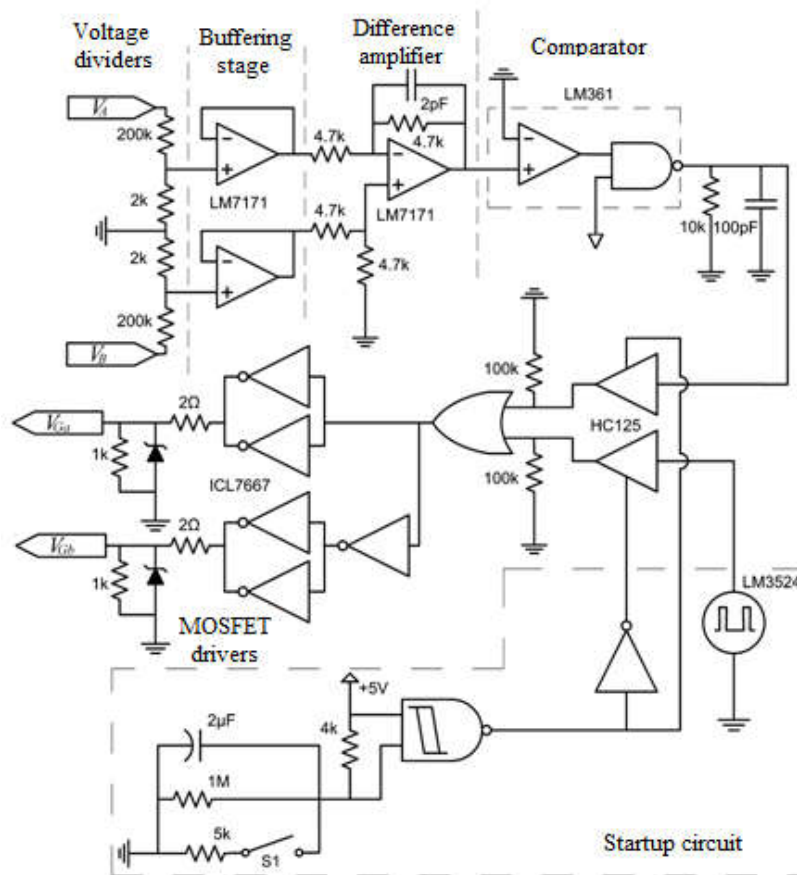
Figure 6.5: Control circuit of the inverter.

(only visible in the time scale of Fig. 6.6(b)), is typically equal to a few tens of ns and depends each time on the given semiconductor. Therefore, as t_d will be considered the time interval from the zero crossing of the output voltage V_o to the termination of the turn-off process of the corresponding semiconductor switch (Fig. 6.6(b)).

The reason that a separate triggering circuit (start up circuit) was built, based on the National Semiconductors integrated LM3524, suitable for PWM control, is that, depending on the losses encountered on the resonant inductors and the load, a disturbance caused by some other method (e.g., a capacitor discharge) can have such a low amplitude, or may decay so fast, that it is not possible to be detected by the control circuit. This is due to the dc offset of the buffering stages and the difference amplifier before the comparator (Fig.6.5).

These stages are fixed to give an acceptable output signal, less than ± 12V, when the supply is ± 15V (so that the on-chip transistors do not saturate), even for the maximum

values of the V_A and V_B voltages, which may be as much as the voltage rating of the MOSFETs (several hundreds of volts). This means that when the voltage $V_o=V_A-V_B$ is only a few volts, the output signals of the buffers to the difference amplifier, as well as the output signal of the difference amplifier to the comparator, have amplitudes comparable
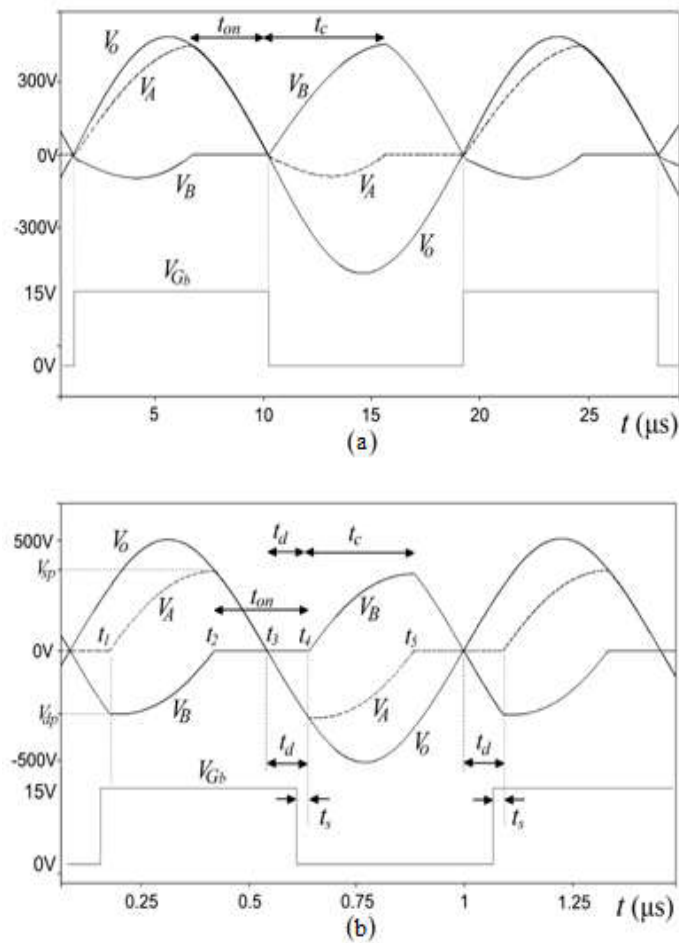
Figure 6.6: Voltages V_A, V_B, output voltage $V_o=V_A-V_B$ and the voltage V_{Gb} at the gate of the switch T_b, as shown by the simulation, for (a) negligible control board delay t_d and (b) non-negligible t_d.

with the output dc component of the integrated LM7171 (typical value 24mV). Eventually, the comparator's input signal may be either desynchronized with the control circuit input signal, or, for very small control circuit input signal, there may be no output at all from the

comparator due to the dc offset of the difference amplifier. With the IC LM3524 we can adjust the duty cycle and the frequency of the trigger pulses to ensure the start up of the inverter in any case.

Moreover, it is very useful if two of the four resistors in the difference amplifier resistor network are variable (trimmers). In this way and with the application of some test signals to the input, prior to the inverter's first operation (just once, at the final stage of the control circuit calibration), it is possible to minimize the output dc offset and the common mode rejection ratio (CMRR).

It is also important to note that the voltage dividers at the input of the control circuit must be properly calculated for the maximum expected voltage at the points A and B. Also, it helps a lot if the resistors for their implementation are mounted on the board, instead of soldered, so that they can be easily replaced if such necessity shows up, such as when applying the test signals mentioned above. It must be emphasized that the use of voltage dividers has two main advantages over the use of Hall voltage probes (LEM components): both the cost of the control board and its size are minimized. Of course, the use of simple voltage dividers is possible here because the topology does not require galvanic isolation between the two circuits (power and control) which have a common ground.

6.4.2. Resonant Tank

The output impedance Z_o of the inverter or, in other words, the impedance between nodes A and B at resonance is given by:

$$Z_o = \sqrt{\frac{2L_a}{(C_m + 0.5C_a)}} = \frac{1}{\omega(C_m + 0.5C_a)} = \omega 2L_a \tag{6.3}$$

with ω being the angular frequency ($\omega = 2\pi f$). If I_{res} is the resonating current, the inductors should be made such that they do not saturate at its peak value, which is:

$$I_{resp} = V_{op}/Z_o \tag{6.4}$$

The dc bias of $I_s/2$ at each inductor is, anyway, much lower compared to I_{resp}. Moreover, for the reasons mentioned earlier, the losses on the switches are practically negligible compared to those on the inductors. It is also important to remember that, with increasing frequency and

for a given current value, the amount of losses (copper and core) occurring in the inductors rises, with a dependence not linear with frequency.

One main issue for the designer to take care of is the construction of the proper inductor L_s that will guarantee a current in the resonant tank with no significant ripple throughout the frequency range that the inverter will operate. At high frequencies, the parasitic capacitances may short circuit the inductor, allowing a major high-frequency ripple of I_s (at the oscillation frequency in the resonant tank). Whereas for an improperly low L_s value, there will be a low frequency oscillation observed on the current I_s and, consequently, on V_{op}, a situation seen in the oscillogram of Fig. 6.7. This low frequency oscillation of V_{op} may be permanent or transient just when a change in I_s is attempted.

About the selection of the proper semiconductor switches and diodes, it may be said that, despite that, under specific conditions, V_{op} can be much higher than the peak voltages encountered at nodes A and B, these components should be selected with voltage ratings at least equal to V_{op}. The maximum difference between V_{op} and peak voltages in A and B occurs when we have a fast control board and low-loss resonant inductors (§6.8).
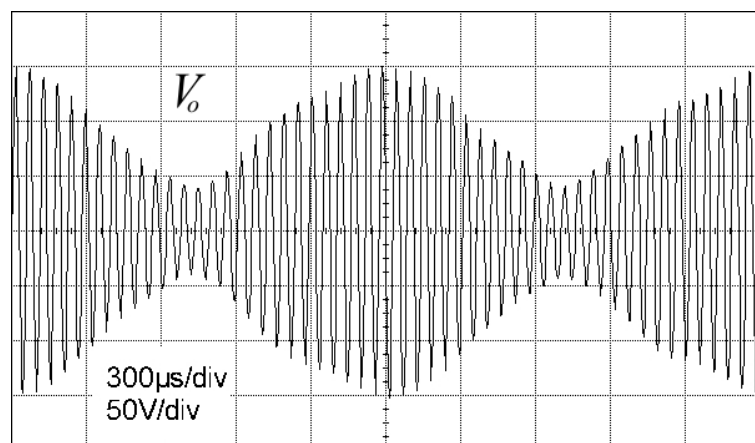
Figure 6.7: Low frequency oscillation, superimposed on the output voltage, when the value of L_s is not sufficiently high and therefore the current I_s cannot remain constant (oscillogram).

6.5. Output voltage quality

For the reliability of the measurements that are to be taken with the use of the inverter, it is a main concern that the output voltage should be harmonic free. Although the topology can be easily driven to offer an ac voltage, the achievement of a clearly sinusoidal waveform is not that simple and is a matter of taking into account several factors.

One issue to be investigated is the appropriate value for the ratio p of the main capacitor value to that of the auxiliary capacitor:

$$p=C_m/C_a \tag{6.5}$$

It is experimentally observed that, the higher the value of p the lower the harmonic distortion at V_o. To understand and illustrate this fact, a series of simulations were performed for various values of the parameter p. From the results of the simulations, Fig. 6.8 shows some waveforms that are relatively hard to record experimentally. The currents at node A are presented and it is clear that as p gets higher the disturbance at the current I_{Cm} of the main capacitor C_m, the voltage of which is the output voltage, is less prominent. Therefore a high value for p is desirable. However, it will be shown in §6.6 that p cannot take an infinitely high value.
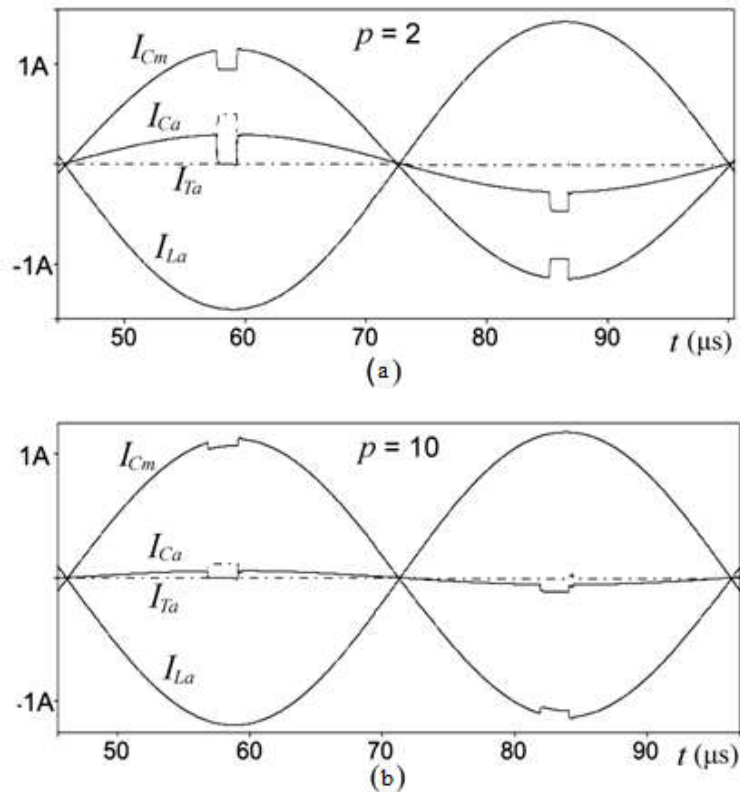
Figure 6.8: Simulated current waveforms at node A for (a) *p=2* and (b) *p=10*.

After several simulations and experimental tests, a choice of *p* between 10 and 20 proved to be satisfactory, to ensure that the sinusoidal oscillation in the resonant tank is maintained (§6.6) and that the output voltage harmonic content –to the extent that it depends on the value of parameter *p*– is acceptable.

The losses of the load and the resonant tank insert a damping factor, which, at a high value, can seriously distort the output voltage. To avoid this problem the inductors should be designed for minimum losses, even at the highest frequencies, and the load impedance Z_L should have a value that is quite higher than Z_o. Regarding the resistive character of the load, thorough experimental investigation indicated that, for a mainly inductive load, it is a fine choice if approximately $Z_L > 5Z_o$, whereas for a mainly resistive load, it has to be at least $Z_L > 15Z_o$. From the expression (6.2) we understand that in order to achieve a specific frequency we can choose from several possible $L_a - C_m$ combinations. Taking (6.3) into account, from the aforementioned discussion, it is evident that, as the resistive character of

the load rises, combinations with low L_a and high C_m are preferable. In Fig. 6.9 we see the output voltage oscillogram for purely resistive load with $R_L=10Z_o$, in which the deviation from the desired sine waveform is evident.

A combination of different capacitances C_a and C_b can seriously distort the output voltage. Such an asymmetry is imposed when, for example, a simple passive probe is used to
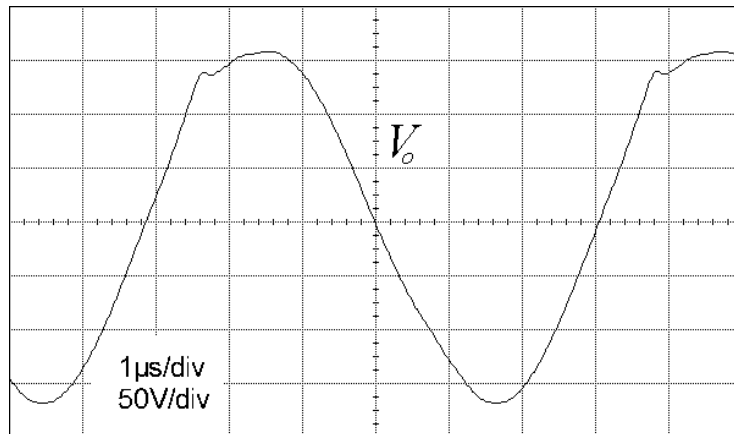
Figure 6.9: The output voltage for clearly resistive load $R_L=10Z_o$ (oscillogram).
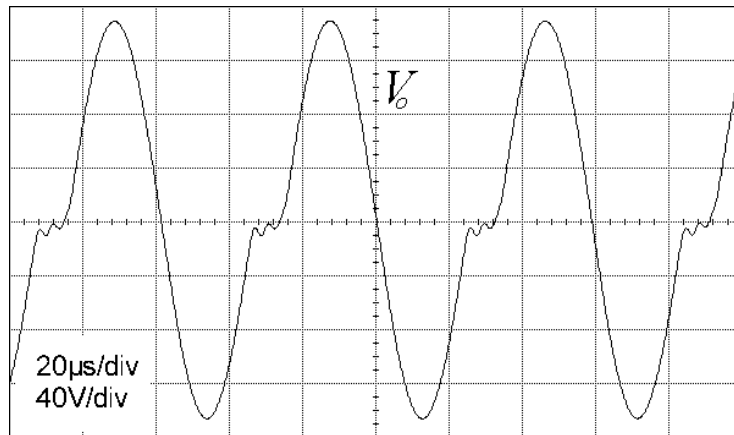
Figure 6.10: Distortion of output voltage due to the parasitic capacity when a passive voltage probe is used (oscillogram).

sense V_o, because its parasitic capacitance comes in parallel to one of C_a or C_b (Fig.6.10). This problem can be overcome if an active differential voltage probe is used.

Different response times of the control board for the rising and the falling edge of the output voltage do not affect the harmonic content of the output voltage (as long as it remains $t_d<T/4$ at both semi-periods, §6.6.3). In the control board designed for a prototype of the converter [162], [164] the comparator response times on the rising and falling edges of its input signal varied by approximately 200ns. In Fig. 6.11 we see the effect of this asymmetry on the voltages V_A and V_B, which shows that the two switches' conduction intervals are not equal due to the difference in the t_{da} and t_{db} delay times of the control circuit. However, in such a case, the amplitude of the current pulses remains equal in both switches (Fig. 6.12) and the only point of caution under these conditions is that the switch with the longer conduction time interval incurs excessive losses compared to the other one. The analysis that follows does not consider such a possible asymmetry. Therefore, it will be assumed that the period T consists of two equal t_{on} conduction intervals (one for each switch) and two equal intervals t_c during which both switches are off (see Fig. 6.6):

$$T=2t_c+2t_{on} \tag{6.6}$$
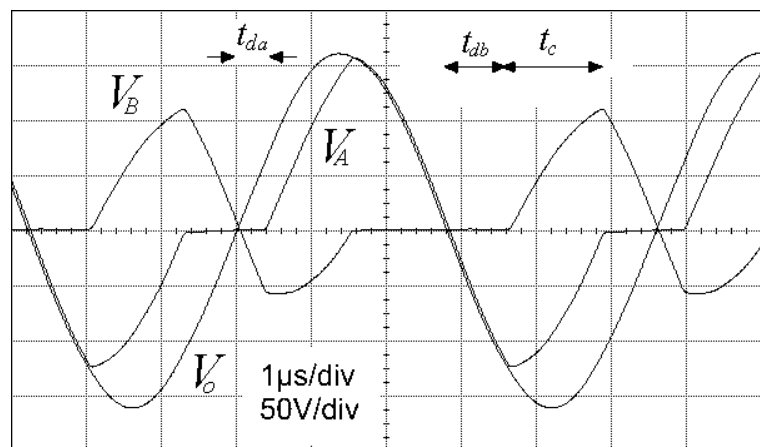
Figure 6.11: Voltages V_A, V_B and V_o with asymmetric operation of the control circuit (oscillogram).
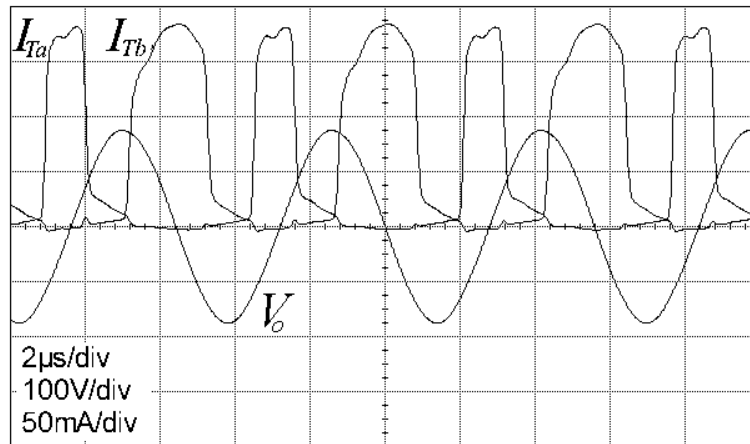
Figure 6.12: Output voltage and current pulses in the semiconductor switches, with asymmetric operation of the control circuit (oscillogram).

6.6. Theoretical and experimental analysis of the inverter operation

6.6.1. General issues

Some power electronic applications, e.g. resonant converters, have started to extend into operating frequencies from several hundreds of kHz up to a few MHz (§3.3.3). For this reason, it would be quite helpful for making test measurements to have an excitation source, like the one presented, operating at these frequencies. In the following, there is an investigation of the limitations of the presented inverter, related to fundamental constructive parameters, so as to reveal the way to extend its operation to a frequency range as wide as possible, while maintaining the output voltage quality within acceptable limits.

We define the time from the zero crossing of V_o to the turn-off of the corresponding switch (switch T_b) as $t_d=t_4-t_3$ and the following time interval, when both switches are off and C_a is charged back to zero voltage, as $t_c=t_5-t_4$ (Fig. 6.6(b)). By examining the charge balance in C_a (since $C_a=C_b$ nothing would change in the analysis if C_b was examined) and by assuming ideal components (inductors and capacitors) and a clearly resistive load R_L, it follows that [23]:

$$\frac{C_a}{2}\sin 2k\pi = \frac{\pi}{4fR_L}\cdot\frac{\lambda}{1-2\lambda} - \frac{C_a}{2}\sin 2\pi(k+\lambda) \qquad (6.7)$$

where, in order to facilitate the analysis, the following symbols have been used:

$$k=t_d/T, \qquad \lambda=t_c/T \tag{6.8}$$

Expression (6.7) takes into account the dc current I_s entering the resonant tank [23]. Although, for the derivation of (6.7), ideal components and a clearly resistive load were assumed, this condition is not a restraint in the analysis that follows, as will be explained in the next paragraph. With (6.7) as the starting point, we will get some useful results.

6.6.2. The case of negligible delay in the control circuit response

In this paragraph is the investigation of the constructive limitations of the proposed inverter in the case when the response time t_d of the control circuit is a negligible fraction of the resonance period T. As will be shown in the following paragraph, this case corresponds to operating frequencies relatively low compared to the maximum operating frequency boundary of the control circuit.

For an open output operation (no-load) and a non-zero frequency, the coils give the main loss factor in the resonant tank and it is true that for any non-zero frequency each of them can be represented with an impedance ωL_a in parallel to a resistance R_{La} (Appendix V), where of course this resistance represents the total losses in the coil (copper and core losses). Studying the resonant current (we ignore the comparatively low current I_s), the two resistances R_{La} and R_{Lb} at the two resonant inductors carry the same current component (we assume inductors with identical characteristics, i.e., $R_{La}=R_{Lb}$ and $L_a=L_b$), and since we are concerned for the open-circuit operation, the sum $R_{La}+R_{Lb}$, which is equal to $2R_{La}$, can take the place of the load resistance R_L in the previous analysis (Fig.6.13):

$$R_L=2R_{La} \tag{6.9}$$
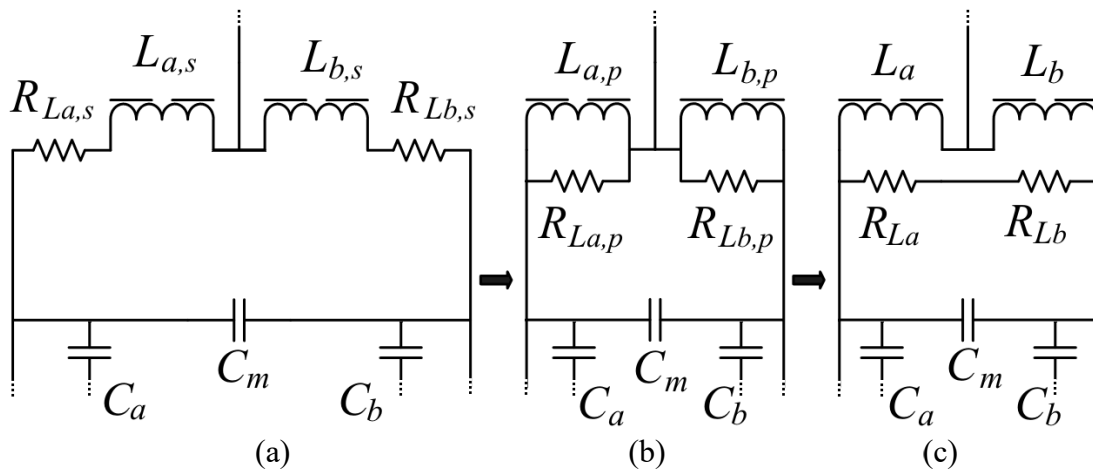
Figure 6.13: The resonant tank with no load connected. Since the two resonant inductors are identical, in the analysis the sum of their equivalent parallel resistances $R_{La,p}+R_{Lb,p}=R_{La}+R_{Lb}=2R_{La}$ can take the place of the load resistance R_L, which is parallel to the main capacitor C_m. In the above conversion it is $R_{La,p}=R_{La}$, $R_{Lb,p}=R_{Lb}$ and $L_{a,p}=L_a$, $L_{b,p}=L_b$ and it is also assumed that $L_{a,s}=L_{a,p}$ and $L_{b,s}=L_{b,p}$ (Appendix V).

If we name g the ratio of the resistance R_{La} of a resonant inductor to its inductive reactance:

$$g=R_{La}/\omega L_a \tag{6.10}$$

(6.9) can be rewritten as follows:

$$R_L = g\omega 2L_a \tag{6.11}$$

It is important to remember that, with increasing frequency, the core and copper losses of a given inductor increase, leading to a drop in g. At resonance, it is (also see (6.3)):

$$\omega 2L_a = \frac{1}{\omega(C_m + 0.5C_a)} \tag{6.12}$$

and given now that the condition $p>>1$ is applied for minimum output-voltage distortion, it follows from (6.12) that:

$$\omega 2L_a \cong \frac{1}{\omega C_m} \tag{6.13}$$

and (6.10) becomes:

$$R_L \cong g\,\frac{1}{\omega C_m} = g\,\frac{T}{2\pi C_m} \tag{6.14}$$

Since t_c is the time interval when none of the switches is in conduction state (Fig. 6.6), the necessary condition to have an oscillation, with the obvious limitation that $D<0.5$ (also see (6.6)), is the existence of an even small interval t_c (it is reminded that it can never be $D=0.5$ due to the capacitors C_a and C_b [23]). This condition can be expressed as:

$$\lambda > 0 \tag{6.15}$$

However, in both experimental observations and simulation results, output-voltage harmonic distortion is clearly apparent at operation with $\lambda<0.04$ due to the high loading (low R_L values) that generally corresponds to this case. Thus, the condition $\lambda>0.04$ ensures an oscillation with an output voltage of low harmonic content, and therefore, the previous condition for securing sinusoidal oscillation in the resonant tank is modified as follows:

$$\lambda > h = 0.04 \tag{6.16}$$

In a case when k can be considered very low compared to λ, even when λ takes low values of the order of h, we may approximate:

$$k \cong 0 \qquad \text{and} \qquad k + \lambda \cong \lambda \tag{6.17}$$

If we substitute (6.5), (6.14) and (6.17) in (6.7) we get:

$$\frac{p}{g} = \frac{1}{\pi^2} \cdot \frac{1-2\lambda}{\lambda} \sin 2\lambda\pi \qquad\qquad 0.04 < \lambda < 0.5 \tag{6.18}$$

The condition $\lambda<0.5$ follows directly from (6.6) (also see (6.20)). Studying (6.18), we are interested in the value of the ratio p/g at the limit where λ approaches zero, which is:

$$\lim_{\lambda \to 0}\left(\frac{p}{g}\right) = \frac{2}{\pi} = 0.637 \tag{6.19}$$

This value can also be read in Fig.6.14, which shows the graphical representation of (6.18), as the intersection of the extension of the graph curve with the p/g axis. At the same figure, the simulation results are presented, giving a corresponding value of approximately 0.70 and the measurements on the inverter giving an approximate value of 0.80. If we set h as the minimum acceptable value for λ, the corresponding marginal p/g values are a bit lower (e.g. from the theoretical curve representing (6.18) the approximate value is about 0.59). From the technical point of view, the case where t_d can be considered negligible refers to a frequency
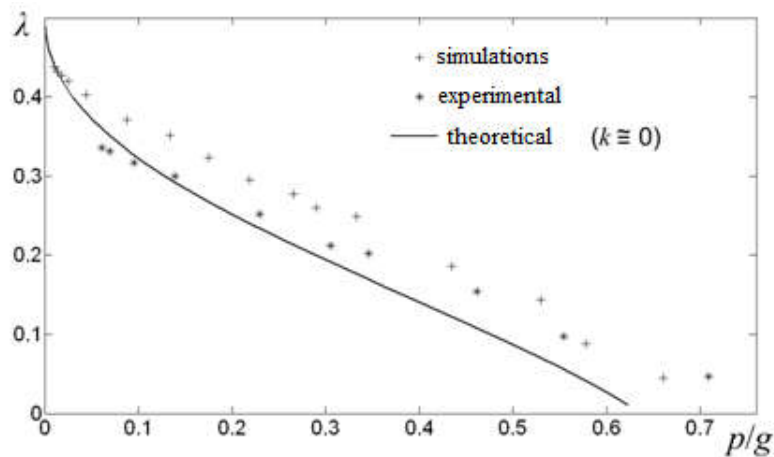
Figure 6.14: Graphical representation of (6.18), experimental investigation, and simulation results.

that is very low in comparison to the maximum frequency that the control board can handle (§6.6.3).Thus, the information given in Fig. 6.14 actually indicates the worst permissible design choices for the resonant tank at relatively low and intermediate frequencies, and the value $p/g=0.637$ should be kept as the most appropriate maximum limit to ensure the sinusoidal oscillation. This result stresses the importance of designing low-loss resonant inductors (with high g value), but also puts a technical restraint on the maximum value of p.

6.6.3. The case of non-negligible delay in the control circuit response

As the operating frequency of the inverter rises, the control board response delay t_d becomes a considerable fraction of the resonance period T. In this paragraph, we investigate the manufacturing constraints of the proposed inverter in this frequency range.

From (6.6) it comes that:

$$\lambda + D = 0.5 \tag{6.20}$$

From (6.7) and (6.20), it comes that with all other parameters kept constant, when R_L rises, as a result, λ rises and D drops. For $R_L \to \infty$ (i.e. for ideal inductors with $g \to \infty$ when we analyze the open-circuit operation) it should be $\lambda \to 0.5$ and $D \to 0$. However, (6.7) was derived in [23] with basic assumption that the power $V_s I_s$ offered by the dc voltage supply is equal to the power V_o^2/R_L delivered on the resistive load. This consideration does not take into account the various non-idealities in the resonant tank (further than the inductor losses that we have included in the R_L value) or on the semiconductor switches. If these non-idealities are taken into consideration the following inequality must be valid:

$$\frac{\pi}{4fR_L} \cdot \frac{\lambda}{1-2\lambda} - \frac{C_a}{2}\sin 2\pi(k+\lambda) > \frac{C_a}{2}\sin 2k\pi \tag{6.21}$$

The condition expressed by (6.21) gets important when p/g drops and puts a restraint on the minimum value of D when $p/g \to 0$. If (6.14) and (6.20) are substituted in (6.7) we get the expression:

$$\frac{p}{g} = \frac{2}{\pi^2}\frac{2D}{1-2D}\sin[\pi(0.5+2k-D)]\cos[\pi(0.5-D)] \tag{6.22}$$

Figure 6.15 contains the plot of (6.22), giving the duty cycle D of the switches as a function of the ratio p/g (D curves), with k as parameter.
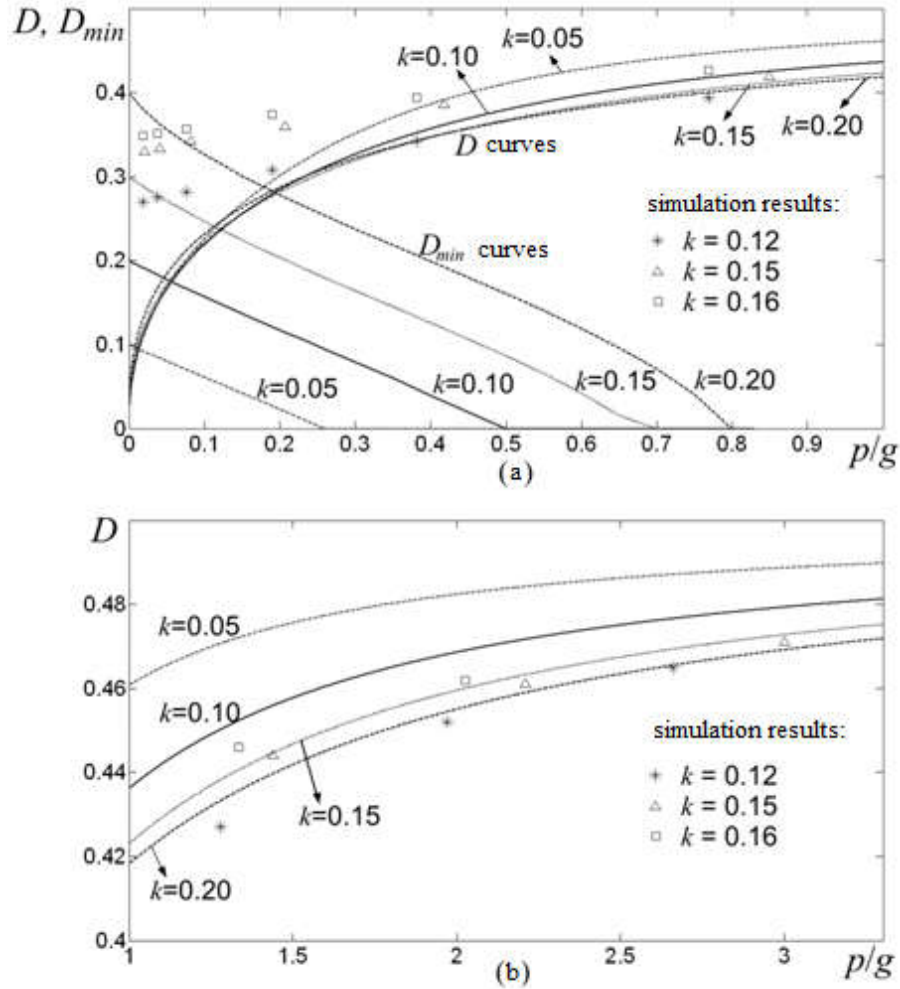
Figure 6.15: Graphical illustration of (6.21) (D_{min} curves) and (6.22) (D curves) and simulation results, with k as a parameter, for (a) $0<p/g<1$ and (b) $1<p/g<3.3$. The region above a D_{min} curve is the region of validity of (6.21).

In Figure 6.15(a) are also plotted the D_{min} curves, that illustrate inequality (6.21), with k as parameter (the same k values as for the D curves) and in which, for a given k, (6.21) is valid at the region of the graph that extends above the corresponding D_{min} curve. At last, in the same figure are the simulation results for k equal with 0.12, 0.15 and 0.16. The simulations for $k=0.12$ and $k=0.16$ are with $p=20$ and those for $k=0.15$ with $p=15$. It can be seen that, at high p/g values (6.22) is valid. In the low p/g range, where the non-idealities of the power part of the inverter get important, (6.21) prevails, and for $p/g \rightarrow 0$, the duty cycle D is a bit higher than $2k$.

187

Another conclusion from the previous discussion is that, for $k \to 0.25$ it is $D \to 0.5$, independently from the specific p/g value (even for $p/g \to 0$). Hence, the following condition expresses the maximum frequency limit that a control board can handle:

$$k < 0.25 \tag{6.23}$$

As an example, with a control board characterized by a response delay $t_d = 0.25\mu s$, the maximum attainable operating frequency can be 1MHz, while if $t_d = 0.5\mu s$ the corresponding frequency is 500kHz. As already mentioned, due to the capacitors C_a and C_b, it can never be $\lambda = 0$ and if operation at a frequency with $k > 0.25$ is attempted, as it has also been experimentally verified, the operation of the inverter continues with $f_s < f_{res}$ and a highly distorted output voltage waveform.

At the high-frequency range of the inverter operation, which is our concern here, we accept that there is an appreciable time delay t_d. Moreover, in search of the limit when $\lambda \to h$ we also assume that $\lambda << k$. Under these conditions, the following approximations are valid:

$$k + \lambda \cong k \tag{6.24a}$$
$$1 - 2\lambda \cong 1 \tag{6.24b}$$

If (6.24a) and (6.24b) are substituted in (6.7), we get the following approximate solution for t_c:

$$t_c = \frac{4R_L}{\pi} C_a \sin 2k\pi \tag{6.25}$$

And if we substitute (6.5) and (6.14) in (6.25) we get the expression:

$$\lambda = \frac{2}{\pi^2} \cdot \frac{\sin 2k\pi}{(p/g)} \tag{6.26}$$

In this way, the necessary condition (6.16) for a sinusoidal oscillation to exist becomes:

$$\lambda = \frac{2}{\pi^2} \cdot \frac{\sin 2k\pi}{(p/g)} > h \tag{6.27}$$

The expression (6.26) and the corresponding inequality (6.27) indicate the maximum operating frequency of the inverter in the case of a non-negligible delay t_d of the control circuit, as defined by the constructive parameters g, p and k. At frequencies for which t_d is not negligible the operation of the inverter is limited by (6.23), which is a necessary condition in any case, otherwise it is limited by (6.27). That is, if the inequality (6.23), which is related solely to parameter k, is satisfied, then the three construction parameters p, k and g must satisfy the condition expressed by (6.27) in order to have a sinusoidal oscillation.

Taking into account the above discussion, we may now conclude that (6.27) implies a limitation at the rise of the value for p, (for which we want a value as high as possible), always dependent on the values of the parameters g and k. It also indicates that, for the achievement of higher frequencies, it is not enough just to have a faster control board (so that (6.23) is satisfied), but also a lower loss resonant tank i.e., carefully designed resonant inductors with high g value even at the targeted high frequencies.

As a primary verification of (6.26), a set of simulations was carried out for k=0.10. The ratio p/g is varied by varying both p and g, and λ is recorded.
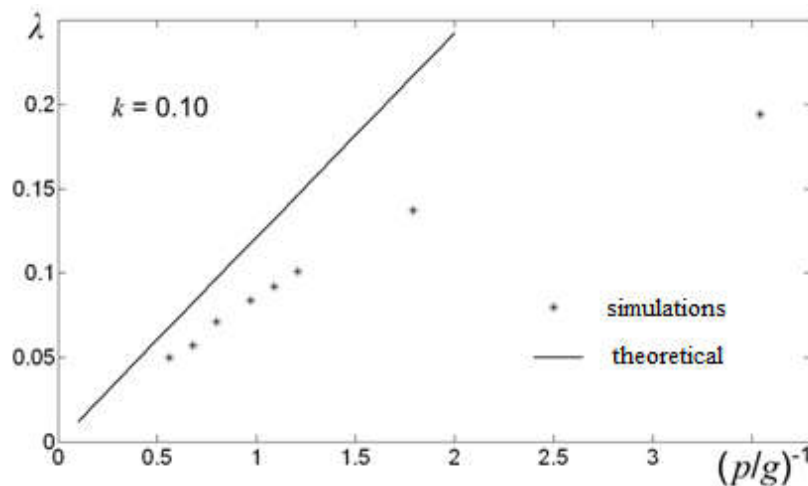
Figure 6.16: Theoretical (eq. 6.26) and simulated variations of the ratio $\lambda=t_d/T$ versus $(p/g)^{-1}$ for k=0.10. Convergence is observed, as expected, for low λ values.

The graph of (6.26) for this k value and the simulation results are shown in Fig. 6.16. It is clear that, as λ approaches the values for which (6.26) was derived ($\lambda \ll k$), the formula and the simulations converge.

Further than this computer-aided verification of (6.26), it was necessary to proceed with some experimental support of its validity. The final improved control board, presented in details in §6.4.1 (Fig. 6.5), in contrast with the original design mentioned above, operates in a perfectly symmetrical manner, thus allowing the experimental verification of (6.26). The method for taking measurements is based on varying parameter p by changing, for constant C_m, the value of C_a. Time t_c is measured on the oscilloscope. From (6.2), it is evident that the frequency remains in a restricted range even for major changes in C_a, as long as it is $C_m \gg C_a$, and thus, since the frequency varies only slightly, parameter g varies only slightly too.

The value of g is determined by measuring the total power consumption in the resonant tank (i.e. in the resonant inductors) as $P_{tot} = \langle V_o \cdot I_{res} \rangle$ and assuming that the L_a inductance, when the resonant inductor is represented as an inductance parallel with a resistor, is the same as in the series representation ($L_{a,p} = L_{a,s} = L_a$, see Appendix V), which was measured using a bridge (details on the method of measuring power consumption can be found in Ch. 7). This latter assumption generally applies to inductors with a sufficiently high value for g. For the inductors used in the specific experiment, g ranged between 4 and 4.5 at the frequencies of measurement (about 250kHz). Given P_{tot}, I_{res}, ω and L_a, we can easily determine $R_L = R_{La}$ and hence g can be determined from (6.11).

Parameter k can be adjusted by connecting some proper value resistors in series with the MOSFET driver output. For the maximum 60Ω of this resistor, a total delay $t_d = 550$ns was achieved. In this experiment the intention was to keep parameter k as low as possible.

In the graph of Fig. 6.17, the points correspond to measurements for k values between 0.118 and 0.135. This is because, as C_a varies, for a given delay t_d, the correlative slight variation of frequency results to slightly different k values, despite any compensatory action with changes in the value of the resistance at the MOSFET driver outputs. A comparison between measurements and the graph of (6.26) shows the convergence of the two for low λ values, the range for which the formula was derived.

It has to be reminded at this point that all the aforementioned analysis refers to the open output case. If a load is connected to the output, the analysis is still valid if the actual value of

g is introduced in the equations. In this case, g is a function of the resonant inductor impedance and of the load impedance too. In the same way, the actual value of p has to be
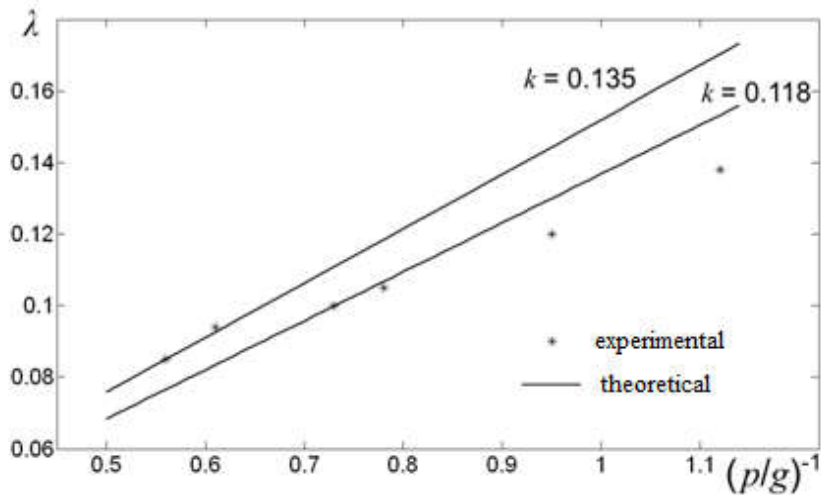
Figure 6.17: Experimental validation of (6.26) that describes the converter's operation for non-negligible control delay t_d at low λ values.

taken into account if the load shows some capacitive character.

Closing this section, we may review the extracted conclusions as follows:

(a) The maximum frequency that the control board can handle is $f_{max}=1/4t_d$, where t_d is the sum of the time delay in the response of the logic part plus the time necessary for the turn-off of the switches.

(b) At low and intermediate operating frequencies (much lower than f_{max}), where t_d can be considered negligible, the operation of the inverter is limited by the condition $p/g<0.637$.

(c) At high frequencies (comparable to f_{max}), given that (6.23) is valid, inequality (6.27) must be satisfied for a sinusoidal oscillation to be possible.

(d) In both cases (b) and (c) the imposed conditions put restraints on the maximum permissible value of parameter p (which otherwise must be as high as possible for minimum output-voltage distortion). They also, indicate the necessity to have a low-loss resonant tank and a fast control board to ensure both the maintenance of a

sinusoidal oscillation and the achievement of the highest possible operating frequencies.

6.7. Optimization of the inverter construction

Having had investigated all the factors that affect the quality of the output voltage and the upper frequency limit of the inverter, the control circuit presented in §6.4.1 (Fig. 6.5) was designed. The investigation of these factors heavily relied on experimental observations on a prototype inverter [162], [164]. The improved electronic circuit has a faster response (compared to that used in the prototype inverter) and components of improved features were selected for the power part in order to extend the frequency range of the inverter further than the 250kHz limit of the prototype, with the output voltage being kept as high as possible at the same time.

Resonant inductors were constructed for high voltage and high frequency operation. The ferrite grade Ferroxcube 3F4 was used, suitable for frequencies even higher than 1MHz. Inductor coils were formed with bunched wire of 0.20mm diameter strands, extra insulated along its full length, since the low number of turns on each inductor ensured a high voltage among adjacent turns.

The improved inverter control circuit (Fig. 6.5) was designed to be simpler and faster than the original by incorporating fewer and faster components. All the ICs in the analog zero crossing detection part, i.e. the operational amplifiers for the implementation of the buffering and the difference amplification stages, as well as the comparator, have been replaced with faster ones. The buffering stage originally connected after the difference amplifier [162], [164] has been completely eliminated. It should be noted that, as the input signals (V_A and V_B voltages) are sinusoidal functions of time, the critical information for selecting the appropriate op-ams in the buffering and amplification stages is in the examined IC's amplitude-phase diagram (Bode diagram) and not in the pulse response also given in the data sheet.

In the digital part that follows, fewer gates have been used to implement the logic of complementary pulses. The total time delay t_d from output voltage zero crossing to the MOSFETs turnoff dropped to about 100ns, from about 500ns in the prototype, making it –theoretically– suitable for frequencies up to 2.5MHz, in accordance with what was

mentioned in §6.6.3. However, the power consumption of the MOSFET drive circuits used (ICL7667) has put a barrier to the uninterruptible operation frequency at 1MHz. Frequencies greater than 1MHz, up to about 1.5MHz, were only possible for short periods of time before the MOSFET drivers overheat and the operation had to be terminated. Note that an improvised forced convection heat sink was used to cool the drivers. Increasing the resistance in series with the output of the MOSFET drivers has only a low effect on limiting the temperature rise of these ICs, as there is also a significant power consumption at their input stage. Moreover, increasing this resistance increases the overall delay t_d, canceling this way the original intention, i.e. the construction of a fast control board. In a future redesign of the control circuit, one possible solution for driving the MOSFETs at such high frequencies (further than the search for a suitable IC) may be the incorporation of resonant drive circuits, as described in [139].

Given the extremely high frequency of operation of the inverter, great attention should be paid to electromagnetic noise and ripple issues in the supply voltages of the logic circuit. Two are the main concerns of the designer:

a) The paths of the currents in the resonant tank should be as short as possible and the power circuit should be sufficiently distant from the control board. Proper space arrangement of the resonant inductors is important as the large current in them and the existence of a gap in the outer legs of their cores contribute to the existence of a large electromagnetic emission from them to any adjacent circuits.

b) The pulse current paths in the control circuit must be of minimum length to avoid as much as possible ripples in the supply voltages due to the self-inductance of the above paths. Such significant currents are those from the drivers to the MOSFET gates.

Given that we want to avoid the creation of a separate supply unit for the MOSFET drivers, which this way could be positioned near the semiconductors, away from the rest of the control circuit, it is understood that the latter requirement runs counter to that for maintaining a sufficient distance between the power and control circuits. What we eventually do is to choose a middle ground solution (in the device developed this distance was about 5cm) by making sure that there are both electrolytic and polyester (MKT) or polypropylene (MKP) bypass capacitors installed right next to the MOSFET drivers.

In the case of the device developed there was no need for electromagnetic shielding of the resonant inductors. However, care has been taken that the current paths, in both circuits, control and power, do not create loops and also that opposite currents are in spatial proximity, thereby severely limiting the creation of unwanted magnetic fields (EMI).

At 1.04MHz, the rms output voltage and the rms resonant current did not exceed 450V and 1A, respectively, due to overheating of the inductors. In accordance with the analysis presented in §6.5 the rms current at some mainly inductive loads tested did not exceed 0.3A. In Fig. 6.18 we see the waveforms of the V_o and V_A voltages at this frequency and in Fig. 6.19 the Fourier spectrum of V_o. From the study of the spectrum of V_o, it comes that the 3rd harmonic component, is kept at –50dB below the fundamental, i.e., less than 0.5% of it.
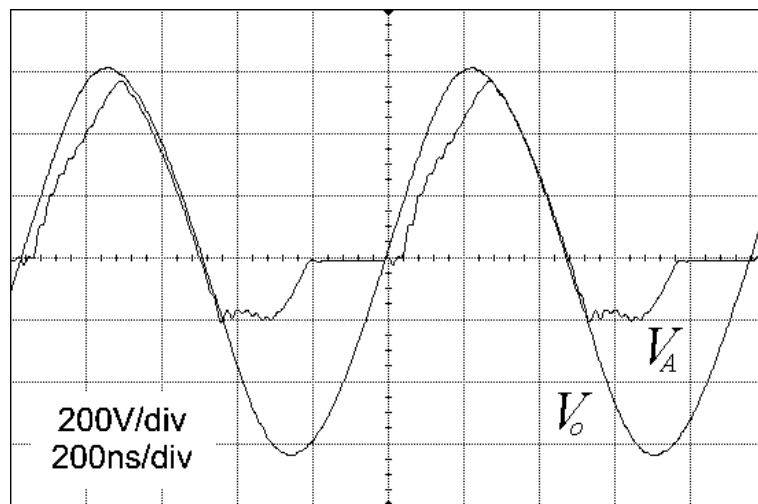
Figure 6.18: Oscillogram of V_A and output-voltage V_o of the inverter at 1.04MHz.
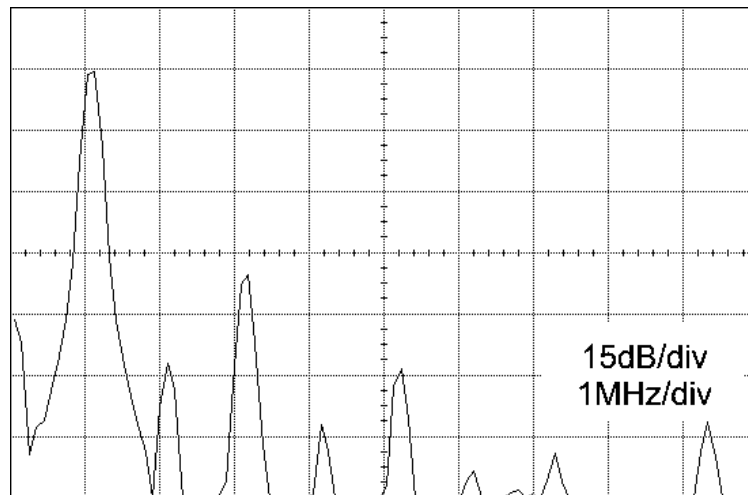
Figure 6.19: Fourier's spectrum of the output voltage at 1.04 MHz operating frequency.

6.8. Maximizing the output voltage of the inverter

In this paragraph, it is shown that the peak output voltage of the presented inverter, under specific conditions, can be up to $\sqrt{2}$ times the voltage rating of the semiconductor switches in the power part and that, in the general case, the MOSFET switches incur higher cut-off voltages than the diodes.

After a T_b conduction time interval, at the time interval (t_4, t_5) (Fig. 6.6), when both switches are off (it is $t_5-t_4=t_c$), the series connection of C_a and C_b (Fig. 6.3) is under V_o voltage. In the general case, it holds true that:

$$\frac{C_a}{2}\frac{dV_o}{dt} >> \frac{I_s}{2} \tag{6.28}$$

Hence, in order to investigate the form of the voltages at the nodes A and B we may neglect the effect of the dc current I_s entering the resonant tank and consider a sinusoidal oscillation of the relevant voltages and currents. Under this scope, it is:

$$V_B(t)=V_{pp}\sin\omega(t-t_4) \qquad \text{and} \qquad V_A(t)=V_{pn}\sin\omega[t-(t_5-T)] \tag{6.29}$$

The values V_{pp} and V_{pn} result from the solution of the following equations (also see Fig. 6.6):

$$V_B(t=t_5) = V_{op}\sin 2\pi(k+\lambda) \tag{6.30a}$$
$$V_A(t=t_4) = -V_{op}\sin 2k\pi \tag{6.30b}$$

and finally it is:

$$V_{pp} = V_{op}\frac{\sin 2\pi(k+\lambda)}{\sin 2\lambda\pi} \tag{6.31a}$$

$$V_{pn} = V_{op}\frac{\sin 2k\pi}{\sin 2\lambda\pi} \tag{6.31b}$$

According to the analysis presented in §6.6.3 the condition $k=D/2$ can only be marginally valid for a power circuit with nearly ideal components and when $p/g \to 0$. In the general case, it is:

$$k<D/2 \Leftrightarrow \lambda<0.5-2k \tag{6.32}$$

If V_{sp} and V_{dp} are the peak cut-off voltages encountered on the switches and on the diodes respectively, we have to consider three different cases:

One is when:

$$k+\lambda>1/4 \quad \text{and} \quad 0<\lambda<1/4 \tag{6.33}$$

$$V_{sp}=V_{op}\sin2\pi(k+\lambda), \qquad V_{dp}=V_{op}\sin2\pi k \tag{6.34}$$

the second case is when:

$$k+\lambda>1/4 \quad \text{and} \quad 1/4<\lambda<1/2 \tag{6.35}$$

$$V_{sp}=V_{pp}, \quad V_{dp}=V_{pn} \tag{6.36}$$

and the third one is when:

$$k+\lambda<1/4 \tag{6.37}$$

$$V_{sp}=V_{op} \quad \text{and} \quad V_{dp}=V_{op}\sin2\pi k \tag{6.38}$$

If we also take into account (6.20) and (6.32), we may easily conclude that, in any of the above cases, it will be:

$$\sin2\pi(k+\lambda)>\sin2k\pi \tag{6.39}$$

and, therefore, it is always $V_{sp}>V_{dp}$.

From the practical point of view, the most interesting case is when V_{sp} gets minimum i.e., quite lower than V_{op}, because this means that a maximum output voltage is attainable within the given voltage rating of the MOSFET switches.

When (6.37) is valid, it generally means that there is a high-loss resonant tank (low R_L values; it is reminded that $R_L=2R_{L\alpha}$ expresses the losses in the inductors if we refer to the open circuit operation) or/and a slow control circuit (high k values). It is $V_{sp}=V_{op}$, and the only way to overcome the limitation imposed by the voltage rating of the switches (and fall

into one of the previous two cases expressed by (6.33) or (6.35)) is to design lower loss inductors <u>and</u> reduce the response time of the control board.

The condition expressed by (6.33) corresponds to a general case with a slow control board, regardless of the specific value of R_L, which may be even high (well-designed low-loss inductors, if we refer to the open output operation). For a reduction of V_{sp} the sum $k+\lambda$ must rise. From the analysis presented in §6.6.3, it is evident that a rise of R_L will only have a restricted effect in the direction of increasing λ. Hence, the main requirement in order to rise the sum $k+\lambda$ is to reduce k by designing a faster control circuit and, further than that, if possible, to also reduce the losses in the resonant tank. Note that, in such a case, a drop of k by Δk would lead to an approximate rise of λ by $2\Delta k$ hence, the sum $k+\lambda$ would rise by about Δk.

At last, (6.35) corresponds to the general case of a quite fast control circuit with low loading at the resonant tank, (i.e., with well-designed inductors at the specific frequency, if we study the open output operation) and V_{sp} is normally well below V_{op}. The maximum V_{sp} cut-off voltage on the MOSFET gets minimum when $k \to 0$ and $R_L \to \infty$.

Note that, given that (6.32) is always valid, in the previous discussion, the maximum possible value for the ratio V_{op}/V_{sp} is $\sqrt{2}$, and that, for given p, any change in the value of R_L is reflected to an inversely proportional change in the value of the ratio p/g.

CHAPTER 7

ISSUES RELATED TO MEASUREMENTS ON MAGNETIC COMPONENTS

7.1. Introduction

At several points in the previous chapters we saw the importance of the experiment in order to confirm a theoretical study or to determine the values of various useful parameters necessary for the application of a theory or method. Following, in this chapter, we will discuss some of the ways in which experimental measurements can be made on magnetic components, as well as a few minute points about this object that need special attention.

When referring to magnetic components, some of the most fundamental issues to which the experiment is called upon to answer are the determination of the copper losses P_{Cu} and the core losses P_{Fe} separately or that of the total losses P_{tot}. In some cases it may be desirable to separate between the specific hysteresis losses $P_{v,hyst}$ and the eddy current losses $P_{v,eddy}$ in the core. Furthermore, the application of some models or methodologies often requires knowledge of some of the ferrite manufacturing parameters, which are not available in the manufacturers' data sheets and therefore need to be derived experimentally. As an example, we mention the various parameters in the hysteresis models (Ch. 2), the thermal resistance R_{th} of a magnetic component (Appendix II) etc. In the following, the parasitic capacitance of the winding will be considered negligible, an approach which is practically correct when the magnetic component has been carefully assembled and when the harmonic content of the current at frequencies corresponding to high order harmonics is also negligible. We start this study with the issue of power loss calculation in a circuit by recording the voltage and current waveforms.

7.2. Determination of the total power loss

7.2.1. General issues

The total power P_{tot} dissipated in a magnetic component is given by:

$$P_{tot} = \frac{1}{T} \int_0^T i_p(t) \cdot v_p(t) \mathrm{d}t \tag{7.1}$$

where $i_p(t)$ and $v_p(t)$ are the current and the voltage in the primary excitation winding, while T is the period of the excitation signal. In cases where technical difficulties prevent direct measurement of v_p, it can be assumed that the voltage $v_s(t)$ in a properly positioned secondary winding is the same (same form and same phase) as that of the primary with a transformation ratio N_s/N_p and thus (7.1) becomes:

$$P_{tot} = \frac{N_p}{N_s} \cdot \frac{1}{T} \int_0^T i_p(t) \cdot v_s(t) \mathrm{d}t = \frac{N_p}{N_s R_m} \cdot \frac{1}{T} \int_0^T v_R(t) \cdot v_s(t) \mathrm{d}t \tag{7.2}$$

where $v_R(t)$ is the voltage on a resistor R_m in series with the primary winding, while the secondary winding is only used to measure the induced voltage v_s (with a practically negligible current) [57]. However, in cases where the core is not excited with sinusoidal waveforms, it is advisable to avoid the use of (7.2), since the magnetic component acts as a frequency filter and the induced voltage waveform appears distorted with respect to the primary voltage. The same is true –in part– even for sinusoidal waveforms, since there is always a distortion due to the nonlinearity of the hysteresis curve, although this nonlinearity can generally be ignored if there is a gap in the core of the magnetic component. Moreover, the approximations made when using (7.2) deviate from the actual conditions when there is another secondary current carrying winding. For a loaded transformer, in order to determine the losses, the input and output active power must be determined and subtracted. Hence, it is more appropriate to separately record $v_p(t)$ to determine the total losses. In any case, after all the preparatory steps have been made, the measurements should be taken within a short time so that the temperature of the magnetic component does not increase significantly, unless it is of our interest to study it at a particular temperature, when it has come in thermal equilibrium with its ambient surroundings. It is reminded that losses in both the core and the winding

vary with temperature. The dependence of copper losses on temperature is an issue discussed in §7.4.

It should be mentioned, however, that even today, calorimetric devices are considered to be the most accurate in determining the total loss dissipated on a magnetic component [28], [115], [118], [169]. In such a device, the magnetic component in question is immersed in the flow of a fluid of given heat capacity inside a thermally insulated tube. The losses are calculated if the fluid flow rate and the fluid temperature increase at the tube exit relative to that at the tube entrance are known quantities. However, this method has almost been abandoned as it presents many technical difficulties. The sample size for example is a critical quantity, since typical calorimetric setups are not usually available in any large size, nor is it simple to make some corresponding improvised setups. The special insulating oil to be used as a calorimetric fluid is also a material not always readily available. Especially for high frequency measurements, another issue that needs to be addressed is the precise knowledge of the effect of the sample connecting terminals on the excitation device, as these will inevitably be relatively long [118]. Finally, we must not forget that the sample to be tested must be a prototype, made solely for the purpose of measurements, since, given its immersion in the calorimetric fluid, for a magnetic component to be used later on the calorimetric procedure is excluded.

Contrary to that, the ability of modern recording systems to acquire data at very high sampling frequencies and digitally store them enables us to process information on voltage and current waveforms. The suitable software for this processing is often integrated into the functions of the acquisition system itself and thus the calculation of losses with eq. (7.1) is facilitated, even for high frequency and high harmonic content waveforms.

7.2.2. Measurements of specific ferrite loss at high frequencies

In the design of magnetic components for power converters, it is a common practice to decrease the amplitude of magnetic induction B_{max} in the core as the frequency increases. This is to keep the total specific losses of the core under a critical value over which overheating occurs (Appendix II). Another fact is that the data sheets provided by the ferrite manufacturers contain information on specific losses up to a frequency limit for which each material is recommended as appropriate. The truth is, however, that magnetic component designers often exceed this boundary by keeping B_{max} sufficiently low and arbitrarily extend the curves contained in the data sheets to approximate the specific losses. The mistake in this procedure is that, as will be explicitly presented in the following, actual losses are quite

higher than expected. Up to the suggested frequency limit, for each specific ferrite grade, losses are mainly due to hysteresis. If, in some cases, they do not increase in a perfectly linear manner with frequency, this is due to the dependence of the hysteresis loop shape on frequency, but also due to the slight increase of eddy currents, which in any case, are kept nearly insignificant. Over the aforementioned frequency limit, electrical conductivity and eventually eddy current losses increase abruptly [140], [142]. For even higher frequencies, the dominance of other loss mechanisms, e.g. excess losses and electromagnetic resonance in the bulk of the core, further increases the power dissipation [22], [60], [104], [124], [133] (see also Ch. 2).

For the ferrite grade Epcos N27, specific loss data are given for frequencies lower than 200kHz [140]. Even so, it is commonly used, with low B_{max} values, up to frequencies double as that, especially in laboratory applications. It is undoubtedly informative to experimentally find the losses for frequencies higher than 200kHz.

Using the current-fed resonant converter presented in Ch.6, a core E42/21/14 with N27 ferrite grade was excited with a sinusoidal voltage at magnetic induction B_{max}=25mT and B_{max}=50mT, at room temperature and for frequencies in the range from 95kHz to 440kHz. In order to avoid a possible temperature increase of the piece under test, each measurement was taken in a short time (a few seconds), and the interval between successive measurements was several minutes. Measurements at frequencies below 200kHz helped verify the measurement method. The current i_p in the excitation winding on the piece under test was measured by sensing the voltage on a shunt low-inductance resistor in series with it. The applied voltage v_p (the output voltage V_o of the converter) sensing was carried out with the help of a differential active probe similar with that used for the current sensing. Using similar active probes for sensing both v_p and i_p (instead of using, for example a Hall effect probe for sensing the current) eliminates the effect of a possible phase-shift error due to the electronic part of these probes [38], [57], [85]. For the frequencies of interest, the inserted error due to parasitic components (capacitance of the probe and inductance of the shunt resistor) was calculated and found negligible. Approximate calculations of the copper losses on the excitation winding indicate that they can be considered negligible compared to the losses on the ferrite (typically, less than 5% of the overall losses). Thus, their accurate separation from the ferrite losses, e.g., with the use of an auxiliary secondary winding, as described in [104] and [118], was judged unnecessary for the purpose of the present experiment. Dissipated power

$P_{tot} \cong P_{Fe}$ was automatically calculated by the data acquisition system (digital oscilloscope HP 54820A Infinium Oscilloscope, 2Gs/sec) as:

$$P_{tot} = \left\langle v_p(t) \cdot i_p(t) \right\rangle \cong P_{Fe} \qquad (7.3)$$

It is necessary to remind here that, with increasing frequency the inductance of the load decreases slightly due to a decrease in the initial permeability of ferrite and its ohmic part increases significantly due to increased losses. Hence, the phase shift between $v_p(t)$ and $i_p(t)$ drops well below 90° and the measurement accuracy improves [115], [148] (see also §7.3.3).

The results of these measurements are shown in Fig. 7.1. The solid lines represent the given curves in the data sheet, their extensions are denoted by the dashed lines, and the
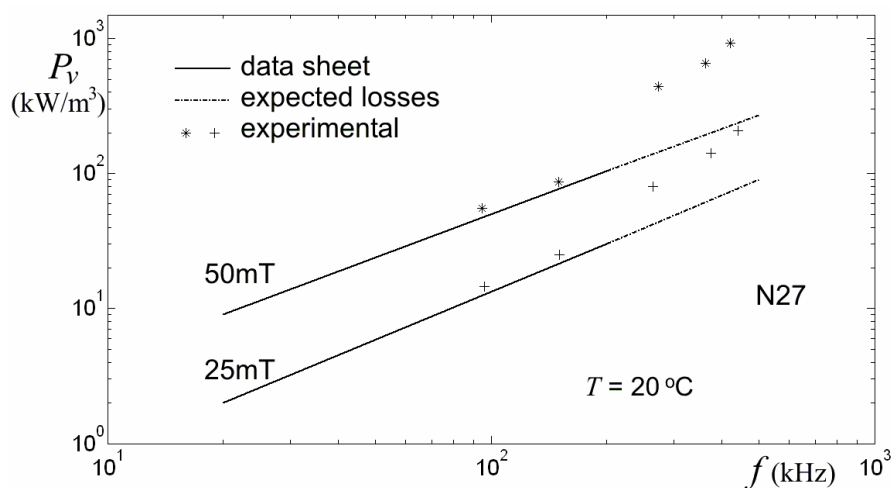
Figure 7.1: Specific losses of N27 material according to data sheet (for $f<200$kHz) and according to experimental measurements.

measurements are shown as experimental points.

It is clear from the graph that, in the range of 400kHz, the specific losses are about three times the expected value, according to the data given for lower frequencies.

7.3. Recording of the hysteresis loop

7.3.1. General issues

Someone may want to know the hysteresis loop of a material for reasons mainly related to the determination, through simple known formulas, of the core losses, but also to the calculation of the magnetic permeability μ, when parameters such as the gap width, the effective cross section and the effective length of the magnetic path within the material are known quantities. We have also seen in the various models for the hysteresis (Ch. 2) some parameters, for the determination of which it is sufficient to know the low frequency hysteresis loop (static loop). Some others need to know the magnetization curve or the non-hysteretic curve, for the acquisition of which there are specific experimental methods.

An example of using the data obtained from the experimental acquisition of the hysteresis loop is the determination of the parameters of Jiles − Atherton model to be imported into the PSpice software [57], [85]. In [85] there is a detailed presentation of the way one can calculate the parameters of Jiles – Atherton model from the hysteresis loop and the manufacturer's data. When the specific material from which the core of the magnetic component is made is not already included in the software libraries, with the import of the correct values for these parameters into the software, the harmonic content of voltages and currents is more accurately described when simulating a circuit. It is also possible to use PSpice to predict the form of the high frequency hysteresis loop [57], [85]. Necessary to note, of course, that this must be done with caution when the piece under test is a ferrite, since Jiles − Atherton model does not refer to soft ferrites. In other words, the import of the experimentally determined parameters of the model into PSpice will not give the actual non-hysteretic curve, neither the actual hysteresis loop. Starting from the experimentally determined values, one has to change them slightly until the predicted curves coincide with the experimental ones.

In the rest of this section, eddy currents losses are considered to be negligible, i.e. we consider ferrites and frequencies below the critical value for which eddy currents become significant, as mentioned in Ch. 2. At the end of the section there will be a reference to the case where the eddy currents cannot be considered negligible.

The classic method to record the hysteresis loop is based on the fact that the induced voltage $v_s(t)$ on a secondary winding with N_s number of turns, located on the core to be measured, is connected to the magnetic induction $B(t)$ by the equation:

$$B(t) = \frac{1}{N_s A} \int v_s(t)\mathrm{d}t \tag{7.4}$$

where A is the area of a turn, given that it is the same for all the turns. It is obvious that, in order to measure $B(t)$ correctly, A must be equal to the cross-sectional area of the core, otherwise the leakage flux affects the measurement. Moreover, in cores with any of the widely used shapes (e.g. E, EI, U), the cross-sectional area varies along the magnetic path, and hence the effective cross-sectional area A_{eff} should be used in the place of A, provided that the measuring winding has only one layer. When applying (7.4), as in the following analysis, we consider an average value for the quantities H and B and we ignore any local variations due to the shape of the core. To minimize the above errors it is more appropriate to use a toroidal core, in which the leakage flux is practically negligible and the cross section constant. Moreover, when it comes to the characteristics of the material it is important that there is no gap. For a core commercially available in two pieces, perfect contact between them is impossible. Of course, the error is low if the two surfaces have been thoroughly cleaned prior to joining and both parts are subject to a sufficiently strong clamping force, as specified by the material manufacturer [140], [142]. However, this problem is also absent from the toroidal core, which consists of one single piece.

The second equation upon which the acquisition of the hysteresis loop is based is the one that links the magnetic intensity $H(t)$ to the core excitation current $i_p(t)$:

$$H(t) = \frac{i_p(t) \cdot N_p}{l_{eff}} = \frac{v_R(t) \cdot N_p}{R_m \cdot l_{eff}} \tag{7.5}$$

where $i_p(t)$ is the current in the excitation winding (primary winding), N_p the turns of the primary winding, R_m a resistance connected in series with the primary winding and $v_R(t)$ the voltage drop on this resistance, while l_{eff} represents the effective length of the magnetic path within the material. The loop is acquired if we record $v_R(t)$ and $v_s(t)$ and, after the appropriate modifications based on the previous equations, project $B(t)$ versus $H(t)$.

Derivation of $B(t)$ waveform presents some additional problems compared to what is necessary for $H(t)$ because $v_s(t)$ must be integrated. Direct integration with the help of the appropriate electrical or electronic circuit (e.g. an integrator based on the use of an operational amplifier) is not the best solution, since recording of the loop is almost always

regarded in a wide range of frequencies and for different parameters each time (e.g. induced voltage), which means that the components of such a circuit (resistances, capacitors, integrated circuits) should differ each time. The best solution is to store $v_s(t)$ and $v_R(t)$ and then process them to draw the loop. Modern high-frequency digital sampling systems, which incorporate complicated computational operations, usually provide the ability to directly integrate and display the result during the measurement.

There is one more special attention point about recording the two waveforms, especially if the frequency is high. It must be ensured that the time delay involved in the information transmission from the experimental set to the recorder is the same for both channels. Otherwise the loop will not correspond to reality, something which can sometimes be visually verified by observing the endpoints of the loop if they happen to be in the saturation region. In order to minimize this error, the two lines of signal transmission to the recorder should be identical, that is, with the same length (same inductance), whereas the appropriate calibration test should be performed at both channels prior to the measurements. The importance of this test becomes even more crucial when the two signals propagate in completely different ways, e.g. when the information for $i_p(t)$ comes from a current probe (measurement of current based on Hall effect) and from the signal amplifier in series, since the electronic part of the amplifier, inevitably introduces a time delay in the transmission of information. Needless to say that, since high frequency and possibly high harmonic content waveforms are to be recorded, the capacitance of the sensing instruments (e.g. voltage probes) should be as low as possible and generally the entire acquisition setup, in all its stages, to be wide band pass. It is noted at this point that the parasitic capacitance of the voltage probes is a major phase delay error factor in the measurement of a signal and often the wide band pass feature does not necessarily mean that over the whole width of this range, even at the high frequency end, the phase delay is negligible. If one has doubts about the specifications of the voltage probe he is using, it is advisable to consult the magnitude-phase diagram (Bode diagram) for its transfer function, when provided by the manufacturer. When this diagram is not given, the equivalent circuit of the probe may be available, so the user has to do the analysis himself.

Figure 7.2 comes from the literature [57] and illustrates the general form of a setup for the recording the hysteresis loop. The excitation source is some circuitry whereby we obtain the desired voltage or current waveform in the primary. We also see that, if necessary, we can measure the voltage and the current in the primary with another independent system, to be able to compare with the main sensing instrumentation.

Before we close this paragraph we will make a reference to the effect of the eddy currents on the experimental recording of the hysteresis loop. In all of the previous analysis about the hysteresis loop we have assumed that the operating frequency, as well as the frequencies of the major harmonics of the magnetic induction, are in the range in which the specific conductance of the core material is very low and thus the eddy currents can practically be neglected (Ch. 2). If the frequency increases beyond this limit (different for each material), the eddy currents developed force us to alter the study. In the previously presented classic method of recording the loop, the magnetic intensity is calculated from equation (7.5). The eddy currents, however, cause their own separate ampere-turn inside the core, resulting in a magnetic field which, according to Lentz's law, opposes the externally applied field due to the current of the excitation winding. The resulting field in any point of the space appears as the sum of the two. So finally, if there are eddy currents, the real magnetic intensity in the core material is not given by (7.5) but by [55]:
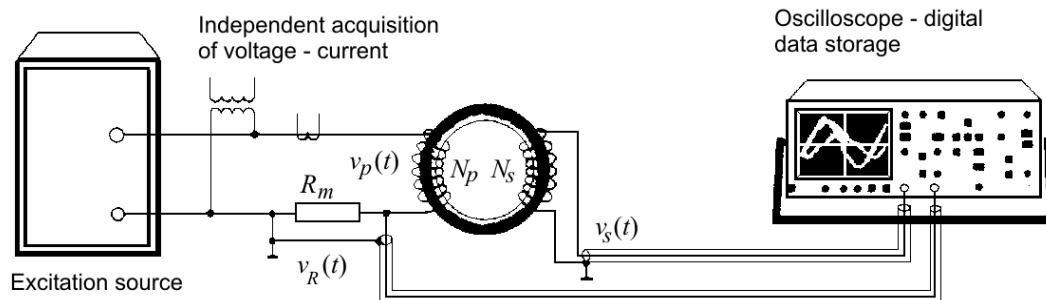
Figure 7.2: Typical setup to record the hysteresis loop [57].

$$H_{real} = \frac{N_p i_p}{l_{eff}} - \frac{k}{N_p l_{eff}} \cdot \frac{\mathrm{d}\Phi}{\mathrm{d}t} \tag{7.6}$$

where H_{real} is the actual value of the magnetic intensity and Φ is the magnetic flux in the cross-section of the core. We may see that in the case of eddy currents, the H resulting from (7.5) is greater than the actual value. The factor k is a function of the specific conductance but also of the geometry of the core and for the direct separation of the hysteresis losses from

the eddy current losses, if we obtain the loop according to (7.5) it is necessary to know it. If not given, it should be experimentally determined in a way that is not so simple and is based on measurements in two dimensions on a thin foil of core material [55]. It is certain that, if the eddy currents are not negligible, the resulting loop from (7.5) is not the actual $B(H)$ loop and the losses calculated by its area give us the sum $P_{hyst}+P_{eddy}$ [55].

7.3.2. Measurements to record the hysteresis loop

The Electromechanical Energy Conversion Laboratory of the Electrical and Computer Engineering Department of the University of Patras has been conducting intensive research since many years on issues related to the study and implementation of electronic power converters for laboratory or industrial purposes. In the context of these studies there have been numerous publications of original work in scientific journals and international conferences. From the accumulated experience it becomes apparent that, whatever the purpose of developing any system with power electronics, quantities such as the efficiency or the harmonic distortion of the waveforms of voltages and currents are of immediate interest. The knowledge of these quantities and some other related data, about which we have made so far extensive reference, may result if we are aware of the hysteresis loop of the ferrite used in the magnetic component cores.

Some of the magnetic core materials used to make transformers and inductors are Epcos N27 and Ferroxcube 3F3 [140], [142]. For these materials, as well as for other commercially available materials, the manufacturers' data cover a wide range of values for the parameters B, f and T (T is the temperature here), in a way not completely satisfactory, since the range of variation of these parameters is not continuously swept, but only by some discrete values. In Fig. 7.3 and Fig. 7.4 [131] for example, we see that the specific losses are given by the manufacturer for only some values of the parameters f and B_{max}. This means that for specific operating conditions we have to interpolate in these diagrams, with the accuracy of the result being, more or less, unknown. Data about e.g. the magnetic permeability are approximate and only for some specific conditions. For example the quantity of particular interest:

$$\mu_\alpha = \frac{1}{\mu_0} \frac{\Delta B}{\Delta H} \tag{7.7}$$

(amplitude permeability) is given for sinusoidal excitation with B_{max}=200mT, f=25kHz and temperatures T=25°C and 100°C. For the effect of the gap on the magnetic permeability, the well known approximate relation is proposed:
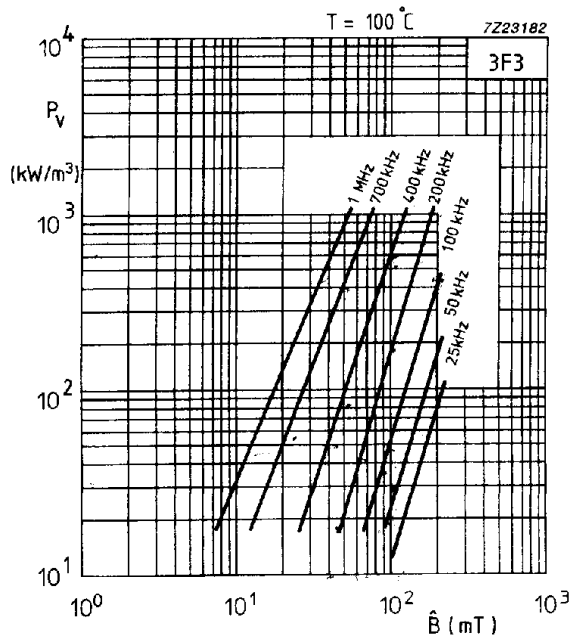
Figure 7.3: Specific losses versus the amplitude of the magnetic induction B_{max}, for a temperature of 100°C, with frequency as a parameter, for the material 3F3 [131].
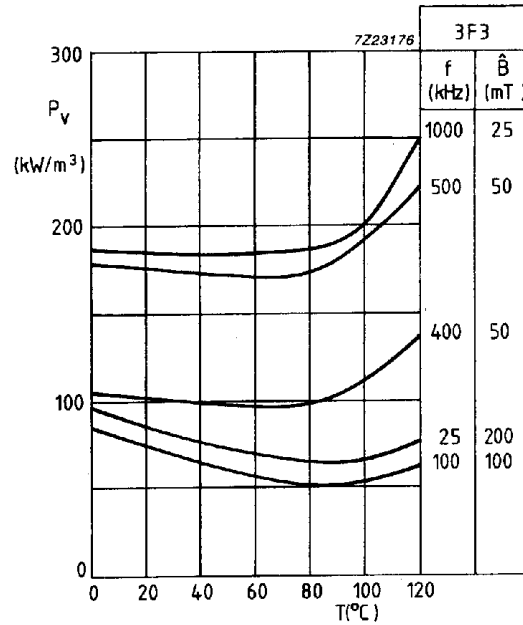
Figure 7.4: Specific losses for various frequency – magnetic induction combinations, as a function of temperature for the material 3F3 [131].

$$\mu_{eff} = \frac{\mu_i}{1+\left(l_g / l_{eff}\right)\cdot \mu_i} = \frac{1}{\dfrac{1}{\mu_i}+\dfrac{l_g}{l_{eff}}} \tag{7.8}$$

where the initial permeability μ_i is equal to μ_α for $\Delta H \rightarrow 0$, that is to say, given by the slope of the magnetization curve for $H \rightarrow 0$. If it is $\mu_i >> l_{eff}/l_g$ from (7.8) the following equation is obtained:

$$\mu_{eff} \cong \frac{l_{eff}}{l_g} \tag{7.9}$$

It is noted that with the insertion of a gap and since the material does not enter saturation, the effective magnetic permeability μ_{eff} becomes equal to μ_a and equal to the differential magnetic permeability $\mu_d = dB/\mu_0 dH$ (eq. 1.7) for any point of the hysteresis loop (see e.g. Fig. 7.6).

It is obvious that we are interested to know the hysteresis loop for the respective excitation conditions that appear during the operation of the various power converters, in order to verify the various assumptions we make about the power consumption of the magnetic components and to see how the gap choice, as well as other design options, affect their properties. It is noted that if the length of the gap gets a high value, comparable to the core cross section dimensions (e.g. on an electromagnet or on a magnetic component due to poor design choices) eq. (7.8) is no more valid and the fringing field appears in such an extent that it is impossible to accurately predict either the effective magnetic permeability or the losses, based on any of the models found in the literature.

At first, measurements were made to acquire the static hysteresis loop. The N27 material loop was measured at low frequency (50Hz) with more emphasis given on examining the capabilities of the recorder available in the laboratory, as well as the problems encountered in recording and processing information. Several problems were encountered such as change of the loop due to core heating in case of delay in measurements, dc-offset in the oscilloscope channels, slight frequency variations of the grid, correct selection of the oscilloscope triggering event etc. The metering setup has the general form shown in Fig. 7.1, where the voltage was supplied by the grid through a transformer and the piece under test to be measured was an E55 core, around the center leg of which, in the coil former, the primary winding was placed and above it (externally) the secondary was placed.

The greatest uncertainty in the measurements is due to the precision with which the value of the shunt resistance for the current sensing is known. The resistor used for this experiment was a low-inductance power resistor (conductive wire, aluminum shell, Arcol Ltd). Its value was measured under constant current conditions, with no significant deviation from the value given by the manufacturer, while there was no significant increase in its temperature during the experiment. Due to this uncertainty, the necessity to use a current probe at low frequencies became apparent, without forgetting the potential problems that this method entails when attempting high frequency measurements. The measurements were taken for

different supply voltages and for different gap widths. Let's see some results and some interesting conclusions which arise.

Figures 7.5 and 7.6 illustrate the hysteresis loops for various excitation levels. The two loops of Fig. 7.5 correspond to the no gap case, while those of Fig. 7.6 are for l_g=0.66mm (the distance between the two E55 halves that make up the core is 0.33mm). In the graphs derived from the oscilloscope, the subdivisions of the axes do not correspond to round numbers, since the axes are scaled when acquiring the oscillogram based on the measured voltages, while the conversion to magnetic induction and magnetic intensity units is made afterwards based on equations (7.4) and (7.5). Moreover, in Fig. 7.6 the graphs have been moved along the horizontal axis, so that they do not overlap and be distinct. The integration of the secondary winding voltage is performed directly by the oscilloscope software.

As already mentioned, with a good clamping of the two pieces that constitute the core we can approximately presume that there is no gap. Thus, for l_g=0, we had the opportunity to observe the change in the form of the hysteresis loop, and in particular the gradual increase in H_c and μ_α, as the excitation magnitude increased starting from low values (Fig. 7.5). These changes are not

easily observed if there is a gap, hence H_c, μ_α remain constant (except in the case of
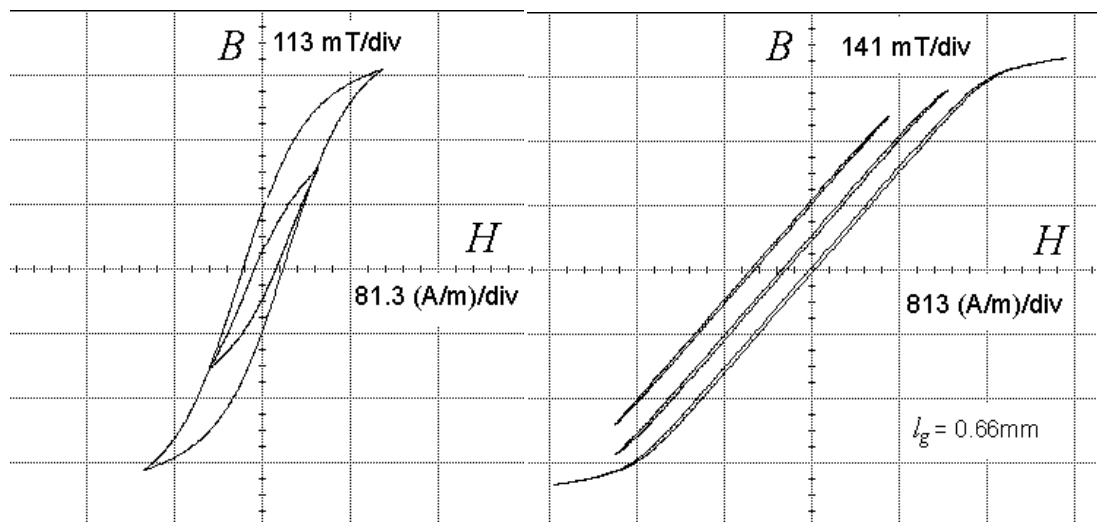
Figure 7.5: Static hysteresis loop of N27 material for two different excitation levels. Measurement on E55 ungapped core, (l_g=0) (oscillogram).

Figure 7.6: Static hysteresis loop of N27 material for several excitation levels. Measurement on E55 core, with gap l_g=0.66mm (oscillogram).

extremely low excitations), same as the differential magnetic permeability (the slope of the loop at various points except its tips).

In Fig. 7.7 we see, for a constant excitation voltage, the variation of μ_α as the gap length varies. Theoretically, as concluded from (7.4), since the amplitude of the excitation voltage remains constant, the amplitude of the magnetic induction should also remain constant. In practice there is a slight decrease in B_{max} as the gap increases (the magnetization inductance decreases), which is due to the decrease of the excitation voltage due to the increase of the excitation current and the consequent voltage drop in the power transformer and the shunt resistor.

The value of the initial magnetic permeability μ_i is given in the data sheet with a 20% tolerance. As we know, gap insertion is a good way to have the effective magnetic permeability μ_{eff} (in the following it is $\mu_\alpha \equiv \mu_{eff}$) determined by equation (7.8) or (7.9) without paying much attention to the exact μ_i value of the material. The accuracy in μ_{eff} calculation from the hysteresis loop was verified with an independent measurement of the
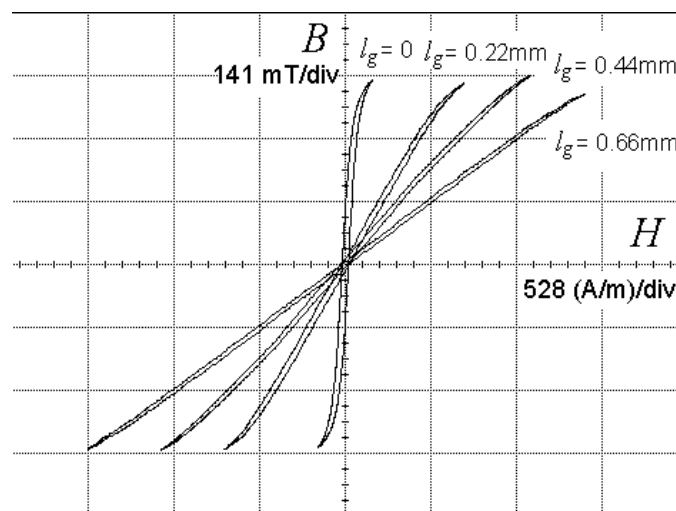
Figure 7.7: Static hysteresis loop of N27 material for constant excitation and for various gap lengths (oscillogram).

inductance L of the excitation winding, found equal to the value calculated on the basis of the expression:

$$L = \frac{\mu_0 \mu_{eff} N_p^2 A_{eff}}{l_{eff}} \qquad (7.10)$$

It is reminded that N_p is the number of turns of the excitation winding. So finally, for the gaps tested (up to l_g=0.88mm), it turns out that (7.9) is generally a bad approximation. The value given by the manufacturer for μ_i is $1800 \pm 20\%$, which means that, for the gaps inserted and with the given value for l_{eff} of the E55 core (123mm), the condition $\mu_i >> l_{eff}/l_g$ cannot be considered as satisfactory. Finally, it is also stated that in this case it is important that there is sufficient clamping force for the two pieces that form the core, so that the length of the gap remains constant, not affected by the mutual attractive force resulting during operation.

Hysteresis losses, as calculated from the shape of the loop for a constant excitation voltage, are expected to be independent of the gap width, since B_{max} and H_c also remain constant [124]. This attribute was confirmed for excitation without saturation, with P_{hyst} varying, always for constant excitation voltage, to values of about $\pm 2\%$ around an average value and with maximum deviation at $\pm 7\%$. Moreover, almost immediately after recording each hysteresis loop (so as the core temperature does not increase), simultaneous acquisition of the current $i_p(t)$ and voltage $v_p(t)$ in the primary winding was performed and with the assistance of the oscilloscope software the instantaneous power as well as its average value for an integer number of periods (eq. 7.1) are calculated and displayed. Having in that way the total dissipated power in the primary and by subtracting from it the ohmic losses $P_{Cu} = i_{p,rms}^2 R_p$ we obtain a value for the hysteresis losses (R_p is the resistance of the primary excitation winding). This value, for a given excitation voltage, generally shows little fluctuations and deviations from the corresponding nearly constant value obtained from the hysteresis loop.

Quantities such as B_r, H_c, μ_a, μ_d can be measured directly on the oscilloscope display since we have the ability to freeze the image and with the help of two cursors we may track the curve reading their coordinates. It is sufficient to know the conversion coefficients of the measured current (with the value of the shunt resistance in the primary being known, the scaling on the screen can be easily adjusted, directly in current units) and of the magnetic flux into magnetic intensity and magnetic induction respectively. However, the area of the loop is of our interest too. Furthermore, the waveforms for the power dissipation must be acquired quickly after the measurement of B_r, H_c. Hence, we prefer to save the hysteresis loop curve for further processing, with the cursors at the appropriate positions on the loop, so

that we can directly measure the power dissipation. As mentioned, converting v_R voltage into i_p current units is done easily by the oscilloscope, with the appropriate conversion at the corresponding channel settings. About the Volt-seconds on the vertical axis, we prefer to convert them into magnetic flux units later on at the computer processing. The value pairs (i_p, Φ), where Φ is the magnetic flux, are stored in two files with different formats, one suitable for reproduction of the waveforms in the oscilloscope (as shown in Fig. 7.5, Fig. 7.6 and Fig. 7.7) and the other one to input these values into any software, such as Excel or Matlab.

Thus, a Matlab code was written to read the value pairs file (i_p, Φ) (converted to H, B values) and some additional information, such as the excitation frequency and geometrical characteristics of the core. Then it calculates the power of hysteresis losses [mW], the specific power of hysteresis losses [kW/m^3], the specific energy of hysteresis per cycle [μJ/cm^{3}cycle], amplitude permeability μ_α, the inductance L of the excitation winding of the magnetic component. If the core has a gap, a saturation check is performed by comparing μ_α with μ_d at a point on the loop with zero magnetic induction.

Since in cases where the frequency is very high we can have a significant effect of the eddy currents and/or a shape change of the loop, μ_α is not calculated from eq. (7.7) but by locating the total chord of the loop. This calculation is done regardless of the position of the loop on the *H–B* plane, that is, even if there is a constant term component for the magnetic induction, as it happens in many applications. The reason is that the ampere-turns of the eddy currents generally come with a phase shift relative to that of the excitation winding and therefore in the loop acquired by measuring on the latter one, the points H_{max} and B_{max} do not coincide (it is reminded here that in the presence of the eddy currents the area of the loop gives the total specific core losses). Also, regardless of this phenomenon, we generally have a change in the shape of the hysteresis loop with the frequency (it appears flattened), notably evident when the gap is absent [38], [75], [85]. One subtle point in building this code is the check of whether the correct settings have been selected when saving the file with the value pairs (i_p, Φ), which should also contain the offsets of the oscilloscope channels, necessary for the correct design of the loop. Hence, in the beginning, if the storage has not been done properly, a relevant message is displayed, otherwise the offsets are read, some additional information is skipped and the numerical data is processed.

In addition to the static loop imprints at 50Hz, the hysteresis loops of the Ferroxcube 3F3 material were also acquired at frequencies from 23kHz to 110kHz. For the excitation of an E-type core (ungapped), which constituted the piece under test to be measured, we used the resonant converter presented in detail in the previous chapter. Figure 7.8 illustrates, for example, the hysteresis loop of Ferroxcube 3F3 material [142] for 23 and 98 kHz, at room temperature, exactly as it appears on the oscilloscope display. With the input of the recorded waveform into the Matlab code mentioned above, we were able to verify the data from the manufacturer about the losses, since at these frequencies the core loss is entirely to hysteresis.
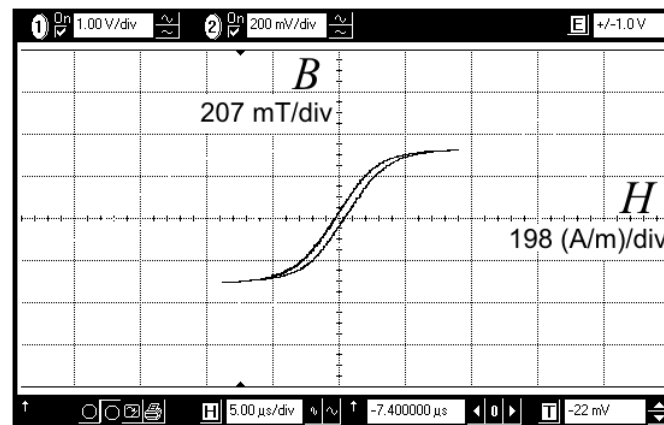
(a)
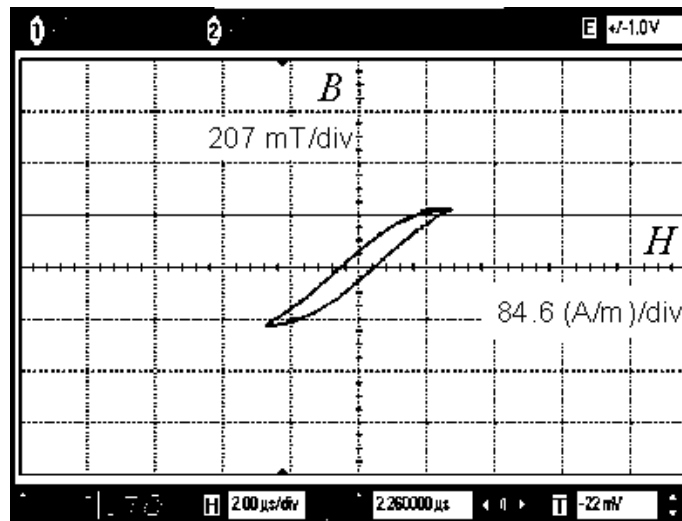
(b)

Figure 7.8: Hysteresis loop of 3F3 material at frequencies (a) 23kHz and (b) 98kHz, as it appears on the oscilloscope display.

7.3.3. Calculation of the phase error in the experimental determination of hysteresis losses

We saw in the above presentation the way the hysteresis loop can be acquired by recording the current $i_p(t)$ of the primary excitation winding and the induced voltage $v_s(t)$ in the secondary measurement winding. Moreover, if there is a reason to determine the copper losses in the primary winding, the hysteresis losses should be subtracted from the total losses calculated from (7.1).

The relation between H and B is generally not linear, but in many cases can be approximated as linear. Such cases are encountered, when a gap is inserted in the magnetic path of the core or when the material used is soft, with a narrow hysteresis loop and a high value for the ratio B_{sat}/B_r. In these cases, if one of the two quantities is sinusoidal then the other one can be considered sinusoidal as well. If, for instance, a sinusoidal voltage $v_p(t)$ is applied to the primary then $B(t)$, $i_p(t)$ and $H(t)$ are also sinusoidal time functions and (7.1) is equivalent to:

$$P_{tot} = v_{p,rms} i_{p,rms} \cos\theta \tag{7.11}$$

where θ is the phase angle between v_p and i_p.

As the frequency increases, there may be some phase error at both the current and the voltage measurements. In general, voltage measurements, with the appropriate equipment, can be very accurate at even high frequencies. Current measurements are more frequently subject to phase errors. When a Hall effect active current probe is used there will be a delay at the information taken due to the propagation delay at the probe system and –mainly– due to the amplifier. Moreover, when a resistor is used to measure the current any slight delay due to the voltage probe used to measure the voltage is generally supplanted by a signal lead dependent on the inductive character of the resistor. In literature there is often a contradiction on the issue of how to accurately acquire current waveforms at high frequencies, as for example in [38] and [85]. While in [85] it is suggested that the active Tektronix A6302 current probe, in combination with the AM503 amplifier of the same manufacturing company is suitable for measurements at frequencies up to 80 kHz without significant phase error, in [38] such an option is categorically rejected and the use of a resistor is applied. This example indicates that great attention should be paid to this issue and that all possible precautions

should be taken to avoid a potential phase error, otherwise one can be led to invalid experimental conclusions.

It is important here to note that for an impedance dominated by one character (here the ohmic), while a secondary character type (here the inductive) appears as a parasitic component with very low effect on the normal operating frequencies of the various impedance analyzers and commercial measurement bridges, this secondary character cannot be detected by the aforementioned devices. More correctly, in search of the parasitic character, measurement with these instruments leads to an incorrect indication. This fact, which is often documented even in the operating manuals of these metering devices, is often overlooked by researchers. Typical operating frequencies of such metering devices range from a few tens of Hz to a few tens of kHz.

Differentiating (7.11) we get:

$$\frac{\mathrm{d}P_{tot}}{P_{tot}} = \frac{\mathrm{d}\cos\theta}{\cos\theta} = -\tan\theta \mathrm{d}\theta \tag{7.12}$$

This simple equation indicates that even a small phase error, when θ is close to 90°, leads to a huge error for the total losses. Given that there is generally an error in determining the phase difference between the quantities $v_p(t)$ and $i_p(t)$, the above finding indicates that it is preferable (if there such an option) that the loss measurements are taken at operating conditions of the magnetic component where θ has a relatively low value and therefore P_{tot} can be measured more accurately.

In the following we show what has to be the correction at the hysteresis loop area when the measuring method applied to acquire the current and the voltage waveform inserts a known phase error. According to what was mentioned previously, we assume a case where both H and B are sinusoidal time functions:

$$B(t)=B_{max}\sin(\omega t) \quad \text{and} \quad H(t)=H_{max}\sin[\omega t+(\pi/180)\varphi], \qquad 90°>\varphi>0° \tag{7.13}$$

where ω is the radial frequency. In Fig. 7.9 is the dependence of the hysteresis loop area $E_h(\varphi)$ on the phase angle φ, normalized at the area E_{h0} corresponding to the case $\varphi=90°$. It is evident that for $\varphi<10°$ it is an approximately linear relation. Subsequently, we represent the ratio H_{max}/H_c of the maximum value of the field intensity to the coercive field as a parameter which we call K_H:
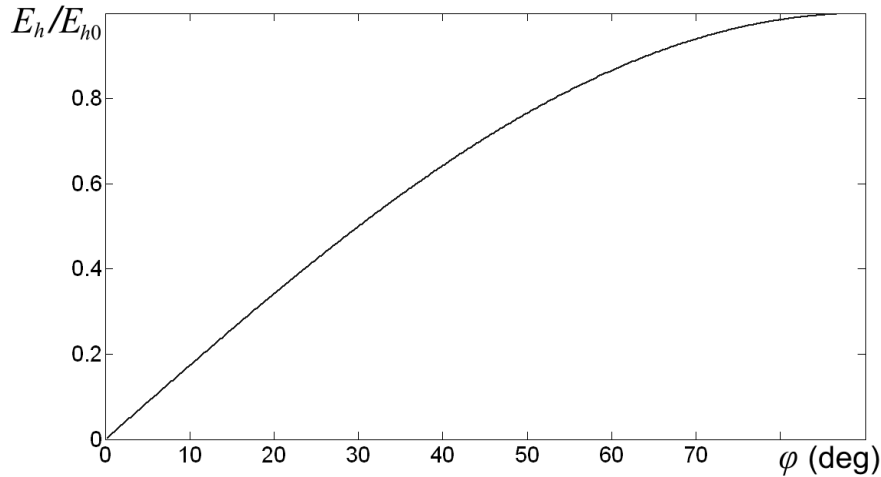
Figure 7.9: Normalized area of the hysteresis loop E_h/E_{h0} as a function of the phase angle φ (eq. 7.13). The area E_{h0} corresponds to $\varphi=90^{\circ}$.

$$K_H = H_{max}/H_c \tag{7.14}$$

The dependence $K_H(\varphi)$ is plotted in Fig. 7.10. In practice, using this diagram, we can determine the phase angle φ between H and B from the measured H_{max} and H_c in the experimental loop. What is left is to determine the ΔE_h correction to the E_h area of the measured loop (cumulative term) when enters a known phase error $\Delta \varphi$:

$$E_{hc} = E_h + \Delta E_h \tag{7.15}$$

where E_{hc} is the corrected value for the loop area. Given the –by approximation– linearity of $E_h(\varphi)$ for angles up to $\varphi=10^{\circ}$, the grid we see in Fig. 7.11 can be plotted. Each curve of the grid in this graph corresponds to a value for the experimental angle φ, as determined from Fig. 7.10, which can be read at the top of the graph, while the horizontal axis corresponds to the absolute value $|\Delta\varphi|$ of the phase error. The correction factor F_{Eh} is given by the relation:

$$F_{Eh} = \frac{|\Delta E_h|}{E_h} \tag{7.16}$$
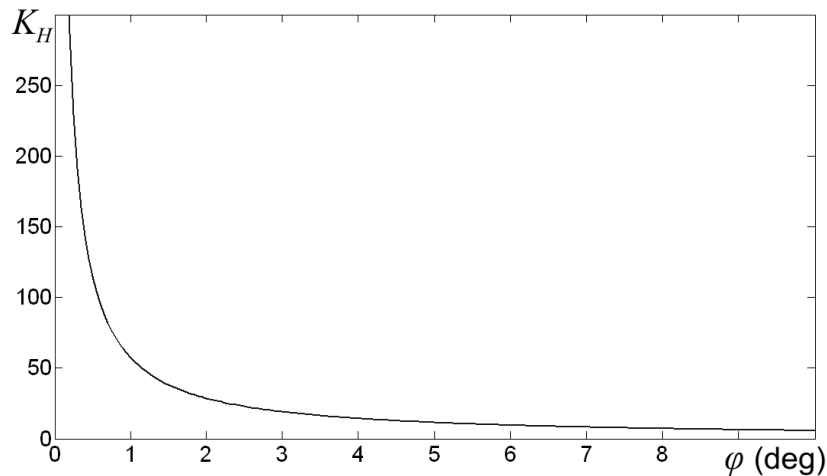
Figure 7.10: Graph of the relation between the parameter $K_H = H_{max}/H_c$ and the phase angle φ.
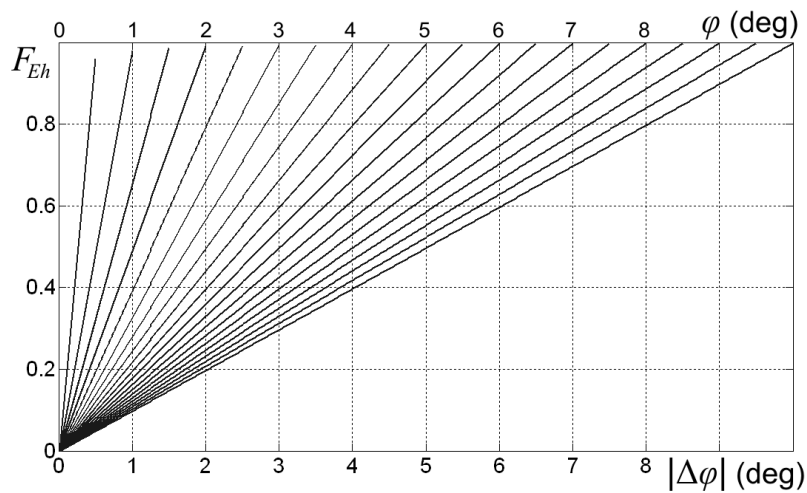
Figure 7.11: The absolute value F_{Eh} of the correction to be made to the experimentally determined area of the hysteresis loop, as a percentage of that (eq. 7.16), for a known phase error $\Delta\varphi$.

it is therefore the absolute value of the ΔE_h correction expressed as a percentage of the measured loop area. When there is a phase lag error in the current measurement the correction should be added to E_h, while the opposite is true if it is a lead error. Hence, the following expressions apply:

$$\Delta\varphi < 0 \quad \Rightarrow \quad \Delta E_h > 0 \tag{7.17a}$$

$$\Delta\varphi > 0 \quad \Rightarrow \quad \Delta E_h < 0 \tag{7.17b}$$

It should be noted that in the previous analysis we considered as negligible the phase delay in the voltage sampling. Otherwise, this should also be taken into account and $\Delta\varphi=0$ will only be valid when both voltage and current measurements are equally time delayed (since voltage measurement is not expected to lead in any case).

In order to verify the validity of the proposed method of correction of the hysteresis losses calculated from the area of the hysteresis loop, the hysteresis loop was taken on a Ferroxcube 3C80 U-I ungapped core. The excitation of the material remained quite far from the saturation levels. With the use of the resonant converter presented in Ch. 6, the core was excited with sinusoidal voltage at 11kHz, low enough to ensure that any possible inductive character of the resistor used to measure the current is negligible. Each time some properly designed inductors were connected in series to the resistor in order to insert a predetermined phase shift in the information obtained for $i_p(t)$. The relatively low frequency also ensures that these inductors behave purely as inductances, while the gap they have ensures that their connection in the excitation winding circuit does not cause any distortion in the current waveform.

Following this procedure, the hysteresis loops shown in Fig. 7.12 were acquired. Loop (a) is the actual one, while (b) and (c) have resulted after the introduction of a particular phase delay $\Delta\varphi$ at $H(t)$ in regard to (a). In Table 7.1 are the quantities related to the three loops where, instead of the loop area E_h, is the result in Watts for the hysteresis losses P_{hyst}, as calculated from the given loop area for the selected U-I core. Attention should be paid to the fact that the quantity $\Delta\varphi$ was calculated (for this specific frequency) on the basis of the inductance each time connected in series with the shunt current metering resistance, while φ for each loop results from Fig. 7.10 based on the K_H value corresponding to the measured loop. This is the reason why if we subtract between the values of φ and the corresponding $\Delta\varphi$ values of the table the results are slightly different.

With any of the three loops as a starting point and with the use of the method described above, the area of any other loop can be calculated with an error that is typically 5% (the final
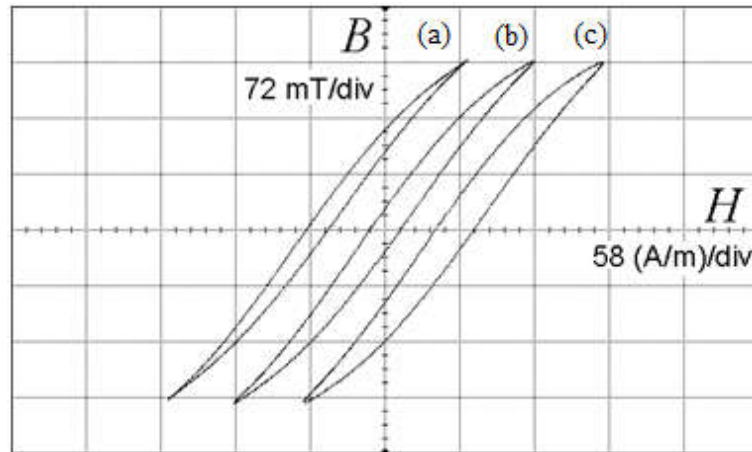
Figure 7.12: Experimental hysteresis loops of the 3C80 grade at a frequency of 11kHz (a) without phase error and (b), (c) with a given phase error $\Delta\varphi > 0$.

TABLE 7.1

The values of $\Delta\varphi$, K_H and φ for the loops of Fig. 7.12, the P_{hyst} result for the hysteresis power loss of the used ungapped U-I core and the calculated losses $P_{hyst,calc}$ according to the proposed method, when the reference loop is the one denoted with brackets.

Loop	$\Delta\varphi$ (deg)	K_H	φ (deg)	P_{hyst} (W)	$P_{hyst,calc}$[a] (W)	$P_{hyst,calc}$[b] (W)	$P_{hyst,calc}$[c] (W)
(a)	0	13.7	4.18	12.4		12.60	13.04
(b)	1.9	9.7	5.91	18.8	18.23		18.70
(c)	3.8	7.0	8.22	24.6	23.93	25.00	

result for the losses $P_{hyst,calc}$ is shown). It is found that this error is not due to some inherent weakness of the method, but mainly due to the accuracy with which one can read the graphs of Fig. 7.10 and Fig. 7.11.

Let us describe an example of the correction calculation: Suppose, that the experimentally measured loop is (c), and it is known that it is obtained with a phase error $\Delta\varphi = +3.8°$. The result for the losses is $P_{hyst} = 24.6$W and we are looking for the actual, corrected losses. From H_{max} and H_c of the loop we find that $K_H = 7$. It is found on the graph of Fig. 7.10 that this value of K_H corresponds to a phase difference between H and B equal to $\varphi = 8.22°$. We consider in Fig. 7.11, with an approximate, visual interpolation, the curve corresponding to this φ value, which for $|\Delta\varphi| = 3.8°$ gives $F_{Eh} \cong 0.47$. The corrected value for losses is equal to $24.6 \cdot (1 - 0.47)$W$= 13.04$W.

In order to verify the validity of the proposed correction method for measurements in cores with gap too, the above experimental procedure was repeated, this time, however, with the insertion of a gap of a total length l_g=0.88mm. If in the previous case considering $H(t)$ and $B(t)$ as sinusoidal quantities was a good approximation now the deviation is really negligible. The hysteresis loops are shown in Fig. 7.13 (loop (d) is the actual one here) and the relevant quantities in Table 7.2. In this case, the error when trying to predict the area of any of the loops in regard to any of them based on the proposed method typically remains below 15%.

In the above method of correcting the phase error in the determination of the hysteresis losses from the hysteresis loop area, $H(t)$ and $B(t)$ were considered sinusoidal quantities, the hysteresis loop was approximated with an ellipse and the whole method was based on the nearly linear relation between the area of the ellipse and the phase angle φ between H and B for low values of φ. In a simplified view we can approximate the shape of the loop as an oblong square. Then, through simple geometrical considerations we end up to the expression:

$$\frac{\Delta E_h}{E_h} = \frac{\Delta \phi}{90} \cdot \frac{H_{max}}{H_c} = \frac{\Delta \phi}{90} \cdot K_H \qquad (7.18)$$

from which we calculate the ΔE_h correction to the area of the hysteresis loop, given all the other quantities. After several measurements it has been shown that (7.18) applies only in those cases where the oblong square can be considered as a good approximation for the shape of the loop. However, this is only true when the core has a gap and the phase error between H and B remains very low (1-2 degrees maximum). Therefore, the correction method based on the graphs of Fig. 7.10 and Fig. 7.11 is more general, whereas (7.18) can be used for a quick correction calculation only in the special cases just mentioned.
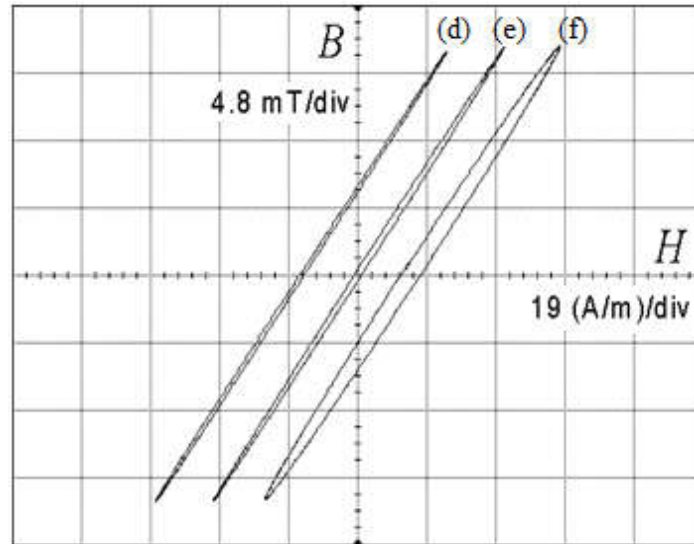
Figure 7.13: Experimental hysteresis loops of the 3C80 grade at 11kHz frequency for U-I core with gap l_g=0.88mm, (d) without phase error and (e), (f) with some given phase error $\Delta\varphi$>0.

TABLE 7.2

The values of $\Delta\varphi$, K_H and φ for the loops of Fig. 7.13, the P_{hyst} result for the hysteresis power loss of the used gapped U-I core and the calculated losses $P_{hyst,calc}$ according to the proposed method, when the reference loop is the one denoted with brackets. Symbol "x" denotes the cases where the corresponding values for F_{Eh} are outside the area of the graph of Fig. 7.11.

Loop	$\Delta\varphi$ (deg)	K_H	φ (deg)	P_{hyst} (mW)	$P_{hyst,calc}$[d] (mW)	$P_{hyst,calc}$[e] (mW)	$P_{hyst,calc}$[f] (mW)
(d)	0	67.9	0.844	91		80	100
(e)	0.55	40.8	1.40	134	150		153
(f)	2.25	18.5	3.12	370	x	x	

7.4. The effect of temperature on the loss measurements on magnetic components

7.4.1. General issues

It has already been reported that the eddy current losses, as well as the form of the hysteresis loop, are temperature dependent and therefore the same applies to total core losses (see eq. 2.9, 2.10 and 2.11) and magnetic permeability. It is therefore important, that in the

various experiments the temperature is known, while in most of the cases it is required to be constant. We have seen that when we want to consider the temperature of the magnetic component constant and equal to the ambient temperature, we try to make the measurement in a short time so as to prevent heating due to losses. In other cases the temperature should be recorded for at least three to four different temperatures, in order to accurately determine the value of the ratio $\Delta T / P_{tot}$, which, as explained in Appendix II, can be considered approximately constant. Even if it is not possible to measure the temperature some other way, with knowledge of the above ratio it may be approximately known if the magnetic component under test has reached thermal equilibrium and the total losses P_{tot} have been determined accurately. It is clarified that the core and winding temperatures in the thermal equilibrium are considered to be approximately equal (Appendix II). The best method to measure the temperature of a magnetic component is to place some thermocouples in the space between the windings and of course between the winding and the core. Surface measurements generally cannot be accurate, unless the thermocouple in contact with the magnetic component is covered with some thermal insulating coating, but without significantly altering the total thermal resistance of the magnetic component to the ambient (so as not to alter the actual operating conditions). Even so, surface measurements cannot substitute measurements at the interior of the assembly. The correct approach is to make measurements at the interior as well as at various points on the surface, in order to have an overall picture of the thermal equilibrium state. In recent years there is a wide use of optical means to record the infrared radiation, which give an excellent picture of the temperature distribution on the surface of the scanned object.

It should also be mentioned that a popular method to determine the temperature of the winding of a magnetic component is the measurement of its resistance at dc. A measurement at a known temperature is required before the operation startup and another one after the thermal equilibrium is reached, e.g. immediately after shutdown, to catch up with the oncoming temperature drop. The operating temperature of the magnetic component is known with an accuracy dependent on the accuracy of measuring the resistance change, if the resistance temperature factor of the conductor is known. As mentioned above, for magnetic component applications, we can assume with a small error that this is the temperature of not only the winding but also that of the core.

It is reminded that the temperature dependence of core losses is a function of the frequency and amplitude of the magnetic induction, different for each material. For some

narrow range of the above two quantities it may be given by an expression, such as (2.10) and (2.11), while for some specific values they are usually given by the manufacturer of the material in the form of some graph, as in Fig. 7.4. As for the temperature dependence of copper losses, it relates to the properties of copper and the frequency in a way that is analyzed in the following paragraph.

7.4.2. Calculation of winding ohmic resistance at high frequencies taking into account the temperature increase

Both during the normal operation of a magnetic component and during experiments to obtain test measurements it is inevitable that the temperature of the piece under test will increase due to losses. We have even seen that the faster the measurements are taken, the lower this increase is and for sufficiently fast processes the temperature can be considered practically unchanged. In any case, it is undoubtedly useful to know the effect of temperature on the variation of the ohmic resistance of a winding at various frequencies.

Chapter 3 summarized various approaches for calculating high frequency losses in the windings of magnetic components, while in Ch. 4 emphasis was given to the classic models of Butterworth, Dowell and Ferreira. It was found that, for circular cross-section conductors, Dowell's model is much more accurate than the other two. Basic parameter for expressing the dependence of the resistance factor F_R from the frequency in the various models is the ratio r/δ of the conductor radius to the skin depth or the ratio h/δ if it is a foil, with h in this case the foil thickness. However, the skin depth, according to eq. (1.3), is a function of the specific conductance σ, which in turn depends on the temperature T as follows:

$$\sigma = \left[\rho_{20}\left(1+\alpha_r\Delta T\right)\right]^{-1} \tag{7.19}$$

where ρ_{20} is the specific resistance at the reference temperature $T_{ref}=20^\circ$C, a_r is the resistance temperature coefficient and ΔT is the temperature rise above T_{ref}. Specifically for copper is $\rho_{Cu,20}=1.694\cdot10^{-8}\Omega$m and $a_{r,Cu}=3.93\cdot10^{-3}$grad^{-1}. The skin depth therefore increases with temperature and higher skin depth means that the current density is distributed over a larger area of the conductor cross-section. That is, since all other parameters remain unchanged, with increasing temperature the effective cross-section of the conductor becomes higher and the ohmic resistance may be lower (we will see that this is true only for some ranges of r/δ parameter). Of course, one should not forget about the change in the dimensions of the

conductor with the temperature, both in the current flow dimension and in the cross-section area. However, taking into account the value of the thermal expansion coefficient of copper ($\alpha_{e,Cu}$=16.6·10^{-6}grad^{-1}), after some simple operations, we find that the effect of temperature on the ohmic resistance due to change of the conductor dimensions (a decrease of resistance) is very low compared to the corresponding effect through the variation of specific conductance and consequently the skin depth at high frequencies. The steps one must follow to correctly calculate the coil resistance at specific temperature and frequency are the following:

(a) Calculate the skin depth δ_T for the given temperature from (1.3) and (7.19).

(b) On the basis of a reliable model for copper losses (e.g. Dowell's) calculate the value of the resistance factor F_R for the particular value of the ratio r/δ, that is, for r/δ_T.

(c) Multiply this value of F_R with the dc resistance calculated for the given temperature.

The dependence of the skin depth on temperature is plotted in Fig. 7.14, in which the temperature is a parameter with a step of 20°C, in a family of curves $\delta=\delta(f)$.

Steps (a) and (b) can be expressed mathematically by the quantity ΔF_{RT}:
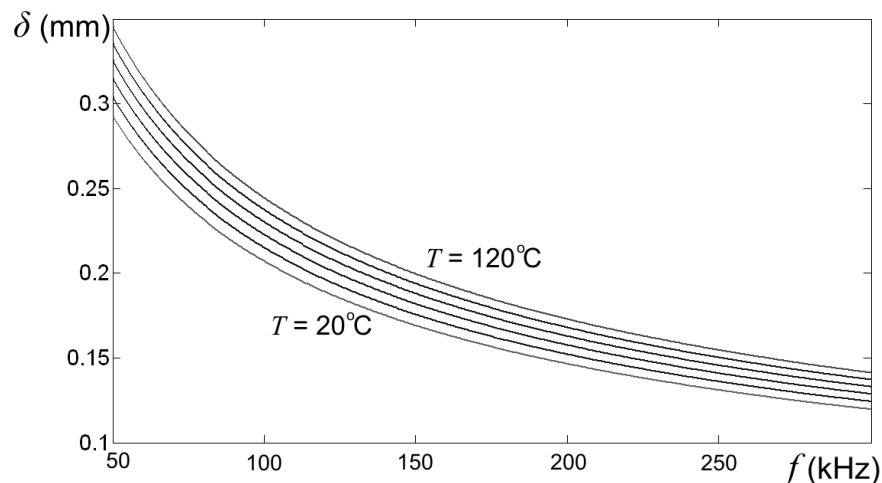
Figure 7.14: Dependence of the copper skin depth δ on the temperature T. The given curves correspond to temperatures 20, 40, 60, 80, 100 and 120°C.

$$\Delta F_{RT} = \frac{\left(1 + a_r \Delta T\right) \cdot F_R\left(\dfrac{r}{\delta_T}\right)}{F_R\left(\dfrac{r}{\delta_{20}}\right)} - 1 \tag{7.20}$$

which equals the correction to be made to the value of the resistance calculated when the temperature effect is ignored and is expressed as a fraction of the latter one. Thus, the actual value R_{ac}^T of the effective resistance at temperature T will be given by:

$$R_{ac}^T\left(\frac{r}{\delta_T}\right) = R_{dc}^{20} \cdot F_R\left(\frac{r}{\delta_{20}}\right) \cdot \left(1 + \Delta F_{RT}\right) \tag{7.21}$$

Attention should be paid to the fact that the skin depths δ_T and δ_{20} refer to the same frequency but at different temperatures (T and 20$^\text{o}$C respectively).

In Fig. 7.15(a) we see the resistance factor F_R as a function of r/δ, as calculated by Dowell's model, with parameter m the number of layers. This graph corresponds to a copper winding at T=20$^\text{o}$C and a layer filling factor η=0.75. From the analysis presented in Ch. 4 we know that for filling factor values higher than 0.75 Dowell's model has a very low error. Moreover, with a dashed line, the resistance factor is plotted for the case of a straight isolated conductor (skin effect).

In Fig. 7.15(b) is the temperature correction factor ΔF_{RT} corresponding to the F_R values obtained from Fig. 7.15(a) (i.e. for η=0.75), expressed as a percentage of them. The correction given in this figure refers to a typical increase in temperature by ΔT=50$^\text{o}$C above the reference temperature T_{ref}=20$^\text{o}$C, while Fig. 7.15(c) corresponds to ΔT=80$^\text{o}$C. Figure 7.16 shows the corresponding graphs for η=0.85.

We observe that at relatively low frequencies the increase of R_{dc} is predominant and the effective resistance increases (compared to the case T=20$^\text{o}$C). At higher frequencies there is an increase in the skin depth and thus the effective resistance decreases if m>1. Finally, for very high frequencies, an increase in resistance is again observed, which, above some value of r/δ is almost constant, independent of the number of layers, similar to that obtained for an isolated conductor with only the skin effect present.

However, maybe the most important remark is that in the frequency band where usually lies the basic harmonic of the current waveform of a magnetic component, that is, at frequencies for which r/δ is approximately equal to unity or even slightly lower, the resistance decreases by about 10–15% if $m>2$. For values of the number of layers m approaching 10 this decrease does not change significantly with increasing m and the same is true for $m>10$, as readily apparent from the relevant investigation. We also observe that by increasing the number of layers, the value of the r/δ ratio at which the minimum ΔF_{RT} appears is decreased. What is not obvious from Figures 15(b) and (c) and 16(b) and (c) is the slight shift of this minimum toward higher r/δ values when the filling factor η increases. Finally, it should be noted that the change in the effective resistance is more significant as the temperature increases, but in practical applications magnetic component temperatures above $80^{\mathrm{o}}\mathrm{C}$ are generally not expected to occur.
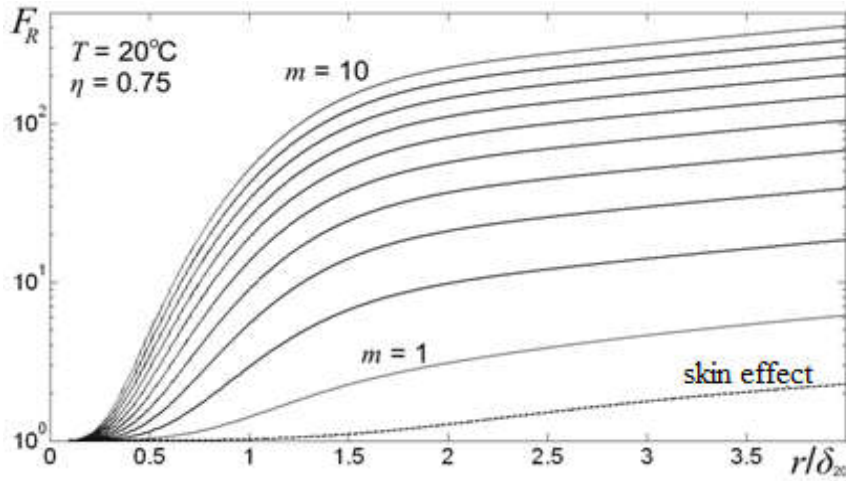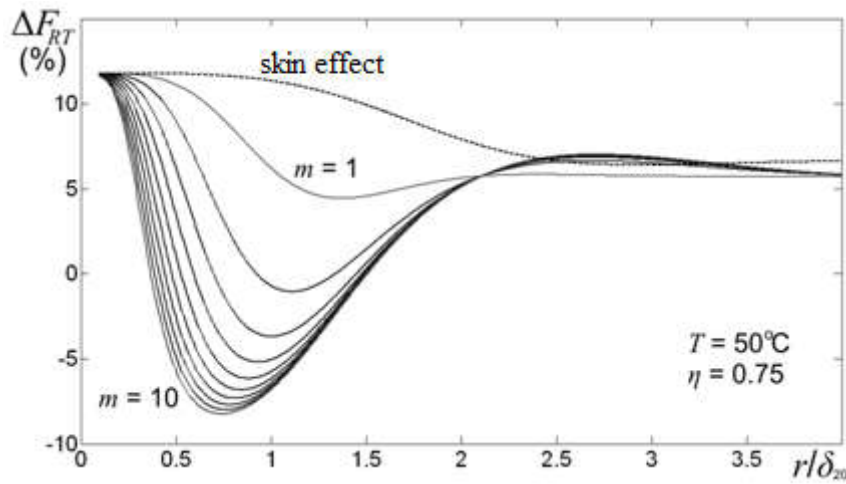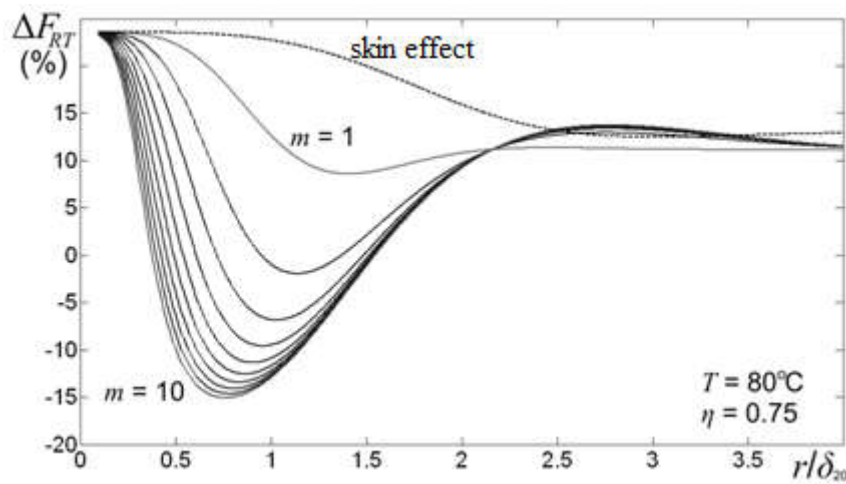
Figure 7.15: The result of Dowell's model for F_R considering that $T=20^{\circ}$C (a), as well as the correction to be made at these values for temperatures $T=50^{\circ}$C (b) and $T=80^{\circ}$C (c), when $\eta=0.75$.
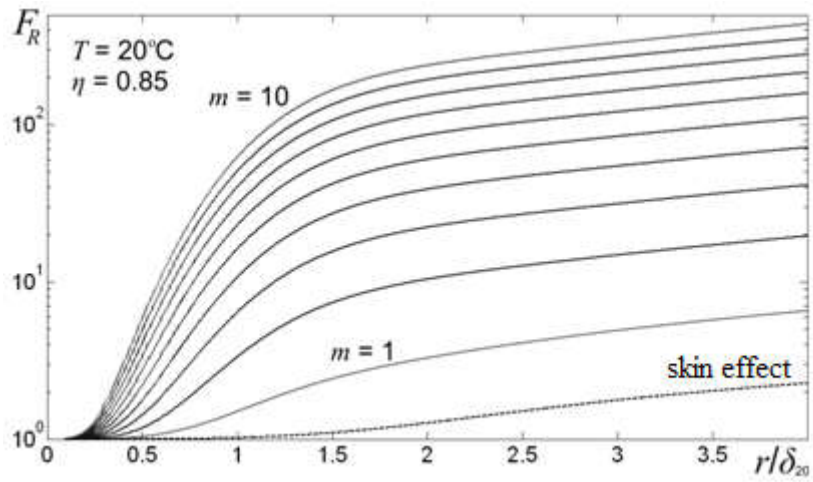
(a)
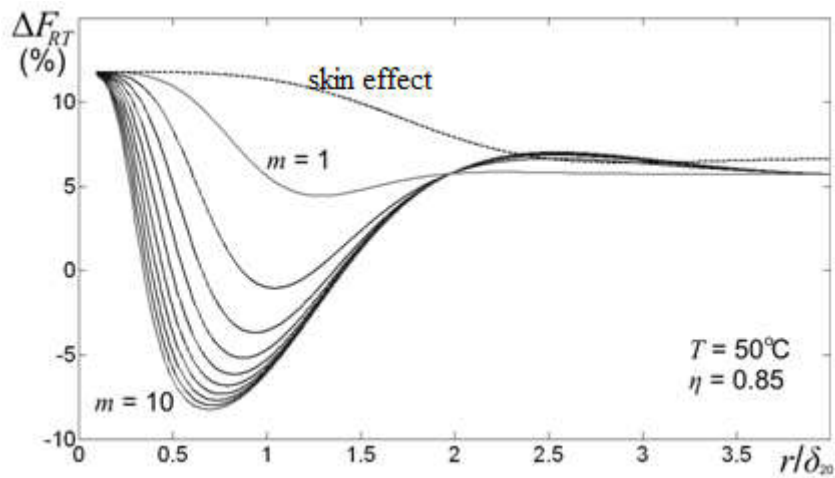
(b)
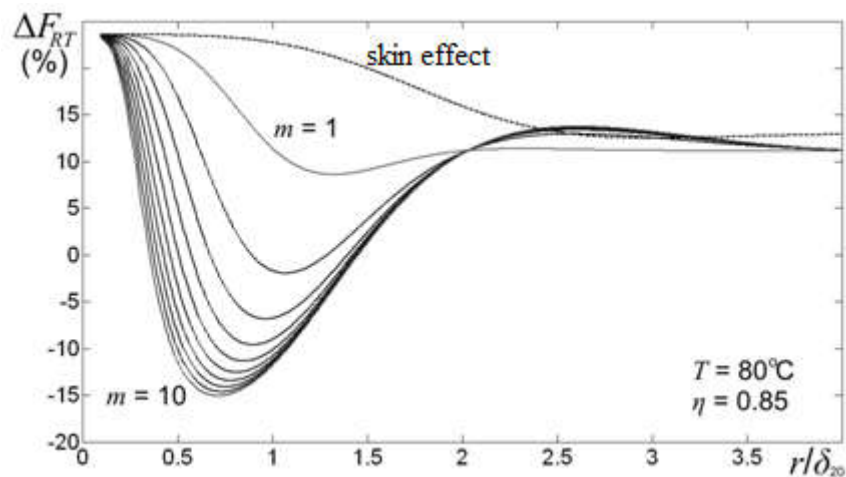
(c)

Figure 7.16: The result of Dowell's model for F_R considering that $T=20°C$ (a), as well as the correction to be made to these values for temperatures $T=50°C$ (b) and $T=80°C$ (c), when $\eta=0.85$.

CHAPTER 8

RECAPITULATION – CONCLUSIONS

8.1. Recapitulation

This dissertation deals with a number of issues directly or indirectly related to the optimization of the design of magnetic components for power electronic applications and the effort to increase the positive factors, with special attention always given to the increase of the efficiency and power density. In order to make the minimization of losses feasible, the appropriate theoretical and practical tools are required for their accurate determination in existing magnetic components, but also for their pre-calculation prior to component fabrication, during the design process. Equally important is the ability to determine critical quantities related to parameters necessary for the application of various models found in the international literature.

Fundamental objectives of the dissertation are the formulation of a new model for the precise determination of high frequency copper losses in magnetic component windings with random arrangement of conductors, the analysis of some two-dimensional effects (edge effect in layered windings and proximity effect in windings with hexagonal conductor arrangement) that occur at high frequencies and contribute significantly to the determination of the effective resistance, as well as the development of a device and a methodology for taking reliable experimental measurements on magnetic components. Of course, an important goal too, but at the same time a necessary background for the achievement of the other goals, is the analysis of the literature related to the issue of losses in magnetic components.

At the beginning of the dissertation there is an introductory presentation of the physical effects that take place in magnetic components. In a simple and comprehensive way the fundamental principles governing the development of eddy currents in conductors under the action of a changing magnetic flux are described, as well as the way that this leads to the appearance of the skin and proximity effects in conductors that carry high-frequency currents. Furthermore, the hysteresis effect in ferromagnetic materials is described qualitatively. In the following are listed, as found in literature, various attempts to describe

231

and quantify the impact that these effects have, with special emphasis on the issue of the power losses they cause during the operation of magnetic components. The classic models for the magnetic hysteresis and the general forms of the expressions commonly used to calculate the core losses are listed, as well as the classic models for calculating the copper losses, but also some different types of approaches, which are based either on analytical solutions or on investigation with finite element software.

Then, with finite element software as the main tool, a detailed investigation is made of the issues related to copper losses in windings that consist of successive layers of conductors. The application limits of the classic models are fully clarified, the deviations of their results from those of the simulations are presented and the reasons for the failure of these models to correctly predict the losses for high frequencies and low values of the filling factor are explained. The edge effect in layered windings is investigated and the increase in losses at the fundamental operating frequency of the magnetic components as well as their decrease at the harmonic frequencies is quantified, while the extent that this effect takes place in the windings as a function of the various geometric parameters and frequency is presented in a descriptive way. Finally, the issue of winding losses is investigated in the case when the round cross-section wires comprising them are positioned in a hexagonal fit, instead of the typically examined square fit that we find in the international literature.

Consequently, a new model is proposed for the calculation of copper losses in windings of magnetic components that present a random arrangement of their conductors. The proposed expression results from the statistical analysis of a large amount of result data from simulations with software that applies the finite element method. The three parameters of the model are directly known to the designer of the magnetic component and hence its application can be implemented very easily by simply replacing their values in the given expression. The fact that the selected geometric parameters for the expression of losses are constant quantities that are easily measurable with great accuracy is brought out as an important advantage of the model that leads to the determination of the final result with very small margins of uncertainty. For the designer who wants to make even easier calculations, oriented just to the fundamental operating frequency range of a magnetic component, an approximate low-frequency expression is provided which also, indirectly demonstrates the physical consistency of the new model in this frequency range. Experimental confirmation of the proposed model is performed for winding geometries, such as those commonly found in industrial and laboratory applications.

Then, in order to offer through the dissertation a complete proposal for reliable measurements, we seek for a way to achieve excitation of magnetic components with high frequency sinusoidal voltage. The purpose of this search is to bypass purchase of commercial devices, which, in addition to a number of technical disadvantages, have a very high cost. After an overview of the topologies that can drive an LC circuit to forced resonance conditions, the current-fed push-pull topology is selected as the most appropriate. The specific converter that is finally proposed is analyzed in depth, in terms of its operating conditions, as they are determined by the values of some constructive parameters, which are related to both the oscillator power circuit and the electronic control circuit. The analysis shows that the values of these parameters are of critical and interrelated importance, both for the expansion of the range of possible operating frequencies, as well as for the reduction of the harmonic content of the output waveform and for the possibility to maximize the output power. The converter manufactured in the present dissertation makes feasible the supply of a magnetic component with sinusoidal voltages of 1MHz frequency and amplitude of several hundred volts, with a harmonic content that is practically negligible.

Finally, there is a presentation of some ways to perform measurements on magnetic components and determine their losses, as well as the values of various parameters related to the magnetic properties of the core. Since phase errors during the record of the voltage and current waveforms are unavoidable, with the most important one that of the current recording, some methods of restraining them are proposed, as well as methods to correct the result when the quantity measured is the area of the hysteresis loop. For those cases where the temperature of the magnetic component varies, it is explained that, at high frequencies, the ohmic resistance of the windings may appear either increased or decreased due to an increase in temperature. Furthermore, the appropriate equations are listed for an easy correction of the value of the effective resistance when it is calculated by any model for copper losses at high frequencies, taking into account the variation in temperature.

8.2. Contribution of the dissertation – original elements

The contribution of the present work in the field of optimizing the design of magnetic components in power electronic converter applications is summarized in the following points:

1. A new analytical model is developed for the accurate calculation of copper losses at high frequencies for magnetic components the windings of which present a random arrangement of the conductors of which they are comprised. A key feature of the new experimentally confirmed model is its simplicity, both in the formulation of the final expression and in the practical determination of its three parameters.

2. Through the detailed investigation of the effect of selected geometric parameters, as well as of the frequency, on ohmic losses of layered magnetic component windings, the accuracy of the results and the application limits of the classic models, on the basis of which these losses are estimated, are determined.

3. The edge effect in layered windings that consist either of copper foils or round cross-section conductors and carry high frequency currents is analyzed and its impact on the total winding resistance is quantified.

4. For windings that consist of round cross-section conductors the effect of the hexagonal conductor arrangement on the effective resistance is analyzed, taking into account the filling factor.

5. The design and assembly of a resonant converter fed by a current source is performed. The converter is suitable for use as a high frequency sinusoidal voltage source for magnetic components, in order to support measurements on them. The result of the theoretical and experimental study of the converter is the appropriate dimensioning of the components in the two circuits (power and control), so that it is possible to optimize its performance, with maximum amplitude and minimum harmonic content of the output voltage, as well as maximum possible operation frequency range. The operation of the converter is achieved at frequencies exceeding 1MHz, satisfying at the same time the former requirements of minimum harmonic content and maximum output voltage amplitude. The operation of the converter is analyzed in depth, both theoretically and experimentally and a series of technical suggestions are provided related to the implementation of its assembly.

6. The various error factors that alter the result of the loss measurements on magnetic components at high frequencies are studied in detail. Some methodologies are proposed for the correction of the result in the determination of the hysteresis losses, when there is a phase error in the acquisition of the waveforms of the magnetic intensity and magnetic induction, as well as in the determination of the effective winding resistance when there is a variation in temperature.

Generally, it can be stated that, through the results and conclusions contained in this work, on the one hand the promotion of scientific knowledge on the subject of losses in magnetic components is achieved and on the other hand a complete book is provided, which contributes significantly to the support of the optimal design of magnetic components in power electronic applications.

REFERENCES

[1]. C. Steinmetz, "On the law of hysteresis", *Am. Inst. of El. Eng. Trans.*, vol. 9, pp. 3–64, 1892, (re-published in *IEEE Proc.*, vol. 72, No 2, 1984).

[2]. J. Maxwell, "A treatise on electricity and magnetism", vol. 2, Oxford – Clarendon Press, art. 689, 1904.

[3]. A. Field, "Eddy currents in large slot-wound conductors", *Proc. AIEE*, vol. 24, pp. 761–788, 1905.

[4]. A. Press, "Resistance and reactance of massed contactors", *Physical Review*, vol. 8, No 4, pp. 417-422, 1916.

[5]. S.Butterworth, "Eddy current losses in cylindrical conductors, with special applications to the alternating current resistances of short coils", *Phil. Trans. of the Royal Society of London*, vol. 222, pp. 57–100, 1922.

[6]. S. Butterworth, "On the alternating current resistance of solenoid coils", *Proc. of the Royal Society of London*, vol. 107, No 744, pp. 693–715, Apr. 1925.

[7]. S.Butterworth, "Effective resistance of inductance coils at radio frequencies", *Exp. Wireless and Wireless Eng.*, vol. 3, p. 203, April 1926, p. 302, May 1926, p. 417, July 1926, p. 483, Aug. 1926.

[8]. F. Preisach, "Uber die magnetische nachwirkung", *Zeitsfur Phys.*, vol. 94, pp. 277–302, 1935.

[9]. E. Bennet, S. Larson, "Effective resistance to alternating currents of multilayer windings", *Trans. of American Inst. of Electr. Engineering*, vol. 59, pp. 1010–1017, 1940.

[10]. R. Medhurst, "H.F. resistance and self-capacitance of single layer solenoids", *Wireless Engineer*, vol. 24, pp. 35-43, Febr. 1947 and pp. 80–92, March 1947.

[11]. A. Sommerfeld, *Electrodynamics*, New York, Academic Press, art. 21, 1952.

[12]. P. Dowell, "Effects of eddy currents in transformer windings", *Proc. IEE*, vol. 113, No 8, pp. 1387–94, Aug. 1966.

[13]. A. Globus, "Universal hysteresis loop for soft ferromagnetic material", *Proc. Europ. Physical Society Conference on Soft Magnetic material*, vol. 2, p. 233, 1975.

[14]. J. Jongsma, "Minimum-loss transformer windings for ultrasonic frequencies", *Philips Electr. Appl. Bulletings*, vol. 35, No 3, pp. 146–163, 1978.

[15]. M. Perry, "Multiple layer series connected winding design for minimum losses", *IEEE Trans. Power App. Syst.*, vol. PAS-98, No 1, pp. 116–23, Jan/Feb 1979.

[16]. M. Schlotterbeck, "Permeability and power losses in ferrite cores on sinusoidal or square wave conditions up to 1 MHz", *Proc. PCI81*, 1981, pp. 37–46.

[17]. L. Bracke, "Optimizing the configuration of ferrite-cored transformers for advanced switched-mode magnetics", *Proc. Powercon 9*, 1982, vol. C-6, pp. 1–9.

[18]. L. Bracke, "Optimizing the power density of ferrite-cored transformers", *Proc. PCI*, Sept. 1982, pp. 56–63.

[19]. W. Rippel, C. McLyman, "Design techniques for minimizing the parasitic capacitance and leakage inductance of switched-mode power transformers", *Proc. Powercon 9*, A1, 1982, pp. 1–12.

[20]. P. Venkatraman, "Winding eddy current losses in switch mode power transformers due to rectangular wave currents", *Proc. Powercon 11*, 1984, Venture, USA, Section A-1, pp. 1–11.

[21]. L. Bonte, J. Campenhout, "A simplified H.F. network representation of power pulse transformers for switch mode dc–dc converters and dc–ac inverters", *Proc. EPE*, 1985, pp. 1.35–1.42.

[22]. G. Bertotti, "Physical interpretation of eddy current losses in ferromagnetic materials", *Journal of Applied Physics*, vol. 57, No 6, pp. 2110–2126, March 1985.

[23]. G. Bruning, "A comparative introduction of a new high voltage resonant oscillator", *Proc. APEC86*, April 1986, New Orleans, USA, pp. 76–78.

[24]. B. Carsten, "High frequency conductor losses in switchmode magnetics", *Proc. HFPC Conf.*, May 1986, Virginia Beach, USA, pp. 155–176.

[25]. M. Ivankovic, "Optimum SMPS transformer design", *Proc. PCI*, June 1986, pp. 183–188.

[26]. D. Jiles, D. Atherton, "Theory of ferromagnetic hysteresis", *J. Magnetism Magn. Mat.*, vol. 61, pp. 48–60, Sept. 1986.

[27]. G. Bertotti, "General properties of power losses in soft ferromagnetic materials", *IEEE Trans. Magn.*, vol. 24, pp. 621–630, 1988.

[28]. D. Conroy, G. Pierce, "Measurement techniques for the design of high frequency SMPS transformers", *Proc. APEC 88*, Feb. 1988, New Orleans, USA, pp. 341–351.

[29]. J. Vandelac, P. Ziogas, "A novel approach for minimizing high-frequency transformer copper losses", *IEEE Trans. Power Electr.*, vol. 3, No 3, pp. 266–277, July 1988.

[30]. T. Nakata, N. Takahashi, K. Fujiwara, M. Nakano, K. Matsubara, "Iron losses of silicon steel under square wave voltage excitation", *Physica Scripta*, vol. 39, pp. 645-647, 1989.

[31]. E. Visser, J. Roelofsma, G. Aaftink, "Domain wall loss and rotational loss in high frequency power ferrites", *Proc. ICF5*, 1989, India, pp. 605-609.

[32]. M. Begger, J. Laval, F. Kools, J. Roelofsma, "Relations between grain boundary structure and hysteresis losses in Mn-Zn ferrites for power applications", *Proc. ICF5*, 1989, India, pp. 619-624.

[33]. J. Keradec, R. Feuillet, J. Perard, "Eddy current losses and H.F. modeling of SMPS transformer", *Proc. EPE*, 1989, pp. 963-965.

[34]. A. Goldberg, J. Kassakian, M. Schlecht, "Finite element analysis of copper loss in 1-10 MHz transformers", *IEEE Trans. Power Electr.*, vol. 4, No 2, pp. 113–123, Jan. 1989.

[35]. A. Goldberg, J. Kassakian, M. Schlecht, "Issues related to 1-10 MHz transformer design", *IEEE Trans. Power Electr.*, vol. 4, No 1, pp. 157–167, Apr. 1989.

[36]. V. Niemela, *et. al.*, "Calculating the short-circuit impedances of a multiwinding transformer from its geometry", *Proc. PESC89*, June 1989, Milwaukee, Wisc., USA, pp. 607–616.

[37]. P. Evans, K. Al-Shara, "Losses in foil-wound secondaries in high-frequency transformers", *IEEE Trans. Magn.*, vol. 25, No 4, pp. 3125–3132, July 1989.

[38]. J. Thottuvelil, T. Wilson, H. Owen, "High-frequency measurements techniques for magnetic cores", *IEEE Trans. Power Electr.*, vol. 5, No 1, pp. 41–53, Jan. 1990.

[39]. F. Fiorillo, A. Novikov, "An improved approach to power loss in magnetic laminations under nonsinusoidal induction waveform", *IEEE Trans. Magn.*, vol. 26, No 5, pp. 2904–2910, Sept. 1990.

[40]. J. Ferreira, "Experimental evaluation of losses in magnetic components for power converters", *IEEE Trans. Ind. Appl.*, vol. 27, No 2, pp. 335–339, March 1991.

[41]. J. Keradec, E. Laveuve, J. Roudet, "Multipolar development of vector potential for parallel wires. Application to the study of eddy current effects in transformer windings", *IEEE Trans Magn.*, vol 27, No 5, pp. 4242–4245, Sept. 1991.

[42]. F. Vadja, E. Torre, "Measurement of output dependent Preisach functions", *IEEE Trans. Magn.*, vol. 27, pp. 4757–4762, Nov. 1991.

[43]. G. Bertotti, "Dynamic generalization of the scalar Preisach model for hysteresis", *IEEE Trans. Magn.*, vol. 28, pp. 2599–2601, Sept. 1992.

[44]. J. Zhu, S. Hui, V. Ramsden, "Discrete modeling of magnetic cores including hysteresis, eddy current and anomalous losses", *Proc. IEE-A*, vol. 140, No 4, pp. 317–322, July 1993.

[45]. W. Hurley, D. Wilcox, "Calculation of leakage inductance in transformer windings", *IEEE Trans. Power Electr.*, vol. 9, pp. 121–126, Jan. 1994.

[46]. N. Dai, F. Lee, "Edge effect analysis in a high-frequency transformer", *Proc. PESC94*, June 1994, Taipei, Taiwan, vol. 2, pp. 850–855.

[47]. J. Ferreira, "Improved analytical modeling of conductive losses in magnetic components", *IEEE Trans. Power Electr.*, vol. 9, No 1, pp. 127–131, Jan. 1994.

[48]. B. Carsten, "Calculating skin and proximity effect conductor losses in switchmode magnetics", *Proc. PCIM'95*, 1995, Nurnberg, Germany.

[49]. M. Bartoli, N. Noferi, A. Reatti, M. Kazimierczuk, "Modelling winding losses in high-frequency power inductors", *Journal of Circuits, Systems and Computers*, vol.5, No 4, pp. 607–626, 1995.

[50]. A. Lofti, F. Lee, "Two-dimensional skin effect in power foils for high-frequency application", *IEEE Trans. Magn.*, vol. 31, No 2, pp. 1003–1006, March 1995.

[51]. A. Sinclair, J. Ferreira, "Optimum shape for ac foil conductors", *Proc. PESC95*, June 1995, Atlanta, USA, pp. 1064–1069.

[52]. M. Amar, R. Kaczmerek, "A general formula for prediction of iron losses under nonsinusoidal voltage waveform", *IEEE Trans. Magn.*, vol. 31, No 5, pp. 2504–2509, Sept. 1995.

[53]. J. Zhu, S. Hui, V. Ramsden, "A dynamic equivalent circuit model for solid magnetic cores for high switching frequency operations", *IEEE Trans. Power Electr.*, vol. 10, No 6, pp. 791–795, Nov. 1995.

[54]. J. Fuzi, "On the Bessel functions occurring in eddy current problems", in *Optimization of electric and electronic equipment*, Brasov, pp. 69–72, 1996.

[55]. M. Temneanu, T. Balan, D. Balan, "Behavioral study of magnetic materials", in*Optimization of electric and electronic equipment*, Brasov, pp. 247–250, 1996.

[56]. O. Bottauscio, M. Chiampi, M. Repetto, "A finite element solution for periodic eddy current problems in hysteretic media", *J. Magnetism Magn. Mater.*, vol. 160, No 1, pp. 96–97, 1996.

[57]. N. Schmidt and H. Guldner, "A simple method to determine dynamic hysteresis loops of soft magnetic materials", *IEEE Trans. Magn.*, vol. 32, No 2, pp. 489–496, March 1996.

[58]. M. Bartoli, N. Noferi, A. Reatti, M. Kazimierczuk, "Modeling litz wire winding losses in high frequency power inductors", *Proc. PESC96*, June 1996, Baveno, Italy, vol. 2, pp. 1990–1996.

[59]. R. Prieto, J. Cobos, O. Garcia, R. Asensi, J. Uceda, "Optimizing the strategy of the transformer in a flyback converter", *Proc. PESC96*, June 1996, Baveno, Italy, pp. 1456–1462.

[60]. G. Skut, F. Lee, "Characterization of dimensional effects in ferrite-core magnetic devices", *Proc. of PESC96*, June 1996, Baveno, Italy, pp. 1435–1440.

[61]. A. Maxim, D. Andreu, J. Boucher, "A new analog behavioral SPICE macromodel of magnetic components", *Proc. ISIE97*, 1997, pp. 183–188.

[62]. I. Mohammed, B. Hashemy, M. Tawffik, "A Fourier descriptor model of hysteresis loops for sinusoidal and distorted waveforms", *IEEE Trans. Magn.*, vol. 33, No 1, pp. 686–691, Jan. 1997.

[63]. A. Boglietti, M. Lazzari, M. Pastorelli, "About the choice of the reference magnetic quantity in presence of non sinusoidal waveforms", *IEEE Trans. Magn.*, vol. 33, No 5, pp. 4002–4004, Sept. 1997.

[64]. A. Maxim, D. Andreu, J. Boucher, "A novel behavioral method of SPICE macromodeling of magnetic components including the temperature and frequency dependencies", *Proc. APEC98*, 1998, Anaheim, USA, pp. 393–399.

[65]. I. Wallace, N. Kutkut, S. Bhattacharya, D. Divan, D. Novotny, "Inductor design for high-power applications with broad spectrum excitation", *IEEE Trans. Power Electr.*, vol. 13, No 1, pp. 202–208, Jan. 1998.

[66]. K. Carpenter, "Simple models for dynamic hysteresis which add frequency-dependent losses to static models", *IEEE Trans. Magn.*, vol. 34, No 3, pp. 619–622, May 1998.

[67]. J. Tellinen, "A simple scalar model for magnetic hysteresis", *IEEE Trans. Magn.*, vol. 34, No 4, pp. 2200–2206, Jul. 1998.

[68]. W. Hurley, W. Wolfe, J. Breslin, "Optimized transformer design: inclusive of high frequency effects", *IEEE Trans. Power Electr.*, vol 13, No 4, pp. 651–659, Jul. 1998.

[69]. L. Dupre, G. Bertotti, J. Melkebeek, "Dynamic Preisach model and energy dissipation in soft magnetic materials", *IEEE Trans. Magn.*, vol. 34, No 4, pp. 1168–1170, Jul. 1998.

[70]. F. Robert, P. Mathys, "Ohmic losses calculation in SMPS transformers: numerical study of Dowell's approach accuracy", *IEEE Trans. Magn.*, vol 34, No 4, pp. 1255–1257, Jul. 1998.

[71]. N. Kutkut, D. Divan, "Optimal air-gap design in high-frequency foil windings", *IEEE Trans. Power Electr.*, vol. 13, No 5, pp. 942–949, Sept. 1998.

[72]. N. Kutkut, "A simple technique to evaluate winding losses including two-dimensional edge effects", *IEEE Trans. Power Electr.*, vol. 13, No 5, pp. 950–958, Sept. 1998.

[73]. A. Schellmanns, K. Berrouche, J. Keradec, "Multiwinding transformers: a successive refinement method to characterize a general equivalent circuit", *IEEE Trans. Instrum. Meas.*, vol. 47, No 5, pp. 1316–1321, Oct. 1998.

[74]. C. Sullivan, "Optimal choice for number of strands in a litz-wire transformer winding", *IEEE Trans. Power Electr.*, vol 14, No 2, pp. 283–291, March 1999.

[75]. L. Dupre, O. Bottauscio, M. Chiampi, M. Repetto, J. Melkebeek, "Modeling of electromagnetic phenomena in soft magnetic materials under unidirectional time periodic flux excitations", *IEEE Trans. Magn.*, vol. 35, No 5, pp. 4171–4184, Sept. 1999.

[76]. J. Lavers, V. Bolborici, "Loss comparison in the design of high frequency inductors and transformers", *IEEE Trans. Magn.*, vol. 35, No 5, pp. 3541–3543, Sept. 1999.

[77]. J. Brauer, J. Ruehl, "Finite element modeling of power electronic circuits containing switches attached to saturable magnetic components", *IEEE Trans. En. Conv.*, vol. 14, No. 3, pp. 589–594, Sept. 1999.

[78]. J. Pleite, R. Prieto, R. Asensi, J. Cobos, E. Olias, "Obtaining a frequency-dependent and distributed-effects model of magnetic components from actual measurements", *IEEE Trans. Magn.*, vol. 35, No 6, pp. 4490–4502, Nov. 1999.

[79]. W. Hurley, E. Gath, J. Breslin, "Optimizing the ac resistance of multilayer transformer windings with arbitrary current waveforms", *IEEE Trans. Power Electr.*, vol 15, No 2, pp. 369–376, March 2000.

[80]. F. Liorzou, B. Phelps, D. Atherton, "Macroscopic models of magnetization", *IEEE Trans. Magn.*, vol. 36, No 2, pp. 418–427, March 2000.

[81]. F. Tourkmani, P. Viarouge, "Accurate analytical model of winding losses in round litz wire winding", *IEEE Trans. Magn.*, vol. 37, No 1, pp. 538–543, Jan. 2001.

[82]. B. Phelps, D. Atherton, "Pinning and minor loops in an inclusive model of ferromagnetic hysteresis", *IEEE Trans. Magn.*, vol. 37, No 1, pp. 517–521, Jan. 2001.

[83]. C. Sullivan, "Computationally efficient winding loss calculation with multiple windings, arbitrary waveforms, and two-dimensional or three-dimensional field geometry", *IEEE Trans. PowerElectr.*, vol 16, No 1, pp. 142–150, Jan. 2001.

[84]. E. Tatakis, N. Polyzos, "A novel method oriented to evaluate the real characteristics of practical boost zero-voltage switching quasi-resonant converters", *EPE Journal,* vol. 11, No 2, pp. 25–33, May 2001.

[85]. R. Garcia, J. Carrasco, J. Espi, E. Dede, J. Castello, "Modeling and simulation of non linerar magnetic cores at high frequencies using PSpice", *EPE Jounal*, vol. 11, No 2, pp. 13–22, May 2001.

[86]. P. Blanken, "A lumped winding model for use in transformer models for circuit simulation", *IEEE Trans. Power Electr.*, vol. 16, No 3, pp. 445–460, May 2001.

[87]. F. Robert, P. Mathys, "A closed form formula for 2-D ohmic losses calculation in SMPS transformer foils", *IEEE Trans. Power Electr.,* vol 16, No 3, pp. 437–444, May 2001.

[88]. N. Polyzos , E. Tatakis , A. Safacas, "A novel method oriented to evaluate the real characteristics of practical buck zero-voltage switching quasi-resonant converters", *IEEE Trans. Power Electr.*, vol. 16, No 3, pp.316–324, May 2001.

[89]. M. Albach, H. Robmanith, "The influence of air gap size and winding position on the proximity losses in high frequency transformers", *Proc. PESC01*, June 2001,Vancouver, Canada, pp. 1485–1490.

[90]. J. Hu, C. Sullivan, "AC resistance of planar power inductors and the quasidistributed gap technique", *IEEE Trans. Power Electr.*, vol. 16, No 4, pp. 558–567, Jul. 2001.

[91]. F. Robert, P. Mathys, J. Schauwers, "Eddy current losses in SMPS transformers: a full-frequency-range review of 2D effects inside the windings", *Proc. EPE01*, Sept. 2001, Graz, Austria, paper on CD.

[92]. M. Prieto, J. Lopera, A. Pernia, J. Martin, F. Nuno, "Arrangement of conductors to obtain turn-coupling in thick-film integrated inductors for power converters", *Proc. EPE01*, Sept. 2001, Graz, Austria, paper on CD.

[93]. E. Waffenschmidt, B. Ackermann, "Size advantage of coreless transformers in the MHz range", *Proc. EPE01*, Sept. 2001, Graz, Austria, paper on CD.

[94]. J. Li, T. Abdallah, C. Sullivan, "Improved calculation of core loss with nonsinusoidal waveforms", *Proc. IAS01*, Sep. 2001, pp. 2203–2210.

[95]. F. Robert, "Eddy current losses: a theoretical discussion of Dowell's layer copper factor", *EPE Journal*, vol. 12, No 3, pp. 9–15, Aug. 2002.

[96]. F. Robert, "A theoretical discussion about the layer copper factor used in winding losses calculation", *IEEE Trans. Magn.,* vol. 38, No 5, pp.3177–3179, Sept. 2002.

[97]. C. Larouci, J. Keradec, J. Ferrieux, L. Gerbaud, J. Roudet, "Copper losses of flyback transformer: search for analytical expressions", *IEEE Trans. Magn.*, vol. 39, No 3, pp. 1745–1748, May 2003.

[98]. A. Podoltsev, I. Kucheryavaya, B Lebedev, "Analysis of effective resistance and eddy-current losses in multiturn winding of high-frequency magnetic components", *IEEE Trans. Magn.*, vol. 39, No 1, pp. 539–548, Jan. 2003.

[99]. X. Nan, C. Sullivan, "Simplified high-accuracy calculation of eddy current loss in round-wire windings", *Proc. PESC04*, June 2004, Aachen, Germany, pp. 873–879.

[100]. G. Lefevre, H. Chazal, J. Perrieux, J. Roudet, "Application of Dowell method for nanocrystalline toroid high frequency transformers", *Proc. PESC04*,June 2004, Aachen, Germany, pp. 899–904.

[101]. Y. Han, W. Eberle, Y. Liu, "New measurement methods to characterize transformer core loss and copper loss in high frequency switching mode power supplies", *Proc. PESC04*, June 2004, Aachen, Germany, pp. 1695–1701.

[102]. W. Roshen, "Winding loss from an air-gap" *Proc. PESC04*,June 2004, Aachen, Germany, vol.2, pp. 1724–1730.

[103]. A. V. den Bossche, V. Valchev, G. Georgiev, "Measurement and loss model of ferrites with non-sinusoidal waveforms", *Proc. PESC04*, June 2004, Aachen, Germany, pp. 4814–4818.

[104]. T. Mthombeni, P. Pillay, "Core losses in motor laminations exposed to high-frequency or nonsinusoidal excitation", *IEEE Trans. Ind. Appl.*, vol 40, No 5, pp. 1325–1332, Sept. 2004.

[105]. K. Laouamri, J. Keradec, J. Ferrieux, S. Catellani, "Design and identification of an equivalent circuit for an LCT component: inventory and representation of losses", *IEEE Trans. Instrum. Meas.*, vol. 53, No 5, pp. 1409–1417, Oct. 2004.

[106]. X. Nan, C. Sullivan, "A two-dimensional equivalent complex permeability model for round-wire windings", *Proc. PESC05*, June 2005, Recife, Brazil, pp. 613–618.

[107]. F. Robert, P. Mathys, B. Valearts, J. Schauwers, "Two-dimensional analysis of the edge effect field and losses in high-frequency transformer foils", *IEEE Trans. Magn.*, vol. 41, No 8, pp. 2377–2383, Aug. 2005.

[108]. T. Brennan, "Proximity-effect loss calculations for a discontinuous-mode PFC inductor utilizing a multifilar winding construction", *IEE Proc. –Electr. Power Appl.*, vol. 152, No 5, pp. 1101–1105, Sept. 2005.

[109]. F. Robert, J. Sprooten, P. Mathys, "Eddy current losses in SMPS transformers round wire windings: a semi-analytical closed-form formula", *Proc. EPE05*, Sept. 2005, Dresden, Germany, paper on CD.

[110]. C. Wang, O. Stielau, G. Covic, "Design considerations for a contactless electric vehicle battery charger", *IEEE Trans. Ind. Electr.*, vol. 52, No 5, pp. 1308–1314, Oct. 2005.

[111]. X. Nan, C. Sullivan, "An equivalent complex permeability model for litz-wire windings", *Proc. IAS05*, Oct. 2005, Hong Kong, vol. 3, pp. 2229–2235.

[112]. M. Borage, S. Tiwari, S. Kotaiah, "Analysis and design of an LCL-T resonant converter as a constant current power supply", *IEEE Trans. Ind. Electr.*, vol. 52, No 6, pp. 1547–1554, Dec. 2005.

[113]. F. Forest, S. Faucher, J. Gaspard, D. Montloup, J. Huselstein, C. Joubert, "Frequency synchronized resonant converters for the supply of multiwinding coils in induction cooking appliances", *IEEE Trans. Ind. Electr.*, vol. 54, No 1, pp. 441–452, Feb. 2007.

[114]. S. Lee, A. Pfaelzer, J. Wyk, "Comparison of different designs of a 42V/14V dc/dc converter regarding losses and thermal aspects", *IEEE Trans. Ind. Appl.*, vol. 43, No 2, pp. 520–530, March 2007.

[115]. C. Xiao, G. Chen, W. Odendaal, "Overview of power loss measurement techniques in power electronics systems", *IEEE Trans. Ind. Appl.*, vol. 43, No 3, pp. 657–664, May 2007.

[116]. R. Casanueva, F. Azcondo, C. Branas, "Output current sensitivity analysis of the LC_pC_s resonant inverter: current-source design criteria", *IEEE Trans. Ind. Electr.*, vol. 54, No 3, pp. 1560–1568, June 2007.

[117]. M. Youssef, P. Jain, "Series-parallel resonant converter in self-sustained oscillation mode with the high-frequency transformer-leakage-inductance effect: analysis, modeling and design", *IEEE Trans. Ind. Electr.*, vol. 54, No 3, pp. 1329–1341, June 2007.

[118]. Y. Han, W. Eberle, Y. Liu, "A practical copper loss measurement method for the planar transformer in high-frequency switching converters", *IEEE Trans. Ind. Electr.*, vol. 54, No 4, pp. 2276–2287, Aug. 2007.

[119]. A. Podoltsev, K. Nilanga, B. Abeywickrama, Y. Serdyuk, S. Gubanski, "Multiscale computations of parameters of power transformer windings at high frequencies. Part I: Small-scale level", *IEEE Trans Magn.*, vol 43, No 11, pp. 3991–3998, Nov. 2007.

[120]. J. Huerta, E. Santamaria, R. Gil, J. Moreno, "Design of the L-LC resonant inverter for induction heating based on its equivalent SRI", *IEEE Trans. Ind. Electr.*, vol. 54, No 6, pp. 3178–3187, Dec. 2007.

[121]. W. Shen, F. Wang, D. Boroyevic, C. Tipton, "High-density nanocrystalline core transformer for high-power high-frequency resonant converter", *IEEE Trans. Ind. Appl.*, vol. 44, No 1, pp. 213–222, Jan. 2008.

[122]. J. Biela, J. Kolar, "Using transformer parasitics for resonant converters – a review of the calculation of the stray capacitance of transformers", *IEEE Trans. Ind. Appl.*, vol. 44, No 1, pp. 223–233, Jan. 2008.

[123]. F. Terman, *Radio Engineer's Handbook*, New York, McGraw-Hill, 1943.

[124]. E. Snelling, *Soft Ferrites - Properties and Applications*, London, Iliffe Books Ltd, 1969.

[125]. C. McLyman, *Transformer and inductor design handbook*, Marcel Dekker Inc., New York 1978.

[126]. Σ. Τραχανάς, *Κβαντομηχανική ΙΙ, Τρισδιάστατα προβλήματα – Κβαντική θεωρία της ύλης*, Πανεπιστημιακές Εκδόσεις Κρήτης, Ηράκλειο, 1986.

[127]. C. Kittel, "Introduction to Solid State Physics", J. Wiley & Sons Ltd, 1996.

[128]. K. Billings, *Handbook of Switchmode Power Supplies*, New York, McGraw Hill, 1989.

[129]. C. Christopoulos, *An introduction to applied electromagnetism*, Wiley, 1990.

[130]. J. Kraus, *Electromagnetism*, McGraw-Hill, 1991.

[131]. *Magnetic Products – Soft Ferrites Data Handbook*, Philips Components, Dec. 1992.

[132]. *Power supply design seminar*, Unitrode Corporation, 1993.

[133]. S. Mulder, *Loss formulas for power ferrites and their use in transformer design*, Philips Components, Feb. 1994.

[134]. Π. Ραΐτσιος, *Μια συμβολή στην ανάλυση του πεδίου σκεδάσεως και της πυκνότητας ρεύματος σε μετασχηματιστές*, Διδ. Διατρ., Παν/μιο Πατρών – Εργ. Ηλεκτρομηχανικής Μετατροπής Ενέργειας, 1994.

[135]. N. Mohan, T. Undeland, W. Robbins, *Power Electronics Converters, Applications and Design*, J. Wiley & Sons, Inc., 1995.

[136]. Α. Κάρτας, *Δυνατότητες υπερφόρτισης μετασχηματιστών ισχύος – ανάλυση και μετρήσεις*, Διδ. Διατρ., Παν/μιο Πατρών – Εργαστήριο Παραγωγής Μεταφοράς και Διανομής Ηλεκτρικής Ενέργειας, 1996.

[137]. *PSPICE 8.0 Reference Manual*, Microsim Corporation, Oct. 1997.

[138]. A. Bossavit, *Computational Electromagnetism*, Academic Press, 1998.

[139]. Ν. Πολύζος, *Νέα γενικευμένη μέθοδος προσδιορισμού των χαρακτηριστικών λειτουργίας των διακοπτικών μετατροπέων ημι-συντονισμού με μετάβαση κατά το μηδενισμό της τάσης*, Διδ. Διατρ., Αρ. 73, Παν/μιο Πατρών – Τμ. Ηλ/γων Μηχ. & Τεχν. Υπολογιστών, 1999.

[140]. *EPCOS Data Sheet Overview*, EPCOS AG, Marketing Communications, P.O Box 801709, 81617, Munich, Germany, Aug. 2001.

[141]. *Opera 2D – User Guide*, Vector Fields Ltd, Kidlington – Oxford, 2003.

[142]. *Data Handbook – Soft Ferrites and Accessories 2005*, Ferroxcube, Sept. 2004.

[143]. A. Van den Bossche, V. Valchev, *Inductors and transformers for power electronics*, CRC Press - Taylor & Francis Group LLC, 2005.

[144]. Κ. Γκουραμάνης, *Επιτρεπόμενη φόρτιση καλωδίων χαμηλής τάσης παρουσία μη γραμμικών φορτίων*, Διδ. Διατρ., Αριστ. Παν/μιο Θεσ/νίκης – Τμ. Ηλ/γων Μηχ. & Μηχ. Υπολογιστών, Εργαστ. Σ.Η.Ε., 2007.

[145]. Ν. Σπύρου, *Ιδιότητες των ηλεκτροτεχνικών υλικών*, Εκδόσεις Παν/μίου Πατρών, 2006.

[146]. Ν. Σπύρου, *Αγώγιμες ιδιότητες των ηλεκτροτεχνικών υλικών*, Εκδόσεις Τζιόλα, 2005.

[147]. Γ. Πρίφτης, Α. Βραδής, Εισαγωγή στη φυσική στερεάς κατάστασης – μέρος Α΄, Εκδόσεις Παν/μίου Πατρών, 2000.

[148]. X. Margueron, J. Keradec, D. Magot, "Analytical calculation of static leakage inductances of HF transformers using PEEC formulas", *IEEE Trans. Ind. Appl.*, vol. 43, No 4, pp. 884–892, Jul. 2007.

[149]. K. Fowler, "Power supply design and distribution", *IEEE Instrumentation and Measurement Magazine*, Dec. 2000.

[150]. *Nikkei Electronics*, vol. 910, October 10, 2005.

[151]. http://www.murata-ps.com (March 2009)

[152]. Α. Σαφάκας, *Ηλεκτρικές Μηχανές Α, Γενικές έννοιες, Μετασχηματιστές, Μηχανές Συνεχούς Ρεύματος*, Εκδόσεις Παν/μίου Πατρών, 2000.

[153]. W. Liu, J. Dirker, J. Wyk, "Power density improvement in integrated electromagnetic passive modules with embedded heat extractors", *IEEE Trans. Power Electr.*, vol. 23, No 6, pp. 3142–3150, Nov. 2008.

[154]. E. Jong, B. Ferreira, P. Bauer, "Toward the next level of PCB usage in power electronic converters", *IEEE Trans. Power Electr.*, vol. 23, No 6, pp. 3151–3163, Nov. 2008.

[155]. W. Li, X. He, "A family of interleaved Boost and Buck converters with winding-cross-coupled inductors", *IEEE Trans. Power Electr.*, vol. 23, No 6, pp. 3164–3173, Nov. 2008.

[156]. C. Sullivan, "Aluminum windings and other strategies for HF magnetics in an era of high copper and energy costs", *IEEE Trans. Power Electr.*, vol. 23, No 4, pp. 2044–2051, Jul. 2008.

[157]. K. Harada, T. Ninomiya, H. Nishi, "Noise suppression characteristics of a dc-to-dc converter", *IEEE Trans. Aerospace Electr. Syst.*, vol. 15, No 2, pp. 260–265, March 1979.

[158]. Γ. Τσέλος, *Σχεδιασμός και κατασκευή διάταξης παραγωγής ημιτονοειδούς τάσης υψηλής συχνότητας, για μετρήσεις χαρακτηριστικών μαγνητικών στοιχείων*, Διπλ. Εργ., Αρ. 230, Εργ. Ηλεκτρομηχανικής Μετατροπής Ενέργειας –Τμ. Ηλ/γων Μηχ. & Τεχν. Υπολογιστών, 2006.

Publications with the participation of the author of this dissertation

[159]. G. Dimitrakakis, E. Tatakis, E. Rikos, "A semi-empirical model to determine HF copper losses in magnetic components with non-layered coils", *IEEE Trans. Power Electr.*, vol. 23, No 6, pp. 2719–2728, Nov. 2008.

[160]. G. Dimitrakakis, E. Tatakis, "High-frequency copper losses in magnetic components with layered windings", *IEEE Transactions on Magnetics,* vol. 45, No 8, pp. 3187–3199, Aug. 2009.

[161]. G. Dimitrakakis, E. Tatakis, "Analysis and design of a current fed resonant converter for sinusoidal excitation of magnetic components in the MHz range", *IEEE Transactions on Industrial Electronics,* vol. 58, No 12, pp. 5411–5423, Dec. 2011.

[162]. G. Dimitrakakis, E. Tatakis, "Analysis and control of a current fed sine wave converter for use in high frequency coil measurements", *Proc. of IEEE International Symposium on Industrial Electronics 2004(ISIE04)*, May 2004, Ajaccio, France, vol. 2, pp. 1267–1272.

[163]. G. Dimitrakakis, E. Tatakis, "Measurement issues related to high frequency sinusoidal excitation of magnetic coils", *Proc.IEEE 35th Annual Power Electronics Specialists Conference (PESC04)*, 21–25 June 2004, Aachen, Germany, vol. 3, pp. 1841–1847.

[164]. G. Dimitrakakis, E. Tatakis, "Generation of high frequency – low distortion sinusoidal voltage, for magnetic coil measurements, using a current fed resonant converter", *11th International Power Electronics and Motion Control Conference (EPE PEMC04)*, 2–4 Sept. 2004, Riga, Latvia, paper on CD, No A42241.

[165]. G. Tselos, G. Dimitrakakis, E. Tatakis, "Analysis and design of a current fed resonant converter applied to high frequency magnetic cores measurements", *17th International Conference on Electrical Machines (ICEM06)*, 2–5 Sept. 2006, Chania, Greece, paper on CD, (No PTM4-14).

[166]. G. Dimitrakakis, E. Tatakis, E. Rikos, "A new model for the determination of copper losses in transformer windings with arbitrary conductor distribution under high frequency sinusoidal excitation", *Proc.12th European Conference on Power Electronics and Applications (EPE07),* Sept. 2007, Aalborg, Denmark, paper on CD, No 589.

[167]. G. Dimitrakakis, E. Rikos, E. Tatakis, "An improved model for the high frequency resistance of non-layered windings", *Proc. of the 39th Annual IEEE Power Electronics Specialists Conference (PESC08)*, 15–19 June 2008, Rhodes, Greece, pp. 4277–4282.

[168]. G. Dimitrakakis, E. Tatakis, "Investigation of high frequency effects on layered coils", *13th International Power Electronics and Motion Control Conference (EPE PEMC 2008)*, 1–3Sept. 2008, Poznan, Poland, paper on CD, No 357.

[169]. G. Dimitrakakis, E. Tatakis, A. Nanakos, "A simple calorimetric setup for the accurate measurement of losses in power electronic converters", *14th European Conference on Power Electronics and Applications, (EPE 2011)*, 30 Aug. – 1 Sept. 2011, Birmingham – UK, No 744.

SYMBOLS – ABBREVIATIONS

In this section the various symbols and abbreviations used in the dissertation are listed, together with the corresponding explanations, in alphabetical order, first those of the Latin and then those of the Greek alphabet. Basically, fundamental quantities are given, while in many cases quantities which result as derivatives of the previous ones through simple mathematical expressions found within the dissertation are omitted. As in the dissertation, the vector quantities appear in bold characters. After the explanation of each symbol – abbreviation, in curly brackets is the number of the chapter in which the specific symbol appears for the first time in the sense given to it in the corresponding explanation ("A" represents the appendixes) and in brackets are the units of the corresponding quantity in the international system of units S.I. (unless it is a dimensionless quantity or a quantity without standard dimensions but dependent on the values of other variable quantities).

As can be seen from the contents of the table below, in a limited number of cases within the dissertation, the same symbols correspond to different quantities. This is due to the fact that many of them come from the international literature and an effort has been made to maintain here the symbols used in the original works. However, thanks to the references made and to the clear definition of the quantities within the text, but also with their explanation in this section, any confusion is avoided. In just a few cases, in order to avoid even a minor possibility of confusion, it was considered appropriate to use symbols in the dissertation different from those found in the original works.

TABLE OF SYMBOLS

A. Symbols from the Latin alphabet

a:	Proportionality constant between h_i and M (Preisach model) {2}
a:	Proportionality constant (Jiles – Atherton model) {2}
a:	Coefficient that correlates the specific core losses with temperature {2}
a:	Constant when calculating the product area AP {A.II}
a:	Constant when calculating copper losses {A.II}
A:	Area of one turn of the measuring winding {7} [m^2]
$\boldsymbol{A}$:	Vector potential {4} [T·m]
A_z:	The vector potential component in the z direction {4} [T·m]
a_n:	The factor of the n-th cosine term of a Fourier series {A.IV}
ac:	Alternating current. Although it normally has a more general meaning, here it is used to describe electric quantities with sinusoidal variation in time {1}
A_{eff}:	Effective cross-section area of a magnetic component core {7} [m^2]
α_e:	Thermal expansion coefficient {7} [grad^{-1}]
AP:	Area product {A.II} [m^4]
a_r:	Resistance temperature coefficient {7} [grad^{-1}]
A_w:	Magnetic component window area {A.II} [m^2]
a_0:	The constant term of a Fourier series {A.IV}
b:	Determination constant of the hysteresis loop (Jiles – Atherton model) {2}
b:	Correlation coefficient between the specific core losses and the temperature {2} [grad^{-1}]
b:	Maximum possible distance between two conductors (parameter) {4} [m]
b:	Parameter that determines the bounding condition when calculating the coordinates of conductors in a random arrangement winding {4} [m]
$\boldsymbol{B}$, B or $B(t)$:	Magnetic induction (magnetic flux density), vector– magnitude {1} [T]
B_{max}	Amplitude of the magnetic induction {7} [T]
$B_{max,opt}$:	Optimal value of the magnetic induction amplitude {A.II} [T]
B_n, B_t:	Normal and tangential (to a surface) component of the magnetic induction {4} [T]
b_n:	The coefficient of the n-th sinusoidal term of a Fourier series {A.IV}

b_p: Value of the parameter (bond) b for which a random distribution of N_m conductors is ensured to fit in a cross-sectional area $X \times Y$ {4} [m]

B_r: Remanent magnetization / residual magnetism (magnetic induction) {1} [T]

B_{sat}:   Saturation magnetization (magnetic induction) {1} [T]

B_x, B_y: Components of the magnetic induction in the x and y direction {4} [T]

$B_{x,max}$, $B_{y,max}$:   The amplitudes of B_x, B_y respectively {4} [T]

c: Correlation coefficient between specific core losses and temperature {2} [grad^{-2}]

C_a, C_b: Auxiliary (resonant) capacitors {6} [F]

C_{cl}, C'_{cl}:   Proportionality constants for the classic specific eddy current losses {2}

C_{ex}, C'_{ex}:   Proportionality constants for the excess specific eddy current losses {2}

C_m: Proportionality constant for the specific core losses {2}

C_m: Main (resonant) capacitor {6} [F]

c_n: The coefficient of the n-th term of a Fourier series when this is expressed only in cosine terms {A.IV}

c_1:   Correlation coefficient between specific core losses and temperature {2}

c_2:   Correlation coefficient between specific core losses and temperature [grad^{-1}]

c_3:   Correlation coefficient between specific core losses and temperature [grad^{-2}]

$C_1(f, T)$:   Proportionality coefficient for the specific hysteresis losses {2}

$C_2(f, T)$:   Proportionality coefficient for the specific eddy current losses {2}

$\boldsymbol{D}$:   Electric displacement (vector) {1} [Cb/m^2]

D: Determinable constant (Globus model) {2}

D: Duty cycle of a periodic pulse current {3}

D: Duty cycle of the power switches {6}

D: Solenoid diameter {4} [m]

d: Diameter of a round cross-section conductor {4} [m]

D_a, D_b: Power diodes of the resonant circuit {6}

dc: Direct current. Although it normally has a more general meaning, here it is used to describe electric quantities with a value invariable in time.

$\mathrm{d}\boldsymbol{l}$, $\mathrm{d}\boldsymbol{s}$:   Vector differentials of length and surface respectively {1} [m]

d_f: Distance of the edge of a winding from the core yoke {4} [m]

DF_R: Relative variation of the resistance factor of a winding due to the edge effect {4} [m]

DF_{Ra}:   Relative variation of the resistance factor of a conductor array due to the edge effect {4} [m]

d_l: Distance (copper-to-copper) between successive layers {4} [m]

d_{ps}:   Distance between primary and secondary winding {4} [m]

d_{sf}:   Distance between the under study secondary winding and the outer leg of the core {4} [m]

D_s: Percentual deviation of the result of a simulation from the average resulting from the results of three simulations {5}

d_t: Distance (copper-to-copper) between adjacent turns of one layer {4} [m]

e: The base of the naperian logarithms (=2.71828...) {1}

$\boldsymbol{E}$:   Electric field intensity {1} [V/m]

E: Deviation of the new model for the winding losses with random conductor distribution from the simulation results {5}

E_h: The hysteresis loop area assuming that $H(t)$ and $B(t)$ are approximately sinusoidal functions {7} [A·T/m]

E_{hc}:   Corrected value for the hysteresis loop area {7} [A·T/m]

E_{h0}:   The hysteresis loop area for 90° phase shift between H and B {7} [A·T/m]

$\boldsymbol{e_r}, \boldsymbol{e_z}, \boldsymbol{e_\theta}$:   The unit vectors in a cylindrical coordinate system {4}

E_R, E_S: Error of the one-dimensional analysis with respect to the results of FEA, for a winding with round and square cross-section conductors respectively {4}

f: Frequency {1} [Hz]

$F(\phi)$:   Statistical distribution of the angle ϕ (Stoner–Wohlfarth model) {2}

F_{Cu}:   The copper filling factor in the cross-section of a winding {5}

FEA: Finite Element Analysis

F_{Eh}:   Absolute value of the phase correction in the hysteresis loop area expressed as a percentage of it {7}

f_{max}:   Maximum possible proper operation frequency of the resonant inverter control circuit {6} [Hz]

F_R: Resistance factor. Expresses the increase in resistance of a conductor carrying a sinusoidal current of a given frequency with respect to its resistance at constant value current conditions {3}

F_{Rn}:   Resistance factor of a conductor at the n-th harmonic frequency of a periodic current waveform {3}

$F_{R,p}$, $F_{R,s}$:   Resistance factor of the primary / secondary windings {5}

$F_{R,skin}$:   Resistance factor of a straight isolated conductor of round cross-section under the influence of the skin effect (sinusoidal current) {A.I}

F_{Rt}:   Resistance factor of a turn of round cross-section solid conductor {5}

F_R^{FEA}:   Resistance factor, as it results from FEA {4}

F_R^{model}:   Resistance factor, as it comes from one of the three classic models for copper losses {4}

$F_R^{with\,EF}$:   Resistance factor of a winding under the act of the edge effect {4}

$F_{Ra}^{with\,EF}$:   Resistance factor of a conductor array under the act of the edge effect {4}

$F_R^{without\,EF}$:   Resistance factor of a winding without the act of the edge effect {4}

$F_{Ra}^{without\,EF}$:   Resistance factor of a conductor array without the act of the edge effect {4}

f_{res}:   Self-resonance frequency (natural frequency) {6} [Hz]

f_s: Switching frequency {6} [Hz]

f_T: Boundary frequency that, in the design of a magnetic component, separates the spectrum in the saturation avoidance region and in the overheating avoidance region {A.II} [Hz]

G: Term describing the proximity effect (Butterworth model) {4}

g: Determinable proportionality constant (Globus model) {2}

$g(F_{Cu}, r/\delta)$:   Corrective function of adjustment of the base equation to the numerical data, in the new model for windings with random conductor distribution {5}

g: Ratio of the parallel equivalent resistance to the inductive reactance of a resonant inductor {6}

$\mathbf{H}$, H or $H(t)$:   Magnetic field intensity, vector– magnitude {1} [A/m]

H: Term describing the skin effect (Butterworth model) {4}

$\mathbf{H_e}$, H_e: Local effective magnetic intensity, vector – magnitude (Jiles – Atherton model) {2} [A/m]

H_c: Demagnetizing force or coercive force {1} [A/m]

h: Conductive foil thickness (in x dimension) {3} [m]

h: Cross sectional side length of the square cross-section conductor{4} [m]

h_c: Demagnetizing force of a particle (Preisach model) {2} [A/m]

$\overline{h_c}$:   Average value of h_c for all the particles (Preisach model) {2} [A/m]

h_i: Intensity of the local interaction field {2} [A/m]

H_{max}: Amplitude (maximum value) of the magnetic intensity {1} [A/m]

H_{real}: Magnetic intensity in the magnetic material in the presence of eddy currents {7} [A/m]

h_{opt}: Optimal conductive foil thickness (in a winding) {3} [m]

$i, i(t)$: Electric current {1} [A]

I_{Cm}: Current in the main capacitor {6} [A]

I_{dc}: The direct component (constant term) in a periodic current waveform {3} [A]

I_{dc}: Direct current source of value I_{dc} {6} [A]

i_{eddy}: Ampere-turns of eddy currents {1} [A]

I_h: The high value in a rectangular periodic current pulse {3} [A]

I_n^{max}: Amplitude of the *n*-th harmonic component in a periodic current waveform {3} [A]

$I_{n,rms}$: RMS value of the *n*-th harmonic component in a periodic current waveform {3} [A]

$i_p(t)$: Primary winding current {5} [A]

I_{res}: Resonant current (rms value) {6} [A]

I_{resp}: Amplitude of the resonant current {6} [A]

I_{rms}: RMS current value {3} [A]

I'_{rms}: RMS value of the time derivative of the current {3} [A/sec]

I_s: Constant current (from a current source) {6} [A]

I_{total}: Total current {1} [A]

$\boldsymbol{J}, J$: Conductivity current density, vector / magnitude {1} [A/m^2]

$\boldsymbol{J_s}$: Imposed currents– power sources (Opera 2D) {4} [A/m^2]

J_{sz}: The component of $\boldsymbol{J_s}$ in the *z* direction {4} [A/m^2]

$\boldsymbol{J_v}$: Currents from external circuits (Opera 2D) {4} [A/m^2]

J_{vz}: The component of $\boldsymbol{J_v}$ in the *z* direction {4} [A/m^2]

K: Constant when calculating the product area *AP* {A.II}

k: Ratio of the delay in the control circuit response to the resonant period {6}

k: Parameter for determining the effect of the eddy currents on the value of the magnetic intensity {7} [A/V]

K_H: Ratio of the amplitude of the magnetic field to the coercive field {7}

K_w: Waveform factor {A.II}

K_1: Proportionality constant in the calculation of the core losses {A.II}

K_1, K_2:   Proportionality coefficients for the classic and the excess specific eddy current losses respectively {2} [(W·sec^2)/(m^3·T^2)] and [(W·sec$^{1.5}$)/(m^3·T$^{1.5}$)] respectively

l: Conductor length {A.I} [m]

l: Solenoid length {4} [m]

L_a, L_b: Resonant inductances {6} [H]

$L_{a,p}$, $L_{b,p}$:   Resonant inductances in the parallel equivalent circuit of the resonant inductors {6} [H]

$L_{a,s}$, $L_{b,s}$:   Resonant inductances in the series equivalent circuit of the resonant inductors {6} [H]

L_{ac}:   Conductor self-inductance under sinusoidal current conditions {1} [H]

$L_{ac,skin}$:   Self-inductance of a straight, isolated conductor of round cross-section under sinusoidal current conditions {A.I} [H]

l_{eff}:   Effective magnetic path length (in the magnetic material of the core of a magnetic component) {2} [m]

l_g: Gap length (in a magnetic component core) {2} [m]

L_p, L_s: Inductance of an inductor in the series and in the parallel equivalent circuit respectively {A.V} [H]

L_s: Inductance of high value {6} [H]

L_t: Resonant inductance connected to the inverter output {6} [H]

l_T: Average turn length of a solenoid winding {4} [m]

L_σ: Leakage inductance coefficient (or leakage inductance) of a transformer {4} [H]

M, M: Magnetization, vector {1} – magnitude {2} [A/m]

M_{rev}:   Magnetization in reversible changes {2} [A/m]

M_s: Saturation magnetization {2} [A/m]

m: Particle magnetization (Preisach model) {2} [A/m]

m: Total number of layers of a winding{3}

m_p, m_s: Number of primary / secondary layers {5}

MMF: Magnetomotive force {3} [A]

N: Number of winding turns of solid, round cross-section conductor {5}

N: Total number of strand turns in a winding with stranded conductor {5}

n: Index for determining the location of a layer of conductors in a winding {3}

n: Order of the harmonic component of a periodic waveform {3}

n:	Number of strands in a stranded conductor {5}
N_c:	Number of turns of a stranded conductor {5}
N_m:	Number of turns randomly distributed over a given cross-section $X \times Y$ when $b=b_p$ {4}
N_p, N_s:	Number of primary and secondary winding turns respectively {5}
P_v:	Specific losses in a magnetic core {2} [W/m^3]
p:	Primary winding {5}
p:	Ratio of the capacitance of the main capacitor to that of the auxiliary capacitor {6}
$p(h_i, h_c)$:	Statistical distribution of h_i, h_c (Preisach model) {2}
P_{ac}:	Eddy current losses in current carrying conductor windings {3} [W]
$P_b(b, F_{Cu})$:	Possibility for a random distribution of conductors with copper filling factor F_{Cu} to occur when the bond value is b {4}
P_{cl}, P_{ex}:	Classic and excess specific eddy currents losses respectively {2} [W/m^3]
P_{Cu}:	Copper loss power (ohmic losses) {3} [W]
$P_{Cu,w}$:	Copper loss power of one winding {A.II} [W]
P_{eddy}:	Eddy current losses {7} [W]
P_{hyst}:	Hysteresis losses {7} [W]
$P_{hyst,calc}$:	Corrected value for the hysteresis losses {7} [W]
P_{Fe}:	Core losses {7} [W]
P_{th}:	Throughput power {A.II} [W]
P_{tot}:	Loss power in the resonant inductors
P_{tot}:	Total loss power (copper and core) in a magnetic component {7} [W]
$P_{v,eddy}$:	Specific eddy current losses {2} [W/m^3]
$P_{v,hyst}$:	Specific hysteresis losses {2} [W/m^3]
p_1, p_2, p_3:	Constants in the expression of the new model for copper losses in windings with random conductor distribution {5}
R:	Radius of the magnetic globule (Globus model) {2} [m]
r:	Radius of a round cross-section conductor {1} [m]
R_{ac}:	Effective conductor resistance to a sinusoidal current {1} [Ω]
R_{ac}^T:	Effective conductor resistance to a sinusoidal current, at temperature T {7} [Ω]

$R_{ac,\,skin}$:	Resistance of a straight isolated round cross-section conductor under the action of the skin effect (sinusoidal current) {A.I} [Ω]
R_{dc}:	Conductor resistance in constant value current conditions (dc resistance) {1} [Ω]
R_{dc}^{20}:	dc resistance of a winding at temperature $T=20^{\circ}$C {7} [Ω]
$R_{dc,p}$, $R_{dc,s}$:	Primary / secondary winding dc resistance {5} [Ω]
$R_{dc,st}$:	dc resistance of one of the strands of a stranded conductor {5} [Ω]
$R_{dc,st\text{-}t}$:	dc resistance of one turn of one of the strands of a stranded conductor {5} [Ω]
RDCLI:	Resonant DC Link Inverter {A.II}
R_{eff}:	Effective conductor resistance for a random periodic current waveform {3} [Ω]
R_L:	Load resistance {6} [Ω]
$R_{L\alpha}$, R_{Lb}:	Parallel equivalent resistances of the resonant inductors {6} [Ω]
R_l:	Transformer short-circuit resistance, at a given frequency, referred to primary {5} [Ω]
$R_{l,dc}$:	Low frequency short-circuit resistance {5} [Ω]
R_m:	Shunt resistance for the current measurement {7} [Ω]
r_m:	Radial coordinate in the cylindrical coordinate system {4} [m]
R_n:	The effective resistance of a conductor to a sinusoidal current with a frequency equal to n times the fundamental frequency of a periodic current waveform {3} [Ω]
R_p, R_s:	Resistance of an inductor in the series and in the parallel equivalent circuit respectively {A.V} [H]
R_p:	Resistance of the (primary) excitation winding {7} [Ω]
R_{th}:	Thermal resistance {7} [grad/W]
s:	Secondary winding {5}
s:	Distance (center-to-center) between adjacent turns of one layer (winding pitch) {4} [m]
S:	Total integration surface {1}
t:	Time {1} [s]
T:	Temperature {2} [grad]
T:	Period of a periodic signal ($=f^{-1}$) {1} [s]
T_a, T_b:	MOSFET power transistors of the resonant circuit {6}

t_c: Time interval (there are two in a period) during which both semiconductor switches are off {6} [s]

t_d: Response delay of the control circuit {6} [s]

t_{da}, t_{db}: Delay (with respect to the zero of the output voltage) in the turn off of the semiconductor switches T_a and T_b respectively {6} [s]

t_f: Fall time of a current pulse {3} [s]

T_h: That part of the period of a rectangular current pulse during which the current has its high value {3} [s]

t_{on}: Conduction time of a power switch component in a period {6} [s]

t_r: Rise time of a current pulse {3} [s]

T_{ref}: Reference temperature (=20$^\text{o}$C) {7} [grad]

t_s: Turn off time of a semiconductor switch

V_A, V_B: Voltage at nodes A and B respectively {6} [V]

V_{dc}: Direct voltage source with value V_{dc} {6} [V]

V_{dp}: Maximum voltage encountered on a diode {6} [V]

V_{GS}: Voltage between the gate and the source of a MOSFET {6} [V]

V_o: Output voltage of the resonant inverter {6} [V]

V_{op}: Amplitude of the output voltage of the resonant inverter {6} [V]

$v_p(t)$: Primary winding voltage {5} [V]

V_{pp}, V_{pn}: Amplitudes of the sinusoidal functions that determine the voltage across a MOSFET and a diode, respectively, when both MOSFETs are off {6} [V]

$v_R(t)$: Voltage on the shunt resistance {7} [V]

V_s: Constant voltage source (variable) {6} [V]

$v_s(t)$: Secondary voltage {5} [V]

V_{sp}: Maximum voltage encountered on a MOSFET {6} [V]

W: Width of a conductive sheet (in dimension y) {4} [m]

W_m: Energy of hysteresis losses per unit volume {1} [J/m^3]

x: The direction perpendicular to the y direction of the axis of symmetry of a magnetic component {1}

X: The thickness of the winding with random distribution of the conductors {5} [m]

$x(f)$: Exponential coefficient of determination of the specific core losses {2}

$x(f, T)$: Exponential coefficient of determination of the specific hysteresis losses {2}

x': Exponential coefficient of determination of the specific hysteresis losses {2}

X_c, X_f:	Winding thickness, at the edges and faces respectively (corners and sides of the cross section), of a coil former for a core with a middle leg of rectangular cross section {5} [m]
X_p, X_s:	Primary /secondary winding thickness {5} [m]
y:	The direction of the symmetry axis of a magnetic component with cylindrical symmetry {3}
Y:	The width of the winding with random distribution of the conductors {5} [m]
$y(f)$:	Exponential coefficient of determination of the specific core losses {2}
$y(f, T)$:	Exponential coefficient of determination of the specific eddy current losses {2}
y':	Exponential coefficient of determination of the specific hysteresis losses {2}
y_e:	Distance in the y direction, inside the copper, from the edge of a winding with copper foils {4} [m]
Y_p, Y_s:	Primary /secondary winding width {5} [m]
Y_w:	Rectangular cross-section window width in a magnetic core {4} [m]
z:	The direction perpendicular to the x–y plane {3}
Z_o:	Output impedance {6} [Ω]

B. Symbols from the Greek alphabet

α:	Constant (exponential) in the calculation of the core losses {A.II}
a:	Coefficient related to the skin effect (Butterworth model) {4}
β:	Constant (exponential) in the calculation of the core losses {A.II}
γ:	Determinable constant (Globus model) {2}
γ:	Coefficient related to the proximity effect (Butterworth model) {4}
δ:	Skin depth {1} [m]
δ_T:	Skin depth at temperature T {7} [m]
δ_{20}:	Skin depth at temperature $T=20^{\circ}$C {7} [m]
δ_1:	Skin depth at the fundamental frequency {3} [m]
ΔB:	Variation (peak-to-peak) for periodic variation of the magnetic induction B {2} [T]
ΔF_{RT}:	Percentual temperature correction in the value of the resistance factor {7}

ΔH: Variation (peak-to-peak) for periodic variation of the magnetic intensity H {2} [T]

Δ_a: Percentual deviation of the low frequency approximation from the full expression for the losses in random distribution conductor windings {5}

Δ_n: Reduced (with respect to δ) optimum thickness of the n-th layer of a conductive foil winding {3}

$\Delta_{optimum}$: Reduced (with respect to δ) optimal thickness of conductive foil winding layers {3}

ε: (Absolute) dielectric constant {2} [F/m]

eq. or ex.: Equation or expression (of the dissertation){3}

ε_r: Relative dielectric constant{2}

ε_0: Dielectric constant of vacuum (=$8.854 \cdot 10^{-12}$) {2} [F/m]

η: Layer filling factor {3}

η_e: Percentage of window filling (in the y direction) in conductive foil winding {3}

η_p, η_s: Primary / secondary winding filling factor {5}

θ: Definition angle of the separating membrane between the two magnetic domains in a magnetic globule (Globus model) {2} [rad]

K_1, K_2: Coefficients related to the proximity effect (Butterworth model) {4}

λ: Ratio to the off time of the semiconductor switches to the resonant period {6}

λ_1, λ_2: Positive constants when N, Y, f, r are constant {5}

μ: (Absolute) magnetic permeability {1} [H/m]

μ_a: (Relative) amplitude magnetic permeability {2}

μ_d: (Relative) differential magnetic permeability {1}

μ_{eff}: (Relative) effective magnetic permeability {2}

μ_i: (Relative) initial magnetic permeability {1}

μ_r: Relative magnetic permeability {1}

μ_0: Magnetic permeability of vacuum (=$4\pi 10^{-7}$) {1} [H/m]

A.: Appendix (of the dissertation) {Symbols – Abbreviations}

ρ_{20}: Specific resistance at 20°C {7} [Ωm]

σ: Specific conductance (conductivity) {1} [$(\Omega m)^{-1}$]

σ: Distribution width (standard deviation) of the distribution $F(\phi)$ (Stoner–Wohlfarth model) {2} [rad]

σ_a: Integer index to determine the relative position of a conductor array {4}

σ_c, σ_i: Distribution widths (standard deviation) for h_c and h_i respectively (Preisach model) {2} [A/m]

Φ: Magnetic flux {7} [V·sec]

ϕ: Angle between the axis of preferred particle orientation and the external field (Stoner–Wohlfarth model) {2} [rad]

$\bar{\phi}$:   Average value of ϕ for the total of the particles (Stoner–Wohlfarth model) {2} [rad]

ϕ_n Phase angle of the n-th harmonic component of a periodic waveform {3} [rad]

φ: Phase shift between quantities H and B {7} [deg]

ω: Radian (or angular) frequency {3} [rad/sec]

ω_n: Radian (or angular) frequency of the n-th harmonic of a periodic waveform {3} [rad/sec]

APPENDIXES

APPENDIX I

The skin effect in an isolated round cross-section conductor

For a straight isolated round cross-section conductor of length l, with cross-section radius r, carrying a sinusoidal current of frequency f and made of material of electrical conductivity σ and magnetic permeability μ, the ohmic resistance is given by the equation:

$$R_{ac,skin} = \frac{l}{\sqrt{2}\pi r \sigma \delta} \left\{ \frac{\text{ber}(q)\text{bei'}(q) - \text{bei}(q)\text{ber'}(q)}{[\text{ber'}(q)]^2 + [\text{bei'}(q)]^2} \right\} \qquad \text{(a.1)}$$

In this equation it is:

$$q = \frac{\sqrt{2}r}{\delta} \qquad \text{and} \qquad \delta = \frac{1}{\sqrt{\sigma \pi \mu f}} \qquad \text{(a.2)}$$

where δ is the skin depth. From (a.1) it results for the resistance factor due to skin effect $F_{R,skin}$ that:

$$F_{R,skin} = \frac{R_{ac,skin}}{R_{dc}} = \frac{q}{2} \left\{ \frac{\text{ber}(q)\text{bei'}(q) - \text{bei}(q)\text{ber'}(q)}{[\text{ber'}(q)]^2 + [\text{bei'}(q)]^2} \right\} \qquad \text{(a.3)}$$

where $R_{dc} = l/\sigma \pi r^2$ is the resistance of the conductor at dc. Correspondingly, if $L_{ac,skin}$ is the inductance factor of the conductor at frequency f, its inductive reactance is given from the equation:

$$\omega L_{ac,skin} = \frac{l}{\sqrt{2}\pi r \sigma \delta} \left\{ \frac{\text{ber}(q)\text{ber'}(q) + \text{bei}(q)\text{bei'}(q)}{[\text{ber'}(q)]^2 + [\text{bei'}(q)]^2} \right\} \qquad \text{(a.4)}$$

where $\omega = 2\pi f$ is the radian frequency. For $r/\delta > 5$ the following approximations can be made:

$$\frac{R_{ac,skin}}{R_{dc}} \cong \frac{r}{2\delta} + 0.26 \qquad \text{and} \qquad \frac{\omega L_{ac,skin}}{R_{dc}} \cong \frac{r}{2\delta} - 0.02 \tag{a.5}$$

The calculation of the quantities that appear in the right-hand side of the equations (a.3) and (a.4) can be facilitated by using the following expressions for the real and the imaginary part of the first order Bessel function:

$$\text{ber}(x) = \sum_{k=0}^{\infty} (-1)^k \frac{1}{((2k)!)^2} \left(\frac{x}{2}\right)^{4k} = 1 - \frac{x^4}{(2\cdot 4)^2} + \frac{x^8}{(2\cdot 4\cdot 6\cdot 8)^2} - \dots \tag{a.6a}$$

$$\text{bei}(x) = \sum_{k=0}^{\infty} (-1)^k \frac{1}{((2k+1)!)^2} \left(\frac{x}{2}\right)^{4k+2} = \frac{x^2}{2^2} - \frac{x^6}{(2\cdot 4\cdot 6)^2} + \frac{x^{10}}{(2\cdot 4\cdot 6\cdot 8\cdot 10)^2} - \dots \tag{a.6b}$$

At this point it is necessary to quote the expansions of the second order Bessel functions appearing in (4.9):

$$\text{ber}_2(x) = \sum_{k=0}^{\infty} (-1)^k \frac{1}{(2k+1)!(2k+3)!} \left(\frac{x}{2}\right)^{4k+4} = \frac{1}{6}\left(\frac{x}{2}\right)^4 - \frac{1}{720}\left(\frac{x}{2}\right)^8 + \dots \tag{a.7a}$$

$$\text{bei}_2(x) = \sum_{k=0}^{\infty} (-1)^{k+1} \frac{1}{(2k)!(2k+2)!} \left(\frac{x}{2}\right)^{4k+2} = -\frac{1}{2}\left(\frac{x}{2}\right)^2 + \frac{1}{48}\left(\frac{x}{2}\right)^6 - + \dots \tag{a.7b}$$

Their first order derivatives with respect to x are represented as ber′, bei′, ber$_2$′, bei$_2$′.

APPENDIX II

Optimal design of magnetic components

The optimal design of the magnetic components cannot be implemented otherwise than taking into account at the same time the core and winding losses, with parallel attention being given to achieving the required value for the inductance, but also to the minimization of the leakage inductance and parasitic capacitance. All this, of course, must be done with the prospect of minimizing the negative factors (e.g. volume, weight, cost and construction time, audio and electromagnetic noise to the environment, etc.) and maximizing the beneficial parameters (e.g. efficiency). In the following we will see some ways to treat the design of a transformer or an inductor as an overall problem.

As presented in chapters Ch. 2 and Ch. 3, the efforts of the several theoretical studies on the subject of losses in magnetic components focus on how to describe in a simple and understandable way effects that in their physics are particularly complex. These efforts are considered successful when the result is a model the parameters of which are easily derived, it is simple to use (always in combination with the capabilities of modern computers) and can accurately describe the various specific effects. The final goal of all these is the optimal choice, by the magnetic components designer, of the core material and shape, of the operation switching frequency, as well as the other parameters related to the winding, in order to maximize the throughput power density and the efficiency, while minimizing the volume and the cost. Compromises between these conflicting requirements lead to the final optimal choices, always under the fundamental requirement of keeping the temperature within acceptable limits. The above design logic of a magnetic component has to take into account all the factors involved (i.e. the core, the winding, but also the rest of the device).

The first thing to consider when designing a magnetic component is that the frequency must remain below a threshold beyond which the losses increase excessively and in an unknown way. In chapters Ch.1 and Ch.2 are mentioned some of the reasons for such a restriction. Such reasons are the abrupt increase in eddy current losses above a specific frequency, the development of standing electromagnetic waves in the core volume and the capacitive currents in the winding which, in non-sophisticated constructions, begin to create problems of losses and current oscillations from relatively low frequencies (a few hundred kHz). Moreover, problems such as the gyromagnetic resonance of the elementary magnetic

dipoles' spin and the resonance of the magnetic domain walls occur at frequencies as low as some MHz. Hence, we conclude that for power converter applications, it is difficult to exceed frequencies of the order of 2MHz without resorting to specific design solutions, such as e.g. the printed circuit magnetic components [34], [35], [90], [92], [93]. Of course, this does not mean that the classic design methods have no application at these frequencies, but, due to the additional effects that take place, the theoretical analysis of the loss variation with the variation of several parameters is not easy, thus the design follows the trial and error procedure of successive tests based on empirical rules, even in the development of industrial products.

There is an increasing dependence of the losses on the frequency, but also on the amplitude ΔB of the magnetic induction. Hence, by increasing the frequency f, ΔB must be reduced for the losses to be kept below a desirable limit. Determination of this may come under the requirement of maximum efficiency. However, in applications where the power handled is of the order of a few hundred watts (e.g. power electronic supplies), it is more important to minimize the volume and this requirement goes (among other things) through the need to keep the supply device temperature at reasonable levels. Otherwise one has to install various cooling devices, of natural or forced heat dissipation, resulting in a significant increase in volume and weight. It is noted here that, in such a device, the components that mainly suffer from temperature rises and to which special attention must be paid are the magnetic components and the semiconductor power components.

It is observed [17], [18], [25], [68] that in a given transformer, the final temperature in the thermal equilibrium state, is approximately proportional to the total amount of losses in it and independent of the P_{Cu}/P_{Fe} ratio of copper losses to core losses, i.e.:

$$\frac{\Delta T}{P_{Cu} + P_{Fe}} \cong \text{constant} = R_{th} \qquad (a.8)$$

The symbol R_{th} for the value of this ratio comes from the term "thermal resistance", since it has dimensions of thermal resistance, as this is defined in physics.

Furthermore, the throughput power P_{th} in a switched-mode power supply transformer is given by the general formula [17], [18]:

$$P_{th} \sim N \cdot A_{eff} \cdot \Delta B \cdot f \sqrt{P_{Cu,w}/R_{eff}} \qquad (a.9)$$

the exact expression of which (the proportionality constant) differs depending on the type of converter and the applied waveforms. In (a.9) A_{eff} is the effective cross-section area, ΔB is the amplitude (peak-to-peak) of the magnetic induction in it, while N, R_{eff} and $P_{Cu,w}$ are the number of turns, the effective resistance (eq. 3.8) and the copper losses respectively, of a transformer winding (e.g. the primary). Equation (a.9) must be combined with the appropriate expression for the core losses as a function of ΔB and *f,* such as e.g. (2.9) and based on the conclusion (a.8) it should be required for the temperature rise not to exceed a specific value.

When designing a magnetic component, it is quite common for the prototype, as it results after various computing approximations, to be an unsatisfactory model. This requires a second attempt and probably even more, until the final result has the desirable characteristics. In laboratory - test applications, where the required specifications are probably not very strict, this procedure may yield the desirable result after a couple of tests, while in an industrial application the designer has to spend more time to achieve the optimal design.

For example, from the calculation of the leakage induction in an transformer with E type core, the logical conclusion is that a winding with fewer layers and therefore a tall and narrow window results in lower leakage induction [12], [19], [132] (see also Appendix III) and lower copper losses at high frequencies [24]. It is also known that with the use of a toroidal core the previous two quantities are minimized [45], [131]. However, in practical applications, the two above tactics are rarely adopted and this is because the problems they create are often more than the benefits they offer. It is obvious that in an electronic device the transformer is probably the bulkiest object and therefore it is imperative that its dimensions remain as small as possible. Moreover, the toroidal core does not allow for the insertion of a gap, since it is commercially available as a single piece, while it has the additional disadvantage that it is not suitable for multiple winding design trials, since the winding and removal of the conductors are quite cumbersome procedures. We do not have the same problem in E cores, because the winding is usually placed on a plastic coil former that can be removed and repositioned very easily. In order to reduce the leakage inductance and for a better behavior at high frequencies, one ends up with options such as, for example, the placement of a core with a cylindrical leg, the appropriate successive interleaving of the windings, as well as other tricks, more or less known the engineers involved in the study, design and assembly of power electronic devices.

As a second example, we will mention the case of designing an inductor to be used as a choke in a dc-to-dc Buck converter. In this converter the main concern of the designer is the

stability of the output DC voltage. This is ensured by a large value L of the choke inductance. However, the maximization of L leads to a massive design, with increased losses too. On the other hand, a reduced value of L, leads to the requirement for high value and (for a given voltage) large size bypass electrolytic capacitors. These large capacitors face problems of mechanical strength, especially under the influence of vibrations and thus often require special installation (e.g. with the addition of elastic materials). Moreover, if the construction of the inductor has not been sufficiently careful or its design has not been correctly calculated, it may exhibit parasitic capacitances, which, in combination with the capacitances of the semiconductor components and the parasitic inductances, may lead to unwanted voltage oscillations on the various components, but also in the output voltage. But something like that, leads to the necessity of additional lower value capacitors at the output (e.g. polypropylene capacitors), but also the placement of more, lower value, bypass capacitors instead of a few higher value ones.

These were some simple examples in order to make it clear that the construction of a magnetic component cannot be a task independent of the implementation of the rest of the circuit. Even after compromising between the several requirements for an overall optimal performance (taking into account all the loss factors), the final options may have completely different criteria (e.g. cost and ease of construction). Further below, we will refer to the theoretical analysis of the correlation between the core losses and the winding losses which are inextricably linked and therefore, for an optimal design, they are considered as a total.

A widely used method (McLyman method [76], [125], [132]) for the design of inductors and transformers is based on the observation that, for a given core, the area A_{eff} of the effective cross-section of the core and the area A_w of the window available for the placement of the windings can be correlated with the parameters of the device according to the expression:

$$AP = A_{eff} A_w = \left(K \frac{VA}{f B_{max}} \right)^a \tag{a.10}$$

where AP is called the area product. Coefficient K is a combination of different constant quantities, VA is the apparent power and α is a constant. Given the required power, for a specific operating frequency, the selection of B_{max} is based on the maximum allowable specific losses in the core, so that the temperature does not exceed a certain limit and using

(a.8) we select the core. A typical value for them is 0.25 W/cm^3, although depending on the size and material of the core, their value can range [93] from 0.1 W/cm^3 (large cores) to 1 W/cm^3 (small cores). It remains for the number N of the winding turns to be determined from the known equation [123]:

$$V_{rms} = K_w N f B_{max} A_{eff} \qquad \text{(a.11)}$$

where K_w is the voltage waveform factor (e.g. K_w=4.44 for a sine-wave and K_w=4 for a square pulse train [68]). The above method may take into account the increase in the winding losses due to eddy currents. For this purpose, a sufficiently accurate value for the R_{eff}/R_{dc} ratio is required (eq. (3.8), (3.15) and (3.16)), which is incorporated in K.

We will now check out the results of a study on the correlation between core and winding losses [68], which ends up to some important conclusions about the ratio of the two losses under the optimal operating conditions of a magnetic component. Similar results are found in [124], [143]. In a given, generally narrow, frequency range and for a fixed temperature, the total core losses can be approximated by an expression of the form:

$$P_{Fe} = K_1 f^a B_{max}^\beta \qquad \text{(a.12)}$$

where the constants K_1, α, β are different for each material, while K_1, also contains the core volume. After a series of reasoning steps and considering equal current density in all the windings (primary and secondaries) if it is a transformer, it follows that the copper losses are given by the equation:

$$P_{Cu} = \frac{\alpha}{f^2 B_{max}^2} \qquad \text{(a.13)}$$

where a is a constant that incorporates the exact value of the R_{dc} resistance of the windings and the ratio R_{eff}/R_{dc} at frequency f, the window copper filling factor and the waveform factor K_w of the current. After some mathematical operations it follows that, for a given frequency, when the magnetic induction takes the value for which will occur minimum losses, it will be:

$$P_{Cu} = \frac{\beta}{2} P_{Fe} \qquad\qquad\qquad\qquad (a.14)$$

while respectively, for a given magnetic induction, it comes that, at the frequency that we will have the minimum losses, it will be:

$$P_{Cu} = \frac{a}{2} P_{Fe} \qquad\qquad\qquad\qquad (a.15)$$

From the previous it becomes clear that the well-known equation $P_{Fe}=P_{Cu}$ for the operating conditions of maximum efficiency, refers to the special case that in (a.12) is $\alpha=\beta=2$, a condition which is generally not valid or applies approximately. An illustrative example is the Ferroxcube 3F3 grade [133], for which the exponents a and b get the values 1.6 and 2.5 respectively for frequencies from 20 to 300kHz, while they are 1.8 and 2.5 for frequencies from 300 to 500kHz. For the 3F4 ferrite grade of the same manufacturer a and b get such values that in some frequency ranges the ideal ratio P_{Fe}/P_{Cu} is of the order of 0.2, thus providing the possibility of a design with fewer turns compared to a design with some other core material.

For each operating frequency there is a value $B_{max,opt}$ for the amplitude of the magnetic induction for which, in normal operation, the total losses are minimum. The amplitude B_{max} should be chosen as high as possible, so that the final design has the minimum possible turns, and therefore a minimum leakage flux, but it must remain well below the saturation levels of the material. A choice of about 10% below B_{sat} is typical to ensure that, even in transient phenomena, the core will not enter saturation (some converters require a larger difference). Therefore, if the calculated $B_{max,opt}$ is greater than $0.9B_{sat}$, either another core should be selected or a magnetic induction of about $0.9B_{sat}$ should be applied, but without the optimal design of the magnetic component that could result with the use of this core. Thus, for every core, there is a frequency f_T below which it is $B_{max,opt}>0.9B_{sat}$ and therefore the optimal design is impossible, so the details of the construction are determined by the requirement to avoid saturation. It is a fact, however, that as the frequency increases in the frequency range beyond f_T where we can achieve optimal design, gradually arise the various other problems, which we have already mentioned, while the profit in throughput power is low. Hence, in practical applications, the switching frequency is finally selected at a value close to f_T. We must also remember that in some resonant topologies (e.g. resonant inverters with dc coupling –

RDCLI) the frequency varies with the load, making it practically impossible to optimally design the magnetic components [65].

In closing this paragraph, we must mention the great contribution of the use of computers in the procedure of optimal design of magnetic components and power electronic converters in general. Given the huge number of parameters to consider, it is important to be able to use circuit simulation software, in which a model or a methodology for calculating the losses can be incorporated in the form of an equivalent circuit [21], [33], [86], [61], [64].

APPENDIX III

Leakage flux in a transformer, MMF diagrams

The leakage flux in a transformer is that part of the magnetic flux that does not completely flow through all the windings and therefore does not contribute 100% to the magnetic coupling between the primary and secondary. In the simple example where the primary and the only secondary are wounded around the middle leg of an E or P type core, one inside, close to the leg and the other externally, above the previous one (Fig. a.1), it is obvious that the flux through the middle leg is 100% coupling flux. As we run the inner winding outwards, the flux in these regions partially connects the two windings, while the flux in the external winding region is purely leakage flux. In the rest of the free space of the window (if the window is not filled with copper along its entire width in the x direction) the flux, although generally not zero, can be considered negligible.

This is a typical quantity of transformers for which various methods of calculation and representation have been proposed, together with corresponding equivalent circuits for the transformer. In the classic and most widely used equivalent circuit, conventionally, it appears divided into primary winding leakage and secondary winding leakage [152]. At some high frequency applications, the leakage inductance is an important factor that lowers the upper
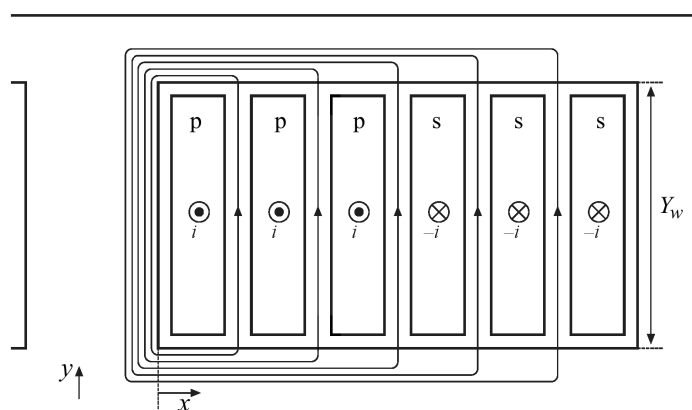

Figure a.1: Approximate representation of the path of the flux lines of the magnetic field at the cross section of a transformer the primary (p) and secondary (s) of which consist of three layers each, each of which carries a total current i. With y the symmetry axis of the winding (and of the core, if it is a P type core) is indicated and with Y_w the width of the window.

limit of the possible operating frequencies or leads to unwanted oscillations, combined with various parasitic capacitances and thus an effort is made to keep it low. In other cases, it is combined with the capacitive components of the transformer to produce a resonant circuit in resonant inverters, without the need to externally connect additional capacitances and inductances [105], [117], [122], [154]. In high power transformers of the grid, it is mainly the leakage that suppresses the short-circuit currents and therefore it is attempted not to be too low during their design.

The leakage flux that penetrates the copper of the windings is responsible for the increase of the copper losses at high frequencies, as it leads to the induction of eddy currents in them. The leakage flux that occupies the copper volume decreases as the frequency increases, but this is generally a low percentage of the total leakage flux and therefore this reduction does not particularly interest magnetic component designers.

With some simple calculations [12], [19], [24], [45] it results that the leakage inductance is lower in a transformer with a high window and a few layers compared to a corresponding transformer of low window and many layers. The assembly of transformers with a high window, however, is generally not desirable. If some leakage decrease is required, a design solution is the appropriate interleaving of the primary and the secondaries, which also reduces the eddy current losses.

The first term in (4.3), which expresses the skin effect, is much smaller than the second one, which expresses the proximity effect, even if $m=1$, where m is the number of layers in the part of the winding under study (portion), which extends between a zero MMF point and another one of maximum MMF. Thus, we can say that the losses are approximately proportional to the square of the number of layers.

In the set of figures of Fig. a.2 we see the MMF diagrams for various cases of interleaving of the two windings, primary and secondary, without any concern here about whether the layers consist of conductive foils or round cross-section conductors. It is obvious that in the layers located in areas of high MMF the development of eddy currents is more intense and consequently the increase of the effective resistance is greater. Thus, layers located in areas of high MMF have higher values for the resistance factor F_R.
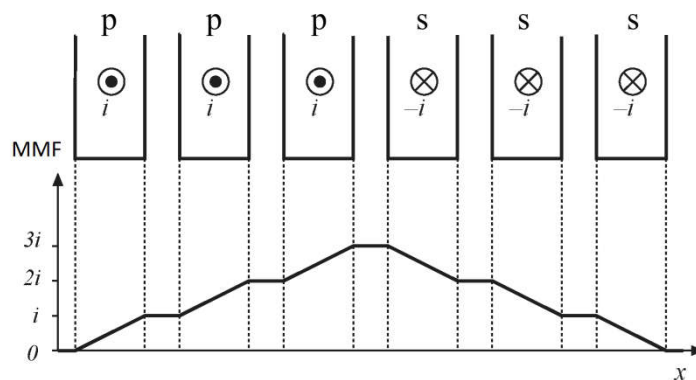
(a)
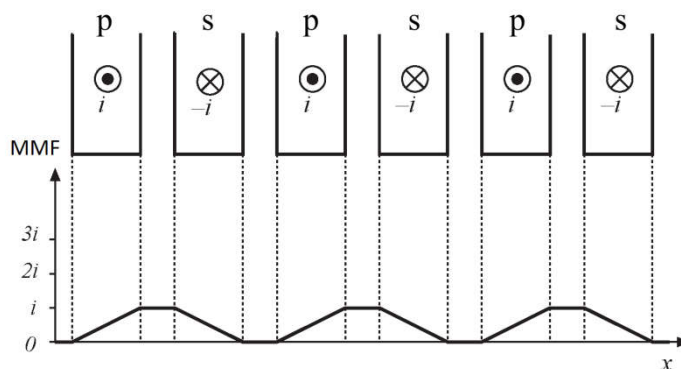
(b)
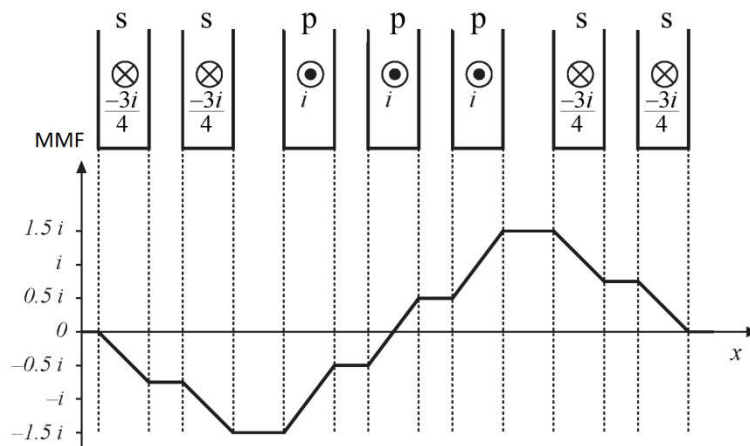
(c)

Figure a.2: MMF diagrams for various cases of interleaving, in a transformer consisting of a primary (p) and a secondary (s) winding.

If there is no edge effect (§3.4.2 and §4.5) turns of the same layer present the same resistance factor, which is obviously equal to the resistance factor of the layer. Correspondingly, in a winding portion extending between zero and maximum MMF, in which the various turns or layers are connected in series and carry the same current, the effective resistance is the sum of the effective resistances of the various turns or layers and the factor resistance is equal to the average of their resistance factors [9], [12], [47]. Obviously, this does not apply to parallel connected windings in which case the known effective resistance calculation models do not apply. From the comparison between Fig. a.2(a) and Fig. a.2(b) it becomes qualitatively obvious that a change in the arrangement of the layers can lead to lower overall losses. From (4.3) it easily results that it is more efficient to select six portions with $m=1$ each, instead of two portions with $m=3$.

Correspondingly, the arrangement of the windings shown in Fig. a.2(c) is preferable (in terms of minimizing the losses) compared to one that would keep the three layers of the primary and the four layers of the secondary separated. We also see in Fig. a.2(c) that a part of the winding may contain a half-integer number of layers (here the primary is divided into two parts with one and a half layers each), i.e. the zero point MMF is located within a layer. In this case nothing changes in the analysis, except from the exact expression that gives the result for the resistance factor F_R [12]. For a large number of layers, however, the relative difference from the result of rounding to the nearest integer number and using (4.3) or even of directly using (4.3), with m now the half-integer number, is small.

So far it was considered that the frequency is not very high and the current density is constant inside the copper at the various points of the winding cross section, hence the MMF changes linearly with respect to x inside the copper. However, for higher frequencies, for which the skin depth becomes comparable to the thickness of the conductors (in the x dimension), the situation is different: The current within a conductor tends to concentrate in the areas of high MMF (Fig. a.3(a)) and the MMF diagram is not a linear function of x within the layers (Fig. a.3(b)). Within a layer, appear currents with a phase shift of up to 180° and the field inside the copper (hence the MMF) can take very low, almost negligible values and thus the magnetic energy inside the copper is reduced significantly. Instead, in the general case, the areas between the layers can be considered as areas of constant MMF.
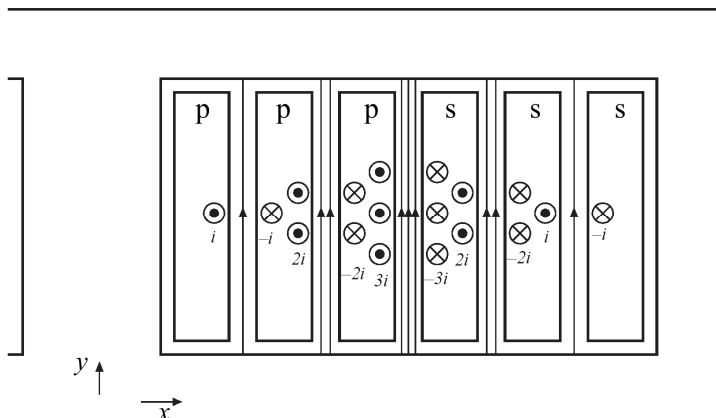
(a)
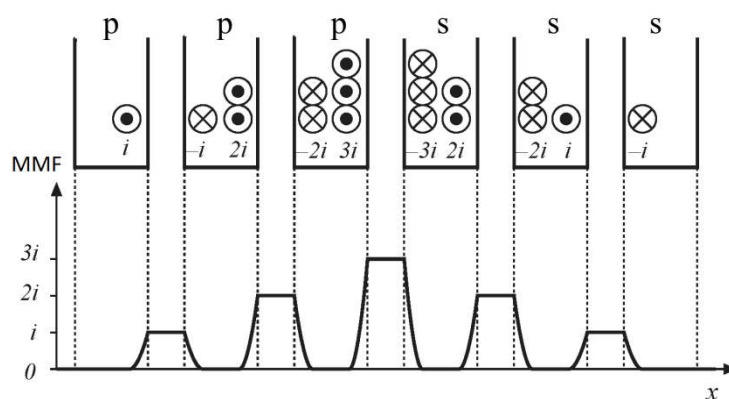
(b)

Figure a.3: For frequencies at which the skin depth becomes comparable to the thickness of the conductors the current density is increased in the areas of high MMF, which is no more a linear function of *x*.

APPENDIX IV

Fourier analysis of a periodic function

Suppose that the function $f(x)$ is periodic with period T. Then, it can be expressed in the form of an expansion from the Fourier series:

$$f(x) = \frac{a_0}{2} + \sum_{n=1}^{\infty}\left(a_n \cos\frac{2n\pi x}{T} + b_n \sin\frac{2n\pi x}{T} \right) \qquad (a.16)$$

where the Fourier coefficients a_n, b_n and a_0 are given by the expressions:

$$a_n = \frac{2}{T}\int_0^T f(x)\cos\frac{2n\pi x}{T}\,dx \qquad (a.17a)$$

$$b_n = \frac{2}{T}\int_0^T f(x)\sin\frac{2n\pi x}{T}\,dx \qquad (a.17b)$$

$$a_0 = \frac{2}{T}\int_0^T f(x)\,dx \qquad (a.17c)$$

and therefore the constant term $a_0/2$ in (a.16) gives the average of $f(x)$. With a few operations, we conclude that (a.16) can be written alternatively as follows:

$$f(x) = \frac{a_0}{2} + \sum_{n=1}^{\infty} c_n \cos\left(\frac{2n\pi x}{T} + \phi_n \right) \qquad (a.18)$$

where:

$$\phi_n = -\tan^{-1}\left(\frac{b_n}{a_n}\right) \qquad \text{and} \qquad c_n = \frac{a_n}{\cos\left[\tan^{-1}\left(\dfrac{b_n}{a_n}\right)\right]} = \frac{b_n}{\sin\left[\tan^{-1}\left(\dfrac{b_n}{a_n}\right)\right]} \qquad (a.19)$$

APPENDIX V

R-L networks

In this section, with the application of some elementary complex analysis, we show that for an ohmic – inductive impedance we can have equivalent representations with an R–L network, either in series or in parallel.

So, let's consider the following two impedances:

$$\boldsymbol{Z_s} = R_s + j\omega L_s \qquad\qquad \boldsymbol{Z_p} = (R_p // j\omega L_p) = \frac{R_p j\omega L_p}{R_p + j\omega L_p} \qquad\qquad (a.20)$$

Provided that it is not $\omega = 0$ or $\omega = \infty$, we can demand for these two impedances to be equal in magnitude and phase. Equating the real and the imaginary parts of these two impedances results in:

$$R_s = \frac{R_p (\omega L_p)^2}{R_p^{\,2} + (\omega L_p)^2} \qquad\qquad L_s = \frac{R_p^{\,2} L_p}{R_p^{\,2} + (\omega L_p)^2} \qquad\qquad (a.21)$$

Thus, for given ω, if R_p and L_p are known R_s and L_s may be directly calculated from (a.21). In the case when the components of the series connection are known and those of the parallel connection are requested, they result from the respective relations:

$$R_p = \frac{R_s^{\,2} + (\omega L_s)^2}{R_s} \qquad\qquad L_p = \frac{R_s^{\,2} + (\omega L_s)^2}{\omega^2 L_s} \qquad\qquad (a.22)$$

while, either from (a.21) or from (a.22), we can easily see that it is:

$$\frac{\omega L_s}{R_s} = \frac{R_p}{\omega L_p} \qquad\qquad (a.23)$$

Moreover, on the basis of (a.22) the observation made in Ch. 6 is supported, according to which if it holds that $R_s << \omega L_s$ or equivalently $R_p >> \omega L_p$ then, without significant error, we can make the approximation $L_p \cong L_s$.

SUMMARY

Power electronic converters are used in a wide range of both low and high power applications. Most of these converters include magnetic components (transformers – inductors), the power losses of which determine in a major degree their efficiency. It is therefore very important to the power electronic converter designers to have available the proper theoretical models and experimental methods for the accurate determination of the magnetic component losses in order to make optimum design choices and achieve an effective energy saving.

The present work has a twofold goal:

a) To investigate the phenomena affecting the copper losses in windings that consist of conductor layers and to develop a new model for the calculation of copper losses in round cross section conductor windings with random distribution of these conductors in the available core window area.

b) To develop a complete methodology of making experimental measurements on magnetic components, through the investigation of the several measurement error factors and to design a resonant converter suitable for the excitation of magnetic components with high frequency sinusoidal voltage.

In the first part of this thesis (chapters Ch. 1, Ch. 2 and Ch. 3) there is a general description of the physical phenomena that take place in magnetic components when a periodically time variable current flows through them, i.e. magnetic hysteresis and eddy currents at the magnetic core material and skin as well as proximity effect at the windings, which are due to the development of eddy currents in them. Moreover, there is an overview citation and critical review of the most important by now theoretical works on these issues which are also widely used for the calculation of the losses related to them.

In the second part of this thesis (chapters Ch. 4 and Ch.5) there is at first a short review of the three classic models for the calculation of copper losses in windings made of layers and then a finite element software is utilized for the investigation of the accuracy and field of application of each of them. It is shown that Dowell's model is much more accurate and that the declination of the models from the real (according to simulations) results are due to their inherent inability to properly take into account the two-dimensional distribution of the

magnetic field and the current density when the frequency increases or when the filling factor value decreases.

The edge effect in layered windings with either round cross section or foil conductors is investigated and a qualitative as well as quantitative description of its effect on the effective resistance is given, showing that there can be an increase in it only at frequencies close to the fundamental frequency of the current waveform. There is also a study about the geometrical extent of the edge effect in the winding volume and it is concluded that the winding is generally affected only on its outer parts, a fact that minimizes the possibility for a hot spot to appear.

Moreover, for layered windings with round cross section conductors, a study is carried out about the difference in the effective resistance between the cases of square and hexagonal fit schemes and it is shown that in the second case there can be an appreciable power loss reduction.

Following this work, is the development of a new model for the calculation of copper losses in round cross section conductor windings with the several turns placed with a random manner in the available core window area, which is a common design choice. For the derivation of the new expression a computer aided curve fitting process has been applied on a large amount of numerical data coming from finite element simulations. The final equation of the model is simple and incorporates only three easily determinable parameters, directly related to known constructive parameters. It is shown that the new expression can also be applied in the case of stranded wire windings. Its sensitivity to the winding height measurement errors is investigated and a low frequency approximation is proposed. At last, the new expression is validated with experimental measurements.

The first work presented in the third part of this thesis (chapters Ch. 6 and Ch. 7) is the design and construction of a resonant converter suitable for the excitation of magnetic components with a clearly sinusoidal voltage of high frequency (up to 1MHz) and amplitude of several hundreds of volts, at several tenths of Watts power level, for the implementation of experimental measurements. The theoretical and experimental investigation of the factors affecting the converter performance reveals the interrelated importance of the design choices in the resonant tank and the electronic control board and leads to the proper component selection in both these circuits so as to expand the operating frequency range, minimize the harmonic distortion and maximize the amplitude of the output voltage.

Following that, there is a description of the methods available to measure the power losses of magnetic components and acquire the hysteresis loop of their magnetic cores. The several error factors are analyzed and measurements are taken in order to determine the power losses and monitor the hysteresis loop of ferrite materials at several frequencies. Some methods are proposed for the correction of the measured hysteresis losses, if these are determined from the area of the hysteresis loop, in the case of a known phase error when recording magnetic intensity or magnetic induction. At last, the reduction with temperature of ohmic resistance at high frequencies is explained and some indicative graphical examples are given for the correction in its calculated value for some typical magnetic component temperature rise values.